Spatial Analysis of Karst Conduit Networks and Determination of Parameters Controlling the Speleogenesis along Preferential Lithostratigraphic Horizons

THÈSE N^{O} 4376 (2009)

PRÉSENTÉE LE 15 MAI 2009

À LA FACULTÉ ENVIRONNEMENT NATUREL, ARCHITECTURAL ET CONSTRUIT
LABORATOIRE DE GÉOLOGIE DE L'INGÉNIEUR ET DE L'ENVIRONNEMENT
PROGRAMME DOCTORAL EN ENVIRONNEMENT

ÉCOLE POLYTECHNIQUE FÉDÉRALE DE LAUSANNE

POUR L'OBTENTION DU GRADE DE DOCTEUR ÈS SCIENCES

PAR

Marco FILIPPONI

acceptée sur proposition du jury:

Prof. A. Mermoud, président du jury
Prof. A. Parriaux, Dr P.-Y. Jeannin, directeurs de thèse
Prof. G. Anagnostou, rapporteur
Prof. K. Föllmi, rapporteur
Dr A. Palmer, rapporteur

ÉCOLE POLYTECHNIQUE
FÉDÉRALE DE LAUSANNE

Suisse
2009

ÉCOLE POLYTECHNIQUE
FÉDÉRALE DE LAUSANNE

Swiss Institute of
Speleology and Karstology

Spatial analysis of karst conduit networks and determination of parameters controlling the speleogenesis along preferential lithostratigraphic horizons

by

Marco Filipponi

Director
Prof. Dr. A. Parriaux and Dr. P.-Y. Jeannin

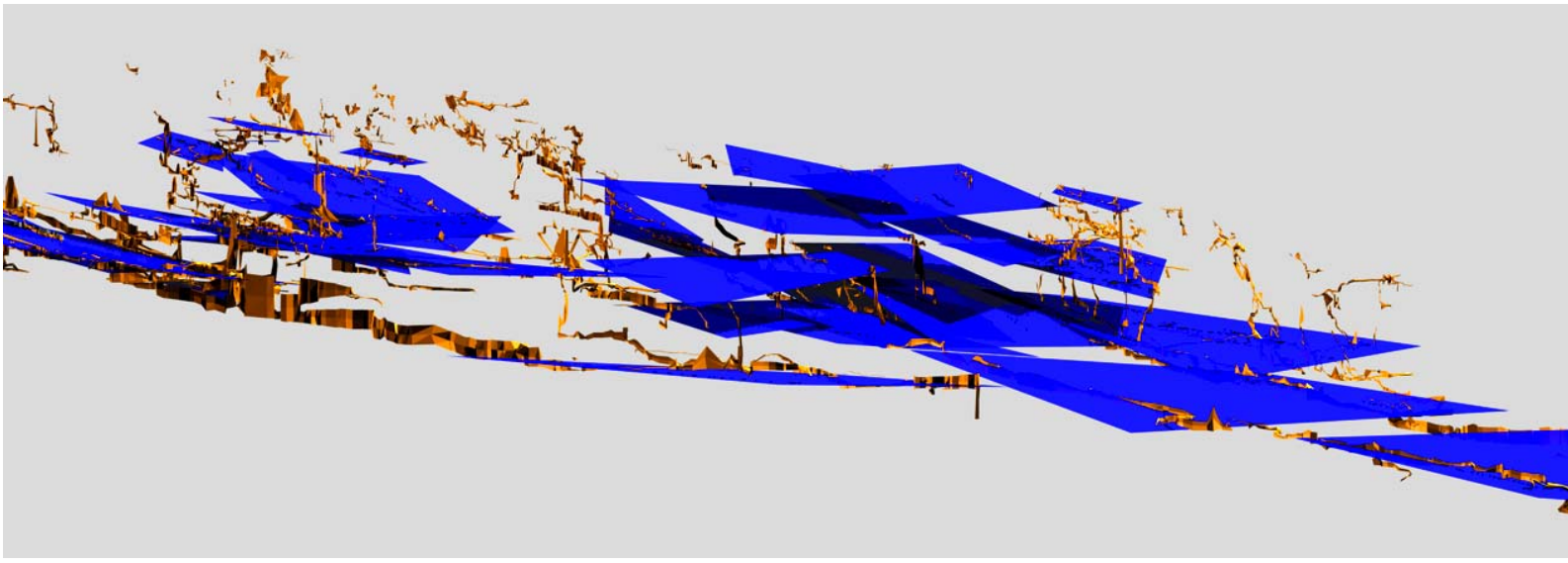

Lausanne – February 2009

- Abstract -

The main objective of this thesis is to improve the understanding of the position and characteristics of karst conduits within a rock massif. Such a characterisation is an important issue in civil engineering and in hydrogeology. Today in practice dissolution voids are considered as random in most cases. However, it is obvious for karst researchers that dissolution void distribution is not random, but defined by parameters controlling the speleogenesis.

We developed a method to analyse the 3D geometry of cave systems in order to demonstrate from a statistical point of view that karst conduits position is not random. The analysis of several among the largest cave systems in the World (more than 1500 km of analysed cave conduits) confirmed for the first time quantitatively that the development and position of karst conduits under phreatic conditions is strongly related to a restricted number of so called inception horizons. An inception horizon – a concept introduced by Lowe (1992) – is a part of a lithostratigraphic succession that is particularly susceptible to the effects of the earliest cave forming processes by virtue of physical, lithological or chemical deviation from the predominant carbonate facies within the formation. We demonstrate that probably less than 10 % of the existing bedding partings of a limestone sequence are inception horizons and guide more than 70 % of the phreatic conduits. Our analysis clearly confirms that the influence of these horizons onto the 3D geometry of cave systems is high.

Based on the 3D analysis of cave systems as well as on field verifications, 18 inception horizons in six cave systems have been selected for field characterisation and sampling in order to identify the properties and processes that makes these particular lithostratigraphic horizons favourable to karstification. Around 200 rock samples from the horizons and the surrounding rock mass have been analysed. The results evidence that inception horizons have a thickness of some centimetres to decimetres and that it is possible to distinguish between 3 types of inception horizons:

- Inception horizons where the cave inception took place **within the inception horizon** (type 1); characterized by a slightly higher primary permeability, pyrite and quartz contents and lower matrix contents than the surrounding rock mass. Usually, fractures propagate through or occur within these horizons.
- Inception horizons where the cave inception took place **at the contact with the inception horizon** (type 2); characterized by a lower primary permeability and carbonate contents, but higher pyrite contents than the surrounding rock mass. Fractures usually are ending at these horizons.
- Inception horizons where the cave inception took place along bedding plane fractures (type 3); already a slippage of just a few millimetres, striation, brecciation and surface irregularities enhance openings along the sliding plane and cause a significant increase in permeability.

Furthermore it can be assumed that for the inception of horizons of type 1 the primary permeability will be the relevant factor at beginning of karstification, whereas both the matrix and the pyrite contents are the key factors during the later phases of cave inception and gestation. Whereas for further cave development the total carbonate content will be crucial.

For inception horizons of type 2, we can assume that the low primary permeability, the clogging of the pores by the clay minerals, the high content of pyrite (production of aggressive solutions within the horizon that concentrates the dissolution along the contact to the surrounding rock) and the ending of the fractures at the horizon are responsible for the enhanced karstification at the contact during cave inception and gestation phases

Using simple hydrogeological numerical modelling we show that an epigenic karstic rock massif can be subdivided into four speleogenetic zones: 1) vadose cave development zone above the water table, 2) the phreatic cave development and 3) gestation zone within the first tens of metres of the phreatic zone and 4) below them the inception zone. Each of these zones is characterized by typical speleogenetic processes as well as dissolution void distribution.

Further, it was possible to explain and reproduce schematically the 3D pattern of different cave systems by using the position and orientation of the inception horizons and the history of the landscape evolution (i.e. the re- and discharge area). This forward analysis provides a first idea of the geometry of the conduits as well as a better understanding of the development of a karst system in time and space (vertical section).

Finally, we evaluated the feasibility to combine the improved inception horizon hypothesis, to predict inception horizons, with other current applied methods to improve the prediction of dissolution voids. Furthermore, we proposed a scientific based risk assessment for underground engineering proposes.

Essentially, it is now evidenced that it is possible to quantify the probability of karst occurrences inside a karst massif by reconstructing the hydrogeolgical history and identifying the few inception horizons that guide the karstification at a regional scale.

Key words

Karstification; Speleogenesis; Inception horizon hypothesis; Spatial distribution; Properties of lithostratigraphic horizons; Prediction of karst conduits.

- Résumé -

Le principal objectif de cette thèse est d'améliorer la compréhension de la géométrie et des caractéristiques des réseaux de galeries au sein d'un massif karstifié. Une telle caractérisation est très importante dans le domaine de l'ingénierie civile et de l'hydrogéologie. Aujourd'hui, les vides de dissolution sont considérés comme étant repartis aléatoirement dans l'espace dans la majorité des cas. Cependant, il est évident pour les karstologues que la distribution spatiale des vides de dissolution n'est pas aléatoire mais définie par des paramètres spécifiques contrôlant la spéléogenèse.

Une méthode permettant d'analyser en 3D la géométrie des réseaux karstique a été développée. Cette approche a pour objectif de démontrer de façon statistique que la position des réseaux karstiques n'est pas aléatoire. L'analyse de plusieurs grands réseaux à travers le monde (plus de 1500 km de galeries) a confirmé pour la première fois quantitativement que le développement et positionnement des conduits sont liés à un nombre restreint d'horizons lithostratigraphiques (horizons d'inception). Un horizon d'inception – concept introduit par Lowe en 1992 – est une unité d'une succession lithostratigraphique particulièrement susceptible aux effets des processus spéléologique au début de la karstification. Ces processus surviennent suite à des changements physiques, chimiques ou lithologiques du faciès carbonaté prédominant au sein de la formation. Nous avons pu démontrer qu'au moins 10 % des bancs d'une séquence carbonatée sont des horizons d'inception et qu'ils guident plus de 70 % des conduits phréatiques. Nos analyses confirment clairement que ces horizons ont une influence importante sur la géométrie 3D des systèmes karstiques.

En nous basant sur l'analyse 3D des réseaux de conduits ainsi que sur des observations de terrain, 18 horizons d'inception dans six réseaux ont été sélectionnés pour être caractérisés in situ et échantillonnés pour identifier les paramètres qui rendent ces horizons lithostratigraphiques favorables à la karstification. A peu près 200 échantillons de ces horizons ainsi que de la roche avoisinante ont été collectés et analysés. Les résultats montrent que ces horizons d'inception ont une épaisseur de quelques centimètres à quelques décimètres et peuvent être classifiés en 3 types:

- Les horizons d'inception dans lesquels l'initialisation de la cavité a eu lieu **au sein même de l'horizon** (type 1): cette unité se distingue de la roche encaissante par une perméabilité primaire légèrement plus élevée, un contenu en quartz et en pyrite également plus élevé et un contenu matriciel moins important. Habituellement les fractures traversent ces horizons ou se produisent en son sein.
- Les horizons d'inception dans lesquels l'initialisation de la cavité a eu lieu **au contact entre l'horizon et la masse rocheuse** (type 2): cette unité se différencie de la roche avoisinante par une plus faible perméabilité primaire et un contenu carbonaté moins important. Le contenu en pyrite quant à lui reste plus élevé. Habituellement les fractures se terminent au contact avec les horizons.
- Les horizons d'inception dans lesquelles la cavité se forme le **long de plans de fractures** (type 3): Un glissement de quelques millimètres sur un plan de fracture produise déjà des ouvertures signifiant et provoquer une augmentation importante de la perméabilité.

De plus, on a supposé que lors de l'initialisation des horizons d'inception de type 1, la perméabilité primaire est le facteur principal, alors que le contenu matriciel ainsi que le contenu en pyrite jouent un rôle important dans la phase tardive de l'initialisation et la gestation. Le contenu en carbonates n'est quant à lui, décisif que pendant la phase du développement de la conduit.

Pour les horizons d'inception de type 2, nous supposons que la faible perméabilité primaire, l'occlusion des pores par des minéraux argileux et le contenu élevé en pyrite, qui favorise la concentration de solutions agressives au contact avec la roche encaissante, sont responsables de la karstification. Celle-ci se développe à partir du point de contact au cours de la phase de l'initialisation et de gestation.

Des simples modèles hydrogéologiques ont montré qu'un massif karstifié épigénique pouvait être divisé en 4 zones distinctes: 1) zone de développement de la cavité vadose au-dessus du niveau piézométrique; 2) la zone du développement phréatique et 3) de gestation dans les 10 premiers mètres de la zone phréatique et 4) au-dessus la zone d'initialisation. Chacune de ces zones est caractérisée par des processus spéléogénétiques ainsi que par une distribution caractéristique des vides de dissolution.

Il a également été possible d'expliquer et de reproduire schématiquement la structure 3D des différents réseaux karstiques, en utilisent le positionnement et l'orientation des horizons d'inception ainsi que l'évolution géomorphologique (soit les zones de recharge et de décharge). Cette analyse donne une bonne première idée sur la géométrie des conduits et permet une meilleure compréhension du développement des complexes karstiques dans le temps et l'espace.

Pour finir nous avons étudié la faisabilité d'améliorer la prédiction des vides de dissolution avec l'hypothèse des horizons d'inception en la combinant avec d'autres méthodes courantes dans le domaine appliqué. Nous proposons, par ailleurs, une évaluation scientifique des risques pour l'ingénierie du sous-sol.

Essentiellement, nos résultats permettent de quantifier la probabilité de rencontrer des réseaux karstiques, au sein d'un massif, en identifiant les d'horizons d'inception et en reconstruisant l'histoire hydrogéologique.

Mots-clés

karstification, spéléogenèse, hypothèse d'horizons d'inception, distribution spatiale, propriétés d'horizons lithostratigraphiques, prédiction de conduits karstiques.

- Table of Contents –

Appendix 1 - Papers and Documents about the Demonstration of Inception Horizon

Siebenhengste Cave System

Evidence of inception horizons in karst conduit networks.

Filipponi M., Jeannin P.-Y., Tacher L., 2009: Geomorphology 106, 86-99.

Totes Gebirge: DÖF-Sonnenleiterschacht, Burgunderschacht

Constraints on alpine speleogenesis from cave morphology - a case study from the eastern Totes Gebirge (Northern Calcacerous Alps, Austria).

Plan L., Filipponi M., Behm M., Seebacher R., Jeutter P., 2009: Geomorphology 106, 118-129.

Lachenstock-Karst

Verstehen der Speläogenese durch 3D-Analyse - Fallbeispiel des Lachenstock-Karstes.

Filipponi M., Dickert A., 2007: 12. Nationtal Congress of Speleology – Switzerland, 46-55.

Nachtrag: Feldnachweis in der Lachenstockhöhle

Nidlenloch

Is it possible to predict karstified horizons in tunneling?

Filipponi M., Jeannin P.-Y., 2006: Austrian Journal of Earth Sciences 99, 24-30.

Feldnachweis und Beobachtungen im Nidlenloch

Grottes aux Fées (CH)

3D Analyse, Feldnachweis und Beobachtungen

Réseau de Covatannaz (CH)

3D Analysis

Kleines Hölloch (D)

3D Analysis

Hirlatzhöhle (A)

3D Analysis

Shuanghedongqun (China)

3D Analysis

Ogof Draenen (GB)

3D Analysis

Appendix 2 – Properties Occurrence Matrices

Appendix 3 -Other Papers

Speläologische Erscheinungen im Zusammenhang mit stratigraphischen Initialfugen.
Filipponi M., 2007: Laichinger Höhlenfreund 42, 21-32.

What makes a bedding plane favourable to karstification? - The role of the primary rock permeability.
Filipponi M., Jeannin P.-Y., 2008: Proceeding of the 4th European Speleological Congress, Spelunca Mémoires, 33: 32-37.

Prediction of karst occurrences by interpreting borehole data within the Inception Horizon Hypothesis.
Filipponi M., Jeannin P.-Y., 2008: Sinkholes and the Engineering and Environmental Impacts of Karst 2008, Proceedings of the 11th Multidisciplinary Conference, Geotechnical Special Publication 183: 120-130.

On the CD (not referenced in the text)

Video-Animations

- Siebehengste-Analyse.wmv
  Animation illustrating on the example of the Siebenhengste Cave System the principles of the developed 3D analysis method of chapter 2.
- -Lachenstock.wmv
  Animation presenting the results of the 3D analysis of the Lachenstock karst. Red dyed cave parts are vadose conduits, the yellow ones phreatic.
- -Nidlenloch.wmv
  Animation presenting the results of the 3D analysis of the Nidlenloch.
- -Shuanghedongqun.wmv
  Animation presenting the results of the 3D analysis of the Shuanghedongqun.
- -GrottesFees.wmv
  Animation presenting the results of the 3D analysis of the Grottes aux Fées.
- -InceptionAndFractures.wmv
  Animation presenting the concept that the main direction of the conduits is determined by the hydrogeological context, their positions by the inception horizons and the conduit courses by the intersection of inception horizons with inception fractures.

Text

- -Filipponi2009.pdf
  Thesis in pdf-format

- 1 -
Introduction and Problem Description

As **karst** is termed a special type of landscape but also a typical hydrogeological system (fig. 1.1). Karst as a landscape develops predominantly by the dissolution of rock and has particular geomorphological features like dolines, karren, caves. Karst as a hydrogeological system is a self-regulated underground dewatering system, which optimises its discharge by the dissolution of the rock mass and develops a drainage system (karst conduits). An overground dewatering system is often widely missing. Karst develops mainly in carbonates (limestone and dolomite), but also in gypsum or halite and rarely in sandstone or quartzite. Around 20 % of the dry and ice-free land consists of karstic rock formations (Ford and Williams, 2007) and it covers large areas especially in China, Europe and USA.

The most spectacular karst features are caves. **Caves** are natural voids in the ground, large enough for human to enter (generally larger than 0.5 m; White, 2002). This definition is arbitrary and subjective, but practical, as it eliminates narrow openings, irrelevant for cave explorers, but it also eliminates dissolution features very significant for hydrologists. As a more general term" **karst conduit**" can be used. It includes all dissolution voids greater than some centimetres in diameter (and therefore also caves). For smaller dissolution features we will use "**dissolution seam**". The development of a cave from a tiny dissolution seam to a cave conduit is described by the **speleogenesis.**

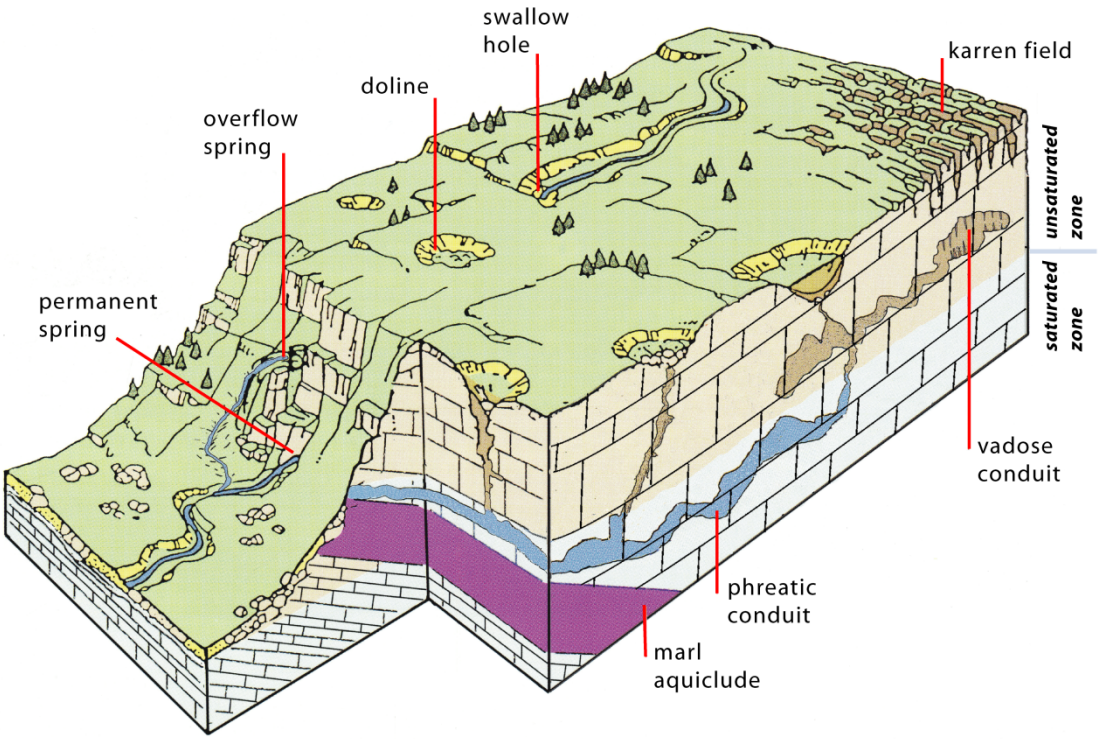

Fig. 1.1: Block diagram of a karst landscape with some typical surface and underground morphological features and their relation to the hydrogeological system (modified after Schaer et al., 1998).

Since the beginning of karst science in the 18th century, attempts have been made to understand and predict the position and geometry of karst conduits (e.g. Lindner, 1841). Such predictions still remain a challenge for various disciplines of Earth Sciences and in particularly for karstology, hydrogeology and civil engineering, for which reaching or avoiding dissolution voids is of high significance.

Karst problems all over the world create huge annual costs as well as social, security-related and environmental problems (e.g. Marinos, 2001; Lolcama et al., 2002; Waltham and Fookes, 2003; Day, 2004; Xeidakis et al., 2004; Casagrande et al., 2005). They are not only related to engineering constructions such as tunnels, buildings or dams but also concern the management and protection of karst groundwater that is in many parts of the world an important or even the only resource of groundwater. The main question beyond many of these problems is to know whether there is a developed network of conduits. If there is, where it is and. in some cases, what its characteristics are (e.g. active/fossil, phreatic/vadose, size). The presently used methods fail due to an insufficient understanding of speleogenesis (e.g. Benson and Yuhr, 1993; Zhang et al., 1993; Veni, 1999; Shofner et al., 2001; Pöttler, 2004; Bakalowicz, 2005).

Research carried out by karst scientists during the last 50 years were dedicated to the understanding of the processes and mainly the time-scale at which dissolution can develop cave systems. The principle of speleogenesis can be described as follow: before the beginning of karst development, any rock mass contains discontinuities, through which rain water infiltrates the underground. The rock being soluble, water dissolves it and enlarges the voids, which become able to accept more water to flow through; i.e. more dissolution to be active and the voids to enlarge faster. This loop is self-developing (positive feedback) until the system of conduits absorbs the total amount of water available from the rain with no significant increase of the hydraulic gradient. At this point, the conduit system is “mature” and will not develop further. Numerical modelling has been used to understand this feedback including the peculiar dissolution kinetics of calcite (e.g. Plummer and Wigley, 1976; Dreybrodt, 1988) and the change of flow conditions from laminar to turbulent when the size of the conduit increases (e.g. Dreybrodt, 1988; Dreybrodt and Siemers, 2000; Gabrovšek and Dreybrodt, 2001; Groves and Howard, 1994; Howard and Groves, 1995; Kaufmann 2003; Jaquet et al., 2004; Dreybrodt et al., 2005). Such models allow for the verification of the basic rules of speleogenesis but so far their applicability to real systems could not be demonstrated.

Whereas many authors contributed to our current understanding of the karstification process, only a restricted number of authors attempted to analyse and understand the geometry of karst conduits (e.g. Waltham, 1971; Palmer, 1974, 1975, 1986, 1989; Jameson, 1985; Lowe, 1992). Karstic rock mass are pervaded by a network of discontinuities; tectonical (joints, faults) and stratigraphical (bedding planes). These are the first flow paths for the groundwater (e.g. Kiraly, 1975; Klimchouk and Ford, 2000).

Discontinuities, which permeability was increased by dissolution, will be addressed in this thesis as **“inception features”** (fig. 1.2). If referred to karstified fractures, we will use **"inception fractures"** (Lowe, 1992 introduced the term “inception links” for inception fractures that link together inception horizons) and for karstified bedding planes **"inception horizons".** *Inception horizons have been defined by Lowe (1992) as lithostraticraphic horizons that are especially favourable to karstification by virtue of physical, lithological or chemical deviation from the predominant carbonate facies.*

Note that in the speleological literature, the use of **bedding planes** is often not the same as in sedimentary geology. While for sedimentologists bedding planes refer to the contact surface of two distinct beds, the term in speleologic literature is often used as equivalent of beds (a layer of sedimentary rock, generally a centimetre or more in thickness, which is distinguishable from adjacent beds - www.glossary.oilfield.slb.com). They are produced by more or less everything that is imaginable, for example changes in sedimentation rate, interruption of sedimentation, changes in seawater chemistry or changes in biodiversity. To be consistent with previous works, we will use bedding plane in the speleological sense.

Although we have a certain understanding of the fundamental speleogenetical processes (e.g. Klimchouk et al., 2000; Dreybrodt et al., 2005), the challenge still exists to understand why only certain discontinuities have been enlarged, i.e. why and how is the karstification selective.

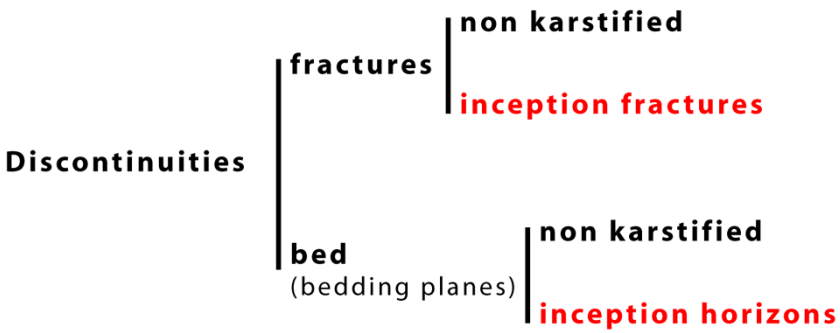

Fig. 1.2: Classification of discontinuities of a karstic rock mass. The challenge is to understand why only some discontinuities are karstified.

In last decades various authors dealt mainly with the development of karst conduits along tectonic discontinuities; for example Eraso (1985) found that fractures parallel to the main stress field are preferentially karstified (fracture strike parallel to $\sigma 1$).

It was the synthetic work of Lowe (1992, 2000) that directed the interest again to the speleogenetic role of stratigraphic discontinuities. He observed like others before (e.g. Rauch and White, 1970; Waltham, 1971; Rauch and Werner, 1974; Palmer, 1974, 1975, 1989; Ford and Cullingford, 1976; Jameson, 1985) that caves develop along a restricted number of bedding planes within the limestone series and introduced the **"inception horizon hypothesis"**. He assumed that the earliest stage of speleogenesis begins at different discrete parts of a rock succession, more precisely along inception horizons which are particularly susceptible to dissolution.

A number of case studies seem to confirm this hypothesis (e.g. Lowe, 1992, 1999; Knez, 1998; Osborne, 1999; Klimchouk and Ford, 2000). However, no major study has been published on this topic providing clear evidence or even any quantitative estimation of the significance of inception horizons in the genesis of cave systems. Up to now, the inception horizon hypothesis was not clearly demonstrated/validated and therefore widely not recognised, albeit existing detailed field observations in caves as well as borehole data supported the idea.

The aim of the present dissertation is to identify and quantify the effects of inception horizons on the genesis of cave systems and to determine the parameters controlling the speleogenesis along them. A short description of the content of the different chapters follows. Notice that each chapter is preceded by an introduction to the state of art, problem description as well as used investigation method.

Chapter 2 describes the identification and quantification of the effect of inception horizons on the genesis of epigenic cave systems in limestone. A method was developed to analyse the geometry of cave systems relatively to the local geological setting and the hydrogeological history. The application of this method to several reference case studies (tab. 1.1) allows demonstrating on a statistical base as well as on direct field observations, that inception horizons play a significant role in speleogenesis. It also appears clearly that the influence of these horizons on the 3D geometry of cave systems is high. For the first time it was possible to confirm quantitatively the speleogenetic role of inception horizons.

In **chapter 3,** we accept the challenge to understand what makes inception horizons favourable to karstification. Some concrete suggestions are expressed in the literature so far (e.g. Lowe, 1992, 2000; Knez, 1998; Pezdič et al., 1998; Florea et al., 2007). However, only little analytical confirmation/evidence has been presented. Therefore, we sampled and analysed more than 200 rock samples of 18 inception horizons in six

cave systems (tab. 1.1) to determine the lithological properties and processes that are involved, and which of them are the most important for speleogenesis.

In **chapter 4,** we add hydrogeological to the lithological aspects for an integral understanding of the speleogenesis along inception horizons in space and time. With simple hydrogeological numerical models, we evaluate both the role of the position and orientation of the inception horizons as well as the history of the landscape evolution (i.e. the re- and discharge area) on the karstification of a rock mass.

The achieved improvements of the inception horizon hypothesis do not only represent a step forward in the understanding of speleogenesis but also for engineering geological purposes. We sketch in **chapter 5** a methodology to quantify the probability of karst occurrences inside a karst massif by identifying the few inception horizons and reconstructing the hydrogeolgical history.

We are convinced that the identification of inception horizons and reconstruction of the hydrogeological history is a good tool, not only for predicting karst conduits, but also for a better understanding of the speleogenesis.

Name of the Cave System	Country	3D-Analysis *Chapter 2*	Analyse of Samples *Chapter 3*		Remarks
			Rock Samples	Gypsum Samples	
Siebenhengste Cave System	Bern, Switzerland	x	x	x	*main case study*
Hölloch & Silbernsystem	Schwyz, Switzerland	x	x	x	
Nidlenloch	Solothurn, Switzerland	x	x	x	*case study in chapter 5*
Réseau des Grottes aux Fées	Vaud, Switzerland	x	x		
Réseau de Covatannaz	Vaud, Switzerland	x	x		
Mammoth Cave System	Kentucky, United States	x		x	
Schönberg Cave System	Oberösterreich, Austria	x			
Shuanghedongqun	Guizhou, China	x			
Hirlatzhöhle	Oberösterreich, Austria	x			
Ogof Draenen	South Wales, United Kingdom	x			
Dachstein-Mammuthöhle	Oberösterreich, Austria	x		x	
Schwarzmooskogel Cave System	Oberösterreich, Austria	x			
Burgunderschacht	Oberösterreich, Austria	x			
DÖF-Sonnenleiterschacht	Obwalden, Switzerland	x			
kleines Hölloch	Allgäu, Germany	x			
Lachenstockhöhle, K10 & Plattenloch	Schwyz, Switzerland	x		x	
Gamsalp-O91	St.Gallen, Switzerland		x		
Sukiloch	Schwyz, Switzerland			x	
Saint-Marcel Cave System	Ardèche, France			x	
Noël Cave System	Ardèche, France			x	

Tab. 1.1: Table of the case studies worked on during this dissertation.

- 2 -
Do inception horizons exist?
–
Demonstration of Inception Horizons

2.1 Introduction

Based on a detailed observation of cave systems and their geological context, different authors (e.g. Rauch and White, 1970; Waltham, 1971; Rauch and Werner, 1974; Palmer, 1974, 1975, 1989; Ford and Cullingford, 1976; Lauritzen, 1988) suggested that caves develop along a restricted number of bedding planes within the limestone series. These observations were synthesised in more recent publications into the inception horizon hypothesis (Lowe, 1992, 2000). This hypothesis assumes that the earliest stage of speleogenesis (in some cases it can even start during the lithification of the carbonate sequence) begins at different discrete parts of a rock succession, more precisely along horizons which are particularly susceptible to dissolution. Such inception horizons are supposed to be especially favourable to karstification by virtue of physical, lithological or chemical deviation from the predominant carbonate facies within the surrounding sequence (Lowe, 1992).

However, no major study has been published on this topic providing clear evidence or even any quantitative estimation of the significance of inception horizons in the genesis of cave systems. Therefore, the inception horizon hypothesis was widely not recognised.

In this chapter, we describe a method which allows the identification and quantification of the effect of inception horizons on cave genesis. The application of this method to several reference sites makes it possible to demonstrate on a statistical base, as well as on direct field observations, that inception horizons exist and play a significant role in determining the position of karst conduits. In other words, we investigate if conduits are distributed randomly along any bedding planes or if we can find some special horizons that were favourable to the development of conduits and what proportion of conduits are related to those horizons.

We are convinced that the evidence of inception horizons is a significant step forward not only for a better understanding of the speleogenesis (chapter 3 and 4) but also for predicting karst conduits (chapter 5).

2.2 Method development and validation on the Siebenhengste Cave System[1]

Unlike many other authors (e.g. Ford and Ewers, 1978; Bögli, 1980; Palmer, 1987; Audra, 1994) we choose to analyse the geometry of cave systems not in two-dimensions (plan view or side view) but in three-dimensional space. Compared to the commonly used 2D analysis of cave systems (e.g. vertical distribution of conduits for the identification of cave levels or plan view to work out the relationship between cave development and fractures) our 3D analysis allowed us to couple the geological and hydrogeological contexts to the conduit network geometry within a carbonate rock mass.

A method of investigation and analysis had first to be designed (fig. 2.1). Therefore, a software tool has been developed for the 3D analysis of the complex geometry of long cave systems. It helps by providing the statistical analysis of the relationship between the conduit network geometry, the geological settings and the hydrogeological context of cave systems. Data necessary for this analysis are descriptions in 3D of the geology (faults and beds) and of the cave (survey data). For the geological model, mainly one reference layer has to be introduced into the model. Very often the base of the limestone series (top of the underlying marls) is used. The analysis follows six steps (fig. 2.1), which are presented on the application to the Siebenhengste Cave System.

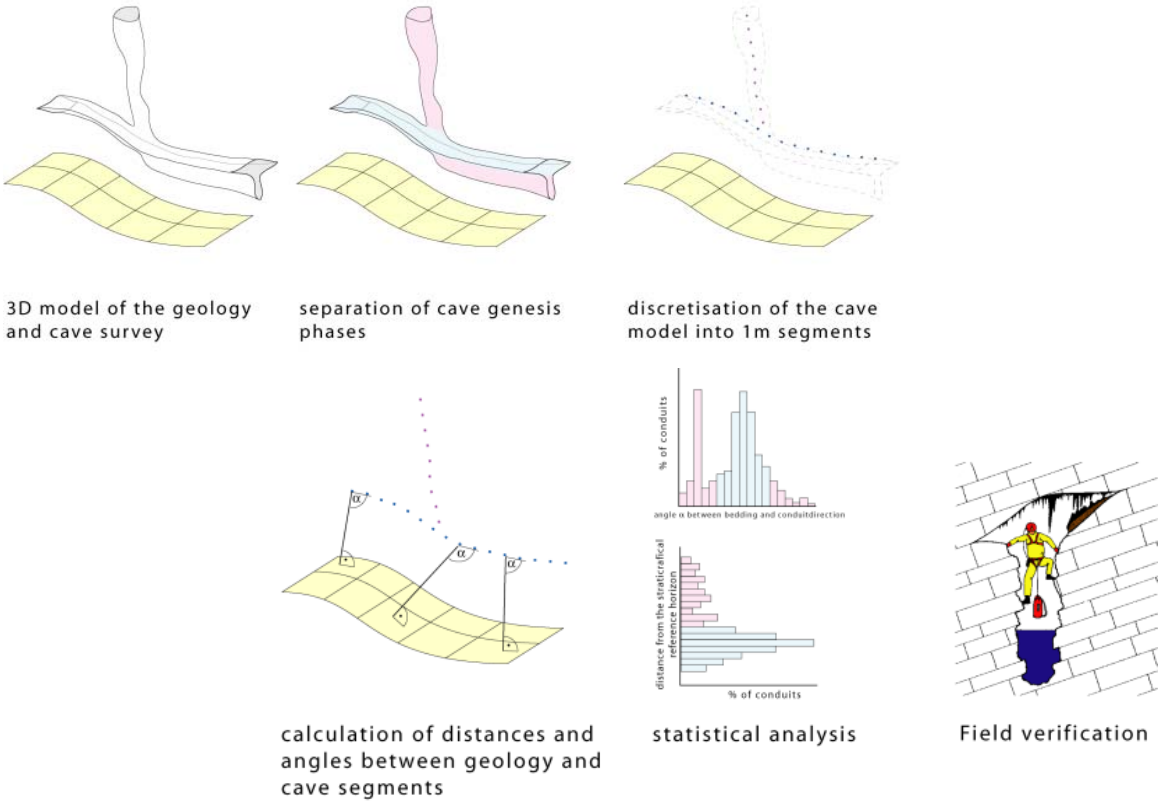

Fig. 2.1: Analysis procedure: The proposed method allows getting statistical evidence of the existence of inception horizons based on cave survey and geological data.

[1] *This chapter is widely equivalent to the chapter "method development" in Filipponi et al., 2009.*

2.2.1 Three dimensional (3D) models of cave conduits and geology

The basic elements of the method are 3D computer models of the geological setting and the cave conduits network (fig. 2.1 panel 1). The quality of the 3D model directly influences the explanatory power of the analysis. A high degree of precision is required in order to be able to define if conduits develop for example along one single stratigraphical horizon (bedding plane). If such an analysis is very easy in a context of flat lying limestone, it is much more challenging in folded areas. For our study and in order to get a high degree of precision, the geological models were based on digital elevation models, geological maps and descriptions, aerial photo interpretations, observations in the cave systems. This allows us to work with a model accuracy for simple geological settings of a few metres and for complex geological settings (folded, faulted, thinning out of the strata etc.) in order of a few decametres.

The VRML visualization technique (Virtual Reality Modelling Language) was originally developed as a 3D standard for the internet and most 3D modelling tools to allow to import and/or export of VRML files. It is also suitable as an exchange file-format between the cave surveying programs (e.g. Toporobot, Survex, Compass, Visualtopo), geological modelling programs (e.g. Geoshape), GIS programs (e.g. Arc-GIS), mathematical and statistical programs (e.g. Matlab) and animation programs (e.g. Cinema4D). This allows developing and analysing relatively efficient 3D models of a karst area/system.

2.2.1.1 The Siebenhengste Cave System

The Siebenhengste Cave System, located North of Interlaken (Switzerland), is one of the most significant cave systems in the World with a length of more than 154 km and a depth range of 1340 m (fig. 2.2) (e.g. Jeannin and Häuselmann 2005). Close to this network are also several other important caves, which so far have not been connected to it through cave exploration. The total length of explored conduits within the area is almost 300 km.

The 154 km of the Siegenhengste Cave System comprise a 3D labyrinthine network of cave conduits, which consists of shaft series linked by subhorizontal conduits, which are in most cases bedding plane guided (fig. 2.2). The 3D model of the cave system was obtained from the cave survey data collected by cavers.

The subhorizontal passages have often a “keyhole” profile cross-section which reflects a multiphase evolution of the conduits, whereas the elliptical upper section of the conduits developed under phreatic conditions, the “canyon” at the bottom was formed under later vadose conditions (fig. 2.14-right).

2.2.1.2 Geology of the Siebenhengste area

The Siebenhengste–Hohgant region belongs to the “Helvetic Border Chain” (Helvetikum). This Cretaceous series consists of a sequence of limestone, marls and sandstone (Ziegler, 1967). The main part of the Siebenhengste Cave System is located in the Schrattenkalk Formation (Barremian to Aptian, Urgonian facies) with a thickness of about 180 m (fig. 2.3). This formation is underlaid by the 30 to 50 m thick Drusberg Marl (Drusbergschichten, lower Barremian) which forms an impervious base. The upper limit of the Schrattenkalk is erosive and thus formed by various types of rocks, depending on the regions. In most places, an Eocene turbiditic series called “Hohgant-series” lies directly on top of the Schrattenkalk. The Hohgant-series can be up to nearly 200 m thick and some of its beds, containing calcareous cement, are karstified.

The Schrattenkalk Formation is a pure shallow marine limestone and can be grouped into six units with variation of ooids content, dolomite–calcite ratio, macrofossils (rudists) and impurities (clay content) (Jeannin, 1989).

The limestone of the Schrattenkalk Formation dips 10° to 30° towards the southeast as a large slab. This dipping slab is cut by a series of faults more or less parallel to the strike of the beds, resulting in E–W horizontal displacements.

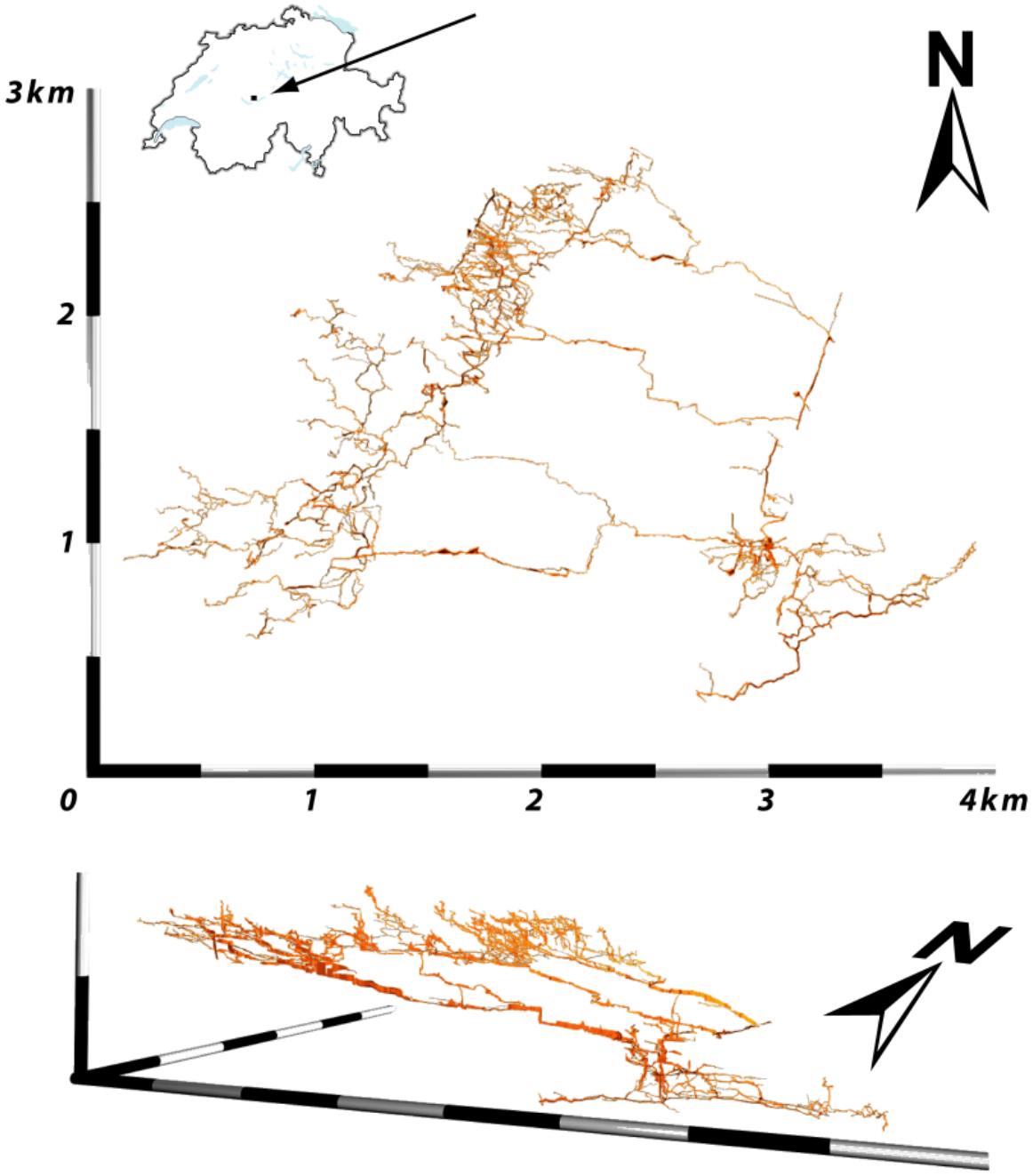

Fig. 2.2: Location and shape of the Siebenhengste Cave System: the complex and maze-like geometry of the conduit network (154 km) can only be analysed within a 3D approach.

The 3D computer model of the geology of the Siebenhengste area is based on digital terrain models (DTM) provided by the Swiss Federal Office of Topography (Swisstopo) on which we superposed geological maps and aerial photos. The inter- and extrapolation of the formation boundaries and the main faults in the underground was done by interpolation of the "outcrops" under consideration of field measurements (dip and dip direction of the feature). The superposition of this model with the 3D model of the cave system (chapter 2.2.1.1) allows refining the geological model by considering also underground observations and measurements (taken within the cave).

For further analysis the study area was subdivided into “homogenous” zones between the main faults (in the Siebenhengste area 7 zones) and for each zone a “stratigraphical reference horizon” was selected (most of the cases the basis of the limestone formation). The statistical analysis of chapter 2.2.4 was done for each zone separately.

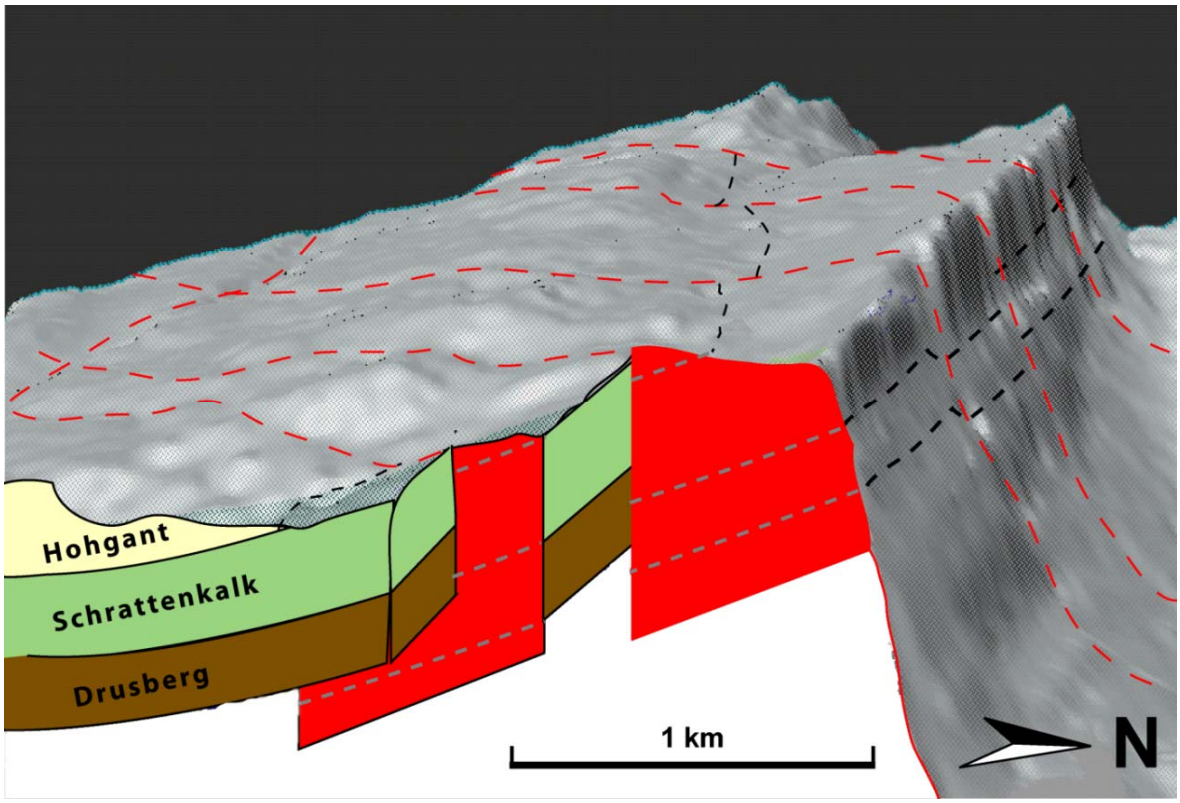

Fig. 2.3: View of the 3D model of the geology and cave conduits of the Siebenhengste region: the Siebenhengste Cave System evolved predominantly in the limestone of the Schrattenkalk Formation which is inclined towards the SE and displaced by some major faults (red dashed lines).

2.2.1.3 Model uncertainty

For the statistical analysis, a high degree of precision is required. For the model of the Siebenhengste area, a radial total uncertainty of about ±25 m can be assumed within the national coordinate system. This error is related on one hand to the geological mapping and modelling, and on the other hand to the precision of the cave survey. The uncertainty of the geological model is about ±15 m, and is mainly related to the extrapolation of the surface observations at depth as well as to the extrapolation of the underground observations down to the base of the Schrattenkalk Formation. The quality of the cave model is quite good and probably within ±10 m. The cave survey is so much interconnected (survey loops) that every cave survey station is related to fixed points at surface by several survey lines, strongly reducing the position uncertainty (e.g. Grossenbacher, 1992). During the discretisation step, it was assumed that the inception of the conduit occurs at the ceiling (see also chapter 2.2.3).

For the analysis of inception horizons, only the relative uncertainty between cave conduits and geology is relevant. As many observations of the geology were made in caves, this uncertainty is smaller than the absolute one, i.e. on the order of 10 to 15 m.

2.2.2 Reconstruction of the hydrogeological conditions

Karst conduits may develop under phreatic as well as under vadose (unsaturated) conditions (e.g. Bretz, 1942). This depends mainly on the position of the conduit within the aquifer: above the water table conduit enlargement is mainly due to vadose processes, whereas below the water table the enlargement is exclusively phreatic. Due to high hydraulic conductivities of karst conduits, the water table lies in a developed karst system (mature) almost horizontally from the karst spring upwards (e.g. White and White, 2001 – lower than 1 m per km). In the phreatic zone the hydraulic gradient is mainly horizontal, linking a recharge area to a discharge area (i.e. spring) (see also chapter 4). Thus, discontinuities parallel to this gradient will be mostly used. They guide the conduits development. Therefore, the relative positions of the recharge and discharge areas are key factors controlling the orientation and position of phreatic conduits. These are usually tubes with an elliptic to round cross-section (fig. 2.13-left) and with a more or less horizontal course, going up and down depending on the initial openings available in the limestone mass (phreatic loops). Flow in vadose conduits is ultimately controlled by gravity; i.e. mainly vertical. As water can only flow downwards, vadose conduits are mainly vertical shafts or pitching, meandering canyons. It is thus important to distinguish purely vadose conduits from phreatic ones, because their orientation and genesis is significantly different. Most karst conduit systems in the World are multiphase; i.e. consist in a series of conduits formed under variable boundary conditions (mainly changing recharge–discharge areas) (e.g. Jeannin et al., 2000). A first challenge in understanding their genesis is to distinguish the respective phases (subset of conduits belonging to a single phreatic zone of a karst system in the past) and their respective characteristics.

A way to start the analysis of a speleological conduit network is to remove all conduits clearly vadose in origin and to draw a histogram of the cumulated length of the remaining conduits by elevation classes (such as suggested by e.g. Bögli, 1980; Palmer, 1987). This should allow for the identification of the main evolution phases of the karst network. In cases of a flat geology this is an easy way to winnow different levels of karst water table. However, in karst systems with a steep or folded geology the conduits may be distributed quite far away from a simple horizontal plane (former water table) (e.g. see appendix 1). It is for this type of situation that our analysis combines speleogenetic phases and geological structure in a 3D model (fig. 2.1 panel 2).

2.2.2.1 Hydrogeological phases of the Siebenhengste Cave System

The cave system has a distinctive labyrinthine character and its complex geometry can only be explained by a series of superimposed flow systems that corresponds to different and more or less independent times and hydrogeological conditions (Jeannin, 1996; Bitterli and Jeannin, 1997; Häuselmann et al., 1999; Jeannin et al., 2000; Häuselmann, 2002). Most of the conduits in the system were formed under phreatic conditions (which include also the epiphreatic zone). Vadose flow has only reshaped the profile of certain passages without fundamentally modifying the overall geometry. The major features resulting from vadose flow conditions are a series of shafts that pass through the limestone series vertically down to the phreatic zone. In certain conduits, it was possible to observe the exact transition point between the former phreatic and vadose zones making it possible to reconstruct the top of paleophreatic zones (e.g. Häuselmann et al., 2003). In the Siebenhengste Cave System it was possible to distinguish five different major paleophreatic zones (Jeannin et al., 2000).

Many of the main conduits were formed quite deep below the water table, e.g. loops deepening more than 250 m below the top of the phreatic zone were observed. It was therefore not an easy task to separate the different phases because conduits of two or even three different phases may occur at the same elevation (fig. 2.4). Thus, the widely used method consisting of looking at the vertical distribution of the conduits to assign a given conduit to a paleo-phreatic phase (e.g. Palmer, 1987), does not work well for this case study. The only way, to assign a given conduit to a paleo-phreatic phase, was to reconstruct, based on the conduit morphology, the logical connections of the known cave conduits in the 3D model with the help of field observations. Thereby, it was possible to reconstruct the conduit networks of the five hydrogeological phases.

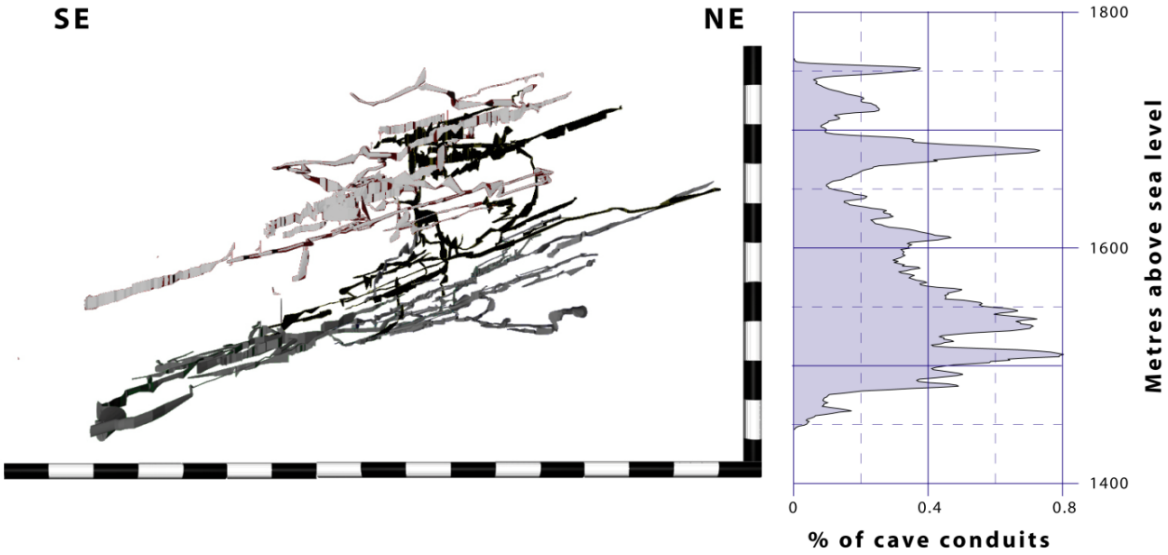

Fig. 2.4: 3D model view of the phreatic conduits of one part of the Siebenhengste Cave System (Zone II) and the corresponding vertical distribution of the conduits. The grey shades in the 3D view indicate three major hydrogeological phases out of five. However, it is difficult to recognise these phreatic phases in the histogram.

2.2.3 Discretising the 3D model

To analyse the 3D model statistically it was necessary to discretise (split the data into discrete intervals) each cave conduit into 1 m long segments (fig. 2.1 panel 3). Properties (direction, dip) of the conduit were assigned to the respective segments. It must be pointed out at this point, that for our analysis we used only the conduit length and not the volume.

In this study, we had to approximate the position of the inception horizon in the conduit cross-section. It was assumed that the ceiling of the conduit is the best approximation of that position. It may be argued that in phreatic elliptic conduits, the inception horizon is often located in the middle of the ellipse. On the other hand in a multi-phased conduit (phreatic tube entrenched by a vadose canyon), the inception horizon is rather located at the ceiling than in the middle of the cross-section. This is the most common case in many of the investigated cave systems, therefore this assumption was used. This is a simple way to get an approximation of the position of a potential conduit inception horizon with an accuracy of a few metres.

The geology was represented by the modelling of a single stratigraphical reference horizon, in most cases the base of the karstified rock formation, i.e. the top of the Drusberg Marls in the case of the Siebenhengste Cave System. This reference horizon was discretised within a mesh of a width of around 5 m. For each grid point the normal vector to the surface has also been calculated.

2.2.4 Statistical analysis

Based on the discretised 3D model, the method used made it possible to quantify the relationship between the geometry of the cave systems, the geological setting and the hydrogeological boundary conditions. With these results, it was possible to describe the relationships with different descriptive statistical methods and to provide quantitative evidences of the role of inception horizons on cave genesis at regional scale.

2.2.4.1 Analysis of the parallelism of conduits to bedding planes

This analysis aims at verifying to what extent conduits are parallel to bedding planes. Based on the 3D model, the developed software tool computes the spatial angle between the directions of the conduit segments and the normal vector of the reference horizon (bedding). Consideration of the normal vectors to the bedding planes means that parallel conduits will have a minimum spatial angle of 90° whereas perpendicular conduits will have a minimum spatial angle of 0°.

Results from Siebenhengste Cave System show angles close to 90° (fig. 2.5), although the dispersion is quite large. The same analysis was applied on a subset of the data, after having removed the vadose conduits from the data set.

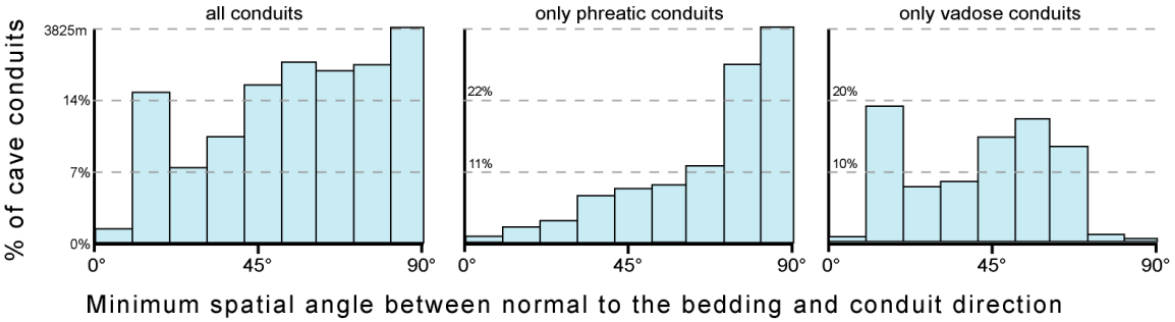

Fig. 2.5: Histogram of minimum spatial angles between the normal to the bedding and the conduit direction in the Siebenhengste Cave System (Zone II). Left: all conduits together showing a central trend around 90°; the peak at low angles corresponds to vertical conduits in the vadose zone. Middle: only phreatic conduits. Right: only vadose conduits.

Concerning the vadose zone, the results show that cave directions are poorly related to the stratigraphy (fig. 2.5, right). However, most parts of the vadose conduits are concentrated in two intervals: 10–20° and 50–60°. The first interval represents the angle between the orientation of the bedding (120/25°) and the orientation of the main joints and faults in this region. This corresponds in fig. 2.2 to the five main straight conduits linking the upper (NE) maze to the lower (SE) maze parts of the system. This direction (intersection between bedding planes and the main joints) is well-marked in the Siebenhengste area because the dip of the bedding planes is rather constant (fig. 2.6). In folded regions, angles would not be so well defined around a single value although caves may have the same type of preferential direction. It is noteworthy that even in the vadose zone some conduits are parallel to the dip of the bedding. These passages correspond to short meander sections linking two shafts.

Concerning the phreatic zone, the histogram of fig. 2.5 shows that karst conduits are predominantly parallel to bedding planes (about 70 % of the phreatic conduits in the Siebenhengste Cave System). As presented above and later in this chapter, this does not imply that fractures have no influence on the development of the conduits.

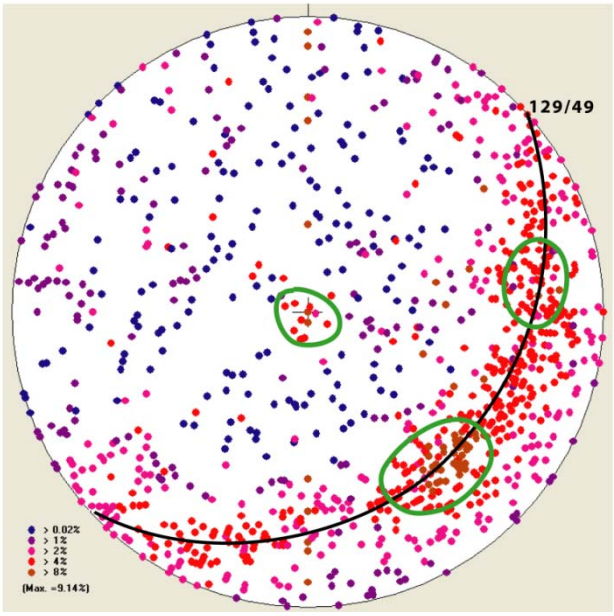

Fig. 2.6: Stereographic analysis of the cave conduit segments orientations in the Siebenhengste Cave System (Zone I). The segments orientation trends within a great circle that is coincident with the dipping of the bedding. Furthermore, the two zone of increased concentration (green bordered) coincident with the intersection between bedding planes and the main joints; the concentration zone in the centre coincident with vadose shafts.

2.2.4.2 Analysis of the existence of favourable bedding planes — or the statistical evidence of the inception horizon hypothesis

In the previous chapter, we showed that most phreatic conduits are developed parallel to bedding planes. In this chapter, we investigate if conduits are distributed randomly along any bedding planes or if we can find some special horizons that were favourable to the development of conduits. In other words we ascertain if there is a statistical evidence of the inception horizon hypothesis (Lowe, 1992).

To do this, our software determines the shortest distance between a conduit segment and the geological reference surface. Histograms of these distances give the percentage of conduits for a given distance from the reference surface, respectively the percentage of conduits in a stratigraphical horizon. Peaks represent horizons where karst development is concentrated (fig. 2.7). A 3D visualisation of the cave system already confirmed the basic idea of inception horizons raised by various authors from qualitative field observations. In the Siebenhengste Cave System it is quite obvious that conduits are concentrated along some specific strata. A more detailed interpretation of the histograms allows separating up to seven different horizons (fig. 2.7 and tab. 2.1).

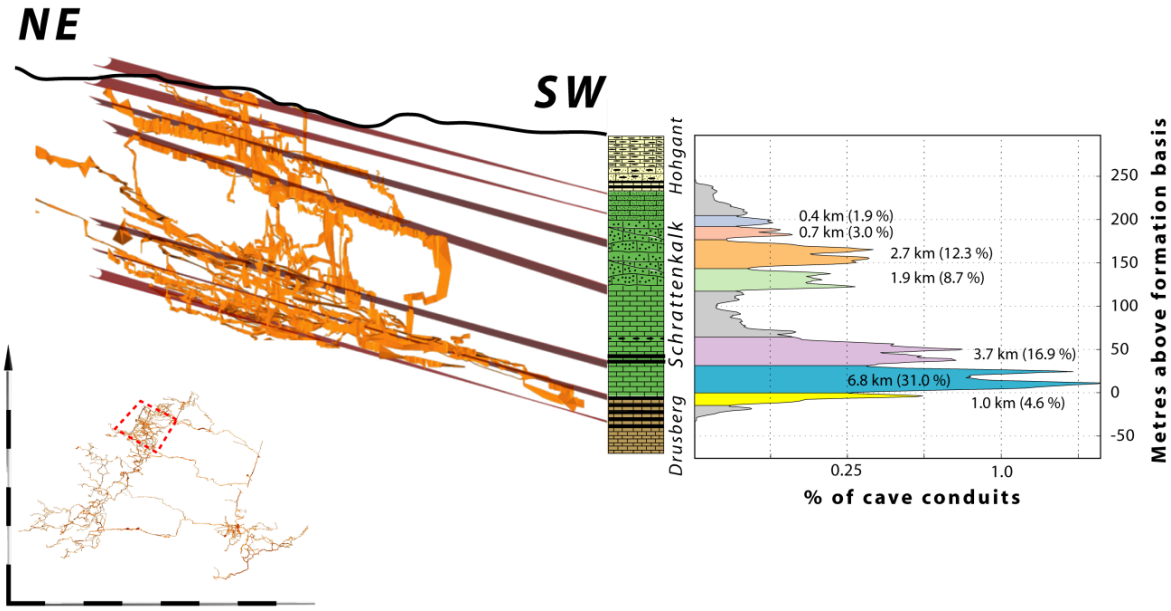

Fig. 2.7: 3D projection of one part of the Siebenhengste Cave System (Zone II). Seven potential "inception horizons" can be identified within the Schrattenkalk Formation. The thickness of the limestone is nearly 180 m.

The respective peaks correspond to a clearly increased cave conduit density compared to a homogeneous distribution of the conduits in the rock mass. About 80 % of the conduits of the Siebenhengste Cave System are restricted to 7 horizons (fig. 2.7). Peaks seem to represent a normal distribution around a given discrete feature. As presented in a more detailed way in chapter 2.2.5 and chapter 3.3, these features are in most cases bedding planes or lithological strata of a thickness of some decimetres or even less. This would reduce the peak width to a very thin range, i.e. about 80 % of the conduits would be developed within only about 0.5 % of the total limestone thickness. The scattering of the data is caused by the uncertainty of the respective positioning in the 3D model. In the example presented here (Siebenhengste Cave System) the uncertainty is in the order of ±15 metres.

The relative size of the peaks only has a limited meaning concerning the properties of the horizons. The presented analysis only takes into account cave conduits that are large enough to be accessible for cavers. In the karstic rock mass, there will be many more karst conduits that are too small to be explored by humans as well as some cave conduits which have not been explored so far.

The real development of the conduit network along a bedding plane is also strongly related to the history of the hydrogeological boundary conditions (e.g. two compartments shifted by a fault may be in different positions relatively to the hydrogeological boundary conditions). This makes some peaks more or less pronounced at different compartments of the cave system (fig. 2.8). From this on, the only reliable conclusion we can make from the histograms is that peaks represent horizons which are preferred for conduit development. The method also makes it possible to define the stratigraphical position of these inception horizons.

An interesting observation is that the shape of the histograms are quite similar when displaying all or only phreatic conduits of a cave system (fig. 2.9). It seems even that peaks appear more clearly when including all conduits. This is because vadose conduits (in most of the cases meanders) of the Siebenhengste Cave System are located along the same bedding planes as those of the phreatic zones previously developed in the analysed rock volume. On the other hand, vadose shafts of the analysed cave network are vertical and in most cases cross the whole limestone series down to its base. Therefore, they produce a more or less homogeneous distribution over the whole limestone thickness.

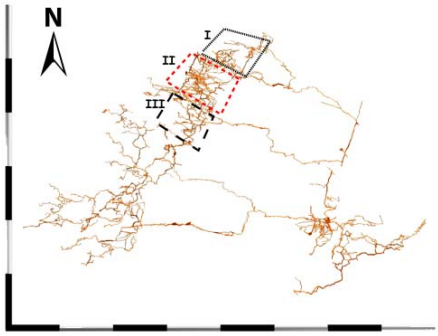

Inception horizon	Zone I	Zone II	Zone III
1	**3.9%** (0.5km)	--	--
2	**2.8%** (0.4km)	**1.9%** (0.4km)	**6.8%** (1.0km)
3	**7.1%** (0.9km)	**3.0%** (0.7km)	**1.9%** (0.3km)
4	**15.9%** (2.1km)	**12.3%** (2.7km)	**7.3%** (1.1km)
5	**16.5%** (2.2km)	**8.7%** (1.9km)	**28.1%** (4.3km)
6	**6.3%** (0.8km)	--	--
7	**21.3%** (2.8km)	**16.9%** (3.7km)	**18.7%** (2.9km)
8	**2.4%** (0.3km)	**31.0%** (6.8km)	**19.4%** (3.0km)
9	**2.9%** (0.4km)	**4.6%** (1.0km)	--
Total	***79.1%*** of 13km	***78.4%*** of 22km	***82.2%*** of 15km

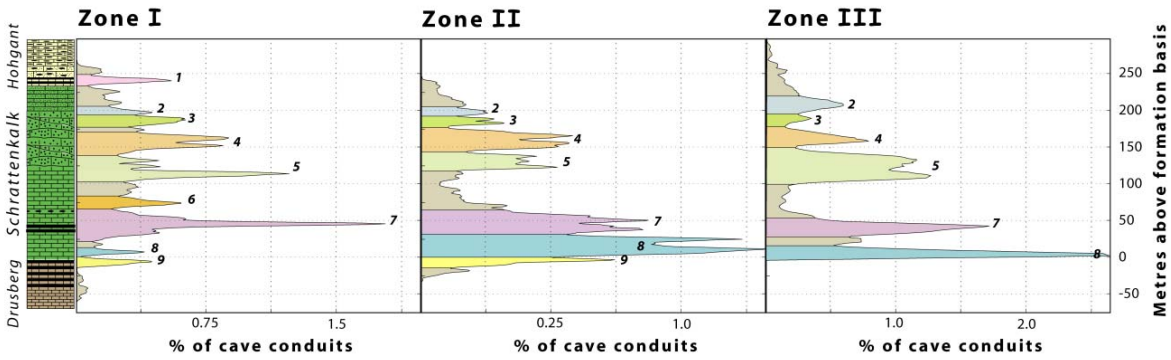

Fig. 2.8: Histograms of three zones of the Siebenhengste Cave System representing the distances from the cave conduits to the base of the Schrattenkalk Formation: The same peaks are differently pronounced in the respective compartments. The table included in the figure gives the percentage of conduit length on the corresponding inception horizon.
Peaks 4, 5 and 7 are present and significant in all three regions. They fit well with the image we have of the conduit distribution in Siebenhengste Cave System. Peak 9 is present when the lowest part of the Schrattenkalk is accessible (to karstification or to cavers) (Zone I and II).

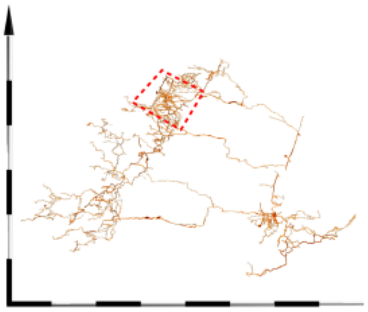

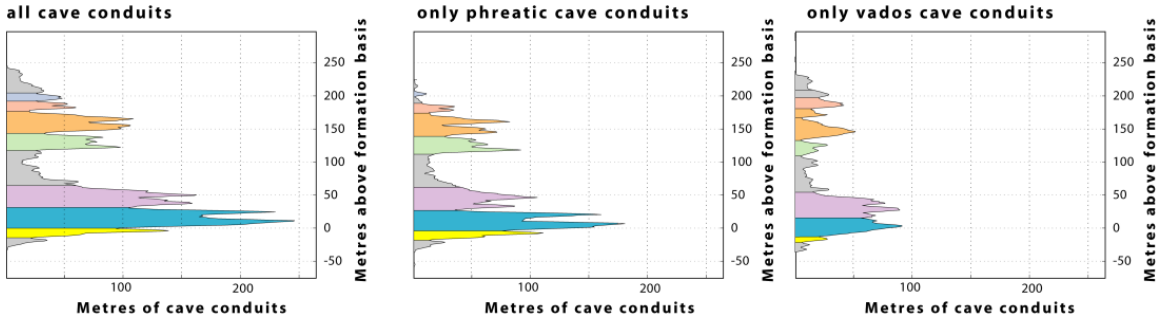

Fig. 2.9: Histogram of the conduit distribution relative to the base of the limestone series: Vadose shafts are evenly distributed across the limestone series and represent therefore a more or less homogeneous conduit distribution, i.e. not really influencing the overall distribution. Vadose meanders between shafts appear to be located along the same favourable horizons as phreatic conduits. (Example of the Siebenhengste Cave System, Zone II).

2.2.4.3 *Analysis of the relationship between the position of the (paleo-)water table and the position of the inception horizons*

With the previous analysis (chapter 2.2.4.2) we showed that most phreatic conduits are developed along a few inception horizons. In this chapter, we investigate if conduits are distributed randomly along an inception horizon or not.

Based on field observations, different authors describe that cave developed preferential near the (paleo-)water table (e.g. Davies, 1960; Palmer 1987). Only a few of them coupled their hydrologic observations with stratigraphical observations within the conduits. For example, Palmer (1987) showed that in the Mammoth Cave (Kentucky, USA) several conduits developed near the intersections of the paleo-water table with the few stratigraphical horizons, which are favourable guiding the cave conduits.

To control this observation/assumption, our software computes frequency maps of the cave segments (%) relative to the altitude (x-axis) and the distance to the lithological reference surface (y-axis). The frequency map of the Siebenhengste Cave System (fig. 2.10 for zone II) shows that conduits are not distributed homogenous along inception horizons. Four peaks of clearly increased cave conduit frequency are reconcilable. The position of the peaks corresponds quite well to the intersection of the inception horizons with the positions to the paleo-water table (chapter 2.2.2). Though the vertical distribution of the conduits only reflects rudimentary the different hydrologic phases of the Siebenhengste Cave System (due to a superposition of phreatic loops and the utilisation of some passages during more than one phase). Better results are obtained in case studies where the conduits corresponding to a given hydrologic phase are clearly vertically displaced from conduits of other phases (e.g. Hölloch, fig. 4.17).

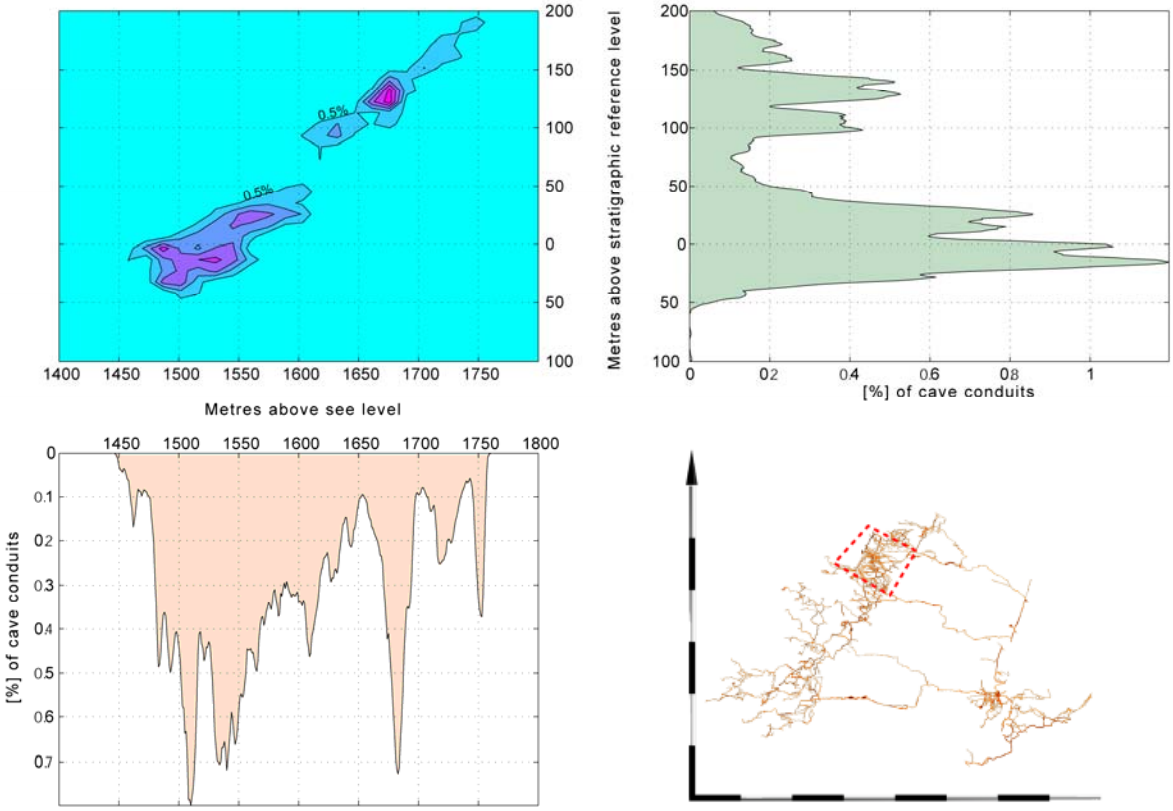

Fig. 2.10: Frequency maps of the cave segments (%) relative to the altitude (x-axis) and the distance to the lithological reference surface (y-axis), contour lines interval 0.5 % of conduits (top left); Histogram of the conduit distribution relative to the stratigraphic reference horizon (top right); Histogram of the conduit distribution relative to their elevation (bottom left): The frequency map shows that an increased number of conduits developed at the intersection of the inception horizons with the paleo-water tables. (Example of the Siebenhengste Cave System, Zone II).

2.2.4.4 *Analysis of the conduit direction*

We demonstrated above that the main part of the phreatic cave conduits are related to a restricted number of stratigraphical horizons. As a next step we analyse the distribution of conduit directions in order to identify potential preferred flow directions along the inception horizons. Under phreatic conditions the flow direction is dominated mainly by the direction of the hydraulic gradient, i.e. is different from the down-dip direction in most cases. For example, it is well known that phreatic conduits display up and down "loops" stretching along the strike of the limestone beds.

The plan view of the Siebenhengste Cave System clearly indicates that preferred directions do exist. Previous studies of the fracture network (Jeannin, 1989) showed that some fractures are preferentially used by cave conduits rather than others. However, this analysis took into account all conduits of the cave system together. In the following analysis, we separated the conduit networks of the respective genetic phases of the system prior to analysing the conduit directions. The idea was to see if changes in the hydraulic gradients according to the respective phases of the cave genesis could significantly change the discontinuities used by conduits.

For the analysis, we compiled rose diagrams of the conduit direction weighted by their length (fig. 2.11). This allows us in a simple way to identify preferential directions. We did not analyse the whole cave system at once but looked at each evolutional phase separately (chapter 2.2.2).

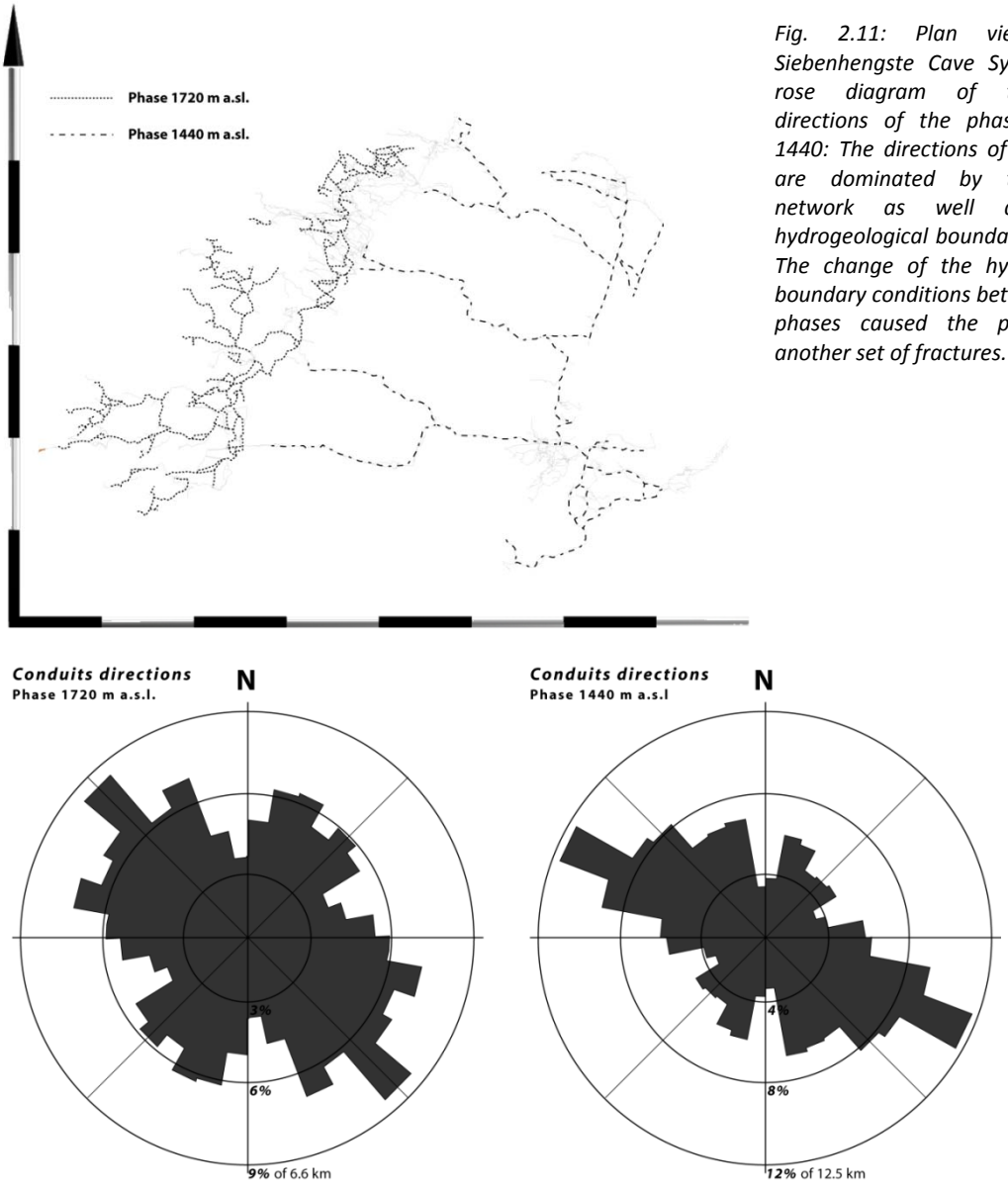

Fig. 2.11: Plan view of the Siebenhengste Cave System with a rose diagram of the conduit directions of the phase 1720 and 1440: The directions of the conduits are dominated by the fracture network as well as by the hydrogeological boundary conditions. The change of the hydrogeological boundary conditions between the two phases caused the preference of another set of fractures.

The rose diagram of the conduits directions, from phase 1720, features two main directions (NW–SE, N–S). These directions are well known from the study of the fracture pattern of the area (Jeannin, 1989). The NW–SE direction corresponds to the direction of the large strike-slip faults that subdivide the area in different shifted blocks (fig. 2.3). The main displacement along those faults were horizontal (probably several hundreds of metres) and the vertical components do not exceed 20 to 40 m. The others directions are associated joint sets.

For phase 1440, the same joint sets are used but the length of conduits along the respective joint sets is significantly different. For this phase, the hydraulic gradient was oriented towards the SE, so that the NW–SE joints were clearly preferred as flow paths.

From this analysis we can conclude that the conduit direction of the phreatic conduits at the regional scale is conditioned by the combination of the hydraulic gradient and the intersection of tectonic fractures with inception horizons. Only intersection lines more or less parallel with the hydraulic gradient will be favourable to conduit development. In some cases, the conduit direction on the inception horizons was not conditioned by the occurrence of fractures (respectively the intersection of inception horizons with fractures), in these cases the conduits followed only the inception horizon.

2.2.5 Field verification of the existence and position of inception horizons

Several parts of the Siebenhengste Cave System were investigated and, in all cases, horizons inferred from the 3D analysis were identified in the field. This clearly showed that inception horizons are much more discrete and localised in the field than obtained by the statistical analysis. In most cases, we think that horizons have a thickness ranging between 2 and 30 cm though they appeared as peaks of 5 to 10 m thickness in the statistical analysis (chapter 2.2.4.2). The width of those peaks is due to the various uncertainties related to the model construction (chapter 2.2.1).

We could observe that at places where a conduit reaches a normal fault, the conduits followed the fault to find the same bedding plane again on the other side of the fault. In some cases, another inception horizon was used.

The seven inception horizons of the Siebenhengste Cave System have different aspects (fig. 2.12):

- The first inception horizon (I) is a fossil-poor bedding plane (some centimetres thick) in the Schrattenkalk sensu stricto. Eye-catching is the network of anastomoses that developed along the bedding plane. The network is so dense in some places that the bedding plane was completely removed.
- The second inception horizon (II) is situated at the contact between the Schrattenkalk-members sensu stricto and “upper oolitic” member. Below this surface, there is a set of close standing joints that seems to end at this contact. Also some evidence of neotectonic movement along the contact could be observed (broken and shifted dripstones).
- Inception horizon three (III) is a 40 to 60 cm thick, very blocky (stromatolitic?) limestone layer.
- Inception horizon four (IV) is a marly horizon of some centimeters thick.
- Inception horizon five (V) is a marly bedding plane (some centimetres thick) of the “Lower Schrattenkalk” member. Many siliceous nodules of some centimetres in diameter are found embedded in the bedding plane.
- Inception horizon six (VI) is a marly layer (some decimetres thick) at the transition between the Lower and Basal Schrattenkalk-members. Conduits related to this horizon are full of cave gypsum formations (crusts, needles, flowers, etc.).
- Inception horizon seven (VII) is a limestone layer (some metres thick) within the marls of the Drusberg-Formation.

Field verifications in the other caves investigated also confirmed the existence of the statistically identified inception horizons (chapter 2.3). However, in some cases, detailed field observations showed that some

conduits also developed along other bedding planes than those identified by the statistical approach. Obviously those bedding planes do not present favourable properties over extended distances and are, therefore, not significant at a regional scale.

A more quantitative analysis and discussion about different field observations along inception horizons in different cave systems is presented in chapter 3.

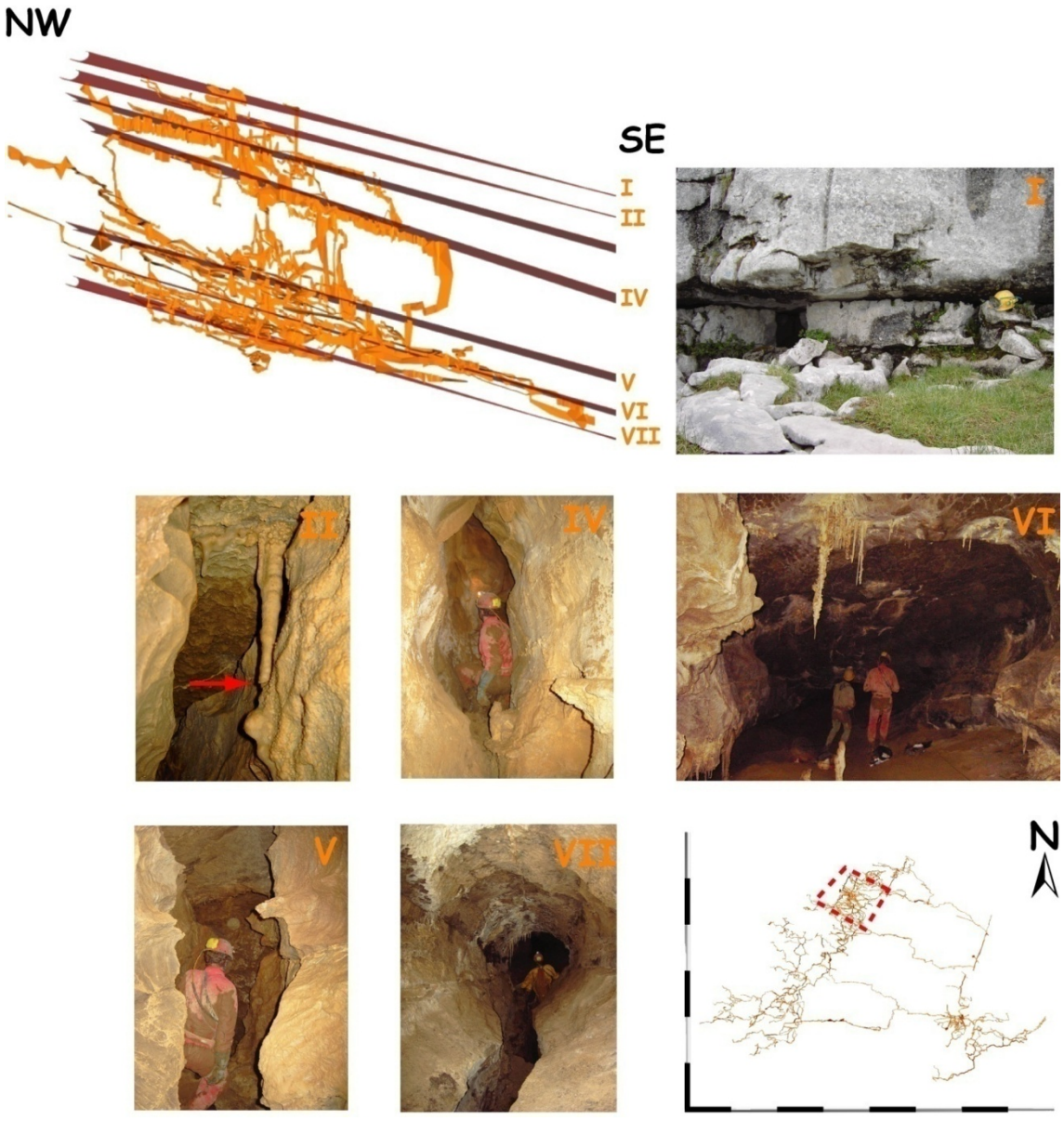

Fig. 2.12: Cave conduits lying on favourable inception horizons. Field verification showed that the karstification began at some discrete stratigraphical horizons (i.e. bedding planes).

2.3 Results from other large cave systems

The statistical method to recognise inception horizons presented above was validated by its application to the Siebenhengste Cave System, where field observations were made to validate the identified inception horizons. The detection method based on the analysis of 3D models is less precise than the direct identification in the field, but allows for a "rapid" analysis of cave systems. We, therefore, applied this method to several other important cave systems from all over the World (tab. 2.1; for the details of the analysis see also appendix 1). This is the first time that such a comparative study has been carried out on such a large number of cave surveys (more than 1500 km of conduits were analysed). The following properties of cave systems were required to be selected for this analysis:

- The explored and surveyed conduit network length should be sufficient (at least 5 km of conduits).
- The respective systems should be representatives of a large panel of geological settings (lithology, tectonics, age…). Nevertheless the analysis been restricted to cave systems developed in limestone and/or dolomite formations.
- Investigated cave systems should were formed only (or at least mainly) by meteoric water karstification (epigenic caves) without or with negligible influence of hydrothermal or hypogenic water.
- The evolution of the investigated cave systems should have occurred mainly under phreatic conditions. This last point is very important because only cave conduits developed under phreatic conditions reflect the initial state of the development of the cave system. By the way, phreatic systems are by far the most common.

The analysis of the parallelism of conduits to bedding planes (chapter 2.2.4.1) clearly showed that in all studied cases the phreatic conduits are parallel to bedding planes. This appears to be independent from the structural context. Nevertheless, cave systems located in a flat lying geological environment have a higher percentage of conduits (e.g. the cave Ogof Draenen with 87 %) that are parallel to bedding planes than systems with more complex geological settings. This is due to the absence of phreatic shafts which can only develop in deeper phreatic conditions. As a general rule, it can be postulated that more than 70 % of the phreatic conduits are parallel to some particular horizons, which in most cases correspond to bedding planes.

The analysis of the inception horizons gives similar results to those obtained for the Siebenhengste Cave System (tab. 2.1). In all cases we could find between two and seven inception horizons. Considering the fact, that horizons are found in all selected cases and that these cases cover a wide range of geological settings as well as hydrogeological boundary conditions, it can be considered that the inception horizon idea is a fundamental principle in cave genesis. Our data even allowed a more quantitative evaluation of the significance of this concept.

The separation of the different peaks was sometimes quite difficult, because the uncertainty of the geological model with respect to the conduit positions was high. This uncertainty is visible on histograms by large peaks. However, as the scattering follows a normal distribution, it is possible to identify the expected stratigraphical position of the inception horizon within a precision of 5 to 20 m. In some cases, where inception horizons are close to each other, peaks may be merged together. In some rare cases with rather complex geological settings (e.g. with a lot of little faults with a displacement of a few metres or slightly folded areas), large peaks were obtained. It was only possible to decompose them with the help of the visualisation of these horizons in the 3D model. From this analysis, it can be concluded that more than 65 % of the phreatic caves (i.e. 90 % of the conduits parallel to the bedding) developed along a very restricted number of stratigraphical horizons. These horizons are in most cases only some decimetre or less thick. This shows the significance of the inception horizon idea for the genesis of cave systems.

The analysis of the conduit directions of the selected cave systems leads us to the same conclusion as for the Siebenhengste Cave System. In all cases, flow directions within (or along) inception horizons are guided by the fracture network, usually the two or three fracture sets which are oriented according to the regional flow direction (controlled by input/output flow conditions). In cases where the landscape dramatically

changed during the evolution of the cave system (e.g. in alpine areas where entrenchment of valleys during glacial periods changed the position of the outlets of the karst system) we could observe that fractures guided the conduit direction change according to the respective outflow conditions. In other words, we could say that the regional hydraulic gradient selects the intersection between fractures and inception horizons which are being karstified. Here, it can be mentioned that inception horizons (i.e. bedding planes) are generally less influenced by the direction changes because, in many cases, hydraulic gradients and inception horizons are both subhorizontal, i.e. parallel, whatever the hydraulic direction can be.

Name of the cave system	Country	Length [m]	Depth [m]	Number of inception horizons
Mammoth Cave System	Kentucky, United States	590'600	115	5
Hölloch & Silbernsystem	Schwyz, Switzerland	193'600 & 37'700	940 890	2-3
Siegenhengste Höhlensystem	Bern, Switzerland	154'000	1340	5-9
Schönberg-Höhlensystem	Oberösterreich, Austria	123'600	1060	4-5
Shuanghedongqun	Guizhou China	106'400	501	2
Hirlatzhöhle Dachstein	Oberösterreich, Austria	95'300	1070	6-7
Ogof Draenen	South Wales, United Kingdom	66'100	100	3
Dachstein-Mammuthöhle	Oberösterreich, Austria	65'800	1200	4-5
Schwarzmooskogel-Höhlensystem	Oberösterreich, Austria	58'200	1030	6-7
Burgunderschacht	Oberösterreich, Austria	20'200	850	6
Schrattenhöhle & Bettenhöhle	Obwalden, Switzerland	19'650	575	2
DÖF-Sonnenleiterschacht	Oberösterreich, Austria	18'200	1055	6
Réseau des Grottes aux Fées	Vaud, Switzerland	12'100	135	3
kleines Hölloch	Allgäu, Germany	9'300	460	3
Wägital Lachenstock, K10, Plattenloch	Schwyz, Switzerland	9'000	270	5
Nidlenloch	Solothurn, Switzerland	7'500	420	4
Lauiloch	Schwyz, Switzerland	4'500	180	1
Réseau de Covatannaz	Vaud, Switzerland	4'450	105	2

Tab. 2.1: Investigated cave systems with the determined number of inception horizons: inception horizons were found in all investigated cave systems.

2.4 Field demonstration – Speleomorphologic Features along Inception Horizons[2]

The statistical analysis of previous chapter 2.2 showed that many conduits are located along a restricted number of inception horizon. These horizons were displayed in the 3D model in order to verify visually their speleogenetical significance. At several places, it has also been verified by field observations or backed-up according to detailed descriptions of the cave passages from the literature. In caves, some typical features and effects can be looked for in order to recognise a bedding plane as an inception horizon.

Depending on the quality of the geological model and the cave survey data we are able to identify by our statistical approach favourable horizons within an accuracy of about ± 10 m. However, this accuracy is not sufficient for various scientific concerns (e.g. elaboration of the key features of inception horizons) or geological engineering (for example, planning a tunnel traces). A higher accuracy can be reached by mapping the inception horizons in the field.

Recognizing the preferred karstified horizons at an outcrop is usually not an easy task. This chapter discuss various speleomorphologic features, which may be encountered along inception horizons. The recognizing of these features allows, not only to improve the accuracy of localisation of the statistically identified inception horizons, but also in cases where not enough cave surveying data are available for a solid 3D analysis (several kilometres surveyed cave conduits are needed), it allows to sequential preferred karstified horizons .

The field identification of the speleomorphologic features discussed in this chapter was used to get the field evidence of the existence of the statistical identified inception horizons. Furthermore, they allow deciding which of the exposed bedding planes within cave passage is most likely the inception horizon. In cave passages with no clear elliptic profile it is sometimes a challenge to recognize the inception horizon. Locally, even multiple bedding planes can show the typical inception horizons features (fig. 2.13), but usually only one bedding plane shows the features over longer distances and is therefore the inception horizon. It should also be noted that not all features need to occur along an inception horizon and that some similar features can be produced by other processes.

Fig. 2.13: Cave passages in the Nidlenloch (Switzerland). Anastomoses was developed along multiple bedding planes, however, some decametres further on, only one bedding plane still has anastomoses along them and can be considered as the inception horizon.

[2] *This chapter is widely a translation of Filipponi, 2007.*

To localise the inception horizons by the statistical analysis of the 3D geometry of the cave systems (chapter 2.2), several kilometres of cave surveying data are necessary. Indeed it is possible to analyse cave data from not connected smaller cave systems, but this can overestimate inception horizons of only local importance (e.g. Veni, 1999). Therefore, it seems to be more efficient and reliable to identify inception horizons in an area with a large number of small caves by mapping and evaluating the above presented speleomorphologic features.

This chapter describes typical geomorphic characteristics recognized on inception horizons of the investigated cave systems. For detailed field observations of the case studies are referred to the appendix 1.

2.4.1 Bedding Plane Conduit

The expression “bedding plane conduit” (in German ”Schichtfugengang“ – e.g. Kyrle, 1923; Trimmel, 1968; Bögli, 1978) is used for caves or cave conduits that are bedding plane guided. They usually have an elliptic or lenticular cross section, whereat the section is often squeezing out into the bedding plane (fig. 2.14-left). This bedding plane can be considered as the inception horizon of regional or local importance depending if the plane guides the cave development at the scale of the rock massive or not.

The cave conduits can have diameters of a few decimetre up to several meters or tens of metres (among them, they will no longer be described as a cave conduits, as for speleologists not passable, but as generalised as karst conduits; see also chapter 2.4.2).

Fig. 2.14: Bedding plane conduits, in red the inception horizon. Left: elliptic conduit cross section in the Petite Grotte aux Fées (Switzerland); Right: key hole profile in the Siebenhengste Cave System (Switzerland).

The classic elliptic shape developed under phreatic conditions, but it may be rework in later vadose phase. Under vadose conditions the conduit floor will gradually be placed deeper and build a canyon –keyhole profile (fig. 2.14-right). In some cases, the vadose canyon becomes morphologically more dominant than the initial elliptic passages, becoming several metres to tens of meters deep (e.g. meandering passages between shafts in alpine caves).

In cave passages with breakdowns, “false” bedding plane passages can occur (e.g. Waltham, 2002; Filipponi, 2003). Especially in thin bedded rock masses, breakdown can produce a “new” elliptical ceiling. This new cavern is located above the original phreatic passages and has no association with inception horizons.

It is needed to clearly distinguish between “bedding plane conduits” (in German “Schichtfugengänge”) and “formation boundary conduits“ (in German “Schichtgrenzgänge“), whereat the later developed along the contact of a karstic with a not karstic rock formation. A classical example of this type of caves is the Seichbergloch (length of 2.2 km and altitude difference of -560 m; Wildhaus, Switzerland) that largely

developed along the formation boundary between the karstic Seewerkalk Formation and not karstifc Garschella Formation (Dickert, 1995).

2.4.2 Anastomoses

As anastomoses are named networks of branching, intersecting, and rejoining channels in a two dimensional system (Slabe, 1995). The network is exposed at the ceiling of a cave passages and/or at the cave conduit walls (fig. 2.15).

Fig. 2.15: Anastomosis in the Mammoth Cave (USA). The inception horizon with the anastomosis is guiding a cave conduit network of length of several kilometres.

In literature various possibilities of the origin/development of the anastomoses are discussed. Among others Ćalić-Ljubojević (2001) proposed that anastomoses that developed along a bedding plane are caused by seepage water that penetrates during floods events from the cave conduit into the bedding plane and flows back during low water time. Therefore, for him the occurrence for anastomoses is only a late speleomorphlogical phenomenon and has no relationship with the early speleogenetic processes.

Another explanatory approach is to consider anastomoses as "proto-caves" (fig. 2.15) (e.g. Ewers, 1966; White, 1988; Lowe, 1992). These authors assume that, at early state of karstification, the ground water flows through a large number of karst conduits along the inception horizons. Only gradually, one conduit becomes more important, prefers the flow thorough and develops faster than the surrounding conduits, whereas the other conduits remain more or less in the proto-cave state. Therefore, the anastomoses can be considered as the “looser” tubes and the main passage as the “victory” tube.

Situations where it takes a relatively long time to develop a clearly preferred drainage conduit, several conduits will grow simultaneously to the size of cave passages (penetrable for speleologists) leading to a labyrinthic network of cave passages along the inception horizon (e.g. Hölloch, Switzerland).

It is difficult to get clear evidences for one or another approach. However, the following facts sustain the "proto-caves-anastomoses" approach:

- The cave passage in which the anastomoses was observed is a bedding plane conduit;
- The cave passage in which the anastomoses was observed is part of a labyrinthine cave network;
- It possible to recognise a network of anastomoses/karst conduits;
- Anastomoses continued at the ceiling of the main cave passage.

In cave passages that are completely filled with cave sediment, water can flow between the sediment and the cave ceiling build structures that are similar to anastomoses (Slabe, 1995). They can be distinguished from “true” anastomoses that they show no connection with a bedding plane (i.e. inception horizon), that is no continuation of the channels in the rock.

2.4.3 Cave Karren

Cave karren are like karren at the surface, channel or rill-shaped corrosive features. They are created by an area-wide wetting of the rock surface and can be found at the floor as well as walls of the cave (Slabe, 1995).

If the upper end of “cave wall karren" are along a bedding plane (fig. 2.16), this suggest that the karren were dissolved by seepage water percolating out of the bedding plane (i.e. inception horizon). Like for the anastomoses there is a debate whether the seepage water is discharging into the cave (Ford and Lundberg, 1987) or whether the water infiltrates during flood events form the cave into the bedding plane and re-infiltrates during low water level (Ćalić-Ljubojević, 2001) .

Structures similar to karren can also develop under sedimentary deposits (Slabe, 1995). They differ from cave wall karren by a less regular rill structure and a less clear upper ending, which is not associated with a bedding plane.

Fig. 2.16: Cave wall karren: The top end of the karren are along an inception horizon. (Hirlatzhöhle, Austria; Photo: Lukas Plan).

2.4.4 Flowstone

If the seepage water percolating out of an inception horizons is under-saturated regarding to the calcite content cave wall karren will develop. Contrary, it the seepage water is oversaturated regarding to calcite, flow stone will precipitate (fig. 2.17).

Fig. 2.17: Flow stone along inception horizons. Left: Hirlatzhöhle, Austria; right: Lauiloch, Switzerland.

2.4.5 Springs

Inception horizons are not only percolated within the phreatic zone (see also chapter 4) by seepage water, but are still under vadose conditions preferential flow phases. Consequently, springs at the surface or within a cave passage are often aligned with inception horizons. These springs can be cave entrances with a spring discharge of several cubic metres per second (fig. 2.18.1), or diffuse spring horizons with many small water outlets (fig. 2.18.2).

Fig. 2.18: Springs along inception horizons. 2.18.1: Karst spring of the Réseau de Covatannaz (Switzerland). 2.18.2: Diffusive spring area along an inception horizon with moisture-loving vegetation. 2.18.3: Small ice waterfall from an inception horizon.

This allows for example, relatively simple the identification of inception horizon at surface outcrops, for example in winter by ice water falls (fig. 2.18.3) or in the summer by an association of moisture-loving vegetation (fig. 2.18.2). In the cave passages are water inlets often associated with cave walls karren (chapter 2.4.3) or flow stone (chapter 2.4.4).

2.4.6 Unroofed Caves

Unroofed caves are caves or cave passages with a missing ceiling that were removed by surface erosion. Therefore, the cave passages are now exposed (fig. 2.19) (Knez and Slabe, 2002). Unroofed caves are mainly horizontal cave passages and are often associated with inception horizons (Šušteršič, 1998) (see also the chapter 2.4.1).

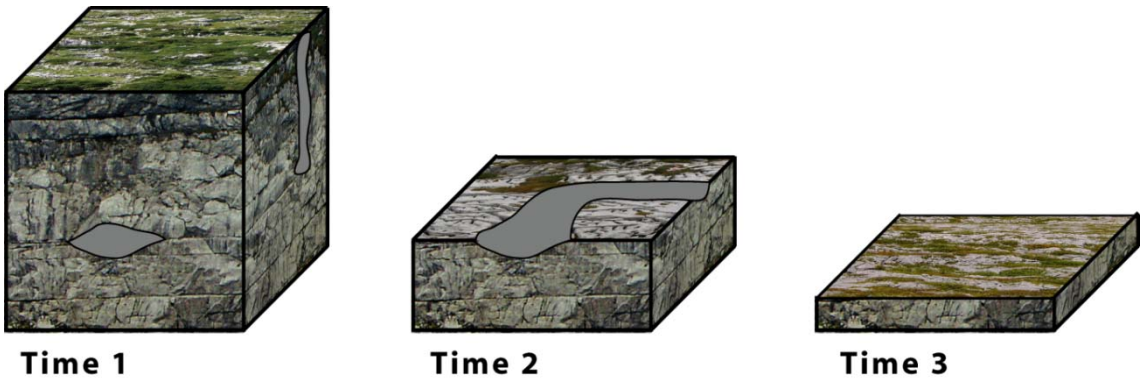

Fig. 2.19: Exposure and destruction of a cave by surface erosion. Time step 2 represents an unroofed cave.

2.4.7 Cave Gypsum

It is common to find cave gypsum as flowers or needles along inception horizons (fig. 2.20).

If the cave gypsum is a re-precipitated sedimentary gypsum, we can suppose that the inception horizons consist at least partly of highly soluble gypsum (e.g. Moggerenschacht, Germany). Contrary, the cave gypsum can also be a by-product of the weathering of pyrite. This weathering can produce aggressive solutions that enhance the karstification at least locally.

The origin of cave gypsum can be determinate by stable isotope analysis (see chapter 3.3.5).

Fig. 2.20: Cave gypsum along an inception horizon. Left: gypsum flowers (Siebenhengste Cave System, Switzerland); right: gypsum needles (Nidlenloch, Switzerland).

2.4.8 Evidence of Neo-Tectonic Movement

In some cases, we observed that the conduit cross section was postponed along an inception horizon and/or broken or shifted dripstones, which give evidence of neotectonic movement (fig. 2.21). The movement along these bedding plane fractures was in the range of a few centimetres to decimetres and occurred after the development of the cave passages.

For a further discussion about bedding plane fractures see also chapter 3.3.3 and chapter 3.6.2.

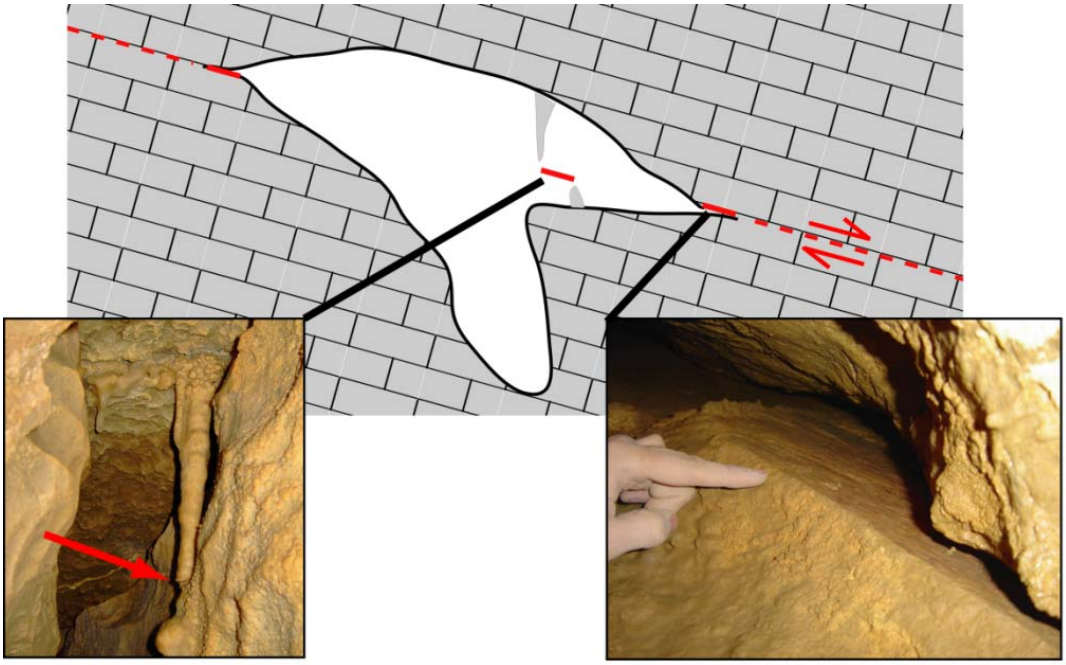

Fig. 2.21: Schematic representation of a conduit cross section with neo-tectonic movement along a bedding plane fracture; left: broken and displaced sinter column (Siebenhengste Cave System, Switzerland); right: Displacement of the upper part of the conduit relative to the lower of around 20 cm, clearly recognisable the slickenside (Nidlenloch, Switzerland).

2.5 Discussion about the existence of inception horizons[3]

The method developed for the analysis of inception horizons in cave systems was validated by the analysis of 18 well documented large cave systems from all over the World, among them the Siebenhengste Cave System being our main test site. The existence of lithostratigraphic horizons along which karst conduits developed preferentially was proved in all examined cave systems. In most cases, we could identify between two and five inception horizons. This analysis confirms the idea of preferential development along some discrete stratigraphic horizons as already introduced by many authors (e.g. Rauch and White, 1970; Palmer, 1989) and named by Lowe (1992). However, the presented method allowed for the first time to provide a clear quantitative evidence of the significance of inception horizons for the genesis of cave systems.

[3] *This chapter is widely equivalent to the chapter "discussion" in Filipponi et al., 2009.*

Our results remarkably show that only a restricted number of inception horizons are used for cave inception at a regional scale: probably less that 10 % of the existing bedding partings are inception horizons and guide more than 70 % of the conduits. It also appeared clearly that the influence of these horizons onto the 3D geometry of the systems is high. However, the method allows only recognising inception horizons with a regional significance (in Lowe, 1992 called major inception horizon). Detailed field observations showed that beside the statistically identified inception horizons, some other inception horizons guided cave passages for only some metres to tens of metres and have only a local significance (some hundreds of m^2; in Lowe, 1992 called minor inception horizon) (fig. 2.22). This also explains the difference between the number of cave conduits parallel to the bedding (in the Siebenhengste Cave System around 70 % of the conduits are parallel to the bedding; chapter 2.2.4.2) and the sum of the conduits length being identified statistically to be on inception horizons (65 %). However, the majority of the bedding plane guided cave passages developed along an inception horizon with regional significance.

To localise the inception horizons by the statistical analysis of the 3D geometry of the cave systems, several kilometres of cave surveying data are necessary. Indeed, it is possible to analyse cave data from not connected smaller cave systems, but this can overestimate inception horizons of only local importance (e.g. Veni, 1999). Therefore, it seems to be more efficient and reliable to identify inception horizons in an area with a large number of small caves by mapping and evaluating the typical speleomorphologic features associated with inception horizons chapter 2.4.

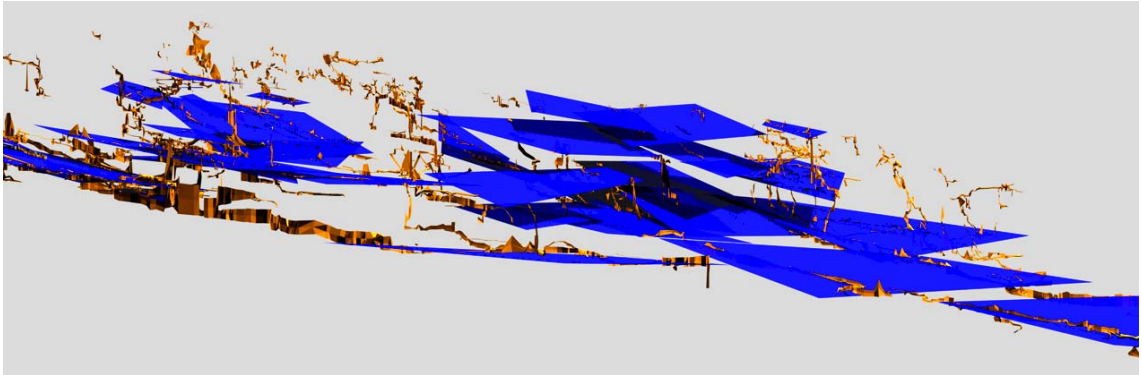

Fig. 2.22: 3D view of zone of the Siebenhengste Cave System with mapped inception horizons of local as well as regional influence.

Knez (1997, 1998) also recognised in the Škocjanske Jame (around 5 km long cave system in Slovenia) only a restricted number of bedding planes to be inception horizons (3 inception horizons of 62 prominent bedding planes in the around 100 m thick limestone sequence). His basic working method was to assign in the field phreatic conduits to the respective stratigraphical horizons.

Palmer (1989) measured with a high degree of precision in the Mammoth Cave region the orientation of about 20 km of conduits and the bedding of the rock at more than 3200 locations. With his field method, he was able to have an accuracy of less than 1°. He could show that around 70 % of the examined conduit passages are discordant to the local dip of the bedding of less than 2°. The conduits were located preferentially along 24 different stratigraphic horizons of which 5 horizons are predominant at the regional scale. Our analysis of the Mammoth Cave data confirmed Palmer's results, providing a supplementary validation of our analysis method. Unfortunately, our method depends on the precision of the cave survey data as well as that of the geological knowledge of the massif investigated. This limited precision is somewhat compensated by the high number of data points available for the analysis.

Similar results have also been published for example by Ford and Ewers (1978). They reported that in Swildons Hole (England) around 70 % of the known passage length where on “bedding planes” (whereof 20 % along bed joint intersection). Jameson’s (1985) structural field analysis on North Canyon of Snedegar Cave (length of around 420 m West Virginia) showed that around 60 % of the conduits are bedding partings

guided (whereof 20 % along bed joint intersection). However, the authors did not delve in details into the stratigraphical position of the conduits.

Field verifications pointed out that those inception horizons are rarely thicker than some decimetres, and in most cases in the order of a few centimetres (see also chapter 3.3). The statistical analysis provides a normal distribution around the position of the inception horizons in the order of some metres to tens of metres, because of the uncertainty of the 3D model. In cases where the inception horizons are very close to each other, it is hard to distinguish them based on the statistical method. Therefore, it is advisable to interpret the histogram with the help of the 3D model and to verify the results by field observations.

Albeit our 3D analysis was restricted only to epigenic caves (caves formed by water recharged from the overlying or immediately adjacent surfaces due to carbonic acid dissolution), it appears that also the geometry of hypogenic karst systems (caves formed by water in which the aggressiveness has been produced at depth beneath the surface, independent of surface or soil CO_2 or near surface acid sources; Palmer, 2000) is guided by a restricted number of stratigraphical horizons (e.g. Klimchouk, 2007). For example, developed the Monte Cucco cave system (Umbria, Italy) along several stratigraphical horizons (Galdenzi and Menichetti, 1995) (fig. 2.23). However, a detailed 3D analysis still needs to be done.

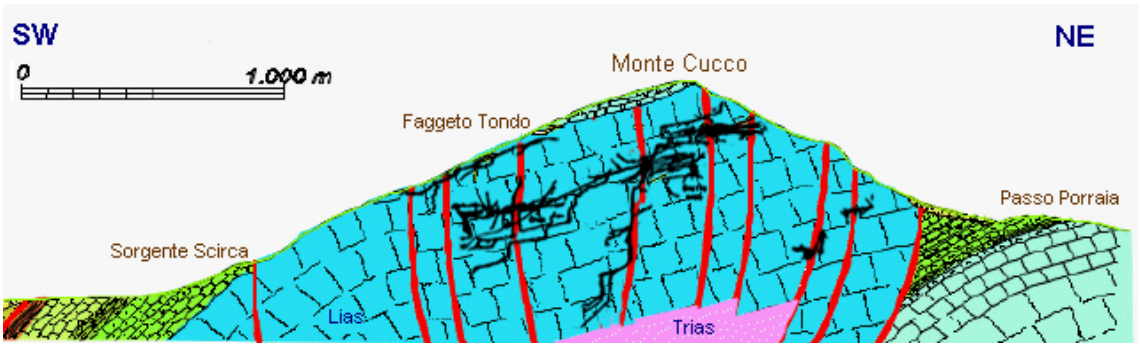

Fig. 2.23: Schematic cross section through the Monte Cucco cave system. Also hypogenic karst systems seem to develop along inception horizons. However, a detailed 3D analysis is still missing. (Figure has been compiled from different figures of www.cens.it).

Davies (1960) suggested that the dip of beds influences the role of the bedding planes for the development of conduits and concludes qualitatively that beds dipping less than around 15° seem to have a clear influence on cave development, whereas beds with a dip between 15 and 80° would have only a restricted influence. The influence of steeper (almost vertical) beds would increase again. Our reference sites cover almost all kinds of bedding orientations, but the role of bedding planes was significant for all of them. This was not only true for phreatic conduits. In cases where bedding is rather steep, vadose conduits preferentially followed beds rather than fractures down to the phreatic zone (e.g. case study of the Nidlenloch (see appendix 1) or from the literature e.g. Osborne, 1999, 2001; Filipponi, 2000; Ford and Williams, 2007). Therefore, we could not confirm Davies observations and we have to conclude that the role of bedding dip is only a subordinate factor.

Compared to fractures, bedding planes often have the advantage of a larger extension, i.e. better continuity (the typical surface area of joints is in the order of some hundreds of square metres; the typical size of bedding planes in the order of square kilometres). They also have the advantage of orientation: most bedding planes are subhorizontal, i.e. parallel to the hydraulic gradient in the phreatic zone. Another advantage compared to fractures is their age (karstification along bedding planes can start during the lithification of the rock mass). However, this does not mean that fractures have no role in cave inception. In most cases fractures control the conduit orientation at local scale and along inception horizons together with the regional hydraulic gradient (fig. 2.24) (e.g. Lauritzen, 1988). In other words, conduits are developed along the intersection between inception horizons and fractures being the most parallel to the hydraulic gradient.

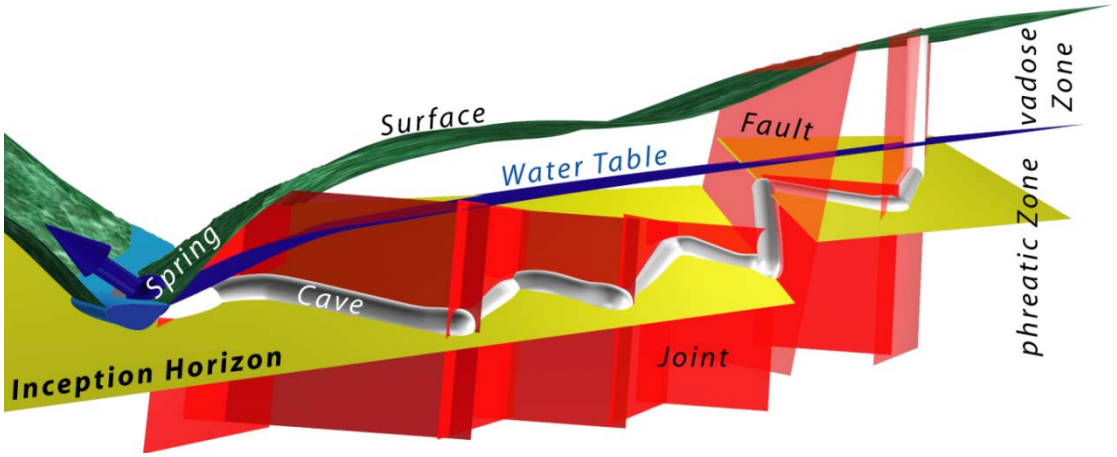

Fig. 2.24: Schematic 3D model of a karst conduit system: The geometry of phreatic conduits is determined by inception horizons (in most cases related to well-marked bedding planes), joints and faults as well as by the hydraulic gradient.

In some cases, cave inception occurs also along fractures that are unrelated to inception horizons. The cave development along these fractures can be induced by "tectonic inception" (tectonics producing a fracture network wide enough to allow turbulent flow; Faulkner, 2006) or by "chemical inception" (dissolution of the fracture surface and gradual enlargement of the fracture width). In our study areas, we could regularly observe that a conduit followed an inception horizon, reached a normal fault, followed the faultto find the same bedding plane on the other side of the fault or to find another inception horizon (fig. 2.24). However, fracture inceptions become dominant when no clear inception horizons are available or if sedimentation structures were obliterated by metamorphism as for example in marbles.

We have seen in chapter 2.2.4 that in the scale of a single cave system, it was not possible to identify the same number of inception horizons in all areas. Therefore, it is not advisable to blindly extrapolate the results of the inception horizon analysis from one site to a neighbouring site. The analysis of the geometry of a karst system should always include the geological as well as the hydrogeological history of the area. This should not only be done for a back-analysis but also for the prediction of the geometry and position of conduits (chapter 5).

The presented methodology is able to detect inception horizons and allows the detection of inception horizons which were favourable not only at the beginning of the karstification of the rock mass but also later when some only slightly opened flow path evolved to form cave conduits. In this analysis, the unavoidable bias remains that the minimum size for a karst conduit is around 0.01 m, while the minimum size for direct exploration (cave) is about 0.5 m (White, 2002). One suspects that there is a very large component of conduits with a scale in the range between 0.01 and 0.5 m, about which we know almost nothing (chapter 4). Unfortunately, we have not been able to include these inexplorable karst conduits in our analysis so far. This is also the reason why the size of the peaks in the histograms in chapter 2.2.4 does not say anything about the relative importance of the respective inception horizons, but gives only the binary answer "yes/no: there is (is not) an inception horizon".

The evidence for inception horizon will also have consequences for the numerical modelling of the evolution of karst systems (e.g. Gabrovšek and Dreybrodt, 2001; Kaufmann, 2002). Up to now, these models used mainly two dimensional networks of initial pathways, for instance a network of fractures enclosed within a rock matrix. The existence of inception horizons will now also justify introducing them into these models, i.e. considering three dimensional networks on initial pathways. It will also be necessary to understand and model the speleogenetical processes along the inception horizons, such as, for example, dissolution processes by sulphuric acid produced by the weathering of pyrite. Furthermore, it is essential to identify the key parameters that distinguish inception horizon related to bedding planes from the far more numerous normal bedding planes and to understand the speleogenetical role of these parameters (chapter 3). Depending on the results, we may be able to simplify the volume (3D) description of initial flow paths.

We are convinced that the identification of inception horizons is a good tool not only for a better understanding of the speleogenesis (chapter 4) but also for predicting karst conduits for engineering proposes (chapter 5).

2.6 Conclusion about the existence of inception horizons

Compared to the commonly used 2D analysis of cave systems (e.g. vertical distribution of conduits for the identification of cave levels or plan view to work out the relationship between cave development and fractures), our 3D analysis allowed us to couple the geological and hydrogeological contexts to the conduit network geometry within a carbonate rock mass. We analyzed more than 1500 km of conduits of some of the most important caves around the World and could show that more than 70 % of the phreatic conduits are located along discrete inception horizons, many of which are bounded by obvious bedding. For the first time, we could quantitatively (statistically) show that the development of karst conduits under phreatic conditions is strongly related to a restricted number of inception horizons.

Our results indicate that the role of inception horizons is often underestimated and that the position of karst conduits at regional scale is not random at all, but mostly constrained by a limited number of inception horizons commonly expressed as prominent bedding planes.

Field verification of some of the statistical identified horizons confirmed the existence of these stratigraphic horizons. They have most of the time a thickness of some centimetres to decimetres. Associated with these horizons we could observe some characteristic features like: anastomoses, karren, flowstones, cave gypsum or the evidence of neo-tectonic movements.

Once the inception horizons are localized/identified we can sample the corresponding bedding planes and analyse the rock with laboratory methods to understand the factors as well as processes that made this particular straticraphical horizon favourable to karstification. This is the major challenge of the next chapter (chapter 3).

- 3 -
What makes an Inception Horizon favourable to karstification?

3.1 Introduction

The analysis of the complex 3D geometry of large cave systems around the World allowed us to get statistical evidence of the inception horizon hypothesis (chapter 2). The analysis clearly confirmed that the influence of these horizons (in most cases between 3 and 5 horizons) onto the 3D geometry of cave systems is high.

However, one main question remains: What makes one specific stratigraphical horizon favourable to karstification and what kind of processes are involved and which of them are the most important? Different descriptions of ”preferred bedding planes” are available in the speleological literature; however the interpretation does usually not consider the whole framework of the inception horizon hypothesis and they are simply discussed as “bedding planes” (e.g. Orndorff et al., 2001). Furthermore, in most cases, one misses a speleogenetical discussion of the observations. Meanwhile, some concrete suggestions are expressed about “why” some parts of the rock succession act as inception horizons but, so far, only little analytical confirmation evidences were presented (e.g. Lowe, 1992; Knez, 1998; Pezdič et al., 1998; Florea et al., 2007).

Lowe (2000) proposes possible reasons for such a higher karstification to be:

- Higher primary porosity of the horizon than the surrounding rock mass.
- Horizon enclosing highly soluble minerals as gypsum: the dissolution or exchange of these minerals causes an elevated ratio of secondary porosity.
- Horizon with sulphide minerals: pyrite or other sulphide minerals can be oxidized and produce H2S or even sulphuric acid, which may turn non aggressive water (moving along the bedding plane) into highly corrosive solutions.
- Horizon of clastic beds: clastic beds such as shales or volcanic clays can be impervious and if thick enough act as a low permeability “screen” along which water will flow preferentially.

Albeit the dissolution process of the rock is one of the fundamental characteristic of karstification they are still insufficiently understood (e.g. Dreybrodt et al., 2005). Only a few researches were done to understand the dissolution of a natural limestone (aggregation of different minerals and typical texture). A majority of them aimed to understand the dissolution rate of various types of limestone and dolomite to classify rock as more or less good karstifable (e.g. Roques and Ek, 1973; Rauch and White, 1977; Eisenlohr et al., 1999; Horoi, 2001). However, none of them deals within the context of inception horizon hypothesis.

Different investigations were done to better understand the weathering and karstification of limestone. Some authors analyzed statistically the lithological properties of karstified rock samples to get the chemical and petrological factors which influence dissolution rate (e.g. Dreiss, 1983, Spate et al., 1985; Plan, 2004). However, it is difficult to compare and/or assembly this published results because the samples are often of unknown stratigraphic position within a given formation or do not take into account the concept of inception horizon hypothesis designing the sampling strategy.

Also laboratory experiments were designed to better understand the process of limestone dissolution (e.g. Rauch and White, 1977; Eisenlohr et al., 1999). Most of them were designed considering that speleogenesis takes mostly place along fractures; therefore, they observed the dissolution on rock surfaces. These results

can only limited be extended to the karstification of inception horizons; that is the dissolution within a porous medium (Noiriel, 2005). Notwithstanding, we can expect that some principal founding will still be valid.

Several characteristics of the rock mass may play a significant role for speleogenesis. It is known that the karst process follows a positive feedback development; the rock being soluble, water dissolves it and enlarges the voids, which become able to accept more water to flow through, i.e. more dissolution to be active and the voids to enlarge faster (Kiraly, 1975). This loop is self-developing until the system of conduits can absorb the total amount of the water available from the rain with no significant increase in the hydraulic gradient. Therefore, we can assume that there are three main aspects that make an inception horizon favourable to karstification (fig. 3.1): Characteristics controlling the flow path (1), controlling the dissolution rate (2) and defining the dissolution capacity of the water (3). The processes under investigation being highly non linear, it is expected that the links are quite complex. Therefore, we can assume that the deviation of the mineralogical and textural composition of the inception horizons within the surrounding sequence will be one of the main factors determining the preferable karstification of the inception horizons.

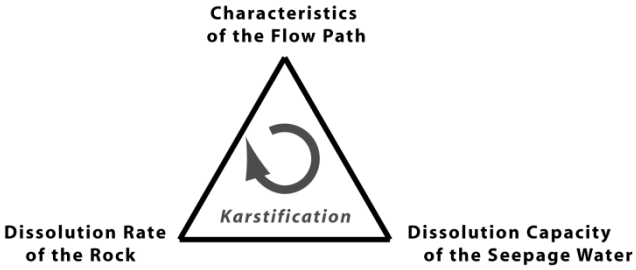

Fig. 3.1: The process of karstification is a positive feedback loop controlled by factors controlling the characteristics of the flow path, dissolution rate and dissolution capacity of the seepage water.

The aim of this study was to investigate the mineralogical and textural diversity of the different types of inception horizons to better understand why these stratigraphical horizons are better karstified as well as the relative importance of the processes during speleogenesis.

The investigation is subdivided into a field (chapter 3.3) and laboratory (chapter 3.4) characterisation of inception horizons.

3.2 Sampling Strategy and Location

In order to understand the reason(s) why a specific inception horizon is used for cave development, we sampled different inception horizons. Based on the 3D analysis of cave systems as well as on field verifications (chapter 2), we selected a set of 18 inception horizons in six different cave systems. Almost 200 micro-cores (3 – 5 cm long, diameter of 2.6 cm) were sampled in order to characterize openings and origin of inception horizons and of the surrounding rock mass. Sampling was designed in a way to approach local as well as regional variations of the selected properties (fig. 3.2). For this purpose at least three samples were taken at a given place of an inception horizon (one sample from the inception horizon and two samples of the surrounding rock mass, one above and one below the inception horizon). For some horizons, several sampling locations were selected in order to assess the regional scale heterogeneity. Most of the samples were drilled parallel to the bedding.

One main challenge in our approach is to assess the characteristics of rock parts, which are no more existing. In fact, the most favourable parts of the rock mass for cave inception were removed during karstification. Despite this bias, one can expect that it will be possible, by choosing appropriate sampling

points, to get at least a qualitative idea of the initial rock properties, or their spatial variation and their role during speleogenesis.

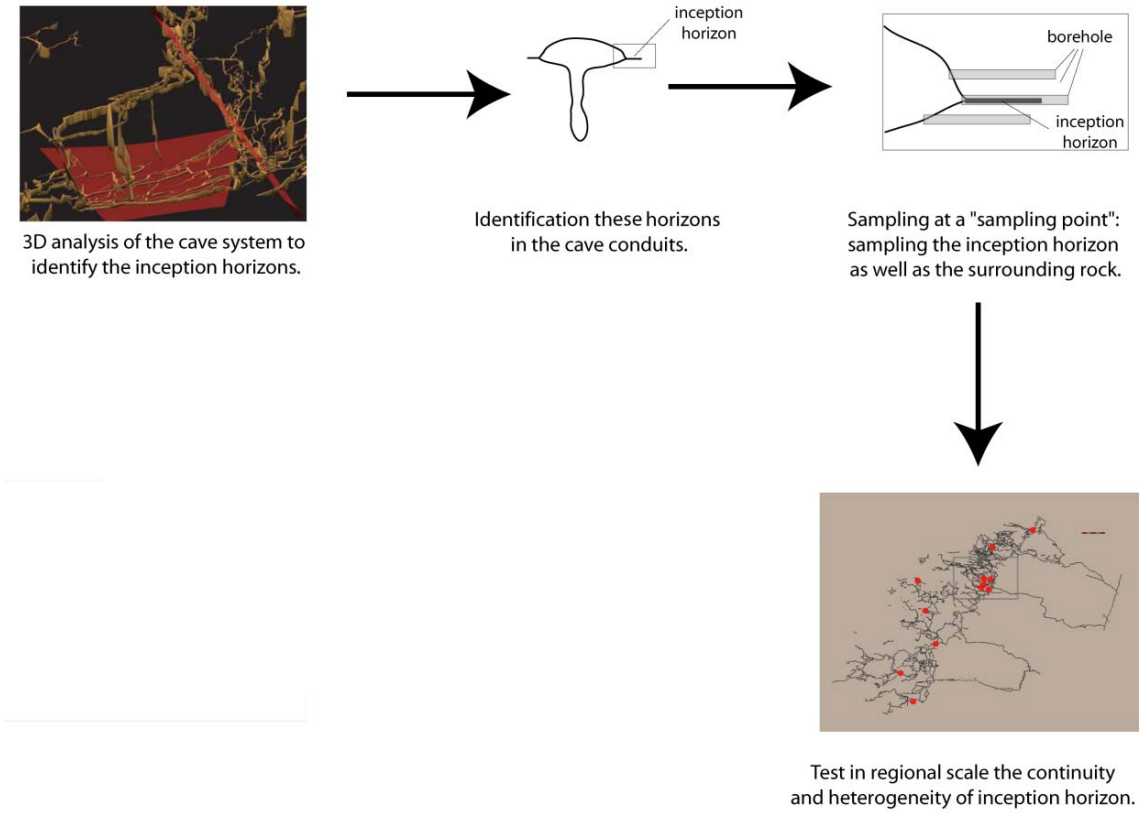

Fig. 3.2: Sampling strategy for the inception horizons. The sampling was designed in a way to approach local as well as regional variations of the inception horizons properties.

Various drilling equipments were tested prior to find the adequate combination for the purpose of the research project and the working condition in caves (size and weight of the equipment to be transported by two persons through a cave, drilling autonomy for at least 10 cores, no waste gas). Finally we used a battery operation power drill (36 V) with a driller allowing to take cores up to 12 cm long (2.6 cm in diameter) associated with a water cooling system (fig. 3.3). We optimized the drilling equipment in a way that it allowed us to sample also in difficult accessible cave parts with a minimum of weight and cooling water as well as accumulator power.

Although we drilled with a short drill pipe, it was sometimes quite tricky to get unbroken cores especially form marly bedding planes. Where it was not possible to drill adequate micro-cores in the field, we collected hand specimens and drilled them in the laboratory.

Fig. 3.3: The drilling equipment: We used a battery operation power drill with a micro-core driller and a water cooling system.

Based on the 3D analysis of cave systems (chapter 2) and on field verifications, we selected a set of inception horizons for further analysis. The selection was constrained mainly by the site accessibility and can be therefore, considered as random. A total of 18 known inception horizons in six different cave systems were sampled and are shortly described below.

3.2.1 Siebenhengste Cave System

Eight inception horizons of the Siebenhengste Cave System (length around 154 km, depth around 1340 m; BE, CH) were selected for sampling (tab. 3.1). For a short description of the cave system be referred to chapter 2.2.1 or in Jeannin and Häuselmann (2005). In all we took samples at 20 sampling points along 8 inception horizons (fig. 3.4 and fig. 3.5).

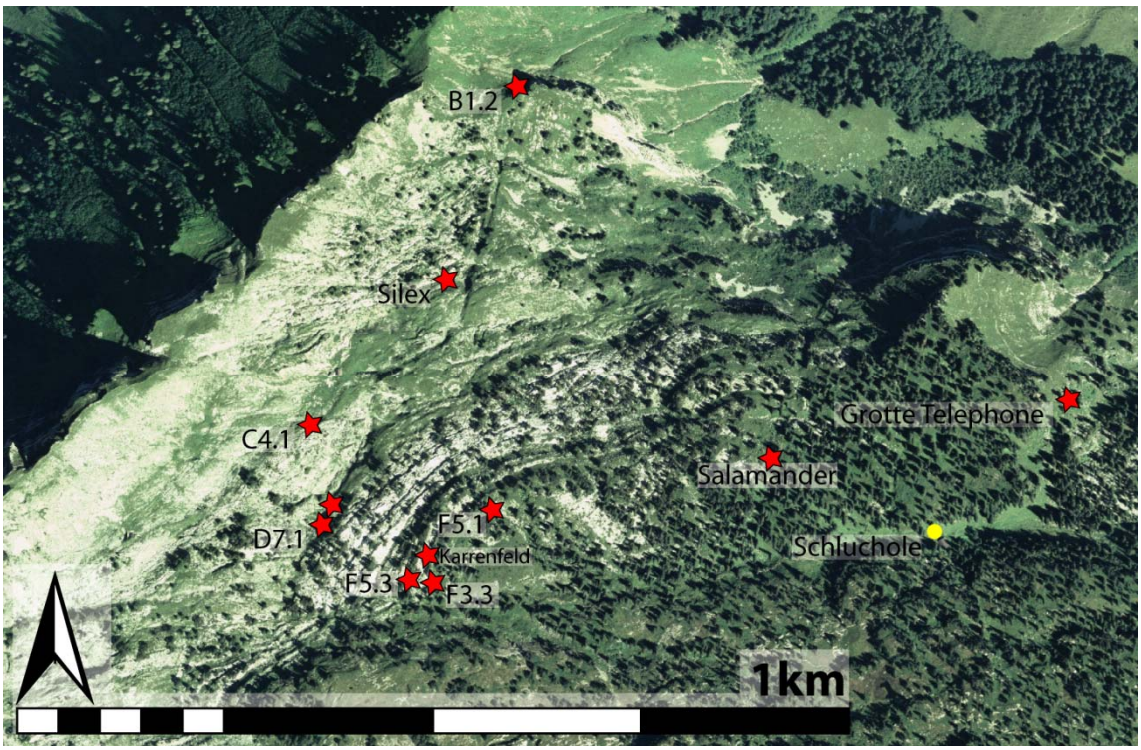

Fig. 3.4: Aerial image of one part of the Siebenhengste area (in fig. 2.8 Zone I and II). The red stars label the position of some sampling points.

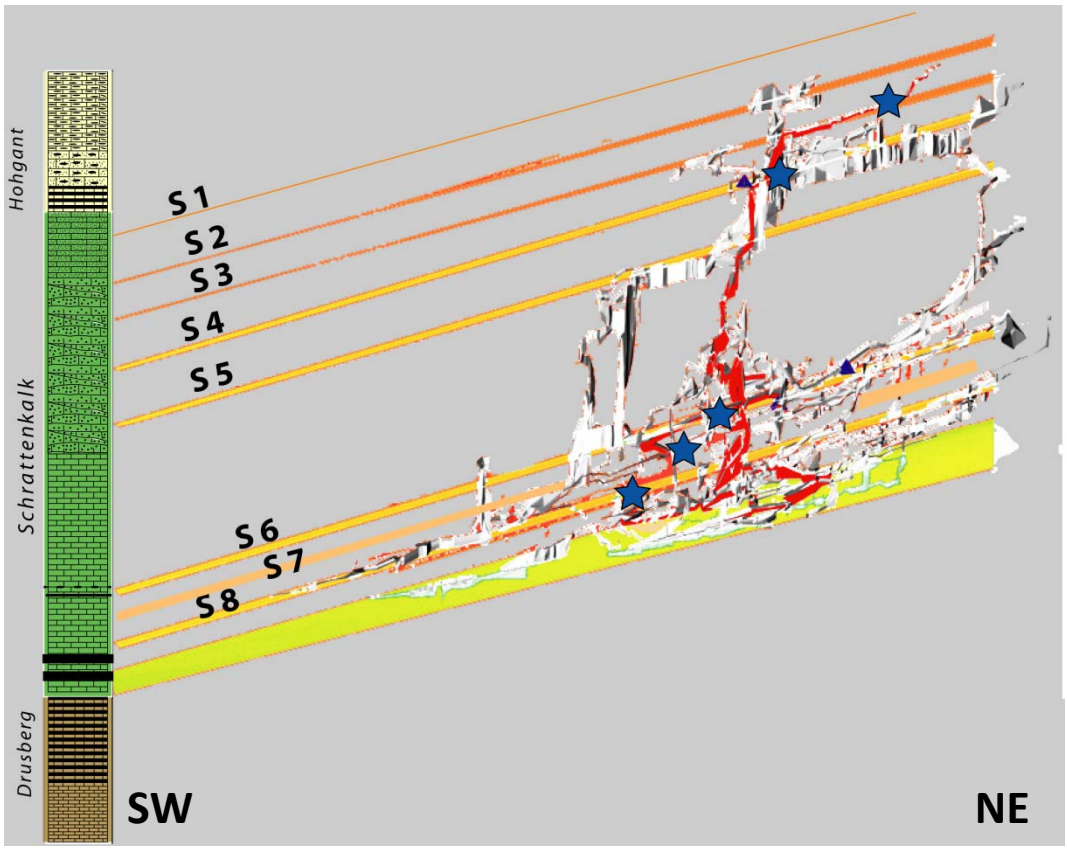

Fig. 3.5: 3D view of one part of the Siebenhengste Cave System (D.7.1 - red dyed cave conduits) with the sampled inception horizons. The blue starts label the sampling points.

Short description of the inception horizons

S1 Inception horizon is a green marl layer.

S2 Inception horizon is some centimetres thick and guides an extensive network of anastomoses.

S3 Inception horizon is a fossil-poor bedding plane (some centimetres thick) in the Schrattenkalk sensu stricto. Eye-catching is the network of anastomoses that developed along the bedding plane. The network is so dense in some places that the bedding plane was completely removed.

S4 Inception horizon is situated at the contact between the Schrattenkalk-members sensu stricto and "upper oolitic" member. Below this surface, there is a set of close standing joints that seems to end at this contact. Also some evidence of neotectonic movement along the contact could be observed (broken and shifted dripstones).

S5 Inception horizon is a 40 to 60 cm thick, very blocky (stromatolitic?) limestone layer.

S6 Inception horizon is a marly horizon of some centimeters thick.

S7 Inception horizon is a marly bedding plane (some centimetres thick) of the "Lower Schrattenkalk" member. Many siliceous nodules of some centimetres in diameter are found embedded in the bedding plane.

S8 Inception horizon is a marly layer (some decimetres thick) at the transition between the Lower and Basal Schrattenkalk-members. Conduits related to this horizon are full of cave gypsum formations (crusts, needles, flowers, etc.).

3.2.2 Hölloch

The Hölloch (length around 193 km, depth around 120 m; SZ, CH) is formed in the Schrattenkalk formation and characterized by a mazy network of superposed cave conduits (e.g. Möckli, 2000). The geological context is rather complex because of alpine displacement, superposition and shearing of the helvetic units.

The 3D analysis of the cave conduits geometry revealed the existence of two to three inception horizons (chapter 2.3). We selected two of them for detailed properties study and sampled each at two sampling points (fig. 3.6 and tab. 3.1).

Short description of the inception horizons

H1 Inception horizon is a 40 to 60 cm thick, very blocky (stromatolitic?) limestone layer with a lot of cave gypsum deposits.

H2 Inception horizon is some centimetres thick marly horizon.

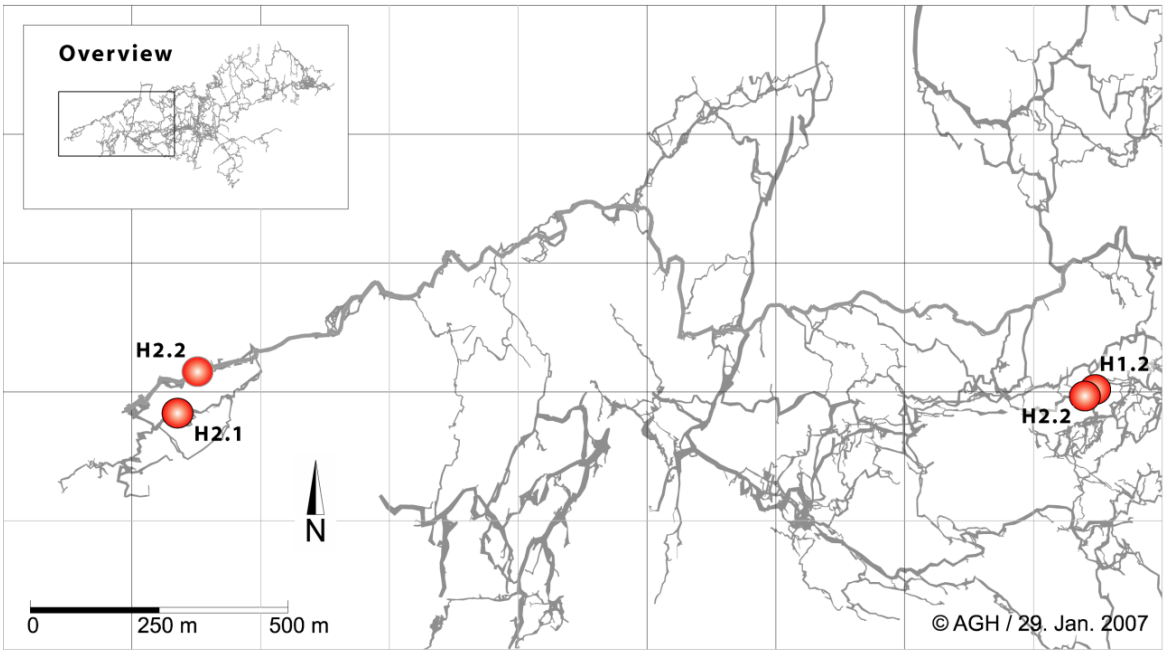

Fig. 3.6: Plan view of the front part of Hölloch. The red circles label the four sampling points.

3.2.3 Nidlenloch

The Nidlenloch (length: 7.5 km, depth: 420 m; SO, CH) is formed in the Sequanian (Malm) Limestone on the northern flank of the Weissenstein fold. The passages follow either the dip of the bedding planes toward the north, or the east-west strike of the beds. Towards the middle of the cave is a horizontal network of partially labyrinthian galleries. Other parts of the cave also have typical phreatic passage networks. The 3D analysis of the cave conduits geometry revealed the existence of four inception horizons, from which we selected three for detailed properties study (fig. 3.7 and tab. 3.1) (see also appendix 1).

Short description of the inception horizons

N1 Inception horizon is a 5 cm thick, very blocky limestone layer with a lot of cave gypsum deposits.

N2 Inception horizon is a 2 to 3 cm thick marly limestone.

N3 Inception horizon is a 40 thick, very blocky limestone with a bedding plane fracture

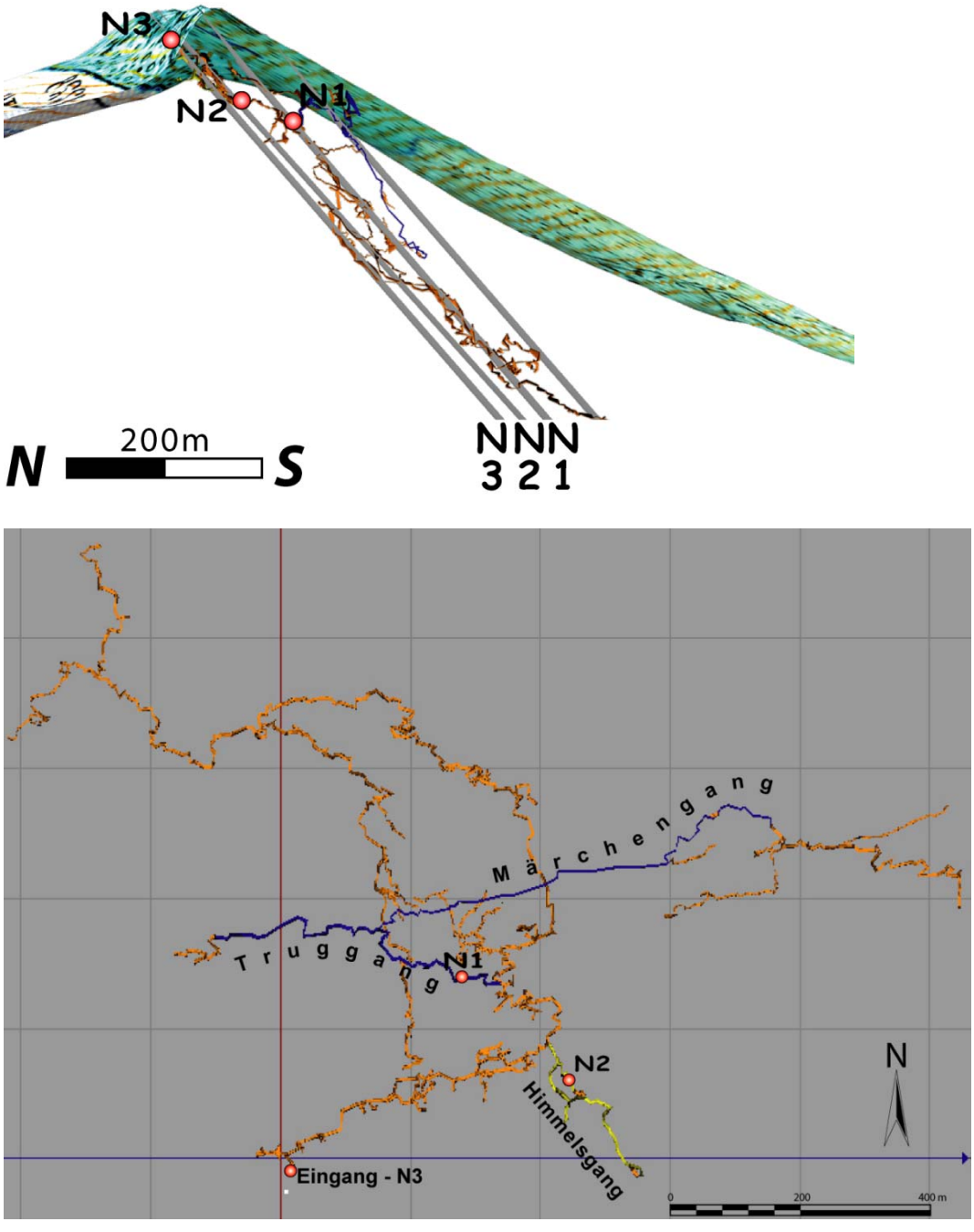

Fig. 3.7: Plan and 3D view of the Nidlenloch. The red circles label the three sampling points.

3.2.4 Réseau de Covatannaz

The Réseau de Covatannaz (length: 4.5 km, depth: 110 m; VD, CH) is formed in the Sequanian (Malm) Limestone. Large portions of the passages follow the subhorizontal bedding planes. The 3D analysis of the cave passages revealed that they are 2 inception horizons of regional importance (chapter 2.3 and appendix 1). Both inception horizons were sampled (fig. 3.8 and tab. 3.8).

Short description of the inception horizons

C1 Inception horizon is a 5 to 10 cm thick layer with a network of anastomoses.

C2 Inception horizon is a 2 to 3 cm thick marly limestone.

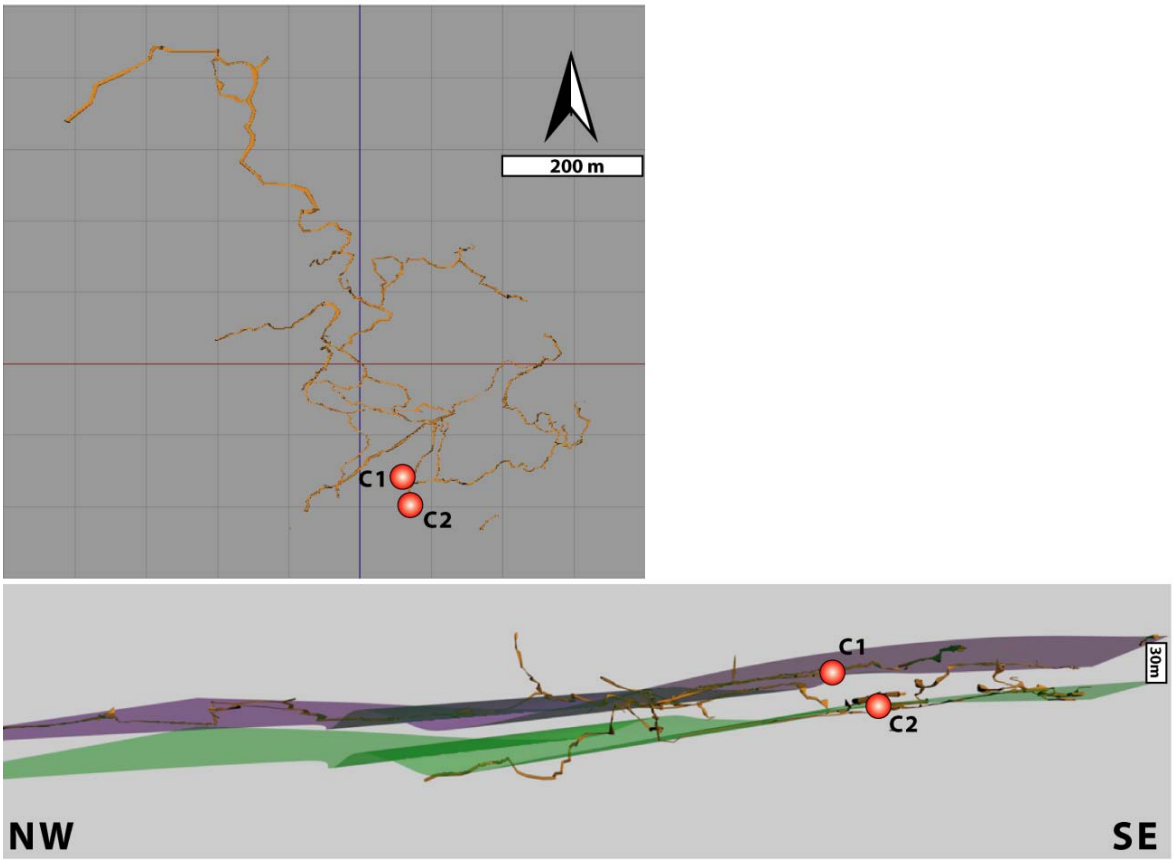

Fig. 3.8: Plan and 3D view with inception horizons of the Réseau de Covatannaz. The red circles label the three sampling points.

3.2.5 Réseau des Grottes aux Fées

The Rèseau des Grottes aux Fèes (length: 13 km, depth: 227 m, still in exploration - status winter 2009; VD, CH) is formed in the Sequanian (Malm) Limestone. Large portions of the passages follow the subhorizontal bedding planes. The cave system can be subdivided by exploration stages into “Ancienne Grande Grotte”, “Novelle Grande Grotte” and “Petite Grotte”. The 3D analysis of cave passages revealed that the cave development was guided at a regional scale by three inception horizons (chapter 2.3 and appendix 1). We sampled all three inception horizons (fig. 3.9 and tab. 3.1).

Short description of the inception horizons

F1 Inception horizon is a 40 to 50 cm thick, very distinct and blocky limestone layer.
F2 Inception horizon is an around 5 cm thick limestone layer with a distinct network of anastomoses.
F3 Inception horizon is a 3 to 5 cm thick marly limestone layer.

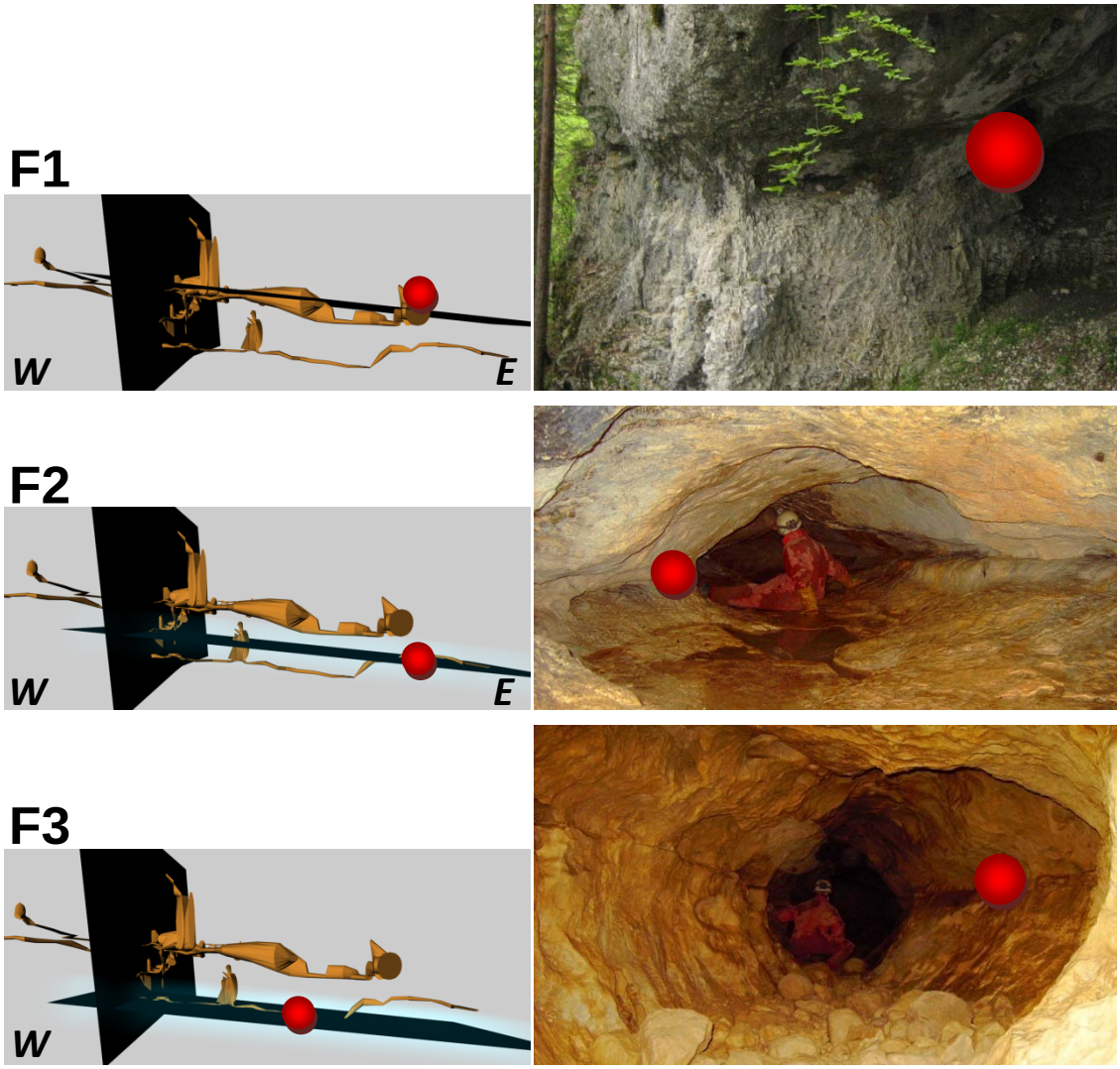

Fig. 3.9: 3D view and photos of the sampling points of the front part of the Réseau des Grottes aux Fées. The red circles label the sampling points.

3.2.6 O91 – Gamsalp

The cave O91-Gamsalp (length: 220 m, depth: 120 m, still in exploration - status fall 2008; SG, CH) is a small cave formed in the Schrattenkalk formation (Stünzi, 2006, 2008). The actual known cave can be subdivided into two parts: a series of subvertical, vadose shafts; at around -40 m below the entrance a subhorizontal, bedding plane guided meander, which is truncated by the shafts (fig. 3.10). We sampled this distinct horizon guiding the meander.

Short description of the inception horizons

G1 Inception horizon is a 5 to 10 cm thick very marly limestone layer.

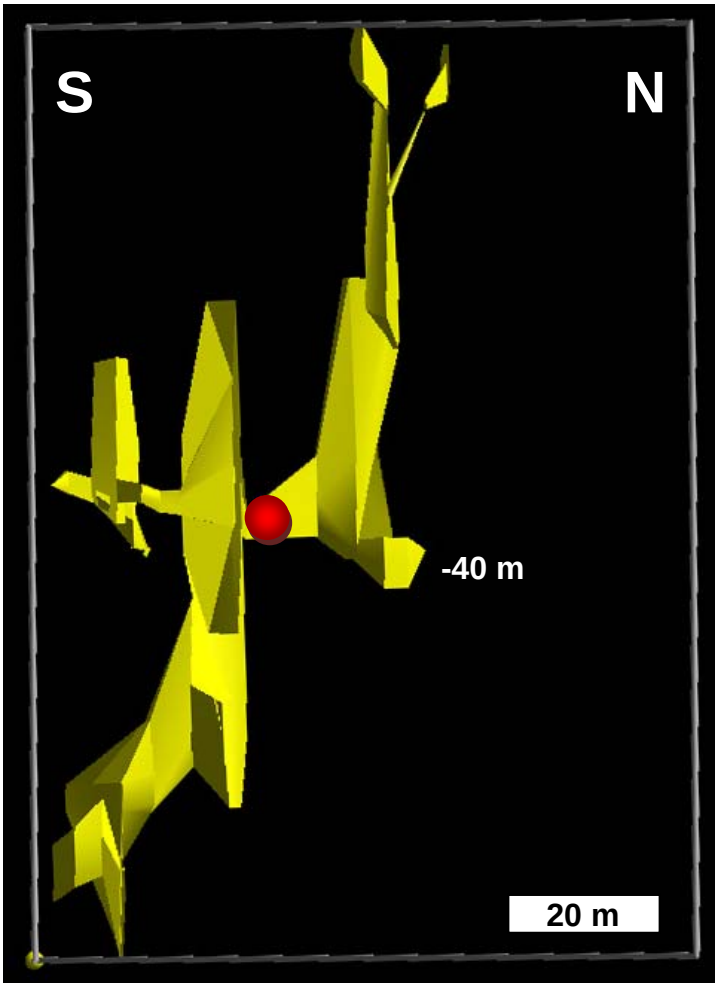

Fig. 3.10: 3D view of the O91-Gamsalp cave. The red circles label the three sampling points.

Name of Incetion Horizon	*Code of the Inception Horizon*	*Type of Inception Horizon*	*Number of Sampling points*	*Number of Rock Samples [total]*	*Number of Gypsum & Pyrite Samples*	*Rock Formation*	*Sample Number*
Réseau de Covatannaz							
Supérieur	**C1**	**1**	**1**	**3**		**Sequanian**	2-04,05,06
Inférieur	**C2**	**2**	**1**	**3**			2-01,02,03
Nidlenloch							
Guanogang	**N1**	**1**	**1**	**3**		**Sequanian**	4-04,05,06
Truggang	**N2**	**1**	**1**	**3**	**3**		4-09,10,11,12
Eingang	**N3**	**3**	**1**	**4**			4-01,02,03
Réseau des Grottes aux Fées							
Ancien	**F1**	**1**	**1**	**3**		**Sequanian**	3-01,02,03
Petite supérieur	***F2***	***1***	***1***	***4***			3-04,05,06,07
Petite inférieur	***F3***	***2***	***1***	***3***			3-08,09,10
Hölloch							
Wasserfalldom	**H1**	**1**	**2**	**18**	**2**	**Schrattenkalk**	5-16,17,18,19 5-20,21,22,23
Schauhöhle	**H2**	**2**	**2**	**12**			5-01,02,03,04,05 5-06,07,08,09
Sibenhengste							
Salamanderschacht	**S1**	**2**	**2**	**18**		**Schrattenkalk**	1-67,68,69,70 (Salamander) 1-78,79,80 (F5.1)
F5.3	**S2**	**1**	**5**	**22**			1-01,02,03 (F5.3) 1-05,04,07,06 (F6.1) 1-74,75,76(F3.3) 1-71,72,73(Karrenfeld) 1-33,34,38,35
Eingang D7.1	**S3**	**1**	**2**	**8**			1-09,10,08,28,11 1-39,40
2te Schichtfuge	**S4**	**2**	**1**	**4**			1-58,59,56,57,60
C4.1	**S5**	**1**	**4**	**24**			1-81,82,83 1-84,85,86,87 1-88,89,90,91 1-92,93,94,95
Balcon	**S6**	**1**	**2**	**10**			1-49,50,52,51 1-22,23,24,25,26,27 (Silex)
Arches	**S7**	**1**	**1**	**4**			1-61,62,63,64
Salle Ami, B1.2	**S8**	**1**	**3**	**14**	**9**		1-53,54,55 1-21,19,20 1-42,45,41,44,43,46,48,47
Gamsalp							
O91	**G1**	**2**	**1**	**3**		**Schrattenkalk**	9-01,02,03,04

Only Gypsum and/or Pyrite Samples		
Lachenstockhöhle (Lachenstock, SZ, CH)	**3**	***Schrattenkalk***
Sukiloch (Bödmeren, SZ, CH)	**4**	***Seewerkalk***
Saint-Marcel Cave System (Ardèche, F)	**2**	***Urgonien***
Noël Cave System (Ardèche, F)	**2**	***Urgonien***
Dachstein-Mammuthöhle (Dachstein, A)	**3**	***Dachsteinkalk***
Mammoth-Cave area (KY, USA)	**6**	***Ste. Genevieve***

Tab. 3.1: Compilation of the sampled inception horizons.

3.3 Field characterisation of Inception Horizons

Before taking samples and looking at the lithologic characteristics of inception horizons, we started with field observations of horizons identified from the 3D analysis of caves systems.

Field observations were used not only to verify the existence of the inception horizons supposed by the statistical analysis but also to provide first indications on why a given stratigraphical horizons became an inception horizon.

Whereas in chapter 2.4 the speleomorphologic features associated with inception horizon were described aimed this chapter to describe inception horizons by assessing where the cave inception took place, the thickness of the horizons, the relation of the inception horizons with fracture occurrence, macroscopic pyrite and cave gypsum occurrence. Unfortunately, the field conditions (e.g. clay smudgy cave walls, flow stone, inception horizon at the ceiling of the conduit) did rarely allow detailed descriptions of sediment structures.

3.3.1 Field evidence of different types of inception horizons

Field observations on cave passages that developed along inception horizons lead us to remark that three kinds of inception horizons can be distinguished (fig. 3.11):

Type 1 - Inception horizons where the cave inception took place **within the inception horizon**;

Type 2 - Inception horizons where the cave inception took place at the **contact with the inception horizon**;

Type 3 - Inception horizons where the cave inception took place **along bedding plane fractures** (interbedded slides).

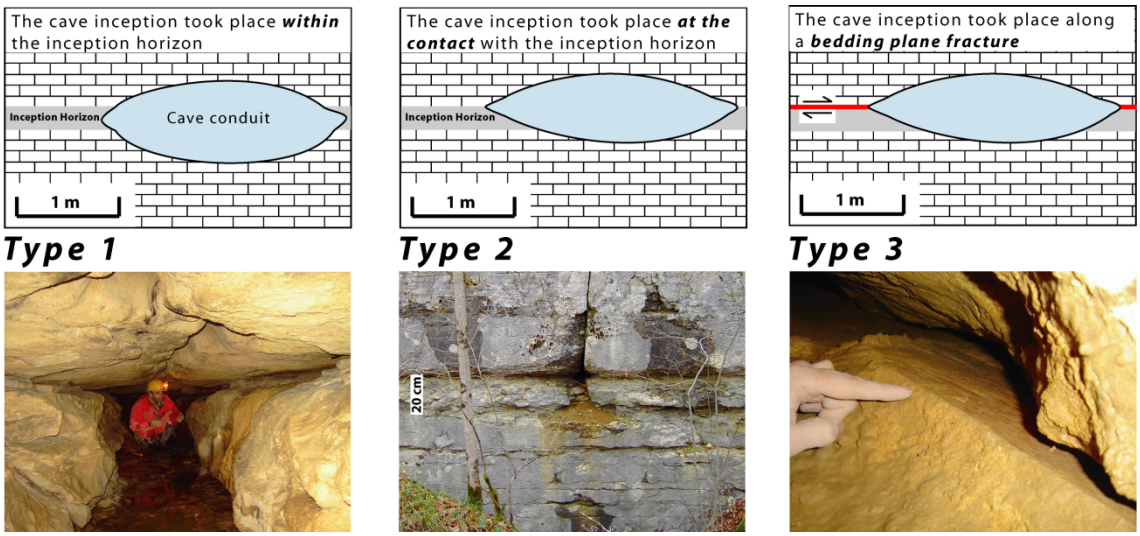

Fig. 3.11: Three kinds of inception horizons can be distinguished: Cave inception may take place within the inception horizon; at the contact with the inception horizon or along bedding plane fractures. For each type, the relationship between the conduit position and the inception horizon is sketched in the upper frame. The lower pictures provide examples from the field.

The distinction between type 1 and type 2 was only possible with the localisation of the squeezing out of the elliptic phreatic cave profile or with the help of anastomoses (a network of branching, intersecting, and rejoining channels in a two dimensional system; Slabe, 1995 – see also chapter 2.4.2). That is, if anastomoses developed along the contact or within a horizon. In cases where we had no clear field evidence that inception horizons took place along the contact, we assumed that the inception took place within the inception horizon.

Conceptually, it is quite easy to recognize inception horizons of type 3; a bedding plane fracture with evidence of slippage (striation) and/or an offset of the conduit cross section (fig: 2.20 and 3.12). However, one of the mayor problems is to distinguish a “bedding plane fracture” from a “dissolution induced fracture”.

A bedding plane fracture is initiated along sedimentary discontinuities (i.e. contrast in mechanical properties; Pollard and Aydin, 1988) (figure 3.12-above); whereas a dissolution induced fracture is initiated along dissolution voids on an inception horizon (figure 3.12-below). Therefore, the fundamental question is to solve: Did the inception of the horizon occur because of a pre--existing bedding plane fracture or was the fracture initiated by the occurrence of dissolution voids along an inception horizon (type 1 or 2)?

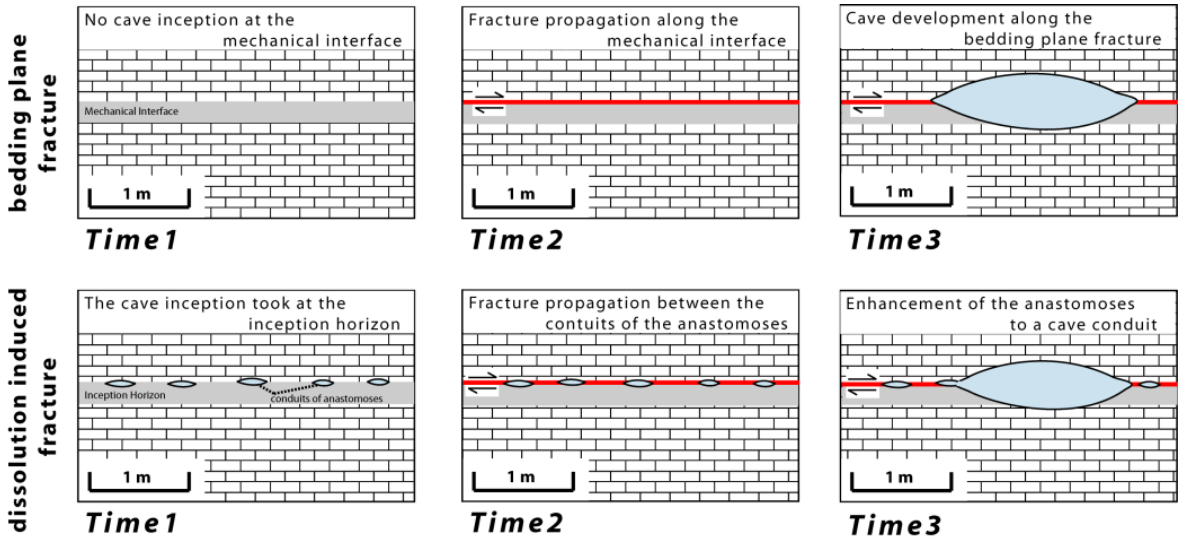

Fig. 3.12: Two different ways of the interaction between bedding plane fractures and cave development. Above: Bedding plane fracture occurs along a mechanical interface and induces the karstification along them. Below: Karstification begins without the occurrences of fractures at the inception horizon; only later a fracture propagates through the karst conduits.

Along various inception horizons we could find evidence of “post cave development phase” movement (i.e. neo-tectonic movement on the inception horizon), like for example broken and shifted dripstones or shifted conduit section (e.g. Filipponi and Jeannin, 2006; Filipponi and Dickert, 2007; Filipponi et al., 2008). The same observations have also been reported for example for Škocjanske Jama (Knez, 1998) or Postojnska Jama (Čar and Šebela, 1998). Nevertheless, these observations do not allow distinguish between bedding plane fracture and dissolution induced fracture, that is, if the fracture already existed before karstification. One indication for bedding plane fracture is the occurrence of cataclasite (fig. 3.13; mechanical fracturing, crushing and rotation of rock fragments induced by tectonic deformation; Micarelli et al., 2006) within the inception horizon (i.e. mechanical interface).

Clear distinction between bedding plane fracture and dissolution induced fracture will be the first step to better understand the speleogenesis along this type of inception horizons. This distinction would allow to reclassify the horizon as inception horizon to type 1 or 2, or in case of a “true” inception horizons of type 3 (bedding plane fracture) the mechanical properties of the horizon can be investigated in more details.

However, already a slippage of just a few millimetres, striation, brecciation and surface irregularities enhance openings along the sliding plane and will cause a significant increase in permeability, and therefore, concentrate the flow and karstification along them.

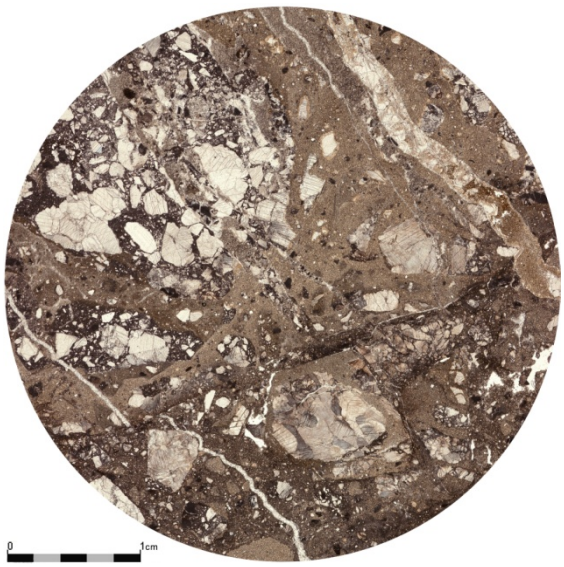

Fig. 3.13: Thin section of an inception horizon of type 3. The occurrence of cataclasite is a clear indication that the bedding plane fracture occurred before the karstification of the horizon.

Of the 18 inspected inception horizons of six cave systems, we observed 12 inception horizons of type 1 as well as 6 inception horizons of type 2 (tab. 3.1.). Attention should be paid that this distribution is by far not representative and depends strongly on the selected cave systems. For further field study as well as sampling we worked only on 18 inception horizons of type 1 and 2. Inception horizons of type 3 were excluded of the sampling.

3.3.2 Thickness of inception horizons

The thickness of the inception horizons vary between some centimetres to several decimetres (fig. 3.14). The data suggest distinguishing inception horizons into a group with a thickness of less than 20 cm and a second of thicker inception horizons. It is to notice that neither inception horizons of type 1 nor type 2 seems to be related with the thickness of the horizon.

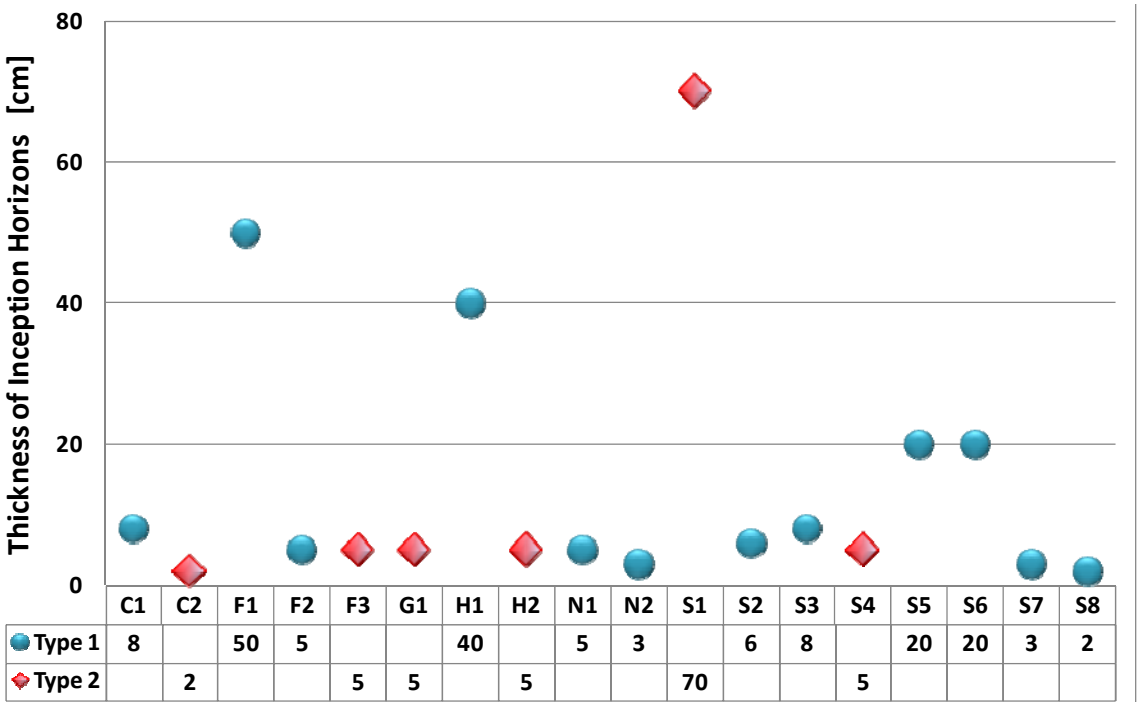

	C1	C2	F1	F2	F3	G1	H1	H2	N1	N2	S1	S2	S3	S4	S5	S6	S7	S8
Type 1	8		50	5			40		5	3		6	8		20	20	3	2
Type 2		2			5	5		5			70			5				

Fig. 3.14: Diagram of the thickness of the inception horizons. The inception horizons are some centimetres to decimetres thick, whereas no relationship between thickness and type of inception horizon is recognisable.

3.3.3 Intersection between fractures and inception horizons

The occurrence of inception horizons does not mean that fractures have no role in cave inception. In most cases fractures control the conduit orientation at a local scale and along stratigraphical inception horizons according to the regional hydraulic gradient. In other words, most phreatic conduits are developed along the intersection between inception horizons and fractures, which are the most parallel to the hydraulic gradient (e.g. Lowe, 1992; Lauritzen and Lundberg, 2000; Filipponi et al. 2008 – see also chapter 2.2.7).

We distinguished between four types of intersections between fractures and inception horizons (fig. 3.15):

- fracture ends at the inception horizon;
- fracture goes through the inception horizon;
- fracture occurs within the inception horizon;
- fracture propagates at the contact inception horizon with the surrounding rock mass (what would be an inception horizon type 3).

In most cases, multiple types of intersections could be observed along an inception horizon. Only a detailed statistical analysis/approach would allow assessing correctly the different occurrences and determine the mechanical properties of the rocks (e.g. Underwood et al., 2003; Cooke et al., 2006). But we contented us with a qualitative assessment of the most obvious intersection type, since the observation conditions in the caves were most of the time difficult. This is due to the fact, that inception horizon often occur at the ceiling of the conduit and therefore, only a limited observation surface was available and/or the wall parts were covered by cave sediments or flowstone.

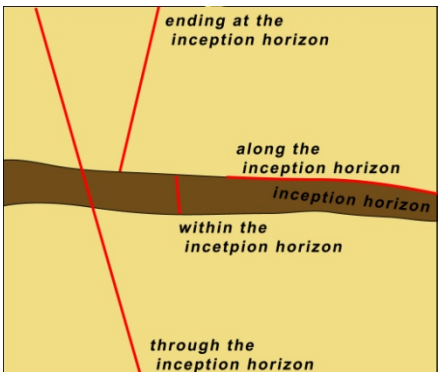

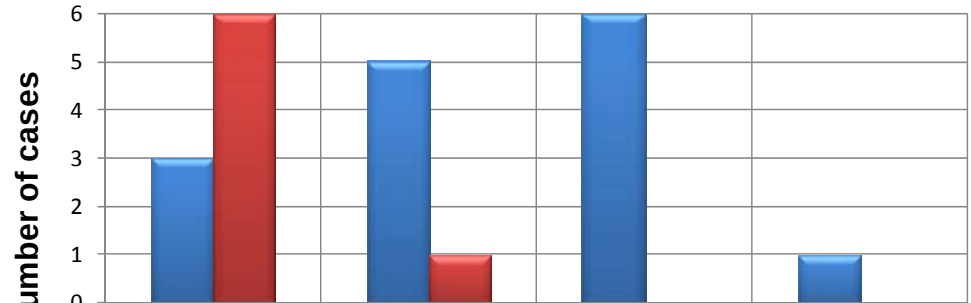

	ending at the inception horizon	through the inception horizon	within the inception horizon	along the inception horizon
Type 1	3	5	6	1
Type 2	6	1	0	0

Fig. 3.15: Relationship between inception horizon type and fracture intersection. Fractures extend more often through or occur within inception horizons of type 1 whereas they end more often at inception horizons of type 2.

Observations along inception horizons of type 1 revealed that fractures ends rarely at this horizons but if the horizons are less thick than around 15 centimetres, fractures go most of the time through the horizon. Contrary, if the horizons are thicker, we can often observe fracture occurrences within the inception horizon (fig. 3.16). This threshold thickness of around 15 centimetres was also observed by others authors (e.g. Narr and Suppe, 1991).

Bedding planes and fractures do not occur at the same time during the history of a rock mass. Whereas the inception of the bedding planes can already start just after the lithification, the occurrence of fractures is a later phenomenon (maybe occurring at the end of cave inception phase – see chapter 3.6 and chapter 6.1). Bedding planes with the largest permeability (inception horizons) just before their intersection by fractures are supposed to give intersections with the highest permeability too, but with values orders of magnitude higher than without fractures (e.g. Kiraly, 1969). What concentrates the flow once more and therefore, also the karstification at the intersection.

Our observations suggest that fractures are often ending on inception horizons of type 2. This was also observed in other studies (e.g. Underwood et al., 2003; Cooke et al., 2006) concluding that shale-rich units within a carbonate sequence often act as “mechanical interfaces” (stratigraphical horizon along which many fractures abut).

There are two predominant mechanisms of fracture termination: ductile deformation of the mechanical interface to resist fracturing; propagation of the “vertical” fracture along the contact (e.g. Pollard and Segall, 1987; Helgeson and Aydin, 1991; Rijken and Cooke, 2001; Cooke et al., 2006). The observations on inception horizons of type 2 correspond more to a mechanical behaviour of type: fracture propagation along the contact; albeit it was not possible to observe this small contact fractures any more (they were destroyed by the development of the cave passages – fig. 6.4-above). This contact fractures would explain the increased flow and therefore, the karstification along the inception horizon fracture contact. If this

would be the main reason why inception horizon of type 2 exists, would this apply for further investigations on the mechanical properties of the inception horizons as well as surrounding rock mass to better characterise the properties of them.

The determination of the most obvious intersection type was done in a very rough way. Nevertheless, we believe that it would be interesting to investigate this topic with a more quantitative approach, for example by image processing of scanned/photographed rock faces (e.g. Underwood et al., 2003; Pötsch et al., 2007).

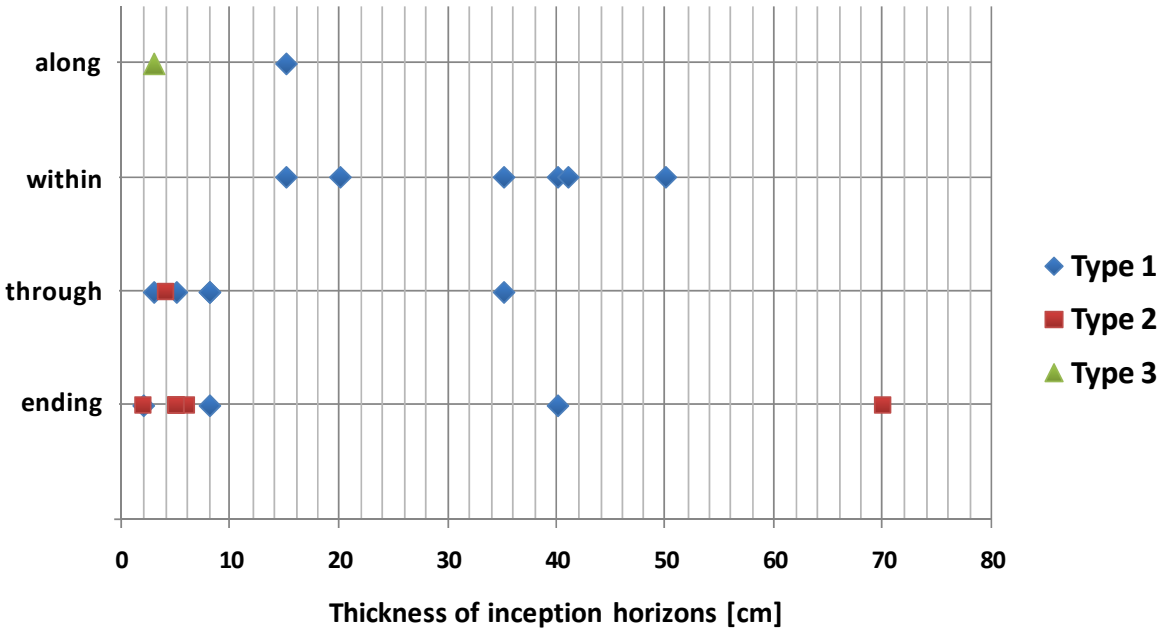

Fig. 3.16: Relationship between inception horizon thickness and fracture intersection. Inception horizons of type 1 that are thicker than around 15 cm often have "inter-horizon" fractures whereas thinner horizons are snapped through by the fractures.

3.3.4 Horizons with macroscopic pyrite enrichments

Several inception horizons have already field evidence of major pyrite deposits within the inception horizons, like for example macroscopic pyrite crystals or weathered pyrite with related dissolution phenomena (fig. 3.17) (for a quantitative discussion about the role of pyrite content of the inception horizons see chapter 3.4.3.2).

Fig. 3.17: Outcrop of a pyrite rich inception horizon (Court, Switzerland). Left above: locally some not weathered pyrite crystals can be found exposed; Left below: the weathering of the pyrite and the associated production of acid solution produced a very porous looking horizon; Right below: within the horizon a cave conduits cropped out, unfortunately the conduit is filled up with clastic sediments and can not be explored to verify if the conduit follows also in distance the inception horizon.

3.3.5 The occurrence and origin of cave gypsum

Within cave conduits that developed along inception horizons, we could frequently observe the occurrence of cave gypsum (tab. 3.2; chapter 2.4.7). Therefore, the question was: can cave gypsum deposits be used as indicator for early speleogenetical processes along inception horizons?

We can distinguish four different types of cave gypsum by the provenience of the sulphur and relate them to different speleogenetical processes:

- **Re-precipitation of sedimentary gypsum** that has been previously dissolved in the rock mass. The speleogenetical indication of this kind of cave gypsum is that the primary gypsum is easy soluble relatively to the surrounding rock mass and causes an elevated ratio of secondary porosity that would favour the evolution of the karstification.
- Reaction between the host limestone and **sulphates** (including sulphuric acid) **derived from oxidized sulphide minerals** (e.g. pyrite). The weathering of sulphide minerals can produce acidic solutions, which can at least locally increase the dissolution capacity and cause an elevated ratio of secondary porosity.

- Reaction between the host limestone and **sulphates** (including sulphuric acid) **derived from hydrothermal sources**. This kind of cave gypsum indicates that speleogenesis took place under hypogenic conditions with a minor role for the karstification of meteoric percolation water.
- Reaction between the host limestone and **sulphates derived from decomposition of organic material in the soil**, and transported by seepage water into the cave (e.g. Choi and Woo, 2005). However, the dissolution capacity of the strong acid is depleted after a relative short flow path (order of some metres), therefore, the influence to the karstification of the whole rock mass is very restricted.

The cave gypsum of the various provenances have characteristic sulphur isotope compositions ($\delta^{34}S$)[1], which allow to distinct them. The isotope compositions are affected by fractionation during biochechemical reactions. The isotope enrichment factor ε[2] express the relation of the isotope composition of the source material to his instantaneous reaction product.

The $\delta^{34}S$ isotope composition of **sedimentary gypsum** is more or less equal to the ratio of the sea water at the time of sedimentation (e.g. Clark and Fritz, 1997; Strauss, 1997). The isotope composition of the sea water is subject to significant fluctuations during the earth history, whereas the $\delta^{34}S$ is most of the time between +10 and +35 ‰ (e.g. Strauss, 1997).

No isotope fractionation occurs during the primary gypsum-to-anhydrite-to-secondary-gypsum transformation (Forte et al., 2005). Also the dissolution and the (re-)precipitation of the gypsum seem to have no or only little influence on the isotope composition of sulphur (peeling principle).

Therefore, the expected sulphur isotope composition of this type of cave gypsum will be similar to those of seawater at the time of deposition of the sedimentary gypsum.

The sulphur isotope value of **pyrite** is primarily determined by the sulphur diffusion during diagenesis into the sediment and by subsequent bacterial reduction to pyrite (Hartmann and Nielsen, 1968). As cause of the preferred reduction of the ^{32}S, pyrite becomes enriched in ^{32}S. Depending on what kind of bacteria are involved, different enrichment factors result (Shen et al., 2001). Is usually not possible to know what kind of bacteria was involved. That is why the factors include a large range (ε -15 to -31 ‰, Buschendorf et. al., 1963; average of ε -40 ‰, Strauss, 1997). Correspondingly, a wide range of the sulphur composition of pyrite is expected (Thode at al., 1952; Buschendorf, 1962).

The sulphur isotope composition of this pyrite-cave-gypsum reflects the source of sulphur and any fractionation effects related to the mechanisms of the oxidation of the sulphide. Unfortunately, there are

---

[1] $$\delta^{34}S(‰) = \left(\frac{R_{sample}}{R_{CDT}} - 1\right) * 1000 = \left(\frac{\frac{^{34}S_{sample}}{^{32}S_{sample}}}{\frac{^{34}S_{CDT}}{^{32}S_{CDT}}} - 1 \right) * 1000$$

Sulphur isotope composition ($\delta^{34}S$). **CDT** *refers to the $^{34}S/^{32}S$-ratio of the standard troilite, an iron monosulfide from the Canyon Diablo Meteroite. $^{34}S_{CDT}/^{32}S_{CDT}$=22.210 (Macnamara and Thode, 1950).*

[2] $$\varepsilon(‰) \approx \left(\frac{R_{product}}{R_{source}} - 1\right) * 1000$$

Definition of the enrichment factor ε

several different conditions, under which the oxidation takes place (pH, temperature, type of bacteria involved). However generally the fractionation is small (around ε -5 ‰; Toran and Hapris, 1989), especially when the entire sulphur source is oxidised, than ε is around 0 ‰ (peeling principle). As next fractionation step follows the reaction of the sulphuric acid with limestone and the by-product of gypsum results as an isotope enrichment factor ε of 0 to -14 ‰ (Hose at al., 2000; Machel, 1992).

Therefore, we can assume that the pyrite-cave-gypsum has an isotope enrichment ε of around 0 to 14 ‰ compared to the pyrite samples, respectively ε of around -40 to -55 ‰ compared to the sedimentary gypsum.

The sulphur isotope composition $\delta^{34}S$ of **sulphates in hydrothermal sources (H_2S)** are in the range of around + 5 ‰ (Taran et al., 1998) and -12 ‰ (Hose at al., 2000). The reaction of the sulphuric acid with limestone and the by-product of gypsum results as an isotope enrichment factor ε of 0 to -14 ‰ (e.g. Hose at al., 2000; Machel, 1992). *Therefore, we can estimate an expected value of the sulphur isotope composition of this type of cave gypsum in the range of $\delta^{34}S$ +5 to around -30 ‰ (e.g. Hill, 2000).*

There are several important sulphur transformation processes occurring in the **pedosphere**. Sulphur in soils exists in organic and inorganic binding forms. Inorganic sulphur may occur in soil solution or as sulphate minerals (e.g. jurbanite, basaluminite). Their isotopic composition is similar to that of sulphate in rainwater (Mayer et al., 1995; range of today atmospheric $\delta^{34}S$ -3 to +9 ‰). Nevertheless, more than 80 % of the total sulphur in soils occurs organically bound. The decomposition of the carbon-bounded sulphur into sulphate can follow different reaction pathway (e.g. Freny and Stevenson, 1966). However, the $\delta^{34}S$ of the pedosphere-sulphurs remains essentially unchanged even if sulphate undergoes this immobilisation-mineralization cycle, since sulphur isotope fraction is small during these transformation processes (around ε +3 ‰; Rees, 1973).
A large isotope fractionation occurs by the reduction of the sulphurs into H_2S in the order of ε -15 to -25 ‰ (e.g. Robertson and Schiff, 1994; Rees, 1973).
As a last step, the reaction of the sulphuric acid with limestone and the by-product of gypsum results as an isotope enrichment factor ε: of 0 to -14 ‰ (Hose at al., 2000; Machel, 1992).
All this means a large range of the expected value for the range of pedosphere-sulphuric gypsum of $\delta^{34}S$ -10 to -50 ‰. The variation of isotope composition of nearby collected gypsum samples will be relevant, because of different reaction ways.

Results of the $\delta^{34}S$ measurements

To evaluate if the cave gypsum deposits within our inception horizons guided conduits can be used as indicator for early speleogenetical processes, the origin the gypsum was determined. Therefore, we measured the isotope composition ($\delta^{34}S$) of cave gypsum samples and pyrite crystals from the inception horizon (if adequate pyrite samples were available) (tab. 3.2). The analysis was not only done on samples from caves/sampling points described in chapter 3.2.1 but also from other caves with strong evidence of inception horizons (some of them have also been included in the statistical identification of the inception horizons in chapter 2).

sampling location	rock formation	rock age	type of sample	δ34S value (per mil CDT) average	min	max	number of samples	d34S value for **sedimentary gypsum** *(Strauss, 1997)*
Siebenhengste Cave System D7.1 - Gallery Francis (BE, CH)	Schrattenkalk	Cretaceous	cave gypsum	**-29.8**	-32.0	-26.3	8	+15 to +20 ‰
			pyrite	-23.0			1	
Hölloch Cave System Briefkasten (SZ, CH)	Schrattenkalk		cave gypsum	**-29.4**	-32.2	-26.5	2	
Lachenstock Cave System Durchschlupf (SZ, CH)	Schrattenkalk		cave gypsum	**-34.3**	-35.5	-33.1	2	
			pyrite	-34.6			1	
Bödmeren Sukiloch (SZ, CH)	Seewerkalk		cave gypsum	**-21.6**	-22.3	-20.8	2	
			pyrite	-19.0	-19.8	-18.2	2	
Ardèche (F)	Urgonien		cave gypsum Saint-Marcel Cave System	**-36.5**	-36.8	-36.2	2	
			cave gypsum Noël Cave System	**-34.1**	-34.5	-33.6	2	
Nidlenloch Cave System (SO, CH)	Sequanian	Jurassic	cave gypsum	**-34.7**	-36.0	-32.5	3	+10 to +15 ‰
Dachstein-Mammuthöhle (A)	Dachsteinkalk	Trias	cave gypsum	**-5.4**	-7.7	-3.6	3	+10 to +30 ‰
Mammoth-Cave area (KY, USA)	Ste. Genevieve	Carboniferous	cave gypsum	**6.5**	3.9	10.1	6	+15 to +20 ‰

Tab 3.2: Results of the $d^{34}S$ measurements on pyrite and cave gypsum samples. The results indicate that pyrite was the sulphur source for the cave gypsum.

Our interest is to evidence if the cave gypsum is re-precipitated from sedimentary gypsum or a by-product of the pyrite oxidation. A hydrothermal sulphur source can be excluded because the caves under investigation are of epigenic and not hypogenic origin (lack of typical hypogenic morphological features, such as the absence of fluvial cave sediments, the typical geometry of the cave conduit network or massy cave gypsum deposits (e.g. Bakalowicz et al., 1987; Hill, 1995; Palmer, 1991, 2002; Klimchouk, 2007). The pedospheric origin can also be neglected (some of the gypsum samples were collected more than 260 m below the surface, therefore, pedospheric sulphur source is rather improbable).

The isotope composition of all cave gypsum samples (tab. 3.2) can be considered as distinct from literature values for sedimentary gypsum of the same age of the rock formation within the cave developed (Strauss, 1997). In return they are very close to the isotope values of the pyrite samples (if measured). This let us conclude that the sampled gypsum comes from the oxidation of pyrite.

Furman et al. (1999) made some $\delta^{34}S$ measurements on sedimentary anhydrite, pyrite and cave gypsum of the Mammoth Cave area. They also concluded that cave gypsum came from pyrite oxidation, albeit the isotope compositions of their and our samples are inconsistent (maybe because of different $\delta^{34}S$ standards?). Furthermore, Palmer and Palmer (1995) observed that most of the major gypsum deposits in the Mammoth Cave are located on or just below major pyrite-rich beds.

In some cave passages, the walls are more or less complied lined with cave gypsum. This is often used as counter-argument for the “pyrite gypsum hypothesis” (fig. 3.18). But Palmer and Palmer (1995) showed with a rough estimation that for building a gypsum crust of 1 cm thickness in a passage of 2 m in diameter

by the oxidation of pyrite, it do not need more than a 1 meter thick zone around the passage (assuming a pyrite concentration of 0.1 %, all pyrite will weather and the sulphur precipitate as gypsum).

Fig. 3.18: Cave passage in the Grotte Saint-Marcel (F). The cave walls are covered with cave gypsum crystals (the red arrow indicates the inception horizon)

The results indicated that the sulphur of the cave gypsum samples from cave conduits guided by inception horizons comes from the oxidation of pyrite. This let us conclude that the karstification along this inception horizons has probably been favoured by the weathering of pyrite and the related production of acidic solutions, which locally increases the dissolution capacity. Such an additional acidic dissolution has a minimal effect on the context of the later passages, but its contribution to the porosity development into the inception horizons can be significant (chapter 3.6).

In chapter 3.4.3.2 we will show that inception horizons are characterised by an increased concentration of pyrite content compared to the surrounding rock mass and that in thin sections we could found associated with pyrite crystals the occurrence of dissolution seams.

Therefore, we can conclude that the occurrence of cave gypsum can be used as indicator for early speleogenetical processes along inception horizons.

3.3.6 The occurrence of stromatolites

Among different textural field observations (e.g. cross bedding or occurrence of fossils) we observed that some inception horizons are stromatolitic (layered accretionary structures formed in shallow water by the trapping, binding, and cementation of sedimentary grains by biofilms of microorganisms – Collinson and Thompson, 1982) (fig. 3.19). The observation that karstification is associated with stromatolitic horizons is frequent in literature (e.g. Goldstrand and Shevenell, 1997; Orndorff et al., 2001; Tipping et al., 2006). However, only a few authors give an explication for the relationship of stromatolite occurrences and speleogenesis, for example are proposed that throughout the stromatolitic limestone an increased concentration of dispersed pyrite could occur (e.g. Goldstrand and Shevenell, 1997).

Fig. 3.19: Example of a stromatolitic inception horizon (Lauiloch, Switzerland).

3.3.7 Conclusion of the field observations

Field observations were not only used to verify the existence of the inception horizons supposed by the statistical analysis but also to provide first indications on why a given stratigraphical horizons becomes an inception horizon.

The observations lead us to conclude that most of the inception horizons are some centimetres to decimetres thick and that three kinds of inception horizons can be distinguished:

Type 1: Inception horizons where the cave inception took place **within the inception horizon**;

Type 2: Inception horizons where the cave inception took place at the **contact with the inception horizon**;

Type 3: Inception horizons where the cave inception took place **along bedding plane fractures**.

We observed (like already other authors before) that phreatic cave conduits are often developed along the intersection between inception horizons and fractures. A detailed study revealed that fractures go in most of the cases through the inception horizons of type 1, if they are thinner than around 15 centimetres; contrary if the horizons are thicker, we often observed fracture occurrences within the inception horizon. The observations on inception horizons of type 2 suggest that fractures are often ending on them. However, it is to remember that bedding planes and fractures do not occur at the same time during the history of a rock mass. Whereas the inception of the bedding planes may begin just after the lithification, the occurrence of fractures is a later phenomenon. A detailed discussion of the speleogenetic importance of fractures will be presented in chapter 3.6.2 and chapter 6.

In cave conduits that developed along inception horizons we could frequently observe the occurrence of macroscopic pyrite crystals/nodules and/or cave gypsum. The results of sulphur isotope composition $\delta^{34}S$ of cave gypsum indicate that the gypsum-sulphur most probably comes from the oxidation of pyrite. This let us assume that the karstification along this particular bedding plane has been favoured by the weathering of pyrite and the related production of acidic solutions. This could at least locally increase the dissolution capacity and contributes to the porosity development in the inception horizons.

3.4 Laboratory characterisation of Inception Horizons

Laboratory investigation on the rock samples aims to characterize the inception horizons as well as the rock mass with regarding to the processes of karstification (fig. 3.1). Therefore, one main concern was to assess the deviation in properties between the inception horizons and the surrounding rock mass. Properties (most of them already mentioned in the literature) that seems to have an effect on one or more karstification processes were selected to be investigated with laboratory methods (tab. 3.3).

The workflow for the laboratory investigations was the following one: after the measurement of the permeability the micro cores were split into two halves; one halve to make thin sections and the other to make powder for calcimetry and XRD analysis. The analysis of the thin sections allowed us to assess the content and composition of the impurities as well as describe the texture of the rock samples (e.g. matrix content, grain size, sorting). Furthermore, the observations on the thin sections allow describing the karstification at microscopic scale (types and origin of the pores).

Following the results of the individual property analysis will be presented and discussed.

	Speleogenetical Aspects			
Investigated Property	Characteristics of the Flow Path	Dissolution Rate	Dissolution capacity of the seepage water	**Investigation Methode**
Primary Permeability	x			gas permeameter
Carbonate Contents				
Total Carbonate		x		automatic calcimeter
Calcite		x		
Dolomite	(x)	x		
Impurities				
Contents of Impurities		x		automatic calcimeter
Clay Minerals	x			XRD
Pyrite			x	XRD as well as qalitative estimation on thin section
Quartz	x			
Gypsum		x		
Texture				
Matrix Type		x		qualitative estimation on thin section
Matrix Contents	x	x		quantitative image processing on scaned thin section
Sparit Contents		x		quantitative image processing on scaned thin section
Type of Components		x		qualitative estimation on thin section
Grain Size	x	x		quantitative image processing on scaned thin section
Sorting of the Grains	x	x		qualitative estimation on thin section
Type of Pores	*for verification*			description of dissolution features on thin section

Tab. 3.3: Table showing the investigated lithological properties, the assumed speleogenetic processes and the used investigation method.

3.4.1 Primary Permeability and Type of Pores

Because of the positive feedback characteristics of karst development, we expect that the initial permeability of the rock or more precisely the permeability distribution within the rock mass, at early stage of cave genesis is a significant parameter (see also chapter 4). It is to expect that inception horizons have a different primary permeability than the surrounding rock mass. Higher permeability would favour the water to flow along this horizon; whereas horizons of l*ower permeability* would act as low permeability “screen” along (or just above) which water would flow preferentially (Lowe, 2000).

3.4.1.1 Primary Permeability

The permeability was measured with an automated gas permeameter (Porous Materials Incorporated, GP-262). The automated gas permeameter measures permeability of porous samples, such as rocks, ranging from 0.1 to 50 milliDarcys (1 mD ≈ 10^{-15} m^2 ≈ 10^{-8} $m/_s$) within an accuracy of 0.5 %.

Unfortunately, it was not possible to use the permeability measurements of all micro cores. Samples with clear secondary permeability voids were removed from the analysis. In some cases, it was possible to identify by a simple visual inspection that dissolution voids or micro fractures were present (fig. 3.20-left). In other cases, thin sections of the micro cores showed occurrences of micro fractures or dissolution voids (fig. 3.20-right). Sometimes it was simply not possible to collect an unbroken core.

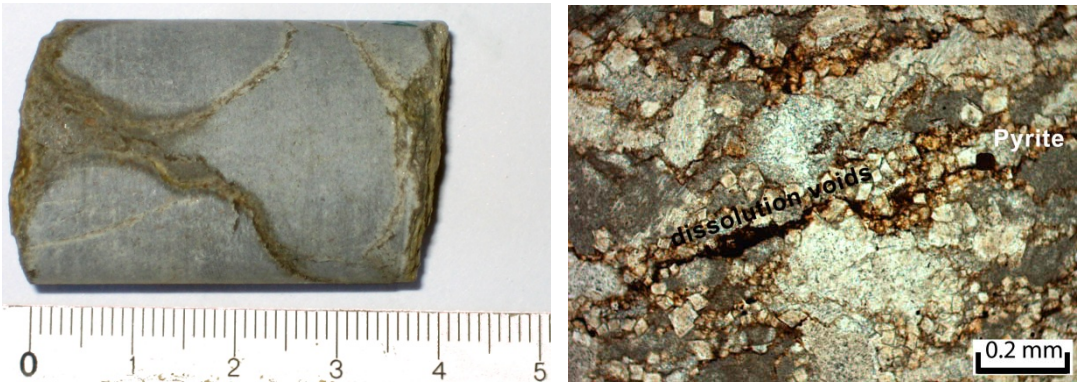

Fig. 3.20: Examples of micro cores that have not been used for permeability measurements because of secondary permeability. The left example shows already by visual inspection evidence of secondary dissolution (karstification). The right example is a thin section view of an inception horizon with microscopic dissolution voids.

The measured primary permeability-values are quite low, generally below 1 mD (tab. 3.3). Permeability-values of the surrounding rock masses have an average of 0.16 mD with a standard deviation of 0.15 mD. Permeability-values where karstification took place within the inception horizon (type 1) have an average of 0.17 mD with a standard deviation of 0.05 mD. In most cases where cave inception took place at the contact with an inception horizon (type 2) the permeability-values of the inception horizons were below the lowest measurement limit of 0.1 mD.

The measured matrix permeability-values are about one order of magnitude lower than published values for other rock masses of the same age (e.g. Edwards Aquifer, Texas, Cretaceous, ~1 mD, measured on core samples - Mace and Hovorka, 2000). However, they are higher than the matrix permeability of other important cave areas such as for examples the Mammoth Cave area (Kentucky, ~0.001 mD, measured on core samples - Worthington et al. 2000).

The primary permeability of a rock mass strongly depends on the diagenesis as well as orogenesis of the rock mass (Wright, 2002). Florea and Vacher (2006) could show that eogenetical carbonates (sediments that have not been buried before exposure; Choquette and Pray, 1970) have a primary permeability higher than 10^{-14} m^2 (~10 mD), whereas telogenetic (exposure and erosion after having been buried; Choquette and Pray, 1970) are usually less permeable. For example, permeability measurements (not sampled within the inception horizon context) of eogenetical limestone formation of the Upper Floridan Aquifer, give a matrix permeability in the order of 10^{-13} m^2 (~100 mD), whereas some strata are more permeable (up to 10^{-11} m^2 (~10^4 mD); Budd and Vacher, 2004). The measurements were done with minipermeameter on cores of 5 cm in diameter (Budd and Vacher, 2004) and are comparable with gas permeameter measurements (Goggin, 1993; Boebe, 1994). Unfortunately, the authors do not describe the rocks and the occurrence of dissolution voids, i.e. one cannot be sure that measured values correspond to the primary (not karstified) permeability of the strata.

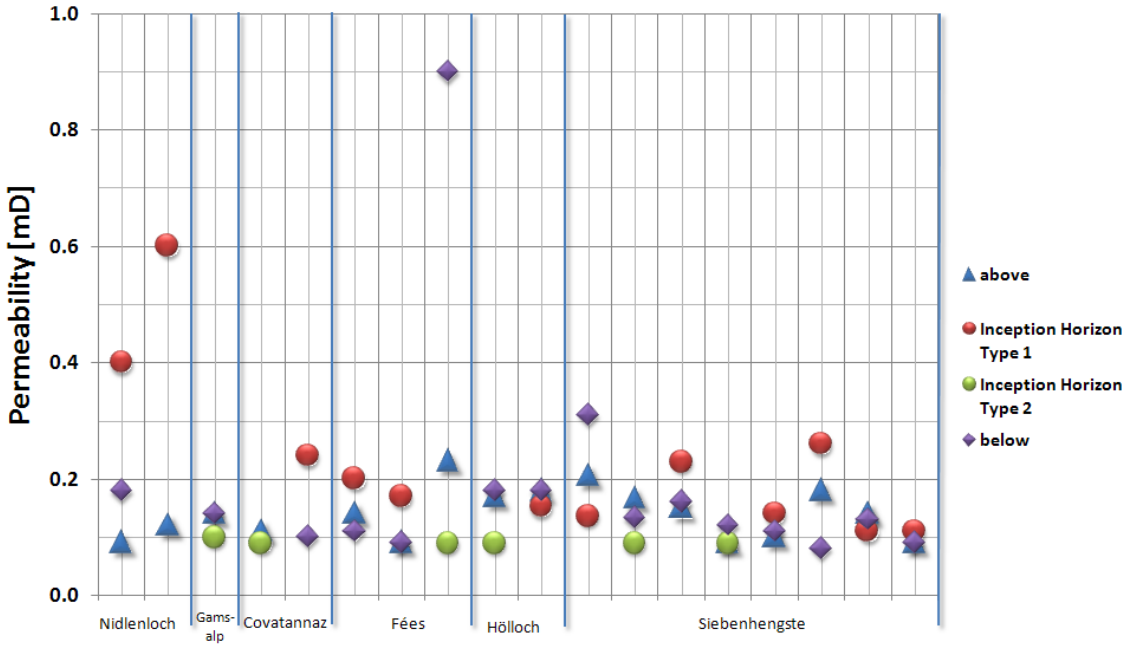

Cave	Cave inception took place	Permeability [mD] above	Permeability [mD] *inception horizon*	Permeability [mD] below
Nidlenloch (SO, Switzerland)	**within**	<0.1	*0.40*	0.18
	within	0.12	*0.60*	no data
Gamsalp (SG, Switzerland)	**at contact**	0.14	*0.10*	0.14
Réseau de Covatannaz (VD, Switzerland)	**at contact**	0.11	*<0.1*	no data
	within	no data	*0.24*	0.10
Réseau des Grottes aux Fées (VD, Switzerland)	**within**	0.14	*0.20*	0.11
	within	<0.1	*0.17*	<0.1
	at contact	0.23	*<0.1*	0.90
Hölloch (SZ, Switzerland)	**at contact**	0.17	*<0.1*	0.18
	within	0.18	*0.15*	0.18
Siebenhengste Cave System (BE, Switzerland)	**within**	0.21	*0.14*	0.31
	at contact	0.17	*<0.1*	0.13
	within	0.15	*0.23*	0.16
	at contact	0.09	*<0.1*	0.12
	within	0.10	*0.14*	0.11
	within	0.18	*0.26*	0.08
	within	0.14	*0.11*	0.13
	within	0.09	*0.11*	0.09

Fig. 3.21: Summary of the permeability measurements. The measured primary permeability-values are quite low, generally below 1 mD and a priori it is not possible to recognise a threshold values that distinguish incepted horizons from not incepted

It was not possible to recognize threshold values that distinguish incepted horizons from not incepted (fig. 3.21). We can suppose that the absolute value of the permeability has only a subordinated significance: It will be mainly the contrast between the properties of inception horizons and the surrounding rock mass which is relevant. For example an inception horizon is expected to develop because it is significantly more permeable than the surrounding rock mass and not because his permeability is higher than a given value.

Considering the contrast of the values (i.e. value of the inception horizon minus value of the surrounding rock mass): numbers above 0 mean that the inception horizon has a higher permeability than the

surrounding rock mass, and numbers below 0 mean that the permeability is lower. Results presented in figure 3.22 makes it possible to distinguish two groups of inception horizons: (1) horizons with a slightly higher permeability than the surrounding rock mass and (2) horizons with a slightly lower permeability. The more or less distinct linear trend in the plot indicates that the rocks above and below the inception horizons are similar and that only the favourable horizon has a different value. The permeability differences are in the order of a few tenth of mD.

A Student's T-Test$_{1\text{-}5\%}$ established that the average of the differences in permeability-values between the inception horizons type 1 and the surrounding rock masses are significant different compared to differences between values of the rock mass above and below the inception horizon.

For type 2 most of the measurements of the inception horizon samples were below the measurement limit of 0.1 mD. Therefore, we considered off-measurement-limit-values as constant with 0.09 mD. But we can assume that the true contrast would be at much higher (fig. 3.22).

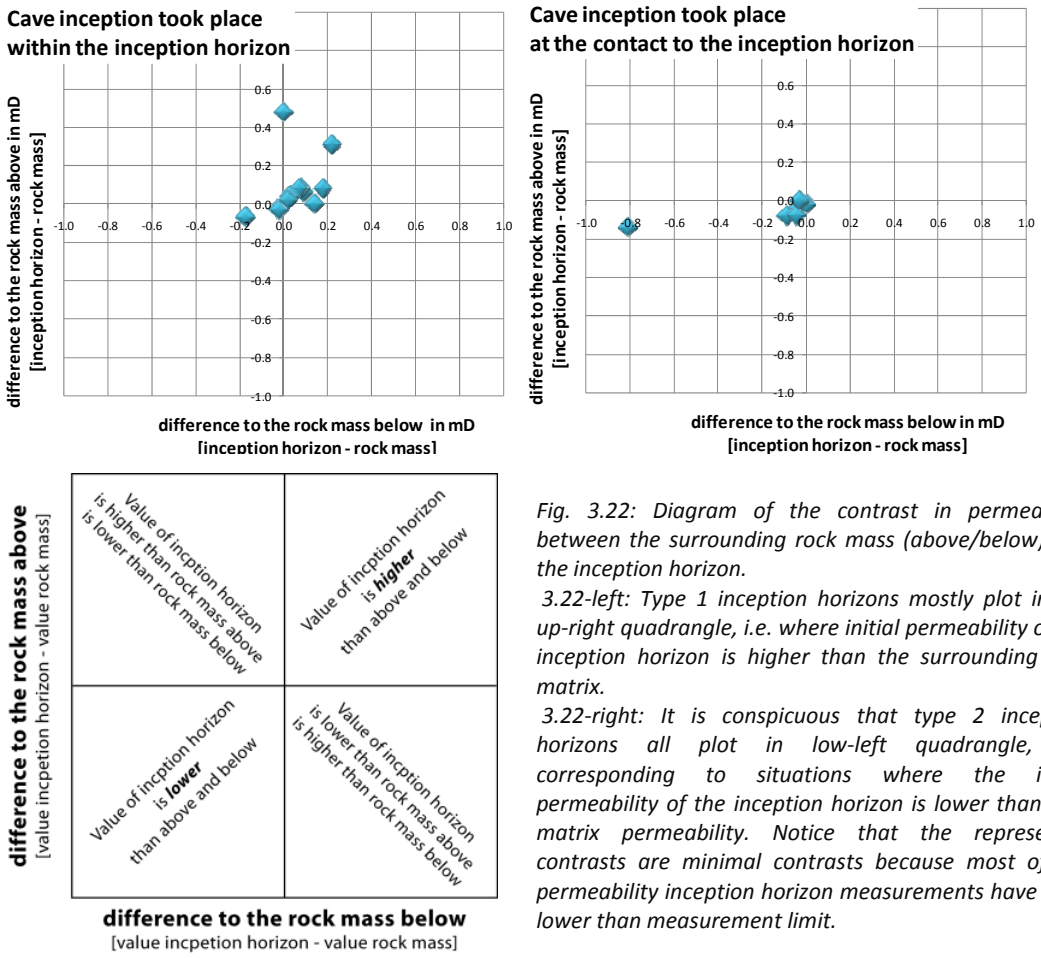

Fig. 3.22: Diagram of the contrast in permeability between the surrounding rock mass (above/below) and the inception horizon.
3.22-left: Type 1 inception horizons mostly plot in the up-right quadrangle, i.e. where initial permeability of the inception horizon is higher than the surrounding rock matrix.
3.22-right: It is conspicuous that type 2 inception horizons all plot in low-left quadrangle, i.e. corresponding to situations where the initial permeability of the inception horizon is lower than rock matrix permeability. Notice that the represented contrasts are minimal contrasts because most of the permeability inception horizon measurements have been lower than measurement limit.

For some inception horizons (tab. 3.1) we took samples at different places to get an idea of the spatial permeability variation. This showed us that the spatial variation of the primary permeability of the inception horizon as well as the surrounding rock mass is higher than the mean difference between the inception horizon and the surrounding rock mass (e.g. fig. 3.23). However, the relative position of the permeability value of the inception horizons remained for all locations consistent (e.g. the values of the inception horizons was at all locations higher than them of the surrounding rock mass).

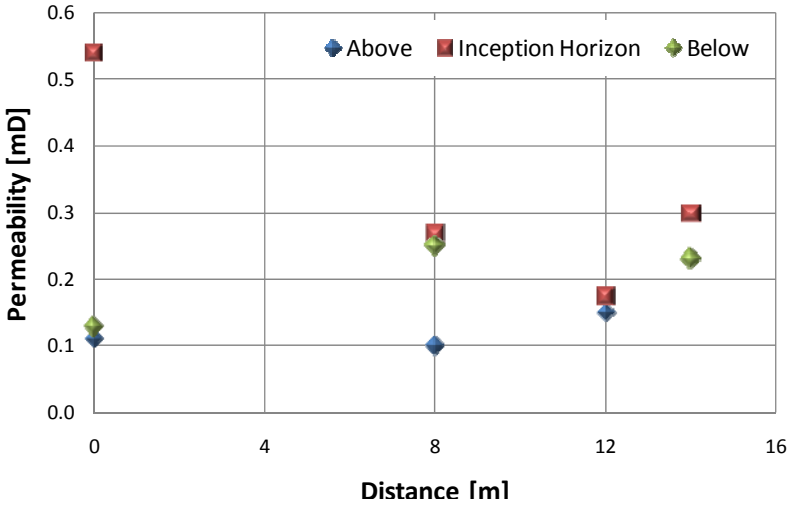

Fig. 3.23: Diagram of the spatial variation of the primary permeability along an inception horizon of type 1. The lateral variance is greater than the difference from the surrounding rock mass to the inception horizon values; however the relative position of the inception horizon sample remains the same for all sampling points (i.e. the value of the inception horizon is higher than them of the corresponding surrounding rock mass).

3.4.1.2 Types of Pores

Among the different pore classifications in use today (e.g. Archie, 1952; Choquette and Pray, 1970) we have used the petrophysical classification proposed by Lucia (1983).

The pores can be subdivided (Lucia, 1983) between *interparticle pores* (pore space located between grains or crystals – matrix pores in Archie, 1952) and *vuggy pores* (visible pores in Archie, 1952). Vuggy pore space is further subdivided based on how the vugs are interconnected into *separate vugs* (vugs that are interconnected only through the interparticle pore network like for example intrafossil pores or shelter pores) and *touching vugs* (vugs that form an interconnected pore system like for example micro fractures and dissolution seams). It is to notice that karst conduits belong in this classification to the touching vugs pores.

We described the pores of our rock samples on the thin sections using an optical microscope. Some of the thin sections were impregnated with blue-dye-stained resin to better recognize the pores.

Only on a few samples we could observe separate vugs, most of the time we observed any vuggy pores at all (interparticle pores are usually smaller than the thickness of the thin sections and/or too small to be identified with an optical microscope). Therefore, we can conclude that the measured permeability is controlled by the interparticle pores, though it was not possible to get a significant correlation between the measured permeability and the matrix partition of the samples (chapter 3.5).

The occurrence of touching vugs was not limited to the inception horizons but was also observed within the surrounding rock mass. However, within the inception horizons the occurrence was significant more frequent than in the surrounding rock mass. At some inception horizon samples it was possible to describe a congeries of touching vugs (fig. 3.24).

The observed touching vugs can be described as dissolution seams (channels/conduits of some tens of micron width and some mm to cm long). Some authors consider this features also as stylolites (e.g. Dewers and Ortoleva, 1994; Graham and Wall, 2006). We suggest considering as stylolites only wave-like interlocking surfaces that contain concentrated insoluble residue such as clay minerals and iron oxides (fig. 3.25). Stylolites are thought to form by pressure solution, which is a dissolution process that reduces pore

space under pressure (http://www.glossary.oilfield.slb.com). The apparent similarity between dissolution seams and stylolites is caused by the fact that pressure dissolution as well as chemical dissolution is preferentially concentrated along the boundaries of the grains.

However, our features are clearly not surfaces but openings (pores). In some cases, we recognized that the dissolution seams ended on pyrite crystals (fig. 3.35), what lead us to conclude, that the dissolution capacity of the seepage water was locally increased by the weathering of the pyrite (see also chapter 3.4.3.2).

The detailed observations of the dissolution seams give us indications where the first dissolution (of the karstification) took place. These observations were used in the following sections to verify the concluded processes related to a given property (for details see in the sections).

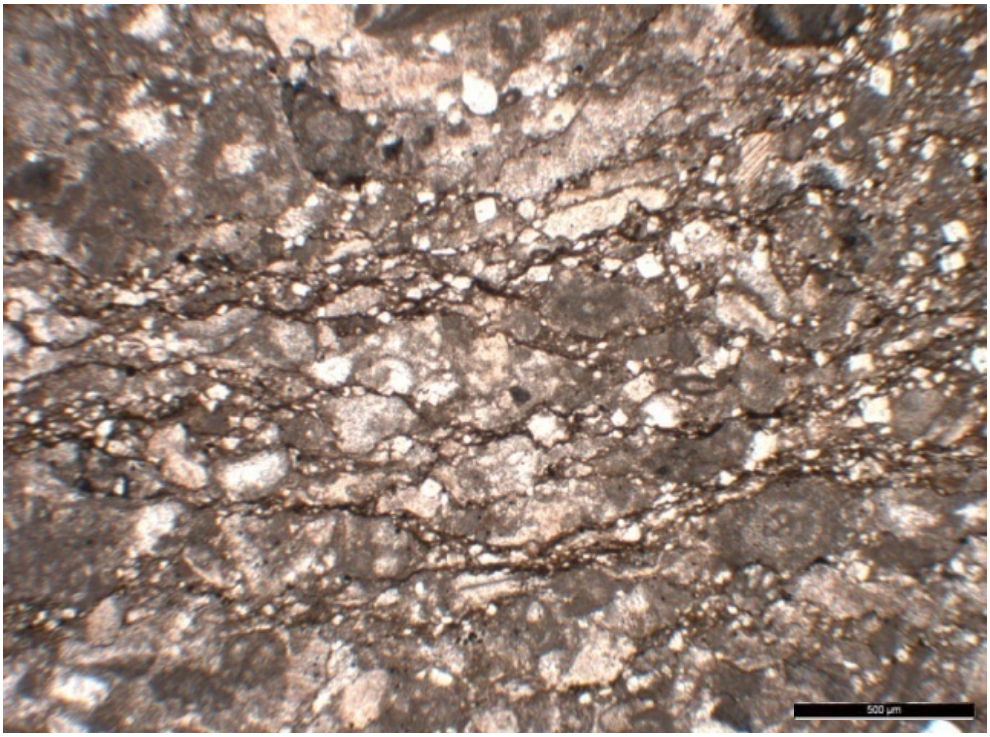

Fig. 3.24: Touching vugs (i.e. dissolution seams). Dolomite-reach layer with micritic matrix, the dissolution seams developed around foraminifera.

Fig. 3.25: Stylolite in a Jurassic limestone. Although some similarities stylolites (wave-like interlocking surfaces that contain concentrated insoluble residue such as clay minerals and iron oxides) should not be confused with dissolution seams (i.e. touching vugs).

3.4.2 Carbonate content

A natural limestone is an aggregation of different minerals whereas calcite and dolomite are the most commune minerals. It is imaginable that the variation in total carbonate, calcite and/or dolomite content can build a favourable horizon for early karstification. However, only a few studies were done within the inception horizon concept; Knez (1998) for example observed a slightly higher level of calcite on the analysed inception horizons from Skocjanske Jame (Slovenia) and deduced that these purer horizons would be “a priori” better soluble than the surrounding rock mass.

Previous work (e.g. Slippel and Glover, 1964; Rauch and White, 1977; Walter, 1985) showed that dolomite is slightly more soluble than calcite in terms of rock volume. In exchange the pure calcite dissolves about 2.5 to 7.5 times faster than dolomite, with the greatest differences at low CO_2 values (Liu and Dreybrodt, 2001). Rauch and White (1977) observed during their laboratory measurements a decreasing of the dissolution rate as percentages of dolomite increased. Nevertheless, the highest dissolution rates are observed for rocks containing about 1 - 2.5 % MgO, these rates are higher than those for magnesium-free rocks. Furthermore, dissolution rate of calcite drops sharply beyond about 60 – 90 % of saturation (e.g. Berner and Morse, 1974; Plummer and Wigley, 1976) and converges asymptotic to saturation; for dolomite this change between linear and asymptotic behaviour occurs already at around 20 – 30 % of saturation (e.g. Herman and White, 1985) and it is assumed to require some years to get in saturation.

It is to notice that this non linear behaviour of the rate close to equilibrium is essential to the origin of karst conduits. If the dissolution rate laws were entirely linear, water penetrating into fissures would attain equilibrium after penetration of only a few metres into the rock because the dissolution rates drop exponentially. In contrast, nonlinear kinetic allows deep penetration into the rock, such that even after distances of kilometres a small, but sufficient solution power exist, which can create conduits (Dreybrodt et al., 2005).

Zupan Hajna (2002, 2003) describes that dolomite content is decreased within the weathered zone of a limestone exposure. This was caused by the difference in dissolution rate between calcite and dolomite. She believes that this process representing an important factor for the cave inception. However, it is to notice that at high saturation the difference in dissolution rate between calcite and dolomite becomes marginal.

Some authors believe that the carbonate content is one of the mayor factors dominating the karstification of a limestone, assuming that the carbonate content is the dominant factor controlling the dissolution rate of the limestone (e.g. Eisenlohr et al., 1999; Rauch and White, 1977; Bögli, 1978). Many field observations done by different authors, in caves all over the World, described that caves or cave passages are mainly guided by “marly bedding plane” (e.g. Glaser, 2005). Unfortunately, these authors give rarely indications where the cave inception took place (within or at the contact).

For the present study, the calcite and dolomite content as well as the total percentage of dissoluble material (sum of both) were measured with an automatic calcimeter (Coretest Systems AC-280, University of Geneva). The measurements are based on the so-called pressure calcimeter principle; i.e. measures the rate of calcium carbonate by the measure of the pressure of the open carbonic gas after a hydrochloric acid injection. The used calcimeter allows measuring 1 gram of pulverised rock sample in the range between 0 and 100 % within an accuracy of 1 %.

As expected, the content of dissoluble minerals (sum of calcite and dolomite) was at most of the cases over 80 weight-% (fig. 3.26). Whereas it is to notice that also the stratigraphical horizons that were addressed in the field as marly horizons had been found to have a high percentage of carbonate content with an average of the calcite content of around 85 weight-% and for dolomite at 5 %.

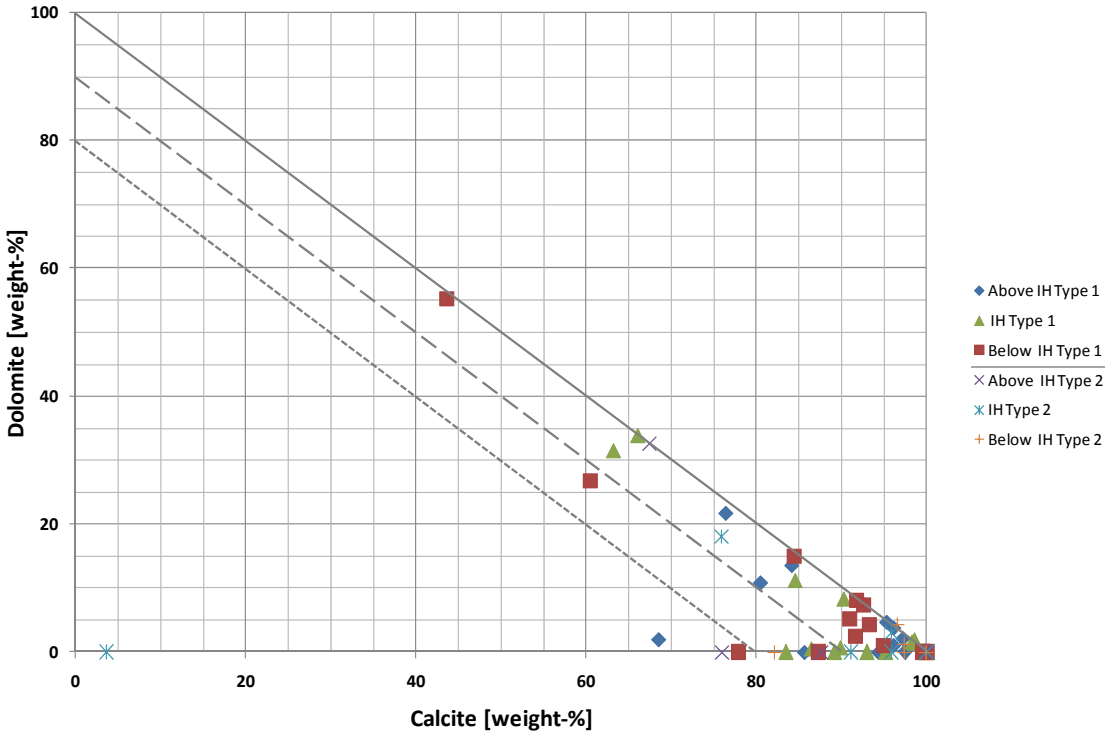

Fig. 3.26: Diagram of the content of calcite against the content of dolomite of the inception horizons and the surrounding rock mass. The total carbonate content (sum of calcite and dolomite) was at most of the cases over 90 weight-percent; a priori it is not possible to recognise a threshold values that distinguish incepted horizons from not incepted.

The view at the absolute values of the measured carbonate content (fig. 3.26) does not allow to distinct neither between inception horizon and not inception horizon samples nor between the different types of inception horizons. Therefore, we can assume that they do not exist a threshold value of carbonate content for recognizing an inception horizon. This is also valid for the calcite and dolomite contentcontent.

Against the expectation the coefficient of determination R^2 of the linear correlation between the calcite, dolomite and total carbonate content of all samples of the sampling points are rather moderate but can be considered for calcite and total carbonate as well as calcite and dolomite as statistically significant correlated ($T\text{-}Test_{1\text{-}5\%}$) (tab. 3.4).

58 Observations

R^2	Total	Calcite	Dolomite
Total	1	0.56	0.02
Calcite	0.56	1	0.30
Dolomite	0.02	0.3	1

T-Test	Total	Calcite	Dolomite
Total		8.5	1.1
Calcite	Ha		4.9
Dolomite	Ho	Ha	

T-Test $_{1\text{-}5\%(60)}$ *1.67*

Ho: The coefficient of determination is not significantly different from 0
=> correlation can be considert as not sigificant.
Ha: The coefficient of determination is significantly different from 0
=> correlation can be considert as sigificant.

Tab. 3.4: Coefficient of determination (R^2) of the linear correlation between the calcite, dolomite and total carbonate contents of all samples of the sampling points and the statistically significant T-Test$_{1\text{-}5\%}$. Albeit the R^2-values are rather moderate, they can be considered as statistically significant for calcite-total carbonate and calcite-dolomite but not significant for dolomite-total carbonate.

To have an idea of the **spatial variation** of the carbonate content along an inception horizon we analysed the values along a single inception horizon (exemplary presented based on the results of inception horizon S2). With a statistical T-Test$_{1\text{-}5\%}$ we verify if there are a significant difference regarding the averages of the value of the rock mass above versus the values of the inception horizon, the same has also been done for the relationship between rock mass below and inception horizon and for control also for the relationship between the rock mass above and below. All this has also been done with a statistical F-Test$_{1\text{-}5\%}$, to see if there are significant differences regarding the variance.

For the **total carbonate content,** the T-Test$_{1\text{-}5\%}$ indicated that the average value of the samples of the inception horizons is significant different from the samples of the rock mass above as well as below (fig. 3.27); whereas no significant difference of the rock mass above and below could be found. This is also true for the significant difference of the variance (F-Test$_{1\text{-}5\%}$). It is to notice that the standard deviation of the values along the inception horizon is in the range of the differences between the measured values of the inception horizon and the surrounding rock mass.

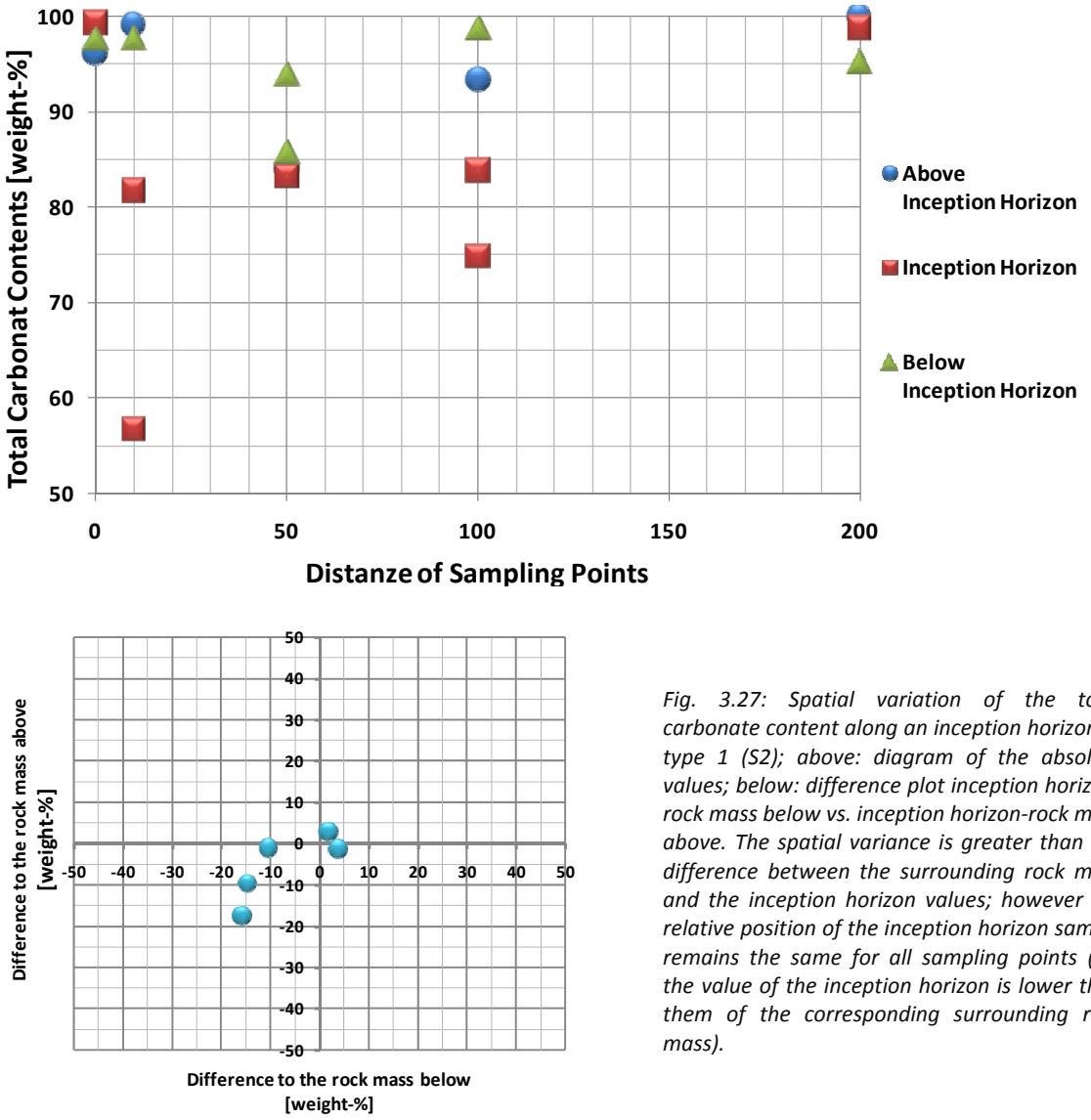

Fig. 3.27: Spatial variation of the total carbonate content along an inception horizon of type 1 (S2); above: diagram of the absolute values; below: difference plot inception horizon-rock mass below vs. inception horizon-rock mass above. The spatial variance is greater than the difference between the surrounding rock mass and the inception horizon values; however the relative position of the inception horizon sample remains the same for all sampling points (i.e. the value of the inception horizon is lower than them of the corresponding surrounding rock mass).

The T-Test$_{1\text{-}5\%}$ as well as the F-Test$_{1\text{-}5\%}$ indicated that there are significant differences in average as well as in variance of the **calcite content** of the samples of the inception horizon and the samples from the rock mass above and below (fig. 3.28). Like for the total carbonate, also for the calcite content the standard deviation of the samples within the inception horizon are in the same order of scale as the differences in absolute values to the surrounding rock mass.

Contrary to that, the statistical tests show no evidence of difference of **dolomite content** neither regarding the average nor the variance (fig. 3.29).

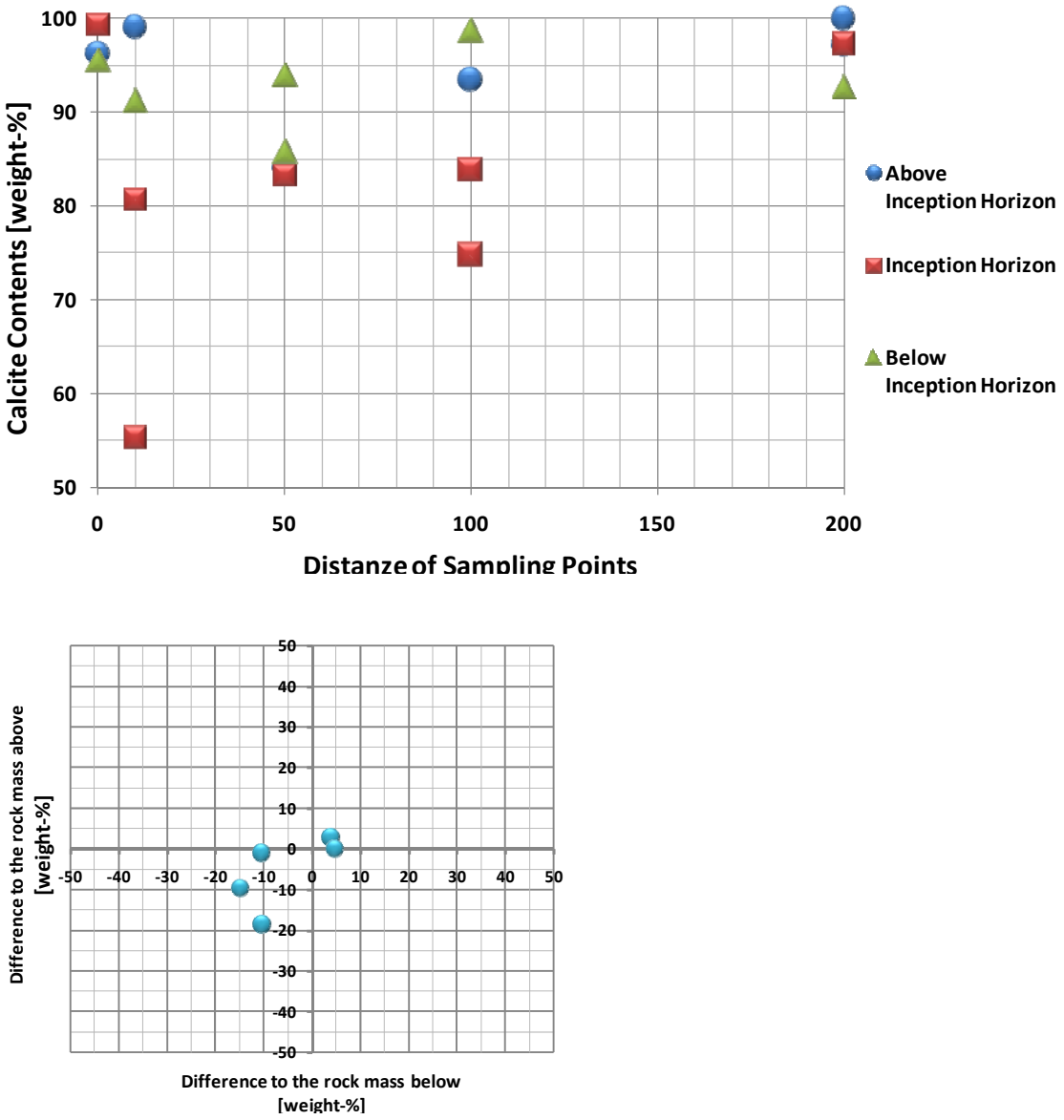

Fig. 3.28: Spatial variation of the calcite content along an inception horizon of type 1 (S2); abve: diagram of the absolute values; below: difference plot inception horizon-rock mass below vs. inception horizon-rock mass above. The spatial variance is greater than the difference between the surrounding rock mass and the inception horizon values; however, the relative position of the inception horizon sample remains the same for all sampling points (i.e. the value of the inception horizon is lower than them of the corresponding surrounding rock mass).

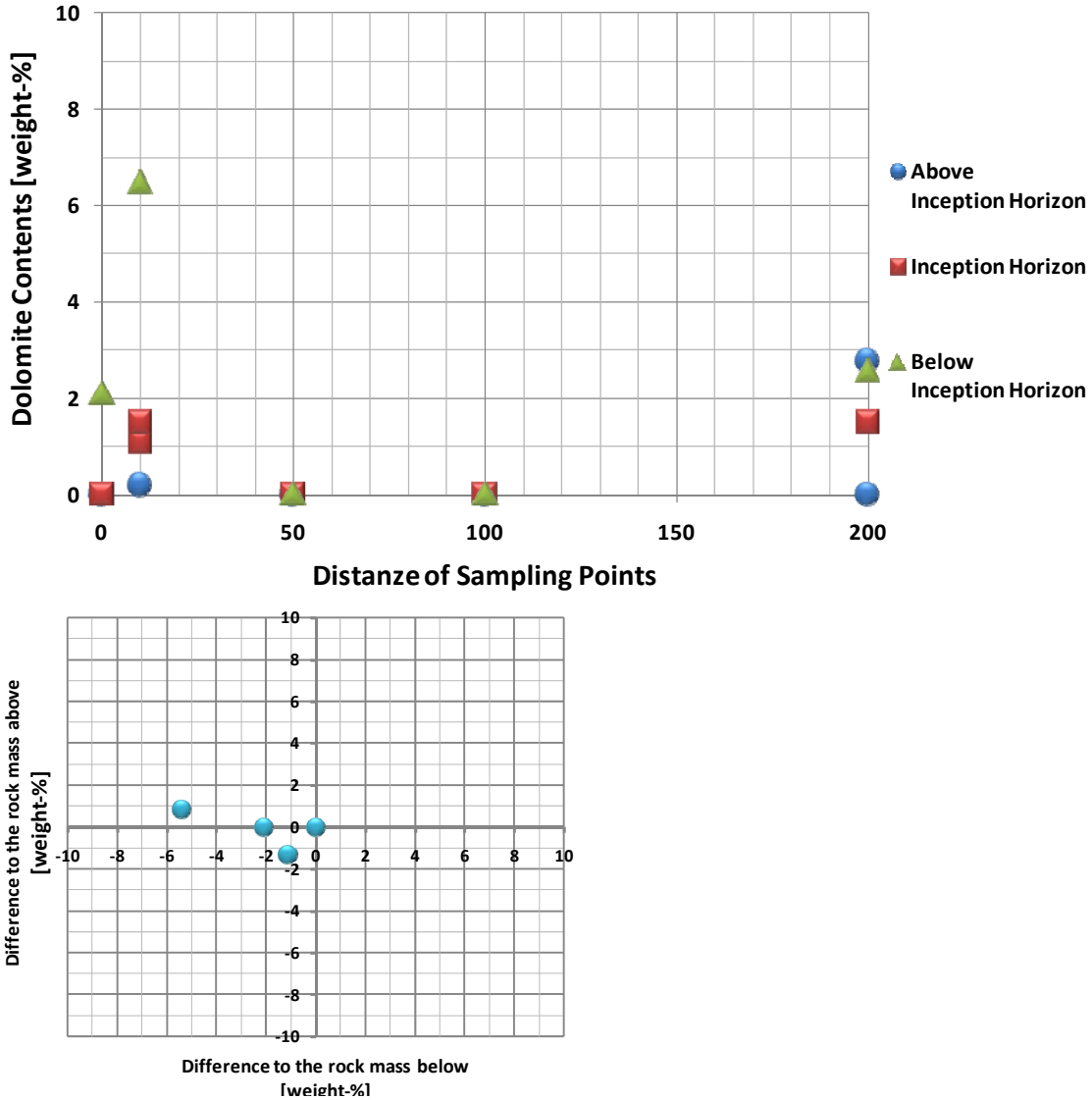

Fig. 3.29: Spatial variation of the dolomite content along an inception horizon of type 1 (S2); above: diagram of the absolute values; below: difference plot inception horizon-rock mass below vs. inception horizon-rock mass above. The spatial variance is greater than the difference between the surrounding rock mass and the inception horizon values; the relative position of the inception horizon sample is not consisted at the different sampling points.

This analysis of spatial variation was done also for other inception horizons of type 1 and 2 getting similar results. We can conclude that there are a significant difference of the mean values of the samples from the inception horizon and the surrounding rock mass for total carbonate as well as calcite contents; for dolomite content no significant difference could be found. This allows us to describe the values of an inception horizon by taking the average of the values of the different sampling points of an inception horizon.

As showed above it was not possible to recognise threshold values to separate the inception horizons values from them of the surrounding rock mass.

The spatial variation of the inception values is in the order of the difference between the values of the inception horizon and the surrounding rock mass. We can suppose that the absolute values as been only of subordinated significance. This and the fact the samples accrue from different lithologies, leads us to consider that mainly the contrast between the properties of inception horizons and the surrounding rock

mass which will be relevant (i.e. value of the inception horizon minus value of the rock mass) (fig. 3.30). Relative values above 0 mean that the inception horizon has a higher content of calcite/dolomite/total carbonate than the surrounding rock mass, and numbers below 0 mean that the content is lower.

Albeit the contrasts between the inception horizons and the surrounding rock mass are slight; in the order of some weight-percentage, they can still be considered as significantly different from 0 (T-Test$_{1\text{-}5\%}$). Even though the standard deviation of the contrast in total carbonate content is slightly higher than for the calcite as well as dolomite content.

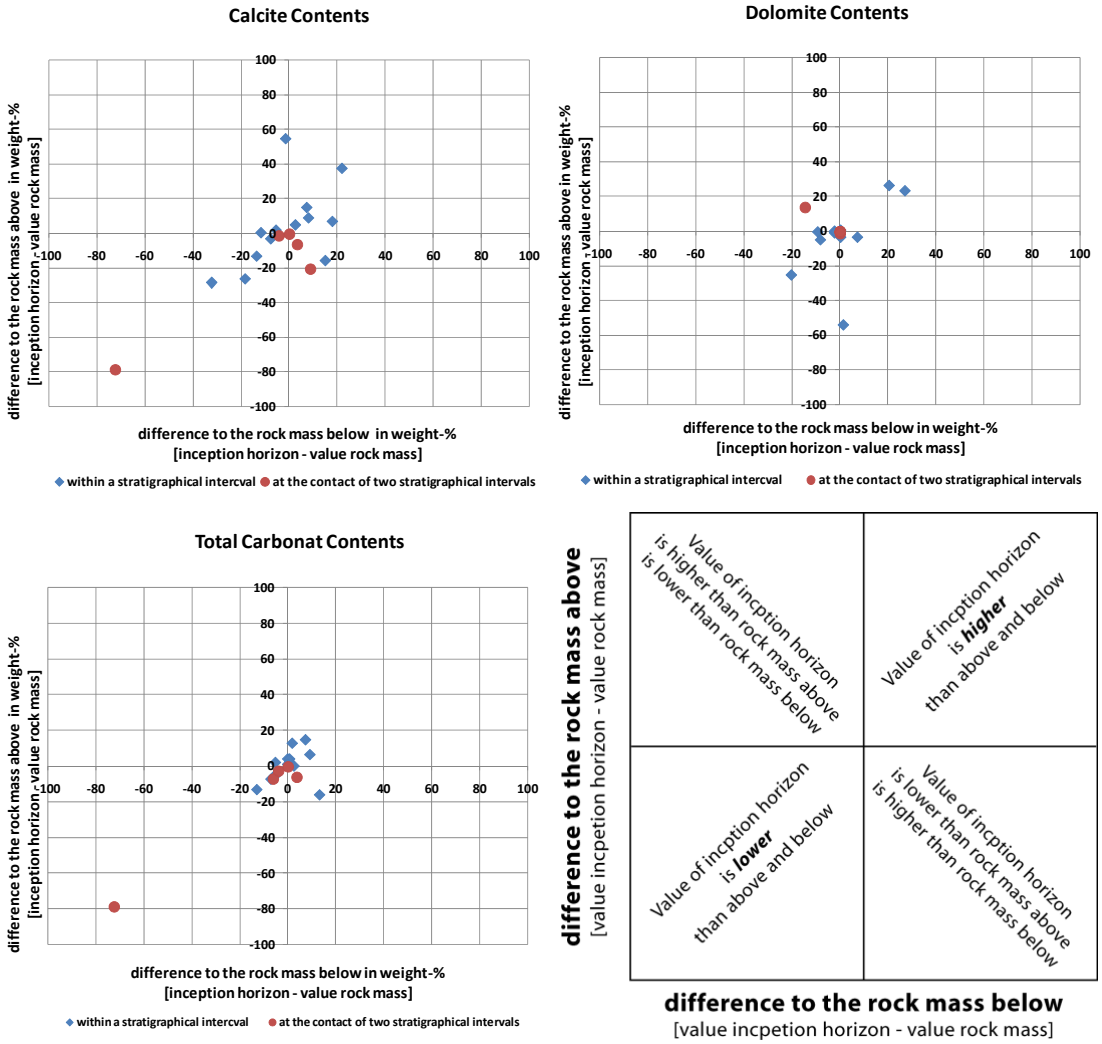

Fig. 3.30: Difference-plots for total carbonate, calcite and dolomite contents. The red points represent inception horizon type 2; the blue points represent inception horizon type 1.

The difference-plots for total carbonate, calcite and dolomite contents suggest a distinct linear trend that would indicate that the rock above and below the inception horizons are similar and that only the favourable horizon has a different value. However, the coefficients of determination R^2 are quite moderate and with a statistical T-Test$_{1\text{-}5\%}$ not to be considered as significant (for inception horizons of type 2 we get significant determination coefficients, however, they are biased by an inception horizon with very low carbonate content; this value were removed for the correlation of all values) (tab. 3.5). Contrary to that shows the correlation between the measured values of the rock mass below against the values of the rock mass above also moderate coefficients of determination but can be considered as significant (T-Test$_{1\text{-}5\%}$) at least for calcite and total carbonate contents and therefore correlated.

	R^2	Dolomite	Calcite	Total	Observations
Difference IH vs. rock mass	All	0.21	0.23	0.09	17*
	IH Type 1	0.34	0.32	0.09	13
	IH Type 2	0.99	0.86	0.98	5
Rock mass above vs. below		0.14	0.57	0.57	18

	T-Values	Dolomite	Calcite	Total	$T\text{-}Test_{(1\text{-}5\%)}$
Difference IH vs. rock mass	All	0.95	1.01	0.60	1.74
	IH Type 1	1.19	1.13	0.57	1.77
	IH Type 2	4.62	2.01	3.54	2.02
Rock mass above vs. below		0.77	1.87	1.87	1.73

	T-Test	Dolomite	Calcite	Total
Difference IH vs. rock mass	All	Ho	Ho	Ho
	IH Type 1	Ho	Ho	Ho
	IH Type 2	**Ha**	Ho	**Ha**
Rock mass above vs. below		Ho	**Ha**	**Ha**

Ho: The coefficient of determination is not significantly different from 0
=> correlation can be considert as not significant.
Ha: The coefficient of determination is significantly different from 0
=> correlation can be considert as significant.

Tab. 3.5: Coefficient of determination (R^2) of the linear correlation between of the difference in for the calcite, dolomite and total carbonate contents and the statistically significant $T\text{-}Test_{1\text{-}5\%}$. For inception horizons of type 1 the R^2-values are moderate, they can be considered as statistically not significant. The high R^2-values and therefore also the significance in the T-Tests are biased by an inception horizon with very low carbonate content. This biased value has been removed for the correlation of all values.
Contrary to that, the correlation between the rock mass below against the rock mass above can be considered as significant for calcite and total carbonate and not significant for dolomite.

The samples of **inception horizons type 1** show in 6 of 12 cases a higher and in 4 cases a lower total carbonate content than the surrounding rock mass. The samples with higher total carbonate compared to the surrounding rock mass indicate a tendency to have a higher calcite and a lower dolomite contents. Whereas the samples with a lower total carbonate content show a tendency to have also lower calcite content but a higher dolomite content (tab. 3.6). It is to notice that the contrast between the surrounding rock mass and the inception horizons are slight and the number of investigated inception horizons quite small, however it was possible to demonstrate with a statistical $T\text{-}Test_{1\text{-}5\%}$ that each of the average difference (IH-surrounding rock mass) of two groups are significantly different from 0.

Calcite Contents [1: highest - 3: lowest]	Total Carbonate [1: highest - 3: lowest] 0	1	2	3
0				
1		*4*		
2		*1*	*2*	
3		*1*		*4*

Dolomite Contents [1: highest - 3: lowest]	Total Carbonate [1: highest - 3: lowest] 0	1	2	3
0				
1		*1*		*3*
2		*1*		*1*
3		*4*	*2*	

Dolomite Contents [1: highest - 3: lowest]	Calcite Contents [1: highest - 3: lowest] 0	1	2	3
0				
1				*4*
2			*2*	
3		*4*	*2*	

Tab. 3.6: The occurrence matrices illustrate the frequencies of combination of two factors. The date of the inception horizons were ranked compared to the values of the surrounding rock mass. Rang 1 means the value of the inception horizon is the highest; rang 3 that the value of the inception horizon is the lowest; rang 2 intermediary value of the inception horizon; rang 0 no difference between inception horizon and the surrounding rock mass.

The samples of **inception horizons type 2** shows in 4 of 6 cases that they have a lower total carbonate content than the surrounding rock mass. The deviation in calcite content could not show a clear tendency and in the most cases neither the rock mass nor the inception horizon had any dolomite content.

3.4.3 Impurities

Typically limestone does not consist entirely of calcite and/or dolomite but has a certain percentage of impurities. These additional minerals consist typically of clastic clay minerals and quartz sand; syndiagenetic mineral formations like for example pyrite or glauconite; under hypersaline conditions highly soluble minerals, such as gypsum can be deposited.

The impurities have different speleogenetical meaning; they can restrain or forward the karstification of an inception horizon by different mechanisms (fig. 3.1).

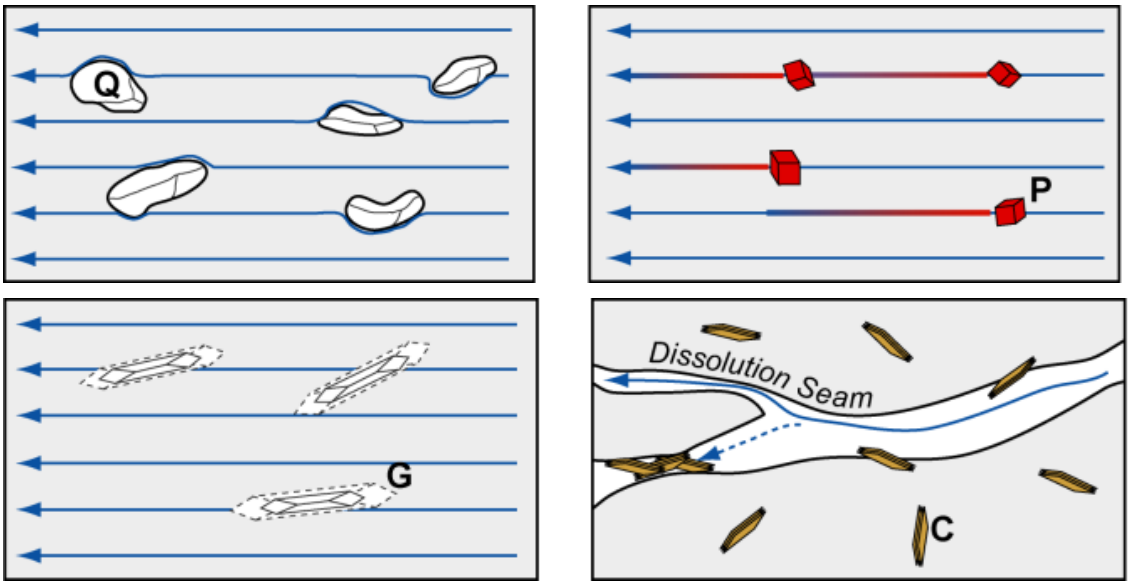

Fig. 3.31: Different speleogenetical meaning of impurities. 3.31.1: Poorly dissoluble minerals like for example quartz grains will concentrate the flow around the grains. 3.31.2: Weathering of certain minerals like for example pyrite can produce aggressive solutions that increase at least locally the dissolution capacity of the seepage water. 3.31.3: highly soluble minerals such as gypsum will dissolve faster than the surrounding rock mass and increase porosity. 3.31.4: Impurities like for example clay minerals can clog flow paths.

Generally it is assumed that the occurrences of **poorly dissolvable minerals** (e.g. clay minerals or quartz grains) decrease the dissolution rates of a carbonatic rock surface (like for example in a fracture or the wall of a cave conduit) by reducing the exposed “reactive surface” of a rock surface (e.g. Rauch and White, 1977, Eisenlohr et al., 1999). However, up to now only a few investigations were done to understand the role of the impurities for the dissolution processes within a porous medium (e.g. Noiriel, 2005), showing that impurities can clog flow paths (e.g. clay minerals) or elsewhere concentrate the flow around poorly dissoluble grains (e.g. quartz grains). High concentrations of quartz sand do not seem to inhibit a priori conduit development, for example contains the cavernous Lolyalhanna Limestone (western Pennsylvania) about 50 % quartz sand (White and White, 2001). Contrary, are cavernous shaley limestones rare. Therefore, it can be assumed that the content of poorly dissolvable minerals can either affect the dissolution rate of the rock mass (macroscopic scale) or affect the microscopic characteristics of the flow path.

Under hypersaline conditions **highly soluble minerals** such as gypsum can be deposited within a carbonate sequence. These minerals are commonly better soluble than carbonates. For example possess gypsum a solubility that is around 10 to 30 times higher than calcite (Bögli, 1978). The dissolution of such minerals can

increase the porosity/permeability of a bedding plane, and favour the water flow along the bedding plane and as such also favour the karstification of the surrounding carbonate rock mass.

Besides that, sulphate minerals can cause the so called "**common ion effect**" (e.g. Dreybrodt, 1988; Ford and Williams, 2007). The common ion effect is: if one of the ions created by dissolution of a given mineral will be introduced from some other source, what causes a reduction of the solubility of that mineral. For calcite and dolomite, this normally implies an alternative source of Ca^{2+} or Mg^{2+} ions. Other carbonate and magnesium minerals are rare, thus the common-ion effect occurs chiefly where Ca^{2+} is furnished by gypsum. These additional Ca^{2+} ions will reduce the dissolution capacity of calcite and increase up to seven times them of dolomite (e.g. Ford and Williams, 2007). Because dolomite dissolves very slowly as it nears saturation (Herman and White, 1985), these dissolution processes are drawn out over long flow distances.

The **weathering of certain minerals** like for example sulphides can produce acidic solutions, which can change the dissolution capacity of the seepage water and may turn nonaggressive water into highly corrosive solutions (e.g. Moore and Druckman, 1981, Lowe, 1992, 2000; Palmer and Palmer, 1995; Goldstrand and Shevenell, 1997; White and White, 2003; Auler and Smart, 2003). The commonest of these mineral is pyrite (FeS_2). Although several authors propose pyrite as a (main) factor for cave inception, there are no quantitative or semi quantitative investigations done on the concentration of pyrite content within inception horizons till now.

The origin of pyrite is related to the diagenesis of marine carbonate mud with an important content of organic materials (Tucker, 1985) and can therefore be assumed to be concentrated within bedding planes.

The oxidation of pyrite is quite complex and still not well understand (Rimstidt and Vaughan, 2003). Simplified the reaction can be written as Equation 1 whereas 1 mol FeS_2 can dissolve 2 mol $CaCO_3$ via H_2SO_4 and other 2 mol $CaCO_3$ by the additional production of CO_2, in other words 1 cm^3 pyrite can dissolve 6 cm^3 of calcite (e.g. Palmer and Palmer, 1995; Bögli, 1978). The reaction is strongly pH-dependent and needs 88 kJ/mol activation energy (Nicholson et al., 1988).

$$FeS_2 + 3.25O_2 + 3.5H_2O \Leftrightarrow Fe(OH)_3 + 2H_2SO_4$$
$$2H_2SO_4^- + H^+ + 2CaCO_3 \Leftrightarrow 2Ca^{2+} + 2SO_4^{2-} + 2H_2O + 2CO_2$$
$$2CaCO_3 + 2H_2O + 2CO_2 \Leftrightarrow 2Ca^{2+} + 4HCO_3^-$$

Equ. 1: Oxidation of pyrite and the dissolution of calcite.

It is assumed that the production of acidic solutions can at least locally increase the dissolution capacity at least locally. These can be observed for example at a microscopic scale (thin sections) where the produced acidic solution causes small dissolution features starting from the pyrite crystals (fig. 3.35), or at a macroscopic scale the dissolution of complied bedding plan parting (fig. 3.17). It can be supposed that this acidy has a minimal effect on the context of the later passages, but its contribution to the porosity development into the bedding plane can be significant.

Already the measurements of the carbonate content showed that our samples have most of the time less than 10 weight-percent of impurities (i.e. non carbonate minerals). Therefore, it was only for some samples possible to measure their mineralogical composition with the XRD-method (resolution of the used facilities at around 5 volume-percent; for a complied decarbonation we did not have enough sampling material) and showed the occurrence of quartz, gypsum and glauconite.

Consequently, we assessed the mineralogical content qualitative by rating the mineralogical content of the thin sections of the inception horizon relatively to them of the surrounding rock mass. The focus was on the content of quartz and pyrite. We addressed all opaque minerals as pyrite independently whether or not it was clearly recognisable the typical cubic shape of pyrite crystals. The thin section estimation of the

mineralogical content of the samples has the disadvantage to only allow to qualitatively quantifying the content. Therefore, we rated the content of the inception horizons relatively to the corresponding surrounding rock mass:

Rang 1) means a higher content of the inception horizon relatively to the surrounding rock mass;

Rang 2) means that the content of the inception horizon is between the content of the rock above and below;

Rang 3) means a lower content of the inception horizon relatively to the surrounding rock mass.

To guarantee an unprepossessed assessment, we ranked the mineralogy content of the thin sections of each sampling point at three independent counting runs and all the time not knowing which of the thin section corresponds to them of the inception horizon.

It is to notice, that the estimated quartz and pyrite contents was most of the cases lower than the measured content of impurities, while measuring the carbonate content. Apart from the difference in recording units (measurements of the carbonate content in weight-percentage, estimation of the content on the thin sections in volume-percentage), we can expect that we have also other impurities than quartz and pyrite, like different kind of clay minerals. However, these minerals are usually too small to be detected with an optical microscope (except some glauconite crystals) and the total content to small low to be detected by the XRD-method.

3.4.3.1 Quartz content

Quartz occurs quite often in our samples, most of the cases in the form of clastic grains. The occurrence is randomly distributed or arranged in thin layers of a thickness of some grains. Associated with them we could often observe small dissolution seams (fig. 3.32). This observation supports the assumption that quartz grains can have an influence of the flow path characteristics in microscopic scale.

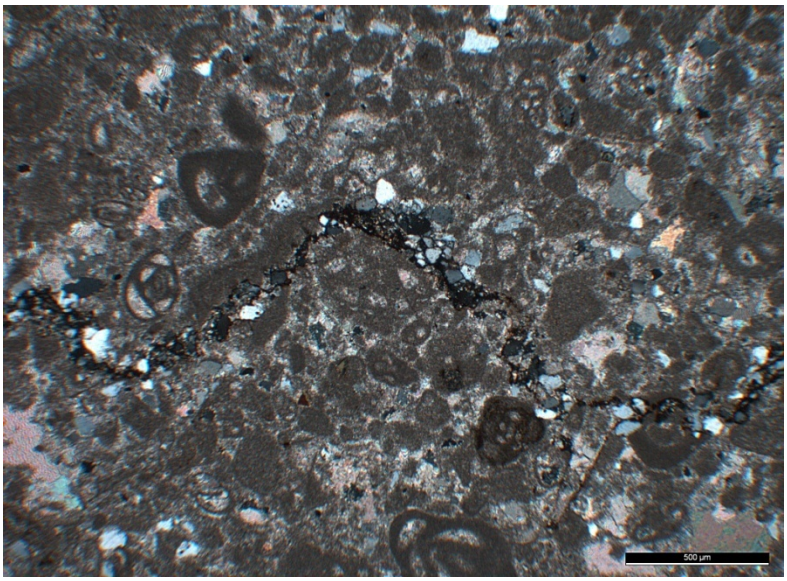

Fig. 3.32: Thin section of an inception horizon sample showing a dissolution seam around quartz grains. The quartz grains concentrated the flow path around the grains and enhanced the locally the dissolution.

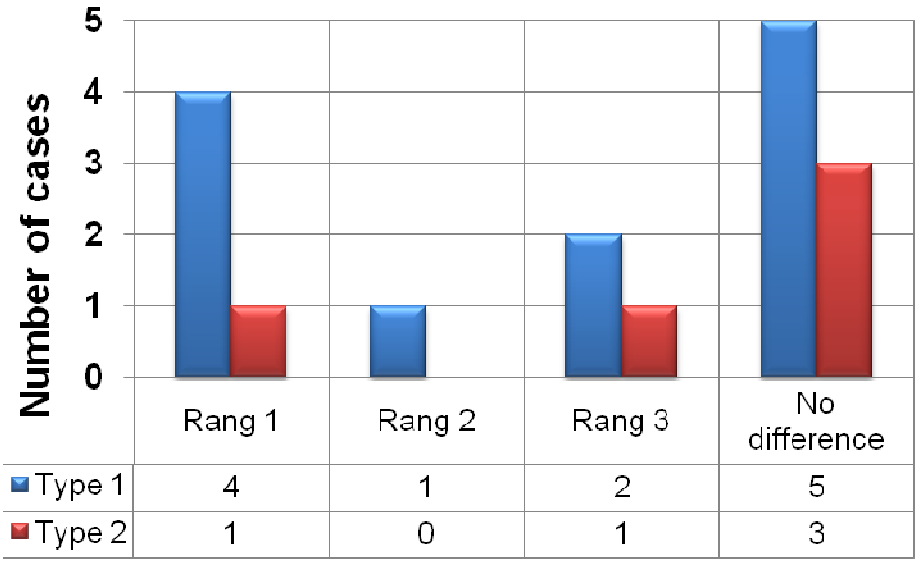

	Rang 1	Rang 2	Rang 3	No difference
Type 1	4	1	2	5
Type 2	1	0	1	3

Fig. 3.33: Diagram showing the rang of the quartz content of the inception horizons samples compared to the samples of the corresponding surrounding rock mass samples (Rang 1: value of inception horizon sample is the highest; Rang 3: value of inception horizon sample is the lowest). Inception horizons of type 1 show no difference to the samples of the surrounding rock mass or are have an increased concentration of quartz content; for inception horizon type 2 no tendency is recognisable.

The assessment of the relative content of quartz shows for 8 inception horizons no significant difference and for other 5 horizons a slight amount in quartz content, only in 3 cases the content of the inception horizons was slight lower than in the surrounding rock mass (fig. 3.33).

Divided up into the different types of inception horizons we can distinguish:

> **for type 1** a first group of inception horizons with a slightly higher content of quartz than the surrounding rock mass and a second group that show no clear difference in content relative to the surrounding rock mass.
>
> **for type 2** most of the inception horizons show no clear difference in quartz content to the surrounding rock mass. Therefore, we can assume that the lower carbonate content of inception horizons type 2 is caused by the occurrences of impurities of clay minerals. This can also be deduced by the missing relationship between the occurrence of quartz and the carbonate content of the samples (chapter 3.5).

To get an idea of the **spatial variation** of the quartz content along an inception horizon we analysed the values along a single inception horizon (exemplary presented based on the results of inception horizon S2). Therefore, we ranked at once the thin sections of all sampling points along the inception horizon (and not like done before each sampling point by them self) (fig. 3.34). The application of a statistical T-Test$_{1\text{-}5\%}$ indicated that the average ranking of the samples of the inception horizons is significant different from the samples of the rock mass above as well as below; whereas no significant difference of the rock mass above and below could be found. While against that the statistical F-Test$_{1\text{-}5\%}$ showed no significant difference for the variance of the ranking.

It is to notice, that the relative ranking of the quartz content at a sampling point was most of the time lower than the surrounding rock mass, what means that the quartz content at the sampling points was most of the time higher than at the corresponding surrounding rock mass samples.

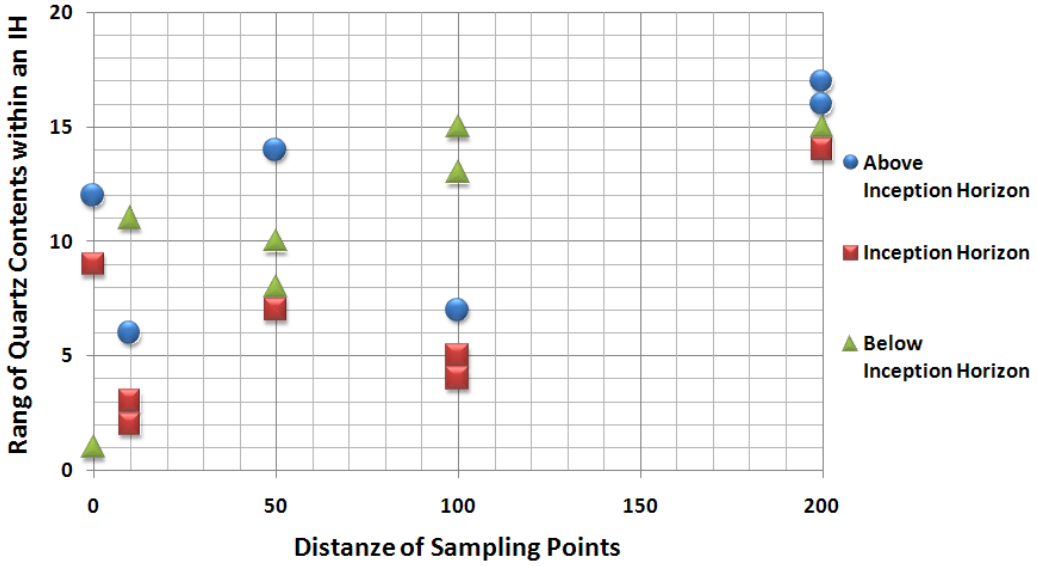

Fig. 3.34: Diagram of the spatial variation of the ranges of the quartz content along an inception horizon of type 1 (all samples of all sampling points were ranged – Rang 1 is the sample with the highest quartz content along the horizon). The inception horizon samples have at almost all sampling points the highest quartz content. (Inception Horizon S2)

3.4.3.2 Pyrite content

Pyrite occurs regularly in our samples, often in the form of small cubic crystals or little opaque nodules (framboids). The pyrite content is in all samples low, most of the time less than 1 volume-% (visual estimation). The occurrence is often randomly distributed through the thin section, whereas a small concentration of pyrite could be observed sometimes on fossils (fig. 3.35-left). It was possible to recognize dissolution seams that started form a pyrite grain/crystal or dissolution holes that suggest that pyrite was weathered away (fig. 3.35-right).

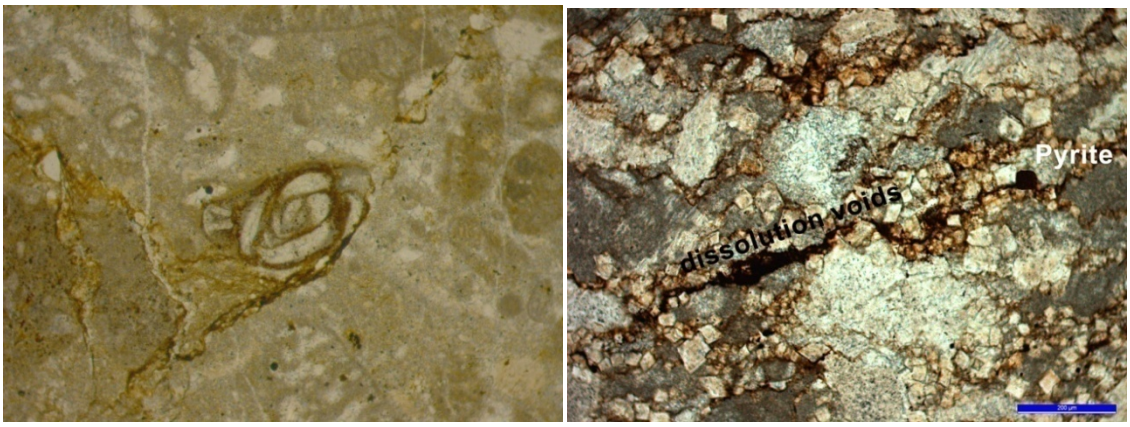

Fig. 3.35: Thin section of pyrite occurrences within the samples. Left: pyrite concentration at a foraminifera. Right: pyrite crystal with a dissolution seam produced probably by the dissolution capacity produced by the production of sulphuric acid of the weathering of the pyrite.

The assessment of the relative content of pyrite showed a clear amount of (microscopically) pyrite within the inception horizons compared to the surrounding rock mass or no difference to the surrounding rock mass when no pyrite was present (fig. 3.36). (For the macroscopic pyrite occurrences along inception horizons see chapter 3.34)

	Rang 1	Rang 2	Rang 3	No difference
Type 1	11	0	0	2
Type 2	4	0	1	0

Fig. 3.36: Diagram showing the ranges of the pyrite content of the inception horizons samples compared to the samples of the corresponding surrounding rock mass samples (Rang 1: value of inception horizon sample is the highest; Rang 3: value of inception horizon sample is the lowest). Inception horizons of type 1 and 2 show a clear increased concentration of pyrite.

To get an idea of the **spatial variation** of the pyrite content along an inception horizon we analysed the values along a single inception horizon (exemplary presented based on the results of inception horizon S2). Therefore, we ranked at once the thin sections of all sampling points along the inception horizon (fig. 3.37).

With a statistical T-Test$_{1\text{-}5\%}$ we could prove that there is a significant difference regarding the averages of the ranking of the inception horizon samples versus the ranking of the rock mass above (below); whereas no significant difference of the rock mass above and below could be found. Contrary to them a statistical F-Test$_{1\text{-}5\%}$ showed no significant difference for the variance of the ranking.

It is to notice, that the relative ranking of the pyrite content at a sampling point was all the time lower than the surrounding rock mass, what means that the pyrite content at the sampling points was all the time higher than at the corresponding surrounding rock mass samples.

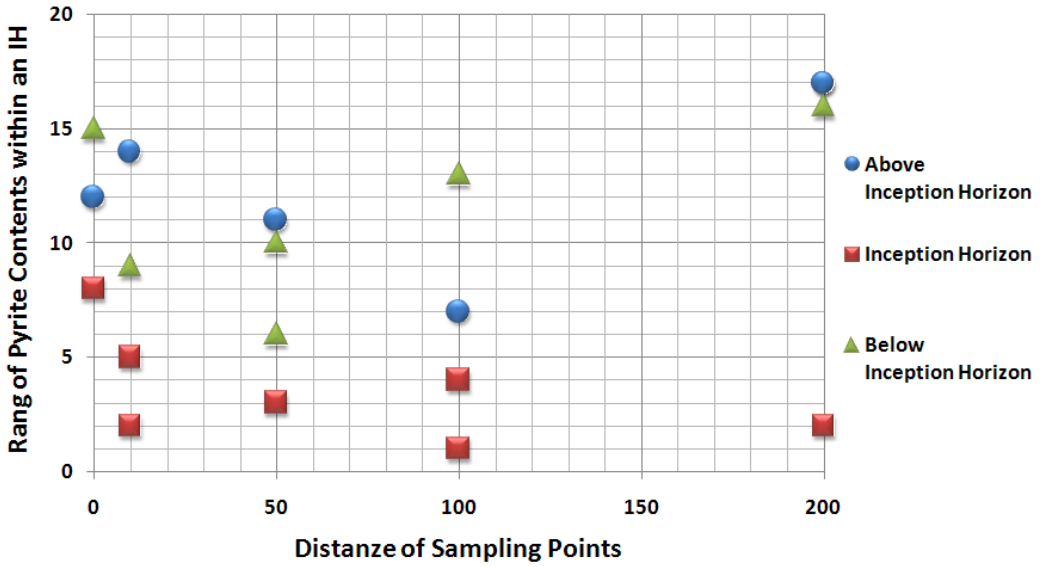

Fig. 3.37: Diagram of the spatial variation of the ranges of the pyrite content along an inception horizon of type 1 (all samples of all sampling points were ranged – Rang 1 is the sample with the highest pyrite content along the horizon). The pyrite content of the inception horizon samples is higher (higher rang) than them of the other samples. (Inception Horizon S2)

3.4.4 Texture of the rock samples

Apart the mineralogical composition, limestones show also a large diversity of texture. The texture describes the general physical appearance of a rock, with respect to the size, size variability, shape and geometric arrangement of its mineral crystals and of its constituent elements

A limestone can microscopically be subdivided into components (e.g. fossils, clastic grains, ooids) and matrix that holds the components together.
The composition of the components of the inception horizons was in the most of the cases not considerably different from them of the surrounding rock mass; foraminifera-rich limestone sometime ooid-rich. Since the inception horizons samples did not show a relevant difference in composition to them of the surrounding rock mass, we did not delve into this aspect. Although some authors reported that that the cave conduits occurred in ooid riches sequences (e.g. Krauthausen and Henne, 1998).

The texture evaluation of our rock samples focused mainly on the matrix type and content, sparite/micrite ratio, size and sorting of the components. The assessment has been done on the thin sections quantitatively or semi quantitatively.

3.4.4.1 Type of matrix

The matrix is the finer grained, interstitial particles that lie between larger particles or in which larger particles are embedded (www.glossary.oilfield.slb.com). In carbonate rocks the matrix consists oftentimes of calcite that precipitated between grains from pore fluids during diagenesis.

The mineralogy composition of the matrix of our samples consists most of the cases of calcite and changed not significantly between the inception horizons and the surrounding rock mass. Nevertheless, it is possible to distinguish by the size of the calcite crystal between two types of matrix: micritic matrix (crystals less than 15 µm) and spartitic matrix (crystals greater than 15 µm).
Previous studies have found that micritic rocks are substantially more soluble than sparitic, this because the area of exposed grain surface is increased (e.g. Sweeting and Sweeting, 1969; Rauch and White, 1977; Dreiss, 1983; Maire, 1990; Eisenlohr et al., 1999). Even though, there are different works done on the subject and some few of them also in terms of the inception horizon hypothesis (e.g. Knez, 1998), the incertitude on the role as well as mechanisms of the type of matrix is still present. Nevertheless, it can be assumed that the matrix type will be significant on the microscopic scale by controlling the dissolution rate.

The analysis of the **types of matrix** showed no remarkably difference between the matrix type of the inception horizons and the surrounding rock mass whereat most of the cases they consist of micritc matrix (fig. 3.38).

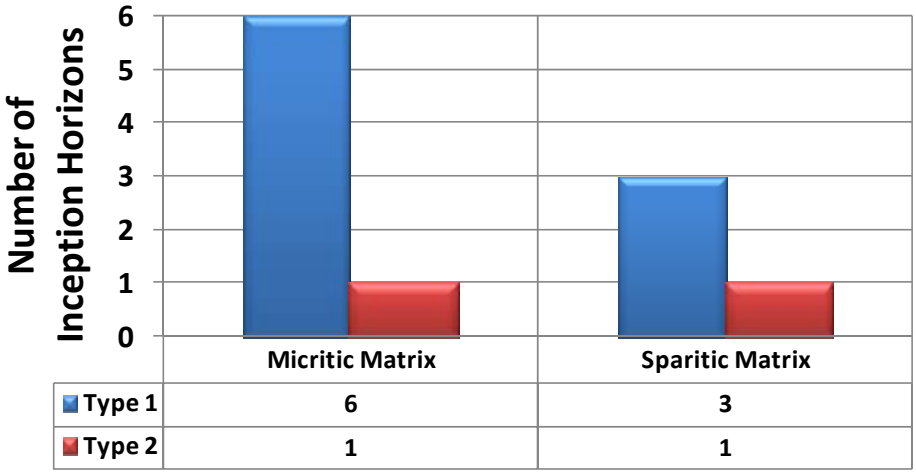

Fig. 3.38: Diagram showing number of inception horizons of type 1 or type 2 with a micritic or sparitic matrix. The diagram shows that in most of the cases the matrix is micritic.

3.4.4.2 Matrix content

Apart the kind of the matrix, we can consider also the matrix content to have an influence on the karstificationon of a rock. Usually, the matrix is more soluble compared to the components albeit both are composed of calcite (e.g. Walter, 1985). The components are for the most part fossils or fragments of fossils (and for a lesser proportion of impurities; see chapter 3.4.3). The poor solubility of the fossils may be caused by a slightly different chemical composition (e.g. a slight silicification or Mg-calcite) or other crystal structure (e.g. Walter, 1985). This different solubility can be observed at different scales: on the macroscopic scale (field observation) where fossils weathered out (fig. 3.39); on the microscopic scale (thin section) where dissolution features can be observed along fossils-matrix contact.

Since we could observe any significant difference in fossil compositions between the inception horizons and the surrounding rock mass (except for the stromatholithic inception horizons – see chapter 3.3.6) we focused the investigation on the matrix content (i.e. the rapport between component and matrix content).

We can assume that the matrix content influences the karstification of an inception horizon by characterising the flow path in microsopic scale as well as affecting the dissolution rate in macroscopic scale (see also chapter 3.6.1).

Fig. 3.39: Example of out weathered fossils (Orbitolinien, Schrattenkalk Formation, Gamsalp, Switzerland). The rock matrix is better dissoluble than the components.

We quantified the **matrix content** by assessing the partition of the matrix in the thin sections. Therefore, we scanned the thin sections and quantify the matrix partition by image processing using JMicroVision (Roduit, 2007). This method allowed us to assess the matrix partition within a reproduction accuracy of around 5 vol-%.

Usually, our limestone samples are quite dense and most of them have between 40 and 70 vol-% of matrix content (matrix supported rocks). The data analysis revealed that the differences between the means (above vs. IH; below vs. IH; above vs. below) are not significantly different from 0 ($T\text{-}Test_{1\text{-}5\%}$); the same is also true for the variances ($F\text{-}Test_{1\text{-}5\%}$). Moreover, there is no evidence for a threshold value of matrix content to identify a given stratigraphical horizon as an inception horizon (fig. 3.40).

Nevertheless, the differences between the inception horizons and the surrounding rock mass are in the order of some 10 vol-% and can be considered as significant ($T\text{-}Test_{1\text{-}5\%}$). Again the data do not suggest the existence of a threshold contrast for an inception horizon (fig. 3.41).

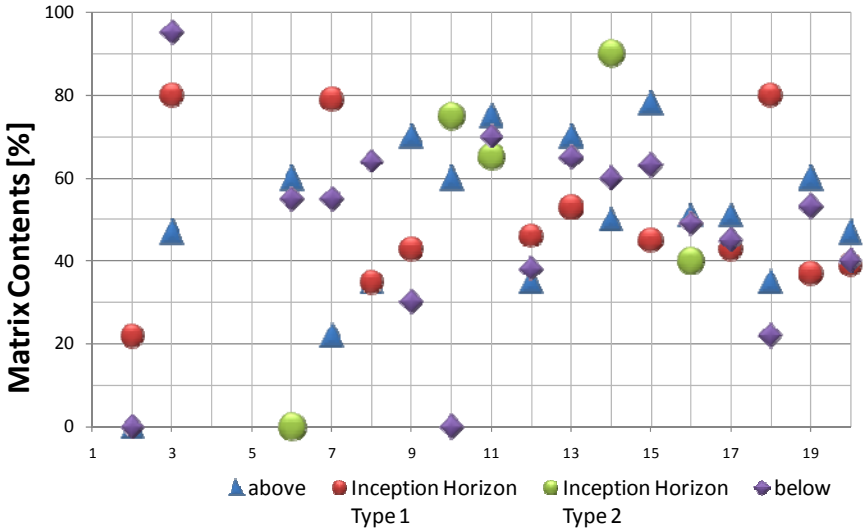

Fig. 3.40: Diagram of the matrix content of the inception horizons and the surrounding rock mass. The matrix content is generally between 40 and 70 vol-%.A priori it is not possible to recognise a threshold values that distinguish incepted horizons from not incepted.

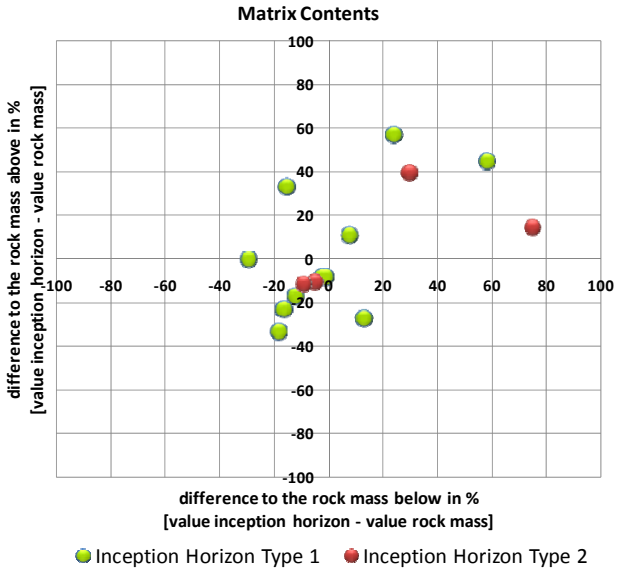

Fig. 3.41: Difference plot of the matrix content between inception horizon and the rock mass below as well as above.

To get an idea of the **spatial variation** of the matrix content along an inception horizon, we analysed the values along a single inception horizon (exemplary presented based on the results of inception horizon S2) (fig. 3.42).

With a statistical T-Test$_{1\text{-}5\%}$ we could not prove that there is a significant difference regarding the averages of the matrix content of the inception horizon samples versus the content of the rock mass above (below); whereas also no significant difference of the rock mass above and below could be found (fig. 3.43).

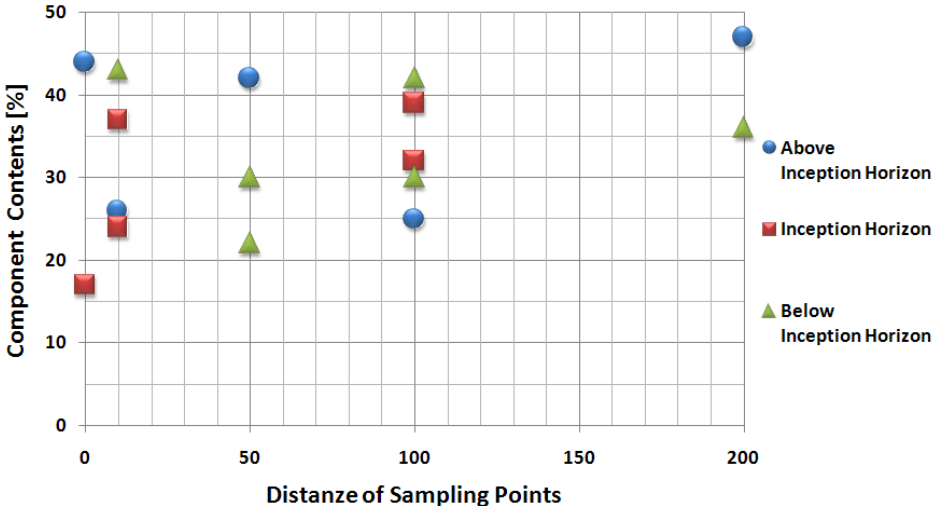

Fig. 3.42: Diagram of the spatial variation of matrix content along an inception horizon of type 1 (S2). No distinction is possible between the inception horizon and the surrounding rock mass samples.

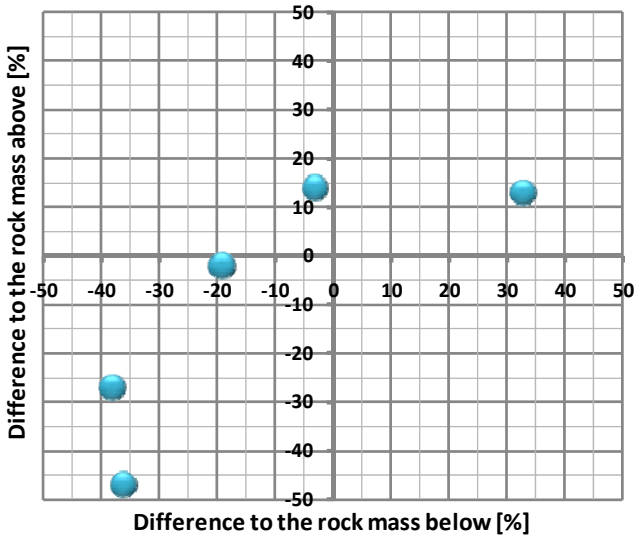

Fig. 3.43: Difference plot of the matrix content between inception horizon and the rock mass below as well as above along an inception horizon of type 1 (S2).

3.4.4.3 Sparite content

Previous studies have found that micritic rocks are more soluble and that solubility decreases substantially where sparite content becomes greater than 40 – 50 % by volume (e.g. Sweeting and Sweeting, 1969; Maire, 1990). Therefore, it is to expect to find a significant contrast in sparite between the inception horizon and the surrounding rock mass. This contrast was considered by some authors (e.g. Lowe, 1992; Ćalić-Ljubojević, 2002) as a characteristic of inception horizons, however without having strong data evidences.

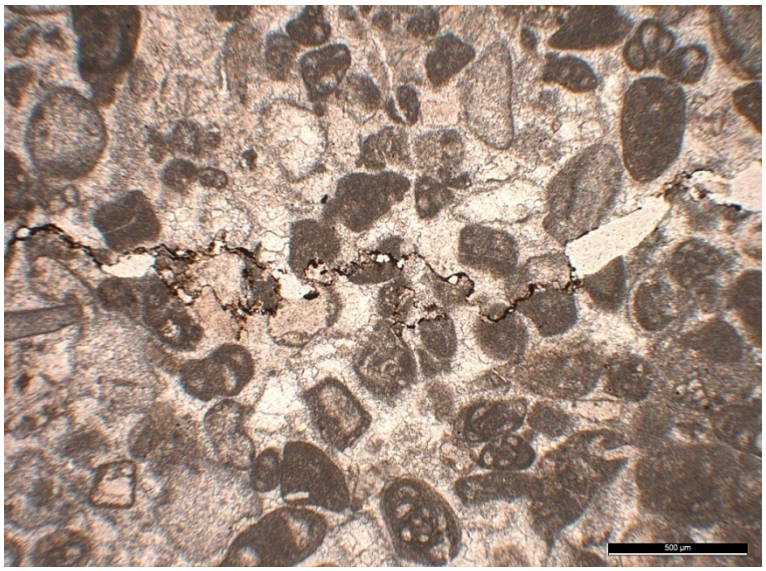

Fig. 3.40: Example of a dissolution seam that developed along the contact between micritc components and sparitic matrix.

We quantified the sparite content of our samples by quantifying the sparite partition by image processing on scanned thin sections using JMicroVision (Roduit, 2007), this allowed us to assess the sparite content within a reproduction accuracy of around 5%.

The assessed thin sections reveal generally a sparite content between 20 and 40 vol-% (fig. 3.45) and therefore below the “sparite knik” (Sweeting and Sweeting, 1969). The detailed data analysis revealed that the differences between the means (above vs. IH; below vs. IH; above vs. below) are not significantly different from 0 ($T\text{-}Test_{1\text{-}5\%}$); the same is also true for the variances ($F\text{-}Test_{1\text{-}5\%}$). Moreover, there is no evidence for a threshold value of sparite content to distinguish incepted horizons from not incepted.

The difference between the inception horizons and the surrounding rock mass is in the order of a few 10 vol-% (fig. 3.46) and can be considered as significant ($T\text{-}Test_{1\text{-}5\%}$). However, again the data do not suggest the existence of a threshold value in difference for an inception horizon; but a slightly majority of the inception horizons have a lower sparite content than the surrounding rock mass (6 of 12 inception horizons of type 1 and 3 of 5 horizons of type 2).

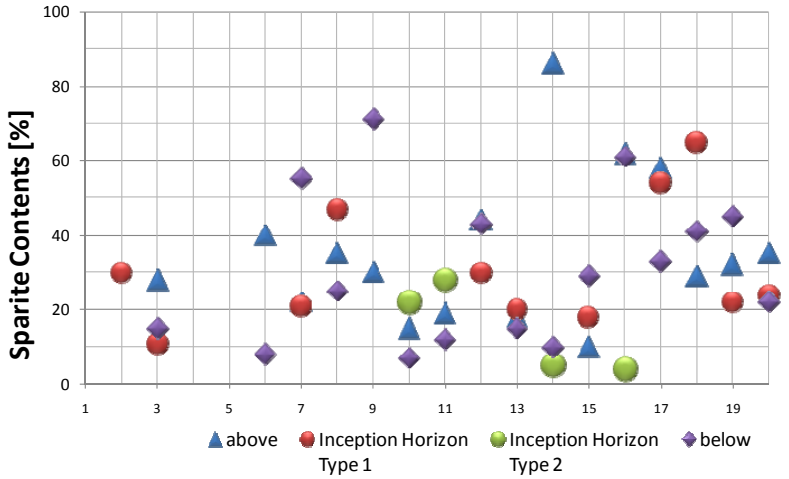

Fig. 3.45: Diagram of the sparite content of the inception horizons and the surrounding rock mass. The sparite content is generally between 20 and 40 %.A priori it is not possible to recognise a threshold values that distinguish incepted horizons from not incepted.

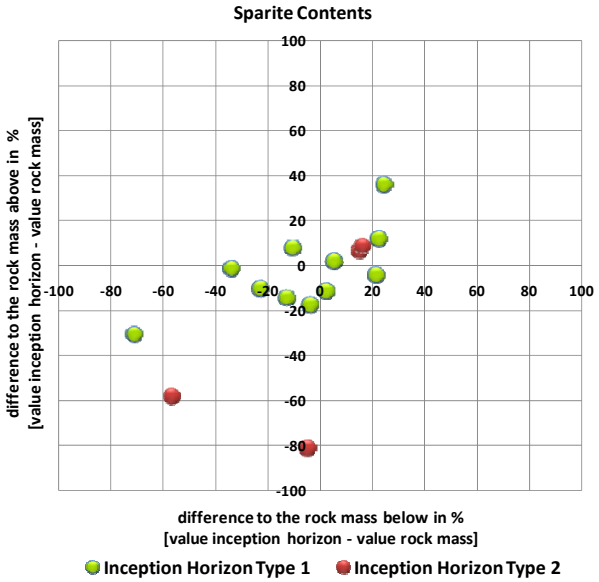

Fig.3.46 : Difference plot of the sparite content between inception horizon and the rock mass below as well as above.

To get an idea of the **spatial variation** of the sparite content along an inception horizon we analysed the values along a single inception horizon (exemplary presented based on the results of inception horizon S2).

With a statistical T-Test$_{1\text{-}5\%}$ we could not prove that there is a significant difference regarding the averages of the sparite content of the inception horizon samples versus the content of the rock mass above (below); whereas also no significant difference of the rock mass above and below could be found (fig. 3.47). Also no tendency was found for the difference of sparite content between the inception horizon and the surrounding rock samples at the sampling points along the inception horizon (fig. 3.48).

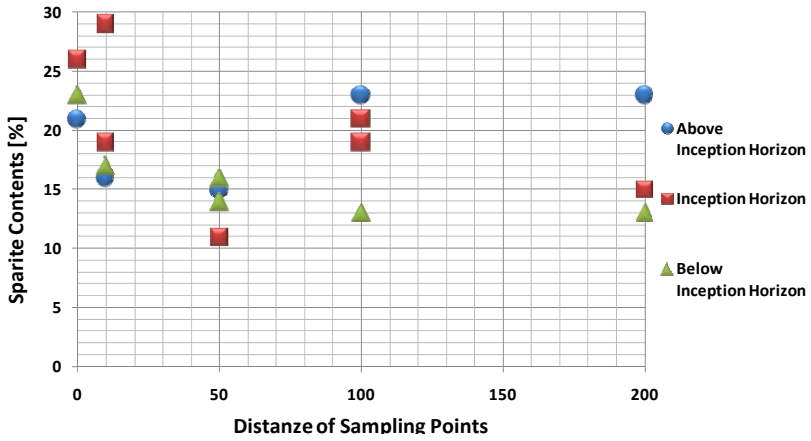

Fig. 3.47: Diagram of the spatial variation of sparite content along an inception horizon of type 1 (S2). No distinction is possible between the inception horizon and the surrounding rock mass samples.

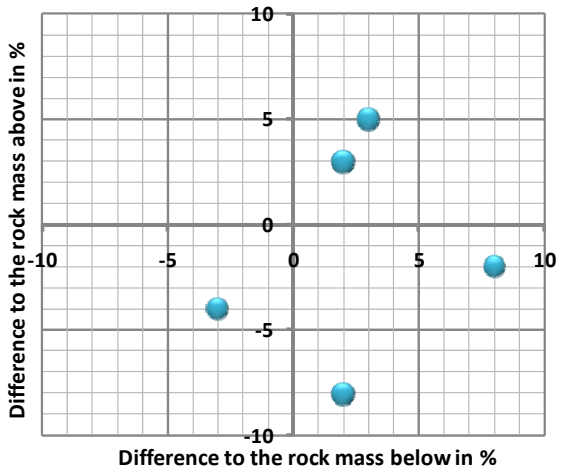

Fig. 3.48: Difference plot of the sparite content between inception horizon and the rock mass below as well as above along an inception horizon of type 1 (S2). No tendency is recognizable in the data points.

3.4.4.4 Grain size and sorting

Generally, it is assumed that the finer the grain size the more soluble a rock tends to be, because the area of exposed grain surface is increased. This is mainly true for the crystal size of the matrix (e.g. Sweeting and Sweeting, 1969; Maire, 1990). For the size of the components this is only restricted valid. Fine grained limestones are sometimes less soluble if the grains are uniform in their size and packing, because surface are than smooth, with exposed grain areas being reduced. Therefore, we can assume that greater the heterogeneity of grain size in a specimen, the greater is the roughness of a dissolving surface (e.g. Noiriel, 2005; Lucia, 2007). All that is true for exposed rock surfaces, like for example in a fracture or the wall of a cave conduit. The relevance of the grain size for the dissolution by a flow through the rock matrix will probably be different, because the selective dissolution will become more significant (e.g. Noiriel, 2005; Brosse et al., 2005).

To estimate variation of the **average grain size** as well as the **grade of grain size sorting** we ranked the images of the inception horizons and the corresponding surrounding rock mass in the order of grain size respectively sorting of the components: Rang 1 means largest grain size respectively best sorted thin section and 3 means smallest grain size respectively the worsted sorted; value 0 means no relevant

difference between the inception horizon and the surrounding rock mass. Of a detailed counting and measuring of the grain size was renounced.

The analysis showed no clear preferred difference of the grain size of the inception horizons compared to the surrounding rock mass (fig. 3.49). This is also valid for the grade of grain size sorting (fig. 3.50), whereas inception horizons of type 1 have a slight tendency to be less well sorted than the surrounding rock mass (5 cases of 10 inception horizons).

Also the correlation between the grain size and the sorting shows no significant relation but only a tendency that samples with a smaller mean grain size are generally better sorted.

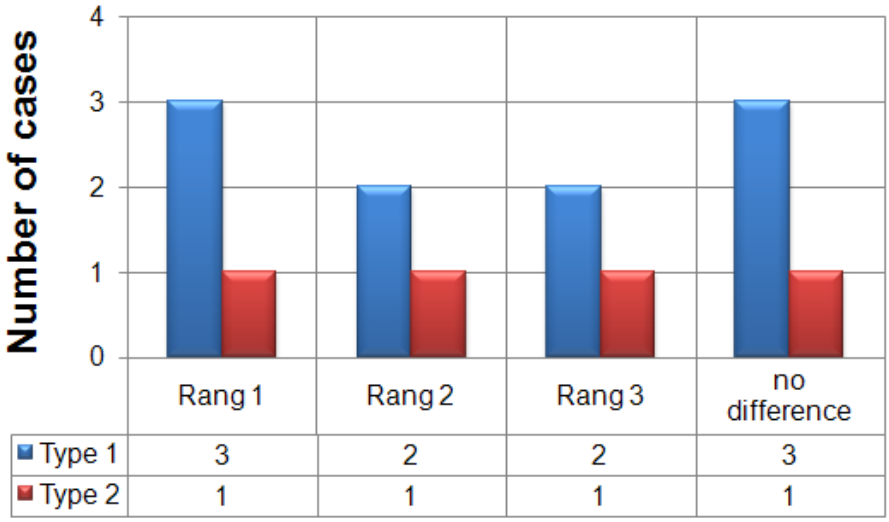

Fig. 3.49: Diagram showing the ranges of the grain size of the inception horizons samples compared to the samples of the corresponding surrounding rock mass samples (Rang 1: size of inception horizon sample is the largest; Rang 3: size of inception horizon sample is the smallest). The data show no clear tendency for the grain size.

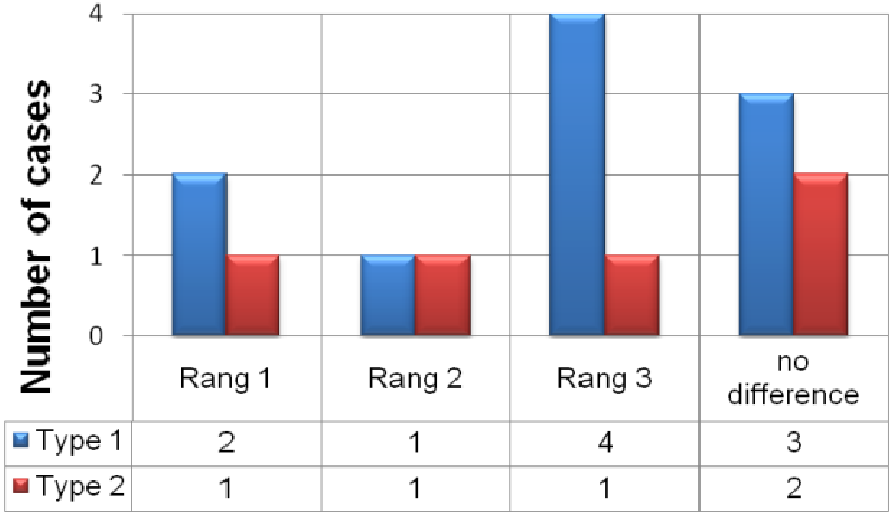

Fig. 3.50: Diagram showing the ranges of the grain sorting of the inception horizons samples compared to the samples of the corresponding surrounding rock mass samples (Rang 1: sorting of inception horizon sample is the best; Rang 3: sorting of inception horizon sample is the worst). The data show a tendency that inception horizons of type 1 are less well sorted than the surrounding rock mass.

To get an idea of the **spatial variation** of the grain size distribution as well as grade of sorting along an inception horizon we analysed the values along a single inception horizon (exemplary presented based on the results of inception horizon S2). Therefore, we ranked the thin sections of all sampling points along the inception horizon (and not like done before each sampling point by them self) (fig. 3.51). With a statistical $T\text{-}Test_{1\text{-}5\%}$ we showed that there are no significant differences regarding the averages of the ranking of the inception horizon samples versus the ranking of the rock mass above (below). This is true for the grain size distribution as well as the grade of sorting.

Also the relative ranking of the average grain size at a sampling point showed no tendency of compared to the surrounding rock mass (fig. 3.52).

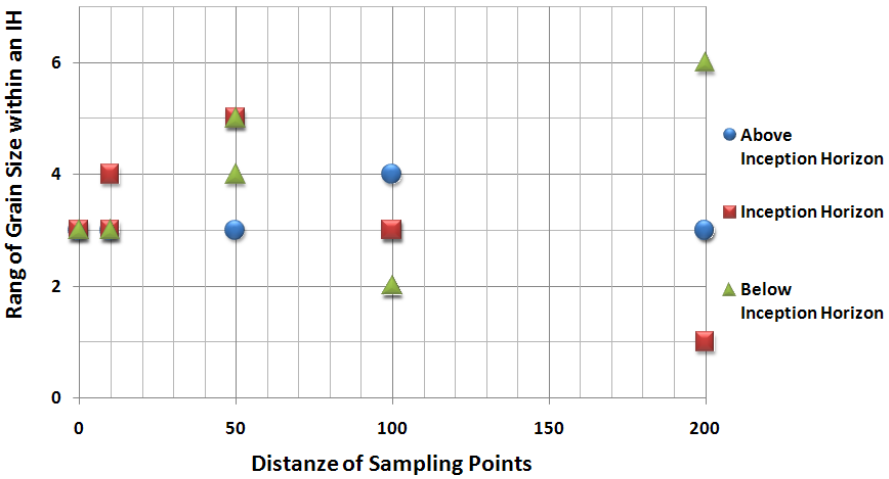

Fig. 3.51: Diagram of the spatial variation of the ranges of the grain size along an inception horizon of type 1 (all samples of all sampling points were ranged – Rang 1 is the sample with the largest grain size along the horizon). No tendency is recognisable. (Inception Horizon S2)

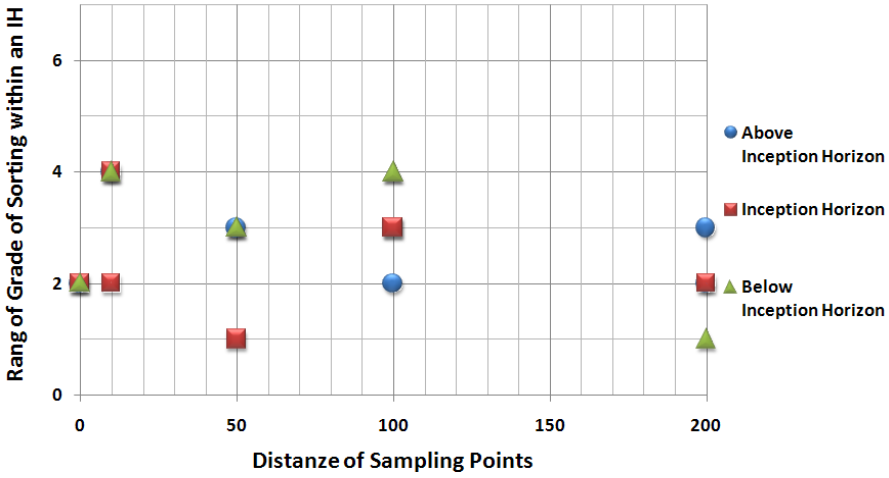

Fig. 3.52: Diagram of the spatial variation of the ranges of the grain sorting along an inception horizon of type 1 (all samples of all sampling points were ranged – Rang 1 is the sample with the best grain sorting along the horizon). No tendency is recognisable. (Inception Horizon S2)

3.4.5 Conclusion of the laboratory analysis

In order to understand the reason(s) why a specific inception horizon is used for cave development, we sampled different inception horizons. Based on the 3D analysis of cave systems and field verifications (chapter 2), we selected a set of 18 inception horizons in six different cave systems. Around 200 micro-cores were sampled and analysed in order to characterize openings, the origin of inception horizons and of the surrounding rock mass. Sampling was designed in a way to approach local as well as regional variations of the selected properties. For this propose, at least three samples were taken at a given place of an inception horizon (one sample from the inception horizon itself and two samples of the surrounding rock mass, one above and one below the inception horizon). For some horizons, several sampling locations were selected in order to assess the regional scale heterogeneity.

Several characteristics of the rock mass play a significant role for speleogenesis: Characteristics controlling the flow path (1), controlling the dissolution rate (2) as well as controlling the dissolution capacity of the water (3).

Some properties appeared to be significantly different at the inception horizons compared to the surrounding rock mass. Others seem not to be significantly different and are therefore, considered as less important for the different karstification of the rocks (tab. 3.7).

For none of the investigated properties it was possible to recognize threshold values that distinguish incepted horizons from not incepted ones. We can suppose that the absolute value of the permeability has only a subordinated significance: it will mainly be the contrast between the properties of inception horizons and the surrounding rock mass which is relevant.

The analyzed samples were extracted from unkarstified places within a rock mass that has been karstified. Along inception horizons, flow paths with the best conditions for karst development were removed. Therefore, the measured values can only minimize contrasts existing at the beginning of the karstification. Nevertheless, we believe that with our sampling strategy we were able at least to qualitatively tackle the trend in variation within the inception horizons as well as compared to the surrounding rock mass. The karstification processes are selective (in microscopic scale still during the phase of cave inception) and concentrates the dissolution/flow along the locally largest dissolution voids/channels/conduits. This will conserve the initially not incepted portion of the inception horizon more or less in the “original” state.

The analysis is based on 18 different inception horizons and therefore only limited representative for all imaginable combination of lithological properties within a limestone (for example horizons with (sedimentary) gypsum are missed). Anyhow, the results give us some good first indications of the key properties as well as processes that occur along the inception horizons.

The measured primary permeability was very low in most of the samples (some 10^{-16} m^2). However, the primary permeability of the inception horizons was significantly different to the surrounding rock mass. This applies for the inception horizons of type 1 (tend to be more permeable) as well as type 2 (less permeable). Observations on the thin sections reveal that this permeability was for most cases due to interparticle pores (matrix pores in Archie, 1952).

The total carbonate content (sum of calcite and dolomite) are in most cases over 80 weight-%. The contrasts between the inception horizons and the surrounding rock mass are significant for the total carbonate content as well as calcite content, but there is no significant difference in dolomite content. Furthermore, we found only a significant correlation between total carbonate and calcite content. While for inception horizons of type 1, we observed horizons with higher and lower carbonate content, all inception horizons of type 2, had a lower carbonate content than the surrounding rock mass. The content of dolomite seems to be a not relevant property.

Most of the impurities are attributable to clay minerals. In addition also quartz and pyrite were often observed, but they represent only a little fraction of the impurities. The contrast in quartz content between the inception horizon and the surrounding rock mass seems to be significant for inception horizon of type 1 (slightly higher quartz content within the inception horizons), but not significant for inception horizons type 2.

In contrast the pyrite content of the inception horizons of type 1 as well as 2 was in almost all cases significantly higher within the inception horizon than at the surrounding rock mass.

For inception horizons of type 1 the matrix type was significantly more often micritic, the matrix content slightly lower and the components less sorted than the surrounding rock mass, but the sparite content as well as the grain size differed not significantly. However, for inception horizons of type 2, none of these properties seem to be significantly different within the inception horizons.

These conclusions suggest that some properties are significant for karstification, but give no weighting among the properties (i.e. which associated processes are more important). This will be the topic of the next chapters 3.5.

Investigated Property	**Significance** [1=significant, 3=not]		**Feature Characteristic** [↑= higher; ↓= lower]		**Speleogenetic Meaning**
	Type 1	**Type 2**	**Type 1**	**Type 2**	
Primary Permeablity	**1**	**1**	↑	↓	Flow Path
Total Carbonate Content	**1** (2 groups)	**1**	↑↓	↓	Dissolution Rate
Calcite Content	**1** (2 groups)	**1**	↑↓	↓	Dissolution Rate
Dolomite Content	**3**	**3**	-	-	Dissolution Rate Flow Path
Quartz Content	**1**	**3**	↑	-	Flow Path Dissolution Rate
Pyrite Content	**1**	**1**	↑	↑	Dissolution Capacity
Matrix Type	**1**	**3**	**Micrite**	-	Dissolution Rate
Matrix Content	**(1)**	**3**	↓	-	Dissolution Rate Flow Path
Sparite Content	**3**	**3**	-	-	Dissolution Rate
Grain Size	**3**	**3**	-	-	Flow Path Dissolution Rate
Sorting of the Grains	**(1)**	**3**	↓	-	Flow Path Dissolution Rate

Tab. 3.7: Summary of the investigated lithologic properties. The table shows which property occurences are statistical significant different within the inception horizon compared to the surrounding rock mass and their characteristic occurrences within the inception horizon (i.e. if the occurrence is tendency higher or lower than at the surrounding rock mass) and their speleogenetic meaning.

3.5 Multivariate statistic to identify types of Inception Horizons

The previous chapter presents the investigation on various lithologic properties (contrast of properties) of the inception horizons and the corresponding surrounding rock mass. The characteristics of some properties turned out to be significant different within the inception horizons compared to the surrounding rock mass, where others show no significant difference and can be therefore considered as not relevant for karstification (tab. 3.7).

Until now, it remains unclear how these significant properties should be weighted. This means, which is the most important property (contrast in property) for the karstification of an inception horizon. Linked to that is the question: if there exist different types of inception horizons that are characterised by a certain combination of properties and therefore have other karstification processes occurring along them.

Already the field observations suggest that 3 types of inception horizons exist: inception horizons where the cave inception took place within the horizon inception (1); at the contact with the inception horizon (2); along bedding plane fractures (3). Whereas only the first two were investigated and sampled during our study. We can assume that the characteristics of these types are different and should be also possible to distinguish them based on property characteristics.

3.5.1 Data preparation

To use the assed data of the laboratory analysis for the statistical treatment we transformed them into equivalent data ranges (some of the original data are ordinary other metric of different order of size). This has been done ones with a transformation to rang data (the value of a the inception horizon has been ranked in relation to the values of the other samples of the sampling point – rang 0: no difference; rang 1: value of the inception horizon is higher than the values of the surrounding rock mass; range 2: value of the inception horizon is intermediary; rang 3: value of the inception horizon is the lowest) and a second time with normalize the mean difference between the inception horizon value and them of the surrounding rock mass ($x_n = \frac{x-\bar{x}}{x_{max}-x_{min}}$) whereat we normalized around 0 ($\bar{x} = 0$) to have all data range comparable.

3.5.2 Occurrence Matrices

The aim of influence factor analysis is to get the relationship of certain combination of factor occurrences. Therefore, we looked at the frequency of combination of two factors (e.g. how often was the carbonate content of inception horizons the lowest and at the same time the pyrite content the highest value compared to the surrounding rock mass). As results we get 55 individual matrices of combinations of two properties (11 properties). This was performed for inception horizons of type 1 and type 2 (appendix 2).

For inception horizons of type 1 the matrices indicates that these horizons have usually increased primary permeability with an micritic matrix and/or an increased pyrite and/or total carbonate content and/or are poorly sorted.

Unfortunately, we probed only a few inception horizons of type 2, therefore we can consider the results of the analysis only as an indication. Nevertheless, the horizons seem to be characterised by a lower primary permeability and a higher pyrite content compared to the surrounding rock mass.

3.5.3 Correspondence Analysis

The correspondence analysis (Benzécri, 1973) is a method of factoring categorical variables and displaying them in a property space which maps their association in two or more dimensions. The results provide information that allows exploring structure of categorical variables. The method is conceptually similar to principal components analysis, but scales the data (which must be positive) in a way that rows and columns are treated equivalently. Where conventional factor analysis determines which variables cluster together, correspondence analysis determines which category values are close together (Greenacre, 1993). This is visualized on the correspondence map, which plots points (categories) along the computed factor axes, which emerge from principal components analysis. Correspondence map provides a graphical display of attributes and individual samples, where the distance between the points is a measure of the similarity (correlation). Groups of sample points characterize members of a specific family; whereas grouping of attributes indicate correlation between attributes.

A complete explanation of this method is present in a number of publications (e.g. Davis, 1986; Greenacre, 1993)

Correspondence analysis is an exploratory and not a confirmatory technique. It makes no assumptions about the distribution of the data (nonparametric technique) and has no requirement on the sample size.

One restriction of the correspondence analysis is that the method can handle only positive values. Therefore, we shifted the value range to be greater than 0.

Missing data were replaced by statistically expected values.

The applied correspondence analysis applied on our data reveals that the first factor (F1 - factor axis, which emerge from principal components analysis) accounts for 46 % and the second factor (F2) accounts for 22 % of the total variation (tab. 3.8). The attribute end-members on the F1 axis are quartz content and primary permeability. The end-members on F2 axis are matrix content and at the other site the sparite and pyrite content. The close position of sparite and pyrite suggests that they should be related together. It is to notice that the first and the second factor represent together only 69 % of the total variation wherefore we interpret also the F1-F3 correspondence map whereat the end-members on F3 axis (16 % of total variation) are sparite content and total carbonate content.

Correspondence Analysis - Rang

		F1	F2	F3	F4	F5
	Eigenvalue	0.04	0.02	0.01	0.01	0.00
	Inertia (%)	46.2	22.4	15.6	12.9	3.0
	Cumulative %	46.2	68.6	84.2	97.0	100.0
Weight (relative)		F1	F2	F3	F4	F5
Matrix Contents	**0.19**	0.00	**0.48**	0.22	0.03	0.07
Sparite Contents	**0.18**	0.01	**0.28**	**0.38**	0.07	0.07
Quartz Contents	**0.12**	**0.74**	0.00	0.01	0.03	0.09
Pyrite Contents	**0.13**	0.00	**0.20**	0.03	0.06	**0.57**
Total Carbonate	**0.19**	0.00	0.04	**0.20**	**0.57**	0.00
Primary Permeability	**0.19**	**0.23**	0.00	0.15	**0.23**	**0.19**

Missing value replaced by expected value

Tab. 3.8: Correspondence analysis of the rang values of the inception horizons. The F1 axis accounts for 46 % and the second F2 for 22 % of the total variation. The attribute end-members on the F1 axis are quartz content and primary permeability and for the F2 matrix content and sparite-pyrite content.

The correspondence maps feature a high clustering of sample points at the centre of the asymmetric plots and the property points radial distributed around them (fig. 3.53 and fig. 3.56). The cluster of sample points

allows not to distinguishing between different groups/types of inception horizons. Not even the distinction between the in the field clearly identified inception horizon types 1 and 2 (see chapter 3.3.1). This is true for the plots on F1-F2 axis as well as for F1-F3 axis. The detachment of the sample point 1c in the F1-F3 axis plot is due to missing of property values.

The property points are well distributed on the axes. At the F1-F2 axis plot the pyrite and sparite content are close together what suggest that they could be related. However, this correlation cannot be confirmed on the F1-F3 axis plot, whereat this plot suggests in return a similarity in matrix and sparite content.

The placement of the property points relative to the cluster of the sample points shows that there is no unique property that controls the behaviour of the samples (sample points cluster around a property point). This means that the characterisation of the cluster is only possible by the use of all properties. However, a stronger influence can be assumed for the total carbonate content as well as the primary permeability and pyrite in a lower order of influence. The missing of a key property is also recognizable by the more or less uniform relative weighting of the properties (tab. 3.8).

The here presented results are based on the "rang scaled" data. However, the analysis done with normalized mean differences gives comparable results.

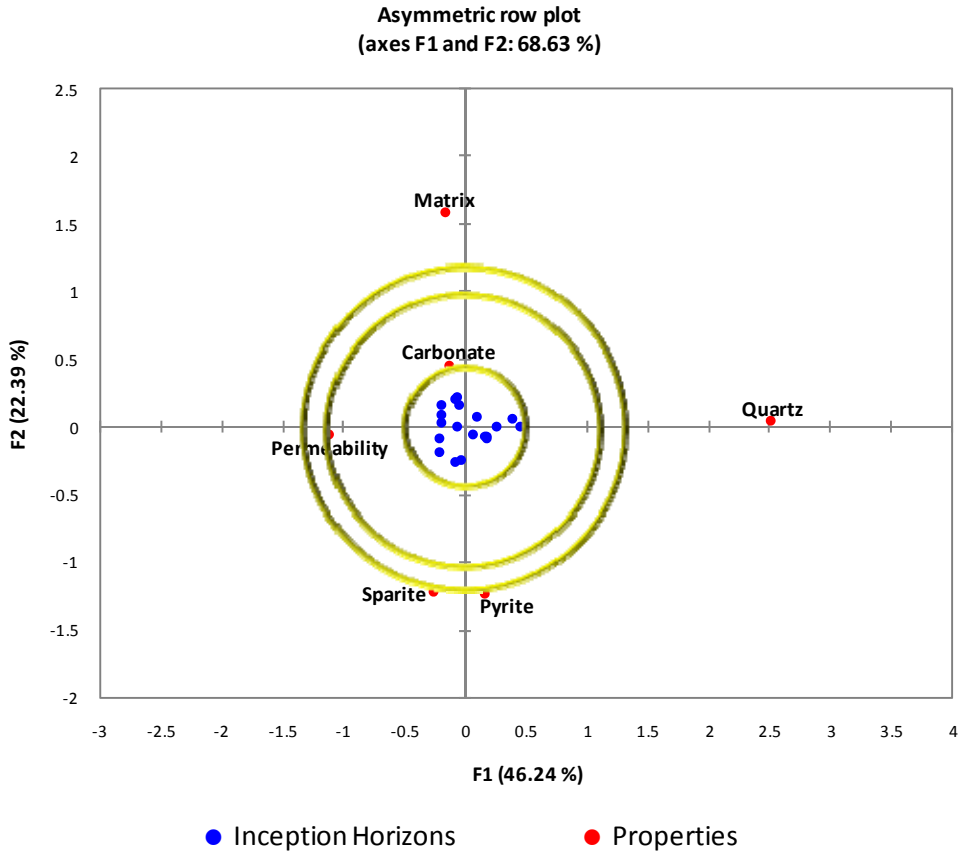

Fig. 3.53: Correspondence map of the F1-F2 axis. The cluster of sample points allows not to distinguishing between different groups/types of inception horizons. The vicinity of the cluster to the property point of carbonate content suggests a strong dependence of them.

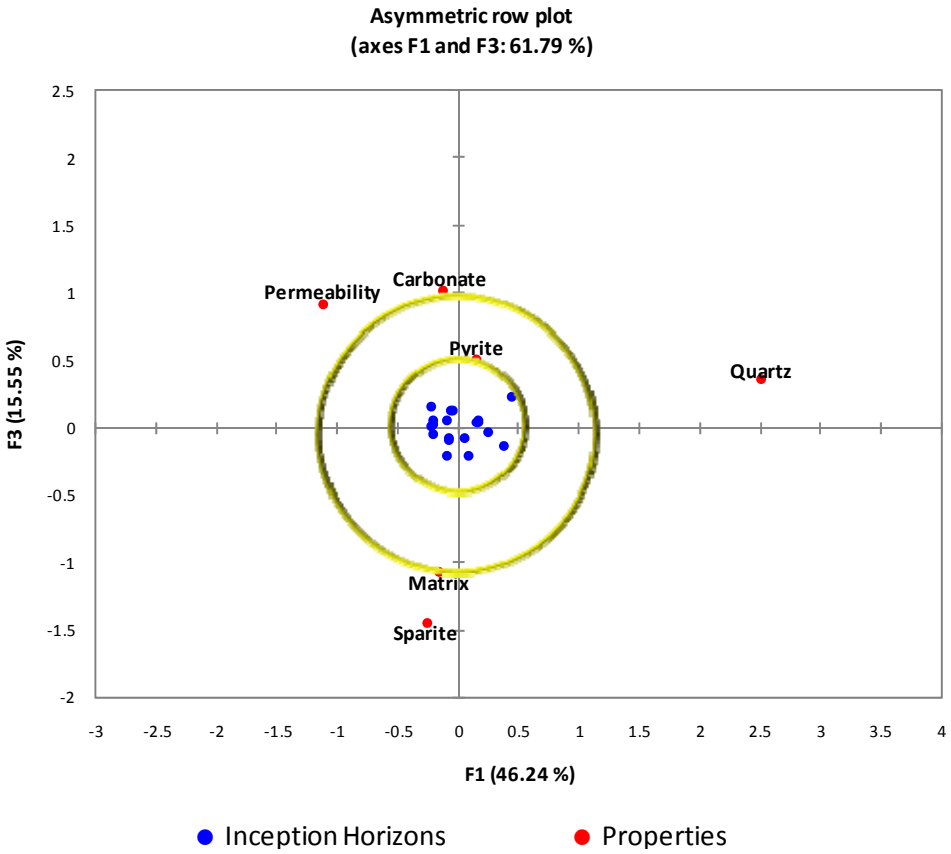

Fig. 3.54.: Correspondence map of the F1-F3 axis. The cluster of sample points allows not to distinguishing between different groups/types of inception horizons. The vicinity of the cluster to the property point of pyrite content suggests a strong dependence of them.

3.5.4 Agglomerative hierarchical clustering

Cluster analysis is an exploratory data analysis method which aims to sorting different "objects" into groups in a way that the degree of association between two objects is maximal if they belong to the same group and minimal otherwise (e.g. Mardia et al., 1979). A number of clustering algorithms were developed, of which we used the agglomerative hierarchical clustering (Ward's method; Ward, 1963). This method starts with every single sample in a single cluster. In successive iterations it agglomerates (merges) the closest pair of clusters by satisfying some similarity criteria (geometric distance in the multidimensional space of the attributes - Euclidean distance), until all data are in one cluster (bottom-up method). The automatic truncation of the number of clusters (dotted line) is based on the entropy and tries to create homogeneous groups. A particularity of the chosen Ward's method is that they do not weight the properties.

For each node in the clustering plot (where a new cluster is formed) we can read the dissimilarity value (i.e. the criterion distance to the next hierarchical cluster), what gives an order of magnitude for the dissimilarity between two hierarchical clusters. The greater the distance the bigger the dissimilarity of the clusters are and contrariwise.

The cluster analysis maps two distinct clusters of inception horizons, which correspond to the distinction of inception horizon type 1 and type 2 (fig. 3.55). This distinction was done very well for type 1 (no error in assignment) and a bit less well for type 2 with three inception horizons that were wrong assigned. This two "main groups" were clustered on the key factor of permeability whereas the permeability of cluster 2 was less permeable (type 2) and cluster 1 more permeable (type 1).

The automatic truncation of the clusters (dotted line) suggests subdividing cluster 1 in two subclusters. These subclusters differ mainly on the content of total carbonate and pyrite (tab. 3.9). However, it is to note, that the dissimilarity of this two subclusters is less distinct than between cluster 1 and 2.

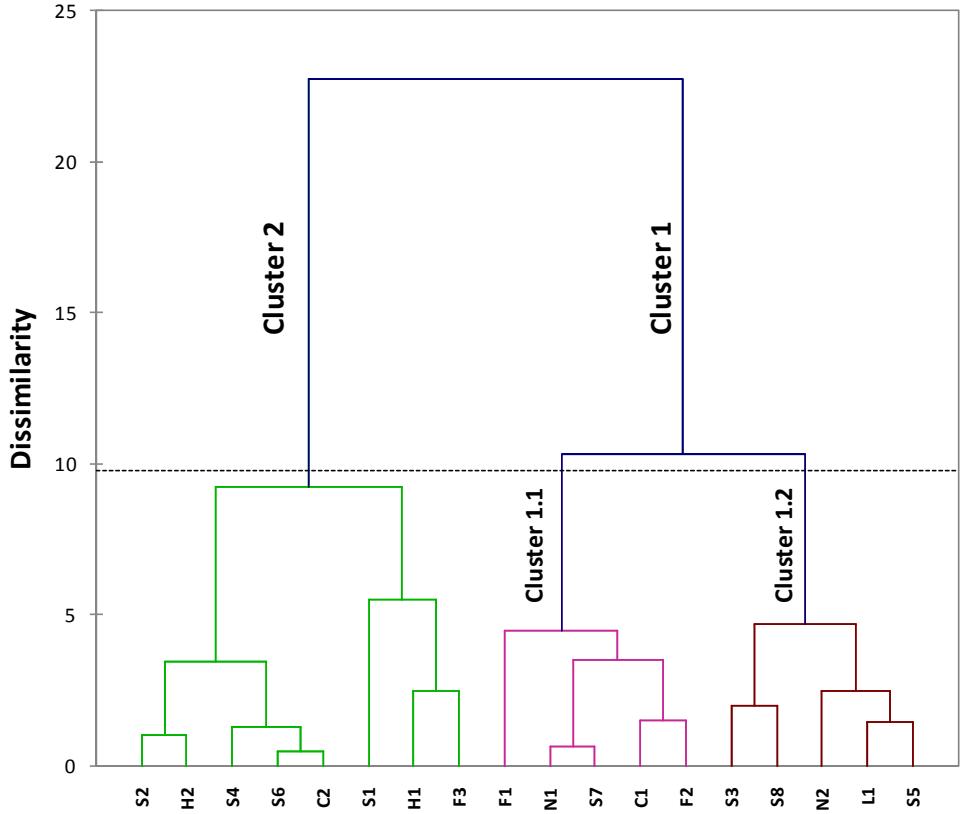

Fig. 3.55: Agglomerative hierarchical clustering. The cluster analysis maps two distinct clusters of inception horizons that correspond to the distinction of inception horizon type 1 and type 2.

Cluster	Name of Incetion Horizon	Type of Inception Horizon	Matrix	Sparite	Quartz	Pyrite	Carbonate	Permeability
1.1	N1	1	-	1	1	1	1	*1*
1.1	C1	1	1	3	0	1	1	*1*
1.1	F1	1	2	1	0	0	3	*1*
1.1	F2	1	2	-	0	0	1	*1*
1.1	S7	1	1	1	1	1	1	*1*
1.2	N2	1	2	3	1	1	3	*1*
1.2	L1	1	-	-	3	1	3	-
1.2	S3	1	3	2	3	1	1	*1*
1.2	S5	1	2	2	2	1	2	*1*
1.2	S8	1	3	2	1	1	1	*1*
2	*H1*	*1*	*1*	*3*	*0*	*1*	*2*	*3*
2	*S2*	*1*	*3*	*1*	*1*	*1*	*3*	*3*
2	*S6*	*1*	*3*	*3*	*0*	*1*	*3*	*3*
2	C2	2	3	2	0	-	3	*3*
2	F3	2	1	1	0	1	1	*3*
2	H2	2	3	1	0	1	2	3
2	S1	2	1	3	1	3	3	*3*
2	S4	2	3	3	-	1	2	*3*

Tab. 3.9: The agglomerative hierarchical clustering of the ranges positions of the inception horizons. The two first order subclusters differ mainly on the contents of total carbonate and pyrite.

3.5.5 Conclusion for multivariate statistics

The employed statistical methods get similar results, while the hierarchical clustering was able to distinguish almost correct between inception horizons of type 1 and 2 (by the main factors total carbonate and pyrite contents), was it not possible do distinguish any groups with the correspondence analyses. Therefore, the correspondence analysis suggest that the primary permeability, the total carbonate, the pyrite and the matrix contents are the "key factors" that distinguishe the inception horizons from the surrounding rock mass.

It is to notice that our statistical conclusions are based only on 18 different inception horizons and is therefore not representative for all imaginable combination of lithological properties within a limestone. Anyhow, the results give us some good indications about the key properties and processes that occur along the inception horizons.

Through the application of statistic we assumed that the processes behind the properties are additive (with a certain weighting of the properties), i.e. the processes occurred simultaneously. However, it is more likely that the processes are successively related, that means that a process can be only dominant during a certain phase of speleogenesis. Therefore, a "time" related weighting of the processes would be more adequate. Nevertheless, the statistical analysis gives some good ideas about the properties (and associated with them which processes) that can be consider as dominant. It will be the topic of the discussion (chapter 3.6.1) to identify the processes and assign them to the different phases of speleogenesis.

3.6 Discussion about the properties of the inception horizons

18 inception horizons in six cave systems were selected for field characterisation and sampled in order to identify the properties and processes that make these horizons susceptible to karstification. The analysis of around 200 rock samples from the horizons as well as surrounding rock mass showed that the characteristics of some properties turned out to be significantly different within the inception horizons compared to the surrounding rock mass, where others show no significant difference and can be therefore considered as not relevant for karstification (tab. 3.7). The challenge will be now to recognize the speleogenetic role of these horizons.

3.6.1 During which speleogenetic phase is a given property the key property? - The Speleogenetic Scale of Influence

Multivariate statistics simply discover structures in data without explaining why they exist and if they really exist (chapter 3.5). Albeit the statistical methods use different weighting of the investigated properties, they assumed that the related processes occurred at the same time. However, it is to expect that during speleogenesis, the importance/role of the parameter(s) will change, because they were consumed (e.g. pyrite or bedding plane with gypsum) or the associated speleogenetical processes become subordinated to others (e.g. primary permeability distribution). Therefore, statistics can only be applied to recognise groups of inception horizons with similar properties/contrast in properties. The challenge would be to recognise for each identified property as well as the associated speleogenetical processes the speleogenetical phases where they are a main or a subordinated speleogenetical factor.

We suggest to approach this challenge with the ”speleogenetic scale of influence". The scale of influence considers the increase in porosity produced by the speleogenetic processes associated to one specific property. For example, the scale of influence of a pyrite crystal is determined by the dissolution capacity of the sulphuric acid, produced by the weathering of the pyrite (i.e. around 6 time the size of the pyrite crystal; e.g. Bögli, 1978). This means that the influence of the pyrite on the speleogenetic process can be assumed to be potentially relevant as long as the size of the pores is smaller than around 6 times the average size of pyrite crystals. After that, the effect of additional dissolution capacity becomes subordinate to other processes. Contrary other processes can only become a dominant factor when the pores have already a certain size, for example, the total carbonate content only has an influence on the dissolution rate of a rock mass when the pore surface is larger than some square millimetres.

We can combine this scale of influence of a property/process with the general concept of the inception horizon hypothesis. The inception horizon hypothesis (Lowe 1992, 2000) distinguishes between three different phases of the development of a karst conduit. The karstification of inception horizons is supposed to start during the so called **cave inception phase** (Lowe 1992, 2000); it can be defined as starting as soon as the pore space increases steadily due to dissolution processes (Filipponi et al. 2008). One may expect that at this early phase the pore size is small (some micrometres - chapter 3.4.1), the dissolution is still low and slow. When relief becomes steeper (upper part of the phreatic zone – see chapter 4), higher gradients do occur, flow becomes increased and therefore also the dissolution (speleogenetic phase of **cave gestation**). *It is to notice that the transition from the cave inception to the gestation phase is not defined by the permeability of the rock mass but by the change of the hydraulic boundary conditions* (see chapter 4). We can assume that at least a pore size of around 0.01 mm (fig. 6.1) is required at this stage to allow a cave development in realistic time scale (chapter 6). The cave gestation phase ends at the time the karst conduit is large enough to allow turbulent flow (breakthrough – changing form laminar to turbulent flow condition – pore size of around 1 cm). From this point on, conduit development is fast and caves can reach human size within a few thousands of years (e.g. White, 1988; Dreybrodt and Siemers, 2000; Palmer, 2002). This corresponds to the **cave development phase**.

We will now discuss the scale of influence of different lithological properties and hypothesize when one specific property, identified in chapter 3.4, becomes dominant factor during speleogenesis (fig. 3.56). Please note that this assignment to the speleogenetic phases is only a rough estimation and need to be refined in the future.

Primary Permeability

The primary permeability determines the initial flow along a horizon. By definition, the primary permeability will be the main factor at the beginning of the karstification process. The permeability measurements and the successive thin section analysis showed that also a small number of secondary pores will increase the permeability substantially. Therefore, we can assume that the scale of influence is quite small. However, we may expect that at this early stage of the karstification, the dissolution is low and slow and therefore the duration of influence will take a long time anyhow.

Total Carbonate Content / Content of Impurities (/Calcite Content)

The total carbonate content (calcite content) affects the dissolution rate of the rock (e.g. Rauch and White, 1977; Bögli, 1978). We can assume that this influence is only relevant when the pore surface is larger than some millimetres square. Below this pore size, the dissolution rate of single minerals will be determinant (selective dissolution). Therefore, we assign the total carbonate content to the end of the speleogenetic phases of cave gestation until the end of the cave development.

Dolomite Content

The dolomite crystals can be considered as poorly soluble compared to the surrounding calcite matrix. The occurrence of dolomite crystals affects in microscopic scale the flow path by representing "obstacles" in the porous rock matrix (dissolution features smaller than the crystal size). This causes a concentration of flow around the crystals and thus a local increase in dissolution. We can assume that this concentration effect will already occur at early stage of karstification (early phase of cave inception) and become insignificant when the pore size reaches approximately the size of the crystals (end of cave inception phase).

In the macroscopic scale (dissolution features larger than the crystal size) the dolomite content affects the dissolution rate of the rock (reducing the dissolution rate; e.g. Liu and Dreybrodt, 2001). Like for the total carbonate content, we can assume that this effect becomes important if the pore surface is larger than some square millimetres (from the end of the cave gestation phase).

Therefore, the dolomite content will enhance the karstification within the inception phase and slow them during the cave development phase.

Content of Clay Minerals

Clay minerals being impurities, they have an effect on the dissolution rate of a rock (see section total carbonate content). Apart that clay minerals can be weathered out of the matrix and clog the pores - in this sense a negative property. This effect may only occur when the pores are large enough to allow a weathering out of the clay minerals, but still small enough to be clogged. This will probably be the case between the end of the cave inception phase and the beginning of the cave gestation. It is important to note that the clogging of cave passages can also occur later by allochthonous cave sediments. However, this need to be distinguished from the autochthonous clogging discussed here.

Pyrite Content

The scale of influence of a pyrite crystal is determined by the dissolution capacity of the sulphuric acid produced by the weathering process (i.e. around 6 time the size of the pyrite crystal, e.g. Bögli, 1978). For the speleogenetic process, this means that the influence of the pyrite can be assumed to be potentially relevant as long as the size of the pores is smaller than around 6 times the average size of pyrite crystals; after that the effect of the additional dissolution capacity becomes subordinate by the other processes.

Quartz Content

Quartz minerals being impurities, they have an effect on the dissolution rate of a rock (see section total carbonate content). Apart that quartz grains affect the flow concentration in the macroscopic scale (up to the scale of the grain size), by presenting an "obstacles" in the permeable rock matrix and causing a concentration of flow. We can consider that this flow concentration occurs already early in speleogenesis (early cave inception phase) and become insignificant when the pore size reaches approximately the size of the grains (end of cave inception phase).

Sedimentary Gypsum

Under hypersaline conditions, highly soluble minerals such as gypsum can be deposited within a carbonate sequence. These minerals are commonly more soluble than carbonates, (gypsum possess a solubility that is around 10 to 30 times higher than calcite; Bögli, 1978). The dissolution of such minerals can increase the porosity/permeability of a bedding plane significantly. This process can occur already at the beginning of the cave inception phase and continue till the speleogenetic phase of cave development. The limiting factor will be the quantity of the available gypsum. In some extreme cases, the gypsum horizon is thick enough to allow the complete cave development within gypsum layer (e.g. Moggerenschacht, Wutachschlucht in South-Germany) in other cases, the horizon is only some millimetres thick and initiates only the cave development along the horizon.

Type of Matrix

The type of matrix (i.e. the crystal size of the matrix) determines the dissolution rate of the matrix: the smaller the crystals the higher the dissolution rate. Therefore, the scale of influence will also be in the same scale (some micrometers) and can be integrated into the speleogenetical phases of early cave inception till early cave gestation.

Matrix content

We have seen that the permeability of our samples was mainly caused by matrix porosity (chapter 3.4.1.2). Therefore, the matrix content is an index for the flow concentration within a rock volume; the lower the content the more concentrated the flow. On the other hand, the calcite matrix has most of the time a higher dissolution rate than the components. For both effects (concentration of flow and higher dissolution rate) we can assume that they are already present at early stage of cave inception phase and will be subordinary processes when the pore size reaches the size of the grains.

Contrary a low matrix content will reduce the dissolution rate at macroscopic scale. Therefore, we can assume that this becomes important if the pore surface is larger than some square millimetres (from the end of the cave gestation phase).

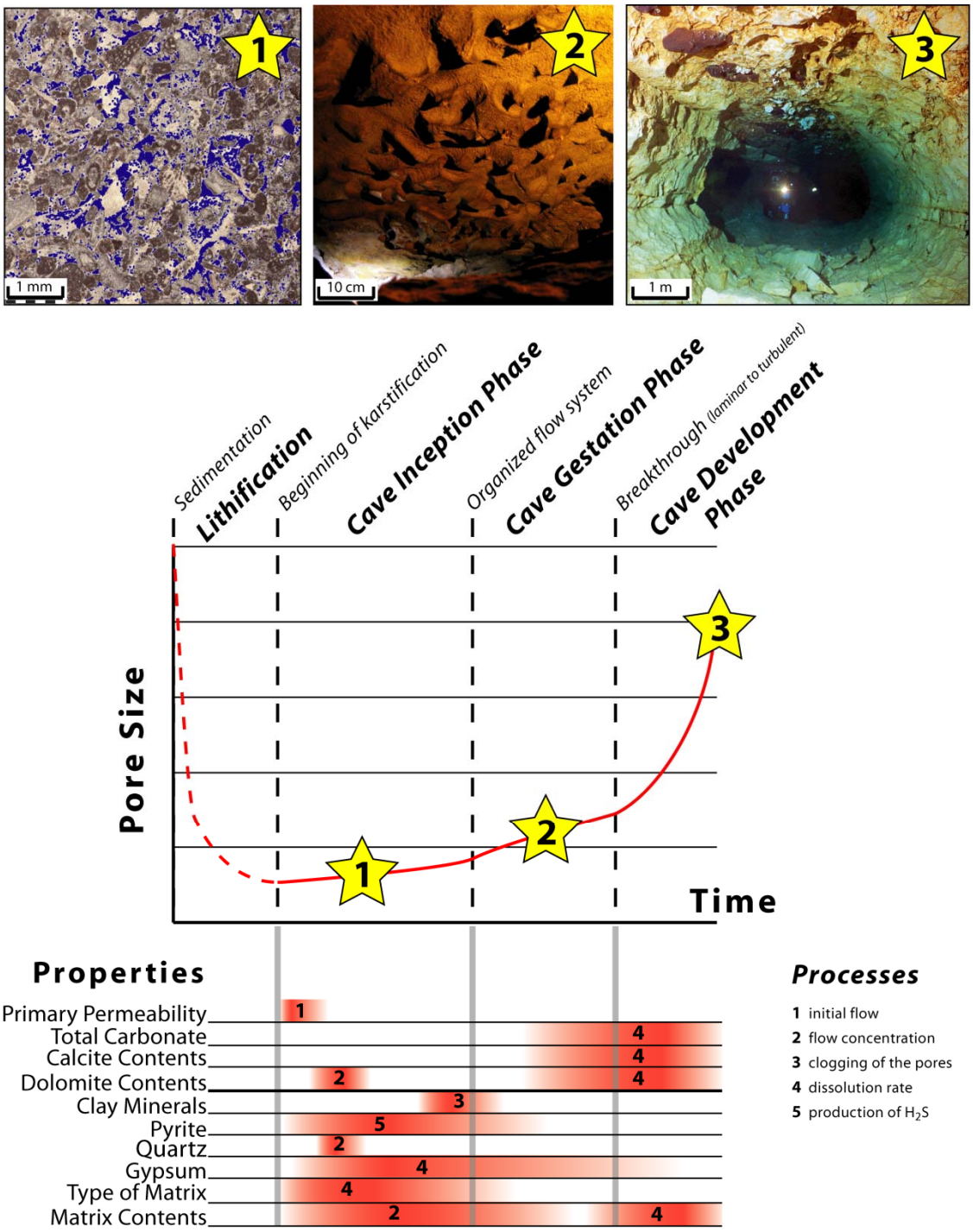

Fig. 3.56: The speleogenetic scale of influence of different lithologic properties. The properties (i.e. the associated speleogenetic processes) are only significant during certain speleogenetic phases.
The beginning of the karstification can be defined by the moment from which the permeability of a pore space increases steadily. During the cave inception phase the pore size is small and the dissolution still slow. During the cave gestation phase the flow becomes increased because of changes in the hydraulic boundary conditions, therefore, also the dissolution will be increased. The breakthrough marks the change from laminar to turbulent flow regime within the conduit; the karst conduit will develop faster and becomes a cave.
3.56.1: dissolution voids on microscopic scale.
3.56.2: network of small karst conduits (anastomoses).
3.56.3: phreatic cave conduit (photo: Steffen Gross).

From the above estimation about the scale of influence and the incorporation into the general concept of the inception horizon hypothesis, we recognize (apart from the special case of gypsum) that the properties are only of importance during certain phases of speleogenesis. Properties, that influence the flow concentration, are rather situated within the cave inception as well as gestation phase; on the other hand, properties that affect the dissolution rate of the rock are supposed to control the speleogenesis rather late during the phase of cave gestation and development.

Furthermore, we can identify which lithologic property tend to be more important at a given speleogenetic phase: the primary permeability for the beginning of the karstification, the pyrite content as well as the matrix content and matrix type for the inception and gestation phase and the total carbonate content for the cave development phase. Please note that these are the same properties that have also been identified by the multivariate statistics to be "key factors".

wereThe scale of influence explains from a lithologic point of view why some horizons are better karstified than others (the hydrogeologic aspects will be discussed in chapter 4). Thus stratigraphic horizons with a low permeability, sparitic matrix and only little pyrite content will take longer to be incepted than high permeable horizons with a micritic matrix and a lot of pyrite. But in both cases, the further development of the cave conduit depends on the total carbonate (i.e. of the dissolution rate of the rock). However it is to notice that horizons with a disfavourable constellation of the properties can also be incepted, they just need more time. The evidence that in a rock mass there are only few horizons with a distinct cave development suggests, that for most of the horizons the time needed to be incepted (i.e. reach a pore size/permeability, that allows a karst conduit development within the cave gestation and development zone; chapter 4) exceed the available time given by the hydrologic boundary conditions (see also chapter 6.1).

We can assume that for the **inception horizons of type 1** (where the cave inception took place within the inception horizon) the primary permeability will be the relevant factor at beginning of karstification. The matrix content and type as well as the content of pyrite are the key factors during the later phase of cave inception and gestation. For further development, the total carbonate content will be crucial. This explains also why we could observe inception horizons of type 1 with a lower primary permeability than the surrounding rock mass. The low primary permeability has been compensated by lower matrix content as well as a higher pyrite content.

For **inception horizons of type 2** (where the cave inception took place at the contact with the inception horizon), we can suggest that the low primary permeability, the clogging of the pores by the clay minerals and the high content of pyrite (production of aggressive solutions within the horizon that concentrate the dissolution along the contact to the surrounding rock) may be responsible for the karstification at the contact (see also chapter 6.1.2).

Although we considered a multitude of processes, some remain abstract away, like for example the hydrocarbon maturation or the shale dewatering, which can provide aggressive fluids for dissolution (e.g. Moore, 1989; Wright, 2002). However, if they occured they will be significant during the burial of the formation (mesogenetic; Choquette and Pray, 1970) and therefore, probably before the beginning of the karstification. However, further investigations on these aspects could be interesting.

3.6.2 The role of fractures within the inception horizons hypothesis

It should be noted that at the above discussion (chapter 3.3.1) ignores the occurrence of fractures. The analysis of chapter 2 showed that a not negligible number of cave conduits developed along the intersection of inception fractures with inception horizons. The occurrence of fractures is in most cases a late phenomenon of the history of a rock mass, most cases after the beginning of karstification. The fractures cause a substantial increase in permeability; whereat horizons with largest permeability just before their intersection by fractures are supposed to give intersections with the highest permeability too, but with value some orders of magnitude higher than without fractures (e.g. Kiraly, 1969). This increase in permeability can be that significant that it allow skipping some speleogenetic phases (fig. 3.5.7). It permits in some "extreme" cases cave development without a significant increase in permeability during cave inception and/or gestation phases (also named as "tectonic inception", if tectonics produces a fracture network wide enough to allow turbulent flow; Faulkner, 2006). However more common is a less increase in permeability of some few orders of magnitude, what still means that it dramatically reduces the time requirement of the gestation phases (chapter 6.1.1).

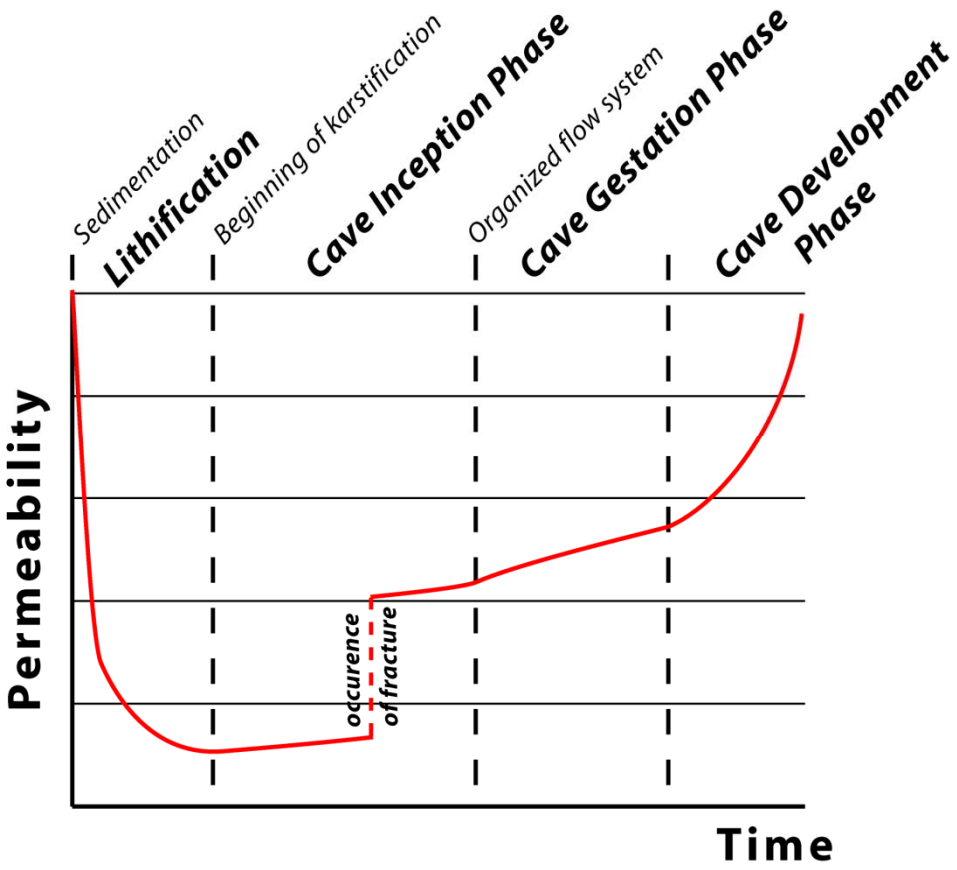

Fig. 3.56: Schematic development of a karst conduit: The fractures cause a substantial increase in permeability and can be that significant that it allow skipping some speleogenetic phases.

3.6.3 Comparison to previous studies

Already some previous studies accepted the challenge to understand the role of the lithologic properties for the karstification processes. The problem to compare the results of these published analyses is that the samples often are from unknown stratigraphic positions within a given formation (other sampling strategy) as well as other choice in the investigated parameters or investigation method. However some consentaneity could be found.

Rauch and White (1977) analysed 17 rock samples (Upper Ordovician, central Pennsylvania). The rock samples were selected from rock units which vary greatly in both lithology and cave development. They measured the dissolution rate of the rock samples on laboratory experiments and compared them with lithological properties (micrite content, grain size of the micrite, sparite content, allochems (carbonate grains), rhombs (only whole euhedral crystals), content in quartz and feldspar and pyrite content). From a principal component analysis, they deduced that the dissolution rate is most strongly associated directly with the percentage CaO and inversely with MgO. This indicates the inverse effect of dolomite content on dissolution rate. Furthermore, they found a strongly inverse relationship between dissolution rate and grain size of the micrite as well as disseminated clay.

The significant difference of this study compared to ours is the different time scale of dissolution, whereas laboratory experiments run for some days to weeks, the natural karstification occurs during millions of years. Therefore, it is to expect that slow processes (like for example the acid production by pyrite weathering) will not appear significant in their analysis (supposed to be the dominate processes in early stages of speleogenesis). In contrast our results reflect a combination of different speleogenetic phases, beginning at early stage of cave inception (see chapter 3.6.1) up to the phase of cave development. However, both results show a clear dominance of the carbonate content. Therefore, we can assume that the carbonate content will probably be one of the most important factors during the speleogenetic phase of the cave development (and the others dominant in other phases).

It is to point out, that Rauche and White (1977) looked at the relation between lithologic properties and dissolution rate and therefore, worked with absolute values whereas in our study we compared incepted horizons with not incepted (i.e. surrounding rock mass) and therefore, looked at contrast in properties.

Goldstrand and Shevenell (1997) analysed 27 samples from two boreholes into the Maynardville Limestone (Oak Ridge, Tennessee). With the correspondence analysis, they looked for the relationship between the measured porosity and lithological properties (content in clay, calcite, dolomite, sparite, micrite). They demonstrated that the attribute porosity plots near the dolomite attribute, indicating a strong correspondence between dolomite and higher porosity. Conversely, samples associated with micrite, sparite, and clay do not correspond with higher porosities.

Compared to the study of Rauch and White (1977) we can assume that the study of Goldstrand and Shevenell (1997) investigate the factors at early stages of karstification (a direct relationship to the development of conduits is missing). Unfortunately, they missed to indicate if the porosity was primary or secondary. Furthermore, the authors conclude that the result reaffirms the petrographic observations that porosity is directly related to dedolomitization of the dolomitic facies.

Dreiss (1983) analysed 59 rock samples (Ordovician-Lower Mississippian carbonates, South Missouri). Her sampling strategy was similar to ours. She observed that in her case studies the conduits had typically a “keyhole type” cross-section (like for example fig. 2.13). She interpreted this profile as a cause of different solution resistivity of the rock. Therefore, she took samples from the resistant wall (most of the time the “canyon” of the keyhole profile), non-resistant wall (the ellipse of keyhole profile) and ceiling. It is to assume that what she describes as a non-resistant wall would be probably for us an inception horizon. On the rock samples, she measured the content in porosity, micrite, sparite, CaO, MgO, insoluble residue, quartz and opaque minerals as well as the size and sorting of the grains.

She analysed the data by the linear discriminant analysis (this statistic method attempts to model the difference between the classes of data by linear combinations of variables) and could group the non-resistant wall samples correctly in one group by the variable of grain size (group of relatively fine-grained samples). The data/method did not allow distinguishing the resistant wall samples from the ceiling samples.

These results are not consistent with ours although we applied similar sampling strategies. While for Dreiss the grain size was the main variable to distinguish the “inception horizons” form the surrounding rock mass, our data showed no evidence of such a tendency for the grain size or a significant difference in grain size between inception horizons and the surrounding rock mass.

Knez (1998) analysed more than 300 thin sections (Skocjanske Jame, Slovenia) of an outcrop with 3 inception horizons (he named them “formative bedding planes”). He concluded that the rock of this three inception horizons is typically damaged (indicating interbedded sliding), has a slightly higher calcite level and a lower porosity than the surrounding rock mass.

The sampling strategy of this study was similar to ours, he sampled and analysed also the inception horizon as well as the surrounding rock mass. However, it is not clear if the tectonic damage of the inception horizon is done by a “bedding plane fracture” or a “dissolution induced fracture” (see chapter 3.3.1).

The "ghost rocks" are described as in-situ, iso-volumetric alteration of limestone with conservation of the rock structure like for example the stratification (Vergari, 1997). These horizons with depleted cohesion are found in quarries (e.g. Vergari and Quinif, 1997), mines (e.g. Wienin and Bruxelles, 2008) or in boreholes up to 100 m of depth (Vergari, 2003). Within the inception horizon hypothesis, we can consider these horizons as an extreme appearance of inception horizons of type 1, that were sufficiently long within the cave inception zone, (chapter 4.4) up to the rock matrix was almost completely dissolved. A particularity of these horizons is that the cave gestation and development phase is not dominated by the dissolution processes but by the mechanical washout of the “residual” rock (e.g. Vergari, 1998; Wienin and Bruxelles, 2008).

Different authors (e.g. Choquette and James, 1988; Bosák et al. 1989; Esteban, 1991; Tinker et al., 1995; Moore, 2001; Muldoon et al., 2001; Ćalić-Ljubojević, 2002; Garasic, 2009) describe that cave development was observed along second or third order cycle boundaries (phenomena named also as “karst stratigraphy”; Bosák, 2002) (fig. 3.58). A sequence stratigraphic cycle is a chronostratigraphic unit defined as a succession of genetically related textures (beds) bounded by marine flooding surfaces and their correlative surfaces by eustatic and glacioeustatic changes in sea level (Lucia, 2007).

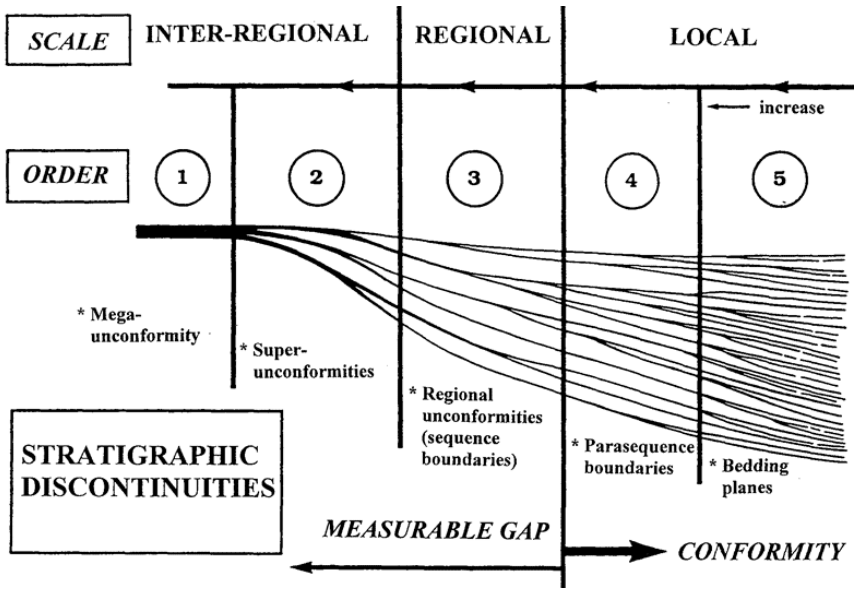

Fig. 3.58: Hierarchy of stratigraphic discontinuities (Bosák, 2002; modified after Esteban, 1991).

A quick literature review on the topic yield that most of these “cycle boundary caves” can be considered as paleokarstic (a karst formed in the past under an earlier erosion cycle and is preserved by burial or suspension of karstification processes [www.speleogenesis.info]). Their developed are in response to freshwater lenses during exposure at the end of the cycles, i.e. at the freshwater-marine mixing zone by the process of mixing corrosion (e.g. Wright and Smart, 1994; Mylroie and Mylroie, 2007). It is to notice that the caves did not develop at the contact itself but some tens of metres below (at the time of exposure, the cycle boundary was the erosive surface, i.e. the karst surface). During exposure “classical” epigenic karstification also occurs (surface karst features, vadose and phreatic cave development) but they seem to be of minor significance. This karstification of poorly lithified limestone is also called syngenetic karstification (Jennings, 1968) and depends on the duration of the exposure, the climatic conditions (mainly rainfall) and the magnitude of the lifting (Budd and Vacher, 1991). During major see level changes (third- or second-order changes), the residence time of the carbonate sediments in the meteoric zone will be long enough, perhaps some few ten thousand years, and the falls will create sufficient topographic relief. As a result, a significant karstification will occur, contrary to shorter cycles (fourth- or fifth-order changes) (Esteban, 1991; Wright and Smart, 1994).

Only a few and contradicting scientific papaers could be found on the question about syngenetic karstification being preserved during deep burial (mesogenetic; Choquette and Pray, 1970) and following uplifting conditions (telogenetic); as well as if and how the paleokarst features will interact with younger karst development (e.g. Schmoker, 1984; Scholle and Halley, 1985; Osborne, 2002; Audra et al., 2007).

The karst areas studied in this thesis can be considered as telogenetic. In some study areas “paleokarst fossils” (lithified sediment filling of cave conduits) could also be observed (fig. 3.59). However, the stratigraphic position of these paleokarst occurrences could not be correlated with any of the identified inception horizons. Therefore, we can assume that syngenetic karstification has a subordinate importance to the later karstification of a telogenetic rock mass. However, it is clear that in eogenetic rock mass (shallow burial, Choquette and Pray, 1970) syngenetic karst features are better preserved and the impact on younger karstification will also be high (e.g. Budd, 2004).

The investigated inception horizons can be considered as fifth- or fourth order changes and therefore, only minor syngenetic karstification is to expect (Wright and Smart, 1994). It is and thus not explained by the karst stratigraphy hypothesis.

Lowe’s (1992) literate discussion about the paleo-karstification and its relationship to cave inception come to a similar conclusion. But he underlines the role of paleo-surfaces and the associated stratigraphic horizon, for example deposit of evaporites, clay layer or organic rich deposits.

Fig. 3.59: Paleokarst conduit on the surface of the Siebenhengste karren field (between the dashed lines). It was not possible to establish a relationship between the paleokarst occurrence and the statistically identified inception horizons.

The comparison with previous studies confirms at least some of our results, especially the role of the carbonate content. However, our results also show clearly the important role of the primary permeability as well as the pyrite content. This is probably due to our sampling and investigation strategy that does not only reflect a single speleogenetical phases but considers different phases (chapter 6.1).

3.6.4 Epigenic or hypogenic caves?

In this thesis, we analysed and sampled cave systems that are considered to have developed under epigenic conditions (caves formed by water recharged from the surfaces due to surface CO_2) (chapter 2.3). Whereas "hypogenic caves are formed by water in which the aggressiveness has been produced at depth beneath the surface, independent of surface or soil CO_2 or other near surface acid sources" (Palmer, 2000). We could show that during early karstification (cave inception phase) the karstification can be enhanced by pyrite weathering acid production, therefore, with a subsurface acid source (chapter 3.4.3.2 and chapter 3.6.1). Should therefore, the caves be reclassified as hypogenic caves?

We think that this is not the case. The distinction between epigenic and hypogenic should only be referred to the cave gestation and development phases. Thus, we suggest to extend Palmer's definition (2000) into: *The speleogenetic processes of the gestation and development phases of* hypogenic caves are characterized by water in which the aggressiveness has been produced at depth beneath the surface, independent of surface or soil CO_2 or other near surface acid sources.

3.7 Conclusion about what makes a bedding plane favourable to the karstification

Field observations lead us to conclude that most of the inception horizons are some centimetres to decimetres thick and that three kinds of inception horizons can be distinguished:

Type 1: Inception horizons where the cave inception took place **within the inception horizon**;

Type 2: Inception horizons where the cave inception took place **at the contact with the inception horizon**;

Type 3: Inception horizons where the cave inception took place **along bedding plane fractures**.

Based on the 3D analysis of cave systems and on field verifications, 18 inception horizons in six cave systems were selected for field characterisation and sampling in order to identify the properties and processes that makes these particular lithostratigraphic horizons favourable to karstification. Around 200 rock samples from these horizons and surrounding rock mass were analysed. Sampling was designed in a way to approach local as well as regional variations properties.

We investigated several parameters controlling the early flow path characteristics, the dissolution rate of the rock and/or the dissolution capacity of the seepage water of inception horizons. Some of the investigated properties are significantly different within the inception horizons compared to the surrounding rock mass. It is to notice that the data did not allow identifying threshold values of the properties or differences to distinguish between inception horizons and surrounding rock mass. Therefore, we suppose that the absolute value of the permeability has only a subordinated significance: It is mainly the contrast between the properties of inception horizons and the surrounding rock mass which is relevant. For example, an inception horizon is expected to develop because it is significantly more permeable than the surrounding rock mass and not because his permeability is higher than a given value.

It is expected that during the karst development the importance/role of the properties(s) will change, because they were consumed or the associated speleogenetical processes become subordinated to others. To recognise for the different spelegenetical processes/properties the speleogenetical phase where they are a main or a subordinated speleogenetical factor, we introduced the ”speleogenetic scale of influence". The scale of influence considers the increase in porosity produced by the speleogenetic processes associated to a property.

The laboratory analysis and the estimation of the speleogenetic scale of influence lead us to conclude that for inception of **horizons of type 1,** the contrast between inception horizons and the surrounding rock mass in primary permeability will be the relevant factor at the beginning of karstification, whereas the contrast in matrix content and type as well as the content of pyrite are the key factors during the later phase of cave inception and gestation phases. For the further cave development phase, the contrast in total carbonate content will be crucial. Fractures propagate in most of the cases through the inception horizons if they are less thick than around 15 centimetres; at thicker horizons, we often observed fracture occurrences within the inception horizon. The fractures are responsible for a substantial increase in permeability, whereat horizons with largest permeability, just before their intersection by fractures, are supposed to give intersections with the highest permeability too, but with value some orders of magnitude higher than without fractures (chapter 6.1). This increase in permeability results in a skipping of certain speleogenetic phases (mainly the cave inception and/or gestation phases).

For inception **horizons of type 2,** we can assume that the low primary permeability, the clogging of the pores by the clay minerals and the high content of pyrite (production of aggressive solutions within the horizon that concentrate the dissolution along the contact to the surrounding rock) compared to the surrounding rock mass may be responsible for the enhanced karstification at the contact during cave inception and gestation phases. Fractures often end at the contact with inception horizon of type 2 and are maybe responsible for fracture propagation along the contact (chapter 6.2). The occurrence of these fractures will increase the permeability along the inception horizons and favour the karstification along them.

Our conclusion is based on 18 different inception horizons and therefore, only limited representative for all imaginable combinations of lithological properties within a limestone (for example horizons with (sedimentary) gypsum are missed). Anyhow, the results give us some good first indications about the properties and processes along the inception horizons, notably for inception horizons of type 1. Further case studies are needed and will help to refine our results to be able to fully describe or even numerical modelling the cave inception phase. Especially for inception horizons of type 2, which were under representative in our sample collection, as well as type 3, which were excluded of our investigation.

- 4 -
The Role of the Position and Orientation of Inception Horizons relative to the hydrogeological Boundary Conditions

4.1 Introduction

The analyses of the 3D geometry of some of the largest speleological conduit networks in the World (in chapter 2) remarkably confirmed and quantified an old idea already developed in the sixties and seventies, that the development and position of karst conduits under phreatic conditions is strongly related to a restricted number of discrete lithostratigraphical horizons (i.e. inception horizons; e.g. Rauch and White, 1970; Waltham, 1971; Rauch and Werner, 1974; Palmer, 1974, 1975, 1989; Ford and Cullingford, 1976; Lauritzen, 1988, Lowe, 1992). It also appeared clearly that the influence of these horizons onto the 3D geometry of cave systems is high (chapter 2). This does not mean that fractures have no role in cave development, but in most cases (inception) fractures control the conduit orientation at a local scale and along inception horizons according to the regional hydraulic gradient (fig. 4.1). In other words most phreatic conduits are developed along the intersection between inception horizons and fractures, which are the most parallel to the hydraulic gradient (chapter 2).

Compared to fractures, inception horizons do represent structures that are present already during lithification of the rock mass whereas fractures do occur most of the time later in the history of the rock mass (chapter 3.6.1). Another factor is that stratigraphical horizons are more likely to be efficient for driving water lateral from the recharge area to the discharge point because they are wider and more parallel to the hydraulic gradient than fractures (chapter 2.2.4.4).

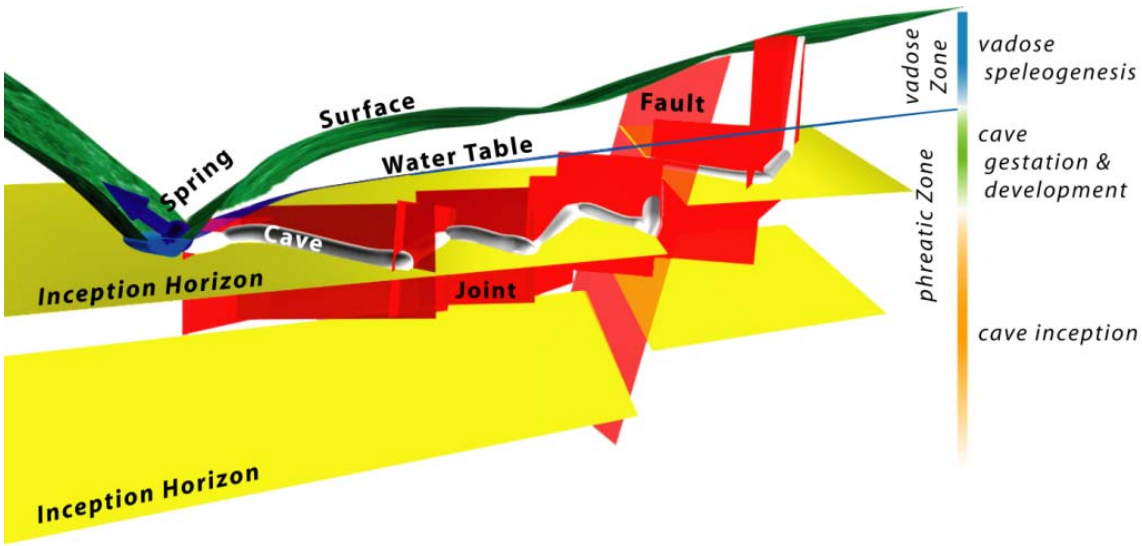

Fig. 4.1: Schematic 3D model of a karst conduit system: The geometry of phreatic conduits is determined by inception horizons, joints and faults as well as by the hydraulic gradient. The inception horizon hypothesis expects that the karstification of a rock mass pass through different speleogenetic phases, whereas different parts of the rock mass are in different karstification state (at the same time).

It is known that the process of karstification follows a positive feedback development; the rock being soluble, water dissolves it and enlarges the voids, which become able to accept more water to flow through, i.e. more dissolution to be active and the voids to enlarge faster (e.g. Kiraly, 1975). This loop is self-developing until the system of conduits can absorb the total amount of the water available from the rain with no significant increase of the hydraulic gradient.

Bosák (2002) noticed that it is not easy to determine the beginning of the karst evolution: "The beginning and the end of the life of living organisms are really clear and can thus be precisely determined and described. On the other hand, to establish the beginning and the end of the life of a karst system is a substantial problem. The dating of karst evolution poses philosophical problems." However, we can assume that the end of the lithification and the beginning of the karstification occur when the rock permeability starts to increase steadily due to dissolution (i.e. dissolution processes > chemical and mechanical compaction) (Fig. 4.2).

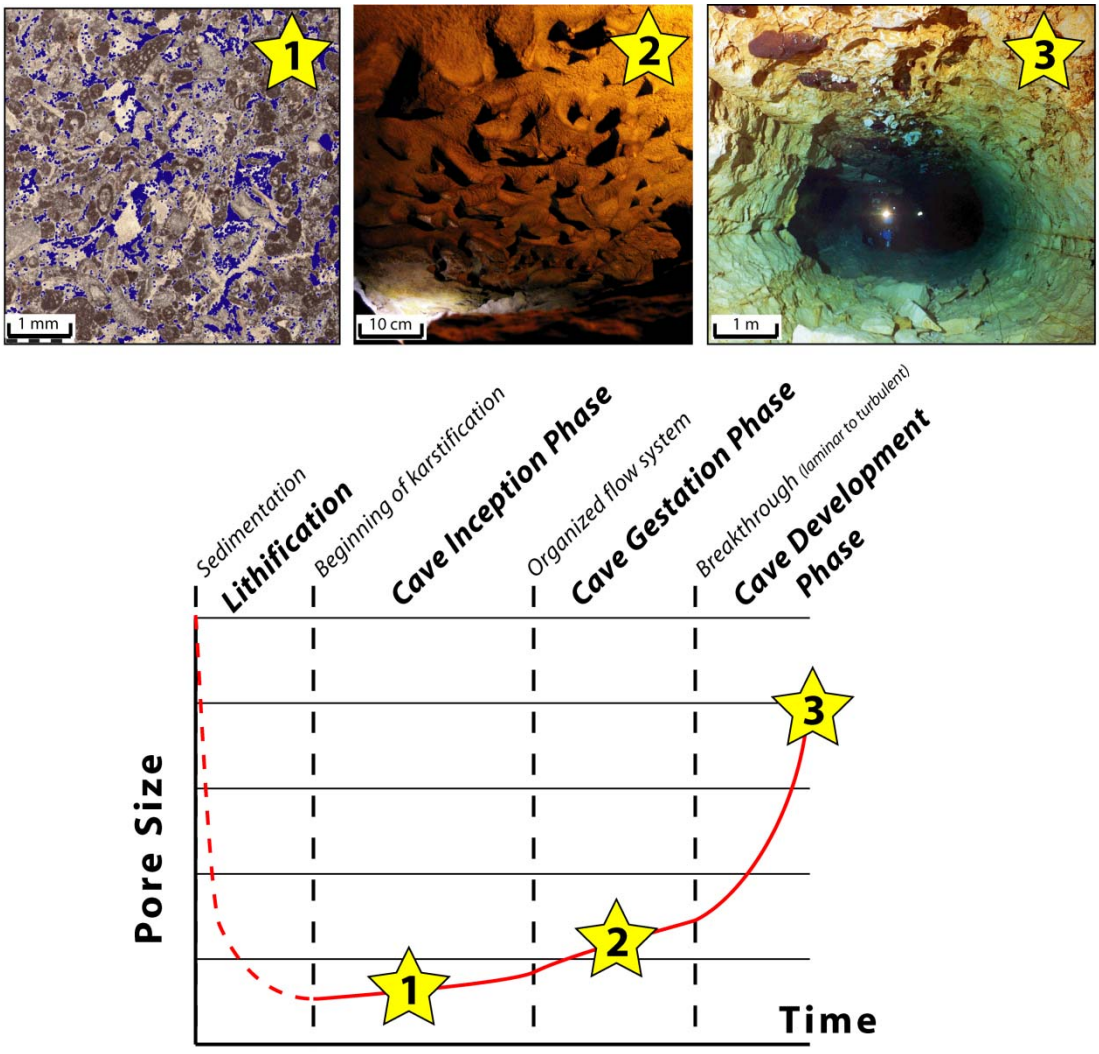

Fig. 4.2: Schematic development of a karst conduit from the sedimentation to present: The beginning of the karstification can be defined by the moment from which the size of the pore increases steadily due to dissolution processes. During cave inception phases the dissolution is low and slow. During the cave gestation phase flow becomes increased because of changes of the hydraulic boundary conditions and the therefore also the dissolution. The breakthrough marks the change from laminar to turbulent flow regime within the conduit; the karst conduits will develop faster and become cave.
4.2.1: dissolution voids on microscopic scale.
4.2.2: network of small karst conduits (anastomoses).
4.2.3: phreatic cave conduit (photo: Steffen Gross).

The inception horizon hypothesis (Lowe 1992, 2000) distinguishes between three different phases of the development of a karst conduit. The beginning of karstification can be defined as soon as the pore size increases steadily due to dissolution processes (Filipponi and Jeannin, 2008; Filipponi et al. 2008). One may expect that at this early phase (cave inception phase) the pore size are small, the dissolution still low and slow and divvuse distributed within various inception features. However, some features tend to increase their permeability slightly faster than others.

When hydraulic gradients become strongly controlled by the respective position of the recharge/discharge areas, the flow becomes organized in order to drain the aquifer. Thus the flow path selects a few horizons which provide the weakest resistance to flow. From this point on conduit development is faster. This phase is called the "cave gestation phase".

After a given time duration some flow path will reach a sufficient size (about 1 cm in diameter) for turbulent flow to occur, what will strongly increase the dissolution kinetics and caves can reach human size within a few thousands of years (e.g. White, 1988; Dreybrodt and Gabrovšek, 2000; Kaufmann, 2002; Palmer, 2002; Dreybrodt et al., 2005). This corresponds to the "cave development phase".

However, it must be pointed out, that this classification of "karstification state" is not applicable to "complex" karst systems synchronously. In fact in most cases different karstification states occur at the same time for a given karst system (Fig.4.3).

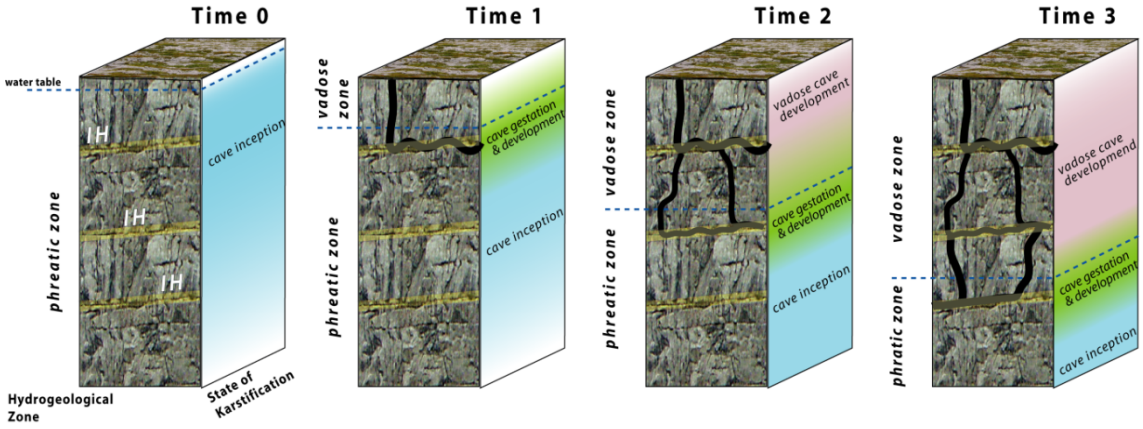

Fig. 4.3: Schematic development of a karst system in time and space (vertical section): Different parts of the system are in a different karstification state at the same time. During cave inception the karstification takes place over the full thickness of the limestone, whereas it is most significant effects in the form of flow paths are concentrated along the inception horizons

Early in the development of a carbonate aquifer (cave inception) under epigenic conditions (caves formed by water recharged from the overlying or immediately adjacent surfaces due to carbonic acid dissolution), all groundwater becomes nearly saturated with dissolved calcite and/or dolomite before it emerges at the surface. The total amount of rock removed along any flow path is nearly independent of chemical kinetics, because the water had enough time to equilibrate with the rock, regardless of dissolution rates (e.g. Palmer, 2002; Dreybrodt et al., 2005). Therefore, we can assume that the main parameter controlling flow and dissolution in this situation is the distribution of the permeability (chapter 3.6.1). This will thus play a significant role for the development of the final 3D pattern of the cave system.

Till now the inception horizon hypothesis is mostly based on field observations and speleogenetical hypotheses on conditions occurring in the early phase of speleogenesis. Direct verifications are difficult, but, considering the significance of the permeability distribution, groundwater flow modelling could help us to understand how cave could develop in these conditions.

There are various speleogenetic numerical modelling publications on the early karstification (e.g. Groves and Howard, 1994; Dreybrodt, 1988; Dreybrodt and Gabrovšek, 2000; Dreybrodt and Siemers, 2000;

Palmer, 2002; Kaufmann, 2003; Sauter and Liedl, 2000; Bauer et al., 2003). Most of them are dealing with the karstification along fracture networks, with initial opening of some 0.1 mm (equivalent permeability of some 10^6 mD). We can assume that this approach is only limited transferable to the early karstification of bedding planes (e.g. Noiriel, 2005). Nevertheless, we suppose that these model results are good to understand the karstification of the cave gestation and cave development phase; therefore after being "prepared" during the cave inception phases (e.g. chapter 3.6.1).

This chapter presents the results of a simple hydrogeology numerical modelling study and addresses following questions: What is the influence of the permeability distribution to the flow conditions at early speleogenetic stages? How to characterise from a hydrological point of view the change between cave inception and gestation phase? What is the role on the flow rate of the position and orientation of inception horizons relatively to the hydrogeological boundary conditions? How influences the geometry of the inception horizons and the landscape evolution the final geometry of the cave system?

4.2 Method and Results

To better understand the influence of permeability distribution to the early karstifcation stages we analysed different scenarios with 2D vertical finite-elements flow models (FeFlow). These model scenarios represents simplified, generic settings that were not designed to account for features of specific field sites but were still found to be useful to gain general insight into the flow conditions during the speleogenetic phases of cave inception and gestation.

The design of the selected scenarios was done within the inception horizon concept, assuming that within a rock mass some stratigraphical horizons are particularly susceptible to the effects of the earliest cave forming processes amongst others due to a slightly higher (or lower) primary permeability than the surrounding rock mass (chapter 3.4.1). Therefore, our numerical model consists of a homogeneous rock mass that is pervaded by horizons with a permeability-contrast with respect to the surrounding limestone. The occurrence of fractures was neglected, presuming that at early stage as well as depth the major fractures occur only with a very low frequency (Hillis, 1998; Ortega et al., 2006) and that the occurrence of fractures would increase the permeability along the inception horizons (chapter 3).

The field and laboratory study of some inception horizons lead us to distinguish three types of inception horizons (chapter 3.7):

1) Inception horizons where the cave inception took place **within** inception horizons. The analyses showed that they correspond to horizons with a slightly higher primary permeability than that of the surrounding rock mass;
2) Cave inception took place at the **contact** between the bedrock and the inception horizons where the primary rock permeability is lower than that of the surrounding rock mass;
3) Cave inception took place along **bedding plane fractures**; already a slippage of just a few millimetres will already cause a significant increase in permeability compared to the surrounding rock mass.

In this chapter we will only model and discuss inception horizons of type 1 and 2. Type 3 is at a hydrogeological point of view similar of type 1 (zone of higher permeability) but the primary permeability is several order of magnitude higher and not related to lithological porosity but to the mechanical weakness of the rock . The measured primary permeability of the inception horizons of type 1 and 2 was generally very low (some 0.1 mD ≈ 10^{-16} m^2), however the contrast between inception horizons and surrounding rock mass was up to ±50 to 70% (chapter 3.4.1).

Our basic model (e.g. fig. 4.4) consists of a 5000 metres long limestone block with a thickness of 500 metres. The width is subdivided in a 800 metres long spring area and a 4200 metres long recharge area. The elevation of the spring area in the respective model scenarios changes between 350 and 260 metres, defining different hydraulic heads at the spring area. The recharge area was taken in most scenarios at 500 metres. At recharge area we kept the hydraulic head constant at land-surface altitude because we can assume that at early stage of karstification the drainage capacity of the massive is lower than the recharge from precipitation; therefore the water table will stay near the surface. No-flow boundary conditions have been assumed for all other boundaries.

The permeability of the limestone massive was assumed to be constant and isotropic, the only exceptions are the two (inception) horizons with a thickness of 1 metre. Their permeability has been varied relatively to the permeability of the rock mass with factors of 0.01; 0.1, 10, and 100. In real world inception horizons have a thickness of some centimetres to decimetres (chapter 3.3.2), because of mesh generation difficulties 1 metre has been assumed to be a reasonable compromise. The permeability of the rock mass was set at 10^{-4} m/s to reduce computing time (in real world some 10^{-9} m/s; chapter 3.4.1); however it is to notice that the absolute value of the permeability has only a subordinate role, more significant are the contrasts to the horizons.

We analysed four geometrical configurations of the horizons: horizontal, dipping towards the spring area, dipping in the opposite direction to the spring area, anticline and syncline structure. For each configuration we had a series of simulations with different combinations of permeability distribution, distance between the inception horizons, distance to the spring area. In all we evaluated more than 100 test runs. The evaluation was based on the hydraulic head distribution and the flow distribution at steady state.

4.2.1 The role of the primary permeability in (deep) phreatic setting

4.2.1.1 Variation in primary permeability

The first set of numerical simulations aimed at understanding the influence of the contrast between the (inception) horizon permeability and the rock mass. Therefore, we used a simple geometric configuration: spring area at 350 m, recharge area at 500 m, horizon 1 at 100 m and horizon 2 at 250 m. The permeability of the horizon was varied in the different runs between 0.01 and 100 times the permeability of the surrounding rock mass.

As expected the finite-element model results show that the vertical distribution of flow depends on the permeability distribution (fig. 4.4 and fig. 4.5). This means that horizons with a X time higher permeability than the surrounding rock mass have also a X time higher flow rate than the surrounding rock mass; or on contrary a X time less permeable horizons have also a X time lower flow rate.

The refraction of the flow lines causes an increased horizontal flow within high permeability horizons but a reduction of horizontal flow within horizons of lower permeability. This is consistent with the theoretical refraction of flow on permeability boundaries $\frac{K_1}{K_2} = \frac{tan\theta_1}{tan\theta_2}$ (Freeze and Cherry, 1979). In other words; flow is horizontal in more permeable horizons and vertical in less permeable horizons (Eaton and Bradbury, 2003).

Low permeability horizons cause not only flow lines to be steeper within the horizon but also flattener in the rock mass below. This should lead to a remarkable flow diminution in the rock mass below the horizon. This decrease mainly depends on the low permeability horizon characteristics (thickness, permeability), but also on the length of the recharge area. However, for the thickness of horizons assumed in our model (1 m) as well as length of the recharge area (length of 4200 m), the flow diminution is not considerable.

Therefore, we can assume that the order of succession of horizons of various permeabilities to have no major effects on the vertical flow distribution (fig. 4.5).

In the model results it can be observed that the flow rate along the (inception) horizons as well as in the surrounding rock mass decreases with the distance to the spring area. In other words the highest flow rate can be observed shortly upstream from the spring area and decreases exponential veering away from there.

	Position	Permeability
Horizon 1	250 m	0.01 * permeability of the rock mass
Horizon 2	100 m	100 * permeability of the rock mass
Spring Area	350 m	
Recharge Area	500 m	

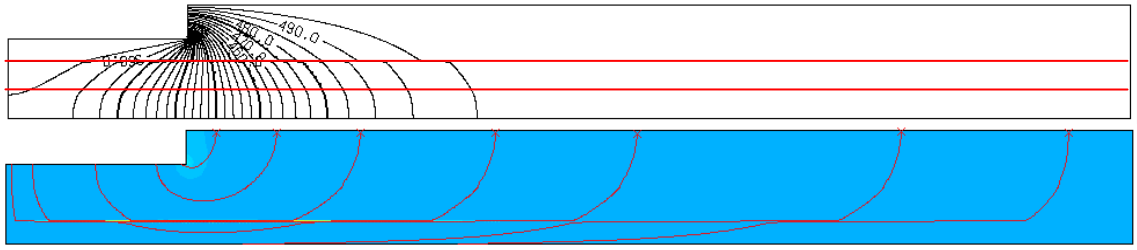

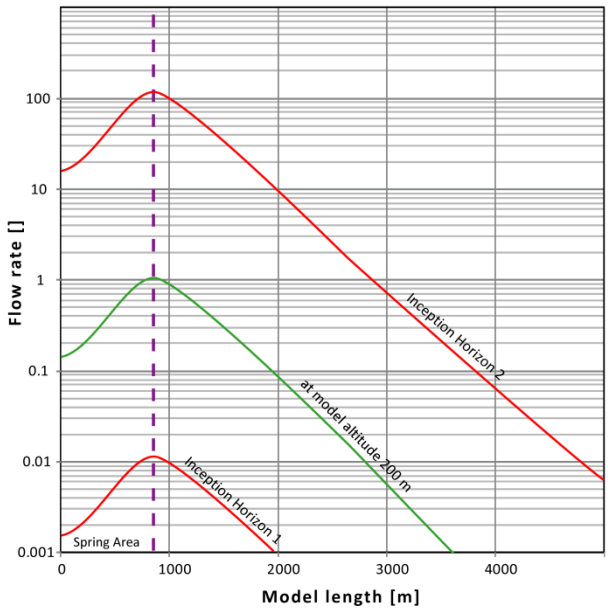

Fig. 4.4: Model scenario with one horizontal inception horizons at 250 m with permeability of 0.01 times the permeability of the surrounding rock mass and a second inception horizon at 100 m with 100 times the permeability of the surrounding rock mass. Spring area is at 350 m and recharge area at 500 m. The plots illustrate the distribution of hydraulic head (top), the flow tracks (middle) and the flow rate along the inception horizons as well as at the rock mass at 200 m (bottom) at steady state.
The results show that the vertical flow distribution is proportional to the permeability distribution.

	Position	Permeability
Horizon 1	250 m	10 * permeability of the rock mass
Horizon 2	100 m	100 * permeability of the rock mass
Spring Area	350 m	
Recharge Area	500 m	

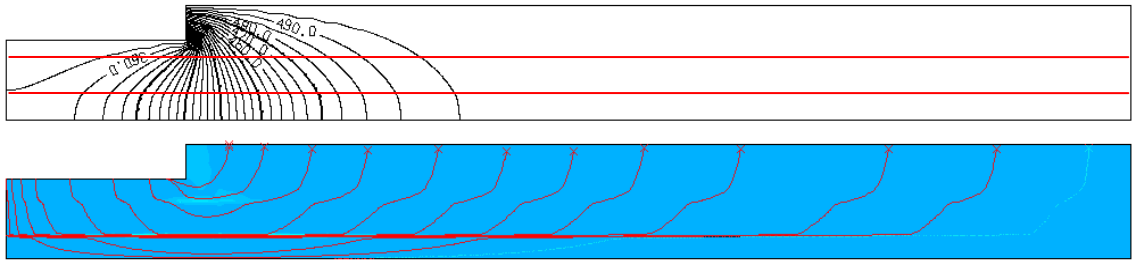

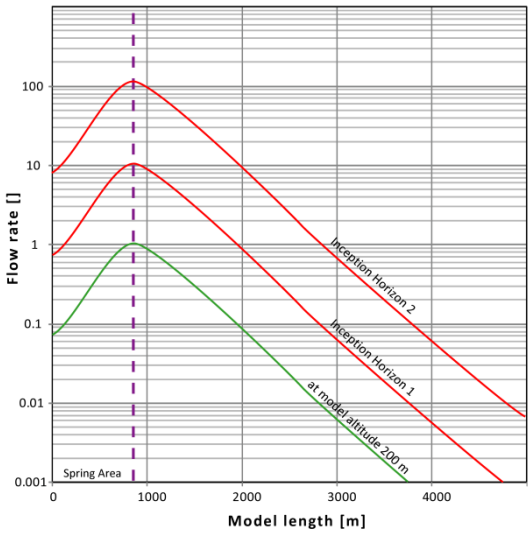

	Position	Permeability
Horizon 1	250 m	100 * permeability of the rock mass
Horizon 2	100 m	10 * permeability of the rock mass
Spring Area	350 m	
Recharge Area	500 m	

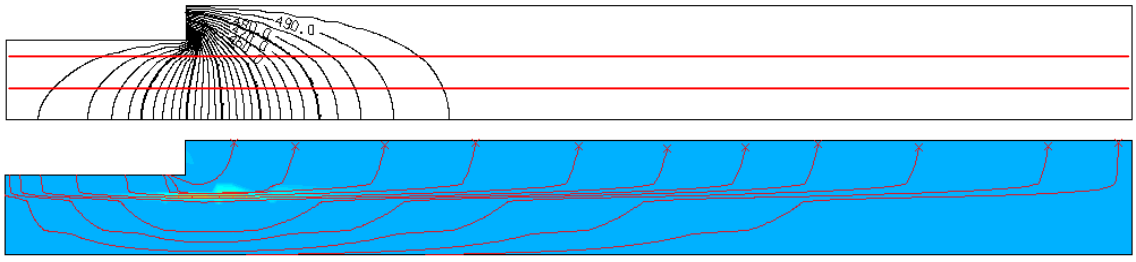

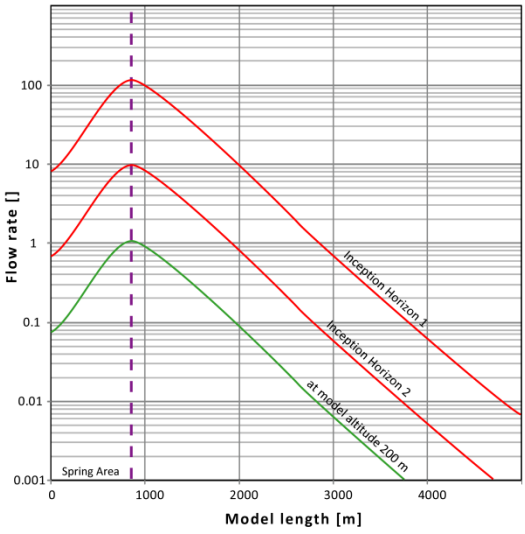

Fig. 4.5: Selected model scenario with one horizontal inception horizons at 250 m with permeability of 10 times (in 4.5.2 - 100 times) the permeability of the surrounding rock mass and a second inception horizons at 100 m with 100 times (in 4.5.2 - 10 times) the permeability of the surrounding rock mass. Spring area at model altitude is 350 m and recharge area at 500 m. The plots illustrate the distribution of hydraulic head (top), the flow tracks (middle) and the flow rate along the inception horizons as well as at the rock mass at 200 m (bottom) at steady state.
The model scenarios show that the vertical flow distribution is proportional to the permeability distribution and is independent of the order of the inception horizons.

4.2.1.2 Variation of the distance between inception horizons

In order to understand the role of the distance between inception horizons on the flow distribution, we analysed scenarios with different distances between horizons (150, 100, 50 and 10 m), whereas the permeability of both horizons was considered to be equal (100 times higher than the permeability of the surrounding rock mass) (fig. 4.6). Results show no dependence of flow distribution on distance between the inception horizons. The vertical flow distribution reflects again only the permeability distribution. *Therefore, we can conclude that the distance between inception horizons seems to have a subordinate role within the (deep) phreatic zone.*

4.2.1.3 Different geometrical settings of the inception horizons

A series of scenarios have been run to see the influence of the geometrical setting of the inception horizons within the phreatic zone. Four different settings have been chosen: dip of the horizons towards the spring area (10°), dip away from the spring area (10°) (fig. 4.7), synclinal and anticline structure (fig. 4.8).

The analysis of the runs showed that geometrical setting has no influence on the vertical distribution of flow rates. In all cases the vertical flow distribution was given by the permeability distribution.

	Position	Permeability
Horizon 1	250 m	100 * permeability of the rock mass
Horizon 2	100 m	100 * permeability of the rock mass
Spring Area	350 m	
Recharge Area	500 m	

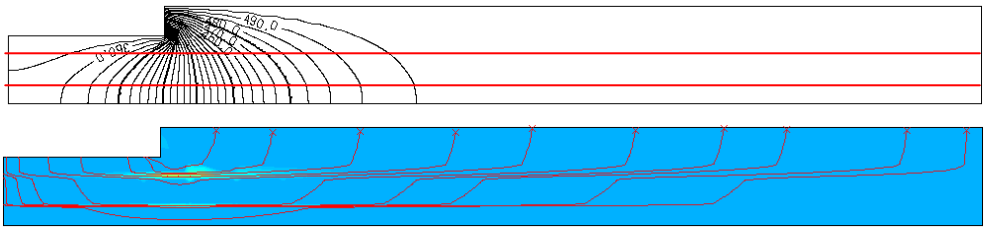

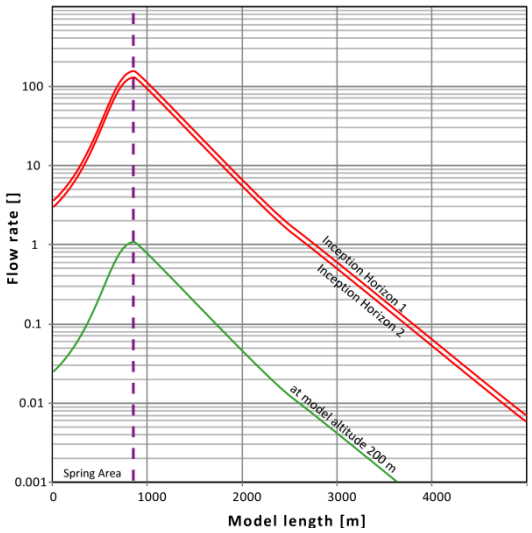

	Position	Permeability
Horizon 1	250 m	100 * permeability of the rock mass
Horizon 2	240 m	100 * permeability of the rock mass
Spring Area	350 m	
Recharge Area	500 m	

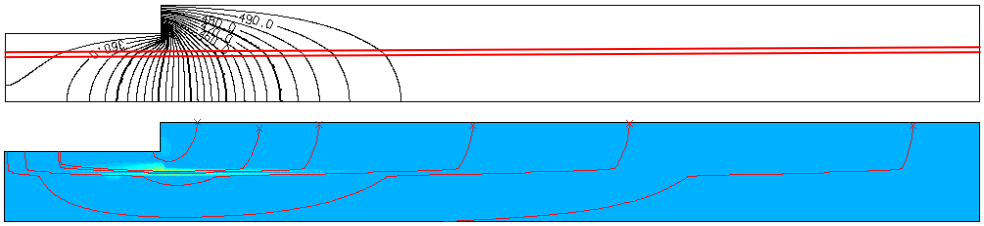

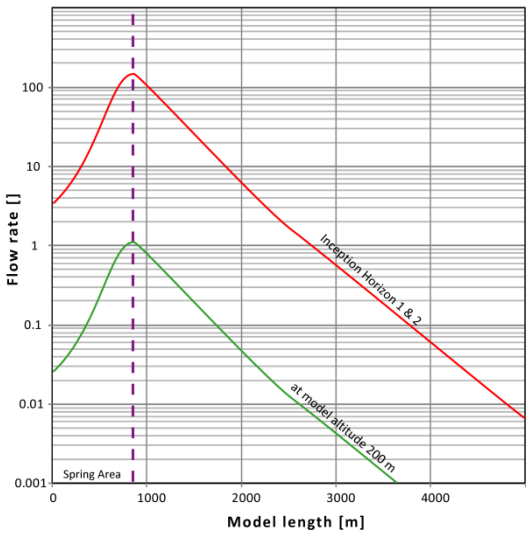

Fig. 4.6: Model scenario with two horizontal inception horizons with a permeability-value a 100 time higher than the permeability of the surrounding rock mass. Spring area at model altitude is 350 m and recharge area at 500 m. In 4.6-above inception horizon 1 is at 250 m and inception horizon 2 at 100 m (distance of 150 m); in 4.6-below lays inception horizon 1 at 250 m and inception horizon 2 at 240 m (distance of 10 m). The plots illustrate the distribution of hydraulic head (top), the flow tracks (middle) and the flow rate along the inception horizons as well as at the rock mass at 200 m (bottom) at steady state.
The results show no dependence of the flow distribution on distance between the inception horizons.

	Position	Permeability
Horizon 1		100 * permeability of the rock mass
Horizon 2		100 * permeability of the rock mass
Spring Area	350 m	
Recharge Area	500 m	

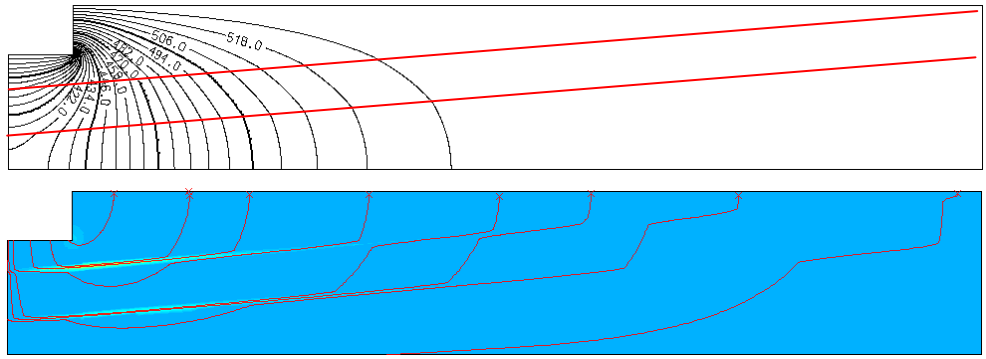

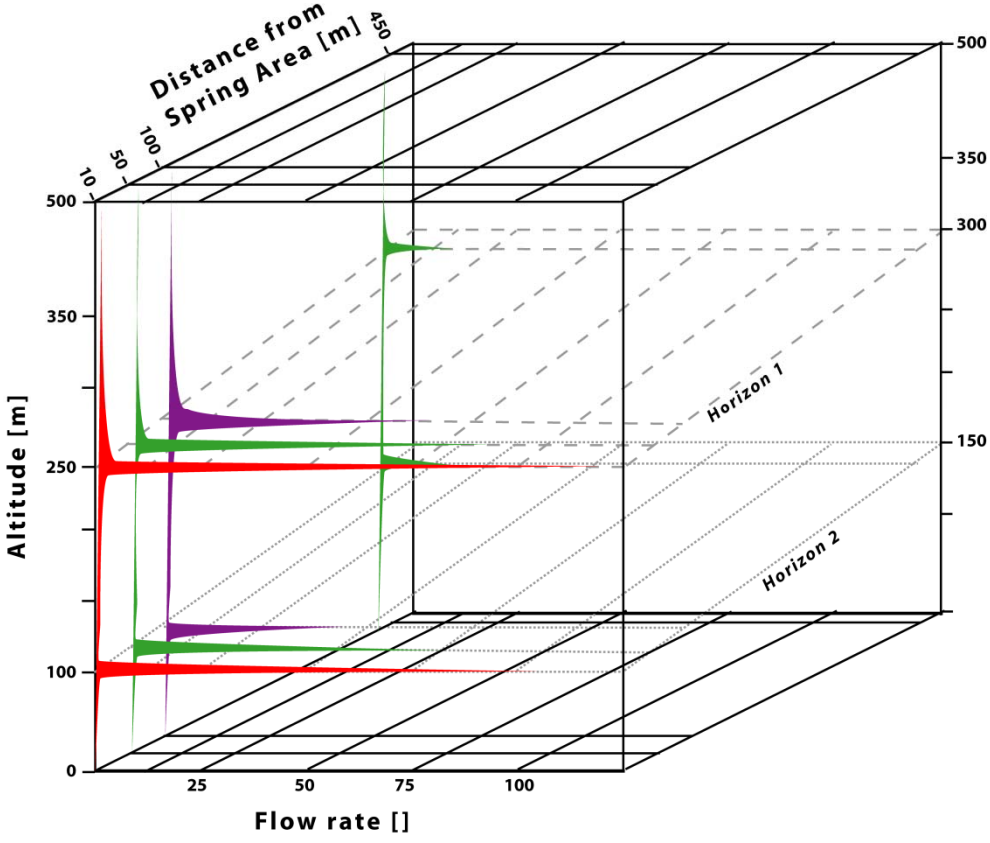

Fig. 4.7: Model scenario with two inclined inception horizons with permeability-values a 100 time higher than the permeability of the surrounding rock mass (distance between the horizons of 150 m). The horizons are inclined with 10° towards the spring area; spring area is at 350 m and recharge area at 500 m. The plots illustrate the distribution of hydraulic head (top), the flow tracks (middle) and the vertical flow rate distribution at different distances from the spring area.
The results show that the geometrical setting has no influence on the vertical distribution of flow rates under (deep) phreatic conditions.

	Position	Permeability
Horizon 1		100 * permeability of the rock mass
Horizon 2		100 * permeability of the rock mass
Spring Area	350 m	
Recharge Area	500 m	

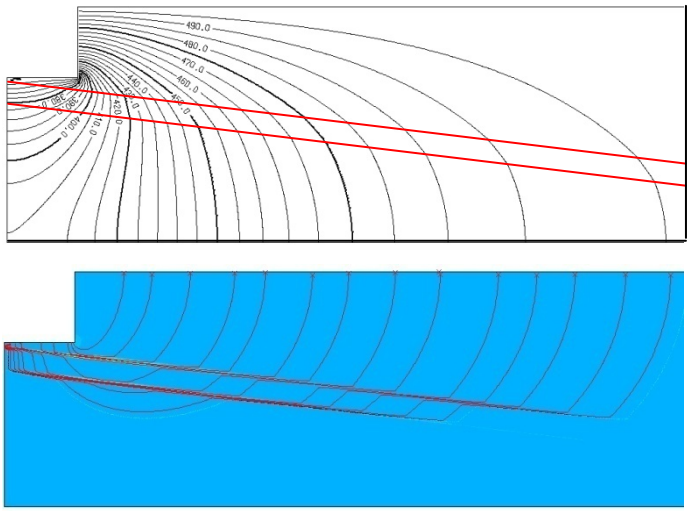

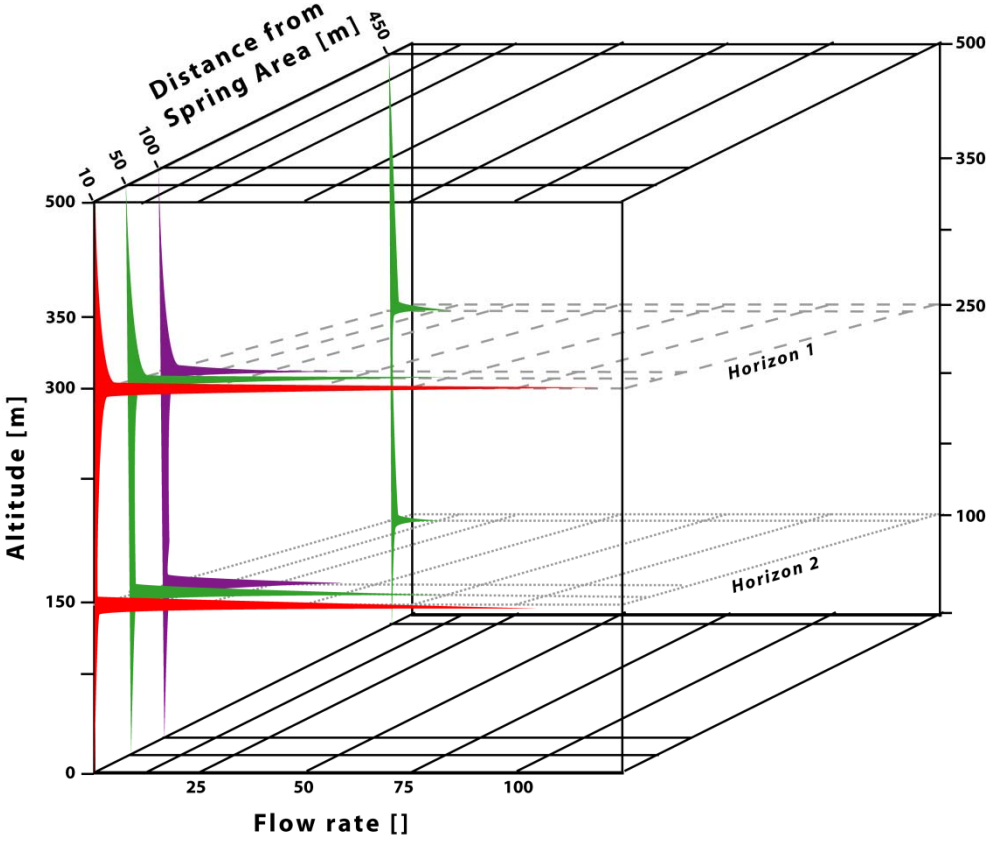

Fig. 4.8: Model scenario with two inclined inception horizons with permeability-values a 100 time higher than the permeability of the surrounding rock mass (distance between the horizons of 150 m). The horizons are inclined with 10° away from the spring area. Spring area is at 350 m and recharge area at 500 m. The plots illustrate the distribution of hydraulic head (top), the flow tracks (middle) and the vertical flow rate distribution at different distances from the spring area.

The results show that the geometrical setting has no influence on the vertical distribution of flow rates under (deep) phreatic conditions.

	Position	Permeability
Horizon 1		100 * permeability of the rock mass
Horizon 2		100 * permeability of the rock mass
Spring Area	350 m	
Recharge Area	500 m	

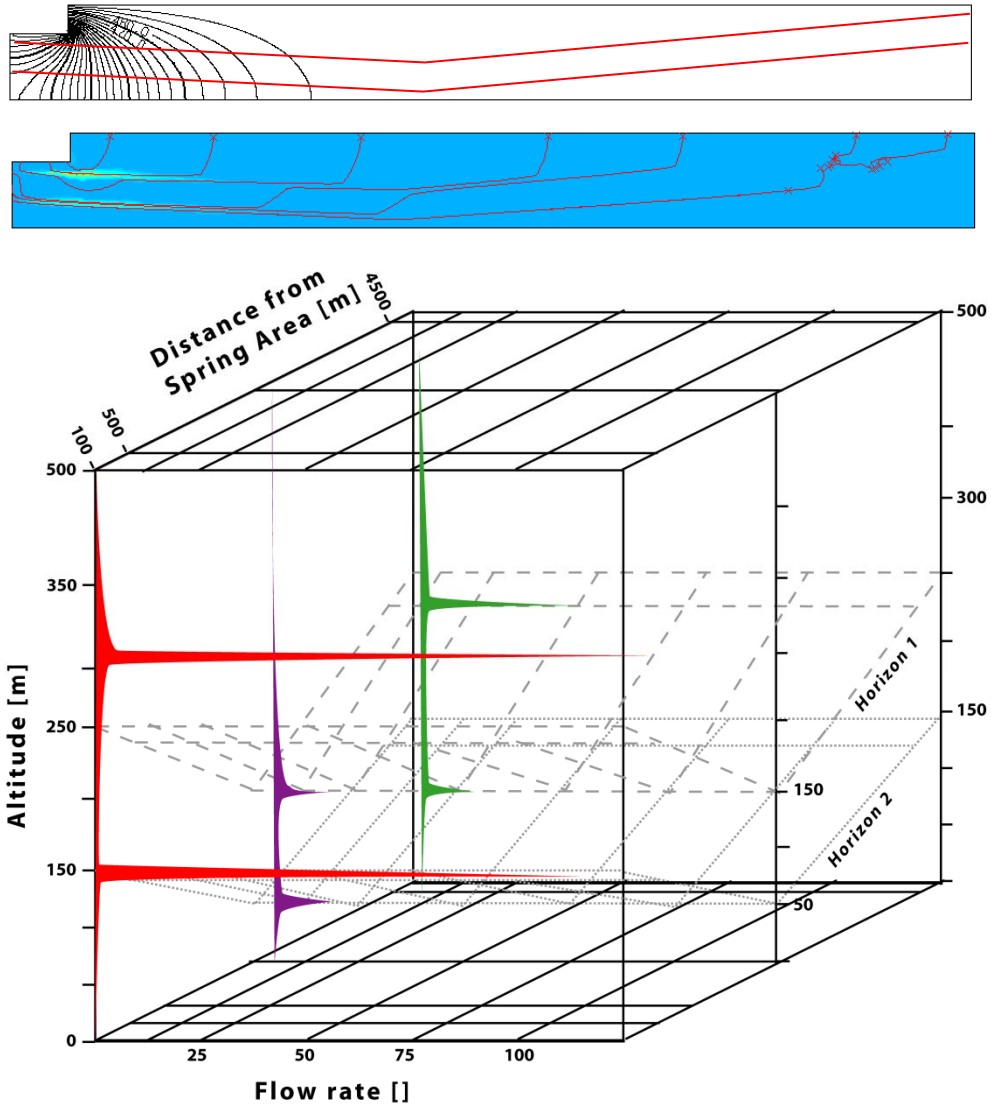

Fig. 4.9: Model scenario with two inclined folded horizons with permeability of 100 times the permeably of the surrounding rock mass (distance of 150 m between the horizons). The horizons draw a syncline structure. Spring area is at 350 m and recharge area at 500 m. The plots illustrate the distribution of hydraulic head (top), the flow tracks (middle) and the vertical distribution of flow rate at different distances from the spring area.
The results show that the geometrical setting has no influence on the vertical distribution of flow rates under (deep) phreatic conditions.

	Position	Permeability
Horizon 1		100 * permeability of the rock mass
Horizon 2		100 * permeability of the rock mass
Spring Area	350 m	
Recharge Area	500 m	

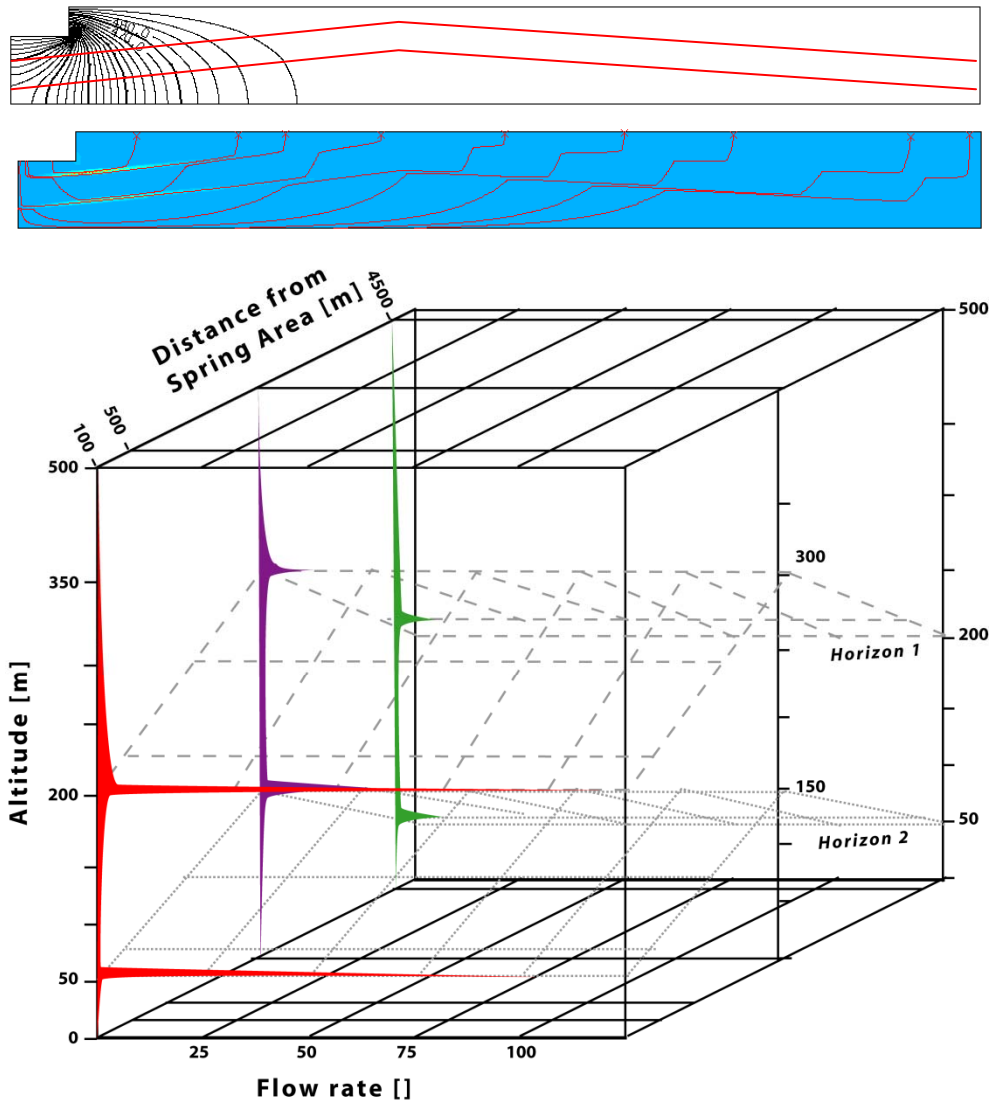

Fig. 4.10: Model scenario with two inclined folded horizons with permeability of 100 times the permeably of the surrounding rock mass (distance of 150 m between the horizons). The horizons draw an anticline structure. Spring area is at 350 m and recharge area at 500 m. The plots illustrate the distribution of hydraulic head (top), the flow tracks (middle) and the vertical distribution of flow rate at different distances from the spring area.
The results show that the geometrical setting has no influence on the vertical distribution of flow rates under (deep) phreatic conditions.

4.2.1.4 The role of the surface roughness of impermeable horizons

Our models show that horizontal flow within horizons of low permeability is reduced (chapter 4.2.1.1), and we could also observe no evidence of increased flow along the top or base of these horizons. However, different authors (e.g. Lowe, 2000) presume that impermeable beds (most of the cases marly strata; i.e. inception horizons of type 2) act as a low permeability "screen" along which water flows preferentially. Please notice that the focus is on "bedding plane conduits" and not at "formation boundary conduit" (chapter 2.4.1).

The surface of such stratigraphical contacts is not completely flat but shows a more or less distinct topography/roughness. The topography of the stratigraphical contacts is related to sedimentation structures such as ripple marks or cut and fill structures or by the heterogenic compaction of the sediments (e.g. Collinson and Thompson, 1982). It is imaginable that this surface roughness causes locally an enhancing in flow. To estimate the effect of surface roughness on the primary flow distribution at the contact we analysed different scenarios with finite element models (fig. 4.11). The basic model consists of a 300 m thick and 1 km^2 wide porous medium with an impermeable bottom boundary with randomly distributed surface roughness with given amplitude. The permeability of the porous medium was set constant at 10^{-4} m/s with a hydraulic gradient of 1 %. The results showed that with amplitude of 5 m we can expect locally a flow concentration up to 30 % relative to the undisturbed flow conditions within the porous medium. However, this concentration diminishes rapidly with decreasing of the amplitude and becoming almost insignificant for roughness amplitude usually observed along the investigated inception horizons (some cm to dm).

The analysis showed that at a vertical distance of around two times the amplitude of the roughness, the flow rate was not influenced by the surface roughness. Furthermore the thickness of the aquifer has no relevance to the flow distribution at the impermeable contact.

Therefore, we can conclude that under low gradient conditions, like they prevail in (deep) phreatic settings, this screen effect is marginal because of the low hydraulic gradient extends parallel to the impermeable horizon. Contrary it is to assume that under vadose conditions this screening effect becomes more relevant (e.g. alpine shaft series with subhorizontal passages between the shafts guided by marly bedding planes).

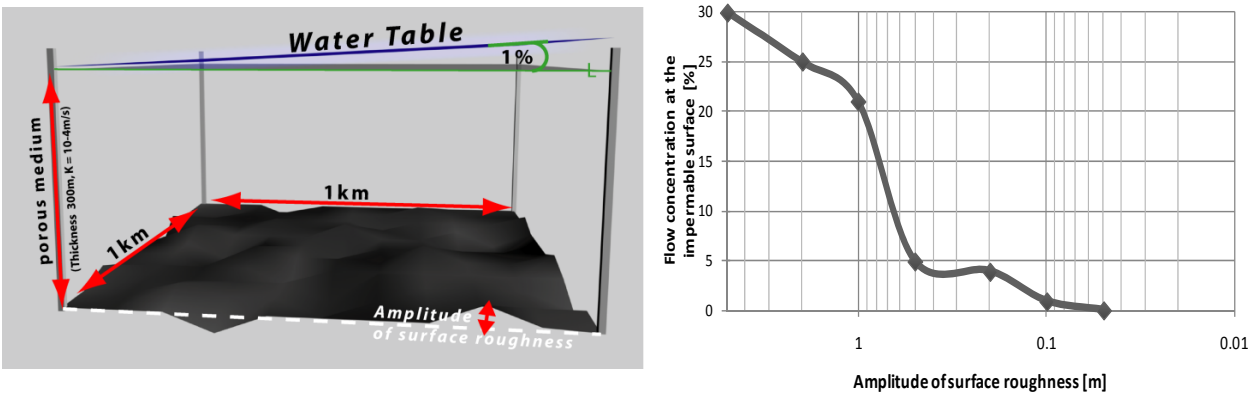

Fig. 4.11: Estimation of the effect of surface roughness of an impermeable horizon on the primary flow. Left: Sketch of the basic settings of the numerical model (variable parameter: Amplitude of the roughness of the impermeable surface). Right: Diagram of flow concentration along the surface versus amplitude of surface roughness. The diagram shows that with increasing of the amplitude flow concentration within the "depression channels" occurs. However, on the amplitude scale of some centimetres to decimetres this effect can be considered as marginal.

4.2.2 The role of the near spring area

Up to now we simulated flow conditions along (inception) horizons that are “far” from the discharge area. The results show that flow concentration is moderate, non selective and only controlled by the initial permeability of the horizons. However, it is to assume that the hydrologic behaviour will change dramatically when one horizon becomes close to the spring area, for instance by incision of the valley floor.

Therefore, we designed a series of simulations to understand the role of the distance between the spring area and the inception horizons to delaminate the “thickness” of the spring influence zone (chapter 4.2.2.1) and another series to recognize the influence of the hydraulic head difference between recharge and spring areas on the thickness and length of the spring influence zone (chapter 4.2.2.2).

4.2.2.1 Variation of the distance between the spring area and the inception horizons

In order to describe the influence of the distance between the spring area and the inception horizons, we analysed the vertical distribution of flow for a series of scenarios with various distances. We assumed a rock massive with two horizontally laying inception horizons (at 100 m and 250 m) with the same permeability (100 times higher than the surrounding rock mass). The distance between the spring area and the uppermost inception horizon has been varied (5, 7, 10, 12, 15, 20, 30 and 50 m).

The finite-element model results show that the flow along (inception) horizons in near spring area is no more proportional to the permeability of the horizon, but decreases with the distance between the spring and the uppermost horizon. Flow in the deepest horizon is still proportional to the permeability difference to the surrounding rock mass. Therefore, the flow rate along the uppermost inception horizon depends on the permeability as well as on the distance to the spring area. However, the spring influence decreases with the distance between the inception horizon and the spring area. It is possible to delineate a zone of spring influence. This zone has a thickness of around 20 to 30 m below the spring area. Within this area the influence decreases exponentially with distance (fig. 4.12).

Further it is to notice that the zone of increased flow is laterally restricted and becomes thinner with distance to the spring area (fig. 4.14). *Based on simulations we can estimate that the lateral elongation of this zone of spring influence is some hundreds of metres depending on the hydraulic head, the contrast in permeability between the rock mass and the more permeable horizon.*

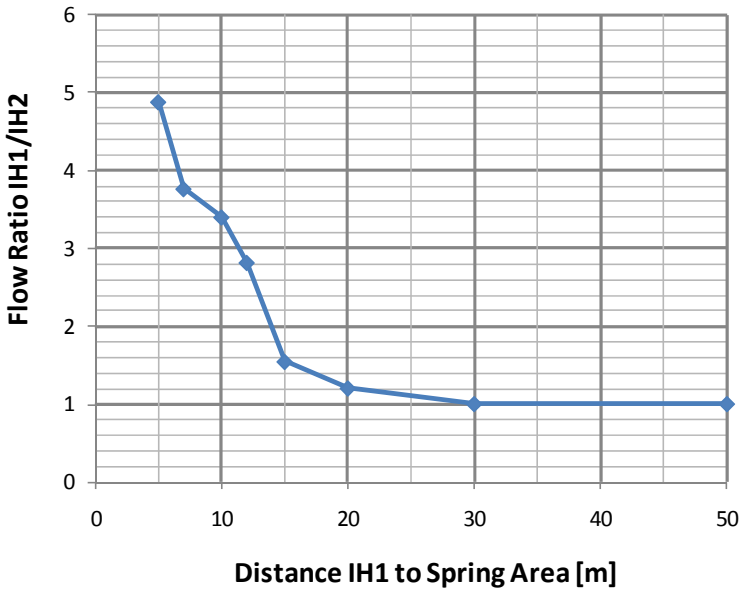

Fig. 4.12: This diagram shows the relationship between the flow rate and the distance of an inception horizon to the spring area. The flow rate is expressed as the ratio to the uninfluenced lowermost inception horizon. The diagram shows that the flow rate is increasing not proportionally with the increasing of the distance; from a distance greater than around 30 m the influence of the distance inception horizon-spring area becomes negligible.

4.2.2.2 *Influence of the hydraulic head difference between recharge and spring areas on the thickness and length of the spring influence zone*

To estimate the influence of the hydraulic head difference between recharge and spring areas on the thickness of the spring influence zone we analysed scenarios with various elevations of the recharge area (at 270, 300, 400 and 500 m). For all scenarios the spring area has been set at 262 m, horizon 1 at 250 m and horizon 2 at 100 m. Both horizons have permeability that is 100 times higher than the surrounding rock mass. *The results show that a decrease in hydraulic head difference induces an increase in flow within the near spring (inception) horizon (fig. 4.13) and that the lateral elongation of the spring influence zone becomes shorter with decreasing hydraulic head difference.*

We can conclude that it exist a zone of spring influence with increased flow depending on the permeably distribution within the zone, distance to the spring area and the prevailing hydraulic head. Beyond this zone the flow distribution is characterized by the permeability distribution. We can assume that within this spring influence zone the cave gestation phase take place (chapter 3.6.1).

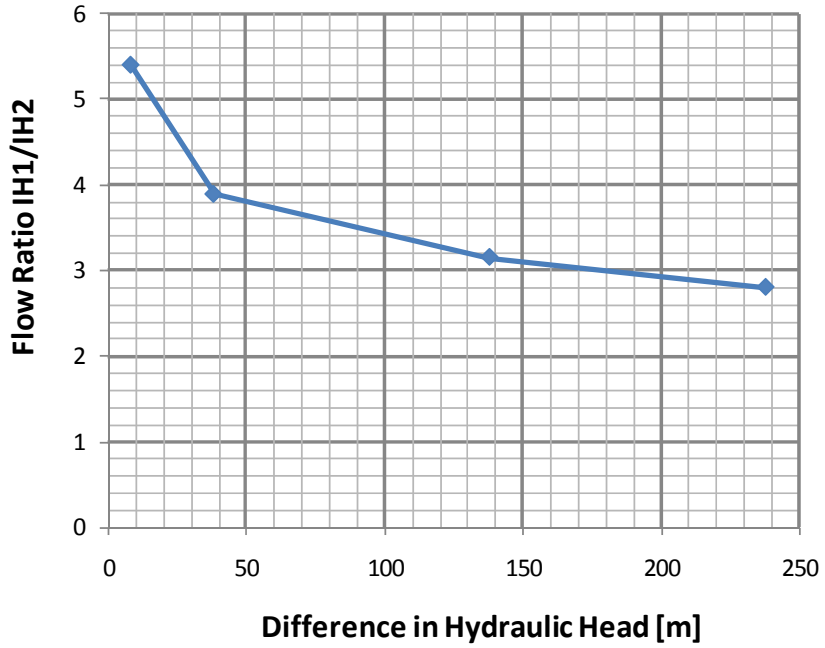

Fig. 4.13: This diagram shows the relationship between the difference in hydraulic head (elevation of the recharge area minus elevation of spring area) and the flow rate along inception horizon 1. The flow rate is measured within the spring influence area delineated in figure 8. The flow rate is expressed as the ratio to the uninfluenced inception horizon 2. The diagram shows the decrease of the flow ratio with increasing hydraulic heads.

	Position	Permeability
Horizon 1	250 m	100 * permeability of the rock mass
Horizon 2	150 m	100 * permeability of the rock mass
Horizon 3	100 m	100 * permeability of the rock mass
Spring Area	265 m	
Recharge Area	500 m	

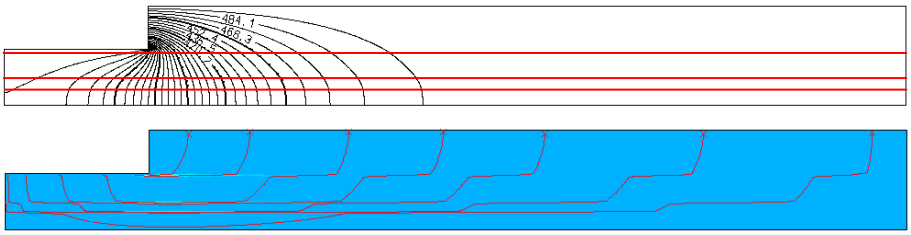

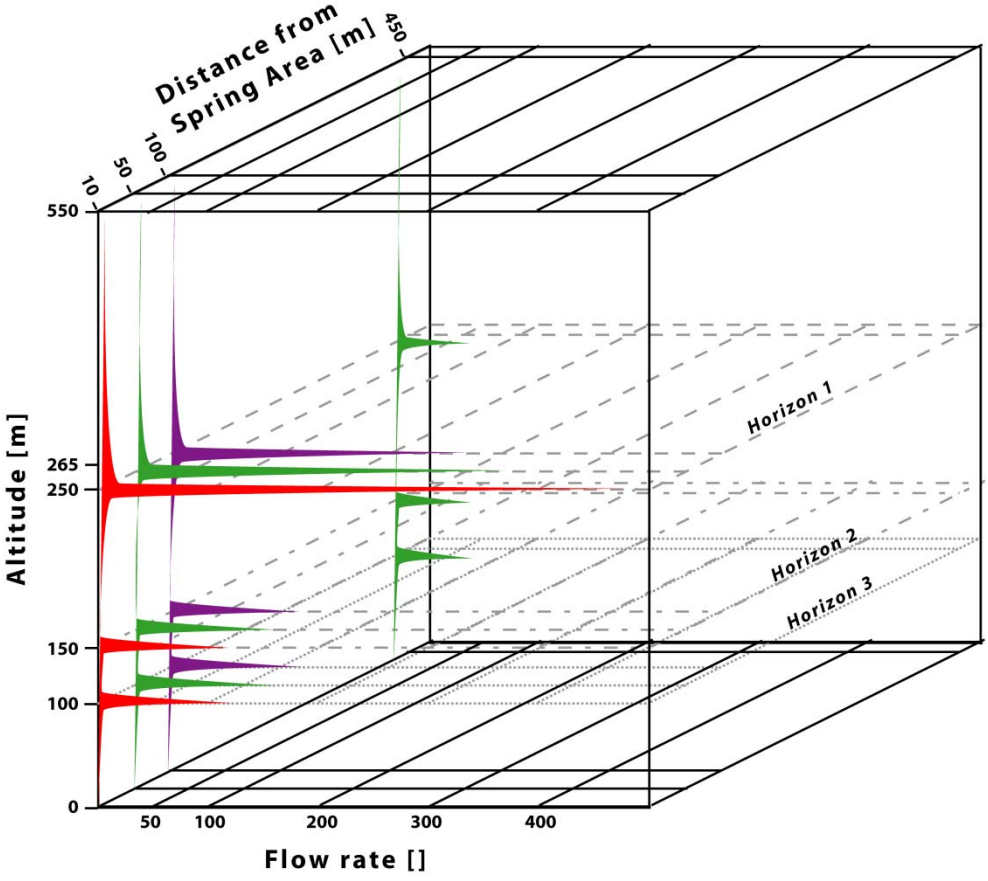

Fig. 4.14: Synthesis of several modelling scenarios. In these models three horizontal inception horizons (at 250, 150 and 100 m of model elevation) with permeability of 100 times the permeably of the surrounding rock mass have been introduced. The spring area was located at a model altitude of 265 m and the recharge area at 500 m. The upper graphic illustrate the distribution of hydraulic head, the middle graphic the flow tracks and the lower graphic the vertical flow rate distribution at different distances from the spring area.
Horizon 1 show in near spring area a strong increase in flow compared to the deeper settled horizons 2 and 3. However, with greater distance to the spring area the difference in flow between horizon 1 and the other two decreases till they become at a distance of around 450 m equal.

4.3 Discussion about the role of the position and orientation of Inception Horizons relative to the hydrogeologic Boundary

The numerical flow simulations show that flow concentration is moderate, non selective and only controlled by the initial permeability of inception horizons as long as they are far enough from the discharge area. The hydrologic behaviour changes dramatically when one inception horizon becomes close to the spring area, for instance by incision of the valley floor. Under these conditions the flow is no more controlled only by the permeability distribution but also by the distance between spring area and inception horizons. Flow is increased in a zone of a thickness of some tens of metres below the spring area and a few hundreds of metres laterally (fig. 4.14).

4.3.1 The speleogenetic role of the cave gestation zone

The finite-element model results show that the flow along (inception) horizons in a spring influence zone is increased. This zone has a thickness of some tens of metres below the spring area and lateral elongation of some hundreds of metres depending on the hydraulic head, the contrast in permeability between the rock mass and the more permeable horizon. From a speleogenetic point of view this zone of spring influence can be considered as the zone where cave gestation and then later (when the flow within the karst conduits become turbulent) the phreatic cave development take place (fig. 4.15).

It is to notice the difference between the cave inception/gestation/development phase, which represents a development stage of a single conduit (dissolution seams for the inception phase; karst conduits for the gestation phase; cave conduits for the development phase), and the inception/gestation/phreatic development/vadose development zone, which represent zones of characteristic flow conditions:

- the **cave inception zone** is characterized by laminar flow under low hydraulic gradient conditions;
- the **cave gestation zone** is characterized by laminar flow under higher hydraulic gradient conditions caused by the "spring influence" and an gradually development of a karst conduit network;
- the **phreatic cave development zone** is characterized by turbulent flow under low hydraulic gradient conditions within karst conduits;
- the **vadose cave development zone** is situated above water table, therefore the cave passages are air and water filled with permanent or occasional water flow during snow melt or rain events. In this zone the flow is ultimately controlled by gravity i.e. mainly vertical. As water can only flow downwards vadose conduits are mainly vertical shafts or pitching, meandering canyons (e.g. Lauritzen and Lundberg, 2000) and are guided by inception fractures as well as inception horizons (chapter 2).

A given dissolution feature can be for example in the cave development zone but still being in the state (size) of the cave inception phase (because a nearby feature was already becoming the main conduit). Therefore, the phase is describing the size as well as the speleogenetic processes within the dissolution feature (chapter 3.6.1) whereas the zone describes the hydrological boundary conditions (and dissolution characteristics distribution along the inception horizon).

Along time, it must be expected that within the "drop shaped" cave gestation zone the hydraulic gradients will flatten down to the spring level because of gradually development of a karst conduit network. Successively the gestation zone will move upstream (fig. 4.15). This flattening is most important when a "victor tube" is large enough to allow turbulent flow (breakthrough; e.g. White, 1988; Dreybrodt et al., 2005) therefore at the change between cave gestation and cave development phase (Lowe, 1992).

The spring for the new upstream moving of the gestation zone will be a "spring" within the developed karst conduits at the "time step" before. In geology with horizontal laying beds the duration of the gestation phase for further gestation zones will be significantly shorter than for the first zone after a valley incision. This because the connection between inception horizon and spring area does not needed to be developed

through the rock mass (i.e. inception fractures)(fig. 4.15). However, this is also true for geology with inclined beds as long as they are not oriented perfectly parallel to the discharge valley (fig. 4.16). For this last situation (probably more theoretical) the upstream moving of the gestation zone is always associated with the speleogenesis "through the rock mass". However, the karstification through the rock mass is mostly along the network of inception fractures (if they link inception horizons also named as "inception links" in Lowe, 1992).

This upstream shifting of the gestation zone reduces also significantly the time required for the cave development. Whereas in conventional connectional models the cave systems develops at once (e.g. Kaufmann, 2002; Palmer, 2002; Dreybrodt et al., 2005) we propose a step by step cave development (step of the size of the gestation zone). The estimation for the breakthrough duration depends among others of the powered conduit length (e.g. Dreybrodt et al., 2005). This powered length causes a significant reduction of the breakthrough time of the step by step karstification ($(a+a)^x >> a^x + a^x$). This reduced time requirement for cave gestation allows for example to develop cave levels of several kilometres of cave conduits in reasonable time scale.

This influence of the near spring area and the upstream moving of the gestation zone are also cognizable in the various numerical speleogenetic models (e.g. Gabrovšek and Dreybdodt, 2001) also if not discussed in details or within the concept of inception horizons. They describe an upstream moving of the "turbulent flow regime" and a flatten of the hydraulic gradient.

Also Ford and Williams (1989 page 178) supposed such a near spring zone (named as "zone of active circulation"). But they give no declaration how they delaminate their zone. Compared to our proposed gestation zone their zone is drawn open at the upstream end.

The lateral shifting of this gestation zone causes a step by step adjustment of the flow path to the new boundary conditions. This numerical observation is also confirmed by cave geomorphologists (e.g. Häuselmann *et al.* 2003; Audra et al., 2007) who described in details the development of phreatic cave systems and observed the same type of stepwise development of new conduits from downstream towards upstream ("soutirage") (fig. 4.15 – time 2.1).

The lateral shifting of the gestation zone by progressive karstification from a given spring position upstream is usually fast compared to valley deepening. However, if valley incision is to fast (e.g. in alpine environment) a new valley may exist before the previous system is developed all the way through the recharge area. This may explain why in some cave systems we can distinguish several incising phases whereas we can hardly distinguish them further upstream (chapter 2.2.4). Therefore, it may happen that the duration of a hydrogeological phase (steady valley position) is not long enough to develop a corresponding "cave level" throughout the whole karst massive.

The jumping behaviour of the valley incision could also be a reason why some potential inception horizons have no regional significance in the development of cave systems: they may have not being long enough in the cave gestation and/or development zone.

4.3.2 Reproduce the 3D geometry of cave systems with the concept of the speleogenetic zones

The above introduced concept of the speleogenetic zones allows reproducing the cave pattern of cave systems within different (simply) geological settings and boundary conditions.

We can illustrate the development of so called "water table caves" in a geological setting with **flat laying bedding** (comparable with the geological setting of areas like for example the Mammoth Cave System, Shuanghedongqun or Ogof Draenen – see appendix 1) (fig.4.15). The conceptual model shows that the conduits develop not at the water table (like the name is suggesting) but at the first suitable inception horizon below the water table (fig. 4.1).

True water table caves are expected to be rare exceptions for situation where the surface spring is on an inception horizon. It will be argued that many springs (cave entrances) can be observed that are on inception horizons, however most of them are high water springs. They develop just after the incision of the valley (fig. 4.15 – Time 2.0, "hanging spring") unlike soutirages developed down to the valley floor (these phenomena can be observed today in many cave systems, e.g. Kristallhöhle Kobelwald, Switzerland - Kürsteiner et al., 2004).
The successive upstream moving of the gestation zone along the lower inception horizon as well as the successive development of the soutirages develops a new cave level.

It is to notice that the only motor for karst development is the hydraulic gradient, which moves through the massif and changes in short (horizontal shifting of the gestation zone) and long (valley incision) time scales.

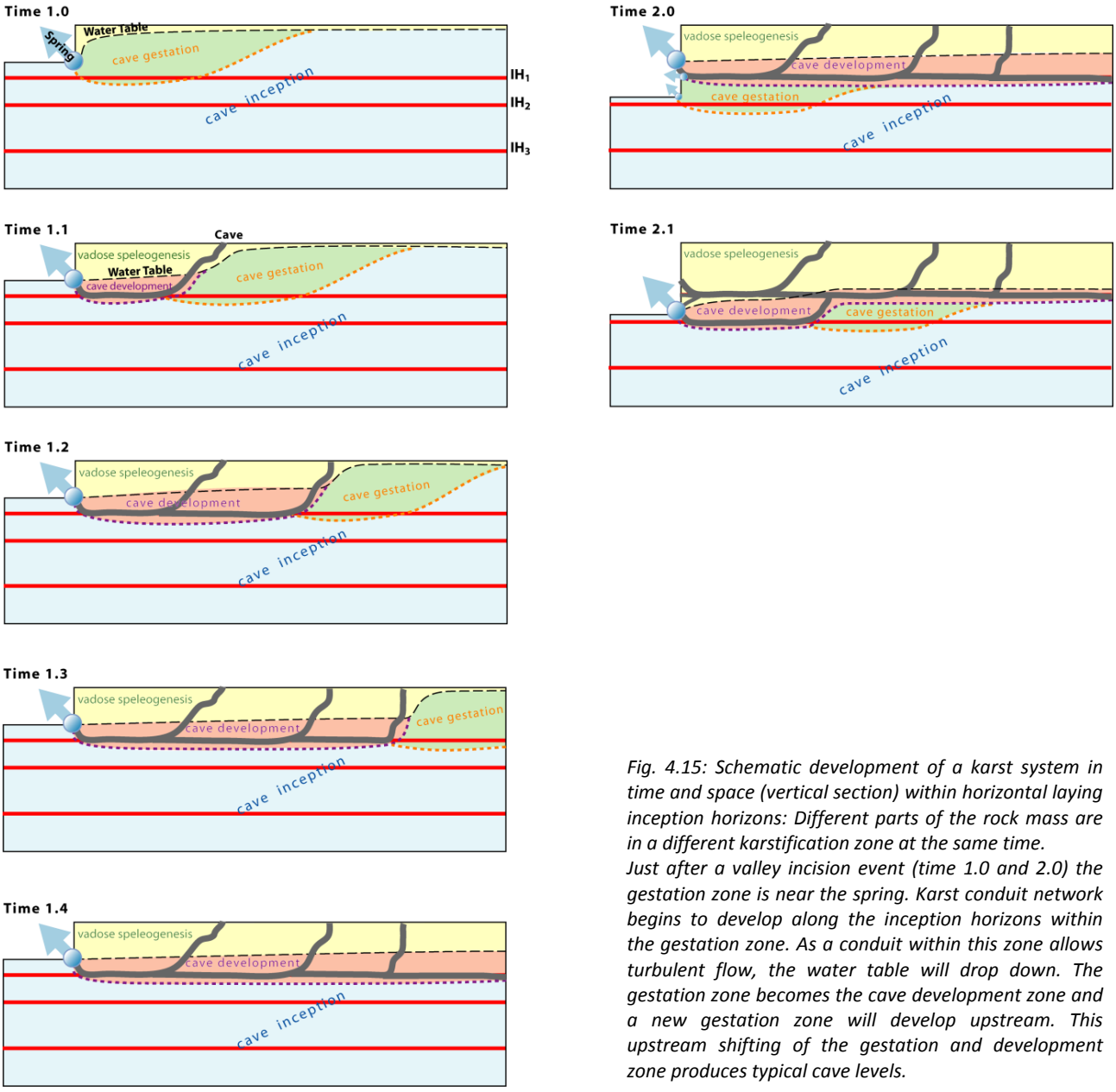

Fig. 4.15: Schematic development of a karst system in time and space (vertical section) within horizontal laying inception horizons: Different parts of the rock mass are in a different karstification zone at the same time.
Just after a valley incision event (time 1.0 and 2.0) the gestation zone is near the spring. Karst conduit network begins to develop along the inception horizons within the gestation zone. As a conduit within this zone allows turbulent flow, the water table will drop down. The gestation zone becomes the cave development zone and a new gestation zone will develop upstream. This upstream shifting of the gestation and development zone produces typical cave levels.

More complex is the situation with **oblique bedding**. As first exercise we will consider the bedding inclined to the spring area that are perfectly parallel to the valley floor (i.e. there exist no oblique outcropping of the inception horizons at the surface) (fig. 4.16). The situation at time steps 1.0 and 1.1 are similar to the previous model (fig. 4.16), the gestation of the first inception horizon as well as the development of the linking flow path between the inception horizon and the spring area. The upstream moving of the gestation zone in time step 1.1 give rise to the gestation of a second inception horizon that need to be linked to the first inception horizon. The link between the inception horizons are manly developed along a network of inception fractures (inception links in Lowe, 1992).

The use of the inception horizons as well as inception links causes a characteristic looping conduit course.

The valley incision between time step 1.3 and 2.0 causes the development of a lower “cave level” that is connected with the upper level by soutirages developing along the inception horizons.

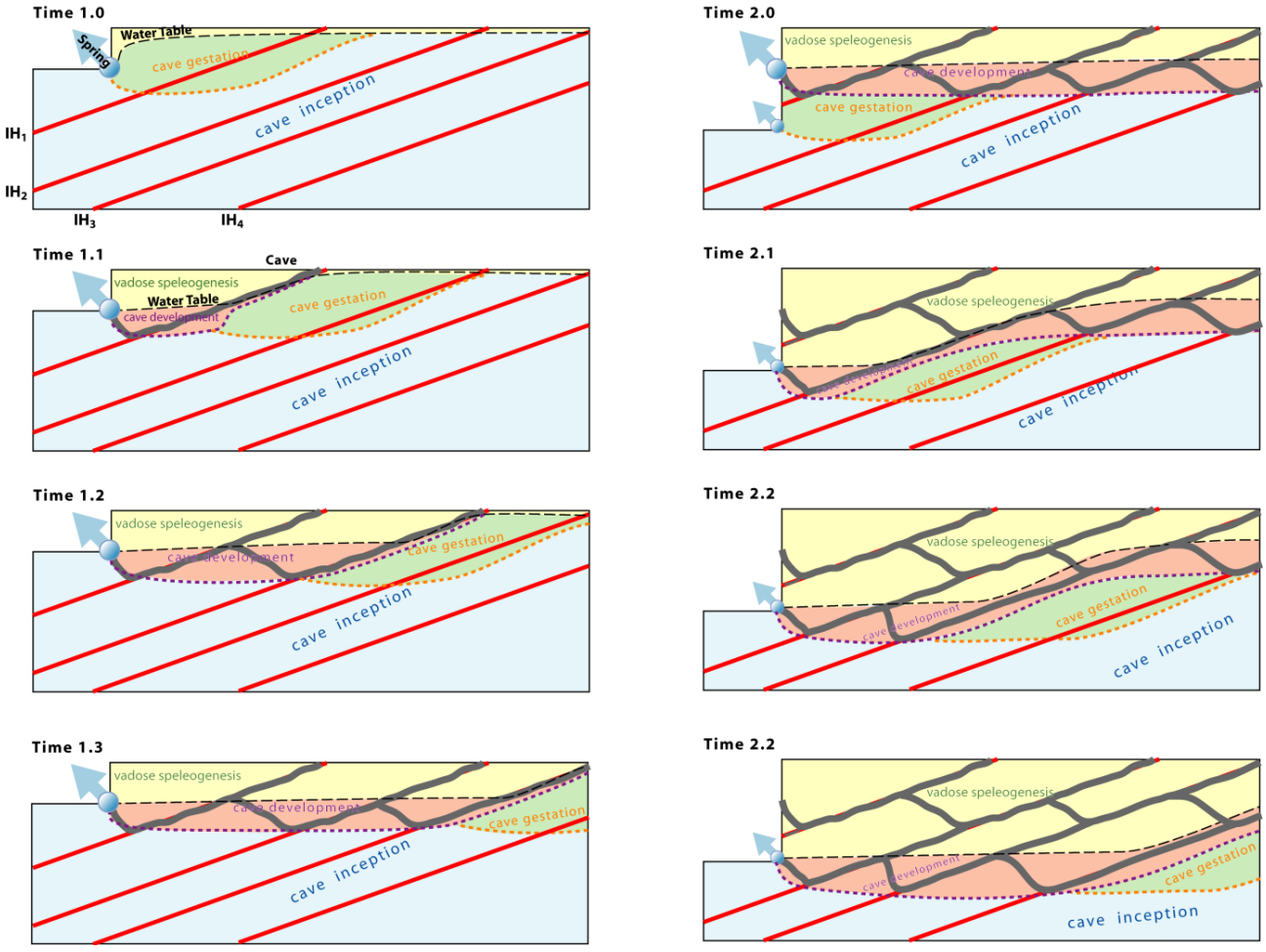

Fig. 4.16: Schematic development of a karst system in time and space (vertical section) within inclined inception horizons towards the spring area and parallel to the valley: Different parts of the massif are in a different karstification state at the same time.

Just after a valley incision event (time 1.0 and 2.0) the gestation zone is near the spring. As a karst conduit network develops within this zone that allows turbulent flow, the water table will drop down. The gestation zone becomes the cave development zone and a new gestation zone will develop upstream. This upstream shifting of the gestation and development zone produces cave levels.

The karst conduit network starts to develop along the inception horizon within the gestation zone. The inclined structure of the inception horizons is responsible for cave develops along different inception horizons what causes the typical phreatic loops develop. Between the inception horizons the conduits develop along inception fractures (inception links).

The above situation with inclined beds that are parallel to the discharge valley is quite theoretical; more often is a **not parallel outcropping** (fig. 4.19). A typical real example for this geometrical situation is the Hölloch (SZ, CH).

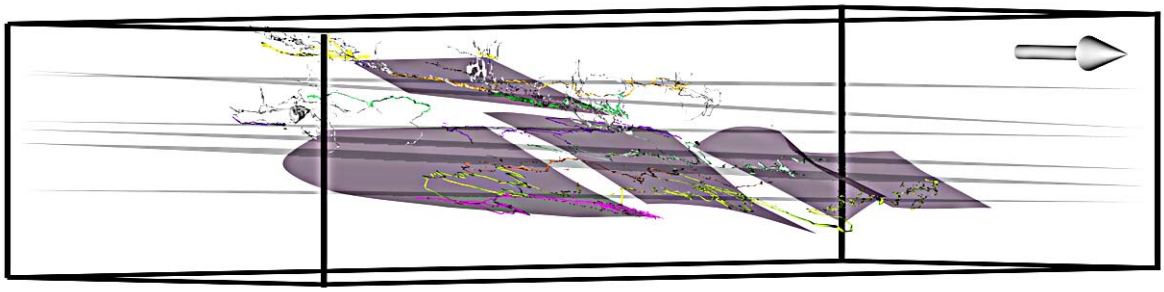

Fig. 4.17: 3D view of the Hölloch (SZ, CH) with inception horizons shifted by faults and the paleo-water tables. The cave conduits developed mainly below the intersection of the inception horizons and the paleo-water tables.

During phase 1 (time 1) a first "cave level" will develop along the upper inception horizon (fig. 4.19). Please notice that at this time the lower inception horizon has no surface outcrop. Since the valley incision (between phase 1 and 2) is not deep enough to expose the lower inception horizon, a second "cave level" will develop along the upper inception horizons with soutirages developing also along the horizon. Only with another valley incision event (between phase 2 and 3) the lower inception horizon will crop out. A third cave level will develop, but this time along the lower inception horizon and the soutirags will develop along the inception fracture network. This assuming that such fractures are present; otherwise the new third cave level will again develop along the upper inception horizon. For this stage also the development of two "independent" cave levels along both inception horizons is imaginable.

It should be notice, that the cave levels on the inception horizons are usually not horizontal, but form more or less distinct (phreatic) loops. These because the conduits develop preferentially along the intersection of the inception horizons and the fracture network (see also chapter 2.7.3 or e.g. Lauritzen, 1988). The amplitude of the loops depends on the orientation of the inception horizon and on the orientation as well as the spacing of the inception fractures (e.g. Ford and Ewers, 1978; Lauritzen, 1988; Ford and Williams, 2007) (fig. 4.18). *Shallow phreatic loops develop at the intersection of sub horizontal orientated inception horizons with wide spaced inception fractures or inclined inception horizon with narrow spaced fracture sets. Contrary deep phreatic loop development need inclined inception horizons with wide spaced fracture sets.*

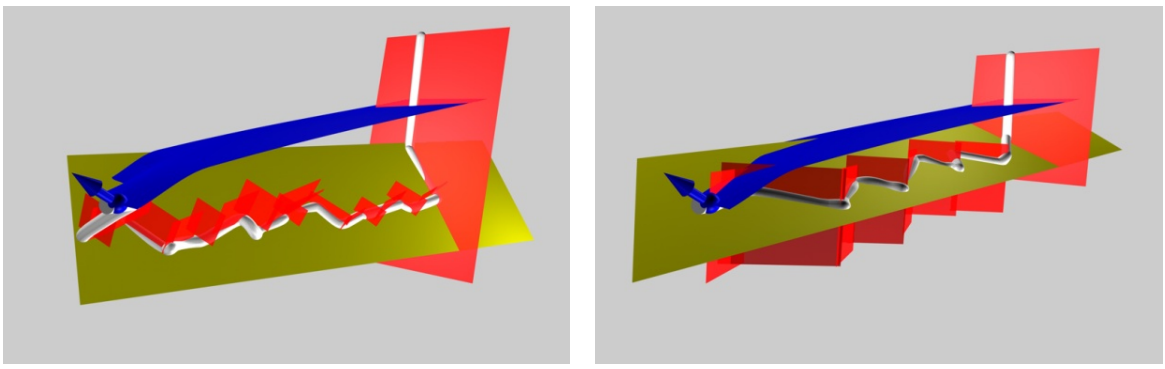

Fig. 4.18: Schematic 3D view illustrating the relationship between the amplitude of the phreatic loops, the orientation of the inception horizon, the orientation as well as the spacing of the fracture network. Left: development of shallow loops in a setting with inclined inception horizon and narrow spaced fracture network. Right: development of shallow loops in a setting with sub horizontal inception horizon and wide spaced fracture network.

We have been able to reproduce the 3D cave pattern of different types of cave systems by using the position and orientation of the inception horizons as well as the history of the landscape evolution (e.g. spring position). This forward analysis provides first ideas of the geometry of the conduits as well as a better understanding of the development of a karst system in time and space (vertical section).

The first steps have been taken to predict the cave pattern of particular case study (introducing also the major joint sets and faults) (chapter 5). However, these forward analysis (and comparison with field observations) has been realized rudimentary till now.

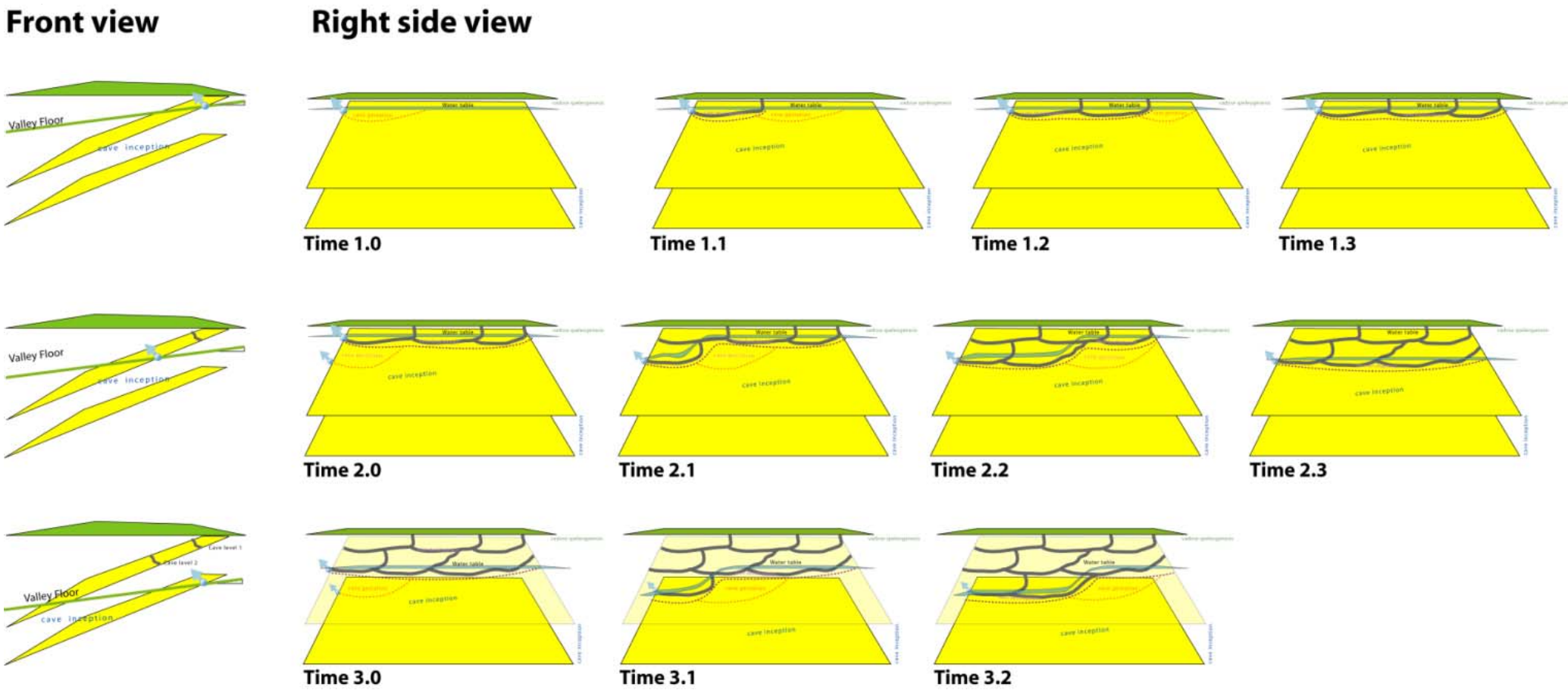

Fig. 4.19: Schematic development of a karst system in time and space (3D view) within inclined inception horizons towards the spring area that crop out at the valley floor: Different parts of the massif are in different karstification state at the same time.

At time 1 cave level develops along the upper inception horizons.

A valley incision event causes a shifting of the spring along the same inception horizon and the development of a second cave level at the same inception horizon (time 2).

Only after another incision event the lower inception horizons crops out and a third cave level develops along the lower inception horizon (time 3)

4.3.3 Conduit size distribution within the speleogenetic zones

Because speleogenesis is selective we can presume that the speleogenetic zones have some typical dissolution voids distributions. The flow concentration along flow path that represent the weakest resistance to the flow will be preferentially used and enlarged (e.g. Kiraly, 1975). This selection is most pronounced within the cave gestation and mainly in the development zone. Some dissolution features will further develop (gestation/development phase) whereas others remain more or less "conserved" at the previous speleogenetic phase. Therefore, dissolution features of previous phases can be found coexistent within a speleogenetical zone.

The understanding of the conduit size distribution within the speleogenetic zones is an important element for the probabilistic prediction of dissolution voids for applied proposes (chapter 5.3).

In the cave inception zone a large number of dissolution seams occur (diameter smaller than some mm). Since the flow rate is small and the dissolution capacity low the different dissolution seams will have similar size. We can suppose that no mayor karst conduits will develop within this zone.

In the cave gestation zone the hydraulic gradient becomes steeper, the flow rate is increasing and the dissolution becomes more selective privileging dissolution seams that are already the largest (i.e. have the highest permeability). Probably less than 0.1 or even 0.01 % of the dissolution seams developed in the cave inception zone will undergo an enlargement to karst conduits (some centimetres).

In the phreatic cave development zone the flow through some karst conduits changes from laminar to turbulent while within the other conduits the flow remains further on laminar (amongst others the flow regime is affected by the conduit size and flow rate (e.g. Worthington, 1999)). The turbulent flow is responsible for a dramatically increase in dissolution rate (e.g. Dreybrodt et al., 2005), increasing the size of these few karst conduits and "concentrates" the flow through them. Again probably only less than 0.1 or even 0.01% of the conduits in the gestation zone will undergo a development to cave conduits (> 0.5 m).

In the vadose cave development zone the flow is affected by gravity i.e. mainly vertical. As water can only flow downwards, vadose conduits are mainly vertical shafts guided by inception fractures or pitching, meandering canyons. The analysis of the 3D geometry of cave systems (chapter 2) revealed among others that the distribution of vadose shafts can be considered as more or less homogeneous (from around 30 m below the surface – e.g. Baroň, 2002), whereas the meanders are guided by inception horizons (chapter 2.2.4).

The presented conduit size distribution within the speleogenetic zones is a very rough estimation at this state of research. Unfortunately it is a serious challenge to obtain size distribution data along inception horizons.

Worthington (1999) calculates the "cave porosity" of some large cave systems (the volume of mapped cave conduits divided by the minimum rectangular block of rock that can contain the cave) and compared them with the measured matrix porosity. For example for the Mammoth Cave System (Kentucky, USA) he reports a matrix porosity of 2.4 % and a cave porosity of 0.06 %. It is to remark that Worthington considered the cave within a rectangular block of rock that can contain the cave (11'000*9'000*90 m) but we could show in chapter 2.3 that around 70 % of the Mammoth Cave System developed along 5 inception horizons. Therefore, we can adjust his value, assuming that the cave distribution along all inception horizons is equal, and estimate a cave porosity density along the inception horizons of around 0.8 %. For comparison we calculated the cave porosity of around 0.1 % along inception horizon number 8 of the Siebenhengste Cave System (fig. 2.8, Zone II). However, these estimations are seriously biased by the fact that no data for karst conduits smaller than about 0.5 m are available (e.g. the karst conduit network of the anastomoses, chapter 2.4.2).

This gap in knowledge can maybe be completed by (borehole) pumping test along inception horizons (e.g. Kresic, 2007) to determinate the dual/triple porosity distribution. It is also conceivable that results of speleogenetic numerical modelling will improve the characteristics of the conduit size distribution within the speleogenetic zones by producing pore size frequency plots (e.g. Rehrl et al., 2008).

4.4 Conclusion

To better understand the influence of permeability distribution in a rock mass for the early karstification flow conditions, we compiled various hydrogeologic numerical models. These model scenarios represent simplified, generic settings that were not designed to account for features of specific field sites but were considered as useful to gain general insight into the flow conditions in pre-karstification and early karstification settings.

The design of the scenarios was done within the inception horizon hypothesis, assuming that within a rock mass, some stratigraphical horizons are particularly susceptible to the effects of the earliest cave forming processes. Primary permeability measurement on such preferential karstified horizons demonstrated that it is possible to distinct inception horizons that have a higher primary permeability than the surrounding rock mass (type 1 and 3) as well as a second type (type 2) of inception horizon with lower permeability (chapter 3). Therefore, our numerical model consists of a homogeneous rock mass that is pervaded by horizons of higher and/or lower permeability than the bulk mass. The occurrence of fractures was neglected.

The results of the numerical simulations allowed us to propose speleogenetic zones with characteristic hydraulic properties and pore size distributions.

The results of the numerical simulations indicate that in the **cave inception zone** ("deep phreatic conditions"), the vertical distribution of the groundwater flow is concordant with the permeability distribution; independent from the geometrical structure and the distance between inception horizons. Generally we can presume that in this zone, the dissolution features are predominantly at the speleogenetical phase of cave inception. Furthermore, we can assume that the karstification takes place over the full thickness of the rock mass but mostly pronounced along flow paths where flow concentration is the highest, i.e. along higher permeability horizons (inception horizons type 1). Horizons with a lower permeability than the surrounding mass (inception horizons type 2) show a reduced horizontal flow rate of the same order than the permeability contrast

The hydrologic behaviour of a given inception horizon changes dramatically when getting close to the spring area, for instance due to a valley incision. Under these conditions, the horizontal flow along the horizon is no more dominated by the permeability distribution alone but also by the distance between the spring area and the horizons. Flow is increased in a drop shaped **cave gestation zone** of some tens of metres in thickness near the spring area and decreases in thickness on a distance of some hundreds of metres. This increased flow also causes an increased rate of karstification. Speleogenetically spoken, we can presume that in this zone, the cave gestation phase will take place. After some time duration flow conditions allow turbulent flow (breakthrough) in this zone. This is the beginning of the cave development phase. Once in the cave developed phase, the hydraulic head of the spring will be propagated upstream to the end of the cave gestation zone, shifting the cave gestation zone upstream. The gestation zone will be moved upstream and the prior cave gestation zone will become the **cave development zone**.

This step by step upstream moving of the cave gestation zone (and phreatic cave development zone) reduces significantly the time requirement for cave gestation and allows, for example, to develop cave levels of several kilometres of cave conduits in reasonable time scale (a few million years).

Based on the concept of the speleogenetic zones deduced of the numerical model results, we were able to reproduce the 3D cave pattern of different types of cave systems by using the position and orientation of the inception horizons and the history of the landscape evolution (mainly the position of the re- and discharge area). This forward analysis provides first ideas on the geometry of the conduits as well as a better understanding of the development of a karst system in time and space (vertical section). It is an important element for the probabilistic prediction of dissolution voids for applied proposes (chapter 5).

- 5 -
Improve the Prediction of Karst Occurrences for Engineering Geological purposes

5.1 Introduction

Karst problems all over the World create huge annual costs as well as social, security-related and environmental problems that are increased due to an insufficient understanding of speleogenesis (e.g. Marinos, 2001; Lolcama et al., 2002; Waltham and Fookes, 2003; Day, 2004; Xeidakis et al., 2004; Casagrande et al., 2005). Problems are not only related to engineering constructions such as tunnels, buildings or dams but also concern the management and protection of karst groundwater that is in many parts of the world an important or even the only resource of groundwater. One way could be to declare karst as not suitable for operating engineered works (declare such areas as highly vulnerable and not predictable). Considering that around 20 % of the dry and ice-free land surface consists of karstic rock formations (Ford and Williams, 2007) and it covers large areas especially in China, Europe and USA such a restrictive statement cannot be applied.

The main question beyond many of these problems is to know whether there is a developed network of conduits and if yes, where it is and in some cases what its characteristics are (e.g. active/fossil, phreatic/vadose, size).

Most ground investigation methods and classifications that are presently available do not introduce speleogenetic considerations (e.g. Zhang et al., 1993; Veni, 1999, 2005; Shofner et al., 2001; Pöttler, 2004; Bakalowicz, 2005; Zabidi and De Freitas, 2006, Xu and Yan, 2004) and consider the karst occurrence as random distributed in space (e.g. Benson and Yuhr, 1993; Tinker and Murk, 1995; Paillet, 2001) (fig. 5.1). These make any inter/extrapolation of observed/detected karst feature almost impossible.

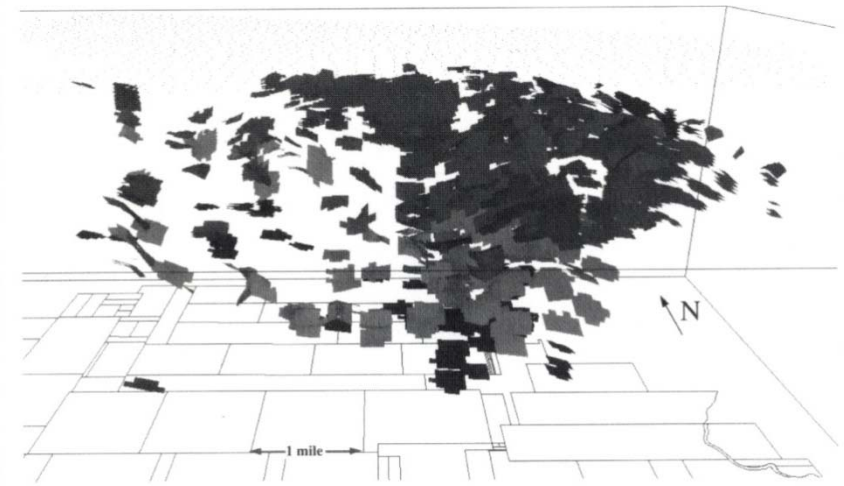

Fig. 5.1: Three-dimensional diagram showing the assumed distribution of caves in the Yates San Andres oil field (Tinker and Murk, 1995). They consider karst occurrence as random distributed in space.

Research carried out by karstologists during the last 50 years showed that the development of dissolution voids is not random. Most efforts were dedicated to the understanding of the processes of speleogenesis. However, only a very restricted number of authors attempted to analyse and understand the geometry of karst conduits i.e. to provide keys for the prediction of conduit positions and characteristics.

A rough prediction of the position of karst conduits can be made by tracing experiments. However, although the map produced by Quinlan and Ray (1981) is a well-known example of this type of prediction, it was drawn in 2D (plan view) and was very imprecise, having an accuracy of only ±500 m. Further, it was based on hundreds of tracing experiments and thousands of borehole data, neither of which are practical for engineering purposes.

An alternative way to address this problem is to study the hydrogeological conditions that prevailed during the karstification of a rock mass. Such studies measure the fracture characteristics (mainly their frequency and orientation) from which conduit directions were derived (e.g. Kiraly, 1968; Jamier and Siméoni, 1979; Eraso and Herrero, 1986; Lauritzen, 1988; Blanc and Nicod, 1990). However, in many cases the authors did not consider the coupling of hydraulic conditions in the speleogenetic process and their methods were limited to descriptions of the relationship between the geological parameters (mainly fractures) and the known conduit directions. Since the influence of non-geological boundary conditions (mainly the respective positions of the recharge areas and the springs) is at least as significant as that of the geology. It was not possible to fully establish and quantify the control that fractures had in the development of the karst conduit networks; i.e. answering the question why only some fractures were incepted. Furthermore it is already challenging to predict/reconstruct the true fracture network (e.g. Jaquet et al., 2004; Dreybrodt et al., 2005). Consequently, this type of approach has a very limited capacity to predict conduit positions (e.g. Zabidi and De Freitas, 2006; Lauritzen, 1988).

Numerical modelling has also been used to understand karstification. Models include the peculiar dissolution kinetics of calcite (e.g. Plummer and Wigley, 1976; Dreybrodt, 1988) and the change of flow conditions from laminar to turbulent when the size of the conduits increases (e.g. Dreybrodt, 1988; Groves and Howard, 1994; Kaufmann 2003; Dreybrodt et al., 2005). So far these models have not often been used for the purpose of conduit prediction, but rather for the assessment of the time duration at which conduits can develop.

In literature a variety of karst classification and karst risk assessments for foundation problems (e.g. sinkhole risk) are presented (e.g. Pöttler et al., 2002; Waltham, 2002; Waltham and Fookes, 2003; Tolmachev and Leonenko, 2005; Kaufmann, 2008; Perlow, 2008) but we could found any classicisation for risk assessments for underground engineers. One exception is Veni (1999, 2005) who analysed cave morphologies in relationship with lithology and hydrologic conditions to derived cave characteristics (probability of occurrence, size and type) of various lithologies. However, his working scale is the rock formation (i.e. rock sequences of some tens to hundreds of metres) therefore his method seems to be more adequate do assess the environmental impact than for engineering geological purposes.

In other words, uncertainty in predictions has not explicitly diminished during the last 50 years and remains very high. Presently there is no real method developed to prediction karstification in regional scale.

Up to now the concept of inception horizons hypothesis (Lowe, 1992) was not clear demonstrated/validated and therefore widely not recognised albeit existing detailed field observations in caves as well as borehole data supported the idea and therefore not introduced into applied karst investigation methods/concepts. However, the clear validation of the inception horizon hypothesis (chapter 2) as well as their enhancements (chapter 3 and 4) will improve significantly the design and interpretation of ground investigation. They will provide a substantial increase in information for engineering purposes as well as for karst hydrogeological investigations. Essentially, it is now possible to quantify the probability of karst occurrences inside a karst massif by identifying the few inception horizons that guide the karstification in regional scale, reconstructing the hydrogeolgical history and winnowing different speleogenetical zones.

This chapter does not present direct results of data analyses because, in our studies, we did not use such data. The aim is to make a quick literature overview to evaluating the impact of the new facts of the inception horizon hypothesis for the design and analysis of karst prediction/detection methods. The overview was encouraging, showing that the inception horizon hypothesis seems to improve consistently the applied karst domains and gives a scientific based justification to inter- and extrapolate data along the extension of certain lithostratigraphical horizons.

5.2 Interpretation of inception horizons from borehole data[1]

In our methodology (chapter 2.2) the identification of regional scale inception horizons is based on cave survey data. However, for many karst regions such data are not available (or are in insufficient quantity and/or quality). In such cases the analysis of boreholes data can be an alternative.

The use of borehole logging data is common in engineering geological investigation programs. These data offer a vertical view of the variation of the physical, chemical or lithological properties of the rock series. In civil engineering borehole data are mainly used for geotechnical purposes. Concerning karst, these data were mainly utilized to detect locally some dissolution voids or areas with increased permeability, or water inflow.

To date occurrences of karst in boreholes were usually considered as randomly distributed in space (e.g. Benson and Yuhr, 1993; Paillet, 2001; Wedekind at al., 2005; Bechtel et al., 2007), which would make any inter-/extrapolations of karst occurrences at a more regional scale almost impossible. It would need around 2500 boreholes to find within an area of 0.01 km^2 a cave (sphere with a diameter of 2.5 m) with a chance of 90 % (Waltham, 2002). The inception horizon hypothesis provides a theoretical framework that allows a new interpretation of borehole data.

Our analyse of the 3D geometry of several large cave systems (chapter 2) show that the development of karst conduits is not random but predictable and linked to the existence of inception horizons. We can postulate that a given inception horizon has a certain continuity along the entire lateral extension of the stratigraphical horizon, since mainly lithological deviations from the predominant carbonate facies are responsible for the fact that a given bedding plane is a potential inception horizon (chapter 3). Therefore, we are convinced that the inception horizon hypothesis improves the potential to extra-/interpolaet locally identified karstified horizons (form the analysis of cave survey data and/or boreholes logging) to a more regional scale.

5.2.1 Methods to identify karstified horizons from borehole data

At least three types of observations can be used to identify/detect inception horizons in boreholes:

1) optical identification of dissolution voids;
2) detection of high porosity zones;
3) identification of zones with a higher permeability.

The following paragraphs shortly present each of them. The choice of the most appropriate method depends mainly on the problem to be addressed, on the required information about the karst system, which is, as well as on the logistical possibilities (Tab. 5.1). For a more detailed presentation and discussion of the different methods please be referred to further reading (e.g. Scott, 1997; Bechtel et al., 2007; Waltham et al., 2005).

[1] *This chapter is widely equivalent to Filipponi and Jeannin, 2008.*

Method			Detection					
			Vuggy Voids	Porosity	Lithology	Water in-/outlet	Permeability	Conectivity
Method	Optical Identification	Core Description	ΩΩ		ΩΩ			
		Televiewer	ΩΩ		Ω	(Ω)		
	Detection of Porosity Zones	Gamma-Gamma-Log		Ω	Ω			
		Temperatur Profile, Flowmeter				ΩΩ	Ω	ΩΩ
	Detection of high Permeablity Zones	Hydraulic Borehole Tests						ΩΩ

Tab. 5.1: Table summarizing the different borehole investigation methods and detected properties (ΩΩ = adequate method; Ω = alternative method - This list is not exhaustive.).

5.2.1.1 Optical identification of dissolution voids

The optical identification is the more intuitive way to recognise karst occurrences. On one hand it is possible to inspect the drilling cores (if available) by eyes, and on the other hand one can use borehole televiewers (visual or acoustic), which provide images of the borehole walls and produce "pseudo cores" (e.g. Cunningham, 2004; Manda and Gross, 2006). Today the resolution of televiewers is comparable to a direct visual inspection, dissolution voids a few millimetres size can therefore be identified.

The size of karst voids typically ranges from microscopic intra granular dissolution features up to cave conduits of several metres in size (chapter 4 and chapter 3.6.1). However, in most cases the size of the intersected karst features in boreholes is smaller than the borehole diameter and they appear as small conduits or as "weathered" stratigraphical intervals.

These observation methods are relatively cheap and fast and make it possible to know the nature of the hydraulic features intersected by the borehole: fracture-like, small dissolution voids or larger karst conduits. They should also allow for recognising lithologic changes (rock fabric, grain size and shape, colour, etc.). However, these methods give any information about the connectivity of the voids.

5.2.1.2 Detection of high porosity zones

Inception horizons are characterized by a concentration of dissolution voids of various sizes, i.e. with a higher (secondary) porosity than to the rock mass. Therefore, any methods allowing for the assessment of the rock porosity are appropriate for the localisation of inception horizons.

Where cores are available the permeability can be measured on them (like we have done in chapter 3.4.1). If they are not available for example the commonly used Gamma-Gamma method can be applied, which gives the density (i.e. porosity) variation along a borehole wall. It seems that this method is also adequate to detect potential inception horizons (e.g. Tipping et al., 2006). Furthermore, this logging method also allows for a rough distinction of the different lithologies intersected by the borehole.

5.2.1.3 Identification of zones with a higher permeability

Most karst voids did not develop as isolated features in the rock mass but are the results of water flowing through fractures and conduits. This means that they belong to an interconnected network of dissolution voids of different sizes. Therefore, inception horizon should display a higher (secondary) permeability than the surrounding rock mass. All available methods able to assess permeability or groundwater in-/outflows in boreholes are therefore interesting for the identification of inception horizons like for example temperature measurements, flowmeter measurements, discrete interval packer tests, etc.

A continuous temperature (or electrical conductivity) profile of the borehole is a simple and fast way to get a first idea about the water movements within an open borehole. Temperature anomalies can be interpreted as water in-/outlets, thus as zones of higher permeability (due to the network of dissolution

voids along inception horizons). However, this method can only be used in boreholes stretching below the groundwater table (phreatic zone).

Flowmeter logging can be used to assess the permeability variations along boreholes by measuring the vertical flow variations within an open borehole (coupled to a calliper log). Electromagnetic flowmeters can measure flows as low as to 0.01 l/s (Paillet et al., 2000; Tipping et al., 2006). Impeller-type flowmeters require several litres per minute in order to produce measurable flow (depending on the borehole diameter). The logging can be done under natural or stressed conditions (either during pumping or injection) and can therefore be also applicable in the vadose zone (above the groundwater table, i.e. unsaturated zone).

Hydraulic borehole tests with packers at discrete intervals of a few metres (or less) provide good measurements of the interval permeability integrating an idea of the borehole neighbouring (depending on the applied hydraulic test) (e.g. Kresic, 2007). Packers are pneumatic or mechanical devices that isolate sections of a borehole by sealing against the borehole wall. These tests should be designed within the concept of the inception horizon hypothesis. It can provide the position of potential zones of higher secondary permeability (which might be due to dissolution processes along an inception horizon). Packer tests are applicable in both the vadose and phreatic zones as multiple or single borehole test.

One possible test configuration is described by Lemieux et al. (2006). They designed pumping and pulse interference tests with pumping or injection of water into one well and measurement of the response in other two wells located 10 to 20 m away. The observation wells were equipped with inflatable packers that isolated the conductive bedding planes (i.e. inception horizons) where responses could be observed.
It is also imaginable to have an inverted configuration: with packer isolated inception horizon with water injection under pressure or water extraction (if highly permeable), simultaneous use of flowmeters in the observation wells.

An important drawback of this group of methods is that they only give the position of potential inception horizons relatively to the top of the borehole. They do not intrinsically provide information about the stratigraphical position of potential inception horizons. A complementary geological survey is therefore necessary. Another weakness is that these methods do not give any information about the nature of the high permeability features (i.e. if they are fractures or dissolution voids).

These methods are quite time consuming and therefore expensive. However, this group of methods is the only one that allows to prove the connectivity/permeability and therefore to describe at least qualitative the state of karstification along the inception horizons

5.2.2 Improve the interpreting of Borehole Data within the Inception Horizon Hypothesis

The above presented borehole geophysic tools are applied to assess the heterogeneity of a karstic rock mass. But how far from the borehole do these methods provide information? Is it founded to correlate logs between boreholes and assume that hydrogeological connections do exist at a regional scale?

In the existing literature different descriptions indicate or even describe the existence of some stratigraphical horizons that are favourable to the karstification in boreholes. They could even be recognized at a regional scale. For examples Paillet and Crowder (1996) describe: “inflow to or outflow from a series of boreholes in northern Illinois was associated with solutionally enlarged bedding plane openings. Many such bedding planes intersected each borehole, but only a few conducted most of the flow. The correlation of these bedding planes was established over borehole separations of about a kilometre”. However, these observations have rarely been interpreted within a speleogeneitcal considerations like for example the inception horizon hypothesis (e.g. Paillet and Crowder, 1996; Yuhr et al., 2008).

The inception horizon hypothesis should be now applied to borehole observations, what would provide a theoretical framework helping for the interpolation of karst occurrences between different boreholes up to a regional scale.

Detailed field observations in caves showed that some conduits developed at a local scale also along other bedding planes than those identified by the statistical (regional) approach (chapter 2). Obviously those bedding planes do not present favourable properties over extended areas and are therefore not significant at a regional scale. For borehole data interpretations this means that an identified karstified stratigraphical horizon can be an inception horizon of local or regional significance (fig. 5.2). The distinction can only be made by correlating horizons recognized in several boreholes and/or in caves or rock outcrops. However, the only way to prove connections at regional scale is to proceed to hydraulic tests between boreholes.

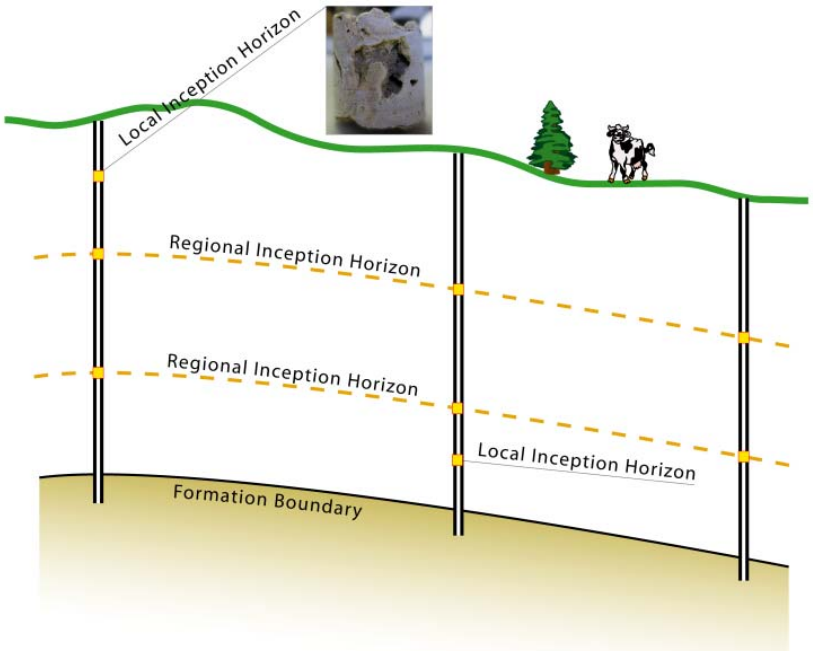

Fig. 5.2: Karstified horizons identified in boreholes can be of local or regional significance. Only the correlation over multiple boreholes allows distinguishing them.

Along karst genesis other factors determine if conduits really develop along them or not (chapter 4). Thus the identification of an inception horizon in a borehole does not mean that this particular horizon really encloses cave conduits (passages with a size larger than around 0.5 m). On the other hand, even for an inception horizon which encloses conduits the measured/observed properties in a borehole do not correspond to properties of the conduits or even of properties of the inception horizon in another borehole (heterogeneity along one single inception horizon, i.e. dissolution features are at different speleogenetic phases – looser and winner tubes). A semi-quantitative extrapolation of any data is not straight forward. Further data are required to estimate if an inception horizon is highly karstified or not (hydrological tests). The development of a conduit network along an inception horizon is strongly related to the history of the (paleo-)hydrogeological boundary conditions (chapter 4). Therefore, a good knowledge of the hydrogeological history of the area as well as of the geological structure is of great help (chapter 5.3).

A strong advantage of boreholes against cave observations is to make possible, with appropriate hydraulic tests, to verify hydraulic connections (i.e. the presence of inception horizons) and characterise them (i.e. size of the karst conduits) around the borehole or at a more regional scale.

The inception horizons hypothesis gives a speleogenetical framework which will help interpretations of borehole data and improve the correlation between boreholes, as well as the extrapolation of “potential inception horizons” over the entire extent of the corresponding stratigraphical horizons.

5.3 Improvements for the karst risk assessment for underground engineering

Many recent tunnel constructions in Switzerland (e.g. Sauges Tunnel, Engelberg Tunnel, Flims Tunnel, La Raisse Tunnel or Alpnach Tunnel) as around the World (e.g. China; Wang and Wang, 2006) have shown that any uncertainties in the geology of the rock volume being tunnelled through, including those related to karst processes, are a major issue, since they may lead to economic, social, security-related and environmental problems. Table 5.2 gives an overview of typical karst-related problems. The main problem beyond these problems is the poor predictability of the location and characteristics (e.g. active/fossil, phreatic/vadose, size, sediment filling) of the karst structures.

Typical problems for tunneling in karst areas

Mainly for limestone and dolostone (gypsum and salt are excluded)

Water

- Massive and abrupt water inflow during boring (« water pocket »)
- Temporary massive water arrival
- Large discharge rates in the unsaturated zone
- Highly variable discharge rates in the unsaturated zone
- Plugging of drainage work by calcite deposition
- Concrete corrosion
- Effect on the discharge rate of neighboring springs
- Effect on the water quality of neighboring springs
- Instabilities/settlements at ground surface due to drainage

Voids

- Instabilities of the tunnel walls, roof and face
- Uncertainty about the stable rock thickness on top of the tunnel (epikarst, soils, conduits)
- Problem for boring/blasting/digging and rock bolting
- Problem for anchoring tunneling-machine
- Other problems (falling down of engines)

Infillings

- Face instabilities
- Sudden debris-flow of karst sediments
- Problem for blasting/digging/boring
- Problem of support of the tunneling-machine
- Problem due to swelling of infillings

Tab. 5.2: Typical civil engineering risks related to karst.

The assessment of karst risks is relevant for the planning, excavation as well as operating of underground structures. Each phase has typical requirements on the site characterization (detailed of risk assessment, available data and budged).

- During the *planning phase* (corresponds in the guidelines of the Swiss Association for Engineers and Architects (SIA) to the preliminary studies and projection phase; SIA-Norm 112) the delimitation of zones with different risk levels will help to decide about location, geometry and dimensioning of the underground construction (e.g. to avoid the most vulnerable zones, Milanovic, 2003) as well as the choice of tunnelling technology ortunnel sections crossing zones of higher risk can be managed in an appropriate way (e.g. by a preliminary recocnassance in front of the working face (Pöttler et al., 2002
- During the *excavation* phase (execution phase in SIA-Norm 112) the karst risk assessment needs to predict and characterize karst conduits (> 1 cm) some meters to tens of metres in front of the

working face to prepare safety measurements (e.g. to control water inrush). The conditions encountered require often constructive and structural measures that should be chosen in a way to be safe and economically interesting (e.g. Marinos, 2001; Milanovic, 2003).

- During the *operating phase* the conditions must be set/controlled in order to guarantee the safety of the construction and workers/users at any moment. Karst hazards related to the potential evolution of nearby karst features should be evaluated too (e.g. a propagation of breakdowns within a karst nearby cave chamber, Waltham et al., 2005)..

In the last years different techniques were developed for the local detection of voids for the excavation and operating phases (e.g. detection of voids a few meters in front of tunnel working faces - e.g. Pöttler et al. 2002; Pesendorfer and Loew, 2004) and controlling of encountered karst structures (e.g. Marinos, 2001; Milanovic, 2003). However, today no method for the prediction of karst occurrences at a more regional-scale is available (i.e for the *planning phase*).

The lack of such a methodology of regional karst risk assessment for an underground structure is due to gaps in understanding speleogenesis but also to a missing transfer of knowledge from karst research to karst applied domains (e.g. Bachus, 2005). Furthermore the social trend to increase the pressure to security, economic and environmental questions will also increase the significance of the *planning* phase.

We are convinced that it is now possible to develop a risk assessment method in regional scale with our improvements of the inception horizons hypothesis:

- clear validation that karstification occurs under phreatic conditions on a limited number of inception horizons (chapter 2);
- showing that the favourable karstification of the inception horizons is due to lithological properties and therefore explicable, identifiable as well as extrapolable along the extend of the whole stratigraphical horizon (chapter 3);
- evidence of the relationship between the spatial placements of the inception horizons, the surface history (valley incision and replenishment) and the geometry of the karst conduit network (i.e. geometry and size) (chapter 2 and chapter 4).

Although the reconstruction of the “true” is not possible yet, will provide the identification of the position of inception horizons in a rock mass as well as the reconstruction of the hydrogeological history (i.e. the position of paleo and present water table) a substantial increase in information for encounter karst occurrences at underground engineering projects.

The risk assessment is based on the assumption that a significant amount of dissolution features occurre along the inception horizons and the delimitation of the four speleogenetic zones (inception, gestation, phreatic development and vadose development - chapter 4) which will characterise the conduit size distribution probability along them.

In the cave inception zone (“deep phreatic conditions”) we assume that the flow and dissolution takes place over the full thickness of the rock mass, and are increased along the horizons of higher primary permeability. However, the flow and dissolution rate are very slight and therefore also the size of the dissolution voids.

The conduit size distribution changes dramatically within the gestation and phreatic development zone (near the water table). Depending on the geometry of the inception horizons relative to the re- and discharge areas and duration of the hydrological phase (time between two valley incision events, i.e. phases where the hydrologic boundary conditions are more or less constant) different geometries and characteristics (size distribution) can be assumed (chapter 4); whereat around 70 % of the conduits developed along the inception horizons and around 30 % along fractures (inception links) (chapter 2).

Flow in vadose cave development zone is ultimately controlled by gravity i.e. mainly vertical. As water can only flow downwards vadose conduits are mainly vertical shafts or pitching, meandering canyons. The shafts development is predominantly guided by fractures. The vertical cave conduit distribution within this zone (below the epikarst) can be considered as almost homogeneous; contrary to that is the development of the meandering passages between shafts often related to inception horizons (chapter 2).

Because the hydrogeological boundary conditions of most cave systems changed during time (mainly the position re- and/or discharge areas by valley incision events) we observe in many cave systems a super position of different phases (i.e. coexistence of voids at different karstification state are close together).

These speleogenetic zones can be reformulated into different probability of karst occurrence and characteristics zones and assign them risk levels ("KarstALEA zones" - aléa is the French word for hazard) (tab. 5.3). It is to notice that for this classification we do not distinguish between the gestation and development zone. Thereby it is possible to subdivide a karstic rock mass into zones of different risk levels by means of the identification of the position of inception horizons in a rock mass as well as the reconstruction of the hydrogeological history.

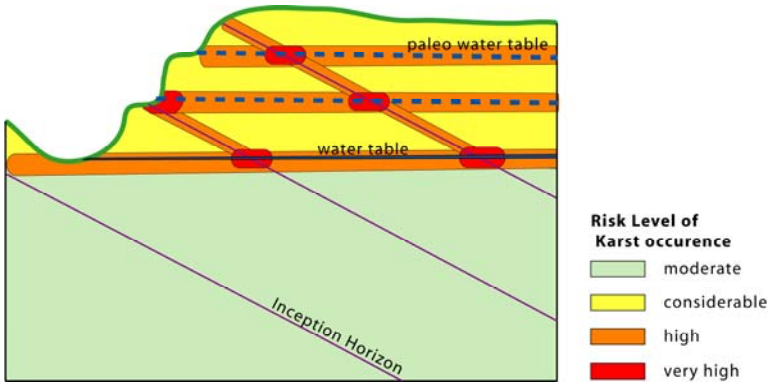

Speleogenetic Conditions	Description	Tunneling Problems			Risk Level
		Water	Voids	Infillings	
incepted	the rock zone is in the deep phreatic zone, dissolution in the size <1 cm are most likely to occur	(x)			moderate
incepted during phreatic phase, maybe vadose cave development	the rock zone is in the vadose zone, dissolution in the size <1cm are most likely to occur but vadose cave conduits (>>1cm) with possible massive water flow during rain events or snow melting can be encountered	(x)	x		considerable
inception horizon with no cave development in the gestation and/or phreatic development zone , probably cave development under vadose conditions	the rock zone is in the vadose zone, dissolution in the size <1cm are most likely to occur but vadose cave conduits (>>1cm) with expected massive water flow during rain events or snow melting can be expected	x	x		high
inception horizon with cave development in the gestation and/or development zone	the rock zone is an inception horizon near the water table, conduits size >> 1cm can be expected	x	x	(x)	very high
inception horizon with cave development in the gestation and/or development zone and probably re-used in vadose conditions	the rock zone is an inception horizon in the vadose zone, conduits size >> 1cm with possible massive water flow during rain events or snow melting can be expected	(x)	x	x	very high

Tab. 5.3: The KarstALEA zones assign risk levels, based on the occurrence of inception horizons and the position of actual and paleo-water table.

A preliminary case-study and coarse validation has been attempted on the Weissenstein Tunnel (3.7 kilometres long railway tunnel between Gänsbrunnen and Oberdorf, Solothurn/Switzerland; constructed in 1908). It crosses the Weissenstein anticline at around 700 metres a.s.l., probably just below the water table. Although the tunnel walls are now concrete-lined the documentation of the tunnel construction (Buxtorf, 1908) indicates that three karst accidents occurred during tunnel construction. They intersect two karst

voids that were filled with sediments, with only a minor water-flow and one void with a larger water inrush, with a discharge of around 80 l/s, (fig. 5.3).

We compared the stratigraphical position of the karst voids encountered during tunnel construction with the stratigraphical position of the statistical identified inception horizon of the nearby Nidlenloch cave system (appendix 1). The tunnel accidents are located along the identified inception horizons of the Nidlenloch cave system (fig. 5.3). According to the Karst-ALEA classification they would belong to the zones of "very high risk level of karst occurrences".

We can thus conclude that in a similar case it would be possible to predict such zones of higher probability of karst occurrences and to be prepared to face such problems and possible to make further preliminary investigations in such tunnel sections.

However, further back as well as forward analysis of different case studies are needed to formulate a real method for the evaluation of the risk of karst occurrence within a massif. But the first results are very encouraging that it will be possible to subdivide a rock mass into useful hazard zones.

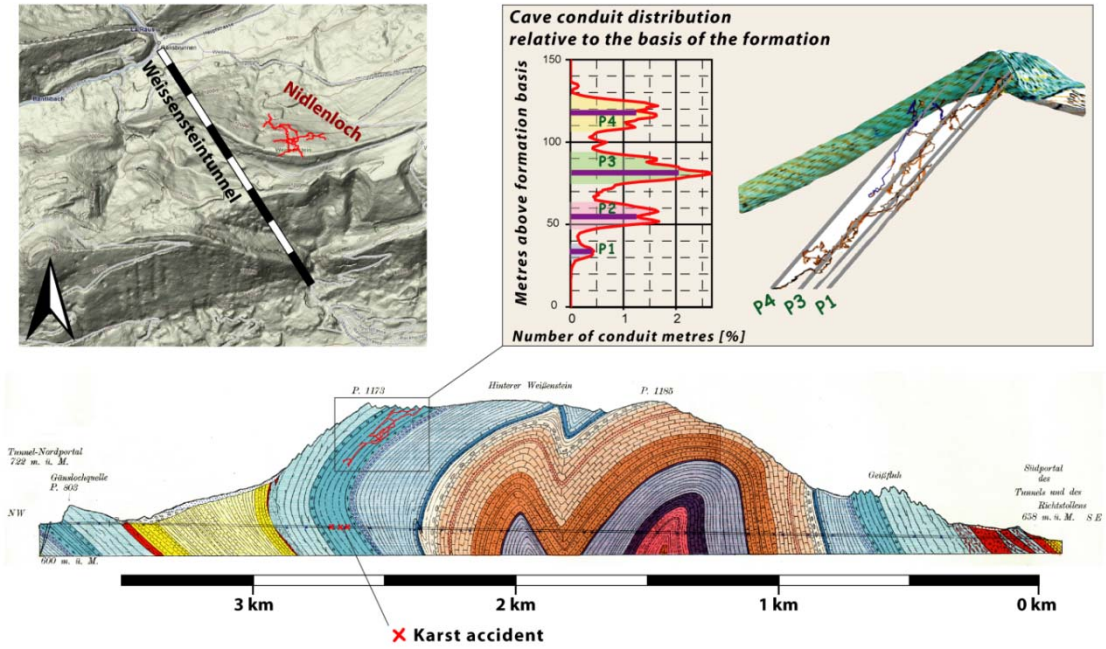

Fig. 5.3: The karst accidents within the Weissenstein railway tunnel are located along inception horizons identified in the nearby Nidlenloch cave system (geological section Buxtorf, 1908).

5.4 Other Applications of the Inception Horizon Hypothesis

The progresses of the inception horizon hypothesis seem to improve also other applications like for example:

- Risk assessment for ground stability due to sinkholes (e.g. Doctor et al., 2008).
- Improve the interpretation of geophysical surveys by reducing the decree of freedoms (e.g. Yuhr et al., 2008).
- Design and interpretation of hyrological tracer tests.
- Improve the cave exploration (e.g. in the Nidlenloch cave system new passages could be found based on the 3D analysis; pers. Com. Tom Hermann, 2009).
- Methods for interpreting carbonate reservoirs.
- Methods for interpreting ore deposits (e.g. Lowe, 1993).

The list is not exhaustive.

Further investigations and case studies are needed improve these applied methods with the transfer of knowledge from the inception horizon hypothesis.

5.6 Conclusion

In this chapter, we evaluated the applicability of the enhanced inception horizon hypothesis to different domains. The results are encouraging, showing that the hypothesis seems to be appropriate for different domains of applied Earth Sciences and engineering. For instance, we showed that the evidence of the existence of the inception horizon justifies/allows interpreting karst occurrences between boreholes and it improves the choice and design of borehole data acquisition.

Furthermore, we showed that the improvements on the inception horizons hypothesis, done in this thesis, allow now to formulate for example a scientific based karst risk assessment for underground engineering purposes.

Many challenges remain in the development of these methods, especially because speleogenesis processes are complex and they highly depend on many factors, which are not always easy to assess (e.g. paleo-hydrogeology). Further developments are required to improve our ability to characterize karstic rock mass. However, we could show that the inception horizon hypothesis has some potential to improve the design and interpretation of site characterisation studies.

Dejenhöhle (GL, CH)

- 6 -
Final Discussion and Conclusion

6.1 Final Discussion about the speleogenesis along inception horizons

We developed a method to analyse the 3D geometry of cave systems in order to demonstrate from a statistical point of view that karst conduits position is not random but related to a restricted number of lithostratigraphic horizons (i.e. inception horizons) (chapter 2). Therefore, our analysis of several among the largest cave systems in the World (more than 1500 km of analysed cave conduits) confirmed for the first time quantitative the inception horizon hypothesis. Up to now, the ideas of the inception horizons hypothesis have been supported by various field observations but no clear demonstration/validation was done and for this reason also not widely recognised.

We could demonstrate that probably less than 10 % of the existing bedding partings of a limestone sequence are inception horizons and guide more than 70 % of the phreatic conduits. These results clearly confirmed that the influence of these horizons onto the 3D geometry of cave systems is high.

Based on the 3D analysis of cave systems and on field verifications, 18 inception horizons in six cave systems were selected for field characterisation and sampling in order to identify the properties and processes that makes these particular lithostratigraphic horizons favourable to karstification (chapter 3). For none of the investigated lithological properties it was possible to recognize threshold values that distinguish incepted horizons from not incepted ones. The absolute values of the properties have only a subordinated significance: it is mainly the contrast between the properties of inception horizons and the surrounding rock mass which is relevant. However, the results evidenced that inception horizons have a thickness of some centimetres to decimetres and that it is possible to distinguish between 3 types of inception horizons:

Type 1 Inception horizons where the cave inception took place **within the inception horizon** are characterized by a slightly higher primary permeability, higher pyrite and quartz contents and lower matrix contents than the surrounding rock mass. Usually, fractures propagate through or occur within these horizons.
The concept of the speleogenetic scale of influence let us assume, that the primary permeability will be the relevant factor at the beginning of karstification, whereas the matrix and pyrite contents are the key factors during the later cave inception phase. The further cave development will be controlled by the total carbonate content.
Fractures along inception horizons of type 1 occur most of the time after the beginning of the karstification. The apparition of fracture will strongly increase the permeability of inception horizons along the intersection with inception horizons and enhance the karstification along the intersection.

Type 2 Inception horizons where the cave inception took place **at the contact with the inception horizon** are characterized by a lower primary permeability and carbonate contents, but higher pyrite contents than the surrounding rock mass. Fractures usually end at these horizons.
We can suppose that the low primary permeability, the clogging of the pores by the clay minerals and the high contents of pyrite (production of aggressive solutions within the horizon that concentrate the dissolution along the contact to the surrounding rock) and the ending of the

fractures at the horizon may be responsible for the enhanced karstification at the contact during cave inception and gestation phases.

Type 3 Inception horizons where the cave inception took place **along bedding plane fractures**; a slippage of just a few millimetres, striation, brecciation and surface irregularities enhance openings along the sliding plane and will cause a significant increase in permeability along mechanical interface that did not undergo significant karstification before the tectonic event.

These results give us some good first indications about the properties and processes along the inception horizons. They allow conceptualising the speleogenesis along inception horizons by combining the lithological properties and the related processes to the hydrological history of a rock mass.

Numerical hydraulic modelling allowed us to distinguish in an epicenic karstic rock mass four different speleogenetic zones with characteristic hydraulic conditions:

- The **vadose cave development zone** is located above the water table.
- The **phreatic cave development zone** is located near the water table. Cave development occurs under low to moderate hydraulic gradient and turbulent flow conditions.
- The **cave gestation zone** is located within the first tens of metres of the phreatic zone and has a length of some hundreds of metres. Karst conduits develop under steep hydraulic gradient but laminar flow conditions.
- The **cave inception zone** is located below the gestation zone with low hydraulic gradient and slow laminar flow. This is the zone in which inception horizons are being prepared.

We concluded that the only motor for karst development is the hydraulic gradient, which moves through the massif and changes in short (horizontal shifting of the gestation zone) and long (valley incision) time scales.

6.1.1 Do we have enough time to develop cave conduits along inception horizons of type 1?

The results of simple hydrogeological numerical modelling study showed that an epigenic karstic rock massif can be subdivided into four speleogenetic zones: (1) the vadose cave development zone above the groundwater table, (2) the cave development and (3) gestation zone within the first tens of metres of the phreatic zone and (4) below them the inception zone (chapter 4).

The distribution of groundwater flow within the inception zone is mainly depending on the permeability distribution and is independent on the geometrical setting and on the distance between inception horizons (chapter 4.2.1). Therefore, karstification takes place throughout the full thickness of the inception zone; whereas it is mostly concentrated along horizons with the highest permeability. At early stage of karstification, it would be more adequate to call them "*potential inception horizons*", because their further development towards conduit development depends on hydraulic conditions occurring at later stage in the cave gestation and development zones.

Primary permeability measurements on micro cores from the inception horizons and of the surrounding rock mass (chapter 3.4.1) showed that inception horizons of type 1 had a primary permeability which was at least 50 to 70 % higher than that of the surrounding rock mass. This means that initial flow velocity through the inception horizons was at least 50 to 70 % higher than through the matrix of the surrounding rock mass. Therefore karstification should also be enhanced. Values are small and contrasts are low compared to the total range of permeability found in a karstified rock. However, this contrast of the initial conditions may be large enough to produce a flow concentration and a preferential development of karst along those horizons. However, one question should be addressed with this context: Is the dissolution rate sufficient within the inception zone to significantly increase the permeability, i.e. to attend a permeability that allows reaching breakthrough within the gestation zone in realistic time-scale?

The application of theoretical dissolution models gives an idea of the time needed for conduits to be developed (e.g. Palmer, 2002; Dreybrodt et al., 2005). These authors give the theoretical estimation for the breakthrough time and a single fracture of a given initial opening (fig. 6.1).

To use these models (that are originally designed to understand the karstification along fractures), we need to estimate the primary pore space within the inception horizons. The microscopic analysis of the pore types (chapter 3.4.1.2) lead us to conclude that the permeability of the samples was controlled by interparticle pores (matrix porosity). They are usually too small to be detected by microscope. Considering our permeability measurements, we will probably not be too far away considering an initial pore opening of some 0.001 mm (Smith et al., 1976). This initial opening would give a breakthrough time of some 10^{13} years (considering the low hydraulic head conditions within the inception zone and on the length of the flow path – chapter 4) (fig. 6.1 - Example). This means that the time duration for breakthrough is longer than the age of the rock itself (10^8 years!). Notice, that in this example the gain in breakthrough duration due to the change in hydraulic gradient between the inception zone and the gestation zone is "only" in the order of 1 million years.

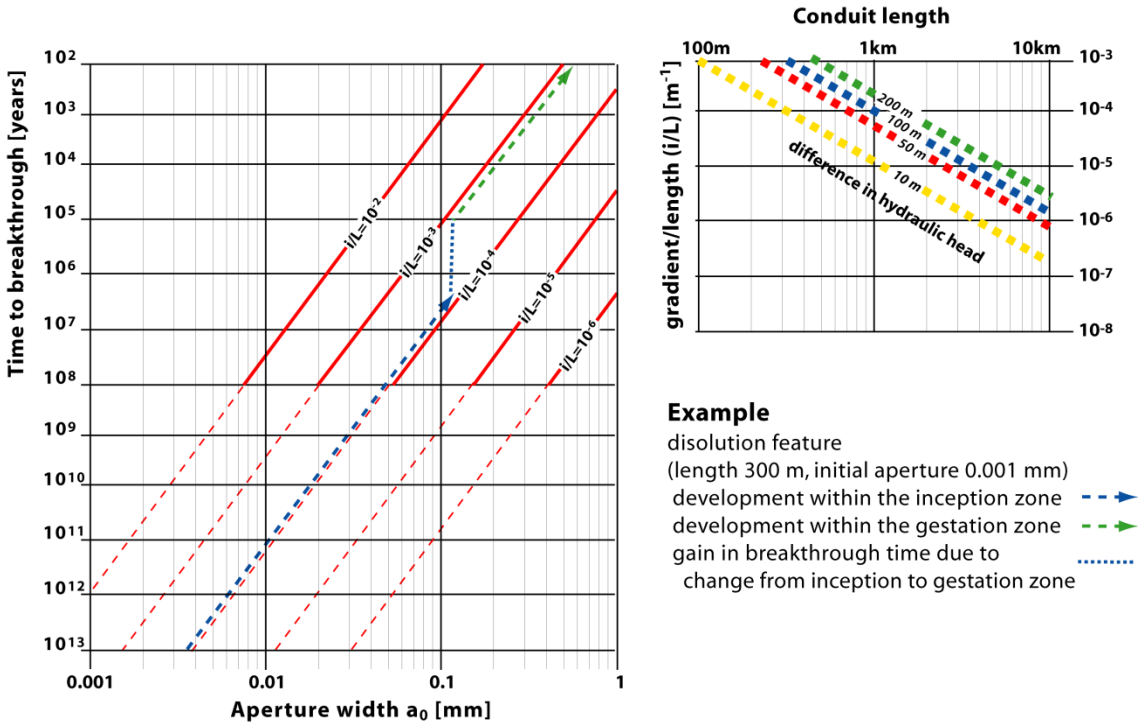

Fig. 6.1: Estimation of the breakthrough time: The diagram gives an estimation of the time required to enlarge a given initial fracture to turbulent breakthrough for different hydraulic gradients as well as flow distance (modified after Palmer, 2002).

There are different reasons for the overestimation of this time duration compared to real conditions:

- The considered primary "pore space" (i.e. measured permeability) is by far a minimum, because the sampling was only possible were inception horizons were still present (chapter 3.4.1). The seepage water was channelled along inception horizons, concentrating flow where the permeability was the highest (i.e. not where samples could be taken). Therefore, we can consider that the obtained breakthrough time as by far a maximum.
- The model assumes that boundary conditions during the karstification do not change (e.g. hydraulic head, Pco_2, water temperature). This assumption is quite consequent because, in reality,

boundary conditions change often according to changes in outside (surface) conditions (climatic and landscape evolution) (chapter 4.2.2).

- The lithological properties of the rock mass may have a strong effect on the dissolution rate (e.g. Eisenlohr et al., 1999) but the understanding of the relationship between the rock properties and the empirical parameter used for the estimation of the breakthrough time is still insufficient to fully consider them (Dreybrodt et al., 2005).
- The model neglects the occurrence of fractures. Inception fractures occur after the beginning of the karstification, whereas the flow along the intersection with inception horizons will drastic increased and therefore, the karstification being enhanced.
- The model was developed for the speleogenesis along fractures, but inception horizons of type 1 should be considered as a porous medium. The flow path within porous medium is characterised by concentrations of flow around insoluble or less soluble grains. The surface available for fluid/rock interactions is higher than in a fracture and therefore, the distribution of grain/crystal size becomes crucial (chapter 3.4.4) (e.g.Noiriel, 2005).
- The model considers only dissolution by epigenic CO_2; other processes occurring during the cave inception phases are missing, for example the production of "acidity" within the inception horizon by weathering of sulphide minerals (production of H_2S) or the decomposition of organic material (production of H_2S and CO_2) (chapter 3.4.3). These processes would at least locally increase the dissolution.

However, we can assume that the theoretical dissolution models in use today are adequate for pore size larger than some 0.1 mm (i.e. cave gestation and development phase). Below this pore size, the dissolution is also influenced by the processes listed above. Further developments are needed to introduce the missing cave inception phase processes into numerical speleogenetic models (e.g. production of additional dissolution capacity by weathering of pyrites) and model an adequate porous medium.

The theoretical dissolution models allow estimating the required size (aperture width) for a dissolution feature to develop to the breakthrough within the gestation zone in realistic time scale (some 10'000 to 100'000 years). For a difference in hydraulic head of 50 m and lengths of the gestation zone of 400 m a dissolution feature opening of some 0.1 mm is required. This means that pore spaces need to be prepared within the inception zone at least to this size. Smaller features will not reach breakthrough before the cave gestation zone moves backwards and the hydraulic gradient will (again) flats down (development zone).

This pore size can be attained by enlarging the primary porosity by processes of the cave inception phases alone (e.g. flow concentration around grains, acid production by pyrite weathering) or being enhanced by the occurrence of fractures. Fractures that intersect inception horizons of type 1 increase the permeability at the intersection of several orders of magnitude.

Field observation evidenced that cave conduits developed mainly at the intersection between inception horizons and inception fractures (e.g. Jameson, 1985; Lauritzen, 1988; Lauritzen and Lundberg, 2000; Filipponi et al. 2008 – see also chapter 2.2.7). The inception horizons of type 1 are often crossed by fractures (chapter 3.3.3). The occurrence of fractures strongly increases the permeability of inception horizons along the intersection of the inception horizons with fractures (e.g. Kiraly, 1969). This increases the contrast between the already incepted horizon and the surrounding rock mass and concentrates the flow and therefore also the karstification at the intersection (fig. 6.2 below). It also reduces the breakthrough time dramatically to a more realistic time scale.

Within some inception horizons of type 1 we could also observe networks of small karst conduits (anastomoses) that have no relation with fractures (chapter 2.4.2). Ewers (1966) already observed that anastomoses are common in areas of poorly jointed limestone. Therefore, we must assume that it is also possible to incept and develop cave conduits along inception horizons of type 1 in realistic time scale without the occurrence of fractures (fig. 6.2 above).

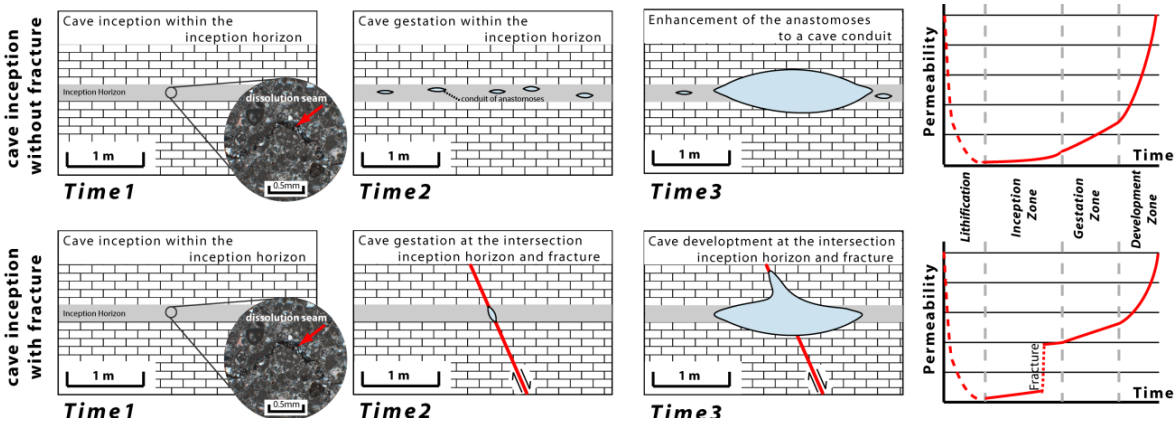

Fig. 6.2: Two different ways of cave development within inception horizons of type 1. Above: Cave inception without fractures where the cave develops by increasing forward from primary pores. Below: Cave develops at the intersection inception horizons with fracture where the permeability is supposed to be highest because of preview cave inception.

We can conclude that the theoretical dissolution models in use today overestimate drastically the duration of the breakthrough time for the cave development along inception horizons of type 1. The models seem to be adequate to describe the speleogenesis within the cave gestation and development phases. For the genesis within the inception phase further developments are required like the flow and dissolution through a porous medium or the acid production within the inception horizon.

6.1.2 Why do caves develop along inception horizons of type 2?

Different authors (e.g. Lowe, 2000, Underwood et al., 2003) presume that inception horizons of type 2 act as a low permeability "screen" along which water flows preferentially, under phreatic conditions. We could not get any numerical evidence of horizontal flow concentration neither within the horizon nor at the contact with the surrounding rock mass (chapter 4.2.1); therefore also no evidence of an increased dissolution zone. The fact that field observations (chapter 2.2.8 and 3.3.1) confirmed the existence of this type of inception horizons lets us suppose that there are other factors than the contrast in primary permeability that controls the early karstification.

Inception horizons of type 2 are characterized by a lower primary permeability and carbonate contents but higher pyrite contents than the surrounding rock mass and fracture termination at the horizon. Therefore, we can suppose that the karstification along the contact may be induced:

- By the production of aggressive solution within the horizon by pyrite weathering that could increase the dissolution at the contact with the surrounding rock mass (chapter 3.4.3.2; fig.6.3-above);
- By the mechanical behaviour of the horizon (i.e. the occurrence of contact fractures) due to the contrast in mineralogical composition (chapter 3.3.3; fig. 6.3-below).

Various authors describe (e.g. Underwood et al., 2003; Cooke et al., 2006) that shale-rich units within a carbonate sequence act as "mechanical interfaces" (stratigraphical horizon along which many fractures abut) and causes a lack of vertical connectivity. They conclude that continued flow along the horizon may promote dissolution along the interface. Dissolution may occur over large areas, resulting in regionally extensive, bed-parallel, high-permeability features. Unfortunately they give no direct explanation why the flow along the contact fracture-inception horizon should be increased compared to the other parts of the fracture within the phreatic zone.

Two predominant mechanisms of fracture termination can be distinguished: ductile deformation of the mechanical interface to resist fracturing (1); propagation of the "vertical" fracture along the contact (2) (e.g. Pollard and Segall, 1987; Helgeson and Aydin, 1991; Rijken and Cooke, 2001; Cooke and Underwood, 2001; Cooke et al., 2006).
The observations on inception horizons of type 2 correspond more to a mechanical behaviour of type "fracture propagation along the contact"; albeit it was not possible to observe this small contact fractures anymore (they have been destroyed by the development of the cave passages) (fig. 6.3-below). These contact fractures would explain the increased flow and therefore, the karstification along the inception horizon-fracture contact.

This requirement of (contact) fractures would involve that the karstification of the horizon only took place with or right after the mechanical wear of the rock massive and therefore quite late compared to karstification history of inception horizons of type 1. The cave inception along these fractures can be induced by "tectonic inception" (tectonics producing a fracture network wide enough to allow turbulent flow; Faulkner, 2006) or by "chemical inception" (dissolution of the fracture surface and gradual enlargement of the fracture width) if the initial fracture width is not enough to allow turbulent flow.

If the mechanical behaviour (i.e. the fracture propagation along the contact) is the main factor inducing the karstification along inception horizons type 2, it would maybe be meaningful to group inception horizons type 2 together with of type 3; that is fracture propagation along stratgraphic horizons with only a moderate karstification within the cave inception phase. At least, this applies for further investigations on the mechanical properties of the inception horizons and the surrounding rock mass.

Nevertheless, along some inception horizons of type 2, we could observe small karst conduits (anastomoses, chapter 2.4.2) that have no relationship with fractures. We should therefore assume that processes can occur along inception horizons of type 2, which increase significantly the permeability during cave inception phase to allow cave development without the occurrence of fractures. For instance, the alteration of some minerals (e.g. pyrite) mainly present along inception horizons could produce aggressive solutions that concentrate the dissolution along the contact to the surrounding rock mass (fig. 6.3-above; chapter 2.4.3.2). It is not necessary that the produced aggressive solution is responsible for the complied inception of the contact. It would also be sufficient when only a small zone of higher permeability is produced early in the cave inception phase. The further development along the contact will follow again the schema of inception horizons of type 1.

Further field investigations and laboratory analysis are required to fully understand the speleogenesis along inception horizons of type 2.

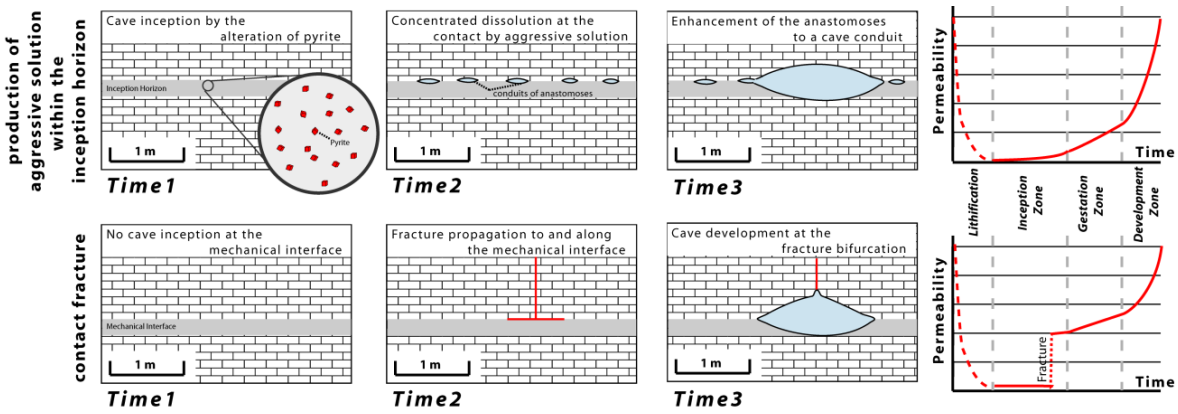

Fig. 6.3: Two different ways of cave development along inception horizons of type 2. Above: Production of aggressive solution within the inception horizons (e.g. by the weathering of pyrite) and the karstification at the contact with the surrounding rock mass. Below: Cave develops along a contact fracture.

6.1.3 What is the nature of inception horizons of type 3?

Conceptually it is quite easy to recognize inception horizons of type 3: a bedding plane fracture with evidence of slippage (striation) and/or offset of the conduit cross section. However, one of the major problems is to distinguish a "bedding plane fracture" (fig. 6.3-above) from a "dissolution induced fracture" (fig. 6.3-centre). That is, if the fracture produces a new "secondary" permeability feature or if the fracture propagation enhances the already existing "secondary" permeability.

We saw that karstification can start already during or just after lithification of the rock mass, whereas fracture can be most of the cases be considered to occur later in the history of the rock mass (chapter 3). Therefore, both bedding plane fracture types can be considered as syn-karstic. However, the distinction is fundamental for the understanding of speleogenesis along this type of inception horizons. In case of the *dissolution induced fracture,* the fracture occurred along an inception horizon that was already a potential inception horizon, i.e. with a significant karstification within the cave inception (and gestation) phase. The tectonic slippage will increase the secondary permeability along the horizon and enhance karstification. In the case of the *bedding plane fracture,* the karstification within the cave inception phase was moderate and the slippage produces a "new" secondary porosity feature. The "horizon" would probably not support cave gestation and cave development phases without the fracture occurrence. *Only bedding plane fractures should be considered as inception horizons of type 3.*

Clear distinction between *bedding plane fracture* and *dissolution induced fracture* will be the first step to better understand the karstification of this type of inception horizons. For bedding plane fracture further investigations on the , the mechanical properties of the rock mass should be considered. Contrary for dissolution induced fracture a re-classification of the inception horizon to type 1 or 2 should be proved and study the litho-chemical properties scheduled.

An invitingly possibility to recognize the nature of these inception horizons would be a lithologic characterisation of the horizons and the surrounding rock mass to see if it would be possible to reclassify the horizon into type 1 or type 2; and if this would not be possible to consider them as inception horizons of type 3. However it is to suppose that the same lithological properties will also be responsible for the mechanical contrast that guides the fracture propagation (e.g. Pollard and Aydin, 1988).

Another possibility to recognise the origin of bedding plane fractures is a detailed microscopic description of dissolution features within the inception horizons; if an increased number of dissolution seems can be observed within the horizon, it is most probable, that it is an inception horizon of type 1, which has been enhanced by the occurrence of the fracture.

Another approach is a detailed structural analysis of the fracture occurrences, i.e. try to reconstruct the tectonic history. However, none of these analyses was done during the present thesis project.

For inception horizons of type 3, we can conclude that a slippage of just a few millimetres, striation, brecciation and surface irregularities enhance openings along the sliding plane and will cause a significant increase in permeability and therefore concentrate the flow and karstification along them.

The fracture can enhance the permeability of already incepted horizons or produce new high permeability feature and therefore concentrate the flow and the dissolution along them. This fracture induced increase in permeability can skip certain speleogenetic phases and in some extreme cases allow the cave development without a significant increase in permeability during cave inception and gestation phase ("tectonic inception" - tectonics producing a fracture network wide enough to allow turbulent flow; Faulkner, 2006). Other extreme cases are fractures which occurred post-cave-development and have no speleogenetic significance (neo-tectonic) (fig. 6.3-below).

As inception horizons of type 3 should only be considered bedding plane fractures; i.e. fracture propagation along stratgraphic horizons with only a moderate karstification within the cave inception phase.

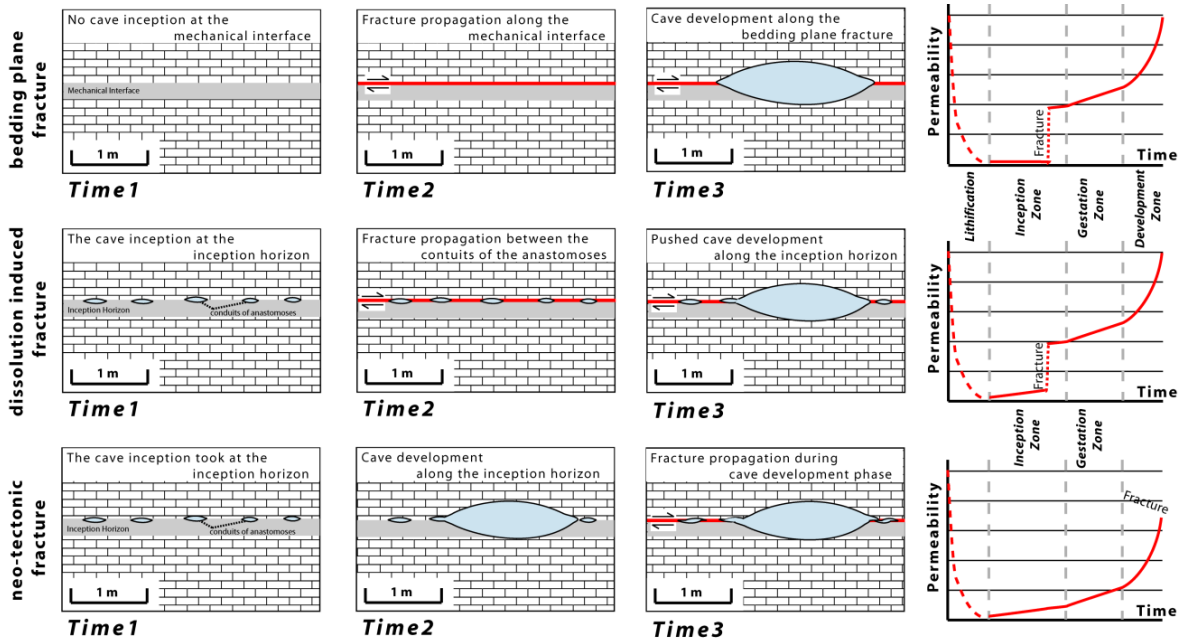

Fig. 6.4: Two different ways of the interaction between bedding plane, fracture and cave development.
Above: Bedding plane fracture occurs along a mechanical interface and induces the karstification along them (=>bedding plane fracture).
Centre: Karstification begins without the occurrences of fractures along the inception horizon; only later a fracture propagates through the karst conduits (=> dissolution induced fracture).
Below: The fracture occurs after the cave conduit was developed (neo-tectonic fracture).

6.1.4 What decides where caves conduits do develop? – The role of the cave gestation zone

The 3D analysis of chapter 2 lead us to conclude that a significant part of caves conduits develop along inception horizons and mainly along the intersection of inception fractures with inception horizons near the (paleo-)water table.

In chapter 3, several lithological properties were indentified to be significantly different within the inception horizons compared to the surrounding rock mass. We also recognised and that the associated processes do only occur within certain speleogenetic phases (chapter 3.XX).

Finally in chapter 4, we recognised that the only motor for karst development is the hydraulic gradient, which moves through the massif.

These findings allow us to formulate a conceptional model of speleogenesis, where the beginning of the karstification can be defined by the moment where the permeability of a rock mass increases steadily due to dissolution. At this stage the hydraulic gradient is low to moderate, the flow is laminar and poorly organised; we are within the inception zone (chapter 4). Dissolution is low, slow, diffuse and distributed within the whole volume of the zone; however some horizons tend to increase their permeability slightly faster than others, preparing the later development of karst conduits. They are becoming potential inception horizons. At this stage, most of the dissolution features are within the cave inception phases, i.e. their karstification is controlled by the primary permeability distribution, the local production of additional of acidity and the dissolution rate of the rock matrix (chapter 3.6.1). If fractures occur, they increase the permeability of certain features (mostly the intersection with inception horizons) and enhance the karstification.

The situation is different near the spring area, where a drop shaped gestation zone (some tens of metres deep and a few hundred metres long) with steeper gradient controls the flow. Flow within this zone becomes organized along previous prepared inception features and a network of karst conduits develops.
However, not all inception features prepared within the previous inception zone will have the same chance for further development; features with already higher permeability (most of the cases the intersection inception horizon with inception fractures) and situated closer to the spring area are privileged (chapter 4). Furthermore the preparation of the inception features within the inception zone needs to be so far as breakthrough can be attained within reasonable time-scale (some 10’000 to 100’000 years) (fig. 6.1) .
Inception features of the cave inception phase will coexist with features of the cave gestation phases. However, only the features within the cave gestation phases will undergo significant further development, the other will remain “conserved” in the inception phase.

Once a karst conduit network is established within the gestation zone that allows turbulent flow (after breakthrough), the dissolution kinetics will strongly increase, the size of the conduits increasing faster and causes a decreasing of the water table to spring level within this zone. The gestation zone will become the development zone. A new gestation zone will take place upstream with regard to the former.

The conduit development in the development zone is fast and caves can reach human size within a few thousands of years (e.g. White, 1988; Dreybrodt and Siemers, 2000; Palmer, 2002). It is mainly controlled by the discharge flow-through and the dissolution rate of the rock mass (i.e. their carbonate contents).

6.2 Achieved results

During this thesis project, different results have been achieved to better understand the spatial arrangement of karst conduit networks and determine parameters controlling the speleogenesis along preferential lithostratigraphic horizons.

- The **3D analysis** of more than 1500 km of cave conduits **confirmed for the first time quantitatively** that the development and position of karst conduits under phreatic conditions is remarkably related to a restricted number of so called **inception horizons**.
- We demonstrated that probably **less than 10 % of the existing bedding partings** of a limestone sequence are inception horizons and **guide more than 70 % of the phreatic conduits**.
- The **field verification** demonstrated that the inception horizons exist and that they have a thickness of some centimetres to decimetres.
- A **conceptual model** could be derived: the karstification develops mainly along **inception horizons** according to the regional **hydraulic gradient**; **fractures** control conduit orientation and position at a local scale along inception horizons
- Based on field observations along the inception horizons and lithologic characterisation of rock samples, it was possible to distinguish between 3 types of inception horizons:
  - Inception horizons where the cave inception took place **within the inception horizon**;
  - Inception horizons where the cave inception took place **at the contact with the inception horizon**;
  - Inception horizons where the cave inception took place **along bedding plane fractures**.
- Based on considerations about the speleogenetic role and scale of influence of lithological **properties of inception horizons**, it was possible to recognize that properties controlling the early flow path as well as producing additional acidity are the main factor during cave inception and early gestation phases, where as the limestone purity and the associated dissolution rates control speleogenesis only in the gestation and cave development phases.
- Simple groundwater flow modelling showed that an epigenic karstic rock massive can be subdivided into four **speleogenetic zones**. Each of these zones is characterized by typical speleogenetic processes as well as a specific dissolution void distribution.
  - The *vadose cave development zone* is located above the water table, where vadose cave development takes place.
  - The *phreatic cave development zone* is located near the water table. Caves development occur under low to moderate hydraulic gradient and turbulent flow conditions
  - The *cave gestation zone* is located within the first tens of metres of the phreatic zone. Cave conduits develop under steep hydraulic gradient but laminar flow conditions.
  - The *cave inception zone* with low hydraulic gradient and slow laminar flow is located below the gestation zone. This is the zone in which inception features are being prepared.
- We showed that the only motor for karst development is the **hydraulic gradient**, which **moves through the massif** and changes in short (horizontal shifting of the gestation zone) and long (valley incision) time scales.
- We demonstrated that it is possible to **explain and schematically reproduce the 3D pattern of different cave systems** by using the position and orientation of inception horizons as well as the history of the landscape evolution (i.e. the re- and discharge area).
- We evidenced the feasibility to combine the improved inception horizon hypothesis with other current applied methods, to improve the prediction of dissolution voids. Furthermore we proposed a **scientific based risk assessment for underground engineering proposes**.

This thesis demonstrated that it is now possible to quantify the probability of karst occurrences inside a karst massif by reconstructing the hydrogeolgical history and by identifying the few inception horizons that guide the karstification at a regional scale.

- Acknowledgments -

I am grateful to my thesis directors Prof. A Parriaux and Dr. P.-Y. Jeannin for giving me the opportunity to immerge into this fascinating thesis project.

This thesis was not possible without the help of numerous cavers, ally, aider helper and gnomes. Thanks a lot for your support!

… Papa and Mami, per avermi fatto vedere che i sogni devono essere presi con rispetto; Petra, meine Schwester auf die ich so stolz bin; Monika, ich sage nur “Dattelpalmenwald in der Morgensonne“; Patty-Phil-Tina, für den Ariadnefaden in den verwinkelten Labyrinthen; my office colleagues Pierre and David to being there for my “petite question a des experts”.

… for the time spend together in the underground: Alex and Florian pour m’avoir ouvert le sous-sol des Siebenhengste; Iris, die sich partout weigerte sich als Massstab fotografieren zu lassen; Daniel, die treue Seele; Oliver, der nicht nur ein Höhlenfreund ist; Fabrice, der Mann, wenn es darauf an kommt; Lorenz, an dessen Wuschelkopf ich nie herangekommen bin; Arnfried, der mir gelernt hat im Feld zu sehen; Häse, der mir die systematische Höhlenforschung näher brachte; Mü (Mirjam), deren Fotos an verschiedenen Stellen in dieser Diss. zu finden sind; Lukas, mein Lieblingsgeograph; Manu toujours a motiver pour une fondu ou une sortie, ou sortie avec fondu...

… for the cave survey data: Höhlenforschergemeinschaft Region Hohgant particularly Alex and Florian Hof; Arbeitsgemeinschaft Nidlenlochforschung particularly Tom Hermann; Arbeitsgemeinschaft Höllochforschung; Ostschweizerische Gesellschaft für Höhlenforschung particularly Andreas Dickert; Arbeitsgemeinschaft für Speläologie Regensdorf; Landesverein für Höhlenkunde in Oberösterreich particularly Lukas Plan; Verein für Höhlenkunde in Obersteier; Arbeitsgemeinschaft Höhle und Karst Grabenstetten, Cambridge University Caving Club; Höhlenverein Sonthofen; Mammoth Cave Cave Research Foundation and all spelunker that spend their time exploring, mapping and document the underground world.

… for the labour facilities: Département de Géologie et Paléontologie de Genève particularly Prof. E. Davaud and J. Chablais; Institut de minéralogie et géochimie Lausanne particularly Prof. T. Vennemann and Dr. J. Spangenberg as well as P. Thélin; L. Gastaldo of the Laboratoire de mécanique des roches EPFL

… for the amity and scientific discussions at the various conferences I could participate during the last four years: L. Plan, P. Audra, J. De Waele, I.D. Sasowsly, J. Kaufmann, T. Wagner, C. Groves, L. Pierce, J.A. Crews, S. Jaillet, B. Sadier …

… for the financial support: Swiss National Foundation for Scientific research (project number 200021-105280 and 200020-116207/1)

- References -

A

Archie G.E., 1952: Classification of carbonate reservoir rocks and petrophysical considerations. American Association of Petroleum Geologists Bulletin 36/2, 278-298.

Audra P., 1994: Karsts alpins. Genèse de grands réseaux souterrains. Exemples : le Tennengebirge (Autriche), l'Ile de Crémieu, la Chartreuse et le Vercors (France). Karstologia Mémoires 5, Grenoble 1 University.

Audra P., Bini A., Gabrovšek F.,Häuselmann P., Hobléa F., Jeannin P.-Y., Kunaver J., Monbaron M., Šušteršič F., Tognini P., Trimmel H., Wildberger A., 2007: Cave and karst evolution in the Alps and their relation to paleoclimate and paleotopography. Acta Carsologica 36/1, 53-68.

Auler A.S., Smart P.L., 2003: The influence of bedrock-derived acidity in the development of surface and underground karst: Evidence from the Precambrian carbonates of semi-arid northern Brazil. Earth Surface Processes and Landforms 28, 157–168.

B

Bachus R.C. ,2005: Geotechnical Analysis in Karst: The Interaction between Engineers and Hydrogeologists. Proceedings of the Multidisciplinary Conference on Sinkholes and the Engineering and Environmental Impacts of Karst, 3-12.

Bakalowicz M., 2005: Karst groundwater: a challenge for new resources. Hydrogeological Journal 13, 148-160.

Bakalowicz M., Ford D.C., Miller T.E., Palmer A.N., Palmer M.V., 1987: Thermal genesis of solution caves in the Black Hills, South Dakota. Bull. Soc. Geol. Am. 99, 729-738.

Baroň I., 2002: Speleogenesis along sub-vertical joints: A model of plateau karst shaft development: A case study: the Dolný Vrch Plateau (Slovak Republic). Cave and Karst Science 29/1, 5-12.

Bauer S., Liedl R., Sauter M., 2003: Modelling of karst aquifer genesis: influence of exchange flow. Water Resources Research 39/10, 1285-1295.

Bechtel T.D., Bosh F.P., Gurk M., 2007: Geophysical methods. In Goldscheider N. and Drew D. (eds): Methods in Karst Hydrogeology. Taylor and Francis, 171-200.

Benson R.C., Yuhr L., 1993: Spatial sampling considerations and their applications to characterizing fractured rock and karst systems. Environmental Geology 22, 296-307.

Benzécri J.-P., 1973: L'Analyse des Données. Volume II. L'Analyse des Correspondences. Paris.

Berner R.A., Morse J.M., 1974: Dissolution kinetics of calcium carbonate in seawater. IV. Theory of calcite dissolution. American Journal of Science 274, 108-134.

Bitterli T., Jeannin P.-Y., 1997: Entwicklungsgeschichte der Höhlen im Gebiet Hohgant - Sieben Hengste - Thunersee (Berner Oberland, Schweiz). – Proceedings of the 12th Int. Congress of Speleology 1, 349-354.

Blanc J.-J., Nicod J., 1990: Les surface karstiques du plateau de Montrieux (Var), (secteur de Valbelle-Morières-Siou Blanc), étude quantitative de la fracturation. Karstologia 16, 17-28.

Boebe M., 1994: Rock permeability determination by using a minipermeameter. Erdöl Erdgas Kohle 110/2, 58-61.

Bögli A., 1978: Karsthydrographie und physische Speläologie. Springer.

Bögli A., 1980: Karst Hydrology and Physical Speleology. Springer.

Bosák P., 2002: Karst process from the beginning to the end: How can they be dated? – In: Gabrovšek (eds.), Evolution of Karst: from prekarst to cessation. Postojna-Ljubliana, Zalozba ZRC, 155-190.

Bosák P., Ford D.C., Glazek J., Horáček I., 1989: Paleokarst. A systematic and regional review. Elsevier.

Bretz J.H., 1942: Vadose and phreatic features of limestone caverns. Journal of Geology 50, 675–811.

Brosse É., Magnier C., Vincent B., 2005: Modelling Fluid-Rock Interaction Induced by the percolation of CO_2-enriched solutions in core samples: the role of reactive surface area. Oil & Gas Science and Technology, 60/2, 287-305.

Budd D.A, Vacher H.L., 1991: Predicting the thickness of freshwater lenses in carbonate paleo-islands: Journal of Sedimentary Petrology 61, 43-53.

Budd D.A., Vacher H.L., 2004: Matrix permeability of the confined Floridan Aquifer. Hydrogeology Journal 12, 531-549.

Buschendorf F., Nielsen H., Puchelt H., Ricke W, 1963: Schwefel-Isotopen-Untersuchungen am Pyrit-Sphalerit-Baryt-Lager Meggen/Lenne (Deutschland) und an verschiedenen Devon-Evaporiten. Geochimica et Cosmochimica Acta 27, 501–523.

Buxtorf A., 1908: Geologische Beschreibung des Weissensteintunnels und seiner Umgebung – Beitrag zur geologischen Karte der Schweiz: Geologische Karte des Weissensteintunnelgebietes 1:25,000. Schweizerische Geologische Kommission, Winterthur, 160 pp

C

Ćalić-Ljubojević J., 2001: Upward growth of bedding –plane anastomoses. 13th International Congress of Speleology Brasilia, 71-73.

Ćalić-Ljubojević J., 2002: Bedding-plane anastomoses as one of the early stages of karst evolution. Acta Geologica Polonica 52/1, 111-115.

Casagrande G., Cucchi F., Zini L., 2005: Hazard connected to railway tunnel construction in karstic area: applied geomorphological and hydrogeological surveys. Natural Hazards and Earth System Sciences 5, 243-250.

Čar J., Šebela S., 1998: Bedding planes, moved bedding planes, connective fissures and horizontal cave passages (Examples from Postojnska Jama cave). Acta Carsologica 27/2, 75-95.

Choi D.W., Woo K.S., 2005: Origin of the gypsum flower in Okgye Cave, Korea. Journal of the Geological Society of Korea 41/4, 451-464.

Choquette P.W., James N.P., 1988: Introduction. In: James and Choquette (eds.): Paleokarst, 1–21.

Choquette P.W., Pray L.C., 1970: Geologic nomenclature and classification of porosity in sedimentary carbonates. American Association of Petroleum Geologists Bulletin 54/2, 207–250.

Clark I., Fritz P., 1997: Environmental isotopes in Hydrogeology. Lewis Publishers.

Collinson J.D., Thompson D.B., 1982: Sedimentary Structures. George Allen & Unwin.

Cook P.G., Herczeg A. L., 2000: Environmental tracers in subsurface hydrology. Springer.

Cooke M.L., Simo J.A., Underwood C.A., Rijken P., 2006: Mechanical stratigraphic controls on fracture patterns within carbonates and implications for groundwater flow. Sedimentary Geology 184, 225-239.

Cunningham K.J., 2004: Application of ground-penetrating radar, digital optical borehole images, and cores for characterization of porosity hydraulic conductivity and paleokarst in Biscayne aquifer, south-eastern Florida. Journal of Applied Geophysics 55, 61-76.

D

Davies W.E., 1960: Origin of Caves in Folded Limestone. Bulletin of the National Speleological Society US 22/1, 3-18.

Day M.J., 2004: Karstic problems in the construction of Milwaukee's Deep Tunnels. Environmental Geology 45, 859-863.

Dewers T., OrtolevaP., 1994: Nonlinear dynamical aspects of deep basin hydrology: Fluid compartment formation and episodic fluid release. Am. J. Sci. 294, 713-755.

Dickert A., 1995: Das Seichbergloch. Höhlenpost 98, 1-56.

Doctor D.H., Weary D.J., Orndorff R.C., Harlow G.E., Kozar M.D., Nelms D.L., 2008: Bedrock Structural Controls on the Occurrence of Sinkholes and Springs in the Northern Great Valley Karst, Virginia and West Virginia. Sinkholes and the Engineering and Environmental Impacts of Karst 2008, Proceedings of the 11th Multidisciplinary Conference, Geotechnical Special Publication 183: 12-22.

Dreiss S.J., 1984: Effects of lithology on solution sevelopment in carbonate aquifers. Journal of Hydrology 70, 295-308.

Dreybrodt W., 1988: Processes in Karst systems: Physics, chemistry and geology. Springer.

Dreybrodt W., Gabrovšek F., 2000: Dynamics of the evolution of single karst conduits – In: Klimchouk, Ford, Palmer and Dreybrodt (eds): Speleogenesis, evolution of karst aquifers, 184-193.

Dreybrodt W., Gabrovsek F., Romanov D., 2005: Processes of Speleogenesis: a modelling approach. Carsologica, ZRC Publishing, Ljubljana.

Dreybrodt W., Siemers J., 2000: Cave evolution on two-dimensional networks of primary fractures in limestone. – In: Klimchouk, Ford, Palmer and Dreybrodt (eds): Speleogenesis, evolution of karst aquifers, 201-211.

Druckman Y., 1981: Burial diagenesis and porosity evolution, upper Jurassic Smackover, Arkansas and Louisiana. American Association of Petroleum Geologists Bulletin 65/4, 597-628.

E

Eaton T.T., 2006: On the importance of geological heterogeneity for flow simulation. Sedimentary Geology, 184, 187-201.

Eaton T.T., Bradbury K.R., 2003: Hydraulic transience and the role of bedding fractures in a bedrock aquitard, southeatern Wisconsin. Geophysical Research Lettres 30/18.

Eisenlohr L., Meteva K., Gabrovsek F., Dreybrodt W., 1999: The inhibiting action of intrinsic impurities in natural calcium carbonate minerals to their dissolution kinetics in aqueous H2O-CO2 solutions. Geochimica et Cosmochimica Acta 63, 989-1001.

Eraso A., 1985: Método de Predicción de las Direcciones Principales de Drenaje en el Karst. KOBIE, Serie Ciencias Naturales 15, 15-165.

Eraso A., Herrero N., 1986: Propuesta de un Nuevo metodo de deduccion de las direcciones principales de drenaje en el karst. Jumar, Madrid.

Esteban M. 1991: Palaeokarst: Practical Applications. In: Wright, Esteban and Smart (eds.), Palaeokarsts and Palaeokarstic Reservoirs. P.R.I.S. Occassional Publication Series 2, 89-119.

Ewers R.O., 1966: Bedding-plane anastomoses and their relation to cavern passages. Bulletin of the National Speleological Society of America 28/3, 133-140.

F

Faulkner T., 2006: Tectonic inception in caledonide Marbles. Acta Carsologica 35/1, 7-21.

Filipponi M., 2000: Forschungsgebiet Gumenalp (Klöntal, GL). Arbeitsgemeinschaft für Speläologie Regensdorf, AGS Info 1/00, 16-47.

Filipponi M., 2003: Die Stabilität von Karsthohlräumen am Beispiel der A.F. Lindner-Halle im Abisso di Trebiciano (Italien). MS thesis, Eidgenössische Technische Hochschule Zürich. http://e-collection.ethbib.ethz.ch/view/eth:26922

Filipponi M., 2007: Speläologische Erscheinungen im Zusammenhang mit stratigraphischen Initialfugen. Laichinger Höhlenfreund 42, 21-32.

Filipponi M., Dickert A., 2007: Verstehen der Speläogenese durch 3D-Analyse - Fallbeispiel des Lachenstock-Karstes. 12. Nationtal Congress of Speleology – Switzerland, 46-55.

Filipponi M., Jeannin P.-Y., 2006: Is it possible to predict karstified horizons in tunneling?. Austrian Journal of Earth Sciences 99, 24-30.
http://www.univie.ac.at/ajes/download/volume_99/filipponi_jeannin_ajes_v99.zip

Filipponi M., Jeannin P.-Y., 2008: What makes a bedding plane favourable to karstification? - The role of the primary rock permeability. Proceeding of the 4th European Speleological Congress, Spelunca Mémoires, 33: 32-37.

Filipponi M., Jeannin P.-Y., 2008: Prediction of karst occurrences by interpreting borehole data within the Inception Horizon Hypothesis. Sinkholes and the Engineering and Environmental Impacts of Karst 2008, Proceedings of the 11th Multidisciplinary Conference, Geotechnical Special Publication 183: 120-130.
doi:10.1061/41003(327)13

Filipponi M., Jeannin P.-Y., Tacher L., 2009: Evidence of inception horizons in karst conduit networks. Geomorphology, 106, 86-99.
doi:10.1016/j.geomorph.2008.09.010

Filipponi M., Hitz O., 2001: Strukturbeobachtungen in Höhlen - Ein Vorschlag für ein Aufnahmeblatt. Schweizerische Gesellschaft für Höhlenforschung, 12. Nationtal Congress of Speleology – Switzerland, 115-118.

Florea L.J., Vacher H.L., 2006: Springflow Hydrographs: Eogenetic vs. Telogenetic Karst. Ground Water 44/3, 352-361.

Florea L.J., Vacher H.L., Donahue B., Naar D., 2007: Quaternary cave levels in peninsular Florida. Quaternary Science Reviews 26, 1344-1361.

Ford D., Cullingford C.H.D., 1976: The Science of Speleology. Academic Press.

Ford D.C., Ewers R.O., 1978: The development of limestone cave systems in the dimensions of length and breadth. Canadian Journal of Earth Science 15, 1783-1798.

Ford D.C., Lundberg J., 1987: A review of dissolutional rills in limestone and other soluble rocks. Catena Supplement 8, 119-140.

Ford D.C., Williams P., 1989: Karst Hydrogeology and Geomorphology. Wiley.

Ford D.C., Williams P., 2007: Karst Hydrogeology and Geomorphology. Wiley.

Forte G.L., Orti F.,. Rosell L, 2005: Isotopic characterization of Jurassic evaporates – Aconcagua-Neuquén Basin (Argentina). Geologica Acta 3/2, 155-161.

Furman F.C., Gregg J.M., Palmer A.N., Shelton K.L., 1999: Sulfur isotopes of gypsum speleothems in the central Kentucky karst system - Indications of pyrite and anhydrite sulfur sources, and sulfuric acid kars tification. MSM Spelunker 42/1, 20-24.

G

Gabrovšek F., Dreybdodt W., 2001: A model of the early evolution of karst aquifers in limestone in the dimensions of length and depth. Journal of Hydrology 240, 206-224.

Galdenzi, S., Menichetti, M., 1995: Occurence of hypogenic caves in a karst region: Examples from central Italy. – Environmental Geology 26, 39-47.

Garasic M. 2009: Karst and caves in post orogenetic carbonate breccias in Croatia. Geophysical Research Abstracts Vol. 11, EGU2009-6872.

Glaser S., 2005: Geologische und hydrogeologische Erkenntnisse aus der Mühlbachquellhöhle. Geologische Blätter NO-Bayern 55, 1-30.

Goggin D.J., 1993: Probe permeametry – Is it worth the effort? Marine and Petroleum Geology 10, 299-308.

Goldstrand P.M., Shevenell L.A., 1997: Geologic controls on porosity development in the Maynardville Limestone, Oak Ridge, Tennessee. Environmental Geology 31, 259-269.

Graham Wall B.R., 2006: Influence of depositional setting and sedimentary fabric on mechanical layer evolution in carbonate aquifers. Sedimentary Geology 184,: 203–224.

Greenacre M.J., 1993: Correspondence analysis in practice. Academic Press.

Grossenbacher Y., 1992: Höhlenvermessung. Swiss Speleological Society.

Groves C.G., Howard A.D., 1994: Early development of karst systems - 1. Preferential flow path enlargement under laminar flow. Water Resources Research 30, 2837-2846.

H

Hartmann M., Nielsen H., 1968: δ^{34}S-Werte in rezenten Meeressedimenten und ihre Deutung am Beispiel einiger Sedimentprofile aus der westlichen Ostsee. Geologische Rundschau 58, 621-655.

Häuselmann P., 2002: Cave Genesis and its relationship to surface processes: Investigations in the Siebenhengste Region (BE, Switzerland). Höhlenforschung im Gebiet Siebenhensgte-Hohgant 6.

Häuselmann P., Jeannin P.-Y., Bitterli T., 1999: Relationships between karst and tectonics: case-study of the cave system North of Lake Thun (Bern, Switzerland). Geodinamica Acta 12/6, 377-387.

Häuselmann P., Jeannin P.-Y., Monbaron M., 2003: Role of epiphreatic flow and soutirages in conduit morphogenesis: the Bärenschacht example (BE, Switzerland). Zeitschrift für Geomorphologie 47, 171-190.

Helgeson D.E., Aydin A., 1991: Characteristics of joint propagation across layer interfaces in sedimentary rocks. Journal of Structural Geology 13 897–911.

Herman J.S., White W.B., 1985: Dissolution kinetics of dolomite: Effects of lithology and fluid flow velocity. Geochimica and Cosmochimica Acta 49, 2017–2026.

Hill C.A., 1995: Sulfur redox reaction: Hydrocarbons, native sulfur, Mississippi Valley-type deposits, and sulfuric acid karst in the Delaware Basin, New Mexico and Texas. Environmental Geology 25/1, 16-23.

Hill C.A., 2000: Sulfuric acid, hypogene karst in the Guadalupe Mountains of New Mexico and West Texas, USA. – In: Klimchouk, Ford, Palmer and Dreybrodt (eds): Speleogenesis, evolution of karst aquifers, 309-316.

Hillis R.R., 1998: The influence of fracture stiffness and the in situ stress field on the closure of natural fractures. Petroleum Geoscience 4, 57-65.

Horoi V., 2001: L'influence de la geologie sur la karstification. Etude comparative entre le Massif Obarsia Closani - Piatra Mare (Roumanie) et le Massif d'Arbas (France). PhD Thesis, Université Paul Sabatier - Toulouse III, France.

Hose L.D., Palmer A.N., Palmer M.V., Northup D.E., Boston P.J., DuChene H.R., 2000: Microbiology and geochemistry in a hydrogen-sulphide-rich karst environment. Chemical Geology 169, 399-423.

Howard A.D., Groves C.G., 1995: Early development of karst systems - 2. Turbulent flow. Water Resources Research 31, 19-26.

J

Jameson R.A., 1985: Structural segments and the analysis of flow paths in the North Canyon of Snedegar Cave, Friars Hole Cave System. MS Thesis, West Virginia University, Morgantown.

Jamier D., Siméoni G.P., 1979: Etude statistique de la distribution spatiale des éléments structuraux dans deux massifs des Alpes helvétique. Conséquences pour l'hydrogéologie karstique. – Bulletin du Centre d'Hydrogéologie, Neuchâtel 3, 1-26.

Jaquet O., Siegel P., Kulbertanz G., Benabderrhamane H., 2004: Stochastic discrete model of karstic networks. Advances in Water Resources 27, 751-760.

Jeannin P.-Y., 1989: Etude Géologique de la Région Burst-Sieben Hengste – Apports de L'étude des cavernes à la connaissance structurale et à la mise en évidence de phases tectoniques quaternaires. MS Thesis, University of Neuchâtel.

Jeannin P.-Y., 1996: Structure et comportement hydraulique des aquifères karstiques. – PhD Thesis, Université de Neuchâtel, Speleo-Projects publishers.

Jeannin P.-Y., Bitterli T., Häuslemann P., 2000: Genesis of a large cave system: the case study of the North of Lake Thun system (Canton Bern, Switzerland). In: Klimchouk, Ford, Palmer and Dreybrodt (eds): Speleogenesis, evolution of karst aquifers, 338-347.

Jeannin P.-Y., Häuselmann P., 2005: Siebenhengste Cave System. In: Culver, White (eds): Encyclopedia of Caves, 500-509.

Jennings J.N., 1968: Syngenetic karst in Australia. In: Williams, P.W. & Jennings, J.N. (Eds): Contributions to the Study of Karst, Department of Geography Publication no. G/5, Australian National University, 41-110.

K

Kaufmann G., 2002: Karst aquifer evolution in a changing watertable environment. Water Resources Research 38/6, 26.1–26.9.

Kaufmann G., 2003: A model comparison of karst aquifer evolution for different matrix-flow formulations. Journal of Hydrology 283, 281-289.

Kaufmann J.E. 2008: A statistical approach to karst collapse hazard analysis im Missouri. Sinkholes and the Engineering and Environmental Impacts of Karst 2008, Proceedings of the 11th Multidisciplinary Conference, Geotechnical Special Publication 183: 257-268.

Kiraly L., 1968: Eléments structuraux et alignement des phénomènes karstiques (région du gouffre du Petit-Pré de St-Livres, Jura vaudois). Bulletin de la Société des Sciences Naturelles de Neuchâtel 91, 127-146.

Kiraly L., 1969: Anisotropie et hétérogénéité de perméabilités dans les calcaires fissurés. Eclogea Geologica Helvetica 62/2, 613-619.

Kiraly L., 1975: Rapport sur l'état actuel des connaissances dans le domaine des caractères physiques des roches karstiques. – In:Burger and Dubertret (eds): International Union Geol. Sci., Series B, 3, 53-67.

Klimchouk A., 2007: Hypogene Speleogenesis: Hydrogeological and Morphogenetic Perspective. National Cave and Karst Research Institute, Special Paper 1.

Klimchouk A., Ford D.C., 2000: Types of Karst and Evolution of Hydrogeologic Setting. – In: Klimchouk, Ford, Palmer and Dreybrodt (eds): Speleogenesis, Evolution of Karst Aquifers, 45-53.

Klimchouk A., Ford D.C., 2000. Lithologic and structural controls of dissolutional cave development. – In: Klimchouk, Ford, Palmer and Dreybrodt (eds): Speleogenesis, Evolution of Karst Aquifers, 54-64.

Klimchouk A., Ford D.C., Palmer D.C., Dreybrodt W., 2000: Speleogenesis, evolution of karst aquifers. National Speleological Society.

Knez M., 1997: Speleogenesis of phreatic channels in bedding-planes in the frame of karst aquifer (Skocjanske Jam Caves, Slovenia). 12th UIS Congress, La Chaux-de-Fonds 2, 279-282.

Knez M., 1998. The influence of bedding-planes on the development of karst caves (a study of Velika Dolina at Škocjanske Jame Caves, Slovenia). Carbonates and Evaporites 13/2, 121-131.

Knez M., Slabe T. 2002: Unroofed caves are an important feature of karst surfaces: examples from the classical karst. Zeitschrift für Geomorphologie 46/2, 181-191.

Krauthausen B., Henne P., 1998: Geologie nd Tektonik des Hirlatzstockes und dessen Umgebung. – In: Buchegger and Greger (eds): Die Hirlatzhöhle im Dachstein. Die Höhle 52, 126-135.

Kresic N., 2007: Hydraulic methods. In Goldscheider N. and Drew D. (eds): Methods in Karst Hydrogeology. Taylor and Francis: 65-92.

Kürsteiner P., Stünzi H., Filipponi M., 2004: Die Kristallhöhle Kobelwald. Verkehrsverein Kobelwald.

Kyrle G., 1923: Theoretische Speläologie. Speläologisches Institut Bundeshöhlenkommission.

L

Lauritzen S.-E. 1988: A Geomorphological Approach to Engineering in Karst. 21st IAH Congress of Karst Hydrogeology and Environment Protection, Guilin, China, 1194-1199.

Lauritzen S.-E., Lundberg J., 2000: Solution and Erosional Morphology. In: Klimchouk, Ford, Palmer and Dreybrodt (eds): Speleogenesis, Evolution of Karst Aquifers, 408-426.

Lemieux J.-M., Therrien R., Kirkwood D. 2006: Small scale study of groundwater flow in a fractured carbonate-rock aquifer at the St-Eustache quarry, Québec. Hydrogeology Journal 14, 603-612.

Lindner, A.F., 1841: Corso sotterraneo del fiume Recca, suo ritrocamento presso Trieste e progetto di trarne un canale a beneficio della città. Finroale del Istituto di Scienze Lettere e Arti e Biblioteca Italiana, 116-121.

Liu Z., Dreybrodt W., 2001: Kinetics and rate-limiting mechanisms of dolomite dissolution at various CO2 partial pressures. Science in China(B)-English Edition 44, 500-509.

Lolcama J.L., Cohen H.A., Tonkin M.J., 2002: Deep karst conduits, flooding, and sinkholes: lessons for the aggregates industry. Engineering Geology 65, 151-157.

Lowe D.J., 1992: The origin of limestone caverns: in inception horizon hypothesis. PhD Thesis, Manchester Polytechnic, United Kingdom.

Lowe D.J., 1993: The Forest of Dean caves and karst: inception horizons and iron-ore deposits. Cave science 20/2, 31-43.

Lowe D.J., 1999: Why and how are caves "organized": Does the Past offer a key to the Present? Acta Carsologica 28/2, 121-144.

Lowe D.J., 2000: Role of stratigraphic elements in speleogenesis: the speleoinception concept. - In: Klimchouk, Ford, Palmer and Dreybrodt (eds): Speleogenesis, evolution of karst aquifers, 65-76.

Lucia F.J., 1983: Petrophysical parametres estimated from visual descriptions of carbonate rocks. Journal of Petroleum Technology 35, 629-637.

Lucia F.J., 2007: Carbonate Reservoir Characterization - An Integrated Approach. Springer.

M

Mace R.E, Hovorka S.D., 2000: Estimating porosity and permeability in a karstic aquifer using core plugs, well tests and outcrop measurements. – In: Sasowsky, Wicks (eds): Groundwater flow and contaminant transport in carbonate aquifers, 93-111.

Machel H.G., 1992: Low-temperature and high-temperature origins of elemental sulfur in diagenetic environments. In: Wessell and Wimberly (eds), Native sulfur developments in geology and exploration, 3–21.

Macnamara J., Thode H.G., 1950: Comparison of the isotopic constitution of terrestrial and meteoric sulphur. Physical Review Letters 78, 307.

Maire R., 1990: La haute montagne calcaire. Karstologia Mémoires, n° 3, 731 p. Thèse d'Etat à Nice. Fédération française de spéléologie & Association française de karstologie.

Manda A.K., Gross M., 2006: Identifying and characterizing solution conduits in karst aquifers through geospatial analysis of porosity from borehole imagery: An example from the Biscayne aquifer, South Florida. Advances in Water Research 29, 383-396.

Mardia K.V., Kent J.T., Bibby J.M., 1979: Multivariate Analysis, Academic Press.

Marinos P.G., 2001: Tunnelling and mining in karstic terrain: An engineering challenge. - In: Beck and Herring (eds): Geotechnical and Environmental Applications of Karst Geology and Hydrology, 3-16.

Mayer B., Feger K.H., Giesemann A., Jäger H.J., 1995: Interpretation of sulphur cycling in two catchments in the Black Forest (Germany) using stable sulphur and oxygen isotope data. Biogeochemistry 30, 31-58.

Micarelli L., Benedicto A., Wibberley C.A.J., 2006: Structural evolution and permeability of normal fault zones in highly porous carbonate rocks. Journal of Structural Geology 28, 1214-1227.

Michalski A., Britton R., 1997: The role of bedding fractures in the hydrogeology of sedimentary bedrock - Evidence from the Newark Basin, New Jersey. Ground Water 35/2, 318-327.

Milanovic P., 2003: Prevention and Remediation in Karst Engineering. Proceedings of the Multidisciplinary Conference on Sinkholes and the Engineering and Environmental Impacts of Karst, 3-30.

Möckli U., 2000: Hölloch - Naturwunder im Muotatal. AS-Verlag.

Moore C.H., 1989: Carbonate Diagenesis and Porosity. Developments in Sedimentology 46, Elsevier Publishing.

Moore C.H., 2001: Carbonate Reservoirs. Porosity Evolution and Diagenesis in a Sequence Stratigraphic Framework. Developments in Sedimentology 55.

Moore C.H., Druckman Y., 1981: Burial diagenesis and porosity evolution, Upper Jurassic Smackover, Arkansas and Louisiana. American Association of Petroleum Geologists Bulletin 65, 597-628.

Muldoon M.A., Simo J.A., Bradbury K.R., 2001: Correlation of hydraulic conductivity with stratigraphy in a fractured-dolomite aquifer, northeastern Wisconsin, USA. Hydrogeology Journal, 570-583.

Mylroie J.R., Mylroie J.E., 2007: Development of the carbonate island karst model. Journal of Cave and Karst Studies 69/1, 59-75.

N

Narr W., Suppe J., 1991: Joint spacing in sedimentary rocks. Journal of Structural Geology 13, 1037–1048.

Nicholson R.V., Gillham R.W., Reardon E.J., 1988: Pyrite oxidation in carbonate-buffered solution: 1. Experimental kinetics. Geochemica et Cosmochimica Acta 52, 1077-1085.

Noiriel C., 2005: Contribution à la determination expérimentale et à la modélisation des différents processus contrôlant l'évolution géochimique, structurale et hydrodynamique des roches fissures carbonatées. PhD Thesis, École des Mines de Paris.

O

Orndorff R.C., Weary D.J., Sebela S., 2001: Geologic Framwork of the Ozarks of South-Central-Missouri – Contributions oto a Conceptual Model of Karst. – In: Kuniansky (eds): U.S. Geological Survey Karst Interest Group Proceedings, Water-Resources Investigations Report 01-40011, 18-24.

Ortega O.J., Marrett R.A., Laubach S.E., 2006: A scale-independent approach to fracture intensity and average spacing measurement. American Association of Petroleum Geologists Bulletin 90/2, 193-208.

Osborne R.A.L., 1999: The inception horizon hypothesis in vertical to steeply dipping limestone: applications in New South Wales, Australia. – Cave and Karst Science 26, 5-12.

Osborne R.A.L., 2001: Halls and Narrows: Network caves in dipping limestone examples from eastern Australia. Cave and Karst Science 28/1, 3-14.

Osborne R.A.L., 2002: Paleokarst: cessation and rebirth? – In: Gabrovšek, (eds): Evolution of karst: from prekarst to cessation, 97-114.

P

Paillet F.L., 2001: Borehole Geophysical Applications in Karst Hydrogeology. – In: Kuniansky (eds): U.S. Geological Survey Karst Interest Group Proceedings, Water Resources Investigations Report 01-4011, 116-123.

Paillet F.L., Crowder R.E., 1996: A Generalized Approach for the interpretation of geophysical well logs in ground water studies – theory and application. Ground Water 34, 883-898.

Paillet F.L., Lundy J., Tipping R.G., Runkel A.C., Reeves L., Green A.J., 2000: Hydrogeologic characterization of six sites in southeastern Minnesota using borehole flowmeters and other geophysical logs. U.S. Geological Survey Water-Resources Investigation Report 00-4142.

Palmer A.N., 1974; Geologic influence on cave passage orientation in Ludington cave, Greenbarrier County, West Virginia. Proc. Of the West Virginia 4th Conference on Karst Geology and Hydrology, West Virginia geol. Survey, 33-40.

Palmer A.N., 1975: The origin of maze caves. Bulletin of the National Speleological Society of America 37/3, 56-76

Palmer A.N., 1986: Prediction of contaminant paths in karst aquifers. Preceding of the Environmental Problems in Karst Terrains and their Solutions Conference, Dublin, Ohio, Natural Water Well Association, 32-53.

Palmer A.N., 1987: Cave levels and their interpretation. Bulletin of the National Speleological Society of America 49, 50-66.

Palmer A.N., 1989: Stratigraphic and structural control of cave development and groundwater flow in the Mammoth Cave region. – In White and White (eds): Karst Hydrology, Concepts from the Mammoth Cave Area, Von Nostrand Reinhold, New York, 293-316.

Palmer A.N., 2000: Hydrogeologic control of cave patterns. – In: Klimchouk, Ford, Palmer and Dreybrodt (eds): Speleogenesis, evolution of karst aquifers, 77-90.

Palmer A.N., 2002: Speleogenesis in carbonate rocks. - In: Gabrovšek (eds.): Evolution of karst: from prekarst to cessation. 43–60.

Palmer A.N., 1991: Origin and morphology of limestone caves. Geological Society of America Bulletin 103, 1-21.

Palmer A.N., Palmer M.V., 1995: Geochemistry of capillary seepage in Mammoth Cave: Proceedings of Mammoth Cave National Park's Fourth Science Conference, 119-133.

Perlow M., 2008: Knowledge based geologic hazard risk assessment for municipal, transportation, energy, and industrial infrastructure. Sinkholes and the Engineering and Environmental Impacts of Karst 2008, Proceedings of the 11th Multidisciplinary Conference, Geotechnical Special Publication 183: 233-242.

Pesendorfer M., Loew S., 2004: Hydrogeologic Exploration during excavation of the Lötschberg Base Tunnel (AlpTransit Switzerland). - In: Hack, Azzam, (eds): Engineering Geology for Infrastructure Planning in Europe. 347-358.

Pezdič J., Šušteršič F., Mišič M., 1998: On the role of clay-carbonate reactions in speleoinception – A contribution to the understanding of the earliest stage of karst channel formation. Acta Carsologica 27/1, 187-200.

Plan L., 2005: Factors controlling carbonate dissolution rates quantified in a field test in the Austrian Alps. Geomorphology 68, 201-212.

Plan L., Filipponi M., Behm M., Seebacher R., Jeutter P., 2009: Constraints on alpine speleogenesis from cave morphology - a case study from the eastern Totes Gebirge (Northern Calcacerous Alps, Austria). Geomorphology 106, 118-129. doi:10.1016/j.geomorph.2008.09.011

Pollard D.D., Aydin A.A., 1988: Progress in understanding jointing over the past century. Geological Society of America Bulletin 100, 1181-1204.

Pollard D.D., Segall P., 1987: Theoretical displacements and stresses near fractures in rock: with applications to faults, joints, veins, dikes, and solution surfaces. - In: Atkinson (eds.) Fracture Mechanics of Rock, 277–349.

Pötsch M., Pischinger G., Bewick R.P., Gaich A. 2007: Geotechnical data collection and analysis in jointed rock – Application of Computer Vision Technology and Metric 3D Images. Felsbau 25/5, 66-73.

Pöttler R., Schneider V., Rehfeld E., Quick H., 2002: Grundkonzept zur Lösung der Karst- und Erdfallproblematik für den Bau von Verkehrswegen. Felsbau 20/3, 10-21.

Pöttler R., 2004: Beherrschung der Karst- und Erdfallproblematik im Tunnelbau. Institut für Geotechnik der Technischen Universität Bergakademie Freiberg.

Plummer L.N., Wigley T.M.L., 1976: The dissolution of calcite in CO_2-saturated solutions at 25°C and 1 atmosphere total pressure. Geoch. Cosmochim. Acta 40, 191-202.

Q

Quinlan J.F., Ray, J.A., 1981: Groundwater basins in the Mammoth Cave region, Kentucky. – Friends of karst, occas. public.1.

R

Rauch H.W., Werner E., 1974: Geological invluence upon cave-passages orientation in Ludingron Cave, Greenribrier Country, West Virginia. Proceedings of the 4th Conference on Karst Geology and Hydrology, West Virginia Geological and Economic Survey, 33-40.

Rauch H.W., White W.B., 1970: Lithologic controls on the development of solution porosity in carbonate aquifers. – Water Resources Research 6, 1175-1192.

Rauch H.W., White W.B., 1977: Dissolution kinetics of carbonate rocks. 1. Effects of lithology on dissolution rate. Water Resources Research 13, 381–394.

Rees C.E., 1973: A study-state model for sulfur isotope fractionation in bacterial reduction processes. Geochimica et Cosmochimica Acta 37, 1141–1162.

Rehrl C., Birk S., Klimchouk A., 2008: Conduit evolution in deep-seated settings: Conceptual and numerical models based on field observations. Water Resources Research 44, (in press). doi:10.1029/2008WR006905

Rijken P., Cooke M.L., 2001: Role of shale on vertical connectivity of fractures in the Austin Chalk, Texas: application of crack-bridging theory. Tectonophysics 337, 117–133.

Rimstidt J.D., Vaughan D.J., 2003: Pyrite oxidation: A state-of-the-art assessment of the reaction mechanism. Geochimica et Cosmochimica Acta 67, 873-880.

Robertson W.D., Schiff S.L., 1994: Fractionation of sulphur isotopes during biogenic sulphate reduction below a sandy forested recharge area in south-central. Canadaian Journal of Hydrology 158, 123–134.

Roduit N., 2007: JMicroVision: un logiciel d'analyse d'images pétrographiques polyvalent. PhD Thesis, University of Geneva. www.jmicrovision.com

Rovey C.W., Cherkauer D.S., 1994: Relation between hydraulic conductivity and texture in a carbonate aquifer – Regional conductivity. Ground Water 32/2, 227-238.

Roques H., Ek C., 1973: Etude expérimentale de la dissolution des calcaires par une eau chargée de CO_2. Ann. Speleol. 28/4, 549–563.

S

Sauter M., Liedl R., 2000: Modeling karst aquifer genesis using a coupled continuum-pipe flow model. - In: Klimchouk, Ford, Palmer and Dreybrodt (eds): Speleogenesis, evolution of karst aquifers, 212-219.

Schaer J.P., Stettler R., Aragno P.O., Burkhard M., Meia J., 1998: Géologie du Creux du Van et des Gorges de l'Areuse. In: Nature au Creux du Van, Editions du Club Jurssien, 143-215.

Schmoker J.W., 1984: Empirical relation between carbonate porosity and thermal maturity - an approach to regional porosity prediction. American Association of Petroleum Geologists Bulltin 68, 1697-1703.

Scholle P.A., Halley R.B., 1985: Burial diagenesis: out of sight, out of mind. In: Schneidermann and Harris (eds), Carbonate cements. Society of Economic Palaeontologists and Mineralogists Special Publication 36, 309–335.

Scott K.W., 1997: A practical guide to borehole geophysics in environmental investigations. Lewis Publishers.

Shen Y., Buick R., Canfield D.E., 2001: Isotopic evidence for microbial sulphate reduction in the early Archaean era. Nature 410, 77-81.

Shofner A.G., Mills H.H., Duke J.E., 2001: A simple map index of karstification and its relationship to sinkhole and cave distribution in Tennessee. Journal of Cave and Karst Studies 63/2, 67-75.

Slabe T., 1995: Cave rocky relief and its speleogenetical significance. Znanstvenoraziskovalni Center Sazu, Ljubljana.

Slippel R.F., Glover E.V., 1964: The solution alteration of carbonate rocks, the effects of temperature and pressure. Geochimica et Cosmochimica Acta 28, 1401-1417.

Smith D.I., Aktinson T.C., Drew D.P., 1976: The hyrology of limestone terrains. – In: Ford, Cullingford (eds): The Science of Speleology, 179-212.

Spate A.P., Jennings J.N., Smith D.I., Greenaway M.A., 1985: The micro-erosion meter: use and limitations, Earth Surface Processes and Landforms 10, 427–440.

Strauss H., 1997: The isotopic composition of sedimentary sulfur through time. Paleogeography, Paleoclimatology, Paleooecology, 132, 97-118.

Stünzi H., 2006: Schachthöhle O91. Arbeitsgemeinschaft für Speläologie Regensdorf, AGS Info 2/06, 23-25.

Stünzi H., 2008: O91 und O92 – Zwischenbericht. Arbeitsgemeinschaft für Speläologie Regensdorf, AGS Info 2/08, 20.

Šušteršič F.. 1998: Interaction between a cave system and the lowering karst surface – Case Study: Laški Ravnik. Acta Carsologica 27/2, 115-138.

Sweeting M., Sweeting S., 1969: Some aspects of the carboniferous limestone in relation to its landforms with particular reference to N. W. Yorkshire and County clare. Revue Géographique des Pays Méditerranéens 7, 201–209.

T

Taran Y., Fischer T.P., Pokrovsky B., Sano Y., Armienta M.A., Macias J.L., 1998: Geochemistry of the volcano-hydrothermal system of El Chichón Volcano, Chiapas, Mexico. Bulletin of Volcanology 59/6, 436-449.

Thode H.G., Kleerekoper H., McElcheran D. 1952: Isotope fractionation in the bacterial reduction of sulfate. Research (London) 4, 581-582.

Tinker S.W., Ehrets J.R., Brondos M.D., 1995: Multiple karst events related to stratigraphic cyclicity: San Andres formation, Yates field, west Texas. - In Budd, Saller, Harris (eds): Unconformities and Porosity in Carbonate Strata: American Association of Petroleum Geologists Memoir 63, 213-237.

Tinker S.W., Mruk D.H., 1995: Reservoir Characterization of a Permian Giant: Yates Field, west Texas. - In Stoudt, Harris (eds): Hydrocarbon reservoir characterization, geologic framework and flow-unit modeling: SEPM Short Course 34, 51-128.

Tipping R.G., Runkel A.C., Alexander E.C., Alexander S.C., Green J.A., 2006: Evidence for hydraulic heterogeneity and anisotropy in the mostly carbonate Prairie du Chien Group, southeastern Minnesota. Sedimentary Geology 184, 305-330.

Tolmachev V.V., Leonenko M.V., 2005: Classification of karstic terrains based on sikhole risk. Soil Mechanics and Foundation Engineering 42/2, 52-55.

Trimmel H., 1968: Höhlenkunde. Vieweg-Verlag.

Tucker M., 1985: Einführung in die Sedimentpetrologie. Enke.

U

Underwood C.A., Cooke M.L., Simo J.A., Muldoon M.A., 2003: Stratigraphic controls on vertical fracture patterns in Silurian Dolomite, northeastern Wisconsin, American Association of Petroleum Geologists Bulletin 87, 121-142.

V

Veni G., 1999: A geomorphological strategy for conducting environmental impact assessments in karst areas. Geomorphology 31, 151-180.

Veni G., 2005: Lithology as a Predictive Tool of Conduit Morphology and Hydrology in Environmental Impact Assessments. Proceeding of the Sinkholes and the Engineering and Environmental Impacts of Karst Conference, 46-56.

Vergari A.,1997: Contraintes paléokarstiques dans l'exploitation du calcaire carbonifère sur le bord nord du synclinorium de Namur en Hainaut occidental. Thèse de doctorat, FPMs.

Vergari A., 1998: Nouveau regard sur la spéléogenèse : le "pseudo-endokarst" du Tournaisis (Hainaut, Belgique). Karstologia 31, 12-18.

Vergari A., 2003: "Gost rocks": a new way for speleogenesis a new key for paleogeographies. Géologie de la France 1, 43-46.

Vergari A., Quinif Y., 1997: Les paléokarsts du Hainaut. Geodinamica Acta 10/4, 175-187.

W

Walter L.M., 1985: Relative reactivity of skeletal carbonates during dissolution: implication for diagenesis. In: Schneidermann, Harris (eds) Carbonate cements. SEPM Special Publication 36, 3-16.

Waltham A.C., 1971: Controlling factors in the development of caves. Transactions of the Cave Research Group of Great Britain 13, 73-80.

Waltham A.C., Fookes, P.G., 2003: Engineering classification of karst ground conditions. Quarterly Journal of Engineering Geology and Hydrology 36, 101-118.

Waltham A.C., Vandenven G., Ek C.M., 1986: Site investigations on cavernous limestone for the Remaouchamps Viaduct, Belgium. Ground Engineering 19/2, 16-18.

Waltham T., 2002: The engineering classification of karst within respect to the role and influence of caves. International Journal of Speleology 35, 19-35.

Waltham T., Bell F., Culshaw M., 2005: Sinkholes and subsidence – Karst and Cavernous Rocks in Engineering Constructions. Springer.

Wang X., Wang M., 2006: Anaylis of the Mechanism of Water Inrush in Karst Tunnels. Proceeding of the Underground Construction and Ground Movement Conference, 66-72.

Ward J.H., 1963: Hierarchical Grouping to optimize an objective function. Journal of American Statistical Association 58/301, 236-244.

Wedekind J. E., Osten M. A., Kitt E., Herridge B., 2005: Combining Surface and Downhole Geophysical Methods to Identify Karst Conditions in North-Central Iowa. Proceedings of the 8th Multidisciplinary Conference on Sinkholes and the Engineering and Environmental Impacts of Karst, 616-628.

White W.B., 1988: Geomorphology and hydrology of karst terrains. Oxford University Press.

White W.B., 2002: Karst hydrology: recent developments and open questions. Engineering Geology 65, 85-105.

White W.B., White E.L., 2001: Conduit fragmentation, cave patterns and the localization of karst ground water basins: the Appalachians as a test case. Theoretical and Applied Karstology.

White W.B., White E.L. 2003: Gypsum weding and cavern breackdown: Studies in the Mammoth cave System, Kentucky. – Journal of Cave and Karst Studies 65/1, 43-52.

Wienin M., Bruxelles L., 2008: Tectonique, Minéralisation, Fantômisation et Karstification dans la Région du „Dôme de Durfort" (Bases Cévennes, Gard) – Note Préliminaire. Ates de la 17e Rencontre d'Octobre, Spéléo-Club de Paris, 95-100.

Worthington S.R.H., 1999: A comprehensive strategy for understanding flow in carbonate aquifers. - In: Palmer, Palmer, Sasowsky (eds.): Karst Modeling: Special Publication 5, The Karst Waters Institute, 30-37.

Worthington S.R.H., Ford D.C., Beddows P.A., 2000: Porosity and permeability enhancement in unconfined carbonate aquifers as a result of solution. – In: Klimchouk, Ford, Palmer and Dreybrodt (eds): Speleogenesis, evolution of karst aquifers, 463-472.

Wright V.P., 2002: Dissolution and porosity development in carbonates. – In: Gabrovšek (eds): Evolution of karst: from prekarst to cessation, 13-30.

Wright V.P., Smart P.L., 1994: Paleokarst (Dissolution Diageneis): Its Occurrence and Hydrocarbon Exploration Significance. - In: Wolf, Chilingarian (eds): Diagenesis, IV, Developments in Sedimentology 51, 477-517.

X

Xeidakis G.S., Torok A., Skias S., Kleb B., 2004: Engineering Geological problems associated with karst terrains: their investigation monitoring, and mitigation and design of engineering structures on karst terrains. Bulletin of the Geological Society of Greece 36, 1932-1941.

Xu R.,Yan F., 2004: Karst geology and engineering treatment in the Geheyan Project on the Qingjiang River, China. Engineering Geology 76, 155-164.

Y

Yuhr L., Kaufmann R.,Casto D., Singer M., McElroy B., Glasgow J., 2008: Karst Characterization of the Marshall Space Flight Center: Two Years Later. Sinkholes and the Engineering and Environmental Impacts of Karst 2008, Proceedings of the 11th Multidisciplinary Conference, Geotechnical Special Publication 183: 98-109.

Z

Zabidi H., De Freitas M.H., 2006: Structural studies for the prediction of karst in the Kuala Lumpur limestone. IEAG 2006, Geological Society of London, 264/1–7.

Zhang Q., Tian S., Mo Y., Dong X., Hao S., 1993: An expert system for prediction of karst disaster in excavation of tunnels or underground structures through a carbonate rock area. Tunnelling and Underground space Technology 8(3), 373-378.

Ziegler M.A., 1967: A study of the Lower Cretaceous Facies Developments in the Helvetic Border Chain, North of Lake Thun (Switzerland). – Eclogae Geologicae Helveticae 60(2).

Zupan Hajna N. 2002: Chemical Weathering of Limestones and Dolomites in a cave environment. IN: Gabrovšek (eds.): Evolution of karst: from prekarst to cessation. Postojna-Lubljana, Založba ZRC, 347-356.

Zupan Hajna N. 2003: Incomplete solution: Weathering of cave walls and the production, transport and deposition of carbonate fines. Carsologica Založba ZRC.

- Appendix 1 -
Papers and Documents about the Demonstration of Inception Horizon

Siebenhengste Cave System

Evidence of inception horizons in karst conduit networks.

Filipponi M., Jeannin P.-Y., Tacher L., 2009: Geomorphology 106, 86-99.
doi:10.1016/j.geomorph.2008.09.010

Totes Gebirge: DÖF-Sonnenleiterschacht, Burgunderschacht

Constraints on alpine speleogenesis from cave morphology - a case study from the eastern Totes Gebirge (Northern Calcacerous Alps, Austria).

Plan L., Filipponi M., Behm M., Seebacher R., Jeutter P., 2009: Geomorphology 106, 118-129.
doi:10.1016/j.geomorph.2008.09.011

Lachenstock-Karst

Verstehen der Speläogenese durch 3D-Analyse - Fallbeispiel des Lachenstock-Karstes.

Filipponi M., Dickert A., 2007: 12. Nationtal Congress of Speleology – Switzerland, 46-55.

Nachtrag: Feldnachweis in der Lachenstockhöhle

Nidlenloch

Is it possible to predict karstified horizons in tunneling?

Filipponi M., Jeannin P.-Y., 2006: Austrian Journal of Earth Sciences 99, 24-30.
http://www.univie.ac.at/ajes/download/volume_99/filipponi_jeannin_ajes_v99.zip

Feldnachweis und Beobachtungen im Nidlenloch

Grottes aux Fées (CH)

3D Analyse, Feldnachweis und Beobachtungen

Réseau de Covatannaz (CH)

3D Analysis

Kleines Hölloch (D)

3D Analysis

Hirlatzhöhle (A)

3D Analysis

Shuanghedongqun (China)

3D Analysis

Ogof Draenen (GB)

3D Analysis

Filipponi M., Jeannin P.-Y., Tacher L., 2009:
Evidence of inception horizons in karst conduit networks.
Geomorphology 106, 86-99.
doi:10.1016/j.geomorph.2008.09.010

Evidence of inception horizons in karst conduit networks

Marco Filipponi[1], Pierre-Yves Jeannin[2] and Laurent Tacher[1]

[1]ICARE GEOLEP, Laboratoire de géologie de l'ingénieur et de l'environnement, Ecole Polytechnique Fédérale de Lausanne (EPFL) ENAC, Switzerland

[2]Swiss Institute of Speleology and Karstology, P.O. Box 818, CH-2301 La Chaux-de-Fonds, Switzerland

Received 27 July 2007; revised 8 July 2008; accepted 18 September 2008.

Abstract

This paper outlines the conclusion from an analysis of 18 large cave systems around the world, comprising more than 1500 km of conduits. The 3D geometry of complex cave systems have been analysed in relation to their geological context as well as their hydrogeological boundary conditions. The methodology allowed for the first time statistical evidence of the inception horizon concept. Thereby it confirms that the development of karst conduits under phreatic conditions is strongly related to a restricted number of so called inception horizons. An inception horizon is a part of a rock succession that is particularly susceptible to the development of karst conduits because of physical, lithological or chemical deviation from the predominant carbonate facies. It passively or actively favours the localisation of dissolutional voids.

The methodology based on detailed geological 3D models and cave survey allowed us to demonstrate the existence of inception horizons in karst conduit genesis. This fact improves significantly the prediction of karst conduits, knowledge that is of relevance for geological engineering problems (e.g. tunnelling, oil industry, hydrogeology) as well as for the scientific understanding of the evolution of karst systems.

Keywords: Karstification; Inception horizon hypothesis; Spatial distribution; Speleogenesis; Prediction of karst conduits; Bedding planes

1. Introduction

Since the beginning of karst science in the 18th century, attempts have been made to understand and predict the position and geometry of karst conduits (e.g. Lindner, 1841). Such prediction still remains a challenge for various disciplines of Earth Sciences particularly for karstology, hydrogeology and civil engineering, for which reaching or avoiding dissolution voids is of high significance.

Karst problems all over the World create huge annual costs as well as social, security-related and environmental problems that are increased due to an insufficient understanding of speleogenesis (e.g. Marinos, 2001, Lolcama et al., 2002, Waltham and Fookes, 2003, Day, 2004, Xeidakis et al., 2004 and Casagrande et al., 2005). Problems are not only related to engineering constructions such as tunnels, buildings or dams but also concern the management and protection of karst groundwater that is in many parts of the world an important or even the only resource of groundwater. The main question beyond many of these problems is to know whether there is a developed network of conduits and if yes, where it is and in some cases what its characteristics are (e.g. active/fossil, phreatic/vadose, size). One way could be to declare karst as not suitable for operating engineered

works (declare such areas as highly vulnerable for pollution). Considering that around 20% of the dry and ice-free land consists of karstic rock formations (Ford and Williams, 2007) and that it covers 100% of large areas especially in China, Europe and USA, such a statement cannot be applied. Most investigation methods that are presently available do not introduce speleogenetic considerations (e.g. Benson and Yuhr, 1993, Zhang et al., 1993, Veni, 1999, Shofner et al., 2001, Pöttler, 2004 and Bakalowicz, 2005).

Research carried out by karstologists during the last 50 years showed that the development of dissolution voids is not random. Most efforts have been dedicated to the understanding of the processes and mainly the time-scale at which dissolution can develop cave systems. Only a very restricted number of authors attempted to analyse and understand the geometry of karst conduits i.e. to provide keys for the prediction of conduit positions and characteristics.

Rough prediction of the geometry of karst conduits can be obtained by tracing experiments. The map produced by Quinlan and Ray (1981) is a famous example of this type of prediction; it is based on hundreds of tracing experiments and thousands of borehole data. However, the position is drawn only in 2D (plan view) and is not precise (± 500 m).

Another way to address this question is to study the hydrogeological conditions that prevailed at the beginning of the speleogenesis (e.g. Kiraly, 1968, Jamier and Siméoni, 1979, Eraso and Herrero, 1986 and Blanc and Nicod, 1990). These authors measured the fracture characteristics (mainly their frequency) and attempted to derive conduit directions from these measurements. However many authors did not consider the coupling of hydraulic conditions in the speleogenetical process and their methods were limited to descriptions of the relationships between the geological parameters (mainly fracture orientations) and the known conduit direction. As the influence of non-geological boundary conditions (mainly the respective position of the recharge areas and springs) is at least as significant for the speleogenesis as that of geology, it was not possible to really understand and quantify the control of fractures on the development of karst conduit networks. Prediction of conduit position was therefore very limited with this type of approach.

Numerical modelling has also been used to understand karstification. Models include the peculiar dissolution kinetics of calcite and the change of flow conditions from laminar to turbulent when the size of the conduits increases (e.g. Dreybrodt and Siemers, 2000). Such models allow the verification of hypotheses and the generation of systems according to a series of various initial/boundary conditions. It has to be noted that so far models have not often been used for the purpose of conduit prediction, but rather for the assessment of the time duration at which conduits can develop. In other words, uncertainty in predictions has not explicitly diminished during the last 50 years and remains very high.

However, careful attention to the published material allows us to find interesting information about the position of conduits. Based on a detailed observation of caves and their geological context different authors (e.g. Rauch and White, 1970, Waltham, 1971, Rauch and Werner, 1974, Palmer, 1974, Palmer, 1975, Ford and Cullingford, 1976 and Palmer, 1989) suggested that caves develop along a restricted number of bedding planes within the limestone series. This idea was developed in more recent publications into the inception horizon hypothesis (Lowe, 1992 and Lowe, 2000). This assumes that the earliest stage of speleogenesis (in some cases it can even start during the diagenesis of the carbonate sequence) begins at different discrete parts of a rock succession, more precisely along horizons which are particularly susceptible to dissolution. Such inception horizons are especially favourable to karstification by virtue of physical, lithological or chemical deviation from the predominant carbonate facies within the surrounding sequence (Lowe, 1992). Possible reasons for such a higher karstification potential are (Lowe, 2000):

- Higher primary porosity of the bedding plane than the surrounding rock mass, so that the bedding plane has a higher initial permeability.
- Bedding plane enclosing highly soluble minerals: under hypersaline conditions highly soluble minerals such as gypsum can be deposited. The dissolution or exchange of these minerals causes an elevated ratio of secondary porosity.
- Bedding plane with sulphide minerals: pyrite or other sulphide minerals can be oxidized and produce H2S or even sulphuric acid, which may turn non aggressive water (moving along the bedding plane) into highly corrosive solutions.
- Bedding plane of clastic beds: clastic beds such as shales or volcanic clays can be impervious and–if thick enough–act as a low permeability “screen” along which water will flow preferentially.

A number of case studies seem to confirm this hypothesis (e.g. Lowe, 1992, Knez, 1997, Knez, 1998, Lowe, 1999, Osborne, 1999 and Klimchouk and Ford, 2000). However no major study has been published on this topic providing clear evidence or even any quantitative estimate of the significance of inception horizons in the genesis of cave systems.

In this paper we describe a method which allows the identification and than the quantification of the effect of inception horizons on cave genesis. The application of this method to several reference sites makes it possible to demonstrate on a statistical base as well as on direct field observations that inception horizons play a significant role in determining the position of karst conduits.

2. Method development and validation on the Siebenhengste Cave System

A method of investigation and analysis had first to be designed (Fig. 1). A software tool has been developed for the analysis of the complex geometry of long cave systems in 3D. It helps by providing the statistical analysis of the relationship between the conduit network geometry, the geological settings and the hydrogeological context of cave systems. Data necessary for this analysis are descriptions in 3D, as complete and precise as possible, of the geology (faults and beds) and of the cave (survey data). For the geological model, mainly one reference layer has to be introduced into the model. Very often the base of the limestone series (top of the underlying marls) is used. The analysis follows six steps (Fig. 1). An application to the Siebenhengste Cave System is presented thereafter as an example.

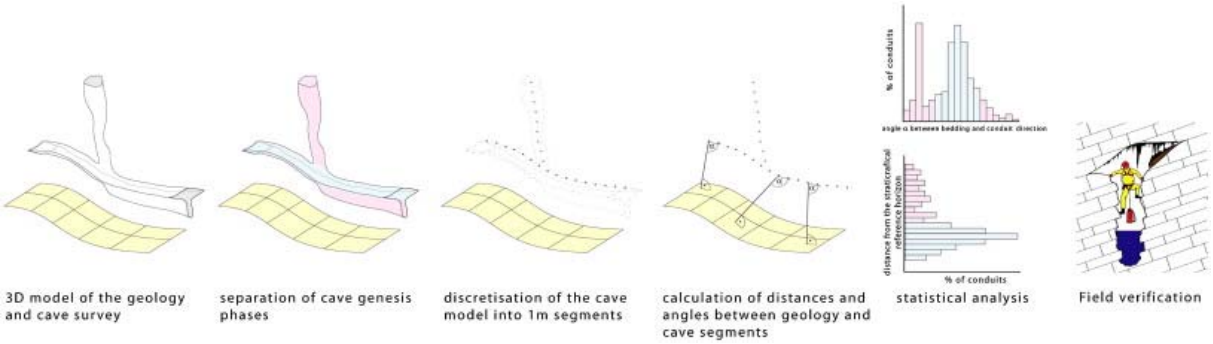

Fig. 1. Analysis procedure: The proposed method allows for getting statistical evidence of the existence of inception horizons based on cave survey and geological data.

The Siebenhengste Cave System

The Siebenhengste Cave System located North of Interlaken (Switzerland) is one of the most significant cave systems in the World with a length of more than 154 km and a depth range of 1340 m (Fig. 2). Close to this network there are also several other important caves, which so far have not been connected to it through cave exploration. The total length of explored conduits within the area is almost 300 km.

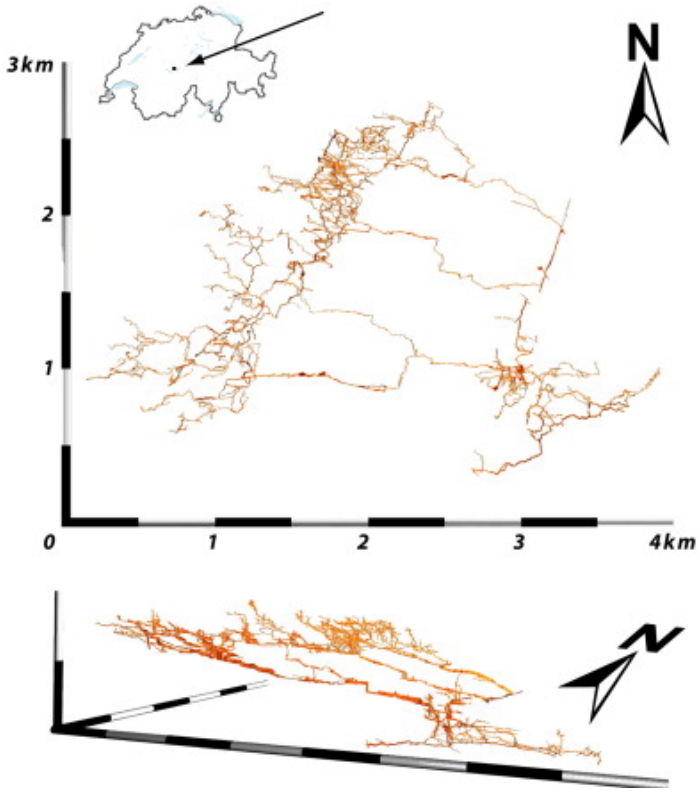

Fig. 2. Location and shape of the Siebenhengste Cave System: the complex and maze-like geometry of the conduit network (154 km) can only be analysed within a 3D approach.

2.1. Three dimensional (3D) models of geology and cave conduits

The approach used requires 3D computer models of the geological situation and cave conduits network (Fig. 1 panel 1). The quality of the 3D model directly influences the explanatory power of the analysis. A high degree of precision is required in order to be able to define if conduits develop for example along one single stratigraphical horizon (bedding plane). If such an analysis is very easy in a context of flat lying limestone it is much more challenging in folded areas. For our study and in order to get a high degree of precision, the geological models have been based on digital terrain models, geological maps and descriptions, aerial photo interpretations, observations in the cave systems, etc. This allows us to work with a model accuracy for simple geological settings of a few metres and for complex geological settings (folded, faulted, thinning out of the strata etc.) in order of a few decametres.

Geology of the Siebenhengste area

The Siebenhengste–Hohgant region belongs to the "Helvetic Border Chain" (Helvetikum). This Cretaceous series consists of a sequence of limestone, marls and sandstone (Ziegler, 1967). The main part of the Siebenhengste Cave System is located in the Schrattenkalk Formation (Barremian to Aptian, Urgonian facies) with a thickness of about 180 m (Fig. 3). This formation is underlain by the 30 to 50 m thick Drusberg Marl (Drusbergschichten, lower Barremian) which forms an impervious base. The upper limit of the Schrattenkalk is erosive and thus formed by various types of rocks, depending on the regions. In most places an Eocene turbiditic series called "Hohgant-series" lies directly on top of the Schrattenkalk. The Hohgant-series can be up to nearly 200 m thick and some of its beds, with calcareous cement, are karstified.

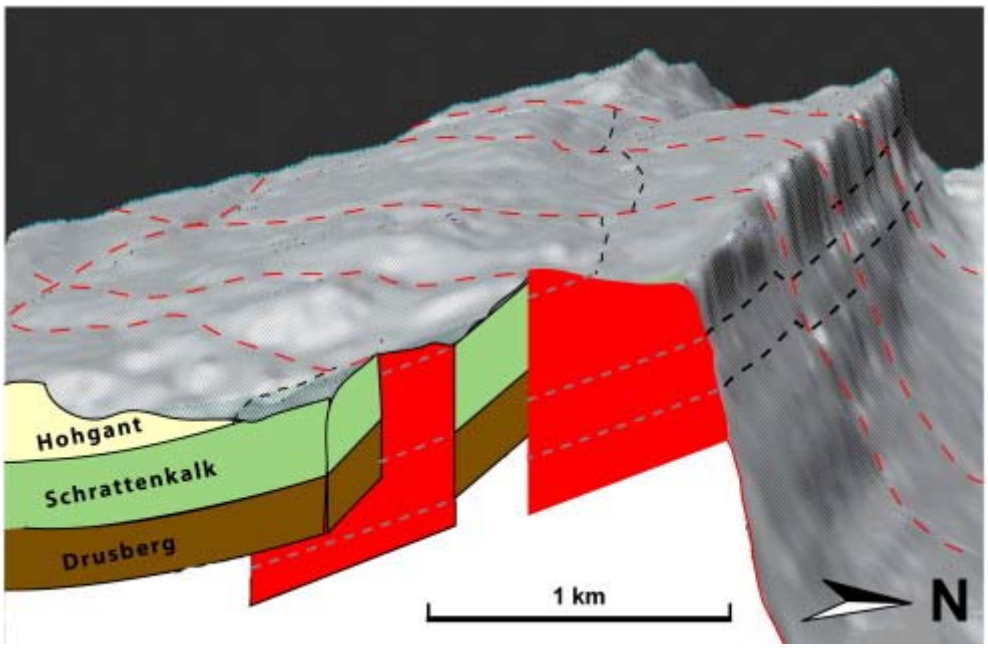

Fig. 3. View of the 3D model of the geology and cave conduits of the Siebenhengste region: the Siebenhengste Cave System evolved predominantly in the limestone of the Schrattenkalk Formation which is inclined towards the SE and displaced by some major faults.

The Schrattenkalk Formation is a pure shallow marine limestone and can be grouped into six units with variation of ooids content, dolomite–calcite ratio, macrofossils (rudists) and impurities (clay content) (Jeannin, 1989).

The limestone of the Schrattenkalk Formation dips 10–30° towards the southeast as a large slab. This dipping slab is cut by a series of faults more or less parallel to the strike of the beds, resulting in E–W horizontal displacements.

Conduits network of the Siebenhengste Cave System

The 154 km of explored cave conduits comprise a 3D labyrinthine network, which consists of shaft series linked by subhorizontal, in most of cases bedding plane guided conduits (Fig. 2). The 3D model of the cave system was obtained by the cave survey data collected by cavers.

The subhorizontal passages have often a “keyhole” profile cross-section which reflects a multiphase evolution of the conduits, whereas the elliptical upper section of the conduits developed under phreatic conditions, the “canyon” at the bottom was formed under later vadose conditions.

Model uncertainty

For the statistical analysis a high degree of precision is required. For the model of the Siebenhengste area a radial total uncertainty of about ± 25 m can be assumed within the national coordinates system. This error is related on one hand to the geological mapping and modelling, and on the other hand to the precision of the cave survey. The uncertainty of the geological model is about ± 15 m, and is mainly related to the extrapolation of the surface observations at depth as well as to the extrapolation of the underground observations down to the base of the Schrattenkalk Formation. The quality of the cave model is quite good and probably within ± 10 m. The cave survey is so much interconnected (survey loops) that every cave survey station is related to fixed points at surface by several survey lines, strongly reducing the position uncertainty (Grossenbacher, 1992). During the discretisation step, it was assumed that the inception of the conduit occurs at the ceiling (see also Section 2.3 “Discretising the 3D model”).

For the analysis of inception horizons only the relative uncertainty between cave conduits and geology is relevant. As many observations of the geology have been made in caves, this uncertainty is smaller than the absolute one, i.e. in the order of 10 to 15 m.

2.2. Reconstruction of the hydrogeological conditions

Karst conduits may develop under phreatic as well as under vadose (unsaturated) conditions. This depends mainly on the position of the conduit within the aquifer: above the water table conduit enlargement is mainly due to vadose processes, whereas below the water table the enlargement is exclusively phreatic. Due to high hydraulic conductivities of karst conduits, the water table lies almost horizontally from the karst spring upwards. In the phreatic zone the hydraulic gradient is mainly horizontal, linking a recharge area to a discharge area (i.e. spring). Thus, discontinuities parallel to this gradient will be mostly used and develop conduits. Therefore the relative position of the recharge and discharge areas is a key factor controlling the orientation and position of phreatic conduits. These are usually tubes with an elliptic to round cross-section and with a more or less horizontal course, going up and down depending on the initial openings available in the limestone mass. Flow in vadose conduits is ultimately controlled by gravity i.e. mainly vertical. As water can only flow downwards vadose conduits are mainly vertical shafts or pitching, meandering canyons. It is thus important to distinguish purely vadose conduits from phreatic ones, because their orientation and genesis is significantly different. Most karst conduit systems in the World are multiphase, i.e. consist in a series of conduits formed under variable boundary conditions (mainly changing recharge–discharge areas). A first challenge in understanding their genesis is to distinguish the respective phases (subset of conduits belonging to a single phreatic zone of a karst system in the past) and their respective characteristics.

A way to start the analysis of a speleological conduit network is to remove all conduits clearly vadose in origin and to draw a histogram of the cumulated length of the remaining conduits by elevation classes (such as suggested by e.g. Bögli, 1980 and Palmer, 1987). This should allow for the identification of the main evolution phases of the karst network and, in cases of a flat geology this is an easy way to winnow different levels of karst water table. However, in karst systems with a steep or folded geology the conduits may be distributed quite far away from a simple horizontal plane (former water table). It is for this type of situation that our analysis combining speleogenetic phases and geological structure in a 3D model has been developed (Fig. 1 panel 2).

Hydrogeological phases of the Siebenhengste Cave System

The cave system has a distinctive labyrinthine character and its complex geometry can only be explained by a series of superimposed flow systems that correspond to different and more or less independent times and hydrogeological conditions (Jeannin, 1996, Bitterli and Jeannin, 1997, Häuselmann et al., 1999, Jeannin et al., 2000 and Häuselmann, 2002). Most of the conduits in the system were formed under phreatic conditions (which include also the epiphreatic zone). Vadose flow has only reshaped the profile of certain passages without fundamentally modifying the overall geometry. The major features resulting from vadose flow conditions are a series of shafts that pass through the limestone series vertically down to the phreatic zone. In certain conduits it was possible to observe the exact transition point between the former phreatic and vadose zones making it therefore possible to reconstruct the top of paleophreatic zones. In the Siebenhengste Cave System it was possible to distinguish five different major paleophreatic zones (Jeannin et al., 2000).

Many of the main conduits were formed quite deep below the water table, e.g. loops deepening more than 250 m below the top of the phreatic zone have been observed. It was therefore not an easy task to separate the different phases because conduits of two or even three different phases may occur at the same elevation (Fig. 4). Thus, the widely used method consisting of looking at the vertical distribution of the conduits to assign a given conduit to a paleophreatic zone does not work well for this case. The only way was to reconstruct, based on the conduit morphology, the logical connections of the known cave conduits in the 3D model with the help of field observations. Thereby it was possible to reconstruct the conduit networks of the five hydrogeological phases.

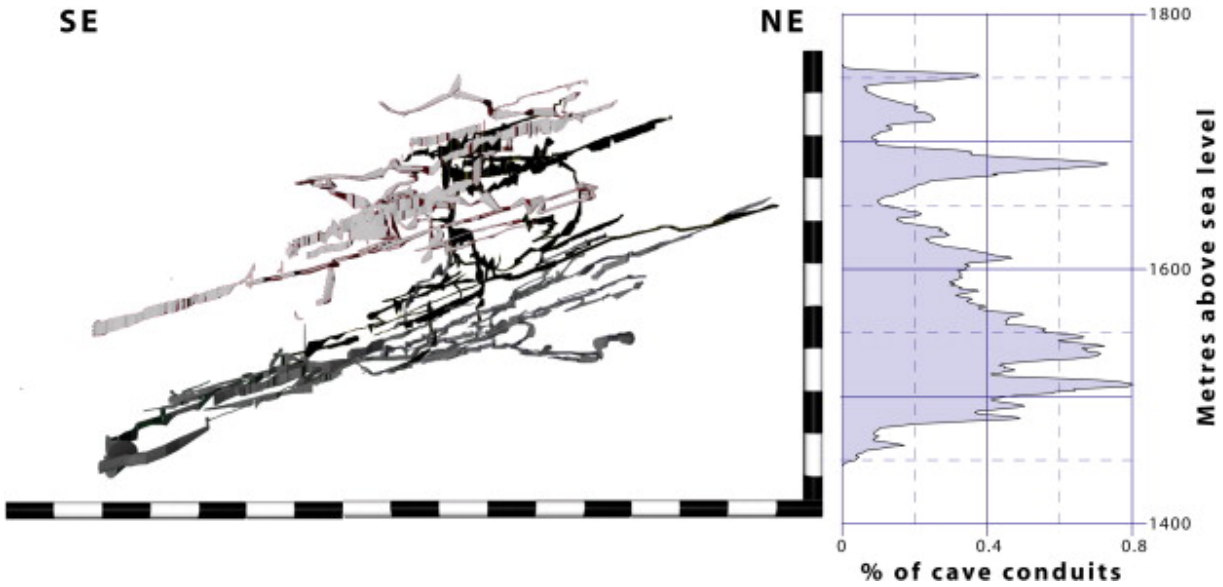

Fig. 4. View of the 3D model of the phreatic conduits of one part of the Siebenhengste Cave System and the corresponding vertical distribution of the conduits. The grey shades in the 3D view indicate three major hydrogeological phases. However it is difficult to recognise these phreatic phases in the histogram.

2.3. Discretising the 3D model

To analyse the 3D model statistically it was necessary to discretise (split the data into discrete intervals) each cave conduit into 1 m long segments (Fig. 1 panel 3). Properties (direction, dip) of the conduit have been assigned to the respective segments. It must be pointed out at this point, that for our analysis we used only the conduit length and not the volume.

For our study we are interested in the position of the inception horizon in the conduit cross-section. It was assumed that the ceiling of the conduit is the best approximation of that position. It may be argued that in phreatic elliptic conduits the inception horizon is often located in the middle of the ellipse. On the other hand in a multi phased conduit (phreatic tube entrenched by a vadose canyon), the inception horizon is rather located at the ceiling than in the middle of the cross-section. This is the most common case in many of the investigated cave systems, therefore this assumption was used. This is a simple way to get an approximation of the position of a potential conduit inception horizon with an accuracy of a few metres.

The geology was represented by the modelling of a single stratigraphical reference horizon, in most cases the base of the karstified rock formation, i.e. the top of the Drusberg Marls in the case of Siebenhengste Cave System. This reference horizon was discretised within a mesh of a width of around 5 m. For each grid point the normal vector to the surface has also been calculated.

2.4. Statistical analysis

Based on the discretised 3D model, the method used makes it possible to quantify the relationship between the geometry of the cave systems, the geological setting and the hydrogeological boundary conditions. With these results it was possible to describe the relationships with different descriptive statistical methods and to provide quantitative evidence of the role of inception horizons on cave genesis at the regional scale.

2.4.1. Analysis of the parallelism

This analysis aims at verifying to what extent conduits are parallel to bedding planes. Based on the 3D model, the developed software tool computes the spatial angle between the directions of the conduit segments and the normal vector of the reference horizon (bedding). Consideration of the normal vectors to the bedding planes means that parallel conduits will have a minimum spatial angle of 90° whereas perpendicular conduits will have a minimum spatial angle of 0°.

Results from Siebenhengste Cave System show angles close to 90° (Fig. 5) although dispersion is quite large. The same analysis was applied on a subset of the data, after having removed the vadose conduits from the data set.

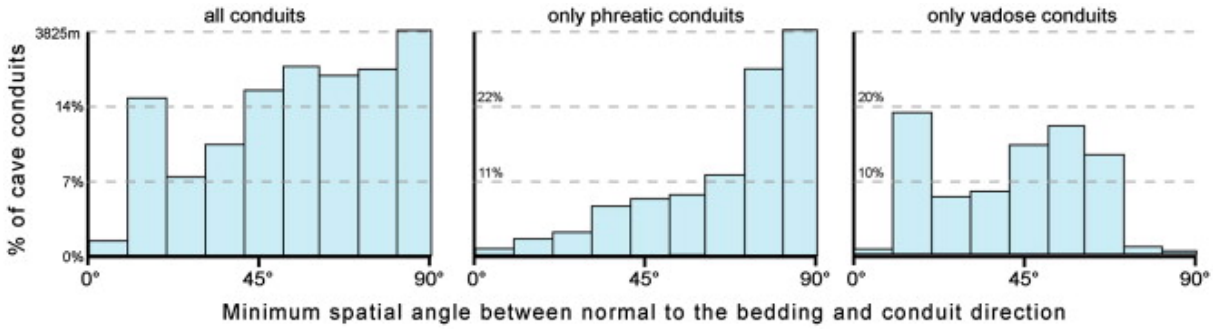

Fig. 5. Histogram of minimum spatial angles between normal to the bedding and conduit direction in the Siebenhengste Cave System (Zone II). Left: all conduits together showing a central trend around 90°; the peak at low angles corresponds to vertical conduits in the vadose zone. Middle: only phreatic conduits. Right: only vadose conduits.

Concerning the vadose zone, the results show that cave directions are poorly related to the stratigraphy (Fig. 5, right). However most parts of the vadose conduits are concentrated in two intervals: 10–20° and 50–60°. The first interval represents the angle between the orientation of the bedding (120/25°) and the orientation of the main joints and faults in this region. This corresponds in Fig. 2 to the five main straight conduits linking the upper (NE) maze to the lower (SE) maze parts of the system. This direction (intersection between bedding planes and the main joints) is well-marked in the Siebenhengste area because the dip of the bedding planes is rather constant. In folded regions, angles would not be so well defined around a single value although caves may have the same type of preferential direction. It is noteworthy that even in the vadose zone some conduits are parallel to the dip of the bedding. These passages correspond to short meander sections linking two shafts.

Concerning the phreatic zone, the histogram of Fig. 5 shows that karst conduits are predominantly parallel to bedding planes (about 70% of the phreatic conduits in the Siebenhengste Cave System). As presented above and later in this paper, this does not imply that fractures have no influence on the development of the conduits.

The analysis of other large cave systems (Table 1) leads to the same type of results.

2.4.2. Analysis of the existence of inception bedding planes — or the statistical evidence of the inception horizon hypothesis

In the previous section we showed that most phreatic conduits are developed parallel to bedding planes. In this section we want to see if conduits are distributed randomly along any bedding planes or if we can find some special horizons that have been favourable to the development of conduits. In other words we want to see if there is a statistical evidence of the inception horizon hypothesis (Lowe, 1992).

To do this our software determines the shortest distance between a conduit segment and the geological reference surface. Histograms of these distances give the percentage of conduits for a given distance from the reference surface, respectively the percentage of conduits in a stratigraphical horizon. Peaks represent horizons where karst development is concentrated (Fig. 6). A 3D visualisation of the cave system already confirmed the basic idea of inception horizons raised by various authors from qualitative field observations. In the Siebenhengste Cave System it is quite obvious that conduits are concentrated along some specific strata. A more detailed interpretation of the histograms allows separating up to seven different horizons (Fig. 6 and Table 1).

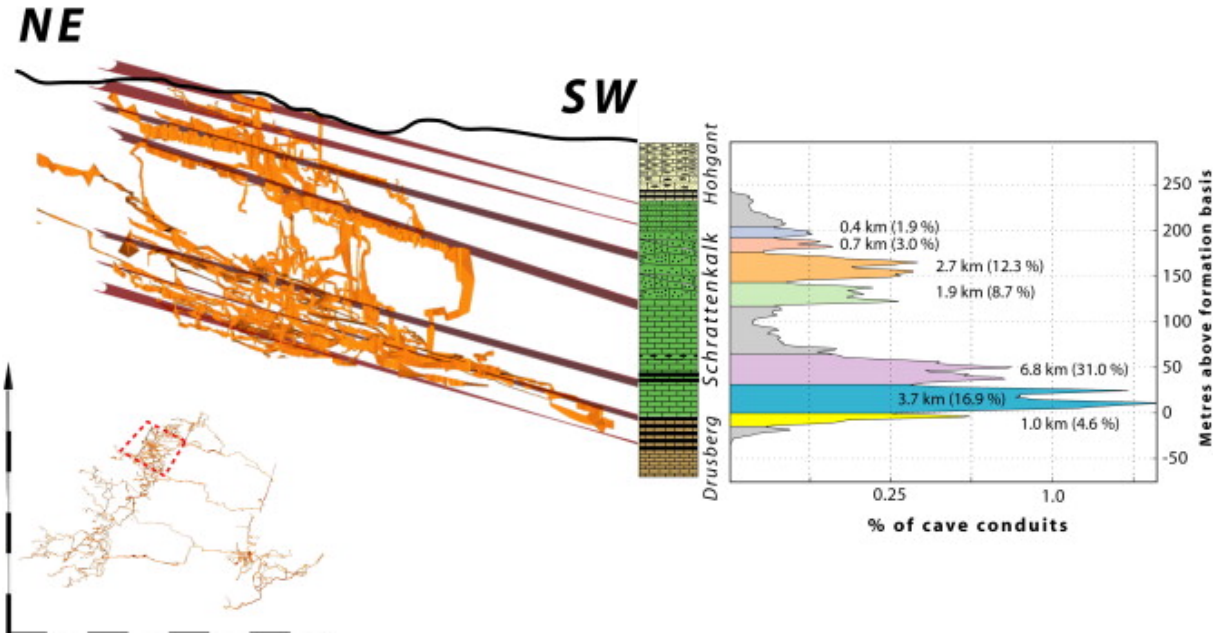

Fig. 6. 3D projection of one part of the Siebenhengste Cave System. Seven potential "inception horizons" can be identified within the Schrattenkalk Formation. The thickness of the limestone is nearly 180 m.

The respective peaks have a clearly increased cave conduit density compared to a homogeneous distribution of the conduits in the rock mass. About 80% of the conduits of the Siebenhengste Cave System are located on 7 horizons (Fig. 6). Peaks seem to represent a normal distribution around a given discrete feature. As presented in a more detailed way in Section 2.5 these features are in most cases bedding planes or lithological strata of a thickness of some decimetres or even less. This would reduce the peak width to a very thin range, i.e. about 80% of the conduits would be developed within only about 0.5% of the limestone thickness. The scattering of the data is caused by the uncertainty of the respective positioning in the 3D model. In the example presented here (Siebenhengste Cave System) the uncertainty is in the order of ± 15 metres.

The relative size of the peaks has only a limited meaning concerning the properties of the horizons. The presented analysis only takes into account cave conduits that are large enough to be accessible for cavers. In the karstic rock mass there will be many more karst conduits that are too small to be explored by humans as well as some cave conduits which have not been explored so far. The real development of the conduit network along a bedding plane is also strongly related to the history of the hydrogeological boundary conditions (e.g. two compartments shifted by a fault may be in different positions relatively to the hydrogeological boundary conditions). This makes some peaks more or less pronounced at different compartments of the cave system (Fig. 7). From this on, the only reliable conclusion we can make from the histograms is that peaks represent horizons which are preferred for conduit development. The method also makes it possible to define the stratigraphical position of these inception horizons.

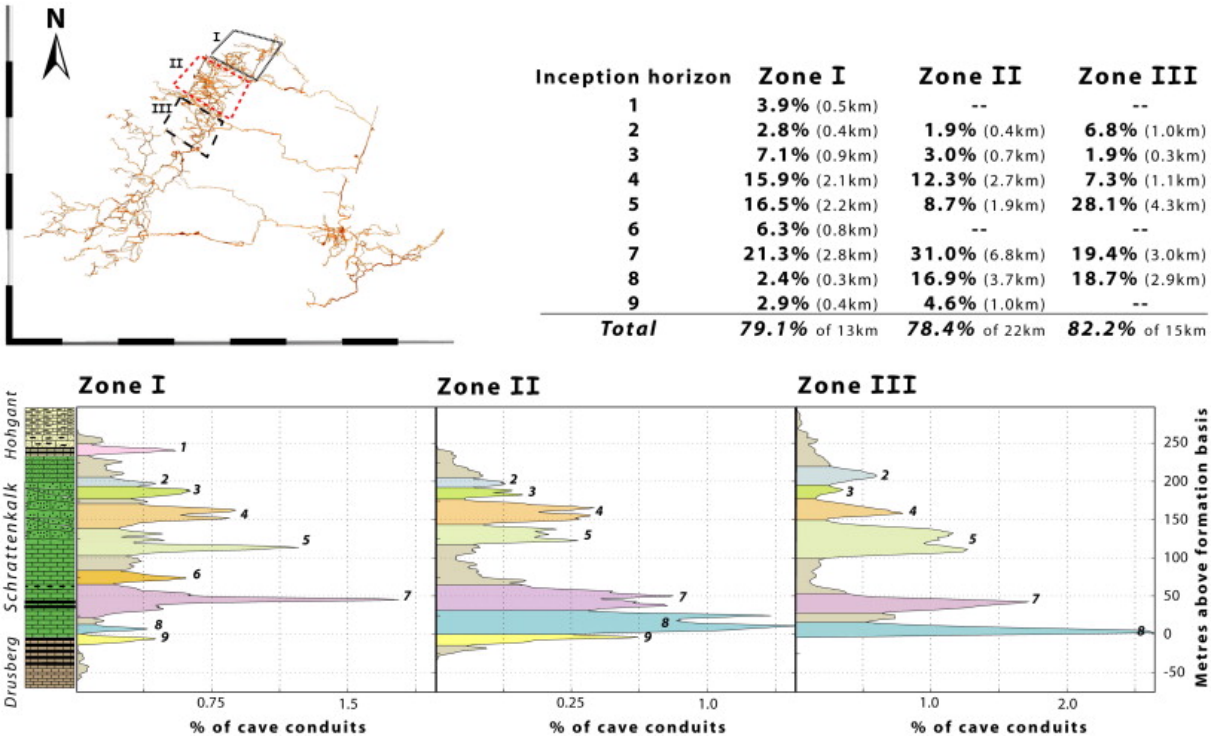

Inception horizon	Zone I	Zone II	Zone III
1	3.9% (0.5km)	--	--
2	2.8% (0.4km)	1.9% (0.4km)	6.8% (1.0km)
3	7.1% (0.9km)	3.0% (0.7km)	1.9% (0.3km)
4	15.9% (2.1km)	12.3% (2.7km)	7.3% (1.1km)
5	16.5% (2.2km)	8.7% (1.9km)	28.1% (4.3km)
6	6.3% (0.8km)	--	--
7	21.3% (2.8km)	31.0% (6.8km)	19.4% (3.0km)
8	2.4% (0.3km)	16.9% (3.7km)	18.7% (2.9km)
9	2.9% (0.4km)	4.6% (1.0km)	--
Total	*79.1%* of 13km	*78.4%* of 22km	*82.2%* of 15km

Fig. 7. Histograms of three zones of the Siebenhengste Cave System representing the distances of the cave conduits relatively to the base of the Schrattenkalk Formation: The same peaks are differently pronounced in the respective compartments. The table included in the figure gives the percent of conduit length on the corresponding inception horizon.

An interesting observation is that the shape of the histograms are quite similar when displaying all or only phreatic conduits of a cave system (Fig. 8). It seems even that peaks appear more clearly when including all conduits. This is because vadose conduits (in the most of the cases meanders) of the Siebenhengste Cave System are located along the same bedding planes as those of the phreatic zones previously developed in the analysed rock volume. On the other hand vadose shafts of the analysed cave network are vertical and in most cases cross the whole limestone series down to its base. Therefore they produce a more or less homogeneous distribution over the whole limestone thickness.

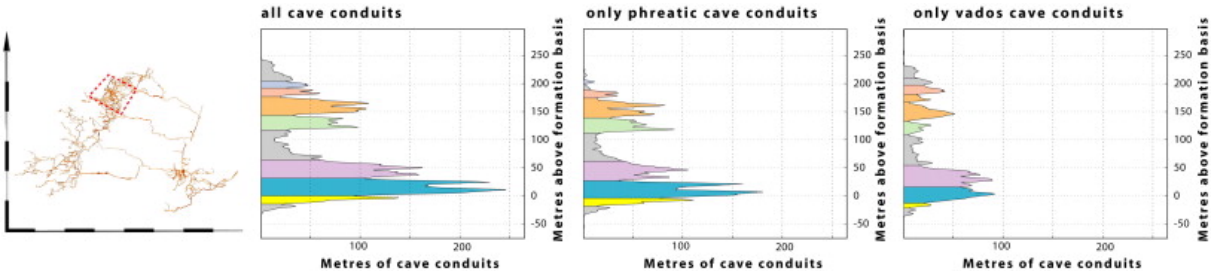

Fig. 8. Histogram of the conduit distribution relative to the base of the limestone series: Vadose shafts are evenly distributed across the limestone series and represent therefore a more or less homogeneous conduit distribution, i.e. not really influencing the overall distribution. Vadose meanders between shafts appear to be located along the same favourable horizons as phreatic conduits. (Example of the Siebenhengste Cave System, Zone II).

2.4.3. Analysis of the conduit direction

We demonstrated above that the main part of the phreatic cave conduits are related to a restricted number of stratigraphical horizons. As a next step we analyse the distribution of conduit directions in order to identify potential preferred flow directions along the inception horizons. Under phreatic conditions the flow direction is dominated mainly by the direction of the hydraulic gradient, i.e. is different from the down-dip direction in most cases. For example it is well known that phreatic conduits display up and down "loops" stretching along the strike of the limestone beds.

The plan view of the Siebenhengste Cave System clearly indicates that preferred directions do exist. Previous studies of the fracture network (Jeannin, 1989) showed that some fractures are preferentially used by cave conduits rather than others. However this analysis took into account all conduits of the cave system together. In the following analysis, we separated the conduit networks of the respective genetic phases of the system prior to analysing the conduit directions. The idea was to see if changes in the hydraulic gradients according to the respective phases of the cave genesis could significantly change the discontinuities used by conduits.

For the analysis we compiled rose diagrams of the conduit direction weighted by their length (Fig. 9). This allows us in a simple way to identify preferential directions. We did not analyse the whole cave system at once but looked at each evolutional stage separately.

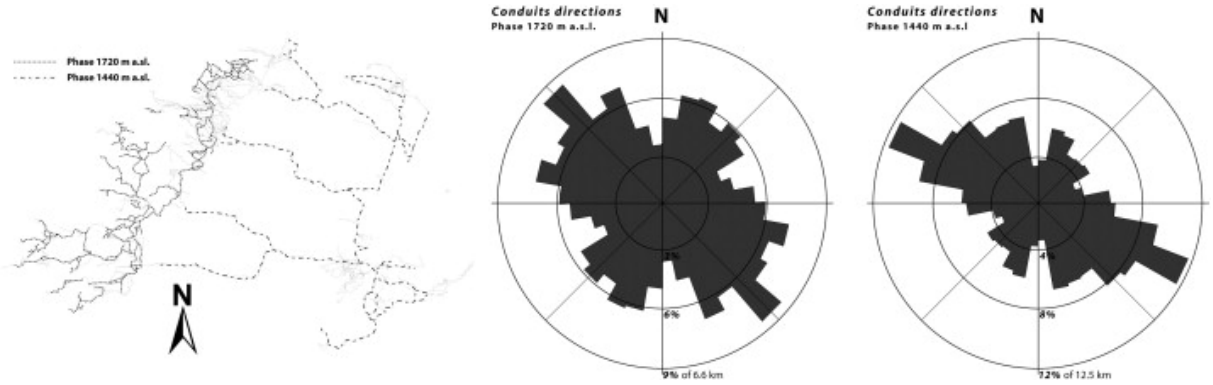

Fig. 9. Plan view of the Siebenhengste Cave System with a rose diagram of the conduit directions of the phase 1720 and 1440: The directions of the conduits are dominated by the fracture network as well as by the hydrogeological boundary conditions, the changing of the hydrogeological boundary conditions between the two phases caused the preference of another set of fractures.

The rose diagram of the conduits directions from phase 1720 features two main directions (NW–SE, N–S). These directions are well known from the study of the fracture pattern of the area (Jeannin, 1989). The NW–SE direction corresponds to the direction of the large strike-slip faults that subdivide the area in different shifted blocks (Fig. 3). The main displacement along those faults has been horizontal (probably several hundreds of metres) and the vertical components do not exceed 20 to 40 m. The others directions are associated joint sets.

For phase 1440 the same joint sets are used but the length of conduits along the respective joint sets is significantly different. For this phase the hydraulic gradient was oriented towards the SE, so that the NW–SE joints have been clearly preferred as flow paths.

From this analysis we can conclude that the conduit direction of the phreatic conduits at the regional scale is conditioned by the combination of the hydraulic gradient and the intersection of tectonic fractures with inception horizons. Only intersection lines more or less parallel with the hydraulic gradient will be favourable to conduit development. In some cases the conduit direction on the inception horizons was not conditioned by fractures (respectively the intersection inception horizon with fractures), in these cases the conduits followed only the inception horizon.

2.5. Field verification of the existence and position of inception horizons

The statistical analysis showed that many conduits are located along the same inception horizon. These horizons have been displayed in the 3D model in order to verify visually their speleogenetical significance. At several places it has also been verified by field observations or backed-up according to detailed descriptions of the cave passages from the literature. In caves, some typical features and effects can be looked for in order to recognise a bedding plane as an inception horizon (e.g. Filipponi, 2007):

- Water inlets in a cave passage, originating from a bedding plane: During and after the main development phase of a karst conduit, the initial inception horizon remains potentially active as a network of interconnected microvoids that conduct water towards the cave.
- Water chemistry of the "bedding plane water inlets": Water coming from an inception horizon may have a particular chemical composition due to the dissolution and exchange processes with minerals of the layer. This particular chemistry of the water can cause two kinds of phenomena: 1) the growth of speleothems such as flowstones, 2) the dissolution of the cave wall and the development of "solution pockets".
- Bedding plane fractures (interbedded slides): Already with a slippage of just a few millimetres striation, brecciation and surface irregularities enhance openings along the sliding plane.
- Bedding plane guided cave passage: If a cave passage follows a bedding plane (i.e. inception horizon) for several hundreds of metres, it can be assumed that this particular horizon was especially favourable. Sometimes the conduit follows a fracture-bedding intersection.
- Anastomoses on a bedding plane: Anastomoses are small channels forming a dense network of small conduits along a plane (Fig. 10) (Slabe, 1995). According to the inception horizon hypothesis, bedding plane anastomoses can be interpreted as a network of karst conduits that have developed during the phase of cave "gestation" before becoming a "victor tube" was able to form a real cave (Fig. 13).

Fig. 10. Anastomoses in the Nidlenloch cave system (Switzerland). Anastomoses are one of the features commonly found in cave passages located along an inception horizon. (Photo: M. Widmer).

Several parts of the Siebenhengste Cave System were investigated and in all cases horizons inferred from the 3D analysis have been identified in the field. This clearly showed that inception horizons are much more discrete and localised in the field than obtained by the statistical analysis. In most cases we think that horizons have a thickness ranging between 2 and 30 cm though they appeared as peaks of 5 to 10 m thickness in the statistical analysis. The width of those peaks is due to the various uncertainties related to the model construction.

In many places we could observe that at places where a conduit reaches a normal fault, it followed the fault to find the same bedding plane again on the other side of the fault. In some cases another inception horizon was used.

The seven inception horizons of the Siebenhengste Cave System have different aspects (Fig. 11):

- The first inception horizon is a fossil-poor bedding plane (some centimetres thick) in the Schrattenkalk sensu stricto. Eye-catching is the network of anastomoses that developed along the bedding plane. The network is so dense in some places, that the bedding plane was completely removed.
- The second inception horizon is situated at the contact between the Schrattenkalk-members sensu stricto and "upper oolitic" member. Below this surface there is a set of close standing joints that seems

to end at this contact. Also some evidence of neotectonic movement along the contact could be observed (broken and shifted dripstones).

- Inception horizon three is a 40 to 60 cm thick, very blocky (stromatolitic?) limestone layer.
- Inception horizon four is a marly horizon of some centimeters thick.
- Inception horizon five is a marly bedding plane (some centimetres thick) of the "Lower Schrattenkalk" member. Many siliceous nodules of some centimetres in diameter are found embedded in the bedding plane.
- Inception horizon six is a marly layer (some decimetres thick) at the transition between the Lower and Basal Schrattenkalk-members. Conduits related to this horizon are full of cave gypsum formations (crusts, needles, flowers, etc.).
- Inception horizon seven is a limestone layer (some metres thick) within the marls of the Drusberg-Formation.

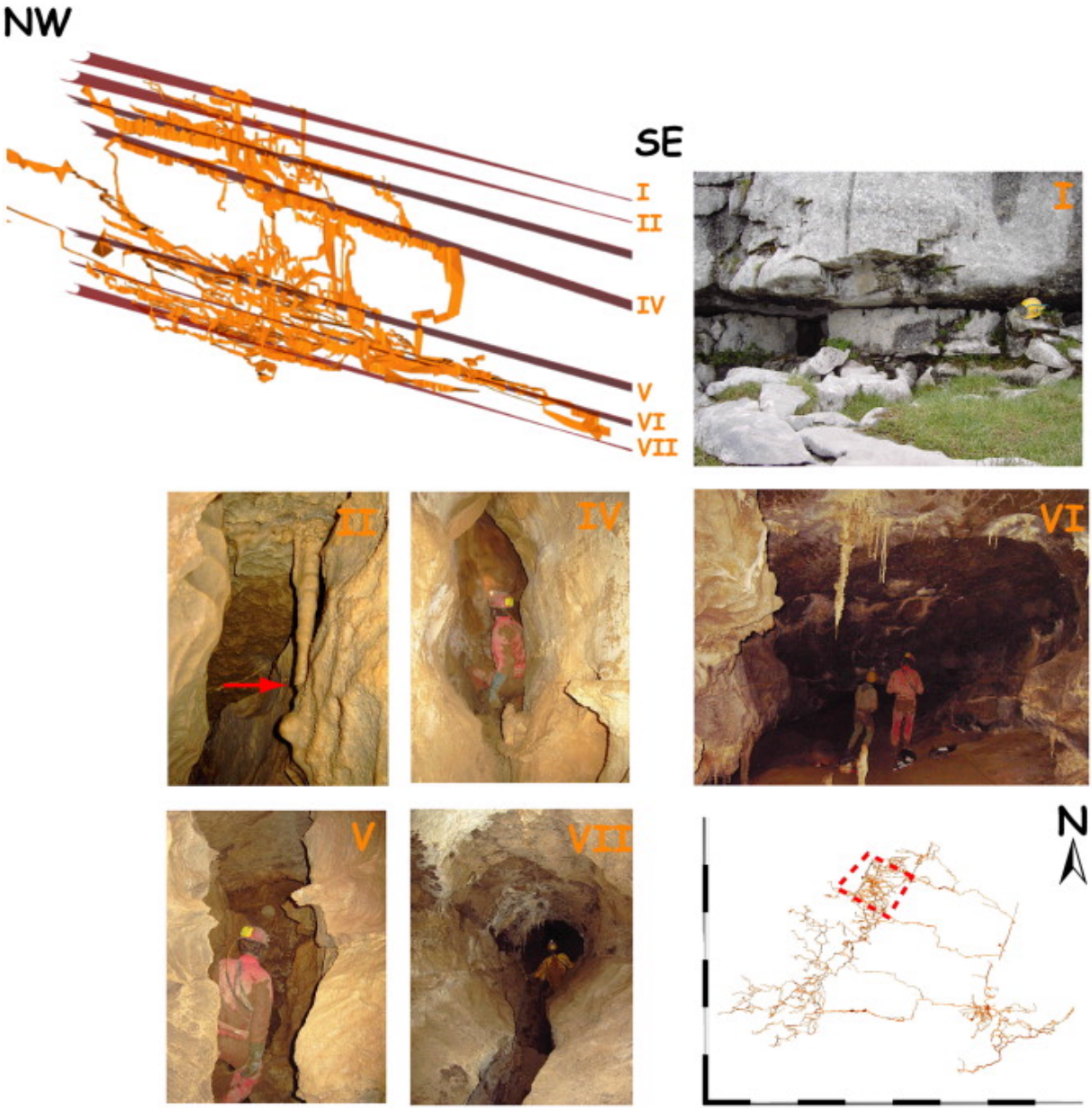

Fig. 11. Cave conduits lying on favourable inception horizons. Field verification showed that the karstification began at some discrete stratigraphical horizons (i.e. bedding planes).

Field verifications in the other caves investigated also confirmed the existence of the statistically identified inception horizons. However in some cases detailed field observations showed that some conduits also developed along other bedding planes than those identified by the statistical approach. Obviously those bedding planes do not present favourable properties over extended distances and are therefore not significant at a regional scale.

3. Results from other large cave systems

The statistical recognition method of inception horizons presented above was validated by its application to the Siebenhengste Cave System. It is less precise than the direct identification in the field, but allows for a "rapid" analysis of cave systems. We therefore applied this method to several other important cave systems from all over the World (Table 1). This is the first time that such a comparative study has been carried out with such a large number of cave surveys (more than 1500 km of conduits have been analysed). The following properties of cave systems were required to be selected for this analysis:

- The explored and surveyed conduit network length should be sufficient (at least 5 km of conduits).
- The respective systems should be representatives of a large panel of geological settings (lithology, tectonics, age…). Nevertheless the analysis has been restricted to cave systems developed in limestone and/or dolomite formations.
- Investigated cave systems should have been formed only (or at least mainly) by meteoric water karstification (epigenic caves) without or with negligible influence of hydrothermal or hypogenic water.
- The evolution of the investigated cave systems should have occurred mainly under phreatic conditions. This last point is very important because only cave conduits developed under phreatic conditions reflect the initial state of the development of the cave system. By the way, phreatic systems are by far the most common.

The analysis of the parallelism clearly showed that in all studied cases the phreatic conduits are parallel to bedding planes. This appears to be independent of the structural context. Nevertheless cave systems located in a flat lying geological environment have a higher percentage of conduits (e.g. the cave Ogof Draenen with 87%) that are parallel to bedding planes than systems with more complex geological settings. This is due to the absence of phreatic shafts which can only develop in deeper phreatic conditions. As a general rule it can be postulated that more than 70% of the phreatic conduits are parallel to some particular horizons, which in most cases correspond to some particular bedding planes.

The analysis of the inception horizons gives similar results to those obtained for the Siebenhengste Cave System (Table 1). In all cases we could find between two and seven inception horizons. Considering the fact that horizons are found in all selected cases and that these cases cover a wide range of geological settings as well as hydrogeological boundary conditions, it can be considered that the inception horizon idea is a fundamental principle in cave genesis. Our data even allow for a more quantitative evaluation of the significance of this concept.

The separation of the different peaks was sometimes quite difficult, because the uncertainty of the geological model with respect to the conduit positions was high. This uncertainty is visible on histograms by large peaks. However, as the scattering follows a normal distribution it is possible to identify the expected stratigraphical position of the inception horizon within a precision of 5 to 20 m. In some cases, where inception horizons are close to each other, peaks may be merged together. In some rare cases with rather complex geological settings (e.g. with a lot of little faults with a displacement of a few metres or slightly folded areas) large peaks were obtained and it was only possible to decompose them with the help of the visualisation of these horizons in the 3D model. From this analysis, it can be concluded that more than 65% of the phreatic caves (i.e. 90% of the conduits parallel to the bedding) have developed along a very restricted number of stratigraphical horizons. These horizons are in most cases only some decimetre or less thick. This shows the significance of the inception horizon idea for the genesis of cave systems.

The analysis of the conduit directions of the selected cave systems leads us to the same conclusion as for the Siebenhengste Cave System. In all cases flow directions within (or along) inception horizons are guided by the fracture network, usually the two or three fracture sets which are oriented according to the regional flow direction (controlled by input/output flow conditions). In cases where the landscape dramatically changed during the evolution of the cave system (e.g. in alpine areas where entrenchment of valleys during glacial periods changed the position of the outlets of the karst system) we could observe that fractures guided the conduit direction change according to the respective outflow conditions. In other words, we could say that the regional hydraulic gradient selects the fractures which are being karstified. Here it can be mentioned that inception horizons (i.e. bedding planes) are generally less influenced by the direction changes, because in many cases

hydraulic gradients and inception horizons are both subhorizontal, i.e. parallel, whatever the hydraulic direction can be.

Name of the cave system	Country	Length [m]	Depth [m]	Number of interception horizons
Mammoth Cave System	Kentucky, United States	590,600	115	5
Hölloch & Silbernsystem	Schwyz, Switzerland	193,600 & 37,700	940	2–3
			890	
Siegenhengste Höhlensystem	Bern, Switzerland	154,000	1340	5–9
Schönberg– Höhlensystem	Oberösterreich, Austria	123,600	1060	4–5
Shuanghedongqun	Guizhou China	106,400	501	2
Hirlatzhöhle Dachstein	Oberösterreich, Austria	95,300	1070	6–7
Ogof Draenen	South Wales, United Kingdom	66,100	100	3
Dachstein– Mammuthöhle	Oberösterreich, Austria	65,800	1200	4–5
Schwarzmooskogel- Höhlensystem	Oberösterreich, Austria	58,200	1030	6–7
Burgunderschacht	Oberösterreich, Austria	20,200	850	6
Schrattenhöhle & Bettenhöhle	Obwalden, Switzerland	19,650	575	2
DÖF- Sonnenleiterschacht	Oberösterreich, Austria	18,200	1055	6
Réseau des Grottes aux Fées	Vaud, Switzerland	12,100	135	3
kleines Hölloch	Allgäu, Germany	9300	460	3
Wägital Lachenstock, k10, Plattenloch	Schwyz, Switzerland	9000	270	5
Nidlenloch	Solothurn, Switzerland	7500	420	4
Lauiloch	Schwyz, Switzerland	4500	180	1
Réseau de Covatannaz	Vaud, Switzerland	4450	105	2

Table 1. Investigated cave systems with the determined number of inception horizons: inception horizons have been found in all investigated cave systems.

4. Discussion

The method developed for the analysis of inception horizons in cave systems was validated by the analysis of 18 well documented large cave systems from all over the World, among them the Siebenhengste Cave System being our main test site. The existence of stratigraphic horizons along which karst conduits developed preferentially has been found in all systems examined. In most cases we could identify between two and five inception horizons. This analysis confirms the idea of preferential development along some discrete stratigraphic horizons as already introduced by many authors (e.g. Rauch and White, 1970 and Palmer, 1989) and named by Lowe (1992). However the presented method allowed for the first time to provide clear quantitative evidence of the significance of inception horizons for the genesis of cave systems.

Our results remarkably show that only a restricted number of inception horizons (i.e. bedding planes) are used for cave inception at a regional scale: probably less that 10% of the existing bedding partings are inception horizons and guide more than 70% of the conduits. It also appeared clearly that the influence of these horizons onto the 3D geometry of the systems is high. However, the method allows only recognising inception horizons with a regional significance (in Lowe, 1992 called major inception horizon). Detailed field observations showed that beside the statistically identified inception horizons some other inception horizons guided cave passages for only some metres to tens of metres and have only a local significance (hundreds of m2; in Lowe, 1992 called minor inception horizon). This explains also the difference between the number of cave conduits parallel to the bedding (in the Siebenhengste Cave System around 70% of the conduits are parallel to the bedding; Section 2.4.1)

and the sum of the conduits length being identified statistically to be on inception horizons (65%; Section 2.4.2). However the majority of the bedding plane guided cave passages developed along an inception horizon with regional significance.

Also (Knez, 1997) and (Knez, 1998) recognised in the Škocjanske Jame (around 5 km long cave system) only a restricted number of bedding planes to be inception horizons (3 inception horizons of 62 prominent bedding planes in the around 100 m thick limestone sequence). His basic working method was to assign in the field phreatic conduits to the respective stratigraphical horizons.

Palmer (1989) measured with a high degree of precision in the Mammoth Cave region the orientation of about 20 km of conduits and the bedding of the rock at more than 3200 locations. With his field method he was able to have an accuracy of less than 1°. He could show that around 70% of the conduit passages examined had discordance to the local dip of the bedding of less than 2°. The conduits were located preferentially along 24 different stratigraphic horizons of which 5 horizons are predominant at the regional scale. Our analysis of the Mammoth Cave data confirmed Palmer's results, providing a supplementary validation of our analysis method. Unfortunately our method depends on the precision of the cave survey data as well as that of the geological knowledge of the massif investigated. This limited precision is somewhat compensated by the high number of data points available for the analysis.

Field verifications pointed out that those inception horizons are rarely thicker than some decimetres, and in most cases in the order of a few centimetres. The statistical analysis provides a normal distribution around the position of the inception horizons in the order of some metres to tens of metres, because of the uncertainty of the 3D model (see also Section 3). In cases where the inception horizons are very close together it will be hard to distinguish them based on the statistical method. Therefore it is advisable to interpret the histogram with the help of the 3D model and to verify the results by field observations.

Albeit our 3D analysis was restricted only to epigenic caves (caves formed by water recharged from the overlying or immediately adjacent surfaces due to carbonic acid dissolution), it appears that also for the geometry of hypogenic karst systems (caves formed by water in which the aggressiveness has been produced at depth beneath the surface, independent of surface or soil CO2 or near surface acid sources; Palmer, 2000) is guided by a restricted number of stratigraphical horizons (Klimchouk, 2007). However a detailed 3D analysis still needs to be done.

Davies (1960) suggested that the dip of beds influences the role of the bedding planes for the development of conduits and concludes qualitatively that beds dipping less than around 15° seem to have a clear influence on cave development, whereas beds with a dip between 15 and 80° would have only a restricted influence. The influence of steeper (almost vertical) beds would increase again. Our reference sites cover almost all kinds of orientation and the role of bedding planes was significant for all of them. It was true not only for phreatic conduits but also in cases where bedding is rather steep vadose conduits preferentially followed beds rather than fractures down to the phreatic zone (e.g. case study of the Nidlenloch (Filipponi and Jeannin, 2006) or from the literature Osborne, 1999, Osborne, 2001 and Ford and Williams, 2007). Therefore, we could not confirm Davies observations and we have to conclude that the role of bedding dip is only a subordinate factor.

Compared to fractures, bedding planes often have the advantage of a larger size, i.e. better continuity (the typical surface area of joints is in the order of some hectares; the typical size of bedding planes in the order of square kilometres). They also have the advantage of orientation: Most bedding planes are subhorizontal, i.e. parallel to the hydraulic gradient in the phreatic zone. Another advantage compared to fractures is their age (karstification along bedding planes can start during the diagenesis of the rock mass). However, this does not mean that fractures have no role in cave inception. In most cases fractures control the conduit orientation at local scale and along inception horizons (e.g. Lauritzen and Lundberg, 2000) together with the regional hydraulic gradient (Fig. 12). In other words conduits are developed along the intersection between inception horizons and fractures being the most parallel to the hydraulic gradient.

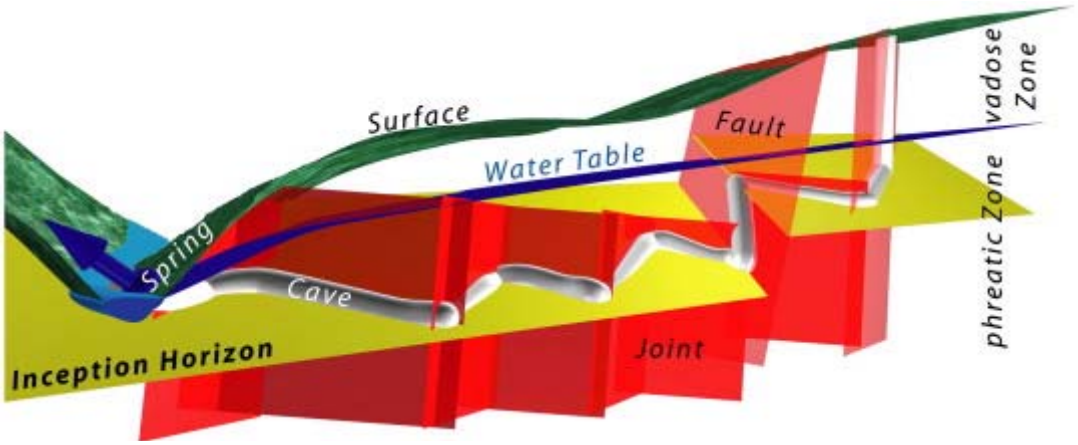

Fig. 12. Schematic 3D model of a karst conduit system: The geometry of phreatic conduits is determined by inception horizons (in most cases related to well-marked bedding planes), joints and faults as well as by the hydraulic gradient.

In some cases cave inception occurs also along fractures that are unrelated to inception horizons. The cave inception along these fractures can be induced by "tectonic inception" (tectonics producing a fracture network wide enough to allow turbulent flow; Faulkner, 2006) or by "chemical inception" (dissolution of the fracture surface and gradual enlargement of the fracture width; Noiriel, 2005). In our study areas we could regularly observe that where a conduit that followed an inception horizon reached a normal fault, it followed the fault to find the same bedding plane on the other side of the fault or to find another inception horizon (Fig. 12). However inception links become dominant when no clear inception horizons are available or if sedimentation structures have been obliterated by metamorphism as for example in marbles.

Bosák (2002) noticed that it is not easy to determine the beginning of the karst evolution: "The beginning and the end of the life of living organisms are really clear and can thus be precisely determined and described. On the other hand, to establish the beginning and the end of the life of a karst system is a substantial problem. The dating of karst evolution poses philosophical problems." However for our approach we can assume that the end of the diagenesis and the beginning of the karstification occur when the rock permeability starts to increase due to dissolution (Fig. 13).

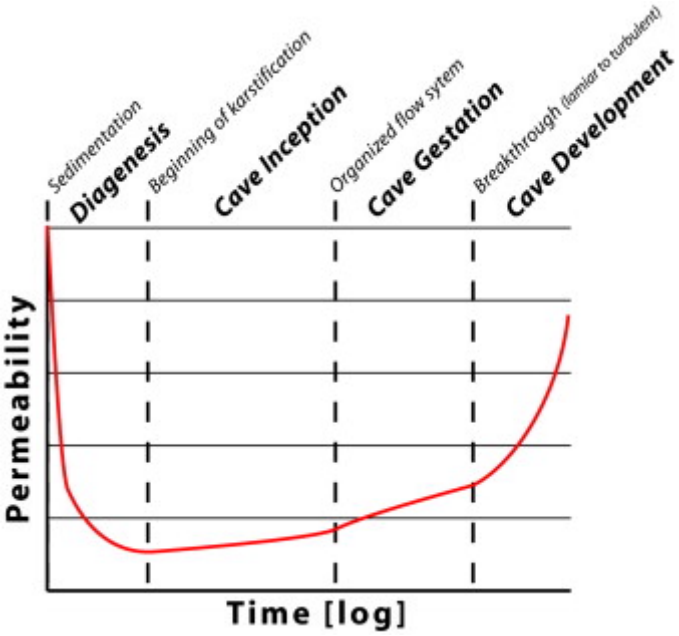

Fig. 13. Schematic evolution of the permeability of a karstic rock mass from the sedimentation to present: The beginning of the karstification can be defined by the moment from which the permeability of the rock mass increases steadily.

One may expect that at the early stage the evolution of small dissolution voids is diffuse and the influence of the hydraulic gradient is restricted. At the same time, hydraulic gradients, which are not steep (margin environment) may change several times. Therefore the diffuse net of proto-conduits is not clearly controlled by any particular hydraulic gradient. Furthermore we can presume that under these conditions the karstification (increasing of the permeability over the whole limestone thickness where the most significant effects in the form of flow paths are concentrated along the inception horizons) prepares the later development of the karst conduits. This may also explain why some karst occurrences can be found in boreholes thousands of metres below sea level (e.g. Lucia, 1999). The very early inception voids should be very tiny and their evolution rather slow; it probably takes some hundreds of thousands to millions of years (Lowe, 1992). It starts during or shortly after the diagenesis of the rock mass and ends when the conditions capable of driving and supporting organized laminar flow are established. This marks the start of the "gestation" phase of cave development (Lowe, 1992). During gestation the relief becomes steeper, higher gradients do occur, that could enhance the development of some preferential flow directions (in most cases) along the inception horizons which have been "prepared" during cave inception. The well known anastomoses are a phenomenon of this phase (Fig. 10). The cave gestation ends at the time a "victor tube" is large enough compared to the others to drain the rock mass efficiently and develops much faster than the other tubes (breakthrough) (White, 1988, Dreybrodt and Gabrovšek, 2000, Kaufmann, 2002, Palmer, 2003 and Dreybrodt et al., 2005).

However it must be pointed out, that this classification of "karstification state" is not applicable to "complex" karst systems synchronously. In fact in most cases different karstification states occur at the same time for a given karst system (Fig. 14).

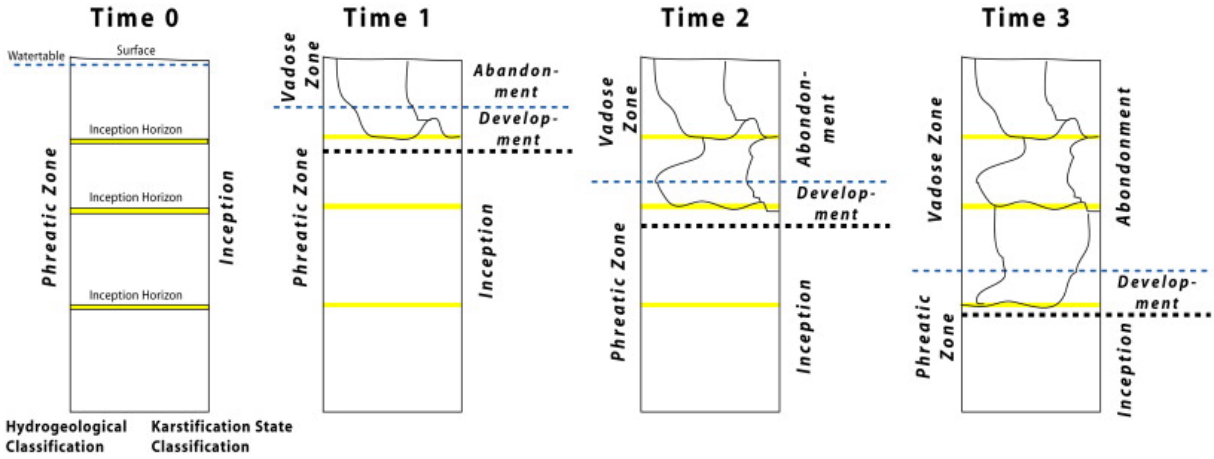

Fig. 14. Schematic development of a karst system in time and space (vertical section): Different parts of the system are in a different karstification state at the same time. *During cave inception the karstification takes place over the full thickness of the limestone, whereas its most significant effects in the form of flow paths are concentrated along the inception horizons. Karstification state of the cave gestation located between the inception and development phase is not represented in this diagram.*

There have been various suggestions concerning why some parts of the rock succession act as inception horizons but, as yet, little analytical confirmation evidence has been presented (e.g. Lowe, 1992, Knez, 1997 and Filipponi and Jeannin, 2006). Is it probably related to some specific properties of the rock mass, which are being investigated as a next step of our research project? A first point that can be stated is that at a given time during early karst development some horizons have a higher hydraulic conductivity than others and are in a favourable situation for allowing conduits to develop. If for any reason there is another pathway which is more favourable than an existing inception horizon (e.g. along a network of fractures) the cave development will not follow this horizon. We have seen in Section 2.4.2 that also in the scale of a single cave system it was not possible to identify the same number of inception horizons in all areas. Therefore it is not advisable to blindly extrapolate the results of the inception horizon analysis from one site to a neighbouring site. But any analysis of the geometry of a karst system should always include the geological as well as the hydrogeological history of the area. This should not only be done for a back-analysis but also for the prediction of the geometry and position of conduits.

The presented methodology is able to detect inception horizons and allows the detection of inception horizons which have been favourable not only at the beginning of the karstification of the rock mass but also later when some only slightly opened flow path evolved to form cave conduits. In this analysis the unavoidable bias remains that the minimum size for a karst conduit is around 0.01 m, while the minimum size for direct exploration (cave) is about 0.5 m (White, 2002). One suspects that there is a very large component of conduits with a site scale in

the range between 0.01 and 0.5 m about which we know almost nothing. Unfortunately we have not been able to include these inexplorable karst conduits in our analysis so far. This is also the reason why the size of the peaks in the histograms in Section 2.4.2 does not say anything about the relative importance of the respective inception horizons, but gives only the binary answer "yes/no: there is (is not) an inception horizon".

One must not forget that inception can also appear during the karst development. For instance, a shear displacement along a bedding plane during a phase of tectonic activity would very probably induce a significant increase in the permeability of this surface and will probably become an inception horizon. Several horizons observed in the field did display such bed to bed shear displacement (e.g. Knez, 1998 and Filipponi and Jeannin, 2006).

The evidence for inception horizon will also have consequences for the numerical modelling of the evolution of karst systems (e.g. Gabrovšek and Dreybrodt, 2001 and Kaufmann, 2002). Up to now these models use mainly two dimensional networks of initial pathways, for instance a network of fractures enclosed within a rock matrix. The existence of inception horizons will now also justify introducing inception horizons (i.e. bedding planes) into these models, i.e. considering three dimensional networks on initial pathways. It will also be necessary to understand and model the speleogenetical processes along the inception horizons, such as, for example, dissolution processes by sulphuric acid produced by the weathering of pyrite. Furthermore it is essential to identify the key parameters that distinguish inception horizon related bedding planes from the far more numerous normal bedding planes, as well as to understand the speleogenetical role of these parameters. Depending on the results we may be able to simplify the volume (3D) description of initial flow paths.

The identification of the position of inception horizons in a rock mass will provide a substantial increase of information for engineering proposes as well as for karst hydrogeological investigations. For example it will help to have a better idea of the geometry of the flow path of a tracing experiment, because it will be possible to assume that the conduits are preferentially located along a given inception horizon. Also for geophysical investigation methods the understanding of inception horizons will help to interpret the results and help to recognise karst conduits.

We believe that the identification of inception horizons is a good tool not only for predicting karst conduits but also for a better understanding of the speleogenesis.

5. Conclusion

Compared to the commonly used 2D analysis of cave systems (e.g. vertical distribution of conduits for the identification of cave levels or plan view to work out the relationship between cave development and fractures) our 3D analysis allowed us to couple the geological and hydrogeological contexts to the conduit network geometry within a carbonate rock mass. We analyzed more than 1500 km of conduits of some of the most important caves around the World and could show for these cases that more than 70% of the phreatic conduits are located along discrete inception horizons, many of which are bounded by obvious bedding. For the first time we could quantitatively (statistically) show, that the development of karst conduits under phreatic conditions is strongly related to a restricted number of inception horizons. An inception horizon is a part of a rock succession that is particularly susceptible for the development of karst conduits because of physical, lithological or chemical deviation from the predominant carbonate facies within the limestone sequence (Lowe, 1992). It passively or actively favours the concentration of dissolution voids.

Our results indicate that the role of inception horizons is often underestimated and that the position of karst conduits at regional scale is not random at all, but mostly constrained by a limited number of inception horizons or their related bounding surfaces, commonly expressed as prominent bedding planes.

By considering this fact together with the other classical parameters of cave development such as the hydrogeological boundary conditions, rain quantity/quality and the main fracture families, we reached a new step along the prediction of the position of karst conduits in a carbonate massif. The next step will be to understand why some particular bedding planes become inception horizons and others do not. This is the major challenge we are investigating in the next steps of our research.

Acknowledgements

This project is supported by the Swiss National Foundation for Scientific Research (project number 200021-105280).

We thank David Lowe and Stephen Worthington for their constructive comments on the manuscript. Special thanks are due to cavers who explored and mapped the cave systems and provided us with the survey data for our analysis. Alex and Florian Hof spent a lot of time discussing and guiding us through the Siebenhengste Cave System.

References

Bakalowicz M., 2005: Karst groundwater: a challenge for new resources, Hydrogeological Journal 13, pp. 148–160.

Benson R.C., Yuhr L., 1993: Spatial sampling considerations and their applications to characterizing fractured rock and karst systems, Environmental Geology 22, pp. 296–307.

Bitterli T., Jeannin P.-Y., 1997: Entwicklungsgeschichte der Höhlen im Gebiet Hohgant–Sieben Hengste–Thunersee (Berner Oberland, Schweiz), Proceedings of the 12th Int. Congress of Speleology vol. 1, pp. 349–354.

Blanc J.-J., Nicod J., 1990: Les surface karstiques du plateau de Montrieux (Var), (secteur de Valbelle–Morières–Siou Blanc), étude quantitative de la fracturation, Karstologia 16, pp. 17–28.

Bögli A., 1980: Karst Hydrology and Physical Speleology, Springer, Berlin.

Bosák P., 2002: Karst process from the beginning to the end: How can they be dated?. In: F. Gabrovšek, Editor, Evolution of Karst: from prekarst to cessation, Zalozba ZRC, Postojna–Ljubliana, pp. 155–190.

Casagrande G., Cucchi F., Zini L., 2005: Hazard connected to railway tunnel construction in karstic area: applied geomorphological and hydrogeological surveys, Natural Hazards and Earth System Sciences 5, pp. 243–250.

Davies W.E., 1960: Davies, Origin of caves in folded limestone, Bulletin of the National Speleological Society 22, pp. 3–18.

Day M.J., 2004: Karstic problems in the construction of Milwaukees Deep Tunnels, Environmental Geology 45, pp. 859–863.

Dreybrodt W., Gabrovšek F., 2000: Dynamics of the evolution of single karst conduits. In: A.B. Klimchouk, D.C. Ford, A.N. Palmer and W. Dreybrodt, Editors, Speleogenesis, evolution of karst aquifers, National Speleological Society, Huntsville (Alabama), pp. 184–193.

Dreybrodt W., Siemers J., 2000: Cave evolution on two-dimensional networks of primary fractures in limestone. In: A.B. Klimchouk, D.C. Ford, A.N. Palmer and W. Dreybrodt, Editors, Speleogenesis, evolution of karst aquifers, National Speleological Society, Huntsville (Alabama), pp. 201–211.

Dreybrodt W., Gabrovšek F., Romanov D., 2005: Processes of speleogenesis: a modeling approach, ZRC Publishing, Ljubljana.

Eraso A., Herrero N., 1986: Propuesta de un Nuevo metodo de deduccion de las direcciones principales de drenaje en el karst, Jumar, Madrid.

Faulkner T., 2006: Tectonic inception in caledonide marbles, Acta Carsologica 35, pp. 7–21.

Filipponi M., 2007: Speläologische Erscheinungen im Zusammenhang mit stratigraphischen Initialfugen, Laichinger Höhlenfreund 42, pp. 21–32.

Filipponi M., Jeannin P.-Y., 2006: Is it possible to predict karstified horizons in tunneling?, Austrian Journal of Earth Sciences 99, pp. 24–30.

Ford T.D., Cullingford C.H.D., 1976: The Science of Speleology, Academic Press, London.

Ford D.C., Williams P., 2007: Karst Hydrogeology and Geomorphology, Wiley, Chichester.

Gabrovšek and Dreybrodt, 2001 F. Gabrovšek and W. Dreybrodt, A model of the early evolution of karst aquifers in limestone in the dimensions of length and depth, Journal of Hydrology 240, pp. 206–224.

Grossenbacher Y., 1992: Höhlenvermessung, Swiss Speleological Society.

Häuselmann P., 2002: Cave genesis and its relationship to surface processes: investigations in the Siebenhengste Region (BE, Switzerland), Höhlenforschung im Gebiet Siebenhengste-Hohgant vol. 6.

Häuselmann P., Jeannin P.-Y., Bitterli T., 1999: Relationships between karst and tectonics: case-study of the cave system North of Lake Thun (Bern, Switzerland), Geodinamica Acta 12, pp. 377–387.

Jamier D., Siméoni G.P., 1979: Etude statistique de la distribution spatiale des éléments structuraux dans deux massifs des Alpes helvétique. Conséquences pour lhydrogéologie karstique, Bulletin du Centre dHydrogéologie Neuchâtel 3, pp. 1–26.

Jeannin P.-Y., 1989: Etude Géologique de la Région Burst–Sieben Hengste–Apports de l'étude des cavernes à la connaissance structurale et à la mise en évidence de phases tectoniques quaternaires. MS Thesis, University of Neuchâtel.

Jeannin P.-Y., 1996: Structure et comportement hydraulique des aquifères karstiques. PhD Thesis, Université de Neuchâtel, Speleo–Projects publishers. Basel.

Jeannin P.-Y., Bitterli T., Häuslemann P., 2000: Genesis of a large cave system: the case study of the North of Lake Thun system (Canton Bern, Switzerland). In: A.B. Klimchouk, D.C. Ford, A.N. Palmer and W. Dreybrodt, Editors, Speleogenesis, evolution of karst aquifers, National Speleological Society, Huntsville (Alabama), pp. 338–347.

Kaufmann G., 2002: Karst aquifer evolution in a changing watertable environment, Water Resources Research 38, pp. 261–269.

Kiraly L., 1968: Eléments structuraux et alignement des phénomènes karstiques (région du gouffre du Petit-Pré de St-Livres, Jura vaudois), Bulletin de la Société des Sciences Naturelles de Neuchâtel 91, pp. 127–146.

Klimchouk A., 2007: Hypogene Speleogenesis: Hydrogeological and Morphogenetic Perspective, National Cave and Karst Research Institute Special Paper 1.

Klimchouk A., Ford D.C., 2000; Lithologic and structural controls of dissolutional cave development. In: A.B. Klimchouk, D.C. Ford, A.N. Palmer and W. Dreybrodt, Editors, Speleogenesis, evolution of karst aquifers, National Speleological Society, Huntsville (Alabama), pp. 54–64.

Knez M., 1997: Speleogenesis of phreatic channels in bedding-planes in the frame of karst aquifer (Skocjanske Jame Caves, Slovenia), Proceedings of the 12th Int. Congress of Speleology vol. 2, pp. 279–282.

Knez M., 1998: The influence of bedding-planes on the development of karst caves (a study of Velika Dolina at Škocjanske Jame, Slovenia), Carbonates and Evaporites 13, pp. 121–131.

Lauritzen S.-E., Lundberg J., 2000: Solution and erosional morphology. In: A.B. Klimchouk, D.C. Ford, A.N. Palmer and W. Dreybrodt, Editors, Speleogenesis, evolution of karst aquifers, National Speleological Society, Huntsville (Alabama), pp. 408–426.

Lindner A.F., 1841: Corso sotterraneo del fiume Recca, suo ritrovamento presso Trieste e progetto di trarne un canale a beneficio della città, Giornale del Istituto di Scienze Lettere e Arti e Biblioteca Italiana, pp. 116–121.

Lolcama J.L., Cohen H.A.,. Tonkin M.J, 2002: Deep karst conduits, flooding, and sinkholes: lessons for the aggregates industry, Engineering Geology 65, pp. 151–157.

Lowe, D., 1992: The origin of limestone caverns: an inception horizon hypothesis. PhD Thesis, Manchester Polytechnic, United Kingdom.

Lowe D., 1999: Why and how are caves organized: does the past offer a key to the present? Acta Carsologica 28, pp. 121–144.

Lowe D., 2000: Role of stratigraphic elements in speleogenesis: the speleoinception concept. In: A.B. Klimchouk, D.C. Ford, A.N. Palmer and W. Dreybrodt, Editors, Speleogenesis, evolution of karst aquifers, National Speleological Society, Huntsville (Alabama), pp. 65–76.

Lucia F.J., 1999: Carbonate Reservoir Characterization, Springer, Berlin.

Marinos P.G., 2001: Tunnelling and mining in karstic terrain: an engineering challenge. In: B.F. Beck and J.G. Herring, Editors, Geotechnical and Environmental Applications of Karst Geology and Hydrology, Swets & Zeitlinger, Lisse, pp. 3–16.

Noiriel, C., 2005: Contribution à la determination expérimentale et à la modélisation des différents processus contrôlant l'évolution géochimique, structurale et hydrodynamique des roches fissures carbonatées. PhD Thesis, École des Mines de Paris.

Osborne R.A.L., 1999: The inception horizon hypothesis in vertical to steeply dipping limestone: applications in New South Wales, Australia, Cave and Karst Science 26, pp. 5–12.

Osborne R.A.L., 2001: Halls and Narrows: network caves in dipping limestone examples from eastern Australia, Cave and Karst Science 28, pp. 3–14.

Palmer A.N., 1974: Geologic influence on cave passage orientation in Ludington cave, Greenbarrier County, West Virginia, Proc. Of the West Virginia 4th Conference on Karst Geology and Hydrology, West Virginia Geol. Survey, pp. 33–40.

Palmer A.N., 1975: The origin of maze caves, National Speleological Society Bulletin 37, pp. 56–76.

Palmer A.N., 1987: Cave levels and their interpretation, National Speleological Society Bulletin 49, pp. 50–66.

Palmer A.N., 1989:Stratigraphic and structural control of cave development and groundwater flow in the Mammoth Cave region. In: W.B. White and E.L. White, Editors, Karst Hydrology, Concepts from the Mammoth Cave Area, Von Nostrand Reinhold, New York, pp. 293–316.

Palmer A.N., 2000: Hydrogeologic control of cave patterns. In: A.B. Klimchouk, D.C. Ford, A.N. Palmer and W. Dreybrodt, Editors, Speleogenesis, evolution of karst aquifers, National Speleological Society, Huntsville (Alabama), pp. 77–90.

Palmer A.N., 2003: Speleogenesis in carbonate rocks. In: F. Gabrovšek, Editor, Evolution of karst: from prekarst to cessation, ZRC Publishing, Ljubljana, pp. 43–60.

Pöttler R., 2004: Beherrschung der Karst- und Erdfallproblematik im Tunnelbau. Institut für Geotechnik der Technischen Universität Bergakademie Freiberg, Freiberg.

Quinlan J.F., Ray J.A., 1981: Groundwater basins in the Mammoth Cave region, Kentucky field trip guidebook 3: Falls Church. In: T.G. Roberts, Editor, GSA Cincinnati, American Geological Institute, Virginia, pp. 457–506.

Rauch H.W., White W.B., 1970: Lithologic controls on the development of solution porosity in carbonate aquifers, Water Resources Research 6, pp. 1175–1192.

Rauch H.W., Werner E., 1974: Geological influence upon cave-passages orientation in Ludingron Cave, Greenribrier Country, West Virginia, Proceedings of the 4th Conference on Karst Geology and Hydrology, West Virginia Geological and Economic Survey, pp. 33–40.

Shofner A.G., Mills H.H., Duke J.E., 2001: A simple map index of karstification and its relationship to sinkhole and cave distribution in Tennessee, Journal of Cave and Karst Studies 63, pp. 67–75.

Slabe T., 1995: Cave rocky relief and its speleogenetical significance, Znanstvenoraziskovalni Center Sazu, Ljubljana.

Veni G., 1999: A geomorphological strategy for conducting environmental impact assessments in karst areas, Geomorphology 31, pp. 151–180.

Waltham A.C., 1971: Controlling factors in the development of caves, Transactions of the Cave Research Group of Great Britain 13, pp. 73–80.

Waltham A.C., Fookes P.G., 2003: Engineering classification of karst ground conditions, Quarterly Journal of Engineering Geology and Hydrology 36, pp. 101–118.

White W.B., 1988: Geomorphology and Hydrology of Karst Terrains, Oxford University Press, New York.

White W.B., 2002: Karst hydrology: recent developments and open questions, Engineering Geology 65 , pp. 85–105.

Xeidakis G.S., Torok A., Skias S., Kleb B., 2004: Engineering geological problems associated with karst terrains: their investigation monitoring, and mitigation and design of engineering structures on karst terrains, Bulletin of the Geological Society of Greece 36, pp. 1932–1941.

Zhang Q., Tian S., Mo Y., Dong X., HaoS., 1993: An expert system for prediction of karst disaster in excavation of tunnels or underground structures through a carbonate rock area, Tunnelling and Underground space Technology 8, pp. 373–378.

Ziegler M.A., 1967: A study of the lower Cretaceous facies developments in the Helvetic Border Chain, North of Lake Thun (Switzerland), Eclogae Geologicae Helveticae 60, pp. 509–527.

Plan L., Filipponi M., Behm M., Seebacher R., Jeutter P., 2009:
Constraints on alpine speleogenesis from cave morphology — A case study from the eastern Totes Gebirge (Northern Calcareous Alps, Austria).
Geomorphology 106, 118-129.
doi:10.1016/j.geomorph.2008.09.011

Constraints on alpine speleogenesis from cave morphology - A case study from the eastern Totes Gebirge (Northern Calcareous Alps, Austria)

Lukas Plan[1], Marco Filipponi[2], Michael Behm[3], Robert Seebacher[4] and Peter Jeutter[4]

[1]Department of Geodynamics and Sedimentology, University of Vienna, Althanstrasse 14, 2A-344, A-1090 Vienna, Austria

[2]Laboratoire de géologie de l'ingénieur et de l'environnement, Ecole Polytechnique Fédérale de Lausanne, EPFL ENAC ICARE GEOLEP, Station 18, CH-1015 Lausanne, Switzerland

[3]Institute of Geodesy and Geophysics, Vienna University of Technology, Gusshausstr. 27-29/1282, A-1040 Vienna, Austria

[4]Verein für Höhlenkunde in Obersteier (Speleologic Society of Upper Styria), A-8983 Bad Mitterndorf, Austria

Received 13 August 2007; revised 27 June 2008; accepted 18 September 2008.

Abstract

The Totes Gebirge is the largest karst massif in the Northern Calcareous Alps (NCA). This paper focuses on the eastern part, where two major multiphase alpine cave systems (Burgunderschacht Cave System and DÖF–Sonnenleiter Cave System) are described with respect to morphology, hydrology, and sediments. The caves consist of Upper Miocene galleries of (epi)phreatic genesis and younger vadose canyon-shaft systems. Morphometrical analyses were used to determine the relevance of (1) cave levels (horizontal accumulations of galleries), (2) slightly inclined palaeo water tables of speleogenetic phases, (3) initial fissures, and (4) inception horizons on the development of the cave systems. (Epi)phreatic cave conduits developed preferentially along vertical faults and along only a restricted number of bedding planes, which conforms to the inception horizon hypothesis. For at least one of the systems, a development under epiphreatic conditions is certain and a hydrological behaviour in the "filling overflow manner" is likely.

Observations in further major cave systems in the Totes Gebirge identify palaeo water tables of speleogenetic phases that show inclinations of 1.5° ± 1°. Analyses of cave levels reveal distinct peaks for each cave but it is hardly possible to correlate these elevation levels between caves of different parts of the karst massif. Therefore, we conclude that cave levels (strictly horizontal) indicate speleogenetic phases or palaeo water tables respectively, but they cannot be correlated with palaeo base levels or on regional scale. An exact correlation between cave development and palaeo base levels at the surface is only possible with inclined palaeo water tables of speleogenetic phases.

For the Totes Gebirge, the inclination directions of the speleogenetic phases imply that palaeo drainage was radial and recharge was autogenic, which is in contrast to observations from other plateaus in the NCA. Differences in fracture properties seem to be the reason for the development of divergent types, according to the Four State Model. A simplified model for cave genesis and surface development in this area since the Upper Miocene is presented.

Keywords: Alpine karst; Cave genesis; Multiphase cave; Cave level; Inception horizon; Morphometrical analyses

1. Introduction

The study of solutional cave systems provides many insights into the evolution of karst massifs and the surrounding landscape (e.g. Kuffner, 1998, Klimchouk and Ford, 2000, Frisch et al., 2002, Audra et al., 2006 and Häuselmann et al., 2007). A frequently used link between subsurface karstification and surface morphology is the concept of "cave levels". In 1909, Sawicki noticed that cave passages concentrate at certain altitudes and introduced the term evolution level ("Evolutionsniveau"; Sawicki, 1909). However, cave levels and their correlation with base levels were highly controversial for a long time. A review of the topic was given by Bögli (1980). Today, however, it is widely accepted that the concentration of solutional cave conduits at certain elevations can be used to study cave genesis in relation to landscape evolution, as fluvial base levels control subsurface cave development (Palmer, 1987). The case study presented here focuses on the largest karst massif in the Eastern Alps of Austria. In the Totes Gebirge area (Fig. 1), several cave levels were already identified in the middle of the last century (Lechner, 1949 and Schauberger, 1956). Later works by (Haseke-Knapczyk, 1989) and (Fischer, 1990) distinguish three major, distinctive levels in the central Northern Calcareous Alps (NCA) that share similar morphological characteristics. Each of them comprises a few hundred metres of altitude, although the absolute elevations differ between the massifs. These were incorporated into a speleogenetic model for the Tennengebirge (Fig. 1) by Audra et al. (2002). The latest comprehensive work was performed by Frisch et al. (2002) who utilise geological correlations, including morphology, tectonics and sedimentology, to specify the ages of the formation of the three levels. The highest, the Ruin Cave Level (~ 2200 ± 300 m a.s.l.) developed between the middle Eocene and Early Oligocene, the Giant Cave Level (~ 1600 ± 500 m) in the Upper Miocene, after the onset of the major uplift of the NCA, and the low lying and often hydrologically active Spring Cave Level (~ 800 ± 300 m) in the Pliocene and Quaternary.

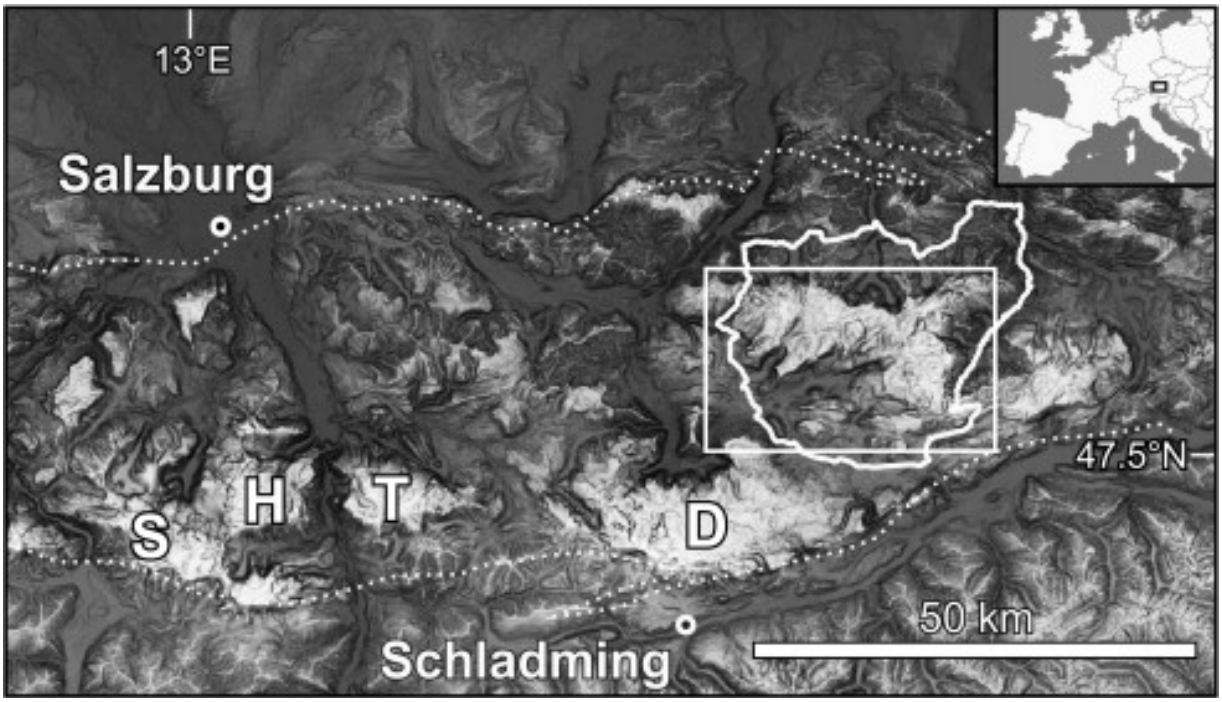

Fig. 1. The Totes Gebirge (white polygon: outline; white rectangle: site of Fig. 2) is located within the central NCA. Greyscale of the background map depicts elevation and slope gradient highlighting elevated plateaus (data base: SRTM); the dotted lines delimit the NCA; other karst massifs: S — Steinernes Meer, H — Hagengebirge, T — Tennengebirge, D — Dachstein. Inlet shows the location within Central and Western Europe.

Here, we focus on two major multiphase (Ford, 2000) cave systems in the eastern Totes Gebirge. Apart from field observations, statistical analyses are used to investigate tectonic fissures as well as inception horizons (Lowe, 1992). Further, horizontal cave levels and slightly inclined water tables of speleogenetic phases are determined; it turns out that a strict differentiation of these phenomena is crucial for the interpretation and correlation with base levels. The paper demonstrates how morphological observations and morphometrical analyses can be used as constraints for models of speleogenesis and subsequent implications for landscape evolution. Further, our analyses provide data that support the inception horizon hypothesis (Lowe, 1992). On a regional scale, we address in particular the question of drainage conditions in terms of allogenic recharge with a sinking river in the south, subsurface flow and reappearance in the north versus autogenic recharge and radial drainage of the karst

massif. Finally, a simplified model for the evolution of cave systems of the Eastern Totes Gebirge since the Upper Miocene is presented.

In this paper, the following definitions are used, distinguishing between four types of planar features which are important for cave evolution: (1) Initial fissures (bedding planes, joints, and faults) are principal structural controls that enable subsurface karstification (e.g. Klimchouk and Ford, 2000); (2) Inception horizons (Lowe, 1992 and Lowe, 2000) are a limited number of stratigraphic horizons or bedding planes that favour cave evolution. Recently, statistical analyses (Filipponi and Jeannin, 2006 and Filipponi et al., 2008-this issue) found strong evidence to support the concept of inception horizons; (3) Cave levels, which we define as accumulation of phreatic galleries at strictly horizontal levels and have been described in many caves (e.g. Palmer, 1987); (4).

The palaeo water table of a speleogenetic phase is a slightly inclined plane that reflects the position of the top of the corresponding genetic phase. In turn, a speleogenetic phase, which is a temporal state, is defined by its springs and the height of the epiphreatic zone (Häuselmann et al., 2003). The minimum height is derived from the connection of the crests of phreatic loops of the corresponding galleries. In contrast, the floodwater table is inferred from canyon-tube-transitions. We avoid the terms tier and storey which have neither a geometric nor a genetic meaning.

There is an ongoing discussion if mature galleries actually form under phreatic (sensu stricto) or epiphreatic conditions (Audra, 1994, Häuselmann et al., 2003 and Ford and Williams, 2007). Since this difference does not affect our study, we use phreatic where the origin is unclear and epiphreatic only if there is clear morphological evidence for such a genesis.

2. Study area

2.1. Geography

The Totes Gebirge (Dead Mountains) karst massif is located on the border between the Austrian provinces of Styria in the south and Upper Austria in the north. The whole mountain range, as defined in Stummer and Plan (2002), covers an area of 642 km2 and is the largest karst massif in the NCA (Fig. 1). The stepped plateau reaches from an altitude of about 1500 m up to the summit (Priel) at 2515 m a.s.l. The massif is surrounded by deeply incised valleys at 400 to 850 m a.s.l. except in the southeast where a saddle separates it from the Warscheneck massif (Fig. 2). Our study focuses mainly on the south-eastern part of the plateau (Fig. 2 and Fig. 5).

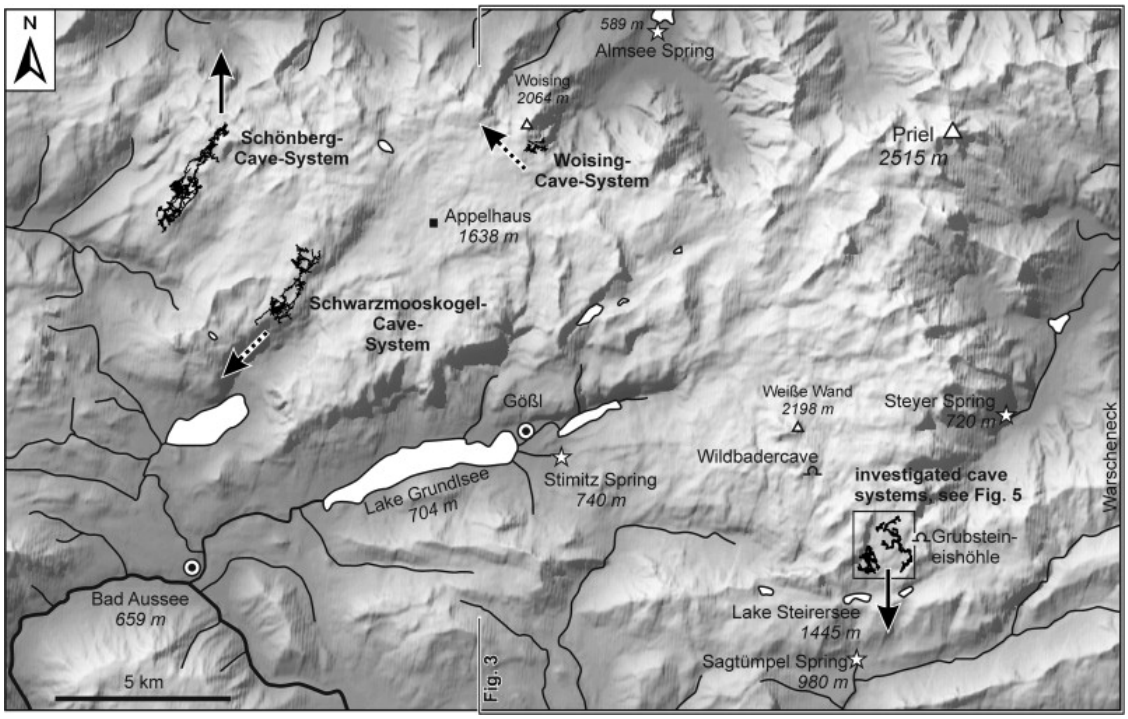

Fig. 2. Shaded digital elevation model of the Totes Gebirge including cave systems, springs, lakes (white areas). Location of the geological overview (Fig. 3) and the study area (Fig. 5) are marked by rectangles. Arrows indicate the dip direction of identified water tables of speleogenetic phases interpreted as palaeo-flow directions (cf. Section 4.5 and 4.6; dotted arrows are uncertain).

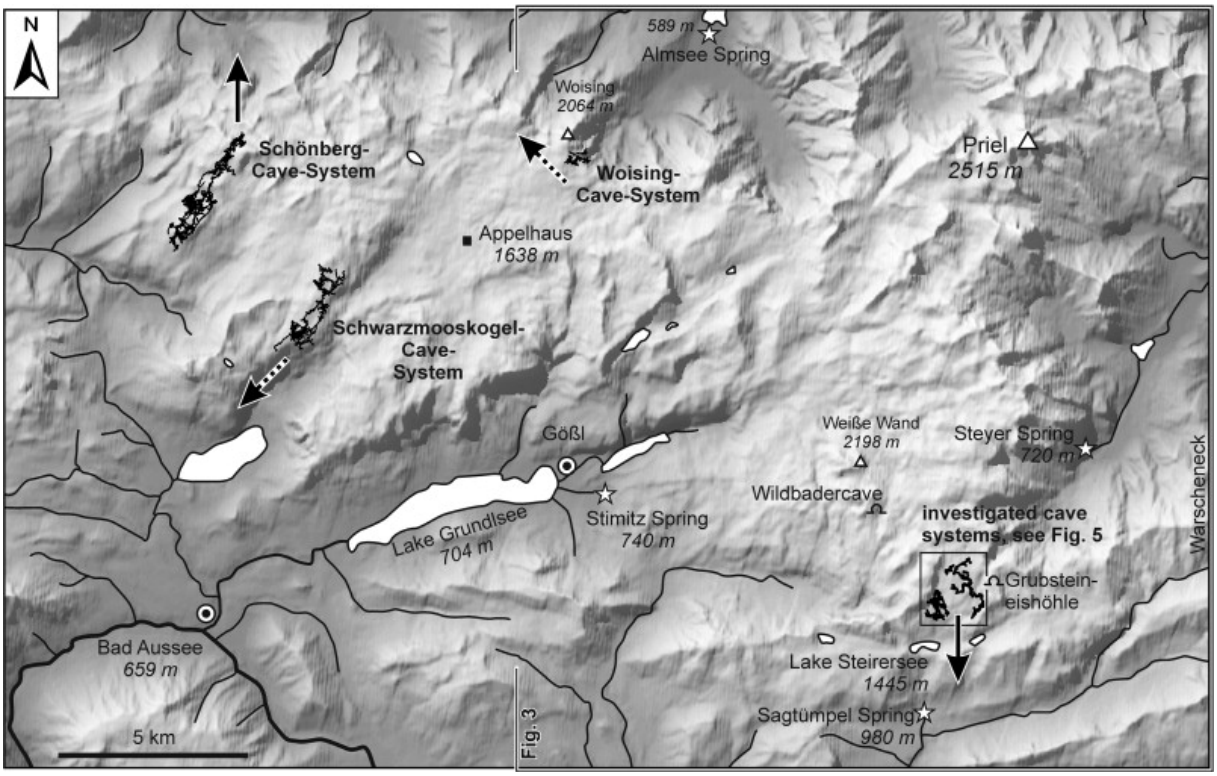

Fig. 5. Plan view of the studied cave systems and dip of the limestone. Arrows point at entrances; stars indicate low lying sumps.

The alpine climate is chilly, with average temperatures around + 7 ° C for the valleys and slightly below zero in the summit regions (Kuffner, 1998). Precipitation is in the order of 1200 mm/a in the valleys and 2500 mm/a in the elevated parts (Baumgartner et al., 1983). On the plateau, snow cover persists for more than 200 days per year.

2.2. Geology

The study area belongs to the Totengebirgs Nappe, which is a part of the Tirolic unit of the NCA. The lithostratigraphy within this area is very homogenous, comprising almost entirely of Upper Triassic limestones of the Dachstein Formation (Fig. 3) in lagoonal facies that are well bedded in the order of few metres. According to Fischer (1964), an ideal bed consists of three layers: a few centimetres of greenish or reddish claystone, a few decimetres of intratidal dolomite, and finally a massive bed of micritic, very pure and fossil-rich limestone. Normally the lowest layer is absent or slickensides indicate tectonic movement along it. Although the Dachstein Formation has a sedimentary thickness of more than 1 km, this value can be significantly exceeded due to internal thrusting. In the area of investigation, the strata dip at 15 to 45° to the southeast. Unlike other parts of the Totes Gebirge, where Jurassic sediments (karstic and non karstic) cover significant areas, only Liassic limestone of the Hirlatz Formation has been preserved as unextended vein fillings (neptunian dikes) in the southeastern part.

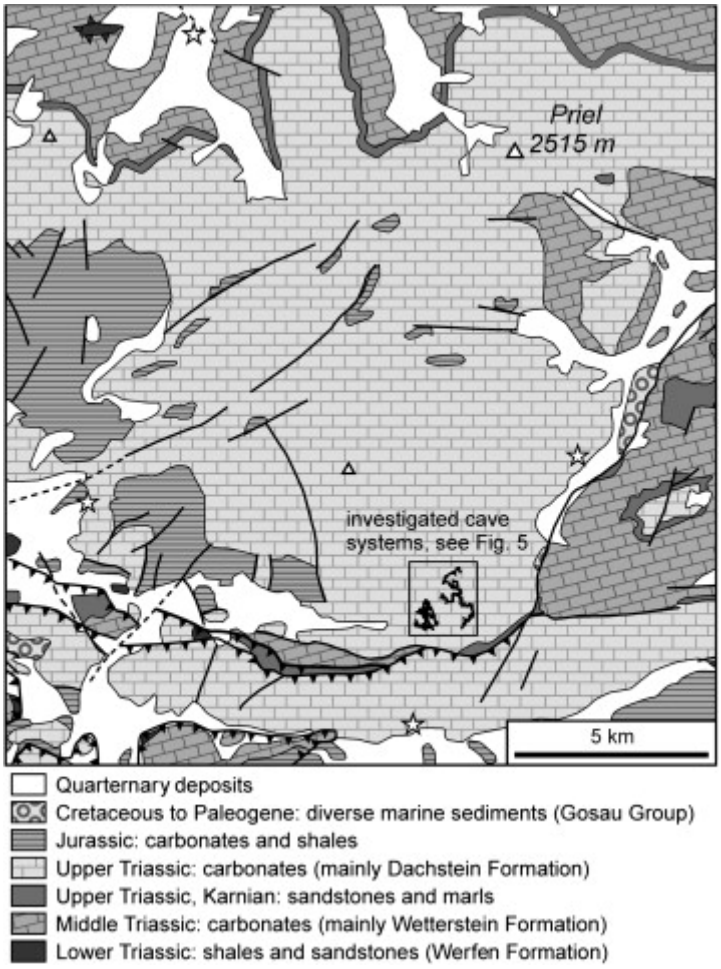

Fig. 3. Simplified geological map (modified after Krenmayr & Schnabel, 2006). For locations and names, see Fig. 2; Stars indicate mentioned springs.

Directly south of the study area, the Totengebirgs Nappe is delimited by the Warscheneck Nappe. Close to the thrust zone, Upper Triassic non-karstic rocks of the Karnian Stage crop out and lead to the development of small lakes (Fig. 2 and Fig. 3, e.g. Steirersee, 1445 m a.s.l.).

The deformation history in the NCA comprises at least five phases of tectonic activity, spanning from the Cretaceous to the present (Linzer et al., 1995). Each period was characterised by a different set of normal, strike–slip and/or thrust faults that have resulted in a complex fault pattern.

In the Oligocene and early Miocene, fluviatile siliciclastic sediments of the Augenstein Formation were deposited over an Eocene hilly palaeo-karst landscape, ("Dachstein Palaeosurface", Frisch et al., 2000 and Frisch et al., 2002). These sediments, possibly up to more than 1 km thick, were removed in the Middle Miocene and only small accumulations of redeposited pebbles ("Augensteine") are found on the plateau today. However, weathering products of the Augenstein Formation are the main source for the clays that are common in the caves. Overall, the relatively simple and homogenous geological settings, favour studies on speleogenesis and the role of planar features in particular.

During the Pleistocene glacial periods, the Totes Gebirge was part of the extensive Alpine ice stream network for at least the latest four major glaciations (Van Husen, 2000). The valleys were filled with up to 1 km thick ice and the glaciers extended up to 50 km to the north and much further to the south. Therefore, the settings can be classified as a "Canadian Type" of alpine karst (in contrast to the Pyrenean Type; Ford and Williams, 2007), in which both the input areas and the springs were occupied by glaciers during cold stages. On the plateau, glacial erosion stripped most of the area and developed staircase pavements (Schichttreppenkarst according to Bögli, 1980; Fig. 4) in the well-bedded Dachstein limestone.

Fig. 4. View over the eastern Totes Gebirge, where Schichttreppenkarst dominates the landscape.

2.3. Karst morphology and hydrology

The impressive karst landscape is characterised by extensive karren fields and truncated shafts that are mainly filled with debris. Only a few elevated areas stood above the massive ice, as nunataks, or just carried ice shields so that large, probably pre-Pleistocene dolines have been preserved. To date, about 1500 caves are registered and explored in the Totes Gebirge, but many areas are still unexplored.

The investigated area is highly karstified and drainage is entirely subsurface. Karst hydrology was studied by several authors, but the results of the tracer experiments by means of Lycopodium spores (Maurin and Zötl, 1964 and Dincer et al., 1972) are not very reliable. Possible discharge areas of the investigated caves are the Steyer Springs in the east (720 m a.s.l.) or the Stimitz Springs in the west (740 m) which both show mean discharges in the order of several hundred litres per second, high discharge variations, and total dissolved carbonates between 75 and 90 mg/l (Zötl, 1961). Drainage to the north (e.g. Almsee 590 m) is unlikely, as aquitard strata (marls and sandstones of the Karnian stage) would have to be crossed. Drainage to the south is impossible as the spring (Sagtümpel spring ~ 980 m) lies higher than the deepest sump of the caves, at 904 ± 10 m.

3. Characterisation of the cave systems

We present observations and data from two cave systems (Fig. 5) with a total length of 42.3 km: the Burgunderschacht Cave System (in the following BUC) and the DÖF–Sonnenleiter Cave System (DÖC). At present, there is neither proof that they were part of a single hydrologic system nor that they were hydrologically separated, although obvious morphological differences suggest analysing them separately. Both cave systems consist of two caves, but the adjacency and morphology of the caves suggest strongly that in each case the two individual caves once formed one cave system. Apart from the host-rock, which is limestone of the Dachstein Formation in lagoonal facies, both cave systems share further similar characteristics which are described in the following sections.

3.1. Common features of BUC and DÖC

3.1.1. Morphology

Most striking is the clear division into vadose shafts and epiphreatic, horizontal galleries. The shafts, of various depths (several meters to 191 m) and often 5 to 10 m or more in diameter, are bound to vertical faults. They are connected by partly narrow meanders that are generally less than few tens of metres long. Most of the meanders lack a phreatic profile on the top. Therefore, they are interpreted as invasion vadose canyons (Ford and Williams, 2007). With depth, the width of the meanders increases.

Most of the sub-horizontal galleries or mazes of phreatic origin are restricted to a small number of altitudinal levels. Their position, many hundred of metres above the present base-level, suggests an old age. The intersection of the shafts with the horizontal galleries seems incidental in almost all cases, except for using the same initial fault. Sometimes, the active vadose systems use the pre-existing phreatic galleries, where keyhole profiles with narrow entrenchments developed, but after a short distance, the vertical path is continued.

Scallops, that allow the palaeoflow direction to be determined, are missing in the phreatic galleries, but paragenetic features are widespread (see Section 3.1.3).

3.1.2. Hydrology

Nearly all cave entrances represent shafts that were truncated by glacial erosion. Therefore, they are not related to the present-day hydrological conditions. Nevertheless, many of the shafts and canyons are fed by streams from micro meanders that enter the vertical system when already some tens of metres below the surface. This behaviour is interpreted as drainage out of a postglacial epikarst. Only one side entrance of the BUC is related to the present hydrological conditions; this directly leads into a narrow canyon of probably postglacial age that is fed by a minor (~ 0.1–10 l/s) surface spring. After some tens of meters, this narrow meander cuts into a pre-existing series of major shafts.

Many of the vadose pits and interconnecting canyons are hydrologically active. As the surface above the caves mainly consists of bare karren fields, response to hydrological events is very rapid. During storm events, rapidly dripping water can turn into waterfalls with flow rates of several tens of litres per second. Generally, the streams unite at depth. In the lower parts of the caves, streams have minimum discharges of few litres per second in winter. Direct observations of the maximum discharge of these low lying streams are not possible, but it is estimated to be in the order of several tens or hundred of litres per second.

The karst water table is at least 1 km below the surface. Until now, only two low lying sumps were reached, but even for the lower one, at 904 m a.s.l., it is not sure if it represents the karst water table since it lies ~ 200 m above the springs that probably drain the area.

3.1.3. Sediments

Three main types of clastic sediments are present in the cave systems: (1) Autochthonous breakdown material is found in several parts of the caves, predominantly where frequent frost wedging occurs. (2) Glacial debris is found at the surface, in particular in depressions, and it completely fills most of the shafts that could represent potential additional entrances. It is a coarse, sub-rounded, and poorly sorted sediment consisting almost entirely of limestone clasts. In the caves, this sediment includes boulders up to 50 cm in diameter and it blocks many shafts and some horizontal passages. It can be observed down to depths of − 300 m but is more frequent at shallower depths. Herrmann (1993, pp. 19–21) presents a simplified model for the small-scale reshaping of the postglacial surface and the transport and redeposition of glacial debris. (3) Fine grained sediments, mainly silts with a high proportion of calcite, are found in most hydrologically inactive parts down to the deepest explored sections. Many horizontal parts were previously completely filled with sediments and many galleries are still blocked. Sediment fill led to the development of paragenetic features like ceiling half tubes, ceiling meanders, and bypasses which are very common. In some sediment profiles, a lamination can be observed that could represent varve layering.

Massive, and most probably pre-Quaternary speleothems, which are known from many other elevated caves in the NCA (e.g. Frisch et al., 2002 and Spötl et al., 2007, pp. 157), are missing. Small, apparently young calcite and aragonite dripstones, as well as hydromagnesite aggregates, have developed at several locations.

Permanent snow and ice fillings occur down to a depth of 250 m. As with glacial debris, many additional possible entrances to the cave systems are completely blocked with firn and ice.

3.2. Individual descriptions

3.2.1. Burgunderschacht Cave System (BUC)

Burgunderschacht (No. in Austrian cave cadastre: 1625/20, length: 20.2 km, depth: − 848 m) and Canyonschacht (1625/382, 2.0 km, − 287 m) are treated as one system as only few tens of meters of passages are missing to link them. The system ranges from 1025 to 1873 m a.s.l. Not less than 38 vertical entrances – many of them hosting massive ice and snow fillings – lead into several series of vadose canyon shafts that intersect with horizontal phreatic passages (Fig. 6 and Fig. 7). Some single shafts have depths of about 100 m and the deepest has a 145 m vertical difference. The lowest point of the system is a sump, reached by French cavers in the 1980 s (Perrin et al., 1983), but surveying data for the deepest parts (below 1307 m a.s.l.) are missing.

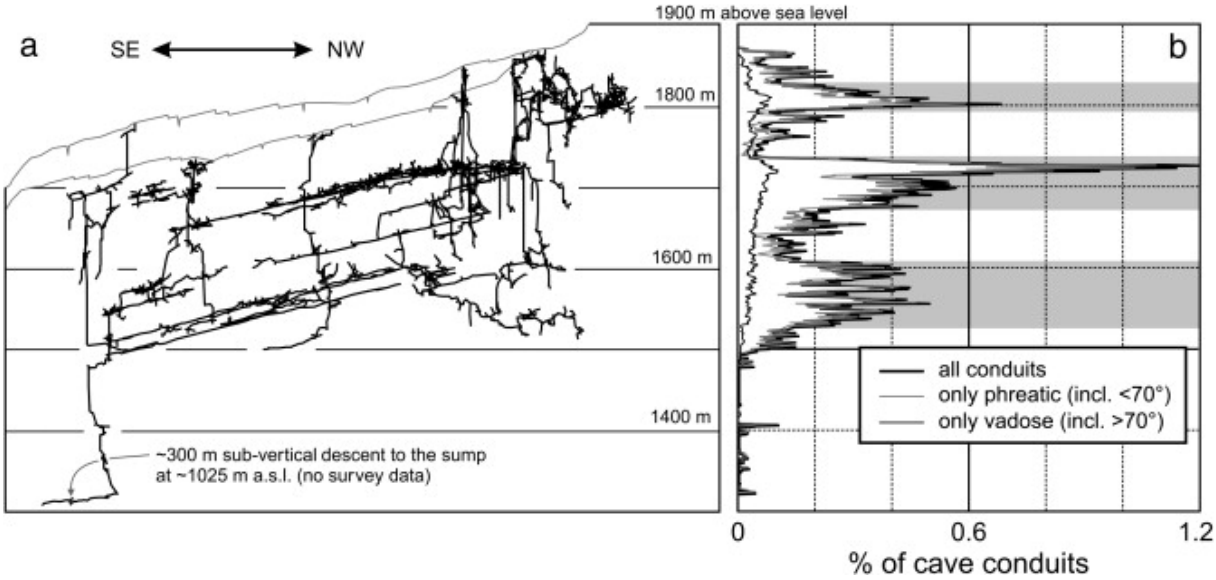

Fig. 6. a. Vertical southeast–northwest section of the Burgunderschacht Cave System (survey traverse only). The apparent tilt towards the southeast indicates the dip (14°) of the bedding (view is sub-parallel to the strike of the bedding). b. Frequency distribution of conduits with respect to elevation (cf. Section 4.1). Grey bars indicate interpreted cave levels.

Fig. 7. Phreatic tube in Burgunderschacht Cave System that formed along the intersection of a bedding plane with a fault (~ 1540 m a.s.l.). The small canyon at the bottom is presently active and is not related to Upper Miocene phreatic development.

Both direct observations in the cave as well as plan views and vertical sections indicate that the cave system has developed along a set of a few parallel directions of vertical faults (mainly strike–slip faults) as well as bedding planes that generally dip at 14° to the southeast (127°). Therefore, inclined (20°–70°) passages are rare (see also Herrmann, 1993, pp. 24). Three phreatic galleries, each showing homogenous morphology throughout, follow the dip of the bedding for at least 100 m of elevational difference. Some parts of the phreatic galleries exhibit angular maze patterns in plan view whilst others represent branchworks. Major horizontal galleries have typical cross-sections of 5–15 m2. Further descriptions are given by Herrmann (1993) and Behm et al. (2007).

3.2.2. DÖF–Sonnenleiter Cave System (DÖC)

Again, the DÖF–Sonnenleiterschacht (1625/379, 18.2 km, − 1054 m) and the adjacent Ozonloch (1625/406, 1.9 km, − 591 m) are regarded a single cave system that ranges from 904 m to 1995 m a.s.l. Four inactive vadose shaft systems intersect with a major sub-horizontal gallery, which lies at 330 to 400 m below the surface (Fig. 8). Shafts are partly very voluminous and up to 191 m deep. Two of the many intersecting vadose canyon shafts were explored further down, whereas in one a final sump was reached at 904 m a.s.l.

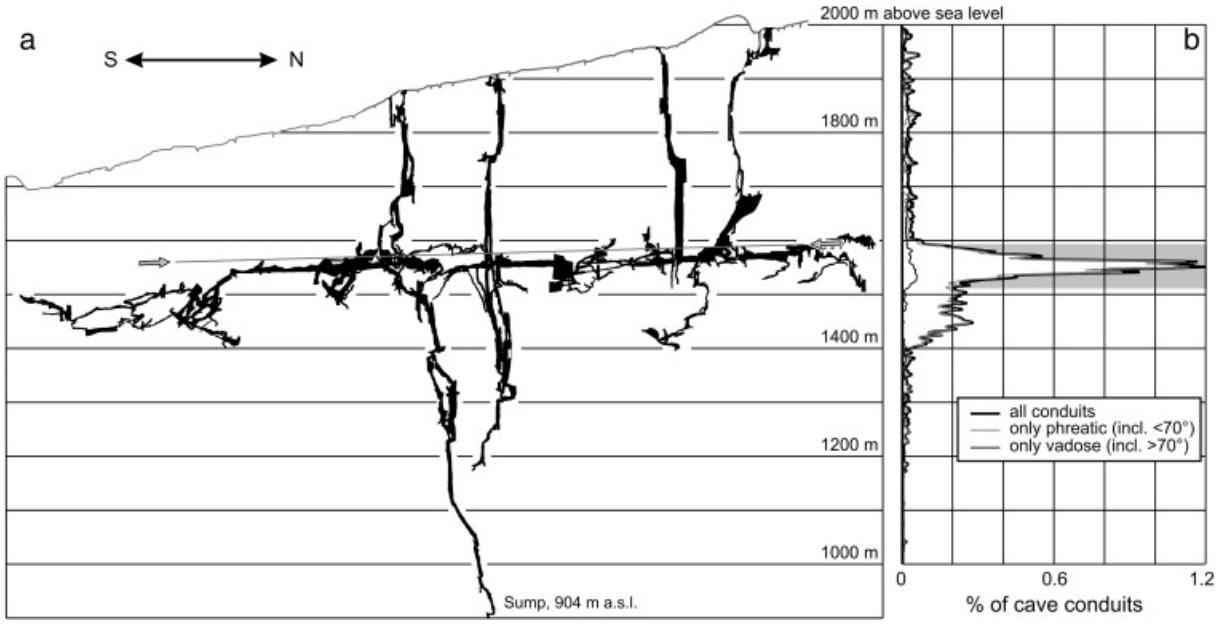

Fig. 8. a. Vertical south–north section of the DÖF–Sonnenleiter Cave System. Arrows and grey line indicate the watertable of a speleogenetic phase inclined with 1.6° to the south. b. Frequency distribution of conduits with respect to elevation (cf. Section 4.1). Grey bars indicate interpreted cave levels.

The almost horizontal main gallery shows a rather homogenous morphology with elliptical cross-sections of roughly 30–50 m2 for a long distance. Several textbook-like examples of vadose entrenchments into crests of upward phreatic profiles (“isolated vadose trenches” according to Ford and Williams, 2007, pp. 232) have developed that clearly indicate epiphreatic genesis. The resulting keyhole profiles are up to 15 m high and the canyons are 1–2 m wide. Several times the gallery loops down some tens of meters along bedding planes or faults and then immediately rises up along other initial fissures to the previous level again. At the bottoms of the loops, small phreatic tubes or mazes lead further down, which are interpreted as soutirages (as defined by Häuselmann et al., 2003; equivalent to undercaptures, Ford and Williams, 2007). The bedding of the limestone dips to the SE (148/25° in the north, 133/35° in the south). More detailed descriptions of the cave system are given by (Jeutter and Seebacher, 1997) and (Jeutter and Seebacher, 2001).

4. Morphometric analyses

We use a method (Filipponi and Jeannin, 2006 and Filipponi et al., 2008-this issue) that gives a quantitative relationship between the conduit network geometry, the geological settings and the hydrogeological context of a cave system. Based on the 3D geometry of the cave system and a geological model, the proposed method is aimed at identifying cave levels, initial fissures, and inception horizons. The geological model is set up by the orientation of the bedding planes, whereas the survey traverse of the entire cave is taken as a proxy for the geometry of the conduits. The frequency distribution of the conduits is calculated with respect to (1) the elevation a.s.l., (2) with respect to the angle between the dip of the conduits and the dip of the strata, and (3) with respect to the normal distance from a pre-defined stratigraphic layer.

We discriminate between vadose and phreatic conduits. The separation is done automatically by classifying all conduits with an inclination of more than 70° as vadose conduits and all the flatter ones as phreatic conduits. In detail, this approach is not entirely accurate because there are also a few phreatic shafts as well as some sub-horizontal vadose passages (e.g. short meander passages between shafts). However, it is an adequate

approximation for this case study, since the separation between vertical, vadose shafts and sub-horizontal, phreatic galleries is very pronounced in the investigated caves.

4.1. Cave levels

Several cave levels are clearly visible in the vertical sections (Fig. 6 and Fig. 8). To analyse them statistically, the complete survey traverse was subdivided into 1 m long segments and their frequency distribution for 1 m height intervals was calculated. A moving average over 5 m was used for smoothing the curves. For BUC, three distinct cave levels, centred at 1800, 1700, and 1560 m a.s.l. can be distinguished (Fig. 6b). In DÖC, major phreatic galleries range from 1400 m to 1600 m but a significant peak is centred at 1550 m a.s.l (Fig. 8b). Further, it is notable that, in both cave systems, vadose conduits are distributed nearly homogenously while only the phreatic conduits show a clear vertical zoning.

The current state of exploration of the caves gives no evidence of further extensive phreatic galleries between 1400 m and the present karst water table at or below ca. 900 m a.s.l. Only from the Wildbadercave (1625/150, 1.6 km, − 874 m; Fig. 2) is a major horizontal system at ~ 1150 m a.s.l. assumed (Pfarr and Stummer, 1988).

4.2. Initial fissures

For the interpretation of the dip of initial fissures, the frequency distribution of the survey traverse shots with respect to the angle between them and the bedding planes (see Sections 3.2.1 and 3.2.2) was calculated. Fig. 9 shows that in both cave systems a large number of conduits are sub-parallel to the dip of the bedding planes. The peaks are more distinct in BUC, which indicates that fewer sets of initial fissures were used. The second maxima represent the vadose shafts that predominantly developed along vertical faults; as bedding is generally steeper in DÖC, this peak is shifted towards a lower angle compared to the BUC.

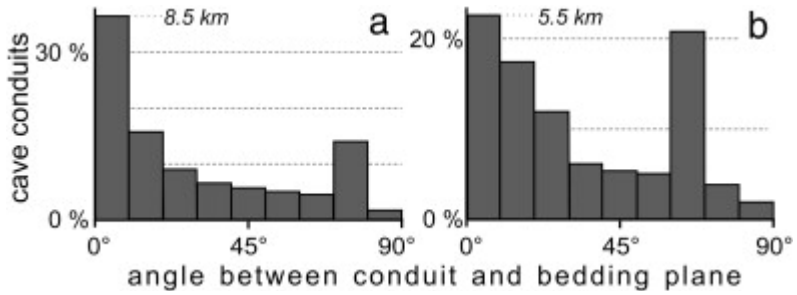

Fig. 9. Angle between conduit and bedding plane: (a) Burgunderschacht Cave System, (b) DÖF–Sonnenleiter Cave System (see text for details).

Further, the frequency distribution of conduits with respect to their azimuth was calculated to check the influence of faults (Fig. 10). In order to eliminate steep survey traverse shots, where the direction may not be representative (e.g. nearly vertical shafts), the horizontally projected segment length serves as proxy. In BUC, we recognise two dominating directions corresponding to the main fault directions. In DÖC, the two recognisable maxima are less pronounced and differ from that of BUC. Overall, both analyses confirm the field observation that phreatic conduits developed preferentially at the intersection of the bedding planes with faults and vadose conduits (mainly shafts) are guided by vertical faults.

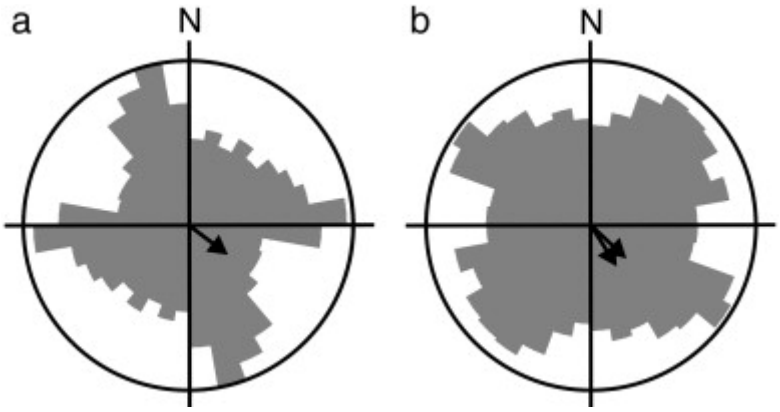

Fig. 10. Symmetrical bidirectional rose diagram of conduit length. Arrows indicates dip directions of the strata. (a) Burgunderschacht Cave System, cumulative length of peak maximum: 1550 m (b) DÖF–Sonnenleiter Cave System, maximum: 1330 m (see text for details).

4.3. Inception horizons

The inception horizon hypothesis (Lowe, 1992) is based on the assumption that within a homogenous carbonate mass, karst conduits develop preferentially along a limited number of stratigraphical horizons. Therefore, the spatial distribution of conduits should be neither uniform nor random, but should exhibit systematic 3D patterns. The distribution of cave conduits relative to the distance from a reference bedding plane are shown in Fig. 11. It is clear that phreatic conduits have developed only along a restricted number of stratigraphic horizons (i.e. bedding planes). Distinct peaks are interpreted as inception horizon. As stratigraphic markers are missing within the Dachstein Formation, it is not possible to establish a specific reference bed within the ~ 1 km thick sequence of limestone. Therefore, we choose a recognisable and distinctive bedding plane within each cave system, although it is not possible to identify the same reference horizon for both systems (BUC and DÖC) as a vertical shift along faults between the two caves is possible.

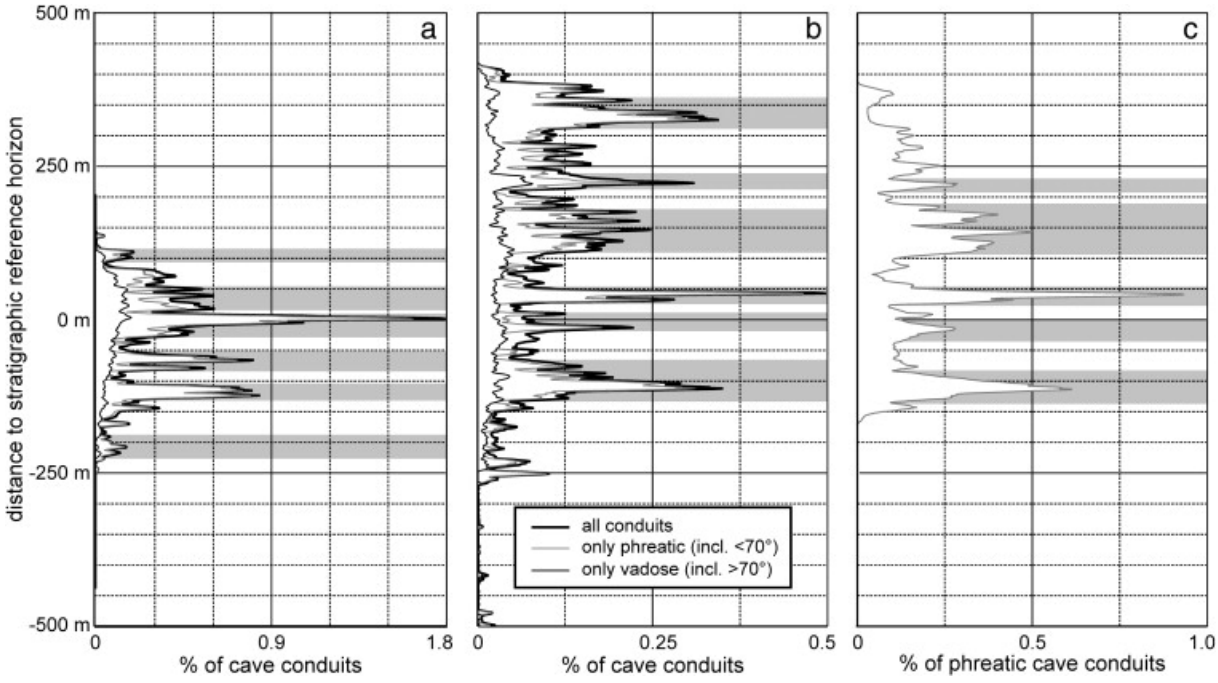

Fig. 11. Frequency distribution of conduits with respect to the normal distance from a reference bedding plane. Grey bars indicate interpreted inception horizons. (a) Burgunderschacht Cave System; (b) DÖF–Sonnenleiter Cave System, (c) Level 1520–1600 m in DÖF–Sonnenleiter Cave System (because of the inclination of the reference bedding plan the range becomes much wider than the 80 m of the analysed height interval).

In BUC vadose shafts are homogenously distributed across the stratigraphic sequence whereas the phreatic conduits developed only along six clearly identifiable inception horizons. In DÖC the stratigraphic distribution of the conduits exhibits six less pronounced inception horizons. Again, vadose shafts are more or less homogenously distributed along the stratigraphic section. The evidence for inception horizons is clearer if only the phreatic conduits lying between 1520–1600 m a.s.l. (Fig. 11c) are analyzed. In this case, it is possible to distinguish five inception horizons.

4.4. Analyses of different cave levels in BUC

In contrast to DÖC, the BUC shows three levels (Fig. 5 and Fig. 6); these have been analysed separately, including histograms of the conduit direction for each level (Fig. 12).

• The level centred at 1800 m a.s.l. (2.7 km of phreatic conduits) developed at the intersection of one inception horizon with NNE–SSW orientated faults. However, the interpretation of only one inception horizon is possibly an artefact since the extension of the conduits is limited due to the intersection of the cave with the surface.

• Level 1700 m (7.0 km) developed at the intersection of two inception horizons with NNW–SSE as well as W–E orientated faults.

• Level 1560 m (5.3 km) developed at the intersection of three inception horizons with NNW–SSE as well as W–E orientated faults.

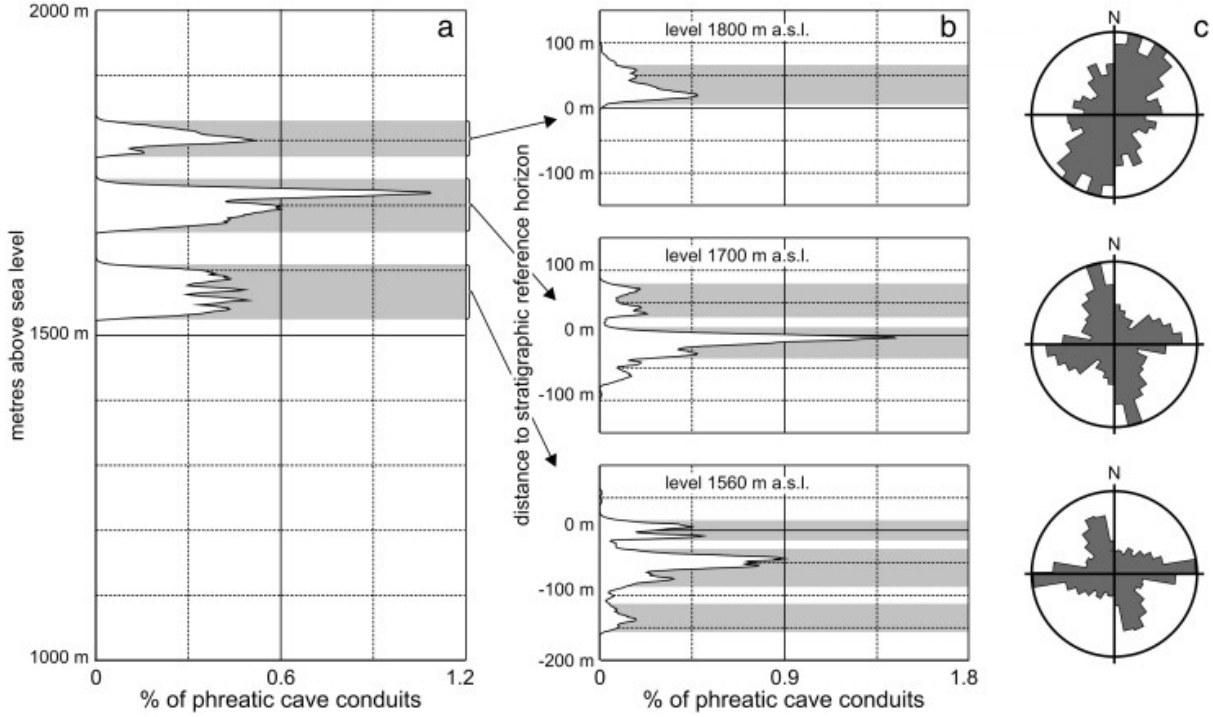

Fig. 12. Histograms of the three levels in Burgunderschacht Cave System. (a) Frequency distribution of the three phreatic conduits interpreted from Fig. 6b with

4.5. Water tables of speleogenetic phases

The 3D-orientation of the water tables of speleogenetic phases were inferred from survey data by analysing various vertical sections of the caves. If linear arrangements of tops of phreatic loops (giving the minimum height of the water table of the speleogenetic phase) were visible, the orientation of the projection plane which shows the steepest inclination of a line connecting the crests of phreatic loops was determined. The direction of the projection plan defines the approximate dip-direction of the palaeo water table and was interpreted as the palaeoflow direction. For BUC no morphologic features that define a watertable of a phase are visible (in contrast to clearly visible dip of the bedding planes; see Fig. 6.). For DÖC a very clear palaeo water table is visible (Fig. 8a) tilted at 1.6° to the south and extending over 1.1 km horizontally and from 1560 to 1590 m a.s.l. vertically.

4.6. Water tables of phases in other cave systems

To compare the orientation of palaeo water tables within other parts of the Totes Gebirge (Fig. 1), further large cave systems were investigated. For Schönberg Cave System (former Raucherkar and Feuertal Cave System, 1626/55; 120.4 km; ± 1060 m; Tenreiter, 2007) a major palaeo water table that extends over 2.4 km and dips at 2.5° to the north (Fig. 13) was detected. This is situated between 1430 and 1530 m a.s.l. A second, minor water table is also present ~ 100 m higher in the cave. Morphometric analyses reveal that Schönberg Cave System developed along four or five inception horizons.

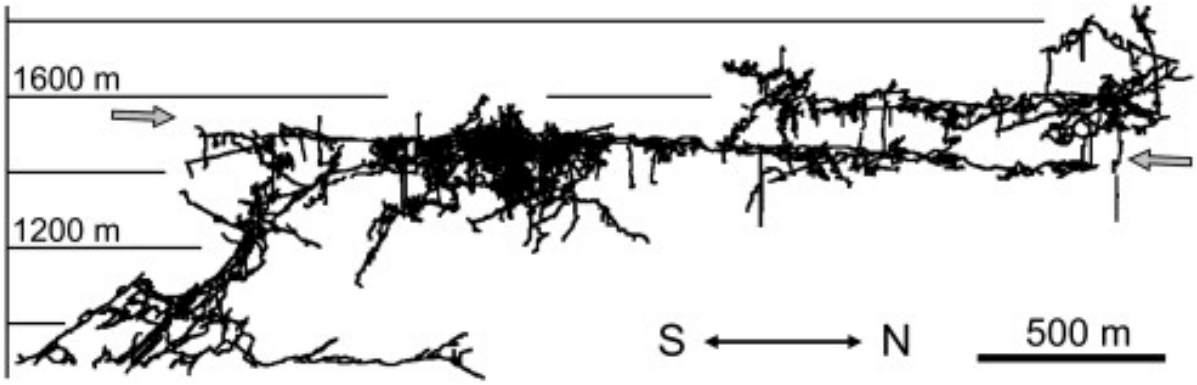

Fig. 13. Vertical S–N section of the Schönberg Cave System. Arrows indicate a speleogenetic phase that is inclined at 2.5° to the north.

In the Schwarzmooskogel Cave System (1623/40; 58.2 km; Winkler, 2004) large breakdown chambers partly obscure the original morphology. However, a potential water table of a phase seems to extend over 2.3 km and dips at 1.6° to the southwest. In this cave system, six inception horizons could be identified (Filipponi and Jeannin, 2006).

For the Woising cave area (1627/74; 10.6 km; Kalmbach and Spahlinger, 2001), a clear planar alignment of loop crests over a distance of 0.5 km is visible. As the inclination of the connecting line is very shallow (0.5°), its interpretation as a northwest-dipping phase at ~ 1650 m a.s.l. is uncertain.

Several caves (Harlacher et al., 2003 and Frank, 2001) near Appelhaus refuge were analysed. Some 26 km of passages at Hüttstatt and Redender Stein developed in Jurassic limestone as well as 15 km of caves in Dachstein limestone (Dellerklapf Cave, 1627/34; Illegal Harem Cave, 1627/42; Klammkogelhöhle 1627/29) do not show significant water tables corresponding to speleogenetic phases. The 2.7 km long Grubsteineishöhle (1625/16; Seebacher, 2001), close to the DÖC, shows morphologic evidence of a phase at ~ 1900 m a.s.l., but due to its short horizontal extent (300 m), the dip-direction cannot be accurately estimated.

5. Discussion

In our study, we analysed cave levels (strictly horizontal accumulation of galleries) and palaeo water tables of speleogenetic phases (slightly inclined). Many former publications tried to correlate cave levels with surface morphology and palaeo base levels (e.g. Kuffner, 1998 and Fischer, 1990). However, it was rarely possible to correlate the levels over regional scale or several cave systems respectively, even within a single karst massif. With the knowledge that phreatic cave passages develop below slightly inclined water tables corresponding to speleogenetic phases (e.g. Häuselmann et al., 2003), it is evident that an observed cave level may be mistaken for a water table of a phase, in particular if the observable horizontal extent is limited. Only detailed observations of cave systems that extend over long distances allow the determination of inclined water tables. Therefore, the term level for horizontal accumulations of galleries at certain altitudes should be used descriptively only. However, the observation of a cave level is an indication that there should be one or more speleogenetic phases within that height interval. Its observation may not be possible because the knowledge of the whole cave system is always limited (state of exploration, sediment fill etc.). This means that cave levels have some genetic relevance but they do not give the exact position of a palaeo water table nor can they be taken as indications for a flat palaeo water table. Therefore, the interpretation and correlation of cave levels is only feasible for large scale levels (in the order of a couple of hundred metres elevation) that may comprise many speleogenetic phases. In

the NCA, three such major cave levels were defined (Haseke-Knapczyk, 1989) and the age of their development was determined by Frisch et al. (2002).

According to their morphology and their elevation between 1400 and 1870 m a.s.l., we identified three levels in the investigated area. The levels are centred at 1810, 1700, and 1560 m a.s.l and are regarded as expression for speleogenetic phases that are part of the Giant Cave Level of the NCA that developed in Upper Miocene times (6 to 10 Ma; Frisch et al., 2002).

Using the classical "Four State Model" (Ford, 1971) in a descriptive way, the BUC can be classified as a phreatic cave with multiple loops while the epiphreatic gallery in the nearby DÖC exhibits water table characteristics with few phreatic loops. Although there are current studies that support other factors responsible for the development of a certain "state" (e.g. discharge conditions; Häuselmann and Gabrovšek, pers. comm.) our studies suggest that the density of initial fissures still is an important factor, which is in accordance with the classical interpretation. For both the angles between conduit and bedding plane (Fig. 9) as well as the conduit directions (Fig. 10), the statistical analyses show more pronounced peaks for the conduits of BUC than of DÖC. This reveals that in BUC there are fewer sets of initial fissures, mainly six distinct inception horizons, which were used during solutional processes for a greater distance. On the other hand, at least for the cave levels at around 1560 m a.s.l., which can be observed in both cave systems, the conduits developed simultaneously, which does not favour the theory of different climate or discharge conditions to develop different states respectively. For BUC, the change of preferred conduit directions at different levels (Fig. 12) indicates that the flow direction or initial fissures have changed over time. This latter could be explained by a change of the stress fields due to the ongoing Alpine deformation, which influences initial fissure properties (aperture, fault rocks etc.). However, the exact reasons for the very local differences in fracture density and measurements of fracture density that are independent of the cave morphology are subject to further studies.

In contrast to the classical Four State Model, we attribute the genesis of the mature galleries, at least for the DÖC, to epiphreatic conditions, as previously suggested by Audra (1994) and Häuselmann et al. (2003). The main gallery of the DÖC is clearly epiphreatic. The soutirages imply that this part developed by the "filling-overflow manner" as it was observed by Häuselmann et al. (2003) in present-day water active caves. For the loops of the BUC, which have elevational differences of at least 100 m, there is no clear morphological evidence for epiphreatic flow. The relatively large elevational differences do not seem outstanding when compared to Audra (1994), who observed epiphreatic loops with a 250 m elevational difference in a cave system in the Tennengebirge (NCA, Cosa Nostra Bergerhöhle).

As small-scale morphological indicators for flow direction are missing, the tilting of the main gallery in the DÖC at 1.6° to the south allows for two interpretations of the palaeoflow direction. (1) Its location in the southern part of the massif, only 10 km north of the margin of the NCA, as well as the large cross-sections areas of the galleries could imply allogenic recharge and a north-directed flow. Similar conditions are very likely for the Dachstein Südwandhöhle at the southern cliffs of the neighbouring Dachstein massif (Seebacher, 2006). This cave is located directly at the southern margin of the NCA and shows north(west) directed palaeoflow. In the Tennengebirge massif, Audra et al. (2002) also suggested allogenic recharge from the south during the development of the Giant Cave Level. However, for the south-eastern Totes Gebirge a north-directed flow together with the observed south-dipping water table of a phase would imply a rotational component during tectonic uplift of more than 1.6°. (2) A south-directed flow according to the dip of the phase would imply autogenic recharge of a large area. The inclination of the palaeo karst watertable of ~ 1.6° matches data by Häuselmann et al. (2003) who observed inclinations of 1.3° to 2.1° in Bärenschacht (Thunersee, Switzerland). Analyses from other cave systems in the Totes Gebirge confirm the magnitude of these angles although Schönberg Cave Systems is slightly steeper (2.5°). Only the inclination of the water table of the phase in Nervensystem Cave seems to be exceptionally low (0.5°) but the horizontal extension of the system is limited. Considering these other cave systems, the dip-directions of the water tables (Fig. 2) are interpreted as palaeoflow directions and generally suggest a radial drainage pattern for the Totes Gebirge in the Upper Miocene. In turn, this implies autogenic recharge. The observations do not support a general north directed palaeoflow with allogenic recharge. Therefore, we reject the idea of north-directed flow and tectonic rotation for the investigated area.

Even though tracer tests by Maurin and Zötl (1964) indicated a radial drainage, we do not take this as support for our model, since the same methods resulted in the same radial pattern for the Dachstein massif (Zötl, 1974), which was subsequently disproved by further tests (Herlicska et al., 1995) that showed north-directed flow.

Nowadays, flow direction within the phreatic zone in the area of investigation is west- or east-directed and therefore perpendicular to that in Upper Miocene. Non-karstic rocks, which presently crop out at ~ 1450 m directly south of the caves, dam the karst close to the southern margin of the plateau. Therefore, the switch in the flow direction must have occurred relatively shortly after the development of the main phase in DÖC which, if extrapolated, intersects with the surface at ~ 1540 m. This, and the fact that the catchment area between the non karstic rock and the study area is very small, would be an explanation for the absence of extensive phreatic galleries below this level.

The fine-grained sediments, which were deposited during very slow flow velocities, are attributed to Pleistocene backflooding. This occurred when the valleys and the discharge points were filled with ice, which lead to several rises of the water table. These interpretations are in accordance with observations by Audra et al. (2002) from Tennengebirge. Also in our area, the slow current and the low chemical aggressiveness of the glacial meltwater that resulted from the suspended calcite rich sediments, restricted speleogenetic action.

Most probably, the widespread paragenetic features developed due to the backflooding, as they occur in many galleries that are filled with fine sediments. Further, old micromorphological structures like scallops were obscured during these periods.

6. Conclusion

Detailed observations of extensive alpine cave systems confirm that (epi)phreatic caves preferentially form below slightly inclined surfaces, the water tables of speleogenetic phases, and not at strictly horizontal levels. At least for alpine caves, inclinations in the order of 1.5° ± 1° seem to be typical for base level related speleogenetic phases that are not controlled by geological inhomogeneities. Therefore, cave levels (horizontal accumulations of galleries) indicate the presence of one or more speleogenetic phases, but they cannot be correlated over large distances or with surface morphology. The delineation of water tables of speleogenetic phases needs in-depth morphological observations and data from cave systems with major horizontal extents.

The two adjacent cave systems investigated show different morphological types with respect to length–depth-development, and to the Four State Model (Ford and Williams, 2007). The main gallery in the DÖF–Sonnenleiter Cave System (DÖC) is a watertable cave with only few loops whilst the three levels in the Burgunderschacht Cave System (BUC) show multiple looping. Statistical analyses of gallery inclination and direction indicate that the BUC formed along a few persistent initial fissures whereas the genesis of the DÖC was guided by less prominent initial fissures. This is in accordance with the explanation of the Four State Model. Further, the simultaneous developments of different states at the same level, which can be observed in both caves, suggest that discharge conditions or climatic factors have no influence on the state for the observed caves. In contrast to the Four State Model development conditions were clearly epiphreatic, at least in DÖC, and not phreatic (sensu stricto) and the loops developed in the filling-overflow manner (Häuselmann et al., 2003).

The Upper Miocene subsurface palaeoflow inferred from the inclinations of the water tables of phases indicate that the Totes Gebirge karst massif was drained radially and recharge was autogenic. This excludes a north-directed through flow of allogenic water as suggested for Tennengebirge and Dachstein.

From the observations above, a simplified genetical model for the caves in the south-eastern Totes Gebirge is deduced (Fig. 14): (a) Upper Miocene: The Dachstein–Surface is already significantly uplifted and speleogenetic phases fed by autogenic recharge develop corresponding to a base level in the south. The cave systems developed along a few inception horizons and faults — phreatic conduits often at the intersection of both. (b) Relative deepening of the base level causes the development of several phases. At least some of them were formed under epiphreatic conditions and behaved in the filling overflow manner. However, the phases differ in type according to the Four State Model as fracturing seems to vary locally. The galleries of both phases (a and b) are part of the Giant Cave Level (Frisch et al., 2002). (c) During Pleistocene glaciations, the Totes Gebirge was covered by massive glaciers of the Alpine ice stream network which eroded the valleys and most of the plateau area. On bedded Dachstein limestone, they formed staircase limestone pavements (Schichttreppenkarst). Back-flooding due to the ice filling of the valleys caused sediment fill and paragenesis in the caves. (d) Pleistocene interglacial (e.g. present conditions): vadose waters enter the old phreatic galleries through the shafts and partly remove the sediment fill. Several cycles of glacial (c) and interglacial periods (d) occur. Galleries of the actual epiphreatic zone, which drain to the east or west, are unknown.

Acknowledgements

This study would not have been possible without the very large amount of data provided by several caving clubs and their representatives. The speleological societies of Upper Styria (VHO) and of Vienna and Lower Austria are in particular thanked for data of the investigated cave systems (BUC and DÖC). Survey data and other information about other major cave systems in the Totes Gebirge were provided by: Max Wimmer and Clemens Tenreiter (Landesverein für Höhlenkunde in Oberösterreich) for Schönberg Cave System; Robert Winkler (data by: Arbeitsgemeinschaft Höhle und Karst Grabenstetten, Cambridge University Caving Club, Forschergruppe Höhle und Karst Franken, Verein für Höhlenkunde in München) for Schwazmooskogel Cave System; Richard Frank and

Uwe Kalmbach (data by Höhlen und Heimatverein Laichingen & Höhlenforschergruppe Nütringen) for the caves around Appelhaus and Woising.

The reviews by Philipp Häuselmann and Philippe Audra improved the manuscript and encouraged discussion. Hugh Rice and Iris Lenauer made improvements to the English.

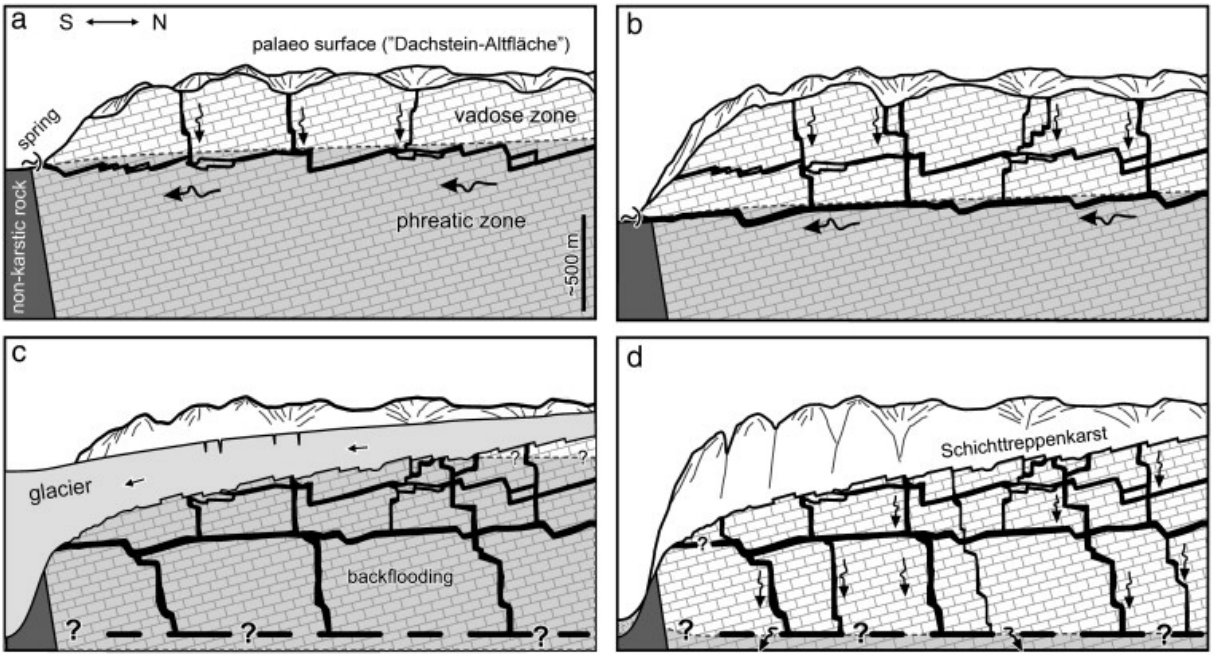

Fig. 14. Simplified genetical model of cave and surface development at the southern margin of the south-eastern Totes Gebirge. For explanation, see text.

References

Audra P., 1994: Karst alpines. Genèse de grands réseaux souterrains. Karstologia Mémoires 5, 280 pp.

Audra P., Quinif Y. and Rochette P., 2002: The genesis of the Tennengebirge karst and caves (Salzburg, Austria), Journal of Caves and Karst Studies 64, pp. 153–164.

Audra P., Bini A., Gabrovsek F., Häuselmann P., Hobléa F., Jeannin P.-Y., Kunaver J., Monbaron M., Sustersic F., Tognini P., Trimmel H. and Wildberger A., 2006: Cave genesis in the Alps between the Miocene and today: a review, Z. Geomorph. 20, pp. 153–176.

Baumgartner A., Reichel E. and Weber G., 1983: Der Wasserhaushalt der Alpen: Niederschlag, Verdunstung, Abfluß und Gletscherspende im Gesamtgebiet der Alpen im Jahresdurchschnitt für die Normalperiode 1931–1960, München-Wien, Oldenbourg.

Behm M., Klampfer A. and Plan L., 2007: Forschungen 1993−2006 im Burgunderschacht (1625/20, Totes Gebirge, Stmk.). Die Höhle 58, pp. 58–68.

Bögli A., 1980: Karst hydrology und physical speleology, Springer, Berlin–Heidelberg (1980).

Dincer T., Payne B.R., Yen C.K. and Zötl J., 1972: Das Tote Gebirge als Entwässerungstypus der Karstmassive der nördlichen Kalkhochalpen (Ergebnisse von Isotopenmessungen), Steirische Beiträge zur Hydrogeologie 24, pp. 71–109.

Filipponi M. and Jeannin P.-Y., 2006: Is it possible to predict karstified horizons in tunneling?, Austrian Journal of Earth Science 99, pp. 24–30.

Filipponi, M., Jeannin, P.-Y., Tacher, L., 2008: Evidence of inception horizons in karst conduit networks. Geomorphology. doi:10.1016/j.geomorph.2008.09.010.

Fischer A.G., 1964: The Lofer cyclothems of the alpine Triassic, Bull. Geol. Surv. Kansas 169 (1964), pp. 107–149.

Fischer K., 1990: Höhlenniveaus und Altreliefgenerationen in den Berchtesgadener Alpen, Mitteilungen der Geographischen Gesellschaft München 75, pp. 47–59.

Ford D., 1971: Geologic structure and a new explanation of limestone cavern genesis, Transactions of the Cave Research Group of Great Britain 13, pp. 81–94.

Ford D., 2000: Speleogenesis under unconfined settings. In: A. Klimchouk, D. Ford, A. Palmer and W. Dreybrodt, Editors, Speleogenesis — Evolution of Karst Aquifers, National Speleological Society, Huntsville, pp. 319–324.

Ford D. and Williams P., 2007: Karst Hydrogeology and Geomorphology, Wiley, Chichester.

Frank R., 2001: Höhlenforschung beim Albert–Appel–Haus im westlichen Toten Gebirge, Mitteilungen des Vereines für Höhlenkunde in Obersteier 19, pp. 118–120.

Frisch W., Székely B., Kuhlemann J. and Dunkl I., 2000: Geomorphological evolution of the Eastern Alps in response to Miocene tectonics, Z. Geomorph. 44, pp. 103–138.

Frisch W., Kuhlemann J., Dunkl I., Székely B., Vennemann T. and Rettenbacher A., 2002: Dachstein-Altfläche, Augenstein-Formation und Höhlenentwicklung — die Geschichte der letzten 35 Millionen Jahre in den zentralen Nördlichen Kalkalpen, Die Höhle 53, pp. 1–36.

Harlacher C., Clemens T. and Sauter M., 2003: Chemische und thermische Reaktion der Wässer von Karstquellen um Hochgebirge (Totes Gebirge, Österreich) auf Niederschlagsereignisse, Bericht der Wasserwirtschaftlichen Planung vol. 84, Steiermärkische Landesregierung, Graz.

Haseke-Knapczyk H., 1989: Der Untersberg bei Salzburg. Die ober- und unterirdische Karstentwicklung und ihre Zusammenhänge, Ein Beitrag zur Trinkwassererforschung, MaB-Reihe vol. 15, Österr. Akademie der Wissenschaft, Wien.

Häuselmann P., Jeannin P.-Y. and Monbaron M., 2003: Role of epiphreatic flow and soutirages in conduit morphogenesis: the Bärenschacht example (BE, Switzerland), Z. Geomorph. 47, pp. 171–190.

Häuselmann P., Granger D.E., Lauritzen S.E. and Jeannin P.-Y., 2007: Abrupt glacial valley incision at 0.8 Ma dated from cave deposits in Switzerland, Geology 35, pp. 143–146.

Herlicska H., Lorbeer G., Humer G., Boroviczeny F., Mandl G.W. and. Trimborn P, 1995; Pilot Project "Karst Water Dachstein", European Commission: Hydrogeological aspects of groundwater protection in karstic areas, EUR 16547 EN, Final report COST Action vol. 65, pp. 21–36.

Herrmann E., 1993: Editor, Die Tauplitz-Schachtzone im Toten Gebirge. Wiss. Beiheft z. Z. Die Höhle No. 44, Verb. Öst. Höhlenforscher, Wien.

Jeutter P. and Seebacher R., 1997: In den Karren: Southern part of the Tauplitz Schachtzone, International Caver 21, pp. 19–28.

Jeutter P. and Seebacher R., 2001: Shaft exploration "In den Karren", Mitteilungen des Vereines für Höhlenkunde in Obersteier 19, pp. 58–62.

Kalmbach U.and Spahlinger W., 2001: Forschungsstand Woising Höhlenpark Totes Gebirge Österreich, Mitteilungen des Vereines für Höhlenkunde in Obersteier 19, pp. 121–124.

Klimchouk A. and Ford D., 2000: Lithologic and structural controls of dissolutional cave development. In: A. Klimchouk, D. Ford, A. Palmer and W. Dreybrodt, Editors, Speleogenesis — Evolution of Karst Aquifers, National Speleological Society, Huntsville, pp. 54–64.

Krenmayr, H.G., and Schnabel, W., 2006: Geologische Karte von Oberösterreich — 1:200.000. Geologische Bundesanstalt, Wien.

Kuffner D., 1998: Höhlenniveaus und Altflächen im Westlichen Toten Gebirge, Wiss. Beiheft z. Z. Die Höhle No. 53, Verb. Österr. Höhlenforscher, Wien.

Lechner J., 1949: Neue karst- und quellengeologische Forschungen im Toten Gebirge, Protokoll der 3. Vollversammlung der Bundeshöhlenkommission, Wien, pp. 32–38.

Linzer H.G., Ratschbacher L. and Frisch W., 1995: Transpressional collision structures in the upper crust: the fold-thrust deformation of the Northern Calcareous Alps, Tectonophysics 242, pp. 41–61.

Lowe D.J., 1992: The origin of limestone caverns: An inception horizon hypothesis. Manchester Metropolitan University, Ph.D. thesis, 512p.

D.J. Lowe, 2000: Role of Stratigraphic Elements. In: A. Klimchouk, D. Ford, A. Palmer and W. Dreybrodt, Editors, Speleogenesis: The Speleoinception concept, Speleogenesis — Evolution of Karst Aquifers, National Speleological Society, Huntsville, pp. 65–76.

Maurin V. and Zötl J., 1964: Karsthydrologische Untersuchungen im Toten Gebirge mit besonderer Berücksichtigung des versorgungswasserwirtschaftlichen Belange im Tauplitzgebiet (Oberösterreich–Steiermark), Österr. Wasserwirtschaft 16, pp. 112–123.

Palmer A.N., 1987: Cave levels and their interpretations, The NSS Bulletin 49 (2), pp. 50–66.

Perrin D., Boibessot D., Motte D. and Palissot J., 1983: Le Burgunderschacht — massif des Totesgebirge — Autriche, Spelunca 9, pp. 22–24.

Pfarr T. and Stummer G., 1988: Die längsten und tiefsten Höhlen Österreichs, Wiss. Beiheft z. Z. Die Höhle 35, Verb. Österr. Höhlenforscher, Wien.

Sawicki L.S., 1909: Ein Beitrag zum geographischen Zyklus im Karst, Geogr. Z. 15, pp. 185–204.

Schauberger O., 1956: Schauberger, Über die vertikale Verteilung der nordalpinen Karsthöhlen, Mitt. d. Höhlenkommission 1955 (2), pp. 21–28.

Seebacher R., 2001: Seebacher, Neue Forschungen in der Grubsteineishöhle Kat. Nr. 1625/16, Mitteilungen des Vereines für Höhlenkunde in Obersteier 19, pp. 67–69.

Seebacher R., 2006: Seebacher, Aktuelle Forschungen in der Südwandhöhle (Dachsteinloch, 1543/28), Stmk/OÖ. Die Höhle 57, pp. 76–89.

Spötl C., Offenbecher K.H., Boch R., Meyer M., Mangini A., Kramers J. and Pavuza R., 2007: Tropfsteinforschung in österreichischen Höhlen — ein Überblick, Jahrbuch der Geologischen Bundesanstalt 147, pp. 117–167.

Stummer G. and Plan L., 2002: Handbuch zum Österreichischen Höhlenverzeichnis, Speldok-10, Verb. Österr. Höhlenforscher, Wien.

Tenreiter C., 2007: Neue längste Höhle Österreichs: Das Schönberg-Höhlensystem (1626/300, Stmk/OÖ). Die Höhle 58, 87–89.

Van Husen D., 2000: Geological processes during the Quaternary, Mitteilung d. Österr. Geol. Ges. 92, pp. 135–156.

Winkler R., 2004: Der Schwarzmooskogel. Karst & Höhle, 2002/2003, Verband d. Deutschen Höhlen u. Karstforscher, München.

Zötl J., 1961: Die Hydrographie des nordostalpinen Karstes, Steirische Beiträge zur Hydrogeologie 1960/61 (2), pp. 53–183.

Zötl J., 1974: Karsthydrogeologie, Springer, Wien.

Filipponi M., Dickert A, 2007:
Verstehen der Speläogenese durch 3D-Analyse - Fallbeispiel des Lachenstock-Karstes.
12. National Congress of Speleology - Switzerland: 46 - 55.

Verstehen der Speläogenese durch 3D-Analyse - Fallbeispiel des Lachenstock-Karstes (Schweiz)

Marco Filipponi[1,3], Andreas Dickert[2]

[1]ICARE GEOLEP, Laboratoire de géologie de l'ingénieur et de l'environnement, Ecole Polytechnique Fédérale de Lausanne (EPFL) ENAC, Switzerland

[2]Ostschweizerische Gesellschaft für Höhlenforschung (OGH)

[3]Arbeitsgemeinschaft für Speläologie Regensdorf (AGSR)

Zusammenfassung

Der Einsatz von 3D-Visualisierungstechnik erlaubte uns visuell und statistisch den Zusammenhang zwischen dem bekannten Höhlensystem und den geologischen und hydrologischen Verhältnisse herzustellen. Die räumliche Analyse der Höhlen des Lachenstock-Karsts erlaubte 2 phreatische Höhlengangniveaus zu unterscheiden, die vorwiegend entlang 2 Hauptkluftrichtungen ausgerichtet sind und sich auf 5 stratigraphischen Initialfugen entwickelten. Dies führt uns zu einem ersten speläogenetischen Modell.

Schlüsselwörter: 3D-Analyse, Speläogenese, stratigraphische Initialfugen (inception horizon), Karsthydrologie

Résume

L'application de technique de visualisation 3D nous a permis d'établir la relation entre la partie connue d'un réseau et ses caractéristiques géologiques et hydrologiques. L'analyse spatiale a permis de différencier 2 niveaux phréatiques s'alignant Je long de 2 directions de fracturation principales et se développant Je long de 5 horizons d'inception. Cela nous mène à un premier modèle spéléogénétique du karst du Lachenstock.

Mots clés: Analyse 3D, spéléogenèse, horizons d'inception, hydrologie du karst.

Einleitung

Der Einsatz der 3D-Visualisierungstechnik VRML erlaubt es, 3D-Modelle eines Karstsystems herzustellen, die nicht nur das Höhlensystem, sondern ebenfalls die Geologie sowie hydrologischen Gegebenheiten darstellen. Dies ermöglicht es auf intuitive Art, die räumlichen Zusammenhänge zwischen Höhlengangnetz, Geologie und Hydrologie zu erkennen. Des Weiteren erlaubt das Diskretisieren des 3D-Modells, die visuell erkannten Zusammenhänge statistisch zu überprüfen.

Im Rahmen der vorliegenden Arbeit wurde die räumliche Verteilung der Höhlengänge des Lachenstock-Karstes (SZ, CH) analysiert, um die Rolle der geologischen Gegebenheiten sowie hydrogeologischen Rahmenbedingungen besser zu verstehen. Das Hauptinteresse lag darin, zu erkennen, ob in der stratigraphischen Abfolge bevorzugt verkarstete Horizonte (so genannte «stratigraphische Initialfugen»; in Englisch «inception horizon», LOWE 1992) existieren.

Methode

Im Gegensatz zu vielen anderen Autoren (z.B. FORD & EWERS 1978, BÖGLI 1980, PALMER 1987, AUDRA 1994) wurde die komplexe Geometrie des Höhlensystems nicht im zweidimensionalen Raum (Planansicht und/oder Längsschnitte), sondern im dreidimensionalen Raum analysiert. Dies erlaubt, die räumliche Verteilung der Höhlengänge in Bezug zu den geologischen Gegebenheiten sowie den hydrogeologischen Rahmenbedingungen zu setzen.

Die VRML-Visualisierungstechnik wurde ursprünglich als 3D-Standard für das Internet entwickelt. Da die meisten 3D-Modelliemngswerkzeuge den Im- und Export von VRML-Dateien ermöglichen, etabliert sich das Dateiformat auch als ein Austauschformat von 3D-Modellen. Es zeigte sich auch geeignete als Schnittstelle zwischen den Höhlenvermessungsprogrammen (z.B. Toporobot, Survex, Compass, Visualtopo), geologischen Modellierungsprogrammen (z.B. Geoshape), GIS-Programmen (z.B. Arc-GIS), mathematisch-statistischen Programmen (z.B. Matlab) sowie Animationsprogrammen (z.B. Cinema4D). Dadurch wird es möglich, relativ effizient 3D-Modelle eines Karstsystems herzustellen. Als Datengrundlage für die Modelle dienten die Höhlenvermessung, digitale Geländemodelle, Luftbildaufnahmen, geologische Kartierungen sowie Feldbeobachtungen an der Oberfläche als auch in den Höhlen.

Um zum Beispiel Aussagen machen zu können, ob sich entlang einer bestimmten Schichtfuge bevorzugt Höhlen entwickelten, ist eine relativ genaues Modell erforderlich, idealerweise im Fünfmeterbereich.

Neben dem qualitativen, visuellen Zusammenhang zwischen Höhlengangverlauf-Geologie-Hydrogeologie wurde dieser auch quantitativ hergestellt, wobei eine Methode zum Einsatz kam, die an der ETH Lausanne in Zusammenarbeit mit dem SISKA entwickelt wurde (FILIPPONI & JEANNIN 2006, FILIPPONI et al. 2008). Das Hauptinteresse der Methode ist das Erkennen von bevorzugt verkarsteten stratigraphischen Horizonten. Als Datengrundlage für die statistische Auswertung dient das oben erwähnte dreidimensionale Modell des Karstsystems.

Das Untersuchungsgebiet

Das alpine Karstgebiet des Wägitals zwischen dem Wägitalersee (Innerthal, SZ, CH) und dem Oberseetal (Näfels, GL, CH) ist rund 20 km2 gross und erstreckt sich vom Wägitalersee (930 m ü.M.) bis hinauf auf rund 2300m ü.M. (Multeriberg) [Abb. 1] Das Landschaftsbild ist ab rund 1500 m ü.M. durch eine ausgeprägte Karrenlandschaft gekennzeichnet.

Seit den 50er-Jahren wird das Karstgebiet durch die Ostschweizerische Gesellschaft für Höhlenforschung (OGH) systematisch erkundet, vermessen und dokumentiert. Das Gebiet zeigt eine ausgeprägte Verkarstung, was sich neben den Karrenfeldern vor allem durch eine Vielzahl von bereits entdeckten Höhlen manifestiert. Bis heute sind 257 Höhleneingänge bekannt und über 21 km Höhlengänge vermessen. Die Höhlen lassen sich grob in zwei Kategorien einteilen (DICKERT 2007):

- Fossil-phreatische, subhorizontale Höhlen,
- Vadose, eher kleinräumige Höhlen mit SchachtMäander-Serien.

Wobei die zweite Kategorie zurzeit eher untervertreten ist. Die vorliegenden Arbeit konzentriert sich auf die drei wichtigsten Höhlen des Lachenstocks (Zone K), die der fossil-phreatischen Kategorie zugeordnet werden können: Lachenstockhöhle, Plattenloch und Zindlenhöhle.

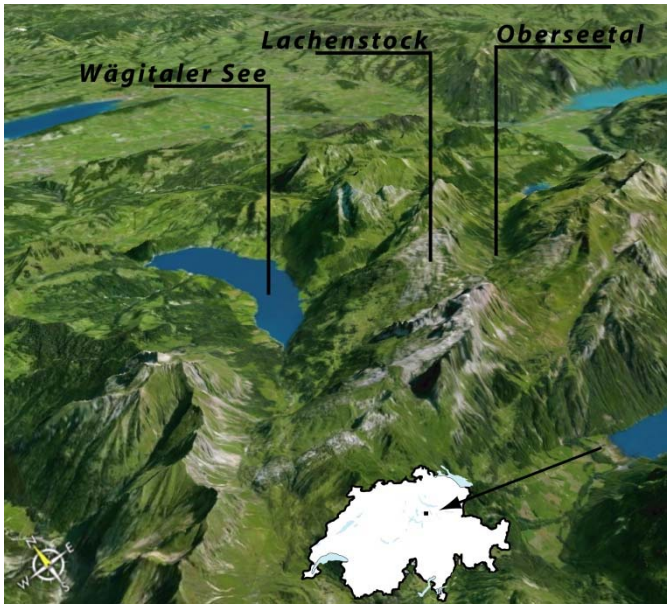

Abbildung 1; *Geografische Lage des Lachenstocks. Schön zu erkennen ist, die nach Westen abfallende Schrattenkalkplatte des Lachenstocks. (Bildquelle: Google Earth)*

Geologische Situation des Lachenstocks

Das Lachenstock-Karstgebiet entwickelte sich hauptsächlich in der gut verkarstungsfähigen SchrattenkalkFormation der Rederten-Decke (Helvetikum) (SCHARDT et al. 1924, OUERHOLZER 1942). Die Formation hat im Untersuchungsgebiet eine Mächtigkeit von rund 200 m und kann in drei Member unterteilt werden (SCHARDT et aL 1924): Unterer Schrattenkalk (rund J00 m), Orbitolinen-Schicht (rund 20 m), Oberer Schrattenkalk (rund 80 m). Die massig gebankte Schrattenkalk-Formation ist weitgehend entlang der ganzen Westflanke des Lachenstocks aufgeschlossen, nur lokal ist die mit erosivem Kontakt im Hangenden befindende, schlecht verkarstungsfähige, sandig-mergelige Garschella-Formation noch erhalten geblieben (z.B. Rädertenalp). Die sich im Liegenden befindenden mergeligen Drusbergschichten sind hingegen nur in der Felswand Richtung Oberseetal sowie Richtung Rädertenstock an der Oberfläche aufgeschlossen. Der Übergang Schrattenkalk-Drusberg ist gekennzeichnet durch eine allmähliche Vermergelung sowie einer Zunahme in Häufigkeit und Mächtigkeit von Mergellagen im eher reinen Kalkstein der Schrattenkalk-Formation.

Strukturell besteht der Lachenstock aus einem Antiklinal-Schenkel (HANTKE 1961) mit einem Schichteinfallen von rund 30° Richtung Westen (290°/30°), wobei im Osten der Schenkel durch eine grosse Verwerfung abgeschnitten wurde, was zur Bildung der steilen Felswand Richtung Oberseetal führte [Abb. 2]. Assoziiert mit der grossen Verwerfung trifft man im Untersuchungsgebiet auf eine Vielzahl von Verwerfungen mit Versatzbeträgen von mehreren Metern bis Zehnermetern.

Um einen Zusammenhang zwischen den geologischen Gegebenheiten, v.a. den Einfluss einzelner stratigraphischer Horizonte, und dem Höhlensystem herzustellen, war es nötig, ein möglichst genaues geologisches Modell herzustellen. Diese hohe Genauigkeit war nur dank den guten Aufschlussverhältnisse an der Oberfläche (Karrenfeld sowie der relativ markant ausgeprägten Orbitolinen-Schicht), den Luftbildaufnahmen sowie den geologischen Beobachtungen in den Höhlen möglich. Es kann angenommen werden, dass das geologische Modell über weite Bereiche eine Genauigkeit im Bereich von 5 bis 10 Metern aufweist.

Für die statistische Auswertung musste eine Referenzfläche eingeführt werden. Obschon der Kontakt Schrattenkalk-Drusberg nur am Rande des Untersuchungsgebiets aufgeschlossen ist, wurde diese gewählt. Wo diese nicht aufgeschlossen war, und diesbezüglich auch keine Beobachtungen in den Höhlen gemacht werden konnten, wurde diese von der Oberfläche in die Tiefe interpoliert.

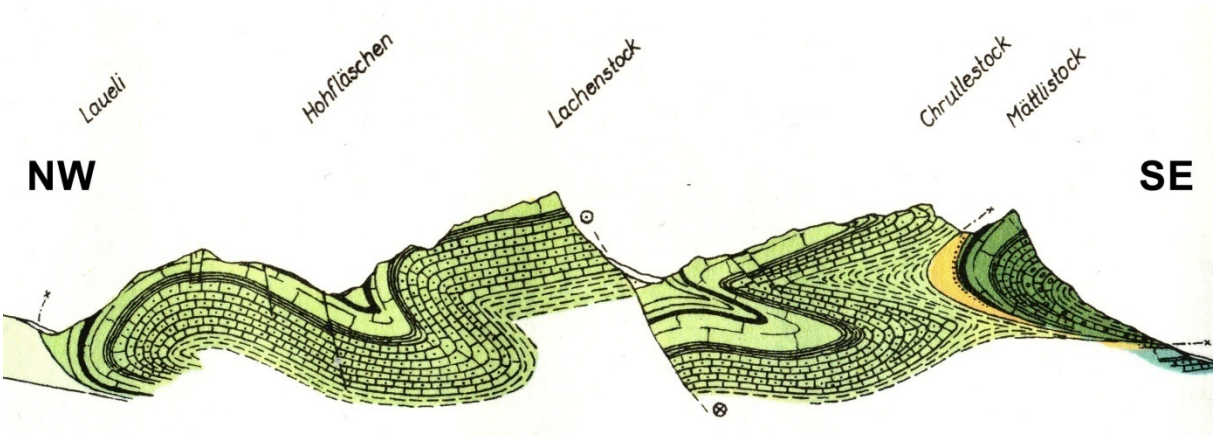

Abbildung 2: Geologisches NW-SE Profil durch das Lachenstockgebiet. Strukturell besteht der Lachenstock aus einem nach Westen einfallendem Antiklinal-Schenkel (aus Hantke 1961).

Die untersuchten Höhlen

Die vorliegende Analyse konzentriert sich auf die drei wichtigsten Höhlen des Lachenstocks [Abb. 3]: Lachenstockhöhle, Plattenloch und Zindlenhöhle.

Lachenstockhöhle *(1740 m ü.M., Länge 5.3 km, Höhenunterschied 193 m)*

Die Lachenstockhöhle ist bis heute die bedeutendste Höhle im Wägital. Die Höhle ist bereits seit den 60er Jahren bekannt. Zwischen 1972 und 1980 wurde durch eine SAC-Gruppe ein Grossteil der heutigen Ausdehnung entdeckt. Die Neubearbeitung durch die OGH geschah ab 1999. Seither wurden mindestens 2 km Neuland erforscht.

Der grossräumige Hauptgang zieht mehr oder weniger gradlinig während rund 800 m in Richtung SE [Abb. 4]. Von diesem zweigt nach rund 450 m der Strudellöchergang in Richtung NE ab, der ausgeprägte phreatische Charakterzüge aufweist (phreatische Gangprofile, Gegensteigungen bis zu 50 m). Erst im letzten Streckenviertel vollzieht der Hauptgang einen markanten Anstieg um 70 m, um bei der T-Junction auf einen NE-SW verlaufenden, horizontalen Höhlengang zu stossen. Sämtliche Fortsetzungen dieses oberen Niveaus zerfasern oder sind mit Sedimenten verfüllt. In die Tiefe enden alle Fortsetzungen in Engstellen oder sonstigen, unüberwindbaren Hindernissen oft in den Drusbergschichten (DICKERT 2001). Im ganzen System existieren zahllose vadose Schacht- und Schlotzonen, welche die alten, phreatischen Gänge kreuzen. Lediglich die Schacht-/Schlotzonen verzeichnen bei Niederschlag oder Schneeschmelze einen bescheidenen Wasserdurchfluss.

Plattenloch K20 *(1927 m ü.M., Länge 1.6 km, Höhenunterschied 208 m)*

Das Plattenloch K20 (DICKERT 2007) besteht aus mehreren vadosen Schacht-Mäander-Serien, die· von der Oberfläche in ein verzweigtes Basissystem führen, von dem wiederum weiter Schächte in die Tiefe fuhren.

Auf -95 m wird die Schichtgrenzfläche Schrattenkalk-Drusberg erreicht. Die Fortsetzung befindet sich vollständig in den Drusbergschichten und ist ein eher kleindimensionierter Mäander, der sich in verschiedene Schachtäste verzweigt.

Zindlenhöhle K10 *(1908 m ü.M., Länge 1.6 km, Höhenunterschied 101 m)*

Die Zindelenhöhle K10 wurde 1979 entdeckt (SENNHAUSER 1982), und über 1 km Ganglänge vermessen. Ab 1999 wurde nach einer Pause die Forschungsarbeit durch die OGH wieder aufgenommen und bei ausgedehnten Neuvermessungen auch einiges an Neuland entdeckt.

Zwei je 25 m tiefe Eingangsschächte führen in ein Netzwerk von horizontalen, relativ geräumigen und ziemlich oberflächennahe verlaufenden Gängen. In den südlichen Höhlenteilen fuhren verschiedene Gänge in tiefere Bereiche und weisen stellenweise labyrinthartigen Charakter auf. Die Höhle besitzt generell einen fossil-phreatischen Charakter mit mässig stark vadoser Überprägung (DICKERT 200 I).

Da bei der Höhlenvermessung durch die OGH grossen Wert auf die Messgenauigkeit gelegt wurde, kann davon ausgegangen werden, dass das 3D Modell des Höhlensystems eine Genauigkeit im Bereich von wenigen Metern aufweist.

Für die statistische Auswertung wurde das Höhlensystem in Segmenten von je einem Meter Länge diskretisiert. Ausserdem wurden die Messpunkte der Höhlenvermessung jeweils an die Höhlengangdecke verschoben, die Richtung und Neigung der Messstrecke zwischen den Messpunkten neu berechnet und anschliessend segmentiert. Jedes Segment(im Folgenden als « Höhlenpunkt » bezeichnet) behielt Angaben über seine Lage, die Gangrichtung und -Neigung.

Das Verschieben der Messpunkte zur Höhlendecke erfolgte als einfache Annäherung der Position des Initials der Höhlengangentstehung.

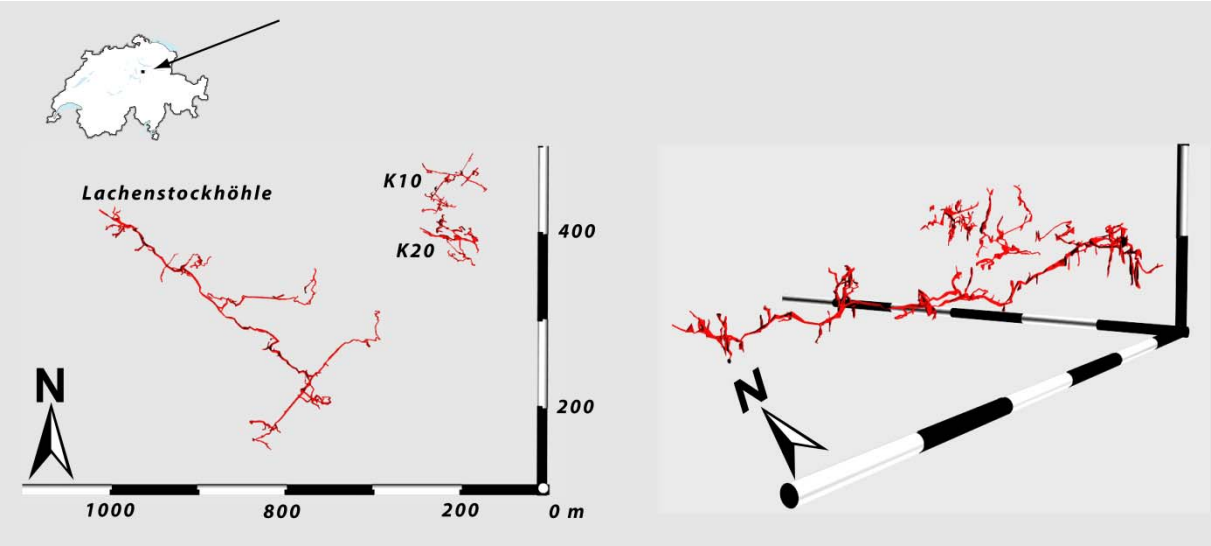

Abbildung 3: *Plan und 3D-Ansicht der Höhlen.*

Abbildung 4: *Grossräumiger, fossil phreatischer Höhlengang in der Lachenstockhöhle (Foto: A. Dickert).*

Einfluss der Geologie auf die Verkarstung des Lachenstocks

Ein verkarstungsfähiges Gebirge kann nicht als homogen betrachtet werden, einerseits gibt es Änderungen in der Lithologie (z.B. leicht mergeligere Lagen, fossilreiche Lagen, Ooid-Lagen, Variation im Mg-Ca-Gehalt, gipsreiche Lagen, Lagen mit Pyrit), anderseits ist das Gebirge mit tektonischen Trennflächen (Klüfte, Verwerfungen) durchzogen. Beide Arten von Inhomogenität spielen eine Rolle bei der Verkarstung (KLIMCHOUK & FORD 2000, FORD & WILLIAMS 2007).

Rolle der tektonischen Trennflächen

Um die Rolle der tektonischen Trennflächen bei der Höhlenentstehung im Lachenstock-Karst abzuschätzen, wurden die Höhlengangrichtungen gewichtet nach der Ganglänge in einem Rosendiagramm dargestellt [Abb. 5]. Im Diagramm treten zwei markante Gangrichtungen zum Vorschein (NE sowie ESE), wobei sich das Gesamtbild nicht wesentlich ändert, wenn nur die vadosen resp. phreatischen Höhlengänge betrachtet werden. Diese Richtungen passen gut zum Streichen der im Luftbild beobachteten und im Feld eingemessenen Klüften und Verwerfungen. Rund 80% der Höhlengänge entwickelten sich entlang dieser beiden Kluftscharen, wobei die ESE Richtung leicht bevorzugt wurde rund 50%.

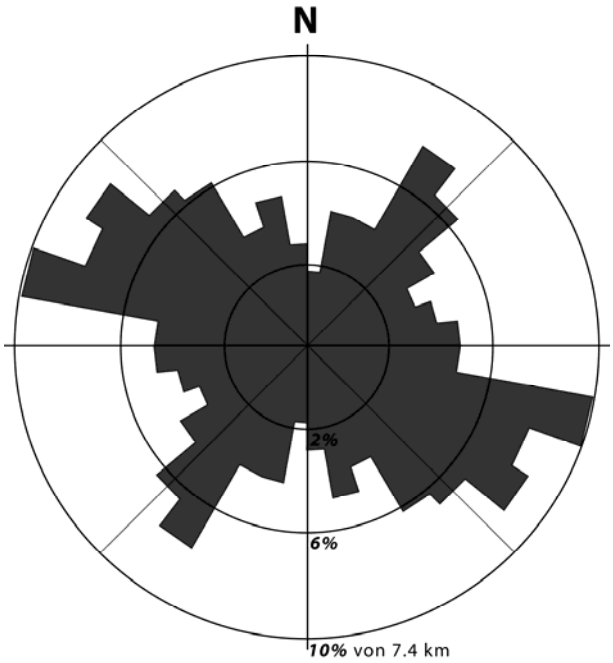

Abbildung 5: *Rosendiagramm der Höhlengänge. Markant treten die zwei Hauptrichtungen (NE, ESE) hervor.*

Rolle der Stratigraphie

Um den Zusammenhang zwischen der Stratigraphie und der Karstentwicklung zu untersuchen wurde in einem ersten Schritt die Anzahl der Höhlengangmeter ermittelt, die parallel zur Schichtung verlaufen. Hierzu wurde für jeden Höhlenpunkt den Winkel (α in Abb. 6) zwischen der Höhlengang-Orientierung und der Normalen zur geologischen Referenzfläche berechnet, und in einem Histogramm der Winkel dargestellt; wobei Höhlengänge die parallel zum Schichteinfallen verlaufen, einen Winkel von 90° aufweisen; senkrecht stehende einen Winkel von 0°.

Histogramm 7/1 zeigt eine markante Häufung an Höhlengängen, die zwischen 80° und 90° zur Normale zur Referenzfläche liegen; also parallel zur Schichtung. Dieses Bild wird noch klarer, stellt man nur die phreatischen Gänge dar (Abb. 7/2), in diesem Fall sind es rund 70%, die parallel sind.

Bereits bei der visuellen Betrachtung des dreidimensionalen Modells des Lachenstock-Karstes ist zu erkennen, dass scheinbar in gewissen stratigraphischen Horizonten vermehrt Höhlengänge vorkommen als in anderen. Um dies zu überprüfen, wurde in einem nächsten Schritt der Abstand (L in Abb. 6) eines Höhlenpunktes zur geologischen Referenzfläche berechnet (resp. zur Basis der Schrattenkalk-Formation). Als Resultat erhält man ein Histogramm der Abstände der Höhlenpunkte zur

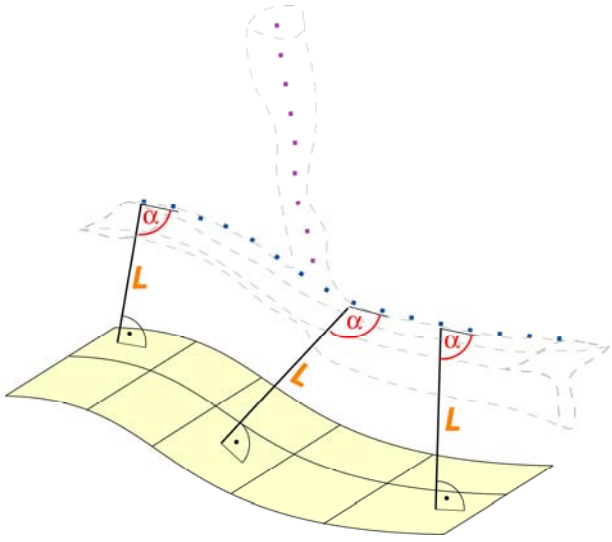

Abbildung 6: *Schematische Darstellungen der Winkel zwischen Normale der geologischen Referenzfläche und dem Höhlengangverlauf (α) sowie des Abstands zwischen Referenzfläche Höhlengang (L).*

Referenzfläche (resp. stratigraphische Position der Höhlenpunkte).

Die Histogramme [Abb. 8] weisen 5 markante Peaks auf, also stratigraphische Horizonte, auf denen vermehrt Höhlengänge vorkommen, In der Lachenstockhöhle sind nur zwei der fünf Horizonte zu erkennen. Dies, weil zum Beispiel die Höhlengänge entlang den fehlenden Horizonten noch nicht entdeckt wurden, oder weil die Gangdimensionen zu klein waren, um sie erkunden und vermessen zu können (Gangdimensionen kleiner als rund 30 cm).

Obschon die Peaks in den Histogrammen rund 10m breit sind, zeigten Feldbeobachtungen, dass es sich bei den bevorzugt verkarsteten Horizonten jeweils um Schichtfugen oder Lagen von wenigen Zentimetern Mächtigkeit handelt. Die Breite der Peaks widerspiegelt die Genauigkeit des 3DModells (Ungenauigkeit des geologischen Modells sowie Höhlenvermessung), jedoch kann angenommen werden, dass der Fehler normal verteilt ist.

Ausserdem zeigten Feldbeobachtungen, dass neben den statistisch relevant bevorzugten Schichten (stratigraphische Initialfugen) noch weitere vorkommen, die jedoch meist nur lokal und nur für wenige Meter die Lage der Höhlengänge beeinflussten.

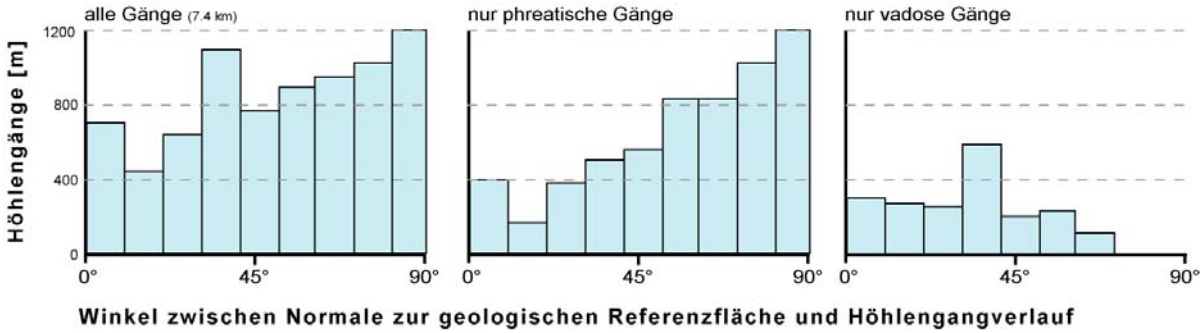

Abbildung 7: Histogramme der Winkel zwischen der Normale zur geologischen Referenzfläche und Höhlengangverlauf. Rund 70% der phreatischen Höhlengänge verlaufen parallel zur geologischen Referenzfläche (resp. orthogonal zu deren Normale; 90°).

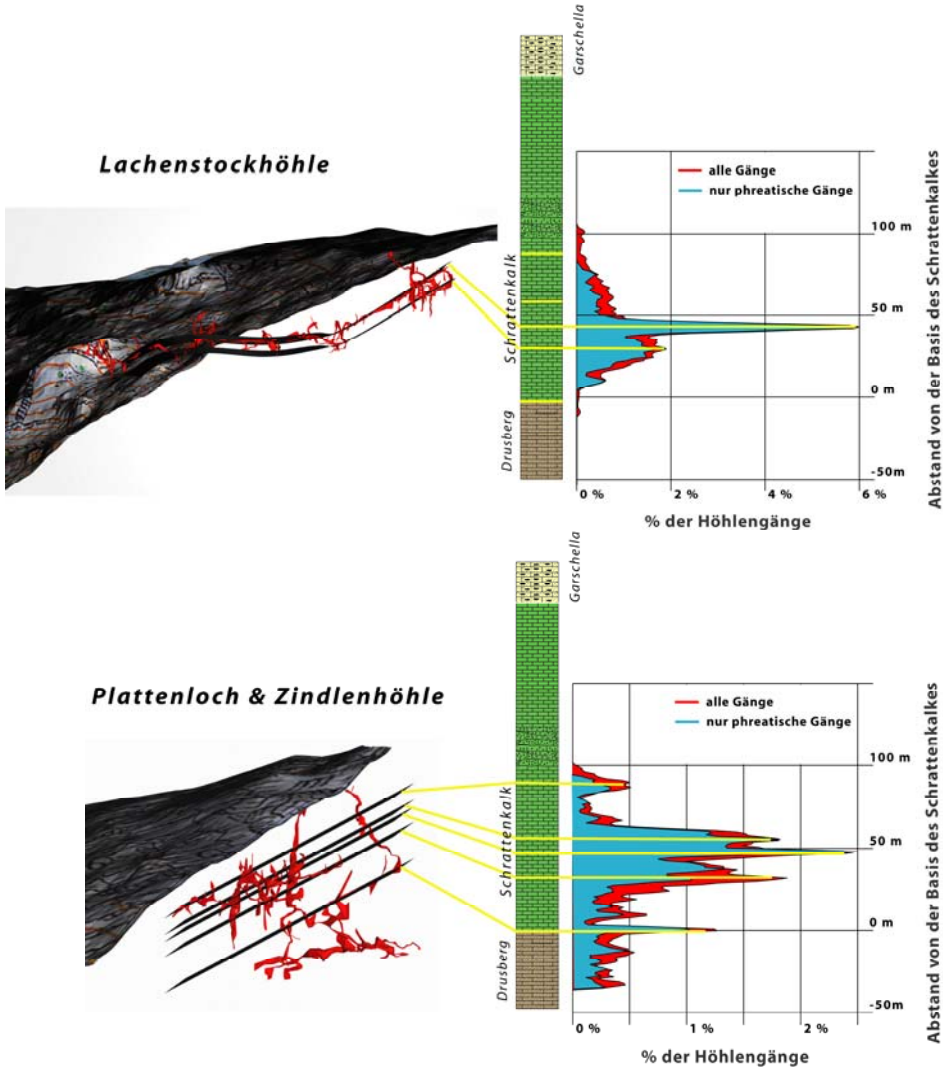

Abbildung 8: Histogramm der Höhlengänge relativ zum Abstand von der Basis der Schrattenkalk-Formation. Die Höhlengänge kommen bevorzugt in 5 stratigraphischen Horizonten vor.

Karsthydrologie des Lachenstocks

Es wird angenommen, dass heute das gesamte verkarstete Gebiet zwischen Schiberg und Schwialppass (also auch das Lachenstock-Gebiet) zu den Karstquellen des Fläschlochs sowie Hundslochs im Talboden des Wägitalersees entwässert (DUERI 1998). Der permanente Karstwasserspiegel liegt demnach heute auf rund 900 m ü.M.. Keine der hier besprochenen Höhlen erreicht diesen Bereich; auch sind keine permanenten Wasserläufe anzutreffen. Hingegen werden bei Niederschlägen oder Schneeschmelze etliche Schachtpartien aktiv. Dennoch weisen die fossilen phreatischen Gänge darauf hin, dass sich die Höhlen mindestens teilweise unter phreatischen Bedingungen gebildet haben.

Die phreatischen Höhlengänge auf verschiedenen Höhlenlagen zeugen von einer mehrphasigen Entwicklung des Lachenstock-Karstes. Um die verschiedenen Phasen zu unterscheiden, wurden eine logisch-visuelle und eine statistische Methode angewendet.

Bei der **logisch-visuellen Methode** wurden die bekannten phreatischen Höhlengänge im dreidimensionalen Höhlenmodell eingefärbt und logisch miteinander verbunden [Abb. 9]. Dies war nicht in allen Regionen gleich gut möglich, da das Höhlenmodell nur die bekannten und vermessenen Höhlengänge beinhaltet und nicht das «wahre» Gesamtbild des Karströhrennetzes. Dennoch war es möglich, zwei unterschiedliche paleo-phreatische Höhlenniveaus zu unterscheiden. Das eine Niveau liegt auf rund 1850 m ü.M. und erstreckt sich vorwiegend in NE-SW Richtung [Abb. 10], während ein zweites auf rund 1750 m ü.M. sich vorwiegend NW-SE orientiert. Es wird vermutet, dass dieser Richtungswechsel mit einem Wechsel des Vorfluterniveaus vom Obersee- ins Wägital zu erklären ist.

Markant ist, dass die phreatischen Höhlengänge nur Gegensteigungen (im Englischen «phreatic loops» genannt) von wenigen Metern bis 10er Metern aufweisen, wohingegen aus ähnlichen alpinen Karstgebieten bedeutet grössere Höhenunterschiede beobachtet bis zu 250 m werden (WORTHINGTON 2003).

Die **statistische Methode** geht von der Beobachtung aus, dass phreatische Höhlengänge oft auf ähnlichen Höhenlagen vorkommen. Es sollte daher möglich sein, mittels Häufigkeitsverteilung der Höhenlagen der Höhlengänge die verschiedenen paleo-phreatischen Höhlenniveaus auszuscheiden.

Die Häufigkeitsverteilung der Höhenlagen der Höhlengänge des Lachenstock-Karstes [Abb. 11] weist zwei deutliche Peaks auf: einen auf rund 1840 und einen auf 1740 m ü.M., was gut mit den visuell bestimmten Niveaus zusammenpasst. Des Weiteren treten noch zwei untergeordnete Peaks auf rund 1800 sowie 1870 m ü.M. auf.

Die Peak-Breite (rund 20 bis 30 m) kommt in diesem Falle nicht durch die Ungenauigkeit des Höhlenmodells zustande (das Höhlenmodell besitzt eine Genauigkeit im Meterbereich), sondern kann als die Gegensteigungen der phreatischen Gänge interpretiert werden, was sehr gut mit den Beobachtungen in den Höhlen zusammenpasst.

Die beiden Methoden führten zu ähnlichen Resultaten. Werden, wie einige Autoren (z.B. BÖGLI 1980, PALMER 1987, AUDRA 1994) vorschlagen, die Höhlenniveaus als die Lage des Karstgrundwasserspiegels betrachtet, würden durch die statistische Methode zwei Phasen zu viel ausgeschieden. Da die vertikale Position eines Höhlenganges nicht nur von der Lage des Karstgrundwasserkörpers abhängt, sondern ebenfalls von der Lage der stratigraphischen Initialfugen, können unter verschieden Konstellationen Höhlenniveaus entstehen, die keinen direkten Zusammenhang mit der Lage des Karstgrundwasserspiegels haben (FILIPPONI et al. 2008). Daher sollte die statistische Methode nur herangezogen werden, um Hinweise über die Lage der Paleo-Karstgrundwasserspiegel zu erhalten, falls diesbezüglich keine oder nur wenige Beobachtungen aus den Höhlen vorhanden sind.

Diskussion und Schlussfolgerung

Die räumliche Analyse der drei zurzeit wichtigsten Höhlen des Lachenstock-Karstgebietes zeigte:

- rund 80 % der Höhlengänge weisen eine Gangrichtung auf, die parallel zu den zwei Hauptkluftrichtungen im Gebiet ist (NE, ESE);
- rund 70 % der phreatischen Höhlengänge verlaufen schichtparallel, wobei 5 stratigraphische Horizonte bevorzugt verkarstet wurden;
- 2 paleo-phreatische Höhlenniveaus konnten ausgeschieden werden, wobei die Höhlengänge des «1750 m ü.M. Niveaus» weitgehend nach ESE orientiert sind und jene des «1850 m ü.M. Niveaus» nach NE.

Diese Resultate führen zu einem konzeptionellen Modell [Abb. I2}, bei dem die Höhlen unter phreatischen Bedingungen bevorzugt am Kontakt Kluftfuge mit einer stratigraphischen Initialfuge; während die regionale

Gangrichtung durch den hydrogeologischen Gradienten bestimmt wird. Nicht alle Schichtfugen sind gleich bevorzugt verkarstet, sondern analog der «Inception horizon» Hypothese können (LOWE 1992, 2000), nur eine diskrete Anzahl von bevorzugt verkarstungsfähigen Schichtfugen vorkommen, so genannten «stratigraphische

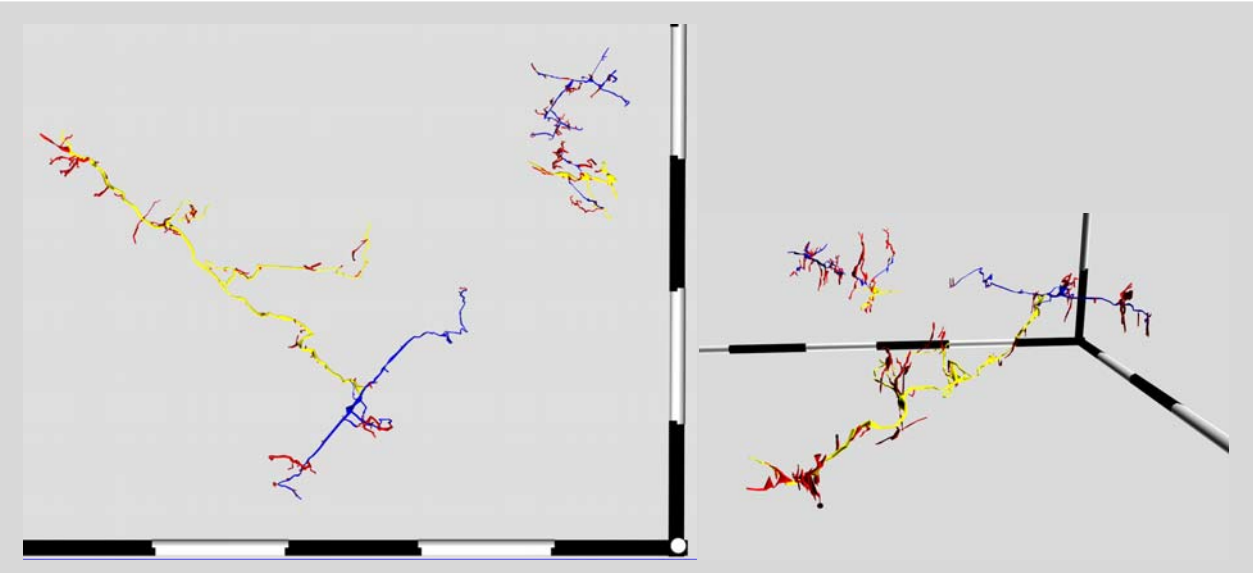

Initialfugen».

Abbildung 9: Mit der logisch-visuellen Methode bestimmtes Netz von phreatischen Gängen. Es konnten zwei Netze von phreatischen Gängen unterschieden werden, eins auf rund 1850 m ü.M. und ein zweites auf 1750 m ü.M..

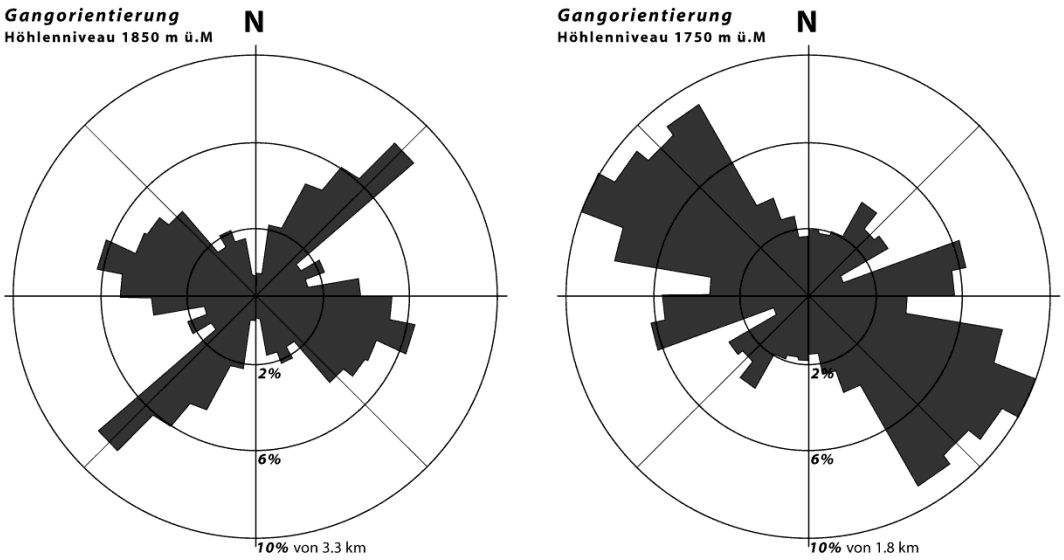

Abbildung 10: Rosendiagramm der phreatischen Höhlengänge des 1850er lind 1750er Niveaus: Während das 1850er Niveau weitgehend NE-SW ausgerichtet ist, dominiert auf dem 1750er Niveau die SE-NE Richtung.

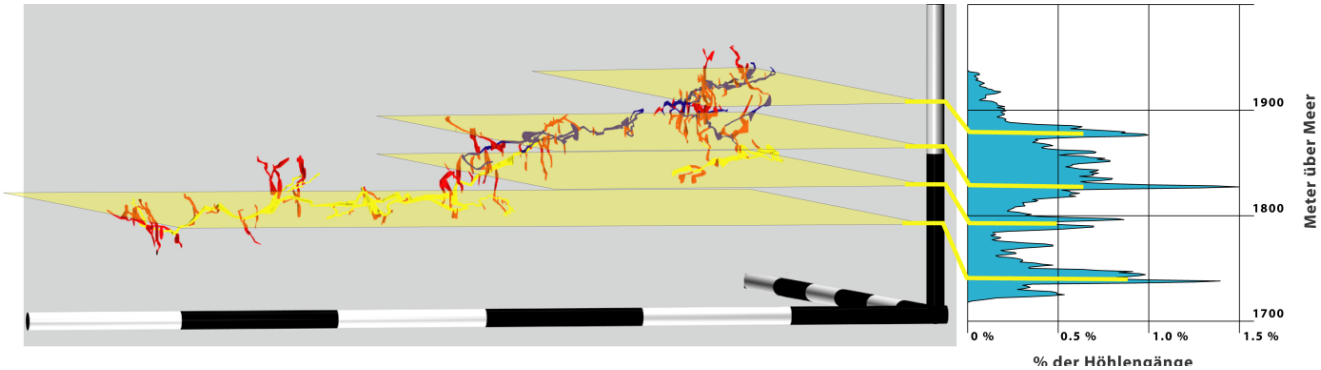

Abbildung 11: Mit der statistischen Methode bestimmte Höhlenniveaus. Das Histogramm zeigt zwei markante Peaks,
die gut mit den visuell bestimmten phreatisc:hen Höhlengang-Niveaus zusammenpassen.

Die stratigraphischen Initialfugen unterscheiden sich von «normalen» Schichtfugen durch ihre bevorzugte Verkarstungsfähigkeit gegenüber dem umgebenden Gebirge. Diese Eigenschaften müssen nicht unbedingt bereits während der Sedimentation oder Diagenese erlangt worden sein (z.B. Gipslagen, Mergellagen, fossilreiche Lagen, Mg-Ca-Gehalt), sondern können auch später während der Initialisierung erworben werden(z.B. Erhöhung der Primärporosität durch Pyrit-Verwitterung). Als die Initialisierung wird jene Zeit zwischen der Diagenese und der Höhlenentstehung (in Englisch development) bezeichnet (LOWE 2000). Während dieser Zeit, die in den meisten Fällen mehrere Millionen Jahre andauern kann, weisen die Lösungshohlräume noch keine bevorzugte Richtung auf. Sie endet mit dem «Durchbruch» (in Englisch breakthrough), bei dem sich das Fliessverhalten im Karströhrennetz drastisch ändern und sich ein gerichtetes Karströhrennetz zu entwickeln beginnt; die eigentliche Höhlenentstehung (DREYBRODT & SIEMERS 2000). Es ist hervorzuheben, dass die Initialisierung und die Höhlenentstehung im selben Gebirge gleichzeitig, jedoch auf verschiedenen Höhenlagen vorkommen können [Abb. 13].

Dies führt uns zu einem vereinfachten speläogenetischem Modell des Lachenstock-Karstes, bei dem fünf verschiedene Phasen unterschieden werden können [Abb. 13]:

- Sedimentation und Diagenese der Schrattenkalk-Formation. Es werden bereits erste Veranlagungen für die spätere Verkarstungen erlangt.
- Während der Initialisierung beginnt entlang der Initalfugen die Verkarstung des Gebirges. Die Verkarstungsprozesse sind sehr langsam und weisen noch eine mehr oder weniger ungeordnete Struktur auf.
- Das Oberseetal hat sich so tief eingeschnitten, dass die Schrattenkalk-Formation aufgeschlossen wird. Es entsteht ein phreatisches Niveau («1850er»), das Richtung Oberseetal entwässert.
- Das Wägital schneidet sich so tief ein, dass es dem Oberseetal das Einzugsgebiet abgewinnt. Es entsteht ein phreatisches Niveau («1750er»), das Richtung Wägital entwässert. Trockenfallen der phreatischen Höhlengänge des 1850er Niveaus.
- Das Wägital schneidet sich tiefer ein und führt zur Bildung einer noch tiefer liegenden phreatischen Phase, deren Höhlengänge jedoch noch nicht entdeckt wurden. Trockenfallen der phreatischen Höhlengänge des 1750er Niveaus.

Die räumliche Analyse des Lachenstock-Karstes erlaubte eine qualitative sowie quantitative Bestimmung des Einflusses der tektonischen und stratigraphischen Trennflächen sowie die Lage des Vorfluterniveaus zum Einzugsgebiet. Dadurch war es möglich, ein erstes speläogenetisches Modell des Lachenstock Karstes zu entwerfen, bei dem die stratigraphischen Initialfugen eine besondere Rolle einnehmen. Als nächste Etappe steht das Verstehen der speläogenetischen Prozesse entlang der

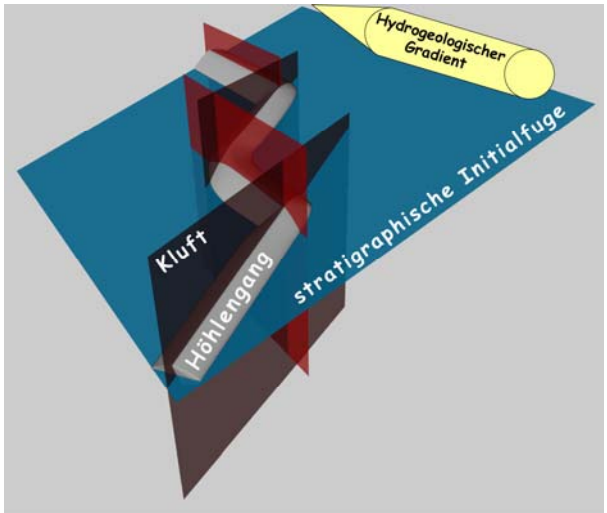

Abbildung 12: Die phreatischen Höhlengänge entwickeln sich bevorzugt entlang dem Kontakt von Klüften mit der stratigraphischen Initialfuge, wobei die regionale Höhlenorientierung durch den hydrogeologischen Gradienten bestimmt wird.

stratigraphischen Initialfugen an, wofür bereits erste Gesteinsproben gesammelt wurden.

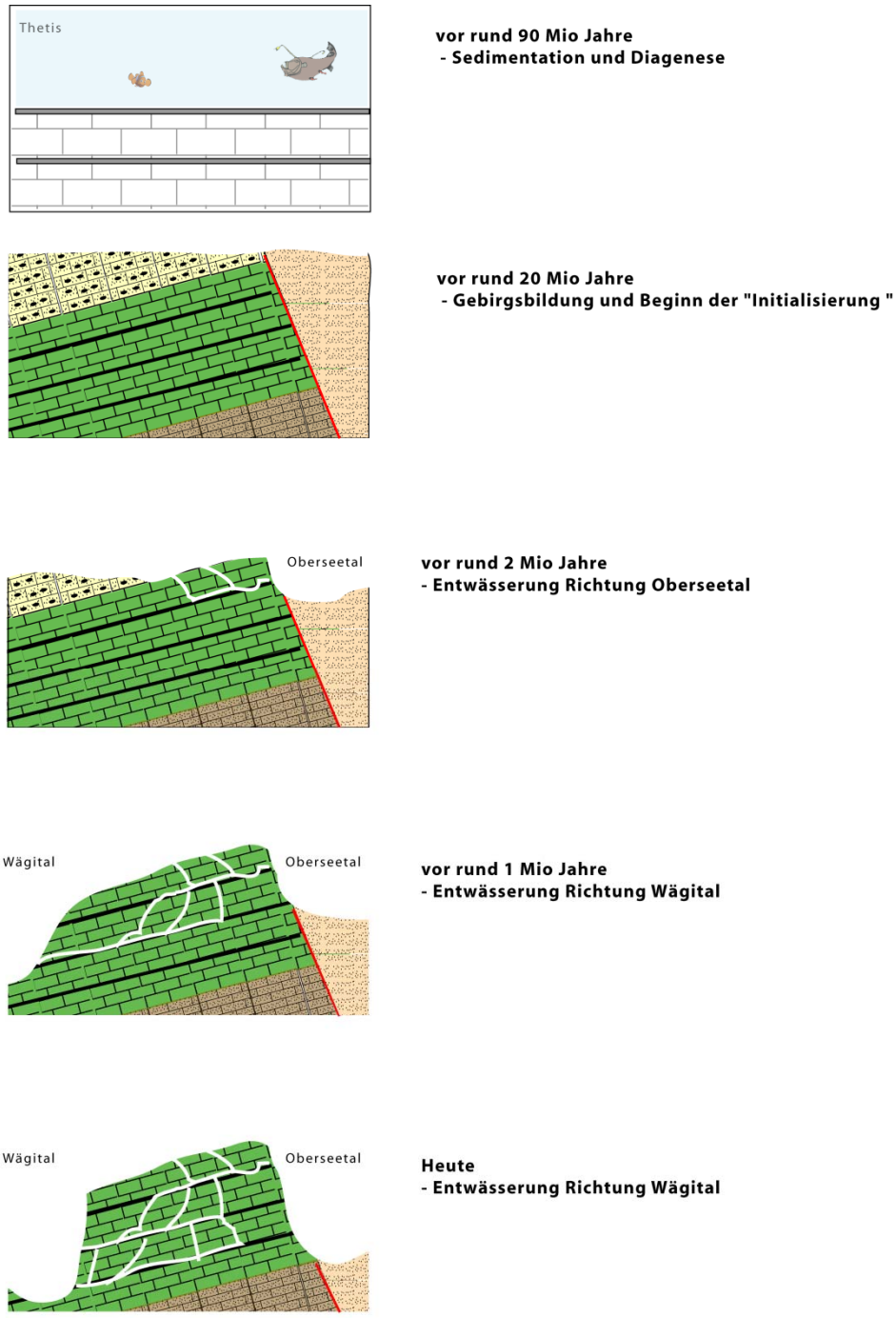

Abbildung 13: Schematische Darstellung der Entwicklung des Lachenstock-Karstes.

Literaturverzeichnis

Audra P. (1994) Karsts alpins. Genèse de grands réseaux souterrains – Exemples le Tennengebirge (Autriche), l'Ile de Crémieux, la Chartreuse et le Vercors (France). Karstologia Mémoires, 5, 280 p.

Bögli A. (1978) Karsthydrographie und physische Speläologie. Springer Verlag, Berlin, 292 p.

Dickert A. (2001) Das Karstgebiet Wägital. Akten des 11. Nationalen Kongresses für Höhlenforschung, Genf, 227-230.

Dickert (2007) Das Plattenloch. Akten des 12. Nationalen Kongresses für Höhlenforschung, Vallée de Joux.

Dueri S. (1998) Das Karstgebiet Wägital – Geologische und hydrogeologische Untersuchungen. Diplomarbeit, ETH-Zürich, 67 p.

Filipponi M., Jeannin P.-Y. (2006) Is it possible to predict karstified horizons in tunnelling? Austrian Journal of Earth Sciences, 99, Wien 24-30.

Filipponi M., Jeannin P.-Y., Tacher L. (2008) Evidence of inception horizons in karst conduit networks. Geomorphology. doi:10.1016/j.geomorph.2008.09.010.

Ford D.C., Ewers R.O. (1978) The development of limestone cave systems in the dimensions of length and depth. Canadian Jour. of Earth Sci., Vol. 15, 1783-1798.

Ford D.C., Williams P. (2007) Karst Hydrogeology and Geomorphology. Wiley-VCH, 576 p.

Dreybrodt W., Siemers J. (2000) Cave evolution on two-dimensional networks of primary fractures in limestone. – In : Klimchouk, Ford, Palmer and Dreybrodt (eds): Speleogenesis, evolution of karst aquifers, 201-211.

Hantke R. (1961) Tektonik der helvetischen Kalkalpen zwischen Obwalden und dem St. Galler Rheintal. Mitteilungen des Geologischen Institutes der ETH und der Universität Zürich, Serie B 16, 210 p.

Klimchouk A., Ford D.C. (2000) Lithologic and Structural Controls of Dissolutional Cave Development. In Klimchouk, Ford, Palmer and Dreybrodt (eds): Speleogenesis, evolution of karst aquifers, National Spelological Society, Huntsville, 60-76.

Lowe D.J. (1992) The origin of limestone caverns: An inception horizon hypothesis. Manchester Metropolitan University, Ph.D. thesis, 512 p.

Lowe D. (2000) Role of stratigraphic elements in speleogenesis: the speleoinception concept. In Klimchouk, Ford, Palmer and Dreybrodt (eds): Speleogenesis, evolution of karst aquifers, 60-76.

Oberholzer, J. (1942) Geologische Karte des Kantons Glarus. Schweizerische Geologische Kommission [Kartenmaterial].

Palmer A.N. (1987) Cave levels and their interpretation. – NSS Bulltin, 49, 50-66.

Schardt H., Meyer H., Ochsner A. (1924) Geologische Karte des Wäggitales und seiner Umgebung 1:25 000. Schweizerische Geologische Kommission [Kartenmaterial].

Schardt H., Meyer H., Ochsner A. (1924) Geologische Profile beiderseits des Wäggitales 1:25 000. Schweizerische Geologische Kommission [Kartenmaterial].

Sennhauser M. (1982) Die Erforschung des K10. Höhlenpost, 31, 16-24.

Worthington S.R.H. (2003) A comprehensive strategy for understanding flow in carbonate aquifer. Palmer A.N., Palmer M.V., Sasowsky I.D. (eds), Karst Modeling: Special Publication 5, The Karst Waters Institute, Charles Town, West Virginia (USA), 30-37, www.speleogenesis.info .

Danksagung

Einen speziellen Dank allen Höhlenforschern, die unermüdlich die Höhlen und Karsterscheinungen des Wägitals erforschen, vermessen und dokumentieren; ohne deren ehrenamtliche Arbeit wäre diese vorliegende Arbeit erst gar nicht möglich gewesen.
Dieses Projekt wurde finanziell durch den Schweizerischen Nationalfonds unterstützt (SNF 200020-116207/1).

Nachtrag

Feldnachweis in der Lachenstockhöhle

In der Schrattenhöhle wurden statistisch 2 Höhlenniveaus identifiziert. Der Feldnachweis bestätigte dieses Resultat und zeigte:

- dass die obere stratigrafische Initialfuge des Typs 3 ist (bedding plane fracture) mit einem neotektonischen Versatz von einigen Zentimetern [Abb. 14];
- dass die untere stratigrafische Initialfuge des Typs 1 ist (Initialisierung im Horizont) [Abb. 15]. An einigen Stellen konnte Höhlengips gefunden werden und geprobt werden (siehe Kapitel 3 dieser Dissertation).

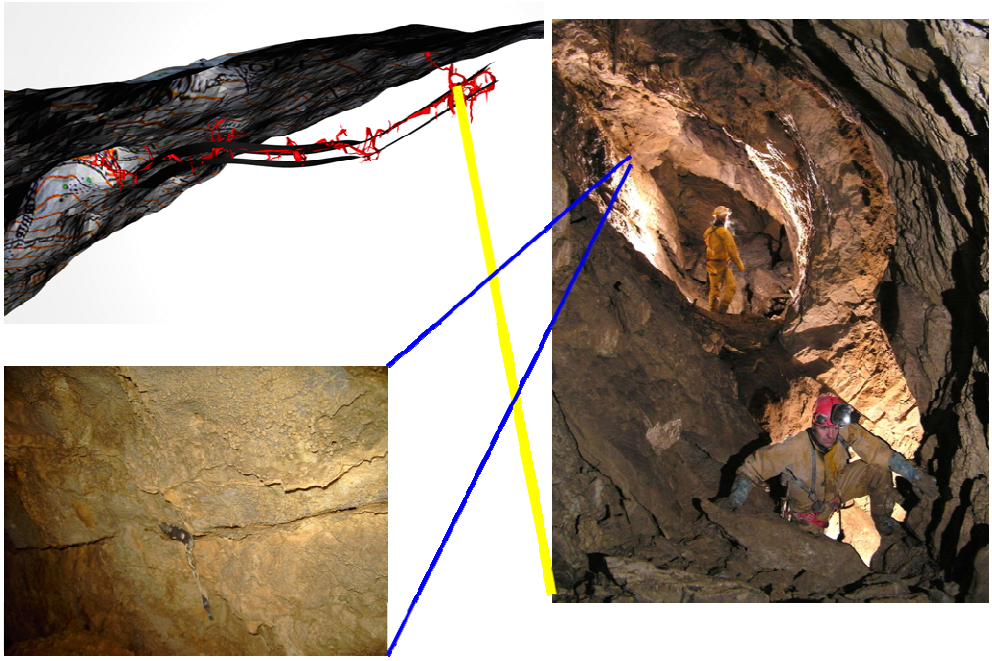

Abbildung 14: Feldnachweis des der Existenz der statistisch identifizierten oberen stratigrafischen Initialfuge Lachenstockhöhle. Initialfuge des Typs 3. (Foto: A. Dickert)

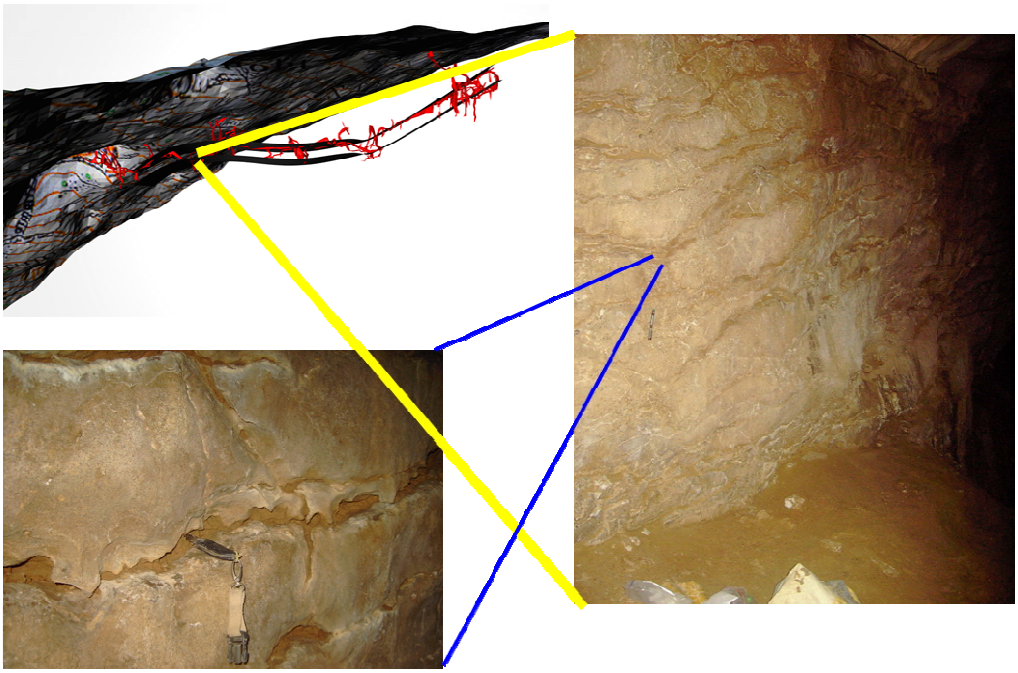

Abbildung 15: Feldnachweis des der Existenz der statistisch identifizierten unteren stratigrafischen Initialfuge in der Lachenstockhöhle. Initialfuge des Typs 1.

AUSTRIAN JOURNAL OF EARTH SCIENCES
[MITTEILUNGEN DER ÖSTERREICHISCHEN GEOLOGISCHEN GESELLSCHAFT]

AN INTERNATIONAL JOURNAL OF THE AUSTRIAN GEOLOGICAL SOCIETY

VOLUME 99 2006

www.univie.ac.at/ajes

EDITING: Grasemann Bernhard, Wagreich Michael

PUBLISHER: Österreichische Geologische Gesellschaft
Rasumofskygasse 23, A-1031 Wien

TYPESETTER: Copy-Shop Urban,
Lichtensteinstraße 13, 2130 Mistelbach

PRINTER: Holzhausen Druck & Medien GmbH
Holzhausenplatz 1, 1140 Wien

ISSN 0251-7493

Is it possible to predict karstified horizons in tunneling?

Marco FILIPPONI[1)*)] & Pierre-Yves JEANNIN[2)]

[1)] GEOLEP, Laboratoire de géologie de l'ingénieur et de l'environnement, Ecole Polytechnique Fédérale de Lausanne (EPFL), Switzerland, marco.filipponi@epfl.ch

[2)] SISKA, Swiss Institute of Speleology and Karstology, Switzerland

[*)] Corresponding author, present address: ENAC ICARE GEOLEP, Station 18, CH-1015 Lausanne, Switzerland, fax: 0041 (0)21 693 63 30, marco.filipponi@epfl.ch

KEYWORDS

prediction of karst conduits
spatial distribution
inception horizons
speleogenesis
tunneling

Abstract

Predicting the position of karst voids for tunnel construction is very important, since they induce economic, social, security-related and environmental problems. Here it is quantitatively show that the development of karst conduits under phreatic conditions is strongly related to a restricted number of so-called inception horizons, related to geological parameters. Thus predicting the position of potential inception horizons (that is, karst conduits) is possible. This is of great interest for engineering geological purposes.

Die Vorhersage der Lage von Karsthohlräumen ist bei Tunnelbauprojekten von großer Bedeutung, da die räumliche Ausdehnung und Orientierung von Hohlräumen zu wirtschaftlichen, gesellschaftlichen, sicherheits- und umweltrelevanten Problemen führen können. Wir konnten quantitative zeigen, dass die Entwicklung von phreatischen Karströhren an so genannten „inception horizons“ gebunden ist. Daher wäre es möglich die Position dieser bevorzugt verkarsteten Horizonte (respektive Karsthohlräume) vorherzusagen, was für ingenieurgeologische Belangen von großem Interesse ist.

1. Introduction

Many recent tunnel constructions in Switzerland (e.g. Sauges Tunnel, Engelberg Tunnel, Flims Tunnel and Alpnach Tunnel) have shown that any uncertainties in the geology of the rock-volume being tunnelled through, including those related to karst processes, is a major issue, since they may lead to economic, social, security-related and environmental problems. Despite this, the prediction of karstic dissolution voids currently lacks a scientific background. Although methods for the detection of such voids a few meters in front of tunnel working faces are being developed (e.g. Pesendorfer & Loew, 2004), no method for their prediction at a more regional-scale is available.

Research carried out by karst scientists during the last 30 years shows that the development of dissolution voids is not random (Kiraly, 1968; White, 1970; Waltham, 1971; Palmer, 1989; Klimchouk & Ford, 2000). However, most efforts have been dedicated to the understanding of the processes and, in particular, the time-scale at which dissolution voids can develop. Only a very restricted number of studies (Palmer, 1989; Lowe, 2000; Klimchouk & Ford, 2000) have attempted to analyse and understand the geometry of dissolution voids (karst conduits in most cases), to provide keys for the prediction of conduit positions, orientations and characteristics.

A rough prediction of the position of karst conduits can be made by tracing experiments. However, although the map produced by Quinlan and Ray (1981) is a well-known example of this type of prediction, it was drawn in 2D (plan view) and was very imprecise, having an accuracy of only ± 500 m. Further, it was based on hundreds of tracing experiments and thousands of borehole data, neither of which are practical during a tunnelling project.

An alternative way to address this problem is to study the hydrogeological conditions that prevailed during the karstification of a rock mass. Such studies measure the fracture characteristics (mainly their frequency and orientation) from which conduit directions were derived (Kiraly, 1968; Jamier & Siméoni, 1979; Eraso & Herrero, 1986; Blanc & Nicod, 1990). However, in many cases the authors did not consider the coupling of hydraulic conditions in the speleogenetic process and their methods were limited to descriptions of the relationship between the geological parameters (mainly fractures) and the known conduit directions. Since the influence of non-geological boundary conditions (mainly the respective positions of the recharge areas and the springs) is at least as significant as that of the geology, it was not possible to fully establish and quantify the control that fractures had in the development of the karst conduit networks. Consequently, this type of approach has a very limited capacity to predict conduit positions.

Numerical modelling has also been used to examine karstification processes. This included the atypical kinetics of calcite dissolution as well as the change of flow conditions, from laminar to turbulent, as the conduit size increased (Dreybrodt & Siemers, 2000). Such models allow hypotheses to be verified and synthetic karst systems to be generated using a range of initial and boundary conditions. However, so far, they have not often been used for conduit geometry prediction, but rather for the assessment of the time duration over which conduits develop. Hence the high uncertainties inherent in predictions of the position of karst conduits have not diminished significantly in the last 30 years.

Examination of published material revealed interesting information about the position of conduits. Rauch & White (1970), Waltham (1971) and later Palmer (1974, 1975, 1989) combined detailed observations of caves and their geological contexts to suggest that caves develop along a restricted number of bedding planes within a limestone series. Although this idea is still adopted in more recent publications (Lowe, 1992, 2000; Osborn,

1999; Klimchouk & Ford, 2000), no qualitative evidence of the existence of such inception horizons, these being the discrete planes within a rock mass that are favourable to karstification, has been documented. Nevertheless, a method which demonstrates the existence of inception horizons has been outlined in this paper. Further, by applying the technique to several case-studies, it has been possible to prove their existence and to quantify their significance. Essentially, it is now possible to quantify the probability of karst occurrences inside a karst massif by reconstructing the hydrogeological history and identifying inception horizons.

2. Methods

On the assumption that karst conduits develop along discrete preferred surfaces within a carbonate mass, then such surfaces (inception horizons) will be either bedding planes or fractures such as joints and faults. If so, then the space close to these surfaces should be more densely occupied by conduits than the remainder of the rock-mass. In other words, the spatial distribution of conduits should be neither uniform nor random, but rather should follow a systematic 3D structure. The geometry of this structure will depend on the hydraulic conditions that prevailed during the development of the karst as well as on the 3D pattern of inception horizons, which, in turn, is a function of the geology.

To analyse the complex geometry of cave systems in 3D, a software tool has been developed which provides a statistical analysis of the relationships between the conduit network geometry, the geological setting and the hydrogeological context of a large cave system. The software determines the shortest distance between a conduit segment and a reference geological surface (in most cases a 3D representation of the bottom of the limestone series) and calculates the distribution as a histogram of cave segments in relation to their distance from the reference horizon. Inception horizons, being horizons where karst development is concentrated, appear as peaks in the histogram, representing preferred distances from the reference horizon (Fig. 1).

To use the program, 3D models of both the cave system and the geology are required; the quality of the models directly influences the precision at which inception horizons can be defined. For instance, a high degree of precision is required to define whether conduits developed along a particular bedding plane in all respective compartments offset by faults. To obtain the necessary precision, geological models should be based on digital terrain models, geological maps and descriptions, air-photo interpretations and observations in the cave systems. The 3D models of the caves are computed from cavesurvey data. The software also calculates the distribution of conduits (cumulate length) with respect to the elevation. This is useful for identifying the various evolutionary stages of the cave system (Palmer, 1987). Once statistically identified as having being highly karstified, these particular bedding planes must be verified by field observations.

3. Results

The analysis described above has been applied to a number of large cave systems from all over the world (Table 1). The systems analysed had several specific properties:

- The explored and surveyed conduit networks have a sufficient minimum length (at least 5 km).
- The systems represent various geological settings (lithology, tectonics, age, etc.). However, the analysis was limited to cave systems in limestone and/or dolomite formations.
- The caves were formed only by meteoric water, without or with only a negligible hypogenic origin (hydrothermal or acidic gas).
- Evolution of the systems took place, at least partly, under phreatic conditions. This is very important, because only conduits developed under phreatic conditions reflect the initial state of cave development.

For these examples, the observed distribution of karst conduits is neither random nor homogeneous but controlled at the regional scale by a limited number of discrete bedding planes and hydrogeological boundary conditions. This documents statistical evidence of the inception horizon hypothesis of Lowe (1992). The number of horizons in the limestone and dolostone sequences studied varied between two and seven.

In contrast to Davies (1960), who postulated that the angle of dip of bedding planes is a key factor in cave development, the present study found no evidence for such a relationship. In all cases, a strong bedding plane bounded network of phreatic karst conduits, independent of the local dip of the bedding, has been found. However, the flow may follow the dip or strike of bedding planes, depending on the prevailing hydrogeological boundary conditions (i.e. recharge/discharge zones).

Further, the data indicates that joints and faults are responsible for the local position and orientation of the conduits within (or along) inception horizons. That is, statistically, most conduits lie at the intersections of joints and bedding planes (Fig. 2).

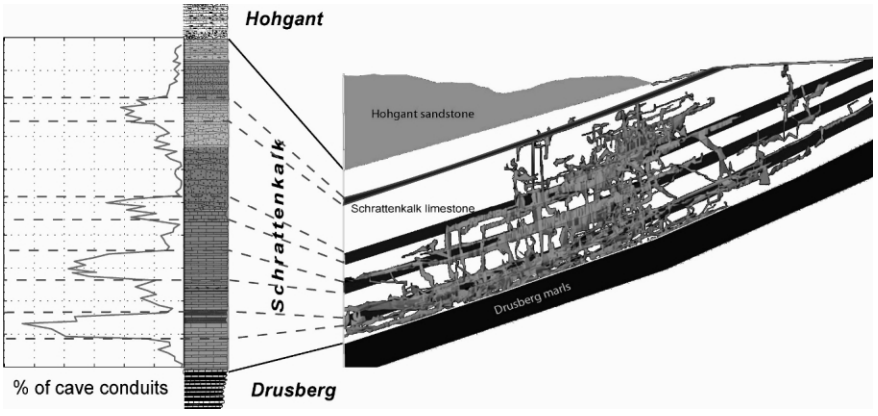

Figure 1: Projection of one part of the Siebenhengste cave system. Four potential inception horizons can be identified within the Schrattenkalk limestone, which is nearly 180 m thick.

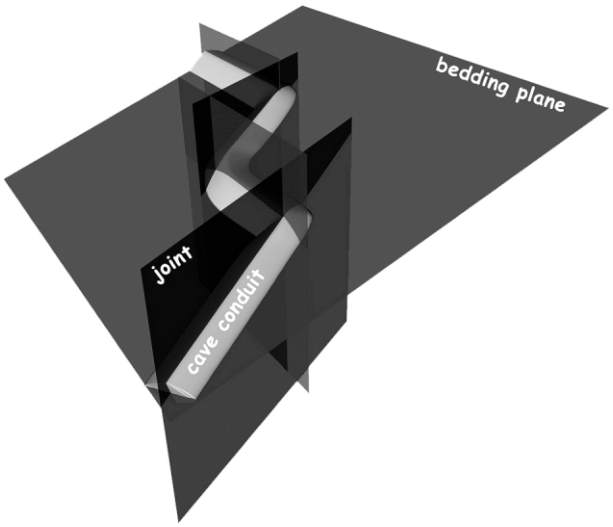

Figure 2: Schematic representation of the role of joint sets and bedding plane for the position and orientation of cave conduits.

In most cases, inception horizons correspond to bedding planes and often the former can be easily recognised in caves. For example, anastomoses (a network of branching, intersecting, and rejoining channels in a two dimensional system; Slabe, 1995) are frequently developed along such preferential planes (Fig. 3). Anastomoses, which are generally formed through dissolution by slow, poorly directed phreatic flows along a discontinuity, represent an important element in the early stages of cave development and are best described as protoconduits. Most protoconduits are abandoned during the later stages of conduit development, when one conduit offers better flow conditions, such that it increases in size at the expense of the others. Anastomoses are evidence of preferential karstification along a given bedding plane; that is, of an inception horizon.

From our field observations as well as from published data (Lowe, 2000) several reasons can be postulated for a bedding plane becoming a potential inception horizon. These reasons apply only partially to fault planes.

- Increased initial permeability. In bulk carbonate sequences, bedding planes may provide the first possible water routes because of a slightly higher primary permeability than the adjacent rock mass.
- Aquicludes. Some bedding planes (e.g. shaly ones) are more impervious (lower permeability) than the surrounding rock mass. They act as aquicludes, and force water to flow at the contact zone with the adjacent carbonate (flow concentration).
- Turning non-aggressive water into corrosive solutions. The weathering of certain minerals, such as sulphides, can produce acidic solutions, which can at least locally increase the dissolution capacity. Such an additional acidic dissolution has a minimal effect in the context of the later stages of passage formation, but its contribution to the initial permeability development of a bedding plane can be significant.
- An increase of the primary porosity of the bedding planes is also possible, through the dissolution of highly soluble minerals such as gypsum, or related to a change in mineralogy as for example dolomitization or dedolomitization, or slight changes in the calcite chemistry (such as high/low magnesium calcite) which strongly affects the mineral stability, or by tectonic slip along the bedding plane.

Note that only a small proportion of the bedding planes present in a carbonate sequence seems to be favourable to karstification; most bedding planes play no significant role in karst development.

4. Case study: the Nidlenloch, Switzerland

The approach used for the examples described in Table 1 is illustrated here in detail with a case-study of Nidlenloch (Switzerland).

4.1 Regional context

The Nidlenloch (length 7,000 m, difference in elevation 420 m; explored by the Arbeitsgemeinschaft Nidlenlochforschung) formed in well bedded oolitic sparitic limestones (Malm) on the northern flank of the Weissenstein anticline, north of Solothurn, in Switzerland. The bedding orientation is essentially constant (092/50° N) and no major faults offset the limestone beds (Fig. 5).

Cave passages follow either the dip of the bedding planes toward the north, or the east-west strike of the beds. A horizontal network of partially labyrinthine passages has been recorded in the central part of the cave. Other parts of the cave also have typical phreatic passage networks. Currently, the cave is traversed by very local or temporary streamlets, which barely contribute to the current karst drainage. Nevertheless, three different palaeophreatic stages have been distinguished (Fig. 4). The first stage, located at ca. 1,200 metres above sea level (a.s.l.), flowed mainly in an W-E direction. The second stage, at ca. 1,100 metres

Figure 3: Anastomosis in the Nidlenloch cave system. (Photo: Mirjam Widmer)

a.s.l. had the same main direction whilst the third phreatic stage, at ca. 950 metres a.s.l, had a predominantly SE-NW flow direction. This change of flow direction was caused by the evolution of the valleys at the surface and, related to this, changes in the hydrogeological boundary conditions. It has been noted that the phreatic conduits of each stage makes loops in the order of some tens of metres of elevation.

Conduits of modest dimensions are often interrupted by breakdown, or low points filled with clay, which reflect the advanced age of the cave. Despite the significant depth of the cave, pits are rare and their depth does not exceed 20 metres. No larger chambers and only rare flowstone speleothems have been found.

4.2 Statistical evidence of the existence of inception horizons

A histogram of the distance of the karst conduits to a geological reference horizon clearly shows some obvious peaks (Fig. 6), indicating that the cave passages are not distributed randomly within the limestone mass, but lie at discrete horizons more favourable to karstification. The peaks indicate that Nidlenloch essentially developed at four stratigraphic horizons; these account for ca. 80% of the surveyed cave conduits.

A stereographic projection of conduit orientations shows that the majority are located in the northern hemisphere and more-or-less lie on the great circle representing the bedding-plane orientation. Two other preferred directions (E-W, N-S), which correspond to two sets of joints, have been identified and can also be seen on a plan view of the cave (Fig. 4).

This analysis indicates that the cave developed mainly at four stratigraphic horizons, along which the conduits followed the intersection of the bedding plane with two predominant joint sets. The direction of conduit development was determined by the hydrogeological context. This was confirmed by a computer generated 3D visualisation of the cave network.

Name of the cave System	Country	Length [m]	Depth [m]	Litology	Number of inception horizons
Mammoth Cave System	Kentucky, United States	579.400	115	Limestone	5
Hölloch & Silbernsystem	Schwyz, Switzerland	192'000 & 37'700	940 890	Limestone	3-4
Siegenhengste-Hohgant Höhlensystem	Bern, Switzerland	171.000	1340	Limestone	5-7
Shuanghedongqun	Suiyang, China	102.000	370	Dolomite and dolomitic limestone	2
Hirlatzhöhle Dachstein	Oberösterreich, Austria	92.940	1010	Limestone	6-7
Ogof Draenen	South Wales, United Kingdom	66.100	100	Limestone	3
Dachstein-Mammuthöhle	Oberösterreich, Austria	65.800	1200	Limestone	4-5
Schwarzmooskogel-Höhlensystem	Oberösterreich, Austria	56.400	1030	Limestone	6-7
Schrattenhöhle & Bettenhöhle	Obwalden, Switzerland	19.650	575	Limestone	2
Réseau des Grottes aux Fées & Grotte de l'Orbe	Vaud, Switzerland	7000 & 6000	135 115	Limestone	3
Hölloch im Mahdtal	Allgäu, Germany	9.300	460	Limestone	3
Wägital Lachenstock, K10, Plattenloch	Schwyz, Switzerland	9.000	270	Limestone	5
Nidlenloch	Solothurn, Switzerland	7.000	420	Limestone	4
Réseau de Covatannaz	Vaud, Switzerland	4.450	105	Limestone	2

Table 1: List of analysed cave systems with the number of statistically identified inception horizons.

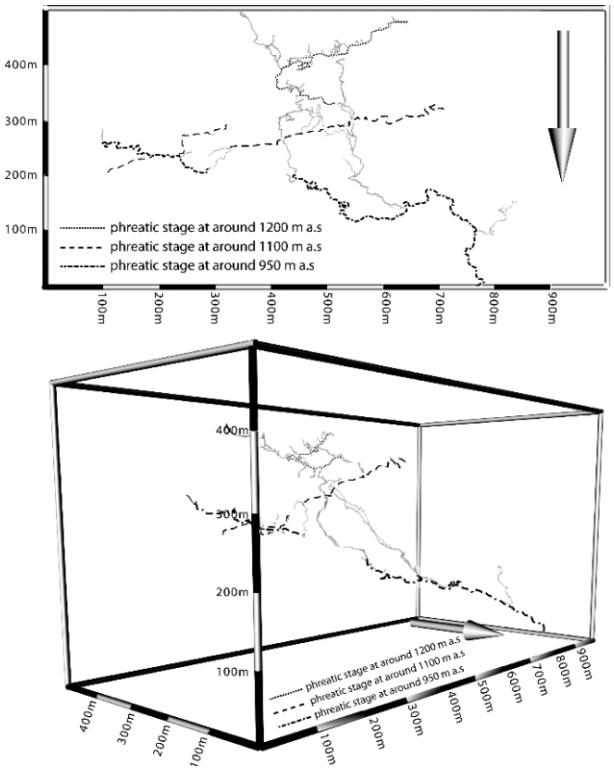

Figure 4: Plan and 3D views of the Nidlenloch: the three different palaeophreatic stages are shown in dashed lines (arrow shows to north).

4.3 Field verification of the inception horizons

Field investigations in the cave confirmed the existence of inception horizons at the positions derived from the cave geometry analysis (Fig. 6). Although the favourable horizons appear in the histograms as peaks of five to 15 metres thickness, in the field they occur along single bedding planes, with a thickness in the order of centimetres to decimetres. This difference is caused by uncertainties in the position of the geological reference surface (± 5 m), in the cave survey (± 5 m) and in the position of the bedding plane within the cave conduit profile (up to ± 2 m).

Detailed observations of the horizons indicated some possible reasons why those specific bedding planes were favourable to karstification. At two horizons, shearing has occurred along the bedding plane after conduit development; probably some shearing also occurred before or during conduit formation. Remarkably, flowers and needles of gypsum have been observed along or nearby the inception horizons. This implies the production of H_2S or possibly H_2SO_4, since the gypsum was probably derived from pyrite. At this stage, however, it is not possible to asses the role of these parameters or even to be sure that they played a significant role in preferential karst development along these horizons.

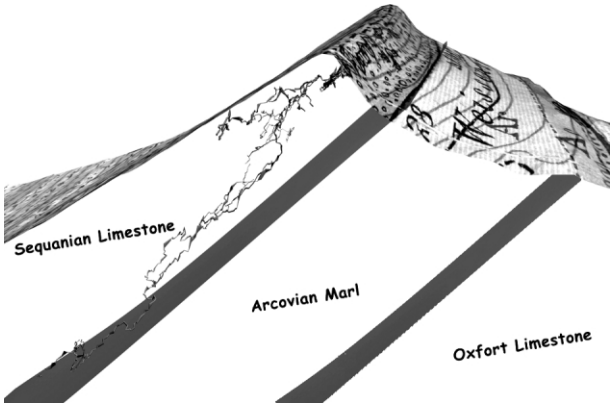

Figure 5: Simplified geology of the Nidlenloch area, with a 3D view of the cave (line of sight towards the NE).

The case-study results have been compared with observations in the nearby Weissenstein railway tunnel, constructed in 1908, which is 3.7 kilometres long and crosses the Wissenstein anticline at around 700 metres a.s.l.. Although the tunnel walls are now concrete-lined, documentation of the tunnel construction (Buxtorf, 1908) indicates that the tunnel crossed karst conduits three times. These were filled with sediments, with only a minor water-flow and once a larger spring, with a discharge of around 80 l/s, was encountered. The stratigraphic positions of these occurrences correspond quite well with the favourable karst horizons determined from analysis of the Nidlenloch cave system geometry.

5 Discussion and Conclusions

An analysis of 14 of the largest cave systems in the world demonstrates that the development of karst conduits under phreatic conditions is strongly related to inception horizons. This is the first clear indication that it is possible to quantify the degree of conduit concentration along such inhomogeneities.

The position of inception horizons can be predicted by documenting the specific properties of bedding planes, as well as of valley and cave evolution. Up to now, a rough idea of the relevant properties of inception horizons has been determined; both tectonic slip along bedding planes and the presence of pyrite are probably significant factors in their development.

Although data from other sites seems to confirm this hypothesis, it is not yet clear if these factors would also apply in other limestone series and other karstification conditions. Consequently, the prediction of karst occurrences remains very challenging.

Compared to the usual 2D analyses of cave systems (e.g. vertical distribution of conduits in order to identify cave levels or plan views to work out the relationship between cave development and fractures) our 3D analysis allowed us to couple the geological and hydrogeological contexts. This has shown that caves evolved along a restricted number of discrete stratigraphic horizons, at which the conduits followed the intersection of the bedding plane with the predominating joint sets. Nevertheless, the main direction of the conduits was determined by the hydrogeological context. On-going studies will likely provide a clear improvement in the prediction of voids in karst massifs, which is especially important for tunnelling or dam construction.

Acknowledgements

This project was supported by the Swiss National Foundation for Scientific Research (project number 200021-105280). Special

thanks are due to the cavers who explored and mapped the cave systems and provided us with their survey data for analysis.

References

Blanc, J.-J. and Nicod, J. 1990. Les surface karstiques du plateau de Montrieux (Var), (secteur de Valbelle-Morières-Siou Blanc), étude quantitative de la fracturation. Karstologia 16, 17-28.

Buxtorf, A. 1908. Geologische Beschreibung des Weissensteintunnels und seiner Umgebung – Beitrag zur geologischen Karte der Schweiz: Geologische Karte des Weissensteintunnelgebietes 1:25,000. Schweizerische Geologische Kommission, Winterthur, 160 pp.

Davis, W. E., 1960. Origin of Caves in Folded Limestone. Bulletin National Speleological Society of America 22, 3-18.

Dreybrodt, W. and Siemers, J. 2000. Cave evolution on two-dimensional networks of primary fractures in limestone. In: Klimchouk, A., Ford, D., Palmer, A. N. and Dreybrodt, W. (eds): Speleogenesis, Evolution of Karst Aquifers. National Speleological Society, Huntsville, 201-211.

Eraso, A. and Herrero, N. 1986. Propuesta de un Nuevo metodo de deduccion de las direcciones principales de drenaje en el karst. Jumar, Madrid, 93 pp.

Jamier, D. and Siméoni, G. P. 1979. Etude statistique de la distribution spatiale des éléments structuraux dans deux massifs des Alpes helvétique. Conséquences pour l'hydrogéologie karstique. Bulletin centre d'hydrogéologie, Université de Neuchâtel 3, 1-26.

Kiraly, L. 1968. Eléments structuraux et alignement des phénomènes karstiques (région du gouffre du Petit-Pré de St-Livres, Jura vaudois). Bulletin la Société des Sciences Naturelles de Neuchâtel 91, 127-146.

Klimchouk, A. and Ford, D. 2000. Lithologic and structural controls of dissolutional cave development. In: Klimchouk, A., Ford, D., Palmer, A. N. and Dreybrodt, W. (eds): Speleogenesis, Evolution of Karst Aquifers, National Speleological Society, Huntsville, 54-64.

Lowe, D. 1992. The origin of limestone caverns: an inception horizon hypothesis. PhD thesis, Manchester Polytechnic, UK, 511 pp.

Lowe, D. 2000. Role of stratigraphic elements in speleogenesis: the speleoinception concept. In: Klimchouk, A., Ford, D., Palmer, A. N. and Dreybrodt, W. (eds): Speleogenesis, Evolution of Karst Aquifers, National Speleological Society, Huntsville, 60-76.

Osborne, R. A. 1999. The inception horizon hypothesis in vertical to steeply dipping limestone: applications in New South Wales, Australia. Cave and Karst Science 26, 5-12.

Palmer, A. N. 1974. Geologic influence on cave passage orientation in Ludington cave, Greenbarrier County, West Virginia. Proceedings of the West Virginia 4th Conference on Karst Geology and Hydrology, West Virginia Geological Survey, 33-40.

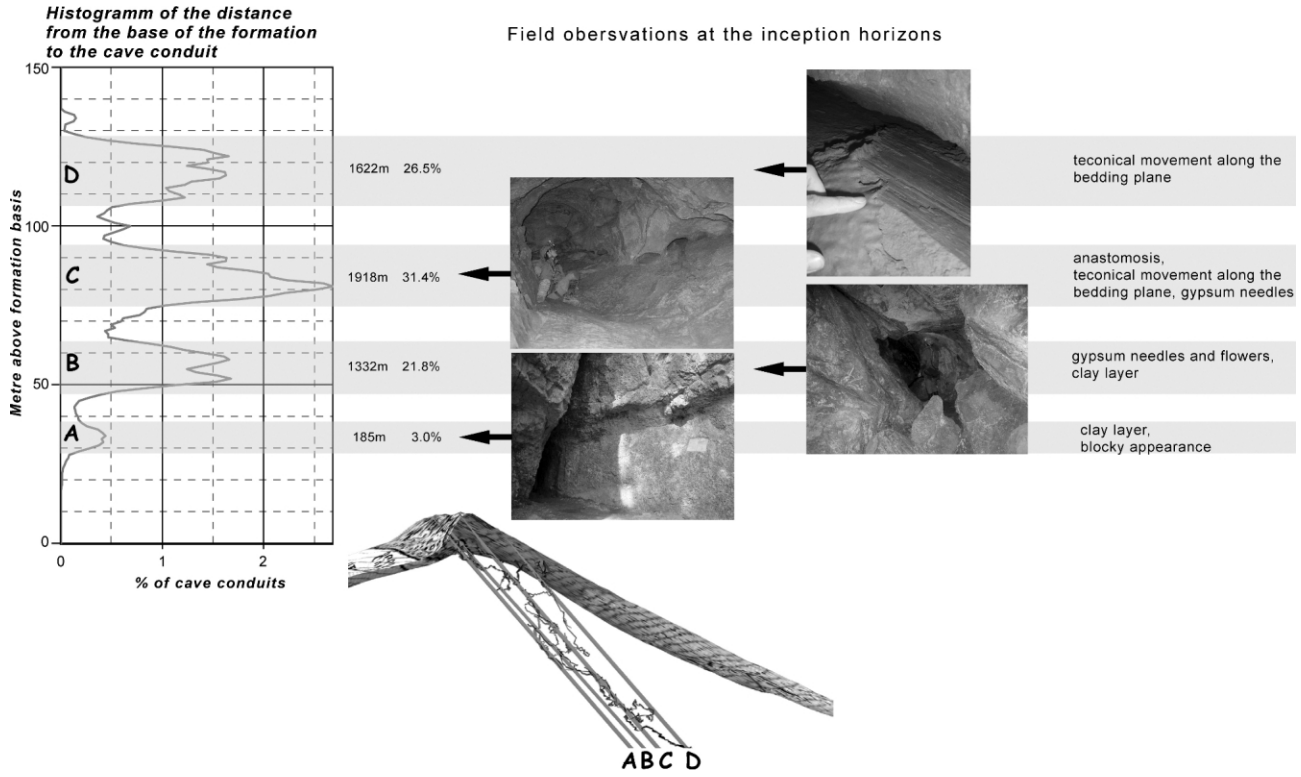

Figure 6: Synopsis of the statistical identification of inception horizons and the geological field identification of them for Nidlenloch.

Palmer, A. N. 1975. The origin of maze caves. Bulletin National Speleological Society of America 37, 56-76.

Palmer, A. N. 1987. Cave levels and their interpretation. Bulletin National Speleological Society of America 49, 50-66.

Palmer, A. N. 1989. Stratigraphic and structural control of cave development and groundwater flow in the Mammoth Cave region. In: White W. B. and White E. L. (eds): Karst Hydrology, Concepts from the Mammoth Cave Area. Von Nostrand Reinhold, New York, pp. 293-316.

Pesendorfer, M. and Loew, S. 2004. Hydrogeologic Exploration during excavation of the Lötschberg Base Tunnel (AlpTransit Switzerland). In: Hack, R., Azzam, R. (eds): Engineering Geology for Infrastructure Planning in Europe. Springer, Heidelberg, 347-358.

Quinlan, J.F. and Ray J.A. 1981. Groundwater basins in the Mammoth Cave region, Kentucky. Friends of Karst, Occasional Publication 1.

Rauch, H. W. and White, W. B. 1970. Lithologic controls on the development of solution porosity in carbonate aquifers. Water Reservoir Research 6, 1175-1192.

Slabe, T. 1995. Cave Rocky Relief and its speleogenetical significance. Znanstvenoraziskovalni Center Sazu, Ljublijana, 128 pp.

Waltham, A. C. 1971. Controlling factors in the development of caves. Transactions of the British Cave Research Association 13, 73-80.

Received: 15. November 2006
Accepted: 20. December 2006

Marco FILIPPONI[1)*)] & Pierre-Yves JEANNIN[2)]

[1)] GEOLEP, Laboratoire de géologie de l'ingénieur et de l'environnement, Ecole Polytechnique Fédérale de Lausanne (EPFL), Switzerland, marco.filipponi@epfl.ch

[2)] SISKA, Swiss Institute of Speleology and Karstology, Switzerland

[*)] Corresponding author, present address: ENAC ICARE GEOLEP, Station 18, CH-1015 Lausanne, Switzerland, fax: 0041 (0)21 693 63 30, marco.filipponi@epfl.ch

- Nidlenloch (CH)-
Feldnachweis und Beobachtungen

Das Nidlenloch (Länge 7.5 km / Höhenunterschied 420 m; SO, CH) ist in den nach Norden abfallenden Schichten der Sequan-Kalke (Malm) im Nordschenkel der Weissenstein-Antiklinale angelegt, die Gänge fallen entsprechend dem Schichtverlauf nach Norden ab oder folgen dem west-östlichen Streichen der Schichten. Im mittleren Teil der Höhle hat sich ein teilweise labyrinthisches Horizontalsystem entwickelt, aber auch in anderen Partien des Nidlenlochs gibt es Ansätze von fossilen, phreatischen Gangnetzen. Heute finden sich nur lokal oder temporär kleine Rinnsale, die bekannten Höhlengänge hat mit der heutigen Karstentwässerung nur am Rande etwas zu tun.

Die generell kleinen bis mittelgrossen Gänge sind, entsprechend dem vermutlichen hohen Alter des Nidlenlochs, recht oft von Verstürzen und lokal von verlehmten Senken geprägt.
Trotz der grossen Höhendifferenz sind Schächte nicht all zu häufig und maximal zwanzig Meter tief, grössere Hallen fehlen ebenso, und auch Tropfsteinschmuck ist selten, jedoch trifft man häufig auf Gipsausblütungen. (nach Wildberger und Preiswerk, 1997)

Ziel der Untersuchungen

Im Rahmen der vorliegenden Arbeit wurde die räumliche Verteilung der Höhlengänge des Nidlenlochs analysiert, um die Rolle der geologischen Gegebenheiten sowie hydrogeologischen Rahmenbedingungen besser zu verstehen. Das Hauptinteresse lag bei der statistischen Identifikation von “stratigraphische Initialfugen“ (in Englisch “inception horizon“; Lowe, 1992), der Feld Verifikation sowie Beprobung der Initialfugen.

Geologisches Modell

Um den Zusammenhang zwischen den geologischen Verhältnissen und der Entwicklung des Nidlenlochs herzustellen wurde ein geologisches 3D Modell des nach Norden abfallenden Schenkels der Weissenstein-Antiklinale erstellt. Hierfür wurde mit GEOSHAPE ein Geländemodell erstellt, auf das in Cinema 4D die geologische Karte (Buxdorf 1908) projiziert wurde. Den Schichtverlauf im Untergrund wurde anhand von Beobachtungen im Nidlenloch selbst interpretiert, wobei der Höhlenverlauf des Nidlenloch von Toporobot ebenfalls in Cinema 4D importiert wurde.
Das so entstandene geologische Modell führt zu einem gleichmässigen Fallen der Schichten Richtung Norden mit einer Neigung von 50° (002/50). Wobei keine Verwerfungen die Schichten wesentlich versetzen. Im Detail kann der Schichtverlauf lokal von diesem idealisierten Modell abweichen (die Messungen der Schichteinfallen variierten zwischen 015/55 und 350/50), dennoch wird angenommen, dass das Modell mit einer Marge von +/- 10m stimmt. Ausserdem wurde angenommen, dass die Schichtmächtigkeit konstant ist, das heisst, kein ausdünnen respektive Mächtigkeitsgewinn der Schichten.

Stratigrafie

Nach Buxdorf 1908 kann der Sequan-Kalkstein (Malm) in drei Schichten gegliedert werden; von unten nach oben:

Cernularis-Schichten: (Mächtigkeit ca. 15m) Mergel und Kalksteinbänke. Kalksteinschichten reich an meist verkieselten Fossilien (Korallen, Seeigeln, …), raues Erscheinungsbild der Kalke

Oolithische Spatkalke: (Mächtigkeit 60-100m) grob- und feinoolithischer, gelegentlich auch spätiger Kalkstein, gut geschichtet, hellgelb bis rotbraune Farbe, z.T. Fossilien von Seeigelstacheln.

Verena-Schichten: (Mächtigkeit ca. 15m) kreidig-weisse fein Oolithe.

Das Nidlenloch erstreckt sich ausschliesslich (?) in den oolithischen Spatkalken.

Quantitative Zusammenhang zwischen der Geologie und der Verkarstung

Bereits qualitativ ist im 3D Modell der geologischen Verhältnisse zwischen dem Einfallen der Schichten und dem Höhlengangverlauf zu erkennen. Um diesen zu quantifizieren wurde ein „kleines“ Programm geschrieben.

Methode und Annahmen

In einem ersten Schritt werden die Vermessungsdaten des Nidlenlochs aufgearbeitet. Es wurde angenommen, dass sich die Höhlengänge an der heutigen Höhlendecke zu bilden begonnen. Dies ist eine sehr grobe Approximation, so wurde gelegentlich beobachtet, dass die Höhlendecke durch Versturz nach oben wanderte oder dass die Initialfuge in der Mitte einer phreatischen Ellipse lag. Jedoch stellst unsere Annahme eine erste und Näherung dar. Daher wurden die einzelnen Messpunkte an die Decke der Höhlengänge verschoben und zwischen denn Messpunkte alle Meter einen Höhlenpunkt gerechnet (X, Y, Z, Richtung, Neigung).

Im nächsten Schritt wurde der Abstand von den Höhlenpunkten normal zu einer Schichtfläche (Referenzfläche) gerechnet und in einem Histogramm dargestellt.

Resultate

Das Histogramm der Abstände der Höhlenpunkte von der Referenzfläche zeigt drei wesentliche Peaks sowie zwei untergeordnete. Dies bedeutet, dass sich das Nidlenloch im Wesentlichen auf drei Schicht(-fug-)en entwickelt hat (rund 70%).

Erstaunen mag die relativ grosse Breite der einzelnen Peaks, die bis zu 15m beträgt, während hingegen in der Höhle selbst die einzelnen Schichtfugen relativ deutlich über weite Strecken verfolgt werden können. Die Breite der Peaks kommt durch die Ungenauigkeit des geologischen Modells sowie der nur angenommenen Lage der Initialfuge an der Decke des Höhlenganges zustande.

Als nächstes wurde den Zusammenhang zwischen der Klüftung, der Schichtung und dem Höhlengangverlauf erstellt. Hierzu wurden die Höhlenpunkte in stereographischer Projektion dargestellt (Richtung und Neigung des Höhlenganges bei jedem Höhlenpunkt).

In der stereografischen Projektion ist zu erkennen, dass eine Mehrheit der Höhlengänge in W-O Richtung verlaufen, sowie ein andere Gruppe von Höhlengängen in NW zeigen. Dies ist ebenfalls in der Planansicht des Nidlenlochs deutlich zu erkennen.

Ausserdem ist auffallend, dass eine Vielzahl von Höhlenpunkten sich in der Nordhalbkugel befindet und sie einen Grosskreis erahnen lassen,der das Schichteinfallen widerspiegelt (Berechnung der

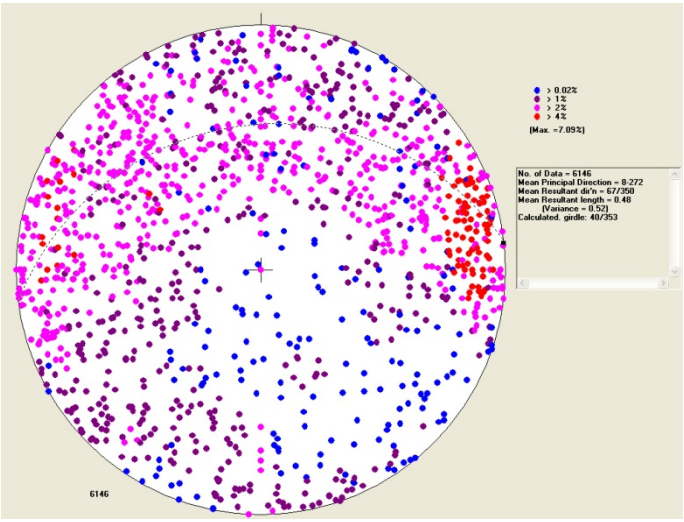

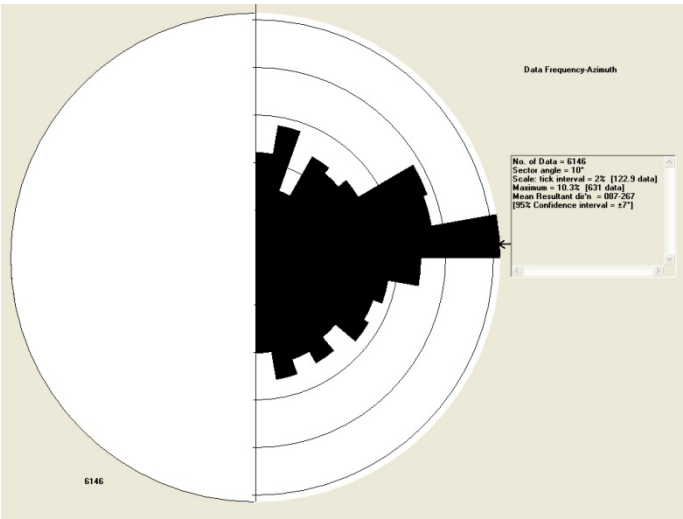

Fläche 353/40). Das heisst, die berechnete Fläche ist leicht steiler als die im Feld gemessene, dies vermutlich als Folge des verschieben der Höhlenpunkte zur Höhlendecke.

Dies alles bedeutet, dass die Schichtung die Lage der Höhlengänge bestimmt, und die Klüftung den lokalen Gangverlauf.

Feldnachweis und Beobachtungen

Feldbeobachtungen 30. März 2006 (Hauptgang bis B1, Himmelsgang)

Am 30. März 2006 konnte ich zusammen mit Mirjam Widmer (AGSR) das Nidlenloch besuchen.

Das Ziel dieser Befahrung war es vom Eingang her dem Hauptgang folgend bis zum B1 das Schichtfallen zu messen und das erstellte geologische 3D-Modell zu überprüfen, Feldnachweis der statistisch identifizierten stratigraphischen Initialfugen, Beschreibung dieser sowie Beprobung.

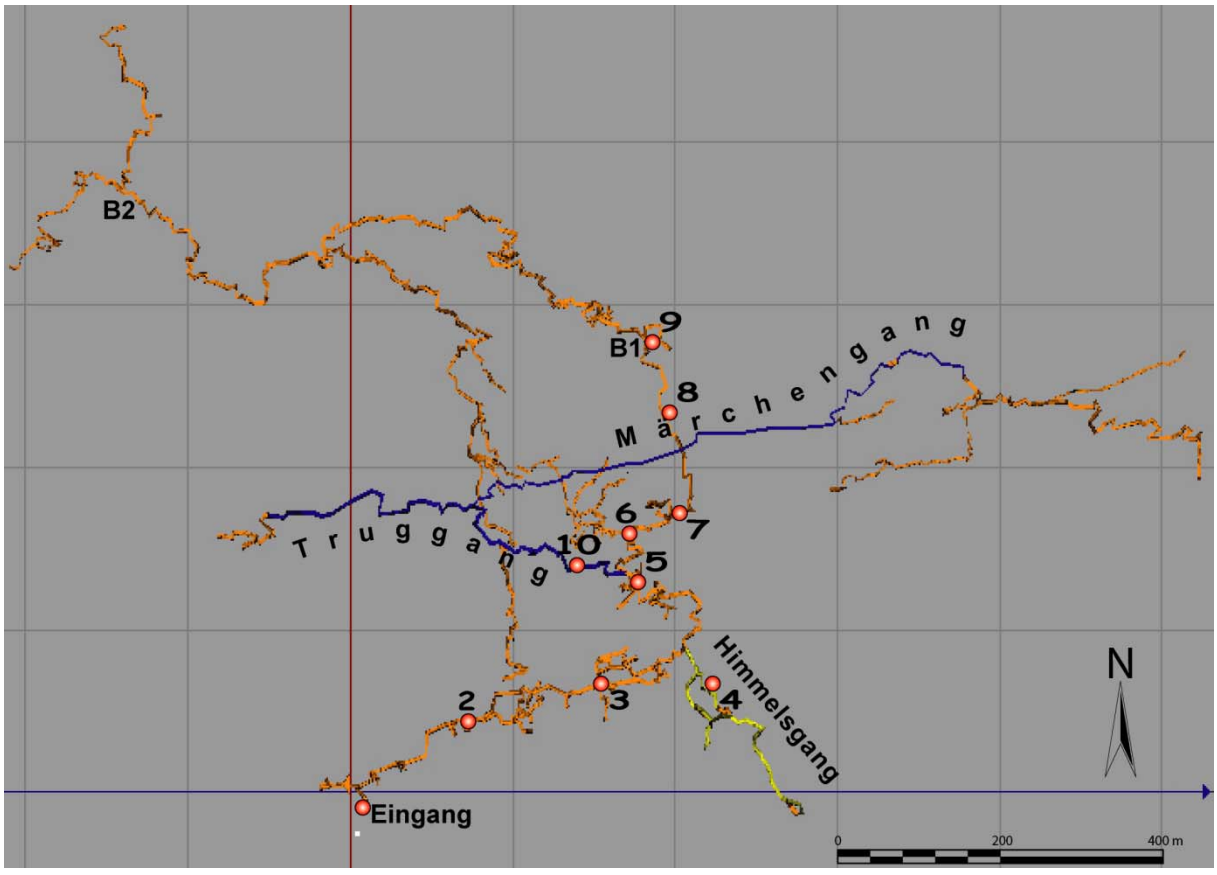

Planansicht des Nidlenlochs mit den beschriebenen Beobachtungspunkten.

1 Höhleneingang. Schichtfallen 015/50. Vor dem Höhleneingang haben wir einen schönen Aufschluss des eher massigen Sequian-Kalkes. Markant ist eine Schichtfuge von rund 50 cm Mächtigkeit, die leicht blockig in der Struktur, z.T. untergrenze von Klüften.

Beprobung an Sampling Point N3

2 Schichtfallen 005/55. Der Höhlengang ist an dieser Stelle sehr hoch, und durch Inkasion geprägt und überhöht. Die Lage der felsigen Gangsohle ist nicht bekannt, jedoch etliche Meter tiefer.
Interessant ist dass die Höhlendecke aus einer Schichtfuge besteht, an der bergwärts kleine Höhlengänge und Anastomose zu beobachten ist, so liegt vermutlich auch der Drachengang an dieser Schichtfuge (?). Auf der Schichtfuge selbst konnte Rutschharnisch beobachtet werden, die nicht durch Inkasionsprozesse entstanden sind, da sie bis in den gewachsenen Fels hinein beobachtet werden können.

3 Region Tropfsteingang. Schichtfallen 015/50. Der Tropfsteingang, der Hauptgang und der Lehmgang liegen auf derselben “Schichtfuge“. Mächtigkeit der Schichtfuge rund 30 cm; Gleitbewegung auf der Schichtfuge (?); das Initial des Höhlenganges scheint an der Basis der Schichtfuge gewesen zu sein; Schichtfuge scheint kompakter als der Umgebene Fels zu sein. Gipsnadeln und –ausglütungen.
An der Decke und z.T. an den Wänden hat es “Fingerlöcher“ >> Entstanden als der Gang vollständig mit Sedimenten gefüllt war(?)

4 Der Himmelsgang und der Guanogang liegen auf derselben Schichtfuge wie der Hauptgang. Schichtfallen 015/45. Interessant ist, dass sich am Ende des Guanoganges, obschon er kleinräumig ist, sich erheblich Inkasionserscheinungen beobachten lassen. Anastomose. Gipsausscheidungen. Guanogang schönes Schlüssellochprofil.

Beprobung an Sampling Point N2 (Fels und Höhlengips)

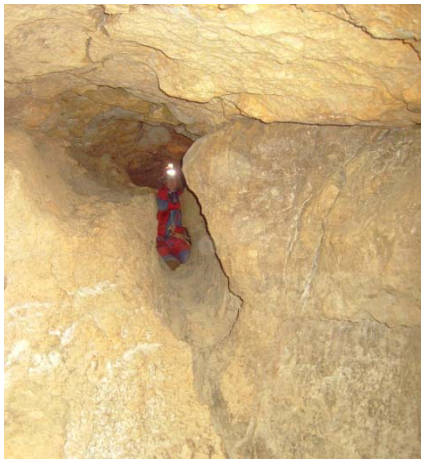

5 Region Labyrinth. Schichteinfallen 010/50. Hier passiert irgendetwas, jedoch bin ich nicht ganz mitgekommen (wechseln der Schichtfuge?)

6 erste Leiter. Schichteinfallen 015/55. Hauptgang und der Einstieg des Schindlerganges liegen auf derselben Schichtfläche. Schacht liegt an einem Bruch 340/75.

7 erste Schächte. Schichteinfallen 015/55.

8 Strudellöchergang. Der Verlauf dieses Höhlenabschnittes wird durch einen Bruch bestimmt 080/55, die eine Serie von Schichtflächen durchschlägt – d.h. Höhlengang ist nicht an Schichtfugen-Kluft-Kreuz entstanden. Gipsausfällungen

9 B1. Schichteinfallen 010/55.

10 Anfang Truggang. Schichteinfallen 010/55. Schöne phreatische Gangprofile. Anastomose. Kolke. Die ersten paar Meter (bis und mit Rutschbahn) liegen auf derselben Schichtfläche wie der Hauptgang. Dann wird die Schichtfuge gewechselt auf eine höhere, jedoch könnte ich visuell die beiden Schichtfugen nicht unterscheiden.

Beprobung an Sampling Point N1

Feldbeobachtungen 1. Mai 2006 (Truggang)

Am 1. Mai 2006 konnte ich zusammen mit Mirjam Widmer (AGSR) das Nidlenloch besuchen.

Das Ziel dieser Befahrung war es die Schichtfugengebundenheit des Trugg- und Märchenganges zu untersuchen. Mit dem Ziel das geologische Modell zu verfeinern und einen Eindruck der Eigenschaften der höhlengangführenden Schichtfugen zu erhalten.

Fotos von mf und mü.

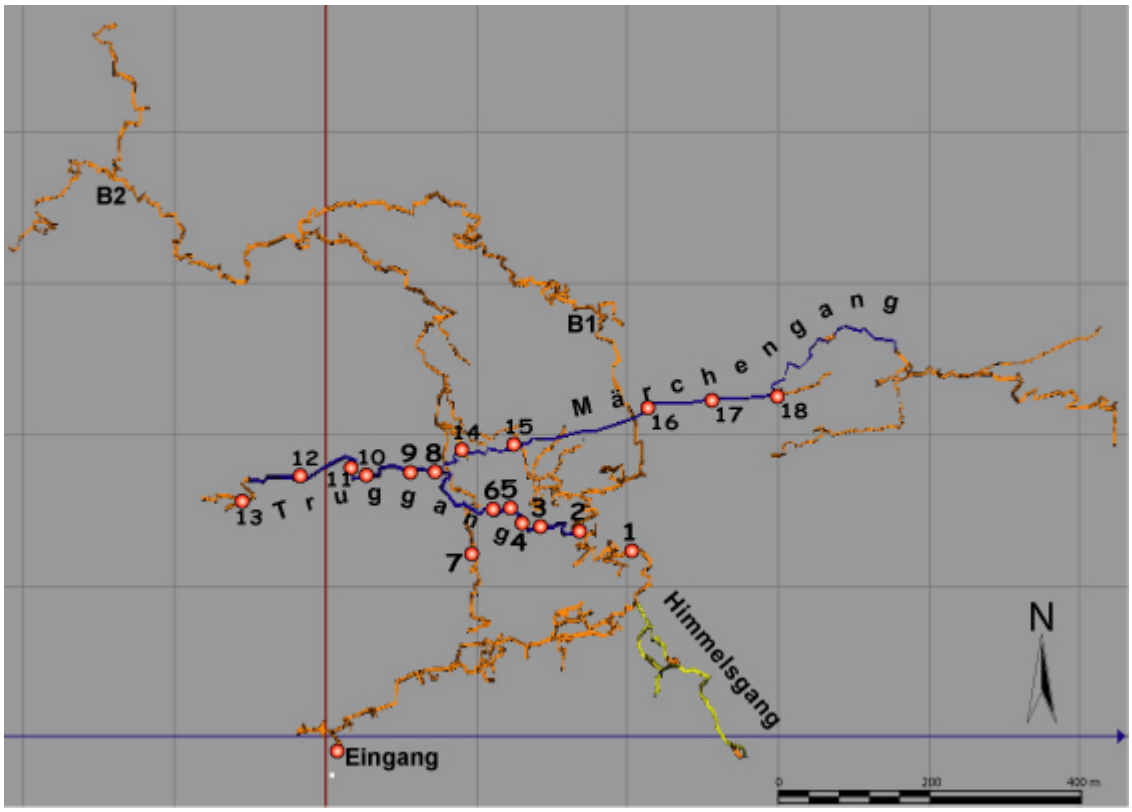

Planansicht des Nidlenlochs mit den beschriebenen Beobachtungspunkten.

1 Kinzelbach's Fall
Der schluchtartige Höhlengang ist hier an einer Verwerfung gebunden, die jedoch nicht gut eingemessen werden konnte: 360/70

2 **Abzweigung Hauptgang ⇔ Truggang**
Schichteinfallen 000/45, Klüftung 060/50
- Der Anfang des Trugganges befindet sich in derselben Schichtfuge wie der Hauptgang. Markant in diesem Gangabschnitt sind die gut ausgeprägten Anastomosen.
- Vereinzelt konnten kleine Harnischflächen auf der Schichtfuge erkannt werden.
- Kondensationskorrosion
- Truggang-Gangprofil: phreatische Röhre

3 Schichteinfallen 000/50
- Höhlengang Schichtfugen gebunden
- entlang Schichtfuge Bewegung >> Harnisch von rund 10-15 cm Richtung Norden.
- an der Decke fossile Schwämme

4 kurzer “Kluft“-gebundener Gangabschnitt
Klufteinfallen 120/45
Höhlendecke stark korrodiert “Kolke“ (?)

5 erneut Schichtgebundenergangabschnitt,
Schichteinfallen 355/45
an der Decke schön zu erkennen die einstiege phreatische Röhre, heutiges Gangprofil: Schlüsselloch

6 **Narrenschacht**

- der Narrenschacht selbst ist an einer kleinen Störung gebunden, die ebenfalls den gleich darauf folgenden Höhlengang bis mitbestimmt 020/50
- Schichteinfallen 005/45
- Fliessfacetten Höhleneinwärts
- Anastomose auf der Störfläche
- Gipsausblütungen auf/in der Störfläche

7 **Sintergang**

Schichtfugen gebunden 340/55

- schöne Harnischflächen, rot gefärbt, hat Sinter zerrissen, Versatz rund 20-25cm Richtung Norden
- Fossilien: Schwämme und Belemniten

9 Für rund 10 m folgt der Höhlengang hier einer Verwerfung 170/60, danach wieder Schichtfugen gebunden
=> Markanter Knick des Ganges

10 Höhlengang Schichtgebunden => Schichteinfallen 355/50
- Leichter Versatz von 1-2 cm,
- Anastomose
- Versturz

11 Höhlengang an Verwerfung 300/40

12 Anastomose auf mehreren Schichtfugen knapp übereinander
Schichteinfallen 010/55

13 Schichtgebunden 005/60
Harnisch Richtung Norden rund 5 cm
Massiggebankter Kalkstein 20-30 cm,
viel Anastomose
Versturz oberhalb der Höhlenbildenden Schichtfuge

14 **Märchengang**
Schichtfugengebunden => 005/55
Anastomose
Gipsausblütungen
Schichtbankung rund 40-50 cm

15 Schichteinfallen 015/45
- Mergellange und Gips, jedoch immer noch dieselbe Schichtfuge auf der sich der Trugg- und Märchengang sich entwickelt hat.
- Anastomose

16 Schichtgebunden => 015/55
Massiggebankter Kalk 40-60 cm
Gibsausfällungen
Bewegung entlang Schichtfuge rund 4-5 cm
Anastomose

17 Schichtfugengebunden => 355/50
Versturz
Anastomose

18 **Oberhalb Märchenschacht**
Massiggebankter Kalkstein 40-60 cm
Kolke
Gipsrosen
Schichtfugengebunden 355/50

Sonstiges in der Rotkäpchen-Halle(?) begegneten wir einem scheuen Pseudoskorpiton(?), vgl. Stalactite 2/2005

Schlussfolgerung

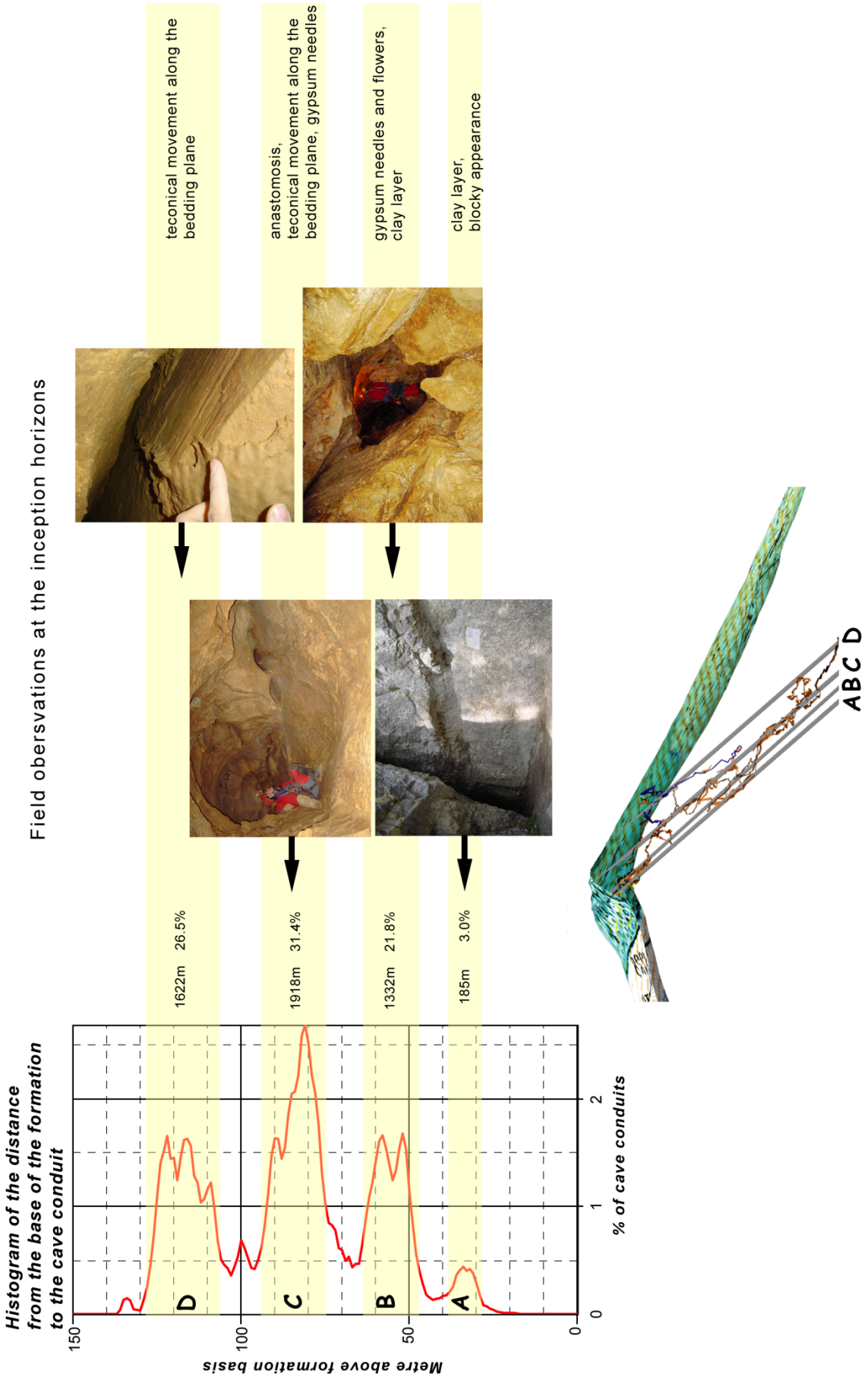

- Grottes aux Fées -
3D Analyse, Feldnachweis und Beobachtungen

Im Rahmen der vorliegenden Arbeit wurde die räumliche Verteilung der Höhlengänge des Grottes aux Fées (Länge 13 km / Höhenunterschied 227 m; VD, CH) analysiert, um die Rolle der geologischen Gegebenheiten sowie hydrogeologischen Rahmenbedingungen besser zu verstehen. Das Hauptinteresse lag bei der statistischen Identifikation von "stratigraphische Initialfugen" (in Englisch "inception horizon"; Lowe, 1992), der Feld Verifikation sowie Beprobung der Initialfugen.

3D Analyse

Die Grottes aux Fées bei Vallorbe erstrecken sich im Sequian-Malm. Die Höhlengänge zeigen typische phreatische Gangprofile. Die Höhlen folgen weitgehend einer Schichtfuge (± 010/05), zwei weitere Schichtfugen scheinen ebenfalls bevorzugt verkarstungsfähig zu sein, sind jedoch der ersteren unterlegen.

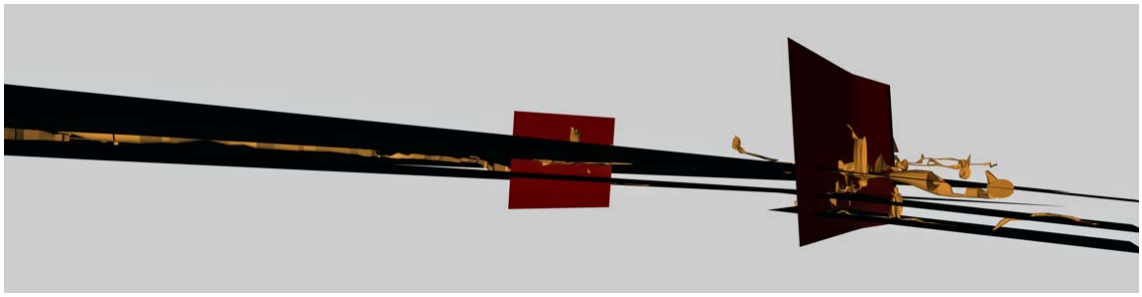

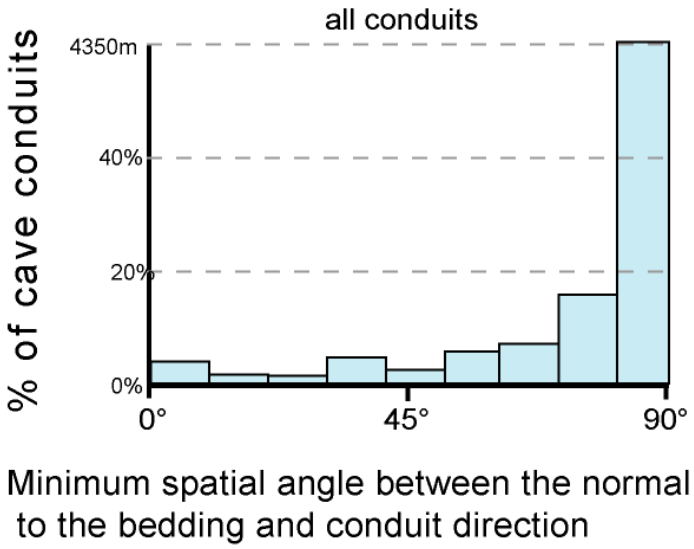

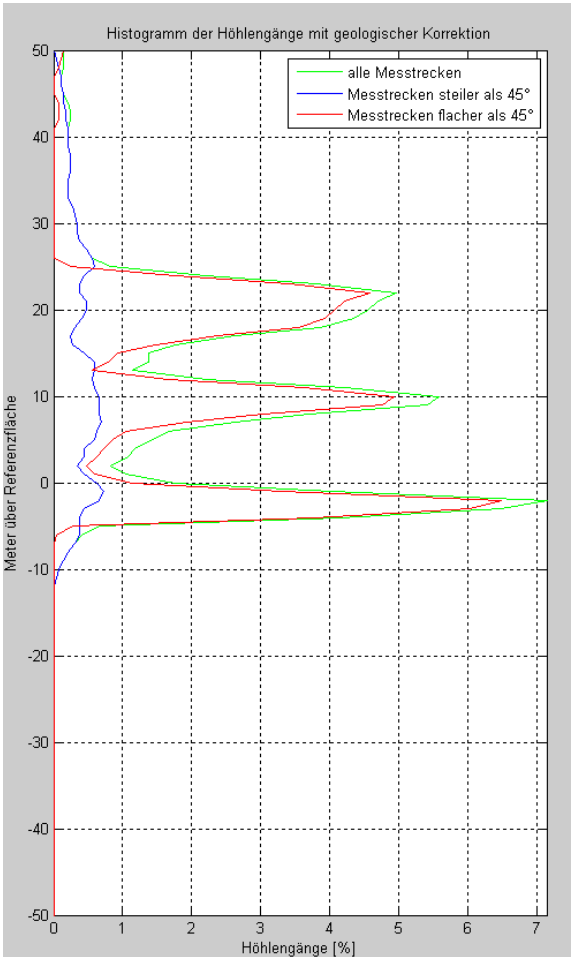

vor der grossen Verwerfung

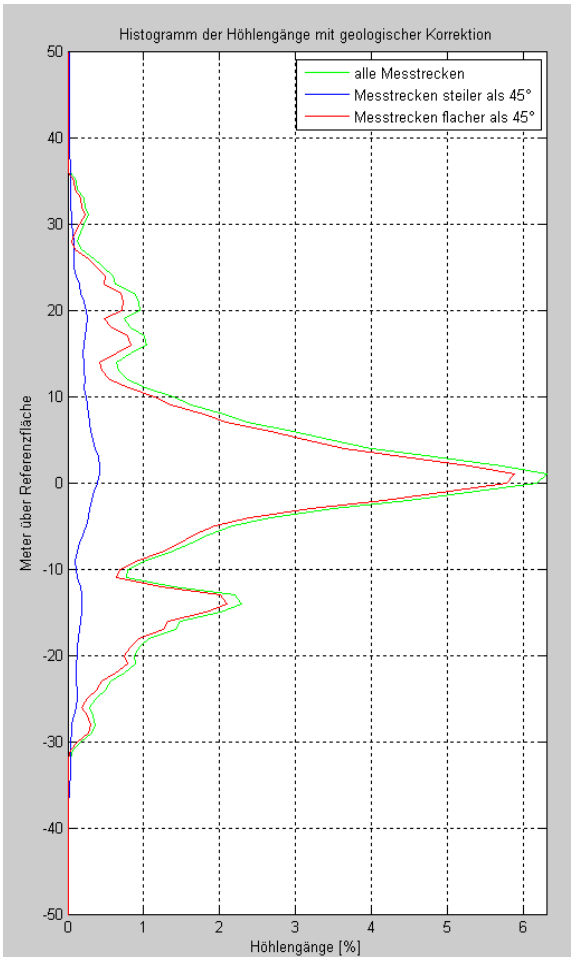

hinter der grossen Verwerfung

- Visuell 3 Horizonte 0Ref; +10m, +25
- > der Gangverlauf selbst ist neben den Schichtfugen Schichtfugen an zwei Kluftscharen gebunden

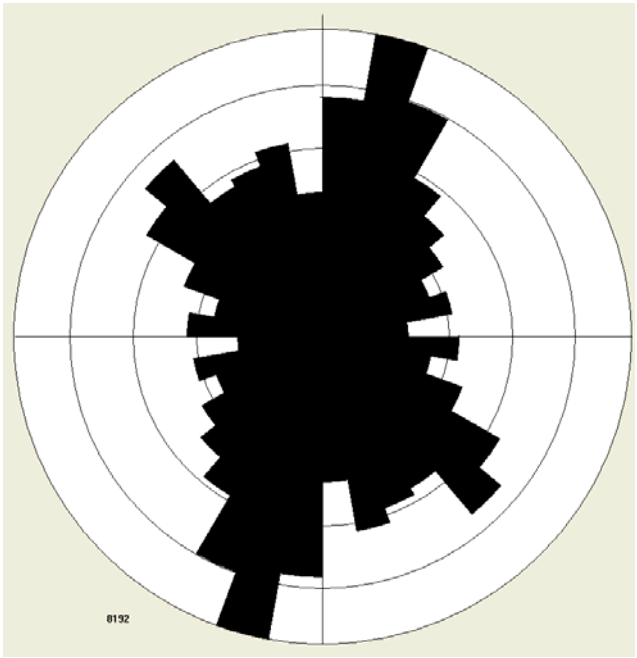

Feldbeobachtungen

Schichtfuge Eingangbereich Grande Grotte au Fée:

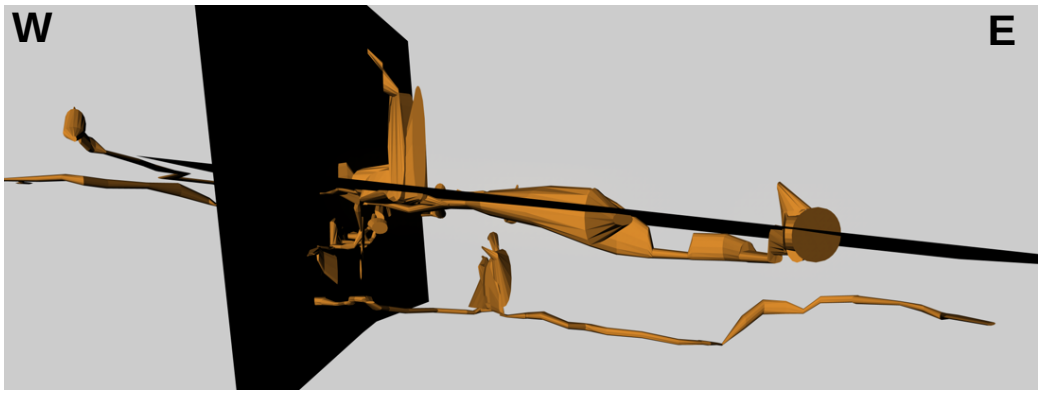

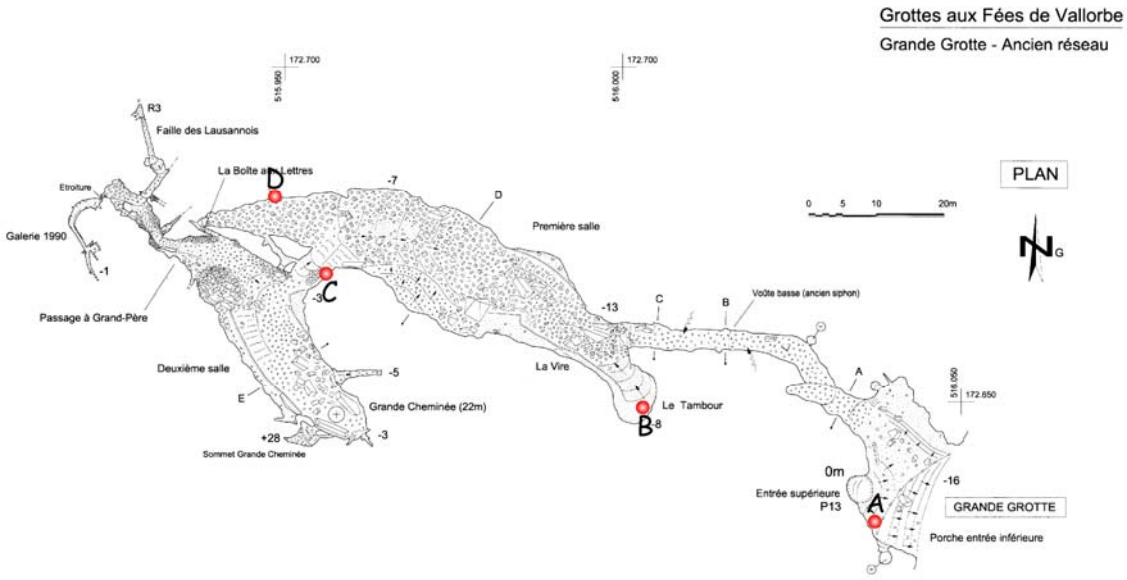

A) Markante Schichtfuge im dm-Bereich, blockiger als Umgebungsgestein, an der Oberfläche weniger Verwitterungsbeständig. Kleines Probestück

B) zwei Horizonte mit Anastomose, viel Wandsinter, keine Anzeichen auf neotektonische Bewegung entlang der Schichtfuge, Höhlendecke stark korrodiert.

C) Schichtfuge weitgehend weggelöst/erotiert, Anastomose, Fels unterhalb der Schichtfuge blockig.

D) Anastomose, Wandsinter.

Schichtfuge Eingangbereich Petite Grotte au Fée:

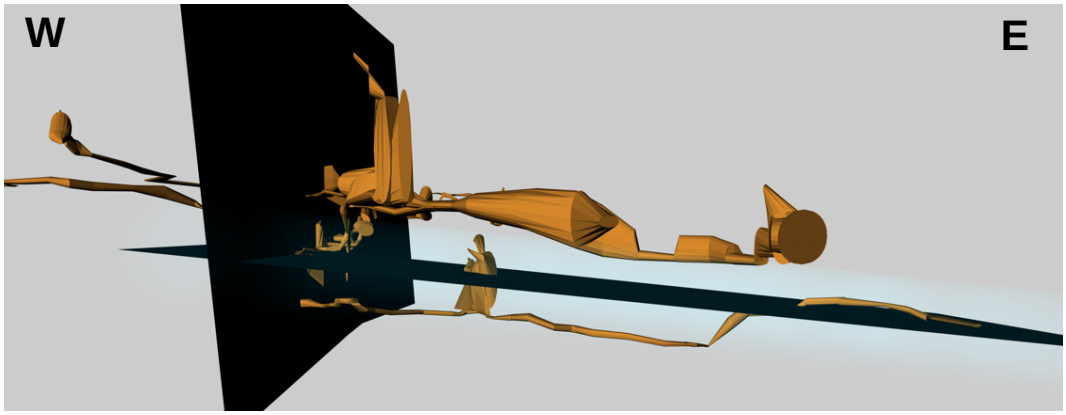

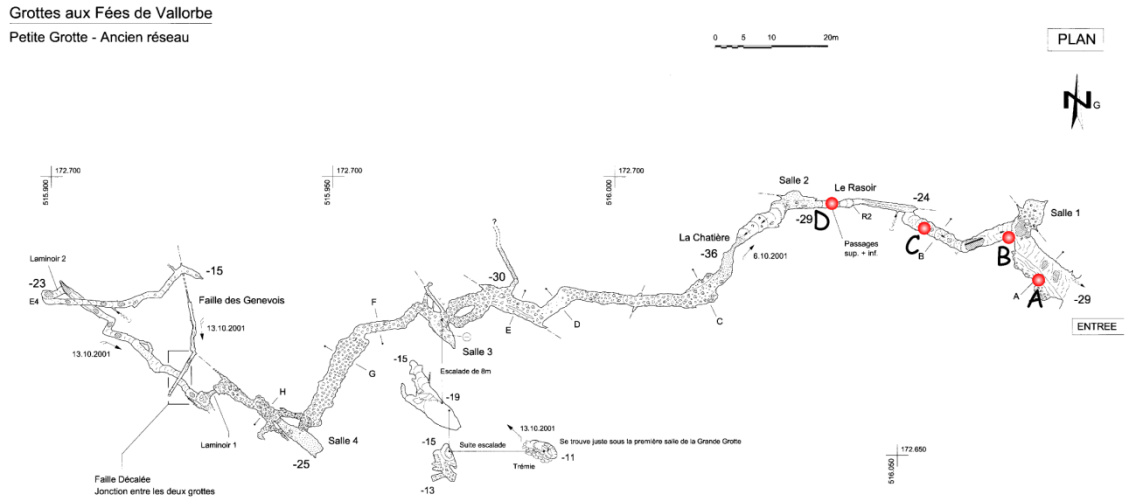

A) relative grosse Fläche mit Anastomose.

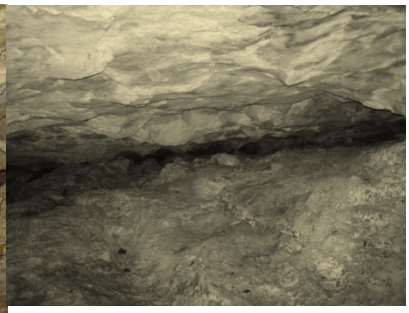

B) Anastomose, Schichtmächtigkeit rund 2-5 cm

C) Anastomose mit kleiner Quelle, Wandsinter => schlecht Schichtfuge nicht beschreibbar. Schönes phreatisches Gangprofil.

D) Höhlengang wechselt Schichtfuge. Höhlengang Kluftgebunden (010/80).

Foto: Mirjam Widmer

Schichtfuge hintere Bereiche Petite Grotte au Fée:

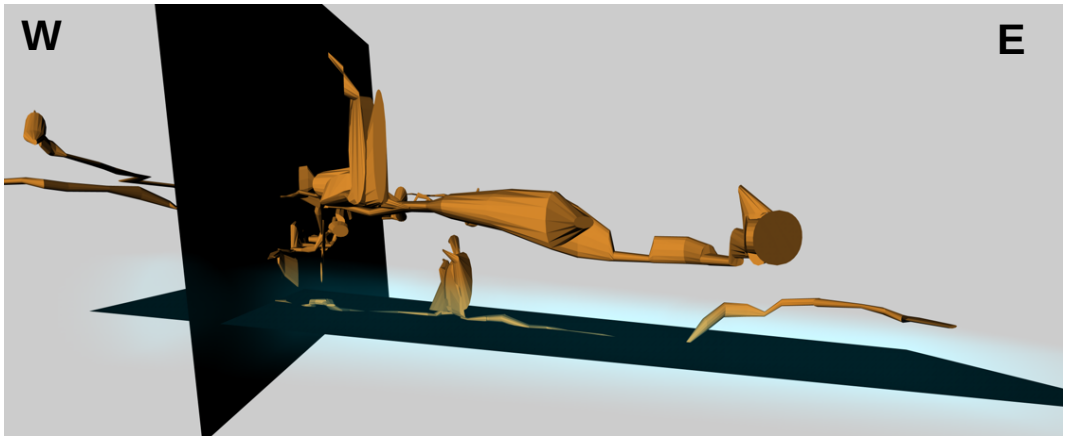

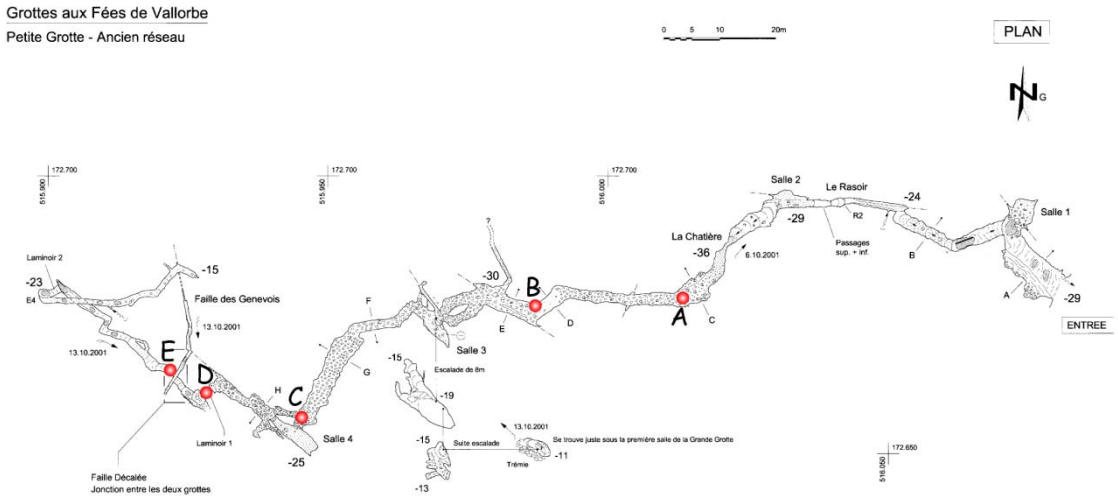

A) Anastomose, markante Schichtfuge, Schichtfugenmächtigkeit 1-5 cm, Anastomose scheint oberhalb der Schichtfuge zu liegen, typisches phreatisches Gangprofil.

Foto: Mirjam Widmer

B) Anastomose, kleine Probenahme, keine Indizien auf Bewegung entlang der Schichtfuge.

C) Höhlengang durch Verwerfung vertikal versetzt worden, ganzer Bereich hier ein wenig labil, viele Versturzblöcke.

D) Wandsinter durch Bewegung entlang Schichtfuge zerbrochen.

E) Höhlengang entlang Verwerfung (300/80) lateral verschoben, vertikaler Versatz im dm Bereich, "lokale" Bewegung entlang Schichtfuge (Verschieben des Gangprofils), Rutscharnisch entlang Verwerfung (?)

Fazit

- Alle drei statistisch bestimmte stratigraphische Initialfugen Schichtfugen konnten in der Höhle wieder gefunden werden.
- Die beobachteten Hinweise neotektonischer Bewegungen scheinen nur lokal zu sein.
- Die Beobachtungen der Schichtfugen war nicht ganz einfach (Wandsinter, keine "frische" Aufschlüsse).

- Réseau de Covatannaz (CH)-
3D Analysis

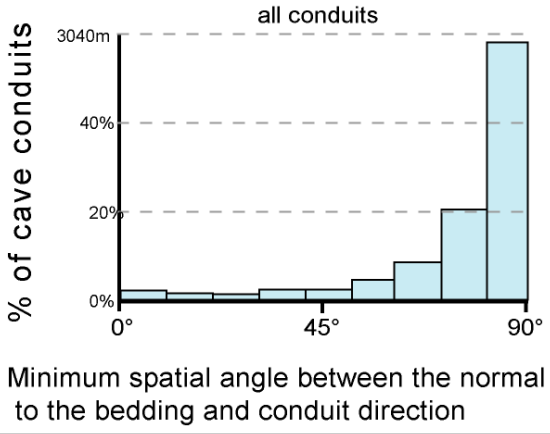

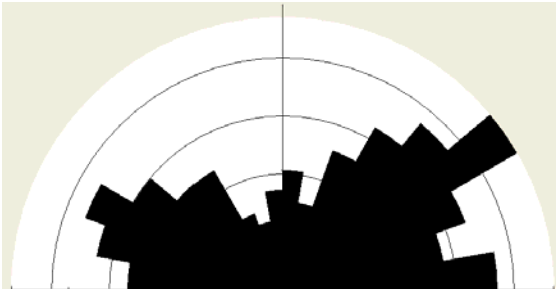

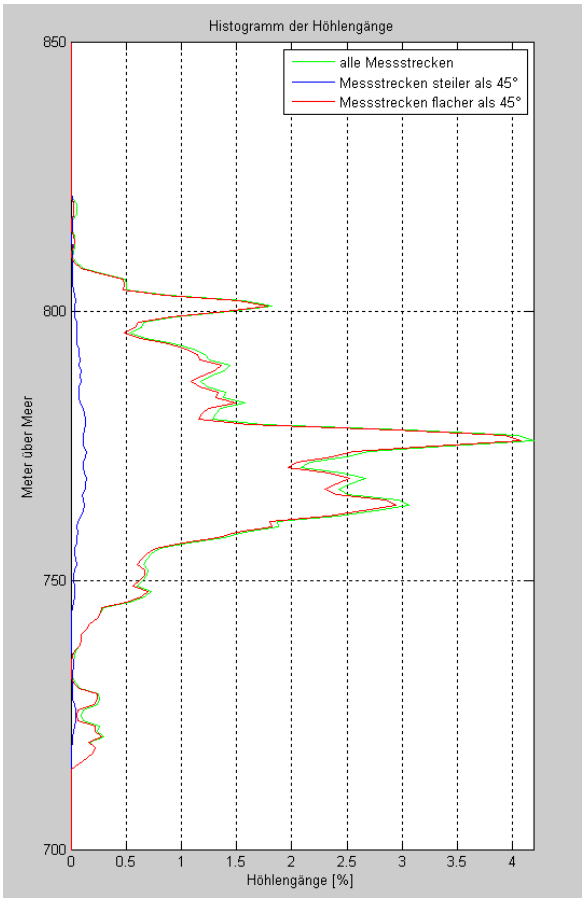

Visuell 2 Zonen mit rund 25m Abstand Visuell Gangrichtungen

- kleines Hölloch (D) -
3D Analysis

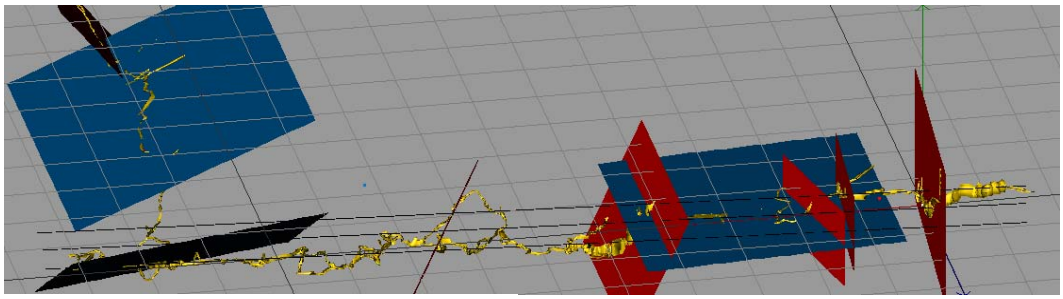

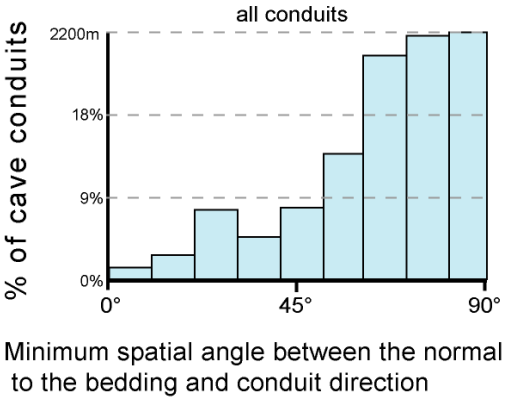

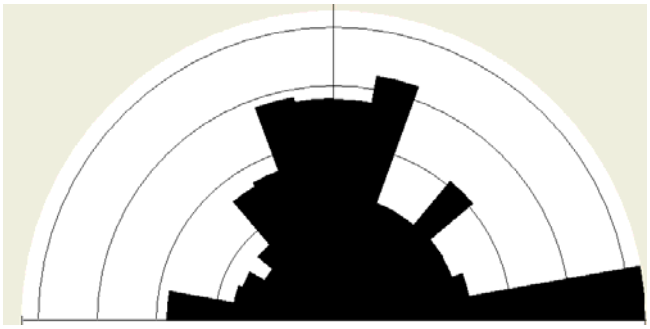

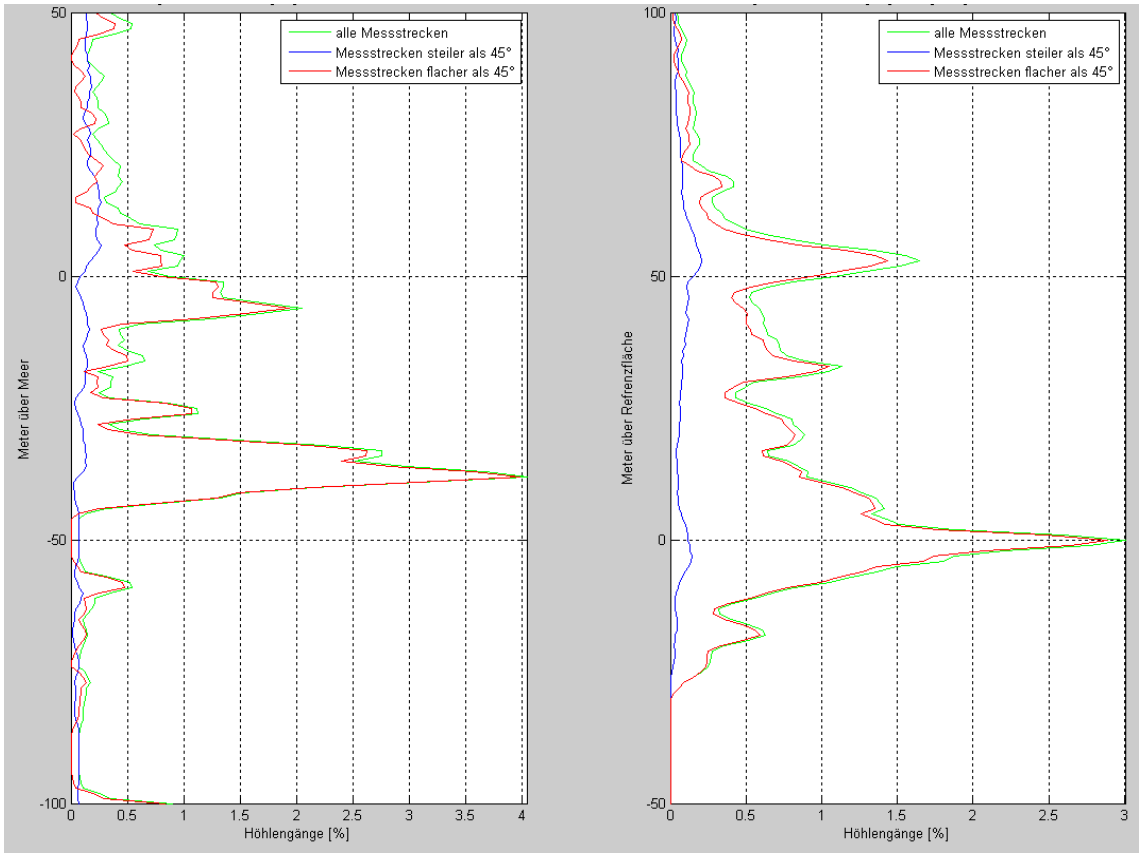

Visuell 3 Horizonte: 0; 26; 50

- Hirlatzhöhle (A) -
3D Analysis

Zone 1.2

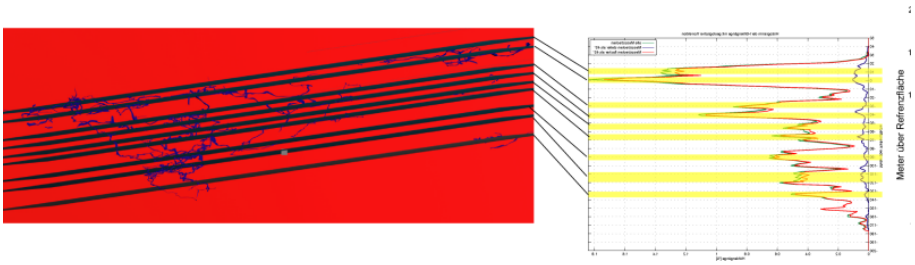

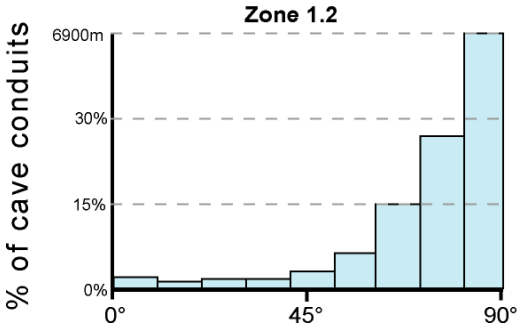

Minimum spatial angle between the normal to the bedding and conduit direction

Zone 2.1

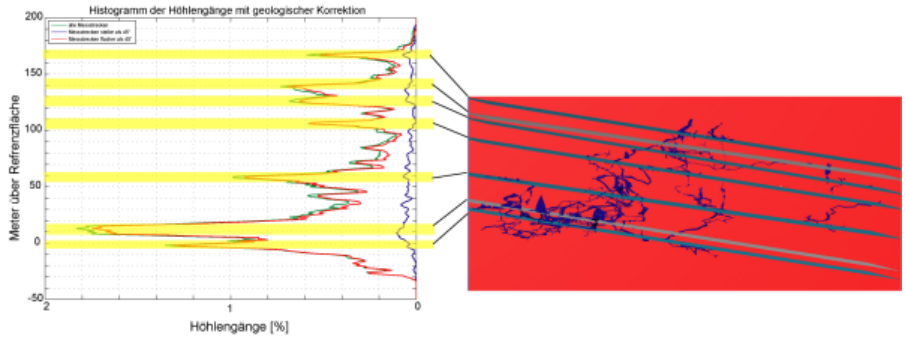

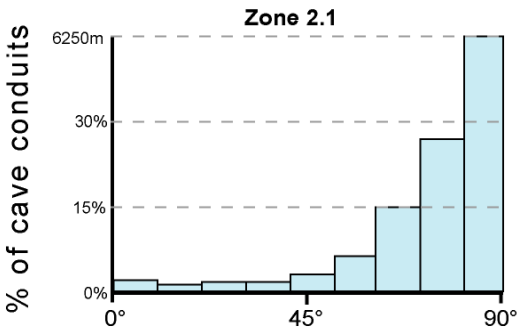

Minimum spatial angle between the normal to the bedding and conduit direction

- Shuanghedongqun (China) -
3D Analysis

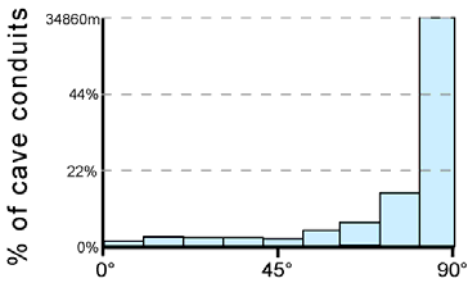

Minimum spatial angle between the normal to the bedding and conduit direction

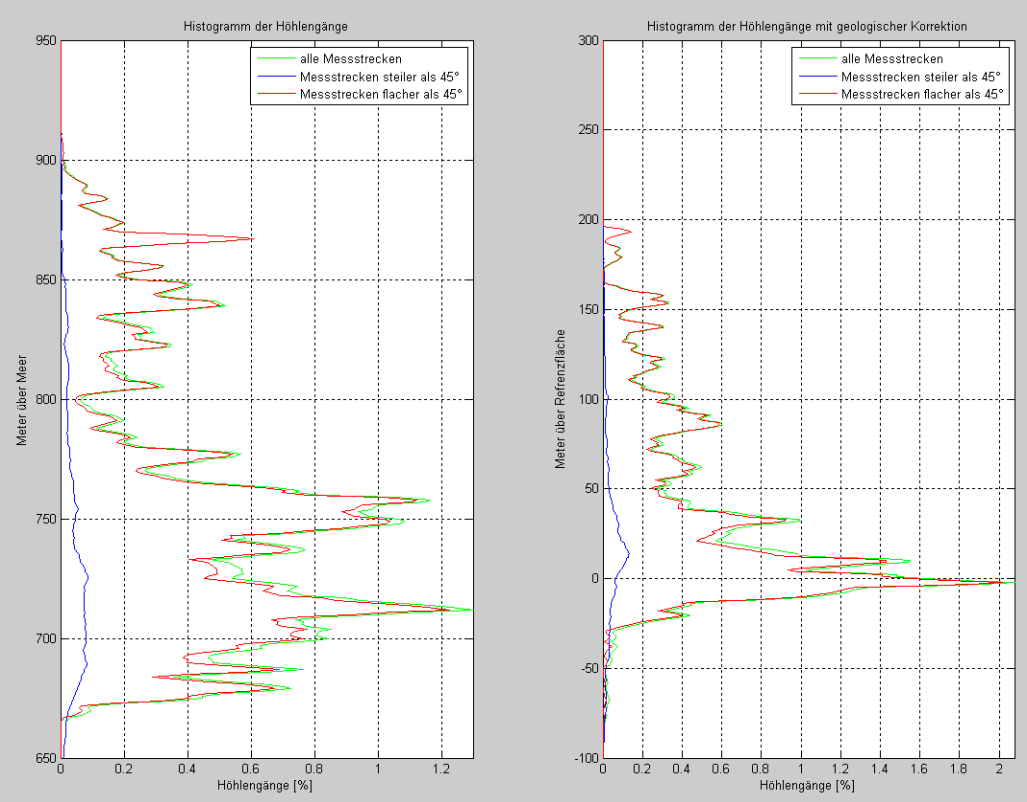

Gangrichtungen

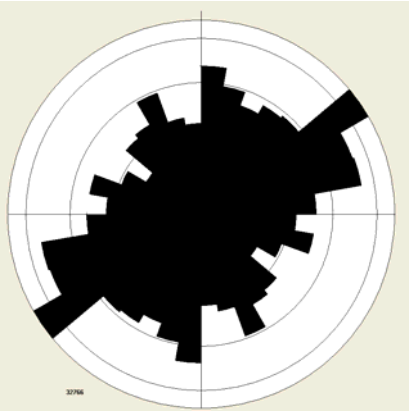

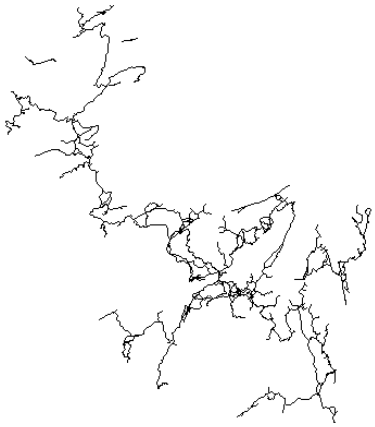

- Ogof Draenen (GB) -
3D Analysis

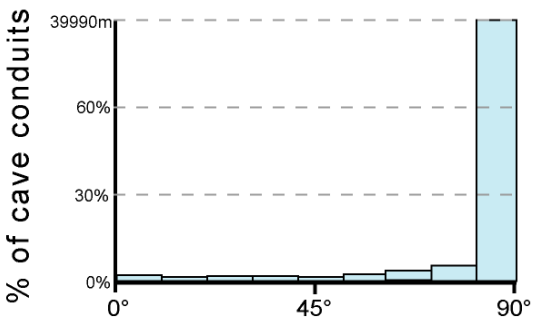

Minimum spatial angle between the normal to the bedding and conduit direction

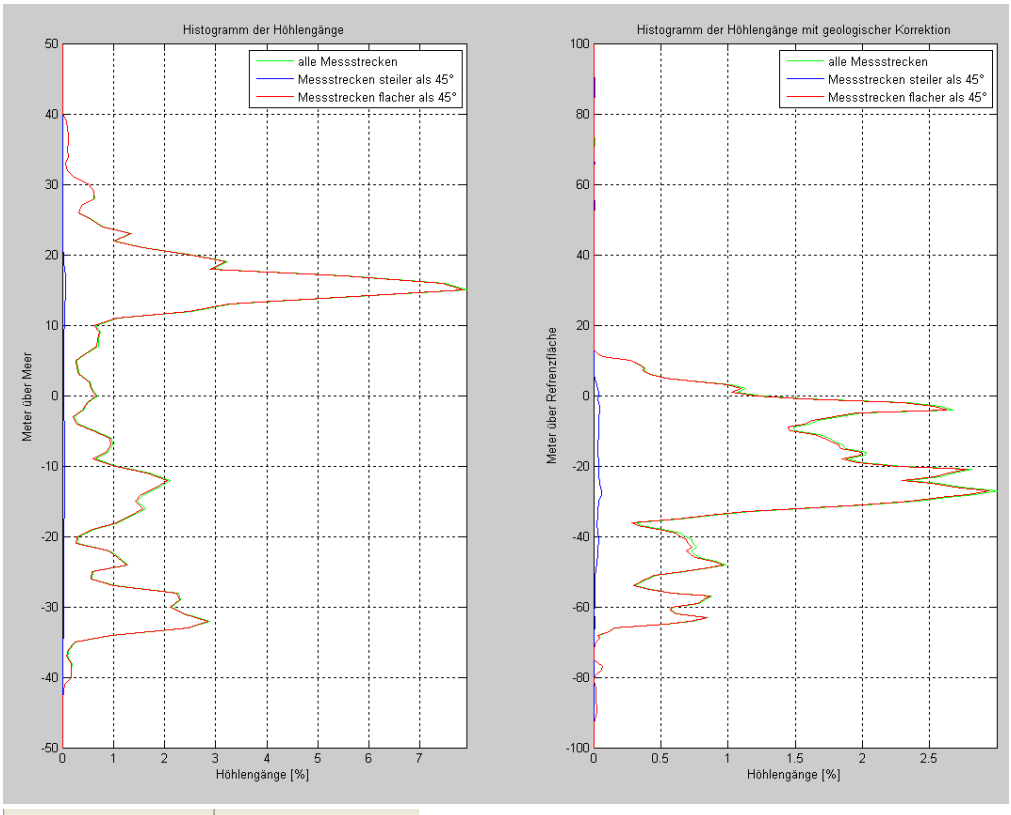

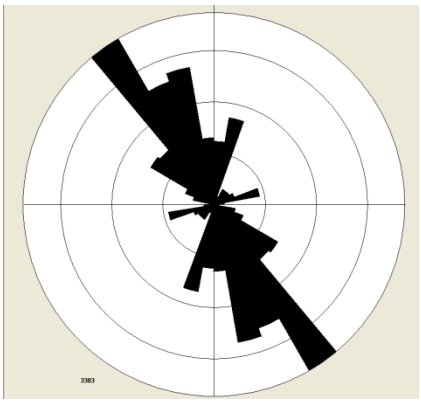

Inception Horizon Type 2

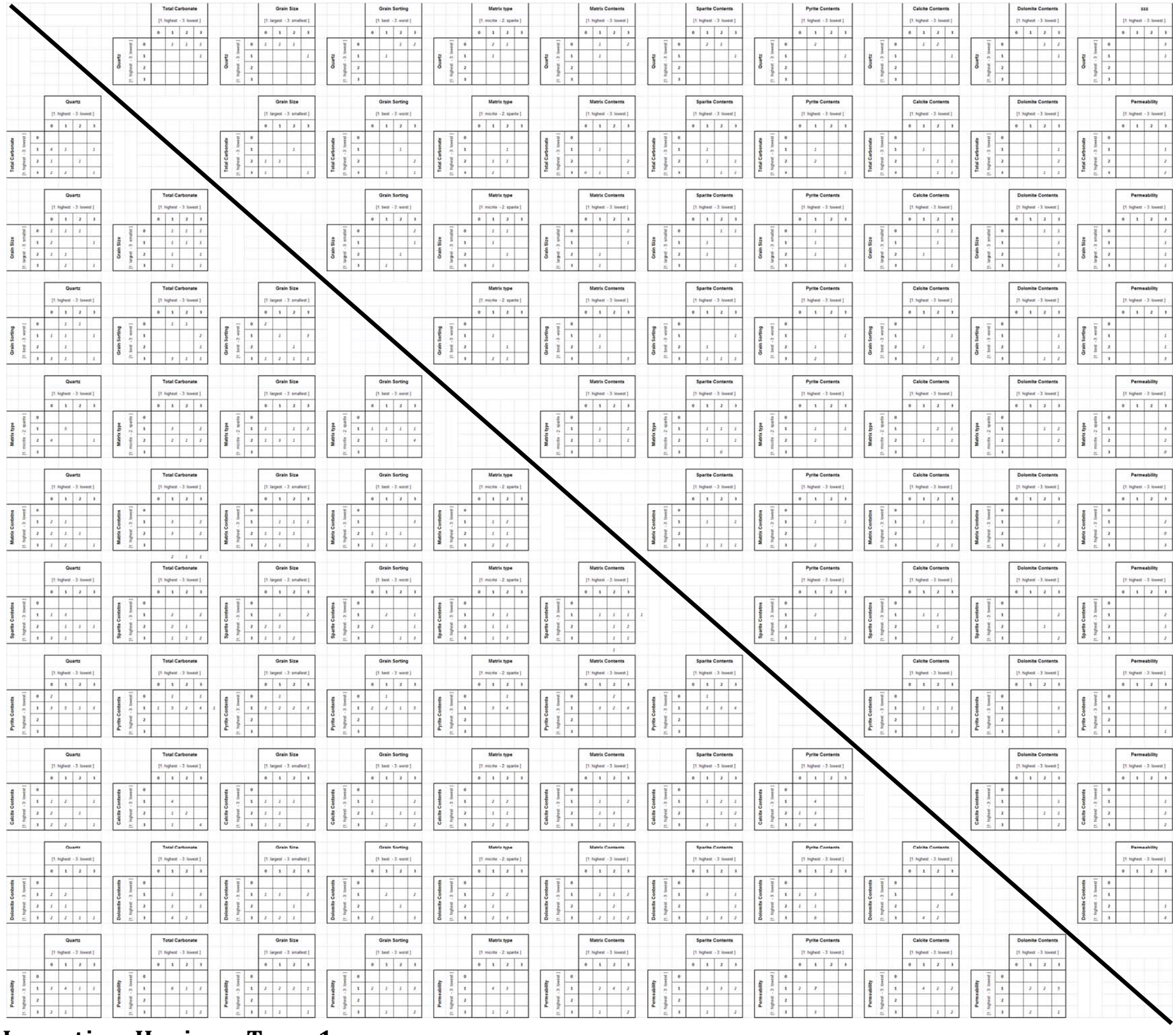

Inception Horizon Type 1

Appendix 2 - Properties Occurrence Matrices

- Appendix 3 - Other Papers

Speläologische Erscheinungen im Zusammenhang mit stratigraphischen Initialfugen.

Filipponi M., 2007: Laichinger Höhlenfreund 42, 21-32.

What makes a bedding plane favourable to karstification? - The role of the primary rock permeability.

Filipponi M., Jeannin P.-Y., 2008: Proceeding of the 4th European Speleological Congress, Spelunca Mémoires, 33: 32-37.

Prediction of karst occurrences by interpreting borehole data within the Inception Horizon Hypothesis.

Filipponi M., Jeannin P.-Y., 2008: Sinkholes and the Engineering and Environmental Impacts of Karst 2008, Proceedings of the 11th Multidisciplinary Conference, Geotechnical Special Publication 183: 120-130.
doi:10.1061/41003(327)13

Laichinger Höhlenfreund, 42. Jahrgang, S. 21 – 32, 13 Abb.; Laichingen 2007

Speläomorphologische Erscheinungen im Zusammenhang mit stratigraphischen Initialfugen

Marco Filipponi

Zusammenfassung

Karsthöhlen entwickeln sich weitgehend entlang von Trennflächen, wobei Schichtfugen eine bedeutende Rolle einnehmen. In der Regel ist nur eine geringe Anzahl von Schichtfugen im regionalen Maßstab bevorzugt verkarstet (in der Regel 3 bis 5), die so genannten stratigraphischen Initialfugen (Englisch „inception horizon“). Assoziiert mit den stratigraphischen Initialfugen können verschiedene speläomorphologische Erscheinungen beobachtet werden, die es ermöglichen, diese Schichtfugen in Feldaufnahmen zu erkennen und ihre speläogenetische Rolle verdeutlichen.
Das Erkennen und Lokalisieren und Kartieren der stratigraphischen Initialfugen (respektive die Position von Karsthohlräumen) ist für verschiedene speläologische, hydrogeologische oder ingenieurgeologische Belange bedeutend.

Einleitung

Karbonatgebirge sind mit einem Netz von tektonischen (Klüfte, Verwerfungen) und stratigraphischen Trennflächen (Schichtfugen, Schichtgrenzen) durchtrennt. Diese stellen die ersten Fließwege für das Grundwasser dar (u.a. KIRALY 1975, KLIMCHOUK & FORD 2000). Wir haben heute ein gutes Verständnis der grundsätzlichen speläogenetischen Prozesse, die während der Entwicklung einer Karströhre (Höhle) entlang jener Trennflächen tätig sind (z.B. KLIMCHOUK et al. 2000, DREYBRODT et al. 2005). Die Herausforderung zu verstehen, weshalb nur gewisse Trennflächen verkarstet werden, bleibt allerdings noch bestehen.

In den letzen Jahrzehnten beschäftigten sich verschiedene Autoren vorwiegend mit der Entwicklung von Karströhren/-höhlen entlang von tektonischen Trennflächen. So stellte zum Beispiel ERASO (1985) fest, dass bevorzugt Klüfte verkarstet werden, welche sich parallel zum Hauptspannungsfeld des Gebirges entwickelten (parallel zu σ_1 streichende Klüfte); oder PALMER (2002), der die Zeit abschätzte, die für die Entstehung einer Karströhre entlang einer Kluft nötig ist. Dabei schienen die stratigraphischen Trennflächen eine untergeordnete Rolle einzunehmen. Erst die Arbeiten von LOWE (1992, 2000) lenkten das Interesse erneut auf die Schichtfugen und führten das Konzept der „inception horizons“ ein. Er erkannte, wie bereits andere vor ihm (z.B. RAUCH & WHITE 1970; WALTHAM 1971; PALMER 1975, 1989), dass sich Höhlen bevorzugt entlang weniger bestimmter Schichtfugen entwickelten, den so genannten stratigraphischen Initialfugen (auf englisch „inception horizon“). Der deutsche Begriff Initialfuge kann irreführend sein, da es sich um (Schicht-)Fugen im weiteren Sinne handelt und auch für Zwischenlagen von einigen Zentimetern bis Dezimetern verwendet wird.

Anschrift des Verfassers : MARCO FILIPPONI, GEOLEP, Laboratoire de géologie de l’ingénieur et de l’environnement, Ecole Polytechnique Fédérale de Lausanne (EPFL) ;
Arbeitsgemeinschaft für Speläologie Regensdorf (AGSR); Korrespondenz: Neugrütstrasse 1; CH-5332 Rekingen – Schweiz; marco.filipponi@epfl.ch

Die stratigraphischen Initialfugen unterscheiden sich von “normalen“ Schichtfugen dadurch, dass sie bevorzugt verkarstet werden. Die Eigenschaften, die diese Lagen besonders verkarstungsanfällig machen, müssen nicht zwingend während der Sedimentation oder Diagenese erlangt worden sein (z.B. Gipslagen, Mergellagen, fossilreiche Lagen, Mg-Ca-Gehalt), sondern können auch später während der Initialisierung erworben werden (z.B. Erhöhung der Primärporosität durch Pyrit-Verwitterung). Als Initialisierung wird jene Zeit zwischen der Diagenese und der Höhlenentstehung bezeichnet (LOWE 2000) *[Abb. 6].* Während dieser Zeit, die in den meisten Fällen mehrere Millionen Jahre andauert, weisen die Lösungshohlräume noch keine bevorzugte Orientierung auf. Die Initialisierung endet mit dem “Durchbruch“ (in Englisch „breakthrough“), bei dem sich das Fließverhalten im Karströhrennetz drastisch ändert (von laminar zu turbulent) und sich ein gerichtetes Karströhrennetz zu entwickeln beginnt (Richtung Vorfluter). Die eigentliche Höhlenentstehung hat begonnen (DREYBRODT & SIEMERS 2000). Es ist hervorzuheben, dass die Initialisierung und die Höhlenentstehung im selben Gebirge gleichzeitig vorkommen können, jedoch auf verschiedenen Höhenlagen. *[Abb. 1] (*FILIPPONI et al. submitted).

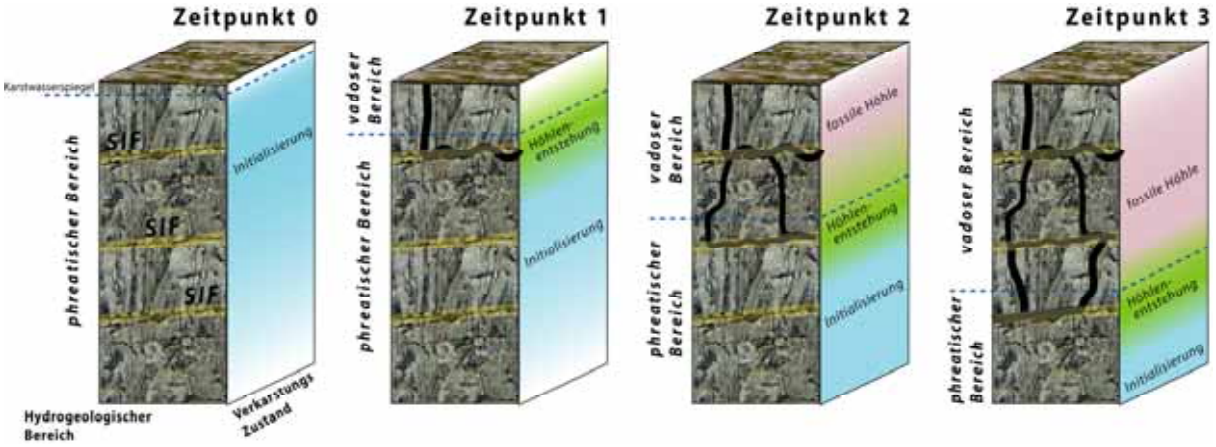

Abb. 1: Schematische Entwicklung eines Karstsystems in Zeit und Raum (vertikaler Schnitt): Verschiedene Bereiche eines Gebirges sind zum selben Zeitpunkt in einem unterschiedlichen Verkarstungszustand. Während der Initialisierung wird die spätere Höhlenentstehung entlang der stratigraphischen Initialfugen vorbereitet.

Im Rahmen einer Doktorarbeit in Zusammenarbeit mit dem Schweizerischen Institut für Speläologie und Karstforschung (SISKA) und der Eidgenössischen Technischen Hochschule Lausanne (EPFL) wurde die Rolle der stratigraphischen Initalfugen während der Verkarstung eines Gebirges genauer untersucht. Hierfür wurde statistisch der Zusammenhang zwischen der Schichtlagerung und der räumliche Anordnung der Höhlengänge von mehr als 15 Höhlensystemen (resp. mehr als 1500 km Höhlengänge) analysiert (FILIPPONI & JEANNIN 2006, FILIPPONI & DICKERT 2007, FILIPPONI et al. submitted). Es zeigte sich, dass sich rund 70% der phreatischen Gänge entlang von Schichtfugen entwickelt haben, wobei nur eine geringe Anzahl Schichtfugen (in der Regel 3 bis 5 stratigraphische Initialfugen) bevorzugt verkarstet wurden [Abb. 2]. Dadurch konnte erstmals die „inception horizon hypothesis“ quantitativ bestätigt werden.

Die Untersuchungen führten zu einem konzeptionellen Modell *[Abb. 3]* (FILIPPONI et al. submitted*)*, in dem sich die Höhlen unter phreatischen Bedingungen bevorzugt am Verschnitt von tektonischen Trennflächen mit einer stratigraphischen Initialfuge entwickeln, während die regionale Gangrichtung durch den hydraulischen Gradienten bestimmt wird.

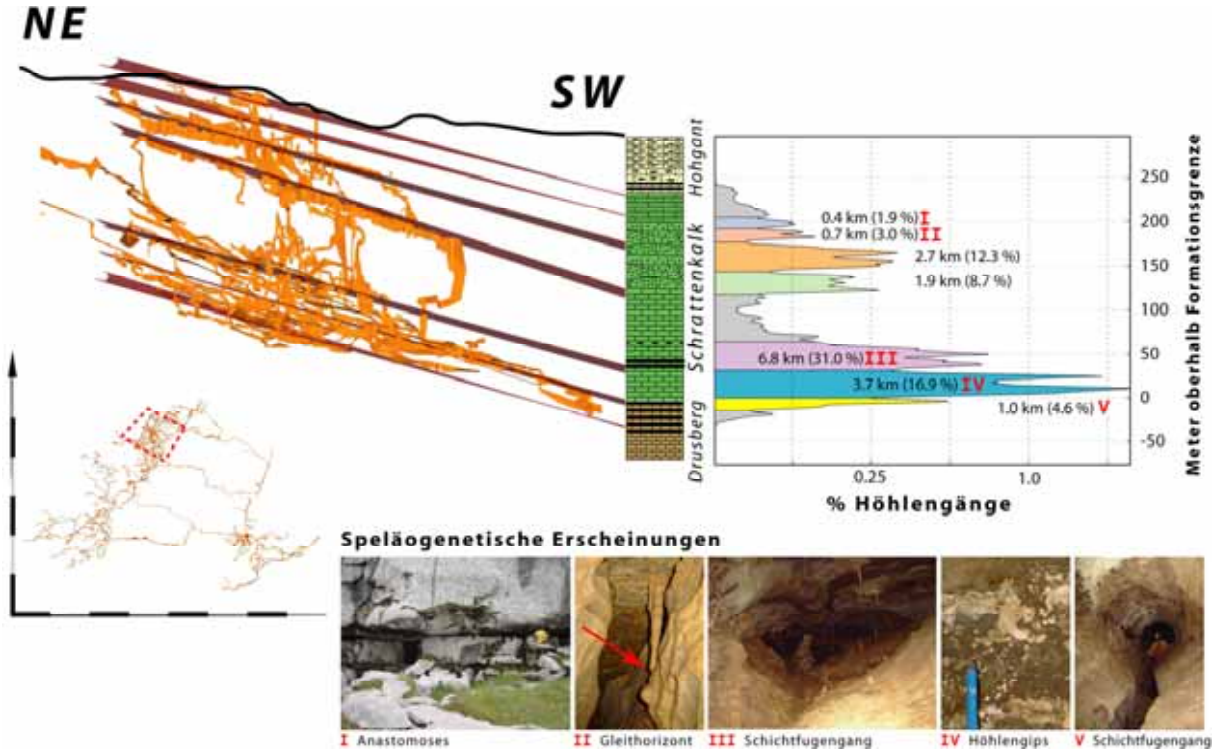

Abb. 2: Histogramm der Abstände der Höhlengange von der Formationsbasis. Die Peaks stellen stratigraphische Bereiche dar, die bevorzugt verkarstet sind (stratigraphische Initalfugen). Der Feldnachweis der statistisch identifizierten Initialfugen zeigte, dass entlang dieser Horizonte verschiedene typische speläomorphologische Erscheinungen festgestellt werden können.

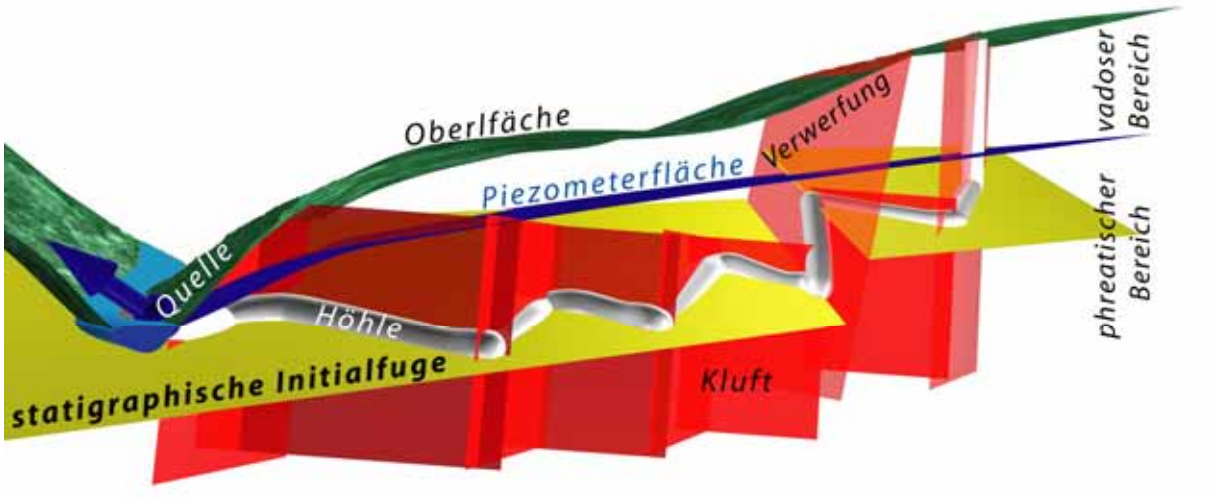

Abb. 3: Schematisches 3D Model eines Höhlensystems: Der Verlauf des phreatischen Höhlenganges wird bestimmt durch die Lage der stratigraphischen Initialfuge, dem Verschnitt mit Klüften sowie dem hydraulischem Gradienten.

Abhängig von der Güte des geologischen Modells sowie der Vermessungsdaten des Höhlensystems lassen sich mit der erwähnten 3D-Analyse die stratigraphische Lage der Initialfugen auf rund ±10 m bestimmen. Diese Genauigkeit reicht jedoch für verschiedene wissenschaftliche (z.B. Ausarbeiten der Schlüsseleigenschaften der Initalfugen) oder ingenieurgeologische (z.B. Planung eines Tunneltraces) Belange nicht aus. Eine höhere Genauigkeit erreicht man durch Kartierung der Initialfugen im Feld. Das Erkennen der bevorzugt verkarstungsfähigen Schichtfugen in einem Aufschluss ist meist nicht einfach. Dieser Artikel möchte die verschiedenen speläomorphologi-

schen Erscheinungen diskutieren, die entlang einer stratigraphischen Initialfuge angetroffen werden können. Die Feldansprache erlaubt es, nicht nur statistisch identifizierte Initialfugen genauer zu lokalisieren, sondern ebenfalls, wo nicht genügend Höhlenvermessungsdaten verfügbar sind für eine zuverlässige 3D-Anaylse (mehrere Kilometerhöhlengänge sind nötig), dennoch ermöglicht bevorzugt verkarstete Bereiche auszuscheiden.

Speläomorphologische Erscheinungen im Zusammenhang mit stratigraphischen Initialfugen

Die im Folgenden beschriebenen speläomorphologische Erscheinungen wurden unter anderem herangezogen, um den Feldnachweis der Existenz der stratigraphischen Initialfugen zu erbringen, die durch die 3D-Analyse der Geometrie der Höhlensysteme identifiziert wurden *(*FILIPPONI et al. submitted*)*. Es ist zu bemerken, dass nicht alle Erscheinungen jeweils an einer bestimmten Initialfuge vorkommen und dass einige Erscheinungen durch verschiede Prozesse entstehen können.

Schichtfugengänge

In der deutschsprachigen Höhlenliteratur hat sich schon früh der Begriff „Schichtfugengang oder –höhle“ durchgesetzt (KYRLE 1923, BÖGLI 1978, TRIMMEL 1968). Er wird für Höhlen verwendet, die entlang von Schichtfugen entstanden sind. Diese weisen meist ein elliptisches oder linsenförmiges Gangprofil auf, während sich das Profil in die Schichtfuge hinein erweitert [Abb. 4]. Wobei es sich bei der Schichtfuge um eine stratigraphischen Initialfuge handelt.

Die Gangprofile können einen Durchmesser von wenigen Dezimetern (darunter werden sie nicht mehr als Höhlengänge bezeichnet, da vom Höhlenforscher nicht befahrbar, sondern als Karströhren; vgl. auch Abschnitt Anastomosen), bis hin zu mehreren Metern aufweisen.

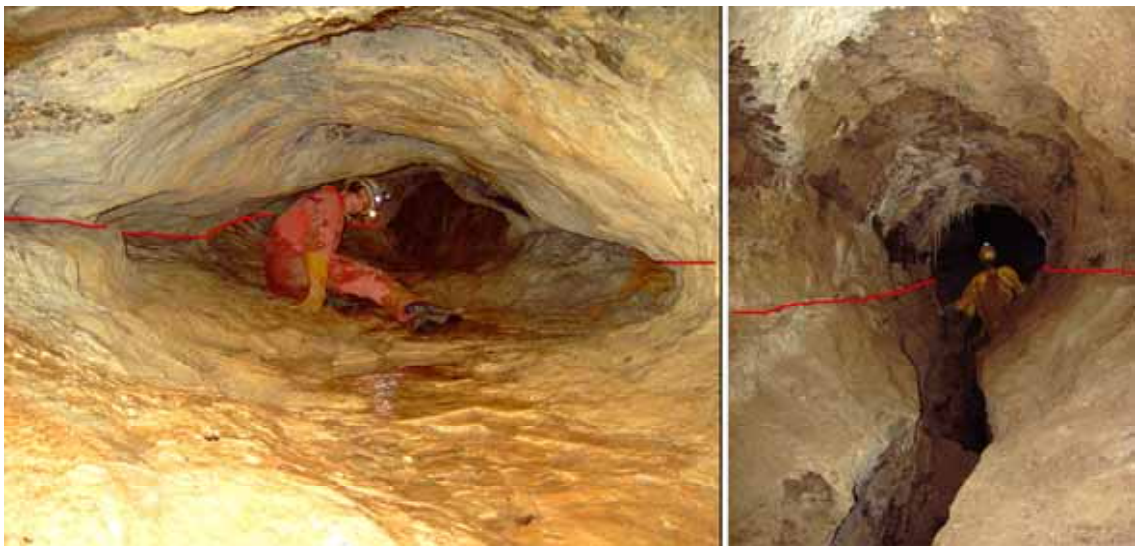

Abb. 4: Schichtfugengänge, in rot die stratigraphische Initialfuge. 4.1 Elliptisches Gangprofil in der Petite Grotte aux Fées, Schweiz; 4.2 Schlüsselloch Profil im Siebenhengste Höhlensystem, Schweiz

Die klassische, elliptische Profilform entstand unter phreatischen Bedingungen, jedoch kann sie in einer späteren vadosen Phase überprägt werden. Dabei wird die Gangsohle allmählich tiefer gesetzt, bis ein so genanntes Schlüssellochprofil entsteht [Abb. 4.3]. In manchen Fällen ist der eingetiefte, vadose Mäander (Bart des Schlüssellochprofils) bedeutender als die Initialellipse. Dieser kann mehrere Meter bis zehner Metern tief sein (z.B. Mäanderpassagen zwischen zwei Schächten in alpinen Höhlen).

In Höhlenpartien, die stark verstürzt sind, kann es zur Bildung von „falschen“ Schichtfugengängen kommen. Vor allem in dünnbankigem Gebirge kann der Versturz zu einem „neuen“ elliptischen Gewölbe führen. Dieser neu entstandene Hohlraum befindet sich oberhalb des natürlichen Hohlraums und hat keinen Bezug zu einer Initialfuge.

Die Schichtfugengänge müssen klar unterschieden werden von Schichtgrenzgängen, wobei sich die letzteren entlang einer Schichtgrenze entwickelt haben, also am Kontakt einer verkarstungsfähigen Gesteinsformation mit einer nicht verkarstungsfähigen. Als Beispiel hierfür sei das Seichbergloch (Länge 2.2 km / Höhenunterschied -560 m; Wildhaus, Schweiz) erwähnt, das weitgehend entlang der Schichtgrenze zwischen der verkarstungsfähigen Seewerkalk- und der nicht verkarstungsfähigen Garschella-Formation entstand (DICKERT 1995).

Anastomosen

Als Anastomosen wird ein Netz von Karströhren bezeichnet, das in einen Höhlengang mündet [Abb. 5] oder an der Decke eines Höhlenganges aufgeschlossen ist [Abb. 6.2]. Die Karströhren weisen einen Durchmesser von wenigen Zentimetern bis Dezimetern auf.

Abb. 5: Anastomosen in der Mammoth Cave (USA). Die statigraphische Initialfuge entlang der sich die Anastomosen entwickelte, ist verantwortlich für ein Höhlengangnetz von mehreren Kilometern Länge.

In der Literatur werden verschiedene Möglichkeiten der Entstehung der Anastomosen diskutiert. So erklärt unter anderem ĆALIĆ-LJUBOJEVIĆ (2001) die Entstehung der Karströhren, die entlang einer Schichtfuge in einen Höhlengang münden, durch Wasser, das während Hochwasserereignissen in die Schichtfuge fließt und bei Niedrigwasser wieder ausfließt. Daher betrachtet er Anastomosen als eine Erscheinung, die erst nach dem Höhlengang entstand.
Ein anderer Erklärungsansatz sieht die Anastomose als „Proto-Höhlen“ [Abb. 6] (u.a. Ewers 1966, WHITE 1988). Dabei wird davon ausgegangen, dass zu Beginn der Höhlenentstehung das Grundwasser durch eine Vielzahl von Karströhren entlang der stratigraphischen Initialfuge fließt. Nur allmählich gewinnt eine Karströhre an Bedeutung, bevorzugt den Durchfluss und erweitert sich stärker als die umgebenden Karströhren. Unter Situationen, bei denen es relativ lange dauert, bis sich eine klar bevorzugte Entwässerungsröhre entwickelt, wachsen mehrere Röhren gleichzeitig zu Höhlengängen heran, was zu labyrinthischen Höhlenpartien führt (z.B. Hölloch, Schweiz).

Oft ist es schwer, Belege für den einen oder anderen Ansatz zu finden. Jedoch weisen folgende Indizien eher auf den zweiten Ansatz, der „Proto-Höhlen-Anastomosen“:

- Ein Höhlengang, in dem die Anastomoses beobachtet wird, ist ein Schichtfugengang;
- Ein Höhlengang, in dem die Anastomoses beobachtet wird, ist Teil einer labyrinthischen Höhlenpartie;
- Es lässt sich ein Netz von Anastomosen/Karströhren erkennen;
- Anastomosen setzte sich an der Höhlengangdecke fort.

In einem vollständig mit Sedimenten gefülltem Höhlengang kann Wasser, das zwischen Sediment und Gangdecke fließt, Strukturen verursachen, die Anastomosen gleichen (SLABE 1995). Sie lassen sich von echten Anastomosen dadurch unterscheiden, dass sie keinen Zusammenhang mit einer stratigraphischen Initialfuge aufweisen, respektive keine Fortsetzung der Kanäle in den Fels erkannt werden können.

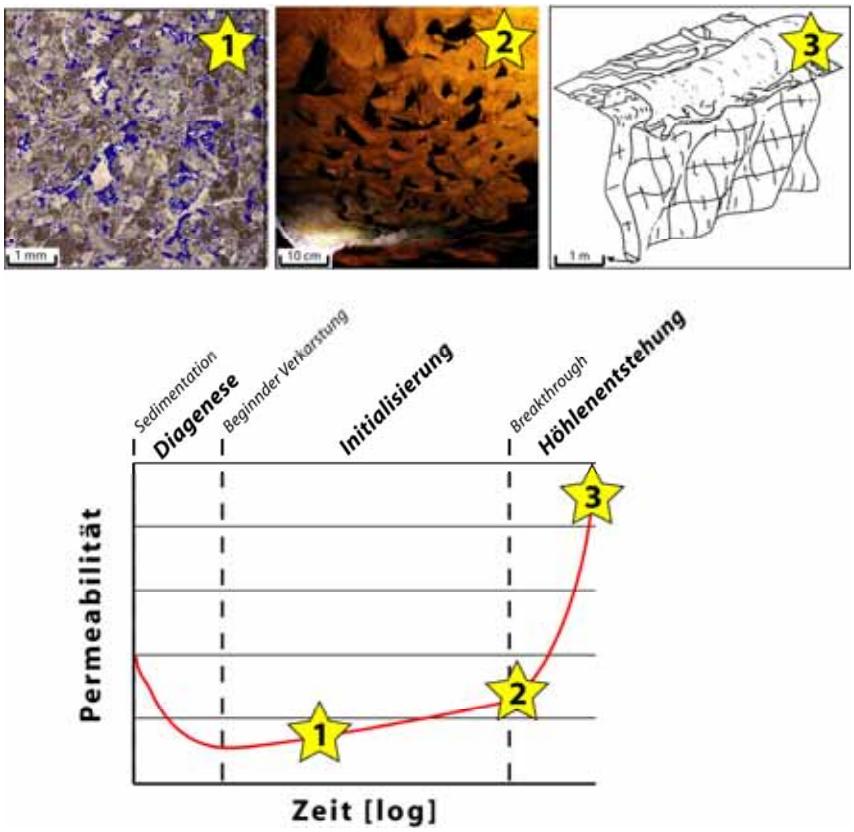

Abb. 6: Entwicklung der Permeabilität eines Gebirges während der Verkarstung: 6.1 mikroskopische, lokale Lösungshohlräume; 6.2 Entstehung eines Netzes von Karströhren (Anastomosen); 6.3 Höhlengang in einem Netz von Karströhren (Abbildung aus FORD & WILLIAMS (2007)).

Höhlenkarren

Höhlenkarren sind wie Karren an der Oberfläche rinnen- oder rillenförmige, korrosive Kleinformen. Sie entstehen durch eine flächenhafte Benetzung der Felsoberfläche und können sowohl an der Gangsohle als auch an der Höhlenwand angetroffen werden (SLABE 1995).

Liegt das obere Ende von „Höhlenwandkarren“ an einer Schichtfuge, lässt dies vermuten, dass die Karren durch Sickerwässer aus einer stratigraphischen Initialfuge entstanden sind [Abb. 7]. Wie bei den Anastomosen wird in der Literatur kontrovers diskutiert, ob es sich dabei um Sickerwässer handelt, die entlang einer stratigraphischen Initialfuge in den Höhlengang gelangten (FORD & LUNDBERG 1987) oder ob Wasser bei Hochwasser in die Schichtfugen geflossen ist und bei Niedrigwasser wieder ausfloss und die Karren bildete.

Karrenähnliche Strukturen können ebenfalls unter Sedimentablagerungen entstehen (SLABE 1995). Diese unterscheiden sich von Höhlenwandkarren durch eine weniger regelmäßige Rillenstruktur sowie eine weniger klare Obergrenze, die zudem nicht auf einer Schichtfuge liegt.

Abb. 7: Höhlenwandkarren: Das obere Ende der Höhlenwandkarren liegt an einer stratigraphischen Initialfuge. (Hirlatzhöhle, Österreich; Foto: LUKAS PLAN).

Höhlensinter

Während bei den Höhlenwandkarren das Wasser aus den stratigraphischen Initialfugen genügend Lösungskraft besitzt, um Karren zu bilden, kommt es auch vor, dass das Sickerwasser in den Schichtfugen mit Kalzium gesättigt ist und es beim Eintritt in den Höhlengang zur Ausfällung von Höhlensinter entlang der Schichtfuge kommt [Abb. 8].

Abb. 8: Sinterablagerung entlang einer stratigraphischen Initialfuge (Hirlatzhöhle, Österreich).

Quellenaustritte

Stratigraphische Initialfugen wurden nicht nur während der Initialisierung oder später während der Höhlenbildung durchflossen, sondern sind meist auch heute noch Fließwege des Sickerwassers durch das Gebirge. Daher liegen Quellaustritte an der Oberfläche oder in einem Höhlengang oft entlang stratigraphischer Initialfugen. Diese Quellen können Höhleneingänge mit einer Schüttung bis zu mehreren Kubikmeter pro Sekunde sein [Abb. 9.1], oder nur diffuse Quellhorizonte mit vielen kleinen Wasseraustritten [Abb. 9.2].

Dies erlaubt es zum Beispiel, relativ einfach Initalfugen in einem Oberflächenaufschluss zu erkennen; zum Beispiel im Winter durch Eiswasserfälle (KNEZ 1998) oder im Sommer durch eine üppige, feuchtliebende Vegetationsvergesellschaftung [Abb. 9.2]. In der Höhle sind zum Teil Wandkarren oder Höhlensinter mit Quellaustritten entlang der Initialfuge assoziiert.

Höhlenruinen

Höhlenruinen (engl. unroofed caves) sind Höhlen oder Höhlenpassagen, deren Überdeckung durch Oberflächenerosion abgetragen wurde und die dadurch an der Oberfläche aufgeschlossen sind [Abb. 10] (KNEZ & SLABE 2002). Bei den Höhlenruinen handelt es sich vorwiegend um horizontale Höhlenpassagen, die, wie ŠUŠTERŠIČ (1998) feststellte, oft entlang einer stratigraphischen Initialfuge angelegt sind vgl. auch Abschnitt Schichtfugengänge). .

Höhlengips

Im Zusammenhang mit stratigraphischen Initialfugen stehen teilweise auch Höhlengipsausblühungen [Abb. 11]. Mehr oder weniger unabhängig von der Erscheinungsform (Nadeln, Blumen, Kruste …) ist in Kalkstein- oder Dolomithöhlen in der Regel der Schwefel das limitierende Element zur Bildung des Gipses ($CaSO_4*2H_2O$). Anhand der Herkunft des Schwefels können vier verschiedene Arten von Höhlengips unterschieden werden (FILIPPONI & JEANNIN 2007) - Die Herkunft des Gipses wird durch δ^{34}S-Isotopenuntersuchungen bestimmt -:

Abb. 9: Quellhorizont entlang stratigraphischer Initialfugen: 9.1 - Karstquelle der Réseau de Covatannaz (Schweiz): 9.2 - Quellhorizont entlang einer Initialfuge mit üppiger, feuchtliebender Vegetationsvergesellschaftung.

Abb. 10: Freilegung und Zerstörung eines Karstgebietes durch die Oberflächenerosion: Zeitpunkt 2 - Höhlenruine.

- **Gips aus der Wiederausfällung von sedimentärem Gips**
  Besteht der Höhlengips aus erneut ausgefallenem sedimentärem Gips, weist dies auf die Möglichkeit hin, dass die Initialfuge mindestens teilweise aus Gips bestand. Da Gips rund 10 bis 30 mal besser löslicher als Kalzit ist (BÖGLI 1978), wird die Verkarstung entlang der gipsreichen Schichtfuge begünstigt (z.B. Moggerenschacht, Deutschland).
- **Gips aus der Verwitterung von Pyrit**
  Die Oxidation von Pyrit (FeS_2) kann zur Bildung von stark korrosiver Schwefelsäure führen, die lokal die Initialisierung der Verkarstung entlang einer pyritreichen Schichtfuge begünstigen kann [Abb. 12] (BÖGLI 1978, WHITE & WHITE 2003). Als „Nebenprodukt" wird teilweise Gips ausgeschieden. Eine solche zusätzliche Erhöhung der Lösungskapazität hat eine geringe Bedeutung für die Entwicklung der Karströhren nach dem "Durchbruch" [vgl. Abb. 6], jedoch kann zu einem frühen Zeitpunkt die primäre Gebirgsdurchlässigkeit lokal erhöht und die Entwicklung von Karsthohlräumen dadurch begünstigt werden (FILIPPONI & JEANNIN 2007).
- **Gips aus hydrothermalem Schwefel**
  Einige Höhlen entstanden unter dem Einfluss von sulfatreichen hydrothermalen Wässern (hypogene Höhlen - GALDENZI & MENICHETTI 1995, HILL 1995), was zur Ausfällung von zum Teil spektakulären Gipsablagerungen führte (z.B. Grotte di Frasassi, Italien, oder Lechuguilla Cave, USA). Diese Art von Höhlengips hat keinen direkten Zusammenhang mit einer stratigraphischen Initialfuge.
- **Gips aus atmosphärischem Schwefel**
  Die Luft besteht unter anderem aus we-

nigen Mikrogramm Schwefeldioxid pro Kubikmeter. Dieser kann durch Niederschlag in den Untergrund gelangen (COOK & HERCZEG 2000) und, wie einige Fälle zeigen, zur Ausfällung von Gips führen (z.B. Okgye Cave, Korea - CHOI & WOO 2005). Diese Art von Höhlengips hat keinen Zusammenhang mit einer stratigraphischen Initialfuge.

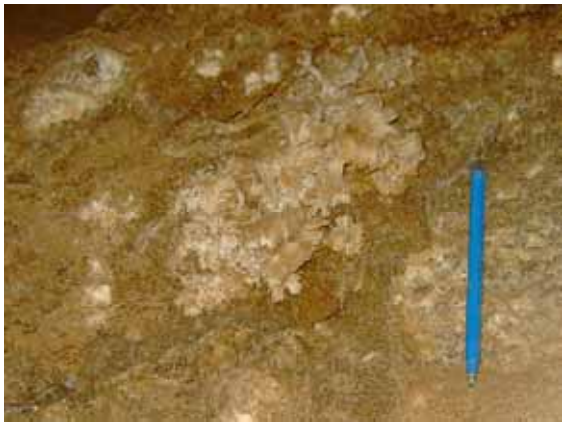

Abb. 11: Höhlengipsausblühung als Nebenprodukt der Pyrit-Verwitterung entlang einer stratigraphischen Initialfuge (Siebenhengste Höhlensystem, Schweiz).

Abb. 12: Dünnschliff einer pyritreichen stratigraphischen Initialfuge: schön zu erkennen ist ein Pyrit-Kristall und von diesem ausgehend ein mäanderartiger Lösungshohlraum (Dünnschliff aus der Schichtfuge vgl. Abbildung 11).

Gleithorizont

In manchen Fällen beobachtet man, wie das Gangprofil entlang einer Schichtfuge verschoben wurde [Abb. 13], wobei es sich oft um die stratigraphische Initialfuge handelt. Die Bewegungsbeträge sind oft im Bereich von wenigen Zentimetern bis Dezimetern.

Leider ist es nur in besonderen Fällen möglich Aussagen zu machen, ob bereits vor der Initialisierung Bewegung entlang der Schichtfuge stattgefunden hat, oder ob diese erst nach dem Beginn der Verkarstung eingesetzt hat.

Diskusison / Schlussfolgerungen

Im vorhergehenden Abschnitt wurden verschiedene speläomorphologische Erscheinungen vorgestellt, die im Zusammenhang mit stratigraphischen Initialfugen stehen. Das Erkennen dieser Erscheinungen im Feld hilft festzustellen, ob und entlang welcher Schichtfugen bevorzugt verkarstet wurde. Jedoch geben diese Feldbeobachtungen nur relativ geringe Hinweise über die Funktion der Schichtfugen für die Verkarstung. Nach LOWE (2000) lassen sich vier mögliche Einflüsse der Initialfugen für die Verkarstung eines Gebirges unterscheiden:

- Erhöhte primäre Permeabilität der stratigraphischen Initialfuge als das Umgebungsgestein und dadurch bevorzugt wasserwegsam,
- geringere primäre Permeabilität als das Umgebungsgestein (z.B. Mergel-/Tonlagen) kann zu einem bevorzugten Grundwasserfluss entlang der Schichtfuge führen,
- besser verkarstungsfähig als das Umgebungsgestein zum Beispiel durch leicht lösliche Mineralien, wie Gips, in einer Schichtfuge,
- die Verwitterung von gewissen Mineralien (z.B. Pyrit) kann lokal zu einer Erhöhung der Lösungskraft führen.

Die Felderkennung der speläomorphologischen Erscheinungen hilft zu entscheiden, welche der in einem Höhlengang aufgeschlossenen Schichtfugen am wahrscheinlichsten die Initialfuge ist. Einmal identifiziert kann die entsprechende Schichtfuge beprobt und im Labor genauer untersucht werden (FILIPPONI et al. 2007). In Höhlengängen ohne ein eindeutiges elliptisches Gangprofil ist es manchmal nicht sehr einfach zu erkennen, ob und entlang welcher Schichtfuge die Höhle entstanden ist. In

manchen Gangabschnitten weisen sogar mehrere Schichtfugen die typischen Merkmale einer stratigraphischen Initialfuge auf und führt zur Frage, ab wann eine Schichtfuge als stratigraphische Initialfugen bezeichnet werden soll.
In einer stratigraphischen Abfolge hat es meistens eine Vielzahl von Schichtfugen, die lithologische Voraussetzungen hätten eine Initalfuge zu sein. Einige werden gar für wenige Meter als bevorzugter Fließweg verwendet, dann jedoch wieder verlassen. Von einer stratigraphischen Initialfuge soll jedoch nur gesprochen werden, wenn die Schichtfuge nicht nur im lokalen, sondern im regionalen Maßstab (größer als 0.1 km^2) die räumliche Anordnung der Höhlengänge mitbestimmt.

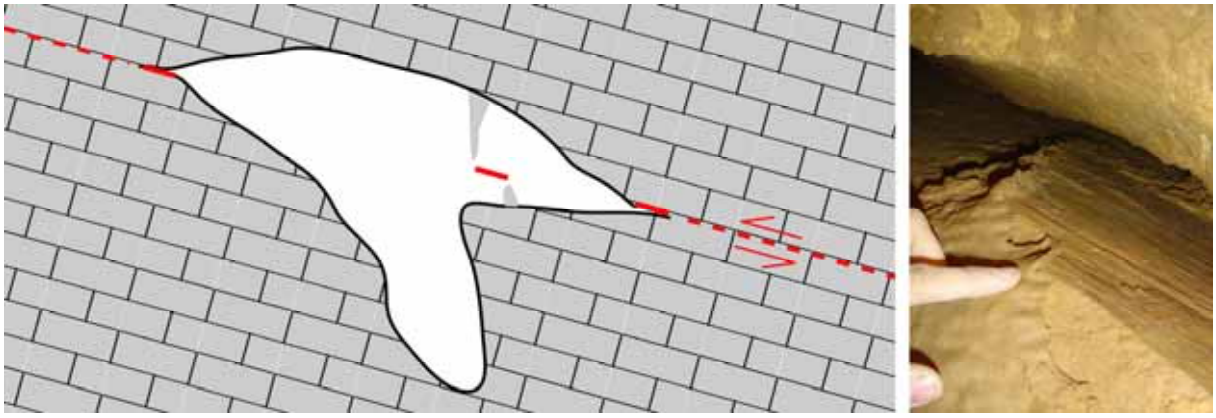

Abb. 13: Neotektonische Bewegung entlang einer stratigraphischen Initialfuge. 13.1: Schematische Darstellung eines verschobenen Gangprofils durch Gleiten entlang einer Schichtfuge; 13.2: Deutlich zu erkennen der Versatz von rund 20cm sowie die Harnischfläche entlang einer stratigraphischen Initalfuge (Nidlenloch, Schweiz).

Benachbarte Höhlensysteme weisen zum Teil unterschiedlich stark ausgeprägte Initalfugen auf (FILIPPONI et al. submitted). In manchen Fällen sind bei nahe beieinander liegenden Höhlen andere Schichtfugen als stratigraphische Initialfuge festzustellen (PLAN et al. submitted). Dies liegt einerseits daran, dass sich die Eigenschaften der Schichtfugen lateral verändern, anderseits hängt es nicht nur von den lithologischen Eigenschaften ab, ob eine Schichtfuge verkarstet wird oder nicht. Denn neben der Lithologie beeinflussen auch die hydrologischen Rahmenbedingungen und biochemische Faktoren die Intensität der Verkarstung einer Schichtfuge (KIRALY 1975). So können entlang einer Schichtfuge unter einem weniger günstigen Kontext nur mikroskopisch kleine Lösungshohlräume entstehen, während ein wenig weiter entfernt die Situation günstiger ist und sich ein ausgeprägtes Höhlengangsystem entwickelt. Diese Zusammenhänge sind jedoch Bestandteil aktueller Untersuchungen.

Zur Ausscheidung der Initialfugen mittels der 3D-Analye von Höhlengängen (FILIPPONI & JEANNIN 2006, FILIPPONI et al. submitted) sind Vermessungsdaten von mehreren Kilometern an Höhlengängen nötig. Zwar ist es möglich, die Messdaten von einem nicht zusammenhängenden Netz von Höhlengängen (resp. Kleinhöhlen) auszuwerten, doch können dabei lokal wichtige Schichtfugen überbewertet werden. Es zeigte sich jedoch, dass diese lokalen Schichtfugen nur bedingt Erscheinungen aufweisen, die auf eine stratigraphischen Initialfuge hindeuten. *Daher erwies es sich als effizient und zuverlässig in Gebieten mit einer Vielzahl von Kleinhöhlen, die stratigraphischen Initialfugen im Feld anhand von speläomorphologischen Erscheinungen zu identifizieren, zu kartieren und auszuwerten.*

Danksagung

Das Forschungsprojekt Karst-ALEA wurde finanziell durch den Schweizerischen Nationalfonds unterstützt (SNF 200020-116207/1).

Schriftenverzeichnis

BÖGLI, A. (1978): Karsthydrographie und physische Speläologie. – 292 S.; Berlin-Heidelberg (Springer).

ĆALIĆ-LJUBOJEVIĆ, J. (2001): Upward growth of bedding –plane anastomoses. 13th International Congress of Speleology, 71-73; Brasilia.

CHOI, D.W., WOO, K.S. (2005): Origin of the gypsum flower in Okgye Cave, Korea. – Journal of the Geological Society of Korea, **41**(4): 451-464; Seoul.

COOK, P.G., HERCZEG, A. L. (2000): Environmental tracers in subsurface hydrology. – 529 S.; Boston (Kluwer Academic Publishers).

DICKERT, A. (1995): Das Seichbergloch. – Höhlenpost, Nr. **98**: 1-56; Zürich.

DREYBRODT, W., GABROVŠEK, F., ROMANOV, D. (2005): Processes of Speleogenesis: A Modeling Approach. – Carsologica, 376 S.; Postojna-Ljubljana.

DREYBRODT, W., SIEMERS, J. (2000): Cave evolution on two-dimensional networks of primary fractures in limestone. – In : KLIMCHOUK, FORD, PALMER & DREYBRODT (eds): Speleogenesis, evolution of karst aquifers, 201-211; Huntsville.

ERASO, A. (1985): Método de Predicción de las Direcciones Principales de Drenaje en el Karst. – KOBIE, Serie Ciencias Naturales, **15**: 15-165; Bilbao

EWERS, R (1966): Bedding-plane anastomoses and their relation to cavern passages.- Bulletin of the National Speleological Society of America. **28**(3): 133-140; Huntsville

FILIPPONI, M., DICKERT, A. (2007): Verstehen der Speläogenese durch 3D-Analyse – Fallbeispiel des Lachenstock Karstes. – 12. Nationaler Kongress für Höhlenforschung: 46-55; Vallée de Joux (Schweiz).

FILIPPONI, M., JEANNIN, P. -Y. (2006): Is it possible to predict karstified horizons in tunneling? Austrian Journal of Earth Sciences, 99: 24-30; Wien.

—— (2007): Cave gypsum an indicator for early speleogenetical processes? Geophysical Research Abstracts, Vol. 9, European Geosciences Union , http://www.cosis.net/abstracts/EGU2007/08499/EGU2007-J-08499.pdf?PHPSESSID=e

FILIPPONI, M., JEANNIN, P.Y., PARRIAUX, A. (2007): From the inception horizon hypothesis to a prediction toll for karstified horizons. – International Conference on Karst Hydrogeology and Ecosystems, S. 16; Boweling Green.

FILIPPONI, M., JEANNIN, P.-Y., TACHER, L. (submitted): Evidence of inception horizons in karst conduit networks. – Geomorphology.

FORD, D.C., LUNDBERG, J. (1987): A review of dissolutional rills in limestone and other soluble rocks. – Catena Supplement, 8: 119-140; Cremlingen-Destedt.

FORD, D.C., WILLIAMS, P. (2007): Karst Hydrogeology and Geomorphology. – 562 S.; West Sussex (Wiley).

GALDENZI, S., MENICHETTI, M. (1995): Occurence of hypogenic caves in a karst region: Examples from central Italy. – Environmental Geology, **26**: 39-47; New York.

HILL, C. (1995): Sulfur redox reaction: Hydrocarbons, native sulfur, Mississippi Valley-type deposits, and sulfuric acid karst in the Delaware Basin, New Mexico and Texas. – Environmental Geology, **25**(1): 16-23; New York.

KIRALY, L. (1975): Rapport sur l'état actuel des connaissances dans le domaine des caractères phsyiques des roches karstiques. – In :BURGER A. & DUBERTRET L. (eds) : Hydrogeology of karstic terrains, International Union of Geological Sciences, Series B 3: 53-67 ; Rotterdam.

KLIMCHOUK, A., FORD, D.C (2000): Lithologic and structural controls of dissolutional cave development. – In : KLIMCHOUK, FORD, PALMER & DREYBRODT (eds): Speleogenesis, evolution of karst aquifers, 54-64; Huntsville.

KLIMCHOUK, A., FORD, D.C., PALMER, D.C., DREYBRODT, W. (2000): Speleogenesis, evolution of karst aquifers. National Speleological Society, – 527 S.; Huntsville.

KNEZ, M. (1998): The influence of bedding-planes on the development of karst caves (a study of Velika Dolina at Škocjanske Jame Caves, Slovenia). – Carbonates and Evaporites, **13**(2): 121-131; New York.

KNEZ, M., SLABE, T. (2002): Unroofed caves are an important feature of karst surfaces: examples from the classical karst. – Zeitschrift für Geomorphologie, **46**(2): 181-191; Stuttgart.

KYRLE, G. (1923): Theoretische Speläologie. – Speläologisches Institut Bundeshöhlenkommission, 353 S.; Wien.

LOWE, D. (1992): The origin of limestone caverns: in inception horizon hypothesis. – PhD thesis, Manchester Polytechnic, UK, 511 S.; Manchester.

—— (2000): Role of stratigraphic elements in speleogenesis: the speleoinception concept. – In : KLIMCHOUK, FORD, PALMER & DREYBRODT (eds): Speleogenesis, evolution of karst aquifers, 65-76; Huntsville.

PALMER, A.N. (1975): The origin of maze caves. – Bulletin of the National Speleological Society of America. **37**(3): 56-76; Huntsville.

—— (1989): Stratigraphic and structural control of cave development and groundwater flow in the Mammoth Cave region. – In White W.B. and WHITE E.L. (eds): Karst Hydrology, Concepts from the Mammoth Cave Area, Von Nostrand Reinhold, 293-316; New York.

—— (2002): Speleogenesis in carbonate rocks. - In Gabrovsek, F. (eds): Evolution of karst: from prekarst to cessation. ZRC: 43-60; Postojna-Ljubljana.

PLAN, L., FILIPPONI, M., BEHM, M., SEEBACHER, R., JEUTTER, P. (submitted): Constraints on alpine speleogenesis from cave morphology - a case study from the eastern Totes Gebirge (Northern Calcacerous Alps, Austria). – Geomorphology.

RAUCH, H.W., WHITE, W.B., (1970): Lithologic controls on the development of solution porosity in carbonate aquifers. – Water Resources Research, 6: 1175-1192; Washington

SLABE, T. (1995): Cave rocky relief and its speleogenetical significance. Znanstvenoraziskovalni Center Sazu, 128 S.; Ljubljana.

ŠUŠTERŠIČ, F. (1998): Interaction between a cave system and the lowering karst surface – Case Study: Laški Ravnik. – Acta Carsologica, 27,(2): 115-138; Ljublijana.

TRIMMEL, H. (1968): Höhlenkunde. – 300 S.; Braunschweig (Vieweg).

WHITE, W.B. (1988): Geomorphology and hydrology of karst terrains. – 464 S.; Oxford (Oxford University Press).

WHITE, W.B., WHITE, E.L. (2003): Gypsum weding and cavern breackdown: Studies in the Mammoth cave System, Kentucky. – Journal of Cave and Karst Studies, **65**(1): 43-52; Huntsville.

WALTHAM, A.C. (1971): Controlling factors in the development of caves. – Transactions of the Cave Research Group of Great Britain. 13: 73-80;

What makes a bedding plane favourable to karstification? – The role of the primary rock permeability

Filipponi Marco (1) ; Jeannin Pierre-Yves (2)

(1) GEOLEP, Laboratoire de géologie de l'ingénieur et de l'environnement, Ecole Polytechnique Fédérale de Lausanne (EPFL), Station 18, CH-1015 Lausanne - Switzerland; marco.filipponi@epfl.ch

(2) SISKA, Swiss Institute of Speleology and Karstology, Case Postale 818, CH-2301 La Chaux-de-Fonds - Switzerland; pierre-yves.jeannin@isska.ch

Abstract

Recent studies on the complex 3D geometry of large cave systems around the World allowed us to get statistical evidence of the inception horizon hypothesis. It clearly confirmed the idea that the development of karst conduits under phreatic conditions is strongly related to a restricted number of so-called inception horizons. An inception horizon is a part of a rock succession that can favour the earliest cave forming processes (LOWE, 1992). It can favour the karstification by physical, lithological or chemical deviation from the predominant carbonate facies within the sequence.

In order to understand the reason(s) why a specific stratigraphical horizon is used for cave development we sampled 18 inception horizons of six cave systems as well as the surrounding rock mass. More than 200 rock micro-cores have been drilled and analysed to determine parameters controlling the speleogenesis, and to provide a better prediction of dissolution voids within a karstic rock mass. The analysis of these cores gives a first idea of the different key properties of inception horizons. This paper only presents and discusses the results of the measurements of the primary rock permeability. The initial permeability contrast is not sufficient to explain alone the concentration of karst development along inception horizons. However it is noticed that two types of inception horizons can be distinguished: type 1, where cave inception took place within the inception horizon and where the permeability of the inception horizon displayed a slightly higher permeability than the surrounding rock mass; type 2, where inception took place at the interface between the inception horizon and the rock matrix, and where the permeability of the inception horizon is slightly lower than the surrounding matrix.

Résumé

De récentes études sur la géométrie tridimensionnelle des grands systèmes karstiques dans le monde ont permis de démontrer statistiquement l'hypothèse des horizons d'inception. Il a été clairement confirmé que le développement des conduits karstiques en milieu phréatique est fortement lié à un nombre restreint de ce qu'on appelle des horizons d'inception. Un horizon d'inception est une partie de la séquence de la roche carbonatée qui peut favoriser les processus du début de la karstification (LOWE, 1992) que se soit par des différences physiques, chimiques ou lithologiques du faciès prédominant.

Afin de comprendre les raisons pour lesquelles certains horizons stratigraphiques sont particulièrement aptes à la karstification, 18 horizons d'inception ainsi que la roche encaissante ont été échantillonné dans six systèmes karstiques. Plus de 200 micro-carottes ont été prises et analysées afin de déterminer les paramètres contrôlant la spéléogenèse, et d'améliorer la prévision des vides de dissolution dans un massif karstique. L'analyse de ces échantillons donne une première idée des différentes propriétés principales des horizons d'inception. Cet article ne présente et ne discute que les résultats des mesures de la perméabilité primaire de la roche. La différence de perméabilité primaire ne suffit pas à expliquer la concentration des conduits karstiques le long des horizons d'inception. Pourtant, il est possible de distinguer deux types d'horizons d'inception : le type 1, dont la perméabilité est légèrement supérieure à la roche encaissante et où le développement initial des conduits se fait au sein même de l'horizon; type 2, dont la perméabilité est légèrement inférieure à la roche encaissante et où le développement initial des conduits se fait à l'interface entre l'horizon d'inception et la roche encaissante.

Keywords
Speleogenesis, Inception horizons, rock matrix permeability

1. Introduction

Along the last few years our research focussed on the analysis of the 3D geometry of several among the largest cave systems in the World (more than 1500 km of analysed cave conduits). It confirmed that the development and position of karst conduits under phreatic conditions is remarkably related to a restricted number of so-called "inception horizons" (FILIPPONI & JEANNIN, 2006; FILIPPONI & DICKERT, 2007; FILIPPONI ET AL., 2008). An "inception horizon" – a concept introduced by LOWE (1992) – is a part of a rock succession that is particularly susceptible to the effects of the earliest cave forming processes by virtue of physical, lithological or chemical deviation from the predominant carbonate facies within the surrounding sequence. Probably less that 10% of the existing bedding partings of a limestone sequence are inception horizons and guide more than 70 % of the phreatic conduits (FILIPPONI ET AL., 2008). Our analysis clearly confirmed that the influence of these horizons onto the 3D geometry of cave systems is high.

However one main question remains: What makes one specific stratigraphical horizon favourable to karstification and what kind of karst inception processes are dominant? Different descriptions of "preferred bedding planes" are available in the speleological literature; however the interpretation does usually not consider whole framework of the inception horizon hypothesis and they are simply discussed as "bedding planes" (e.g. ORNDORFF ET AL., 2001). Furthermore, in most cases one misses a speleogenetical discussion of the observations. On the other hand in hydrogeological domain research some effort is dedicated in understanding the relation between hydraulic conductivity and texture in carbonate aquifers (e.g. ROVEY & CHERKAUER, 1994; MICHALSKI & BRITTON, 1997; MULDOON ET AL., 2001). These studies demonstrate the existence of links between some specific stratigraphical horizons and zones of elevated hydraulic conductivity. However the question to know if this permeability is primary or due to dissolution voids (karstification) was not addressed. Meanwhile some concrete suggestions are expressed about "why" some parts of the rock succession act as inception horizons but, so far, little analytical confirmation evidences have been presented (e.g. LOWE, 1992; KNEZ, 1997; PEZDIČ ET AL., 1998; FILIPPONI & JEANNIN, 2006).

Several characteristics of the rock mass may play a significant role for speleogenesis. It is known that the karst process follows a positive feedback development; the rock being soluble, water dissolves it and enlarges the voids, which become able to accept more water to flow through, i.e. more dissolution to be active and the voids to enlarge faster (KIRALY, 1975). This loop is self-developing until the system of conduits can absorb the total amount of the water available from the rain with no significant increase of the hydraulic gradient. Therefore we can assume that there are three main aspects that make an inception horizon favourable to karstification (fig. 1): Characteristics controlling the permeability (1), controlling the dissolution rate (2) as well as defining the dissolution capacity of the water (3). The processes under investigation being highly non linear, it is expected that the links are quite complex.

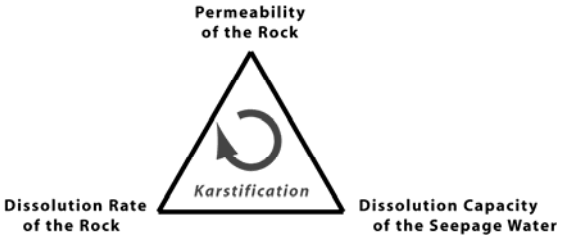

Fig. 1: The process of karstification is a positive feedback loop controlled by factors controlling the rock permeability, dissolution rate and dissolution capacity of the seepage water.

The purpose of this paper is to assess and characterize the primary permeability of inception horizons and to verify if it could be the main factor controlling the development of inception horizons and cave development. Therefore samples along 18 inception horizons of six cave systems were collected. An empirical (statistical) approach has been applied and is presented in the paper. In the discussion part of the paper the statistical results have been linked to a process-oriented approach.

2. Sampling the Inception Horizons

One main challenge in our approach is to assess characteristics of parts of the rock, which are no more existing. In fact the most favourable parts of the rock mass for cave inception have been removed during karstification. Despite this bias one can expect that it will be possible, by choosing appropriate sampling points, to get a qualitative idea of the initial rock properties, or their spatial variation as well as of their role during speleogenesis.

Based on the 3D analysis of cave systems (FILIPPONI & JEANNIN, 2006; FILIPPONI & DICKERT, 2007; FILIPPONI ET AL. 2008) as well as on field verifications, we selected a set of inception horizons for further analysis. A total of 18 known inception horizons in six different cave systems were sampled.

Field observations lead us to remark that three kinds of inception horizons can be distinguished (figure 2):

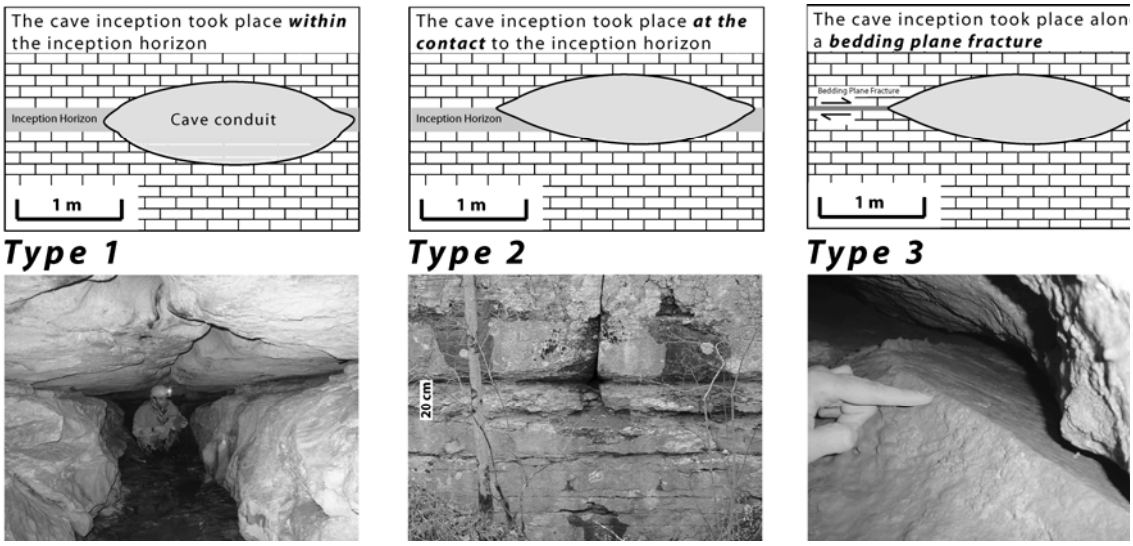

Fig. 2: Three kinds of inception horizons can be distinguished: Cave inception may take place within the inception horizon; at the contact to the inception horizon or along bedding plane fractures. For each type the relation between the conduit position and the inception horizon is sketched in the upper frame. The lower picture provides examples from the field.

Inception horizons where the cave inception took place within the inception horizon (1); at the contact to the inception horizon (2); along bedding plane fractures (3) (interbedded slides). The two first types are linked to lithological properties and the third type to rock mechanical processes.

This paper presents and discusses only results of the permeability measurements of the first two types of inception horizons. The permeability of inception horizons with interbedded slides has not been taken into consideration because the reason for the development of the inception horizon is more obvious: a slippage of just a few millimetres striation, brecciation and surface irregularities enhance openings along the sliding plane and will cause a significant increase in permeability compared to the surrounding rock mass. However an elaborated discussion will be the topic of a further paper.

More than 200 micro-cores (3-5 cm long, diameter of 2.6 cm) have been sampled in order to characterize openings and origin of inception horizons as well as of the surrounding rock mass. Sampling was designed in a way to approach local as well as regional variations of the selected properties. For this propose at least three samples have been taken at a given place of an inception horizon. For some horizons several sampling locations have been selected in order to assess the regional scale heterogeneity.

3. Results

Because of the positive feedback characterising karst development, we expected that the initial permeability of the rock or more precisely the permeability distribution within the rock massif, at early stage of cave genesis is a significant parameter. It is expected that inception horizons have a different permeability than the matrix of the surrounding rock mass. Higher permeability would favour the water to flow through this horizon; whereas horizons of lower permeability would act as low permeability "screen" along (or just above) which water would flow preferentially.

Therefore we measured the permeability of the samples in order to compare their primary permeability. The permeability was measured with an automated gas permeameter (Porous Materials Incorporated, GP-262). The automated gas permeameter measures permeability of porous samples, such as rocks (GOGGIN, 1993), ranging from 0.1 to 50 milliDarcys (1 mD $\approx 10^{-15}$ m^2 $\approx 10^{-8}$ m/s) within an accuracy of 0.5%.

Unfortunately it was not possible to measure the primary permeability of all micro cores. Samples with clear secondary permeability voids have been removed from the analysis. In some cases it was possible to identify by a simple visual inspection that dissolution voids or micro fractures were present. In other cases thin sections of the micro cores showed occurrences of micro fractures or dissolution voids. Sometimes it was simply not possible to collect an unbroken core.

The measured matrix permeability-values are quite low, generally below 1 mD (table 2). Permeability-values of the surrounding rock masses have an average of 0.16 mD with a standard deviation of 0.15. Permeability-values where karstification took place within the inception horizon (Figure 2, type 1) have an average of 0.17 mD with a standard deviation of 0.05. In all cases where cave inception took place at the contact to an inception horizon (Figure 2, type 2) the permeability-values of the inception horizons were below the lowest measurement limit of 0.1 mD.

Beside the very low values found for type 2 inception horizons it was not possible to distinguish other groups of the values (for example the existence of a minimal permeability value that would be necessary for an inception horizon to develop).

It is to point out that the absolute value of the measured properties has only a subordinated significance: It is mainly the contrast between the properties of inception horizons and the surrounding rock mass which is relevant. Regarding permeability an inception horizon is expected to develop because it is significantly more permeable than the surrounding rock mass and not because his permeability is higher than a given value.

Cave	Cave inception took place	Permeability [mD]		
		above	*inception horizon*	below
Nidlenloch (SO, Switzerland)	**within**	<0.1	*0.40*	0.18
	within	0.12	*0.60*	no data
Gamsalp (SG, Switzerland)	**at contact**	0.14	*0.10*	0.14
Réseau de Covatannaz (VD, Switzerland)	**at contact**	0.11	*<0.1*	no data
	within	no data	*0.24*	0.10
Réseau des Grottes aux Fées (VD, Switzerland)	**within**	0.14	*0.20*	0.11
	within	<0.1	*0.17*	<0.1
	at contact	0.23	*<0.1*	0.90
Hölloch (SZ, Switzerland)	**at contact**	0.17	*<0.1*	0.18
	within	0.18	*0.15*	0.18
Siebenhengste Cave System (BE, Switzerland)	**within**	0.21	*0.14*	0.31
	at contact	0.17	*<0.1*	0.13
	within	0.15	*0.23*	0.16
	at contact	0.09	*<0.1*	0.12
	within	0.10	*0.14*	0.11
	within	0.18	*0.26*	0.08
	within	0.14	*0.11*	0.13
	within	0.09	*0.11*	0.09

Tab. 1: Summary of the permeability measurements.

Considering the relative values (i.e. value of the inception horizon minus value of the rock mass) numbers above 0 mean that the inception horizon has a higher permeability than the surrounding rock mass, and numbers below 0 mean that the permeability is lower. Results presented in Figure 3 makes it possible to distinguish two groups of inception horizons: (1) horizons with a slightly higher permeability than the surrounding rock mass and (2) horizons with a slightly lower permeability. The more or less distinct linear trend in the plot indicates that the rocks above and below the inception horizons are similar and that only the favourable horizon has a different value. The permeability differences are in the order of a few

tenth of mD. However a Student's t-Test established that the average of the differences in permeability-values between the inception horizons type 1 and the surrounding rock masses are significant different (level of 95 %) compared to differences between values of the rock mass above and below the inception horizon.

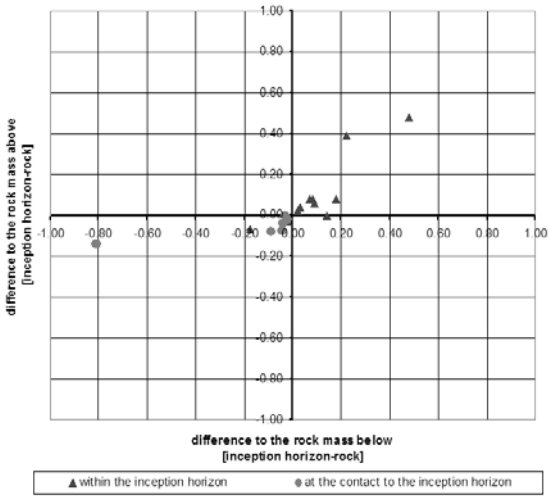

Fig. 3: Diagram of the difference in permeability between the inception horizon and the surrounding rock mass (above/below). It is conspicuous that type 2 inception horizons (dots) all plot in low-right quadrangle, i.e. corresponding to situations where the initial permeability of the inception horizon is lower than rock matrix permeability. Type 1 inception horizons mostly plot in the up-left quadrangle, i.e. where initial permeability of the inception horizon is higher than the surrounding rock-matrix.

4. Discussion

In order to understand why karst occurred only along some specific stratigraphical horizons it is necessary to understand processes of early stage of speleogenesis. The so called period of the "cave inception" can be defined as starting as soon as the permeability of the rock mass increases steadily due to dissolution processes. One may expect that at this early stage of the evolution dissolution is low and slow, therefore contrasts in permeability are still moderate and the influence of the hydraulic gradient is restricted. In other words flow is still diffuse and distributed within the whole rock mass. However some horizons tend to increase their permeability slightly faster than others, preparing the later development of karst conduits (e.g. LOWE, 1992; FILIPPONI ET AL., 2008). When relief becomes steeper, higher gradients do occur, what reorganizes the flow path and selects a few horizons which provide the weakest resistance to flow (i.e. in which are parallel to the hydraulic gradient). This phase of cave gestation ends when the first conduit is big enough to produce a change from laminar to turbulent flow all across the karst system ("breakthrough"). From this point on conduit development is fast and caves can reach human size within a few thousands of years. This corresponds to the phase of cave development (e.g. DREYBRODT ET AL., 2005).

In cases where cave inception took place within the inception horizon (type 1) samples of the inception horizon displayed a slightly higher permeability than the surrounding rock mass (9 of 12 inception horizons). The reason for that is that this slight difference in permeability was sufficient to concentrate flow and dissolution along those planes.

Darcy's equation gives a linear relationship between flow rate and permeability. Therefore the difference in flow rate between inception horizons and the surrounding rock mass is in the order of ±50 to ±70%. This means that flow velocity through the inception horizons is 50 to 70 % higher than through the matrix of the surrounding rock mass and therefore that karstification should also be enhanced. Although values are small and contrasts are low compared to the total range of permeability found in a karstified rock, this contrast of 50 to 70 % of the initial conditions may be large enough to produce a flow concentration and a preferential development of karst along those horizons.

Some theoretical background makes it possible to estimate the minimal time duration required for developing a network of karst conduits from initial state to turbulent breakthrough (e.g. DREYBRODT ET AL., 2005, PALMER, 2000). These authors give the theoretical breakthrough time (duration of the gestation phase) for a single fracture assuming that boundary conditions during the karstification do not change (e.g. hydraulic head, Pco_2, water temperature). This latter assumption is quite consequent because, in reality, boundary conditions change often according to changes in outside (surface) conditions (meteorological, climatic and landscape evolution). However the estimated breakthrough time gives an order of magnitude of the time required for the development of a karst conduits.

In this model we introduced the initial aperture width of the initial fracture by calculating the equivalent permeability of a single fracture. The measured permeability of our samples correspond to an equivalent single fracture width of around $3*10^{-5}$ mm, what would give a breakthrough-time of more than 10^{16} years (depending on the hydraulic gradient as well as on the length of the flow path) (figure 4). Note that a change in the water temperature and/or partial pressure of CO_2 would change the breakthrough time of one order of magnitude at the most. The lithological properties of the rock mass (EISENLOHR ET AL., 1999) may have a stronger effect. Obviously our understanding of the relationship between the rock properties and the empirical parameter used for the breakthrough time estimation is still not sufficient (DREYBRODT ET AL., 2005).

In order to see if the permeability difference between the inception horizons and the surrounding rock mass can explain the concentration of karst development along inception horizons, we assumed that those have the same lithological properties as the surrounding rock mass. Therefore in this hypothesis the variation in primary permeability would be the only reason for a faster karstification of the inception horizons. If so, we can use the figure 4 to roughly estimate the breakthrough time duration. Using the measured permeability time durations are several orders of magnitude higher than the age of the rock (10^8 years). We could thus conclude that the contrast and absolute values of the primary permeability is, in most cases, not the main factor that makes a stratigraphical horizon favourable to karstification. However we know that our data set is biased.

The above discussed estimation of the breakthrough time does not take into account other factors than the primary

permeability, assuming that the permeability distribution within the inception horizon is homogeneous, i.e. that no variations in litholotical properties occur at a microscopic scale and that the karstification takes place all over the horizon.

Field observations show that cave conduits mainly developed at the intersection between bedding planes and fractures (e.g. JAMESON, 1985; LAURITZEN & LUNDBERG, 2000; FILIPPONI ET AL. 2008) i.e. bedding planes are dominant but fracture still play a role. One reason for this field evidence could be that fractures occur later in the history of the rock mass, i.e. during the speleogenetic phase of the cave gestation or even later during the cave development phase. The intersection of bedding plane horizons by fractures increases the permeability along intersection lines (KIRALY, 1969) by orders of magnitude.

Our data show that in the six inception horizons of type 2 (inception took place at the contact to the inception horizon), permeability is slightly lower than in the surrounding matrix, meaning that the bedding plane had act as a low permeability "screen" along which water flew preferentially. However under low gradient conditions, like they prevail during the speleogenetical phase of cave inception, this screen effect is probably marginal because the low hydraulic gradient extends parallel to the inception horizon.

5. Conclusion

The analysis of the 3D geometry of conduit networks of different large cave systems around the World showed that the development and position of karst conduits under phreatic conditions is remarkably related to a restricted number of so called "inception horizons". To understand why those particular stratigraphical horizons are favourable to karstification we sampled 18 inception horizons as well as the surrounding rock mass of six cave systems and measured their primary rock permeability.

The measured primary permeability is generally very low (some 0.1 mD ≈ 10^{-16} m^2). However a correlation could be established between cases where cave inception took place within the inception horizon (inception horizon type 1), in which permeability is slightly higher than that of the surrounding rock mass. In inception horizon of type 2 (inception horizons where cave inception took place at the contact) permeability of inception horizons is lower than that of the surrounding rock mass.

A theoretical approach linking the initial permeability of an inception horizon and the time duration required for turbulent breakthrough to occur has been attempted. It shows that the contrast in primary permeability between the slightly more permeable inception horizons and the surrounding rock mass can not explain the cave development along inceptions horizons. The permeability is so low that it would take billions of years to reach turbulent breakthrough. Thus the observed permeability values will not allow a karst conduit to develop in reasonable geological time scale (age of the rock ~10^8 years).

However three facts are not taken into consideration in this theoretical approach:

1) Bedding planes and fractures do not occur at the same time during the history of a rock massif. Whereas the inception of the bedding planes begins just after the diagenesis, the occurrence of fractures is a later phenomenon (maybe occurring during the phase of gestation). Our permeability measurements reflects the situation before the beginning of the karstification (i.e. at the beginning of the inception phase), whereas the permeability of an inception horizons at the end of the inception phase will probably be at least one order of magnitude higher.

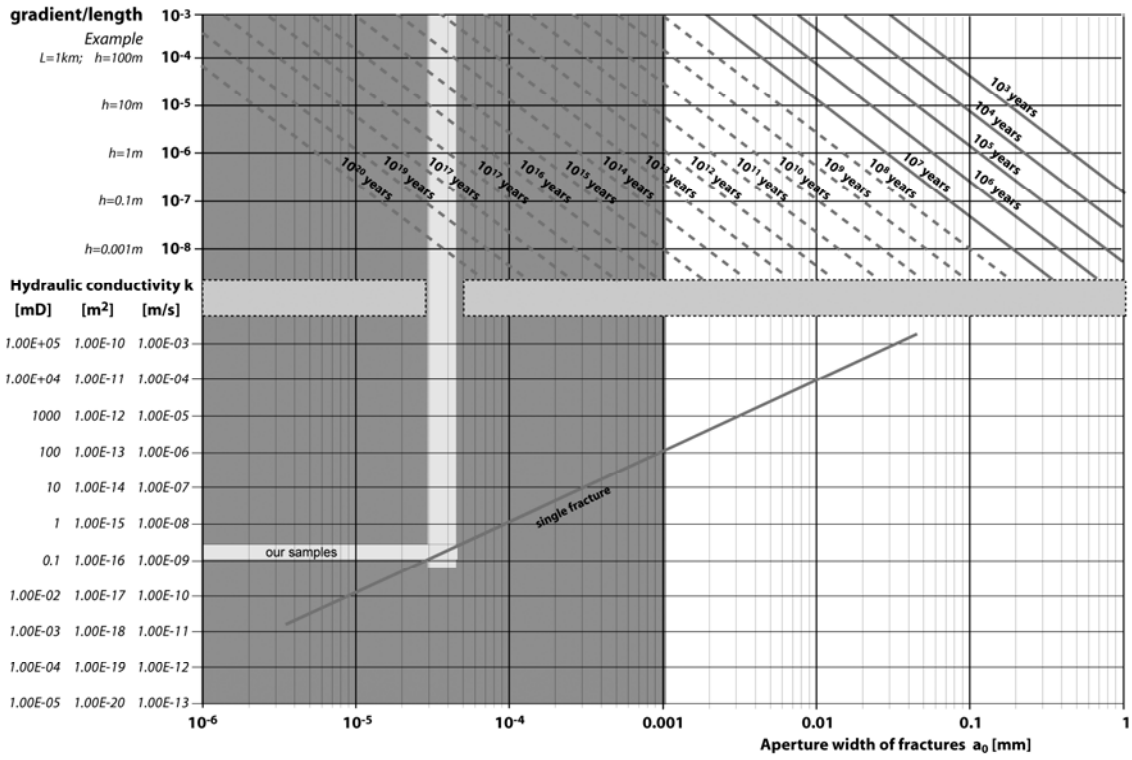

Fig. 4: Estimation of the breakthrough time: The lower part of the diagram shows the relationship between the permeability and the aperture width of an equivalent single fracture. The upper part of the diagram gives an estimate of the time required to enlarge a given initial fracture to turbulent breakthrough for different hydraulic gradients as well as flow distance. Dashed lines are extrapolations of a graphic given by PALMER (2000).

2) The initial permeability of bedding planes inception horizons is low (as measured), but inception horizons are often intersected by fractures. Bedding planes with the largest permeability (inception horizons) just before their intersection by fractures are supposed to give intersections with the highest permeability too, but with values orders of magnitude higher than without fractures.

3) In this paper our analysis focused on permeability measurements. Several other parameters are supposed to play a significant role in the inception hypothesis. Contrasts in dissolution rate (e.g. Mg-Ca contents) and/or increasing of the dissolution capacity of the seepage water (e.g. by the weathering of pyrites) could significantly influence the inception process. Samples showing indications of those processes have been removed from our data set in order to assess the initial permeability (without any dissolution process), what produces a significant bias.

Further investigations are being carried out in order to fully address the characterisation and weighting of the key parameters that make a bedding plane favourable to karstification.

Acknowledgements

This project is supported by the Swiss National Foundation for Scientific research (project number 200020-116207/1).

We would like to thank collaborators of the Department of Geology and Palaeontology of the University of Geneva for the use of their laboratory.

Literature

DREYBRODT W., GABROVSEK F., ROMANOV D. (2005) Processes of Speleogenesis: a modelling approach. Carsologica, ZRC Publishing, Ljubljana.

EISENLOHR L., METEVA K., GABROVSEK F., DREYBRODT W. (1999) The inhibiting action of intrinsic impurities in natural calcium carbonate minerals to their dissolution kinetics in aqueous H2O-CO2 solutions. Geochimica et Cosmochimica Acta 63, 989-1001.

FILIPPONI M. (2007) Speläologische Erscheinungen im Zusammenhang mit stratigraphischen Initialfugen. Laichinger Höhlenfreund, 42 : 21-32.

FILIPPONI M. & DICKERT A. (2007) Verstehen der Speläogenese durch 3D-Analyse - Fallbeispiel des Lachenstock-Karstes. 12. Nat. Cong. of Speleology - Switzerland: 46-55.

FILIPPONI M. & JEANNIN P.-Y. (2006) Is it possible to predict karstified horizons in tunneling? Austrian Journal of earth sciences, 99: 24-30

FILIPPONI M., JEANNIN P.-Y., TACHER L. (2008) Evidence of inception horizons in karst conduit networks. Geomorphology, (accepted).

GOGGIN D.J. (1993) Probe permeametry – Is it worth the effort? Marine and Petroleum Geology 10, 299-308.

JAMESON R.A. (1985) Structural segments and the analysis of flow paths in the North Canyon of Snedegar Cave, Friars Hole Cave System. MS Thesis, West Virginia University, Morgantown.

KIRALY L. (1969) Anisotropie et hétérogénéité de perméabilités dans les calcaires fissurés. Eclogea Geologica Helvetica 62/2, 613-619.

KIRALY L. (1975) Rapport sur l'état actuel des connaissances dans le domaine des caractères phsyiques des roches karstiques. – In:Burger and Dubertret (eds): International Union Geol. Sci., Series B, 3, 53-67.

KNEZ M. (1997) Speleogenesis of phreatic channels in bedding-planes in the frame of karst aquifer (Skocjanske Jam Caves, Slovenia). 12th UIS Congress, La Chaux-de-Fonds 2, 279-282.

LAURITZEN S.-E. & LUNDBERG J. (2000) Solution and Erosional Morphology. . – In: Klimchouk, Ford, Palmer and Dreybrodt (eds): Speleogenesis, Evolution of Karst Aquifers, 408-426.

LOWE D. (1992) The origin of limestone caverns: in inception horizon hypothesis. – PhD Thesis, Manchester Polytechnic, United Kingdom.

LOWE D. (2000) Role of stratigraphic elements in speleogenesis: the speleoinception concept. – In: Klimchouk, Ford, Palmer and Dreybrodt (eds): Speleogenesis, evolution of karst aquifers, 65-76.

MICHALSKI A. & BRITTON R. (1997) The role of bedding fractures in the hydrogeology of sedimentary bedrock - Evidence from the Newark Basin, New Jersey. Ground Water 35/2, 318-327.

MULDOON M.A., SIMO J.A., BRADBURY K.R. (2001) Correlation of hydraulic conductivity with stratigraphy in a fractured-dolomite aquifer, northeastern Wisconsin, USA. Hydrogeology Journal, 570-583.

ORNDORFF R.C., WEARY D.J., SEBELA S. (2001) Geologic Framwork of the Ozarks of South-Central-Missouri – Contributions oto a Conceptual Model of Karst. – In: Kuniansky (eds): U.S. Geological Survey Karst Interest Group Proceedings, Water-Resources Investigations Report 01-40011, 18-24.

PALMER A.N. (2000) Hydrogeologic control of cave patterns. – In: Klimchouk, Ford, Palmer and Dreybrodt (eds): Speleogenesis, evolution of karst aquifers, 77-90.

PEZDIČ J., ŠUŠTERŠIČ F., MIŠIČ M. (1998) On the role of clay-carbonate reactions in speleoinception – A contribution to the understanding of the earliest stage of karst channel formation. Acta Carsologica 27/1, 187-200.

ROVEY C.W. & CHERKAUER D.S. (1994) Relation between hydraulic conductivity and texture in a carbonate aquifer – Regional conductivity. Ground Water 32/2, 227-238.

Filipponi M., Jeannin P.-Y., 2008:
Prediction of karst occurrences by interpreting borehole data within the Inception Horizon Hypothesis.
Sinkholes and the Engineering and Environmental Impacts of Karst 2008, Proceedings of the 11th Multidisciplinary Sinkhole Conference, Geotechnical Special Publication 183: 120-130.
doi: 10.1061/41003(327)13

Prediction of karst occurrences by interpreting borehole data within the Inception Horizon Hypothesis

Marco Filipponi[1] and Pierre-Yves Jeannin[2]

[1] GEOLEP, Laboratoire de Géologie de l'Ingénieur et de l'Environnement, Swiss Federal Institute of Technology Lausanne (EPFL), CH-1015, Lausanne – Switzerland, +41 (0)21 693 42 60, marco.filipponi@epfl.ch.
[2] SISKA, Swiss Institute of Speleology and Karstology Research, Switzerland CH-2301 La Chaux-de-Fonds – Switzerland, pierre-yves.jeannin@isska.ch.

ABSTRACT

The use of borehole logging data is common in engineering geological investigation programs. These data offer a vertical view to the variation of the physical, chemical or lithological properties of the rock series. Concerning karst, the interpretation of borehole data has been, so far, mainly restricted to the detection and characterisation of dissolution voids, which have been usually considered as randomly distributed in space and therefore any prediction of karst occurrences at a more regional scale was supposed as not possible.

Our research focussed on the analysis of the 3D geometry of several of the largest cave systems in the World (almost 1500 km of analysed cave conduits). It showed that the development and position of karst conduits under phreatic conditions is remarkably related to a restricted number of so called “inception horizons”. An “inception horizon” – a concept introduced by Lowe (1992) – is a part of a rock succession that is particularly susceptible to the effects of the earliest cave forming processes.

This concept provides a theoretical framework in which the interpretation of borehole data can be used to characterize and predict karst occurrences up to a regional scale.

INTRODUCTION

Karst occurrences and hazards create worldwide huge annual costs as well as social, security-related and environmental problems because of difficulties related to their exceptionally complex internal structure and flow patterns (e.g., Marinos 2001; Waltham and Fookes 2003; Day 2004; Xeidakis et al. 2004). Problems are not only related to engineering constructions such as tunnels, buildings or dams but concern also the

management and protection of karst groundwater, that is in many parts of the World an important or even the only resource of groundwater. The main question beyond many of these problems is to know whether there is a developed network of karst conduits; if yes, where; and in some cases what are the main conduit characteristics (e.g. active/fossil, phreatic/vadose, size). A better understanding of speleogenesis is required to address these questions.

Over the last 20 years many cave and karst scientists suggested that conduits preferably develop along a restricted number of discrete stratigraphical horizons (i.e. bedding planes; e.g., Rauch and White 1970; Ford and Cullingford 1976; Palmer 1989). Based on this observation Lowe (1992) developed the "inception horizons hypothesis" (IHH). An inception horizon (IH) is a part of a rock succession that is particularly susceptible to the effects of the earliest cave forming processes by virtue of physical, lithological or chemical deviation from the predominant carbonate facies within the surrounding sequence. Following this idea the position of inception horizons could be predicted, i.e. the position of horizons with an elevated probability of karst occurrences. However until recently there was no clear evidence of the existence of these horizons or at least of their significance in a probabilistic point of view.

Since 2005 we analysed the 3D geometry of several large cave systems from all around the World in order to show that the development of karst conduits is not random but predictable and linked to the existence of inception horizons. Furthermore we sampled different inception horizons as well as the surrounding rock mass to determine parameters controlling the speleogenesis and we could show that they can be recognized and possibly identified from borehole data.

The use of borehole logging data is common in engineering geological investigation programs. These data offer a vertical view of the variation of the physical, chemical or lithological properties of the rock series. In civil engineering borehole data are mainly used for geotechnical purposes. Concerning karst, these data were mainly utilized to detect locally some dissolution voids or areas with increased permeability, or water inflow. To date occurrences of karst in boreholes have been usually considered as random (e.g., Benson and Yuhr 1993; Paillet 2001), which would make any inter/extrapolations of observed features almost impossible. The inception horizon hypothesis provides a theoretical framework that allows for a new interpretation of borehole data.

This paper shows that the inception horizon hypothesis allows for making prediction of karst occurrences at local to regional scale and it sketches how borehole logging data can improve, in this framework, the characterization of karst systems for hydrogeolgical, engineering geology or petroleum industry proposes.

EVIDENCES SUPPORTING THE INCEPTION HORIZON HYPOTHESIS

Until recently, the concept of the inception horizon hypothesis (Lowe 1992) was not widely recognised and no clear demonstration of its validity was available, albeit existing detailed field observations in caves supported the idea that caves develop along a restricted number of stratigraphical horizons (i.e. bedding planes) (Rauch and White 1970; Ford and Cullingford 1976; Palmer 1989). In order to provide a demonstration of

the concentration of karst development along some specific lithological horizons within a limestone series we developed a methodology based on geological 3D models and cave survey data. This method brought a statistical evidence of the existence of inception horizons (Filipponi and Jeannin 2006; Filipponi et al. 2008). The analysis was based on 18 large cave systems from all around the World, which included more than 1500 km of conduits. It confirmed that the development of karst conduits under phreatic conditions is strongly related to a restricted number of inception horizons (in most cases between three and five horizons within a karst massive) (fig. 1): Probably less that 10% of the existing bedding partings of a limestone sequence are inception horizons and guide more than 70 % of the phreatic conduits (Filipponi et al. 2008). Therefore it appeared clearly that the influence of these horizons on the 3D geometry of cave systems is high. Direct observation of those horizons in caves (Filipponi 2007) showed that most horizons have a thickness of some centimetres to decimetres meaning that the conduits started its development along the inception horizon, whereas the conduit accessible today became much higher than the initial horizon.

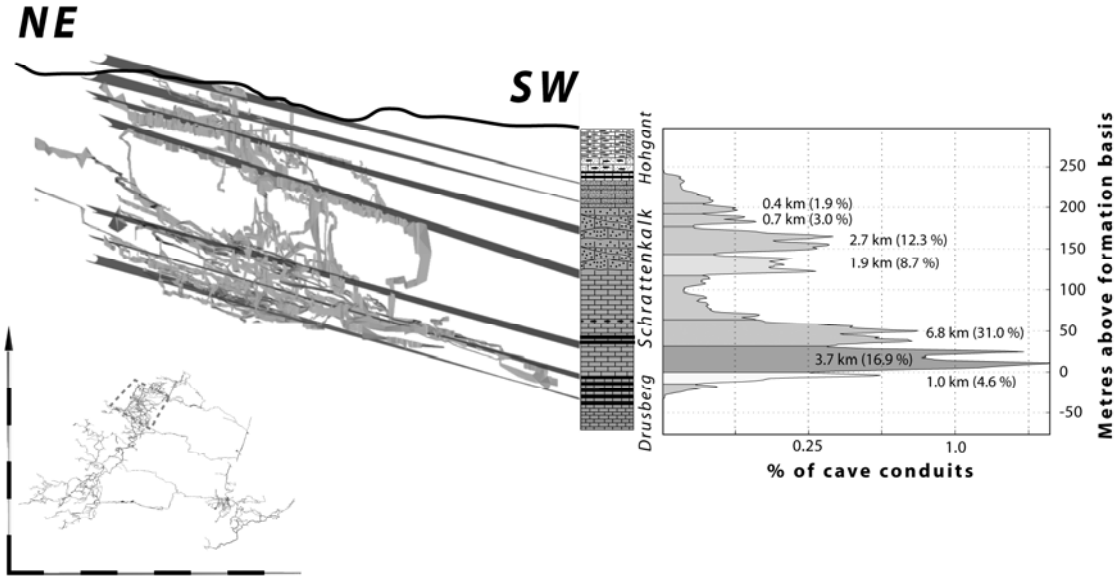

Fig. 1: Horizontal projection of one part of the Siebenhengste cave system (Switzerland, length 154 km). Up to seven potential "inception horizons" can be identified within the Schrattenkalk limestone formation. Total thickness of the limestone is nearly 180 meters.

Although quite efficient our methodology encloses some bias. One problem is that it is based exclusively on conduits which are large enough for men to pass through (>50 cm), but the minimum size for a karst conduit is around 0.01 m. The number and cumulated length of conduits smaller than 0.5 m is probably very high, but is poorly known to date. We are therefore not able to include them in our 3D analysis. However, the occurrences of anastomoses along some inception horizons (anastomoses are small channels (2-10 cm in diameter) forming a dense network of small conduits along a plane; Slabe 1995) allows us to assume that they are also located preferentially along the identified inception

horizons and that it is mostly a question of time and boundary conditions that limited the size and geometry of the voids (e.g., Filipponi and Jeannin 2008a). It can thus be assumed that a significant amount of karst occurrences of different sizes is concentrated along some discrete inception horizons. A careful observation showed that conduits mainly follow the intersection lines between the horizon and the predominating joint sets. The main direction along which conduits are developed is determined by the hydrogeological gradient, i.e. along the intersection lines, which are sub-parallel to the hydraulic gradient (fig. 2).

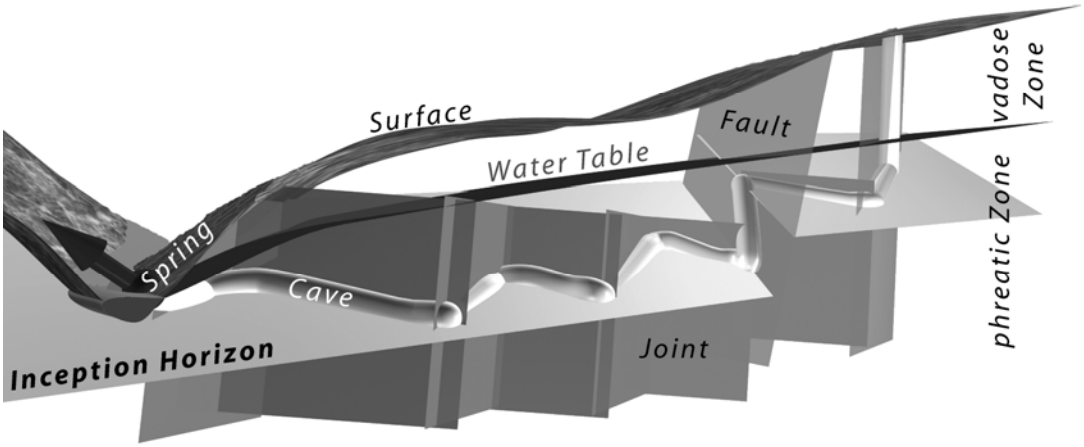

Fig. 2: Schematic 3D model of a karst conduit system: The geometry of phreatic conduits is determined by inception horizons (in most cases related to well-marked bedding planes), joints and faults as well as by the hydraulic gradient.

Why a particular horizon was so favourable for karstification? To address this question we sampled and analysed more than 200 rock samples from different inception horizons as well as from the surrounding rock mass (Filipponi and Jeannin 2008b). We can assume that there are three main properties of inception horizons that make one particular bedding plane especially favourable to karstification; 1) properties that define the permeability, 2) properties that control the dissolution rate, and 3) properties controlling the dissolution capacity of the water. The processes under investigation being highly non linear, it is expected that the links between these properties is quite complex. The rock samples of inception horizons and of the surrounding rock matrix are currently being analysed considering these three properties. Our first results allow us to expect some properties for which deviations of inception horizons compared to the surrounding rock mass are observed. At this stage the carbonate content, the primary permeability and the presence of pyrite seem to be relevant (Filipponi and Jeannin 2007; Filipponi and Jeannin 2008b).

It seems thus that mainly lithological deviations from the predominant carbonate facies are responsible for the fact that a given bedding plane is a potential inception horizon. Therefore we can postulate that a given inception horizon has a certain continuity along

the entire lateral extension of the stratigraphical horizon.

This conception of karst massifs improves the potential extrapolation/interpolation of locally identified inception horizons (form the analysis of cave survey data and/or boreholes logging) to a more regional scale. It proves that karst occurrences should not be considered as random, but can be assessed in a more precise way.

HOW CAN INCEPTION HORIZONS BE IDENTIFIED FROM BOREHOLE DATA

In our methodology the identification of regional scale inception horizons is based on cave survey data. However, for many karst regions such data are not available (or are in insufficient quantity and/or quality). In such cases the analysis of boreholes data can be an alternative.

At least three types of observations can be used to identify/detect inception horizons in a borehole: 1) optical identification of dissolution voids; 2) detection of high porosity zones, and 3) identification of zones with a higher permeability.

The following paragraphs shortly present each of them. The choice of the most appropriate method depends mainly on the problem to be addressed, on the information about the karst system, which is required, as well as on the logistical possibilities.

Optical identification of dissolution voids

The optical identification is the more intuitive way to recognise karst occurrences. On the one hand it is possible to inspect the drilling cores (if available) by eyes, and on the other hand one can use borehole televiewers (visual or acoustic), which provide images of the borehole walls (e.g., Cunningham 2004; Manda and Gross 2006). Today the resolution of televiewers is comparable to a direct visual inspection. Dissolution voids a few millimetres large can therefore be identified.

The size of karst voids typically ranges from microscopic intra granular dissolution features up to cave conduits of several metres in size. However in most cases the size of the intersected karst features in boreholes is smaller than the borehole diameter and they appear as small conduits or as “weathered” stratigraphical intervals.

These observation methods are relatively cheap and fast and make it possible to know the nature of the hydraulic features intersected by the borehole: fracture-like, small dissolution voids or larger karst conduits. They should also allow for recognising lithologic changes (rock fabric, grain size and shape, colour, etc.). However these methods give any information about the connectivity of the voids.

Detection of high porosity zones

Inception horizons are characterized by a concentration of dissolution voids of various sizes, i.e. with a higher (secondary) porosity than to the rock mass. Therefore any methods allowing for the assessment of the rock porosity are appropriate for the localisation of inception horizons.

The commonly used Gamma-Gamma method gives the density (i.e. porosity) variation along a borehole. It seems to be also adequate to detect potential inception horizons (e.g.,

Tipping et al. 2006). Furthermore, this logging method also allows for a rough distinction of the different lithologies cut by the borehole.

Identification of zones with a higher permeability

Most karst voids cannot grow as isolated features in the rock mass but are the results of water flowing through fractures and conduits. This means that they belong to an interconnected network of dissolution voids of different sizes. Therefore inception horizon should display a higher permeability than the surrounding rock mass. All available methods able to assess permeability or groundwater in/outflows in boreholes are therefore interesting for the identification of inception horizons. For example temperature measurements, flowmeter measurements, discrete interval packer tests, etc.

A continuous temperature (or electrical conductivity) profile of the borehole is a simple and fast way to get a first idea about the water movements within an open borehole. Temperature anomalies can be interpreted as water in-/outlets, thus as zones of higher permeability (due to the network of dissolution voids along inception horizons). However this method can only be used in boreholes stretching below the groundwater table (phreatic zone).

Flowmeter logging can be used to assess the permeability variations along boreholes by measuring the vertical flow variations within an open borehole (coupled to a calliper log). Electromagnetic flowmeters can measure flows as low as to 0.01 l/s (Paillet et al. 2000; Tipping et al. 2006). Impeller-type flowmeters require several litres per minute in order to produce measurable flow (depending on the borehole diameter). The logging can be done under natural or stressed conditions (either during pumping or injection) and can be therefore also applicable in the vadose zone (above the groundwater table).

Packer tests with discrete intervals of a few metres (or less) provide good measurements of the interval permeability integrating an idea of the borehole neighbouring (depending on the applied hydraulic test) (Lemieux et al. 2006). It can therefore provide the position of potential zones of higher secondary permeability (which might be due to dissolution processes along an inception horizon). Packer tests are applicable in both the vadose and phreatic zones.

A big drawback of this group of methods is that they only give the position of potential inception horizons relatively to the top of the borehole. They don't intrinsically provide information about the stratigraphical position of potential inception horizons. A complementary geological survey is therefore necessary. Another weakness is that these methods do not give any information about the nature of the potential inception horizons identified (are they due to fractures or dissolution voids). These methods are quite time consuming and therefore expensive.

DISCUSSION

The use of borehole logging data is common in engineering geological investigation programs. Borehole geophysics presents several tools that may be applied to assess the heterogeneity of a karstic rock mass. But how far from the borehole do these methods

provide information? Is it founded to correlate logs between boreholes and assume that hydrogeological connections do exist at a regional scale?

In the existing literature different descriptions indicate or even describe the existence of some stratigraphical horizons that are favourable to the karstification in boreholes. They could even be recognized at a regional scale. For examples Paillet and Crowder (1996) describe: "[…] inflow to or outflow from a series of boreholes in northern Illinois was associated with solutionally enlarged bedding plane openings. Many such bedding planes intersected each borehole, but only a few conducted most of the flow. The correlation of these bedding planes was established over borehole separations of about a kilometre […]".

The inception horizon hypothesis (Lowe 1992) was confirmed by a statistical analysis of different large cave systems (Filipponi et al. 2008) as well as by field observations in caves (e.g., Filipponi 2007). This approach should be now applied to borehole observations, what would provide a theoretical framework helping for the interpolation of karst occurrences between different boreholes up to a regional scale.

Detailed field observations in caves showed that some conduits developed at a local scale also along other bedding planes than those identified by the statistical (regional) approach (Filipponi et al. 2008). Obviously those bedding planes do not present favourable properties over extended areas and are therefore not significant at a regional scale. For borehole data interpretations it means that an identified karstified stratigraphical horizon can be an inception horizon of local or regional significance. The distinction can only be made by correlating horizons recognized in several boreholes and/or in caves or rock outcrops. However the only way to prove connections at regional scale is to proceed to hydraulic tests between boreholes.

The inception horizon hypothesis allows for assessing the position of potential karst conduits. However along karst genesis other factors determine if conduits really develop along them or not. Thus the identification of an IH in a borehole does not mean that this particular horizon really encloses conduit. On the other hand, even for an IH which encloses conduits the measured/observed properties in a borehole do not correspond to properties of the conduits or even of properties of the IH in another borehole (heterogeneity along one single IH). A semi-quantitative extrapolation of any data is not straight forward. Further data are required to estimate if an IH is highly karstified or not. A good knowledge of the hydrogeological history of the area as well as of the geological structure is needed (Filipponi and Jeannin 2008a).

As mentioned the development of a conduit network along an inception horizon is strongly related to the history of the hydrogeological boundary conditions (e.g. two compartments shifted by a fault may be in different positions relatively to the hydrogeological boundary conditions and thus enclose different conduits networks). This is illustrated by the 3D analysis of large cave systems where the cumulated conduit length along an inception horizon considerably varies in different compartments of the same cave system (Filipponi et al. 2008). An explanation to this fact is given by the following brief description of the speleogenesis process. It assumes that characteristics of an IH are defined quite early along the speleogenesis process. i.e. during the so called period of the "cave inception", which can be defined as starting as soon as the permeability of the rock

mass increases steadily due to dissolution processes (e.g., Lowe 1992; Filipponi et al. 2008), i.e. straight after the rock diagenesis phase (fig. 3). Karst conduits occur later when voids are large enough and connected to allow turbulent flow and a much quicker dissolution. At this stage of speleogenesis some IH are more favourable (more parallel) to flow towards the outlet of the system than others. Therefore only a subset of IH is used by conduits. According to landscape evolution, the outlet of the system moves along time and new conduit systems are developed under other flow conditions, which may change the IH used by conduits. Therefore a good knowledge of the paleohydrology and geology can be very helpful for assessing conduits positions and characteristics.

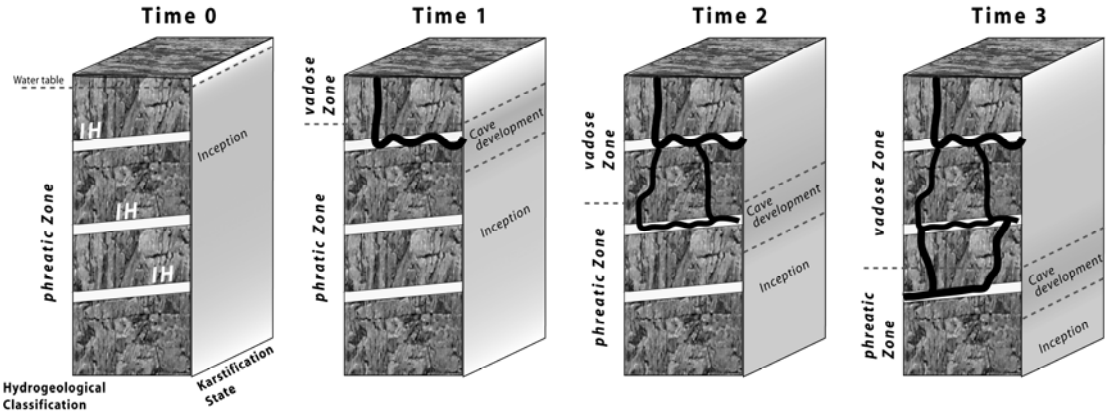

Fig. 3: Schematic development of a karst system in time and space (vertical section): Different parts of the system are in a different karstification state at the same time.

A strong advantage of boreholes against cave observations is to make possible, with appropriate hydraulic tests to verify hydraulic connections (i.e. the presence of IH or even conduits) at a regional scale. These tests should be designed within the concept of the inception horizon hypothesis. One possible test configuration is described by Lemieux et al. (2006). They designed pumping and pulse interference tests with pumping or injection of water into one well and measurement of the response in other two other wells located 10 to 20 m away. The observation wells were equipped with inflatable packers that isolated the conductive bedding planes (i.e. inception horizons) where responses could be observed. Due to the complex and highly heterogeneous nature of karst more sophisticated tests are supposed to be designed for covering the wide range of possible situations.

CONCLUSION

The detailed 3D analysis of large cave systems around the World demonstrates that the regional development of karst conduits under phreatic conditions is strongly related to a restricted number of stratigraphical horizons (i.e. normally between three and five inception horizons). Detailed field and laboratory investigation of these horizons confirmed the inception horizon hypothesis, considering that the occurrences of those

horizons are due to lithological deviations from the predominant carbonate facies within the surrounding sequence.

This leads to a conceptual model of karst in which karst conduits develops preferentially along certain stratigraphic horizons (i.e. inception horizons). The main direction of the conduits is determined by the hydrogeological context. Therefore conduits will develop at the intersection lines between IH and joints, which are sub-parallel to the regional hydraulic gradient. Characteristics of the dissolution voids depend on the local hydrogeological history (e.g. active/fossil, phreatic/vadose, size).

The inception horizons hypothesis gives a speleogenetical framework which will help interpretations of borehole data and improve the correlation between boreholes, as well as the extrapolation of "potential inception horizons" over the entire extent of the corresponding stratigraphical horizons.

This paper does not present direct results of borehole data analyses because, in our studies, we did not use such data. The aim is here to encourage this type of study because a quick look at the literature is encouraging, showing that the inception horizon hypothesis seems applicable. Thus the purpose of this short paper is to inform and encourage people to look at borehole data within the context of the IHH. We are currently working at the development of an applied method for dealing engineering problems in karst (including the application of the IHH) and anyone is welcome to share his experience with the authors.

Many challenges remain in this development, especially because speleogenesis processes are complex and they highly depends on many factors, which are not always easy to assess (e.g. paleohydrogeology). Further developments are required to improve our ability to characterize karst aquifers.

However, the identification of the position of inception horizons in a rock mass provides a substantial improvement for the assessment of a karst system. Furthermore we believe that the identification of inception horizons by the combined analysis of cave survey data and borehole data is a good tool for predicting karst occurrences, what is very important for the management and protection of karst groundwater.

ACKNOWLEDGEMENTS

This project is supported by the Swiss National Foundation for Scientific Research (project number 200020-116207/1).

LITERATURE

Benson R.C., Yuhr, L. (1993). "Spatial sampling consideration and their applications to characterizing fractured rock and karst systems". *Environmental Geology* 22: 296-307.

Cunningham, K.J. (2004). "Application of ground-penetrating radar, digital optical borehole images, and cores for characterization of porosity hydraulic conductivity and paleokarst in Biscayne aquifer, south-eastern Florida." *Journal of Applied Geophysics* 55:

61-76.

Day, M.J. (2004). “Karstic problems in the construction of Milwaukee’s Deep Tunnels.” *Environmental Geology* 45: 859-863.

Filipponi M. (2007). “Speläologische Erscheinungen im Zusammenhang mit stratigraphischen Initialfugen.” *Laichinger Höhlenfreund* 42: 21-32.

Filipponi, M., Jeannin, P.-Y. (2006). “Is it possible to predict karstified horizons in tunneling?” *Austrian Journal of Earth Sciences* 99: 24-30.

Filipponi, M., Jeannin, P.-Y. (2007). “Cave gypsum an indicator for early speleogenetical processes?” *Geophysical Research Abstracts*, EGU General Assembly, Vienna, Austria: (CD-ROM).

Filipponi, M., Jeannin, P.-Y. (2008a). “Possibilities and limits to predict the 3D geometry of karst systems within the inception horizon hypothesis.” *Geophysical Research Abstracts*, EGU General Assembly, Vienna, Austria: (CD-ROM).

Filipponi, M., Jeannin, P.-Y. (2008b). “What makes a bedding plane favourable to karstification? – The role of the primary rock permeability.” *4th European Speleological Congress*, Vercors, France: (accepted).

Filipponi M., Jeannin P.-Y., Tacher L. (2008). “Evidence of inception horizons in karst conduit networks.” *Geomorphology*: (accepted).

Ford, D., Cullingford, C.H.D. (1976). The Science of Speleology. Academic Press. 593p.

Lemieux, J.-M., Therrien, R., Kirkwood, D. (2006). “Small scale study of groundwater flow in a fractured carbonate-rock aquifer at the St-Eustache quarry, Québec.” *Hydrogeology Journal* 14: 603-612.

Lowe, D. (1992). The origin of limestone caverns: in inception horizon hypothesis. PhD Thesis, Manchester Polytechnic, United Kingdom, 511 p.

Manda, A.K., Gross, M. (2006). “Identifying and characterizing solution conduits in karst aquifers through geospatial analysis of porosity from borehole imagery: An example from the Biscayne aquifer, South Florida.” *Advances in Water Research* 29: 383-396.

Marinos, P.G. (2001). “Tunnelling and mining in karstic terrain: An engineering challenge.” - In: Beck and Herring (eds): Geotechnical and Environmental Applications of Karst Geology and Hydrology: 3-16.

Paillet, F.L. (2001). “Borehole Geophysical Applications in Karst Hydrogeology.” - In Kuniansky (eds): U.S. Geological Survey Karst Interest Group Proceedings, Water Resources Investigations Report 01-4011: 116-123.

Paillet, F.L., Lundy, J., Tipping, R.G., Runkel, A.C., Reeves, L., Green, A.J. (2000). “Hydrogeologic characterization of six sites in southeastern Minnesota using borehole flowmeters and other geophysical logs.” U.S. Geological Survey Water-Resources Investigation Report 00-4142.

Paillet, F.L., Crowder, R.E. (1996). “A Generalized Approach for the interpretation of geophysical well logs in ground water studies – theory and application.” *Ground Water* 34, 883-898.

Palmer, A.N. (1989). “Stratigraphic and structural control of cave development and groundwater flow in the Mammoth Cave region.” – In White W.B. and White E.L. (eds):

Karst Hydrology, Concepts from the Mammoth Cave Area, Von Nostrand Reinhold, New York: 293-316.

Rauch, H.W., White, W.B. (1970). “Lithologic controls on the development of solution porosity in carbonate aquifers.” *Water Resources Research* 6: 1175-1192.

Slabe, T. (1995). Cave rocky relief and its speleogenetical significance. Znanstvenoraziskovalni Center Sazu, Ljubljana, 128 p.

Tipping, R.G., Runkel, A.C., Alexander, E.C., Alexander, S.C., Green, J.A. (2006). “Evidence for hydraulic heterogeneity and anisotropy in the mostly carbonate Prairie du Chien Group, south-eastern Minnesota.” *Sedimentary Geology* 184: 305-330.

Waltham, A.C., Fookes, P.G. (2003). “Engineering classification of karst ground conditions.” Quarterly Journal of Engineering Geology and Hydrology 36: 101-118.

Xeidakis, G.S, Torok, A., Skias, S., Kleb, B. (2004). “Engineering Geological problems associated with karst terrains: their investigation monitoring, and mitigation and design of engineering structures on karst terrains.” *Bulletin of the Geological Society of Greece* 36: 1932-1941.

- Curriculum Vitae -

Personal data

Surname	**Filipponi**
First name	**Marco**
Date of Birth	**03. June 1976, in Baden (CH)**

Education

2005 - 2009	PhD candidate at the Swiss Federal Institute of Technology in Lausanne (EPFL)
2001 - 2003	Fachstudium in Earth Sciences at the Swiss Federal Institute of Technology in Zurich (ETHZ) (equivalent M. Sc.)
1998 - 2001	Grundstudium in Earth Sciences at the Swiss Federal Institute of Technology in Zurich (ETHZ) (equivalent B. Sc.)
1996 - 1998	Gymnasium in Baden, Economics (equivalent A level college)
1993 - 1996	College of Economics in Baden (Switzerland)

Research Interests

Speleogenesis

Stability of karst conduits

Cave climatology

Selected Publications

Filipponi M., Jeannin P.-Y., Tacher L., 2009: Evidence of inception horizons in karst conduit networks. Geomorphology 106, 86-99.

Filipponi M., 2006: Karstwanderführer Gamsalp: Entdecken - Kennenlernen - Verstehen. Ortsgemeinde Grabs.

Filipponi M., 2003: Die Stabilität von Karsthohlräumen am Beispiel der A.F. Lindner-Halle im Abisso di Trebiciano (Italien). MS thesis, Eidgenössische Technische Hochschule Zürich. http://e-collection.ethbib.ethz.ch/view/eth:26922

Filipponi M., 2003: Das Höhlenklima der Schrattenhöhle (Schweiz) – Auswertung einer 10 jährigen Messreihe. Eidgenössische Technische Hochschule Zürich, Institut für Atmosphäre und Klima. http://e-collection.ethbib.ethz.ch/cgi-bin/show.pl?type=semarb&nr=45